

AD-A129 773

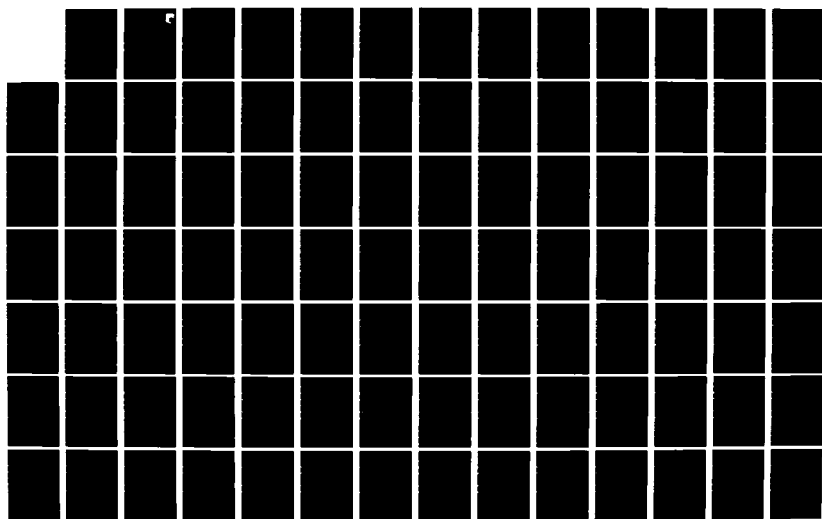
MAGNA (MATERIALLY AND GEOMETRICALLY NONLINEAR ANALYSIS)
PART 1 FINITE ELE (U) DAYTON UNIV OH RESEARCH INST
R A BROCKMAN DEC 82 UDR-TR-82-111 AFWAL-TR-82-3098-PT-1
F33615-88-C-3483

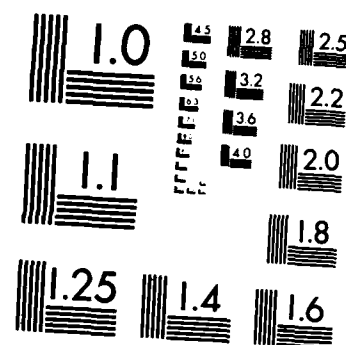
1/8

UNCLASSIFIED

F/G 12/1

NL





MICROCOPY RESOLUTION TEST CHART
NATIONAL BUREAU OF STANDARDS-1963-A

ADA 129773

AFWAL-TR-82-3098, Part I

(This report supersedes AFWAL-TR-81-3181, dated February 1982)

MAGNA (Materially and Geometrically Nonlinear
Analysis)

Part I - Finite Element Analysis Manual

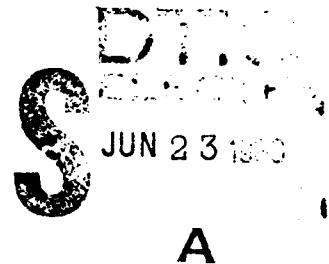


R. A. Brockman

University of Dayton Research Institute
300 College Park Avenue
Dayton, Ohio 45469

December 1982

Final Report, March 1980 - December 1982



Approved for public release; distribution unlimited.

FLIGHT DYNAMICS LABORATORY
AIR FORCE WRIGHT AERONAUTICAL LABORATORIES
AIR FORCE SYSTEMS COMMAND
WRIGHT-PATTERSON AIR FORCE BASE, OHIO 45433

DTIC FILE COPY

83 06 21 062

NOTICE

When Government drawings, specifications, or other data are used for any purpose other than in connection with a definitely related Government procurement operation, the United States Government thereby incurs no responsibility nor any obligation whatsoever; and the fact that the government may have formulated, furnished, or in any way supplied the said drawings, specifications, or other data, is not to be regarded by implication or otherwise as in any manner licensing the holder or any other person or corporation, or conveying any rights or permission to manufacture, use, or sell any patented invention that may in any way be related thereto.

This report has been reviewed by the Office of Public Affairs (ASD/PA) and is releasable to the National Technical Information Service (NTIS). At NTIS, it will be available to the general public, including foreign nations.

This technical report has been reviewed and is approved for publication.




ROBERT E. MCCARTY
Project Engineer



CHARLES A. BABISH, III
Acting Group Leader
Subsystems Development Group

FOR THE COMMANDER


SOLOMON R. METRES

Director
Vehicle Equipment Division

"If your address has changed, if you wish to be removed from our mailing list, or if the addressee is no longer employed by your organization please notify AFWAL/FIER, W-PAFB, OH 45433 to help us maintain a current mailing list."

Copies of this report should not be returned unless return is required by security considerations, contractual obligations, or notice on a specific document.

UNCLASSIFIED

SECURITY CLASSIFICATION OF THIS PAGE (When Data Entered)

| REPORT DOCUMENTATION PAGE | | READ INSTRUCTIONS BEFORE COMPLETING FORM |
|--|-----------------------|--|
| 1. REPORT NUMBER AFWAL-TR-82-3098, Part I | 2. GOVT ACCESSION NO. | 3. RECIPIENT'S CATALOG NUMBER |
| 4. TITLE (and Subtitle) MAGNA (Materially and Geometrically Nonlinear Analysis) Part I - Finite Element Analysis Manual | | 5. TYPE OF REPORT & PERIOD COVERED Final Report March 1980 - Dec. 1982 |
| 7. AUTHOR(s) R. A. Brockman | | 6. PERFORMING ORG. REPORT NUMBER UDR-TR-82-111 |
| 9. PERFORMING ORGANIZATION NAME AND ADDRESS University of Dayton Research Institute 300 College Park Avenue Dayton, Ohio 45469 | | 8. CONTRACT OR GRANT NUMBER(s) |
| 11. CONTROLLING OFFICE NAME AND ADDRESS Flight Dynamics Laboratory (AFWAL/FIER) Air Force Wright Aeronautical Laboratories Wright-Patterson Air Force Base, OH 45433 | | 10. PROGRAM ELEMENT, PROJECT, TASK AREA & WORK UNIT NUMBERS Prog. Ele. 62201F Proj. 2402, Task 240203 Work Unit 24020332 |
| 14. MONITORING AGENCY NAME & ADDRESS (if different from Controlling Office) | | 12. REPORT DATE December 1982 |
| | | 13. NUMBER OF PAGES 692 |
| | | 15. SECURITY CLASS. (of this report) Unclassified |
| | | 15a. DECLASSIFICATION/DOWNGRADING SCHEDULE |
| 16. DISTRIBUTION STATEMENT (of this Report) Approved for public release; distribution unlimited. | | |
| 17. DISTRIBUTION STATEMENT (of the abstract entered in Block 20, if different from Report) | | |
| 18. SUPPLEMENTARY NOTES The computer program contained in this technical report is theoretical and in no way reflects any Air Force owned software programs. | | |
| 19. KEY WORDS (Continue on reverse side if necessary and identify by block number) Nonlinear Structural Analysis MAGNA Finite Element Analysis Aircraft Windshield Plasticity Numerical Analysis | | |
| 20. ABSTRACT (Continue on reverse side if necessary and identify by block number) The finite element program MAGNA (Materially And Geometrically Nonlinear Analysis), developed for the nonlinear static and dynamic analysis of complex three-dimensional structures, is described. This program is applicable to large structural response problems involving bars, membranes, beams, plates, shells, and three-dimensional solids, experiencing large displacements, finite strains, large rotations, and plastic deformation. The theoretical basis of MAGNA and the numerical procedures employed | | |

DD FORM 1473
1 JAN 73

EDITION OF 1 NOV 65 IS OBSOLETE

UNCLASSIFIED

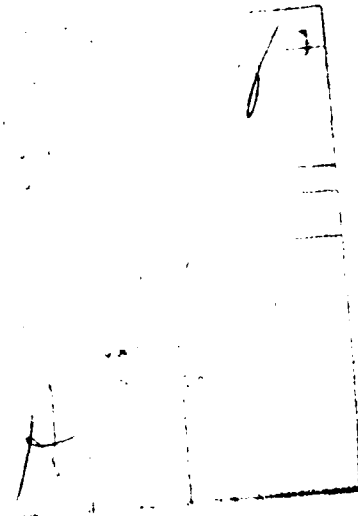
SECURITY CLASSIFICATION OF THIS PAGE (When Data Entered)

UNCLASSIFIED

SECURITY CLASSIFICATION OF THIS PAGE(When Data Entered)

Block 20 (concluded)

are described in detail. Several sample analyses are presented to demonstrate the range of capabilities of the program. Instructions are provided for operating the program, modifying storage capacity, preparing input data, estimating computer run times, and interpreting the output. Computer graphics utilities available for the display of input data and analysis results are also described.



UNCLASSIFIED

SECURITY CLASSIFICATION OF THIS PAGE(When Data Entered)

FOREWORD

This report describes the finite element solution program MAGNA, developed at the University of Dayton Research Institute, Dayton, Ohio. Development of the program was performed between January, 1978 and December, 1982, by the Analytical Mechanics Group (Dr. F. K. Bogner, Leader) within the Aerospace Mechanics Division (D. H. Whitford, Supervisor) of the Research Institute.

This work effort was accomplished under Project 2402, "Vehicle Equipment Technology," Task 240203, "Aerospace Vehicle Recovery and Escape Subsystems," Work Unit 24020332, "Computer Aided Design of Bird-Resistant Transparencies for USAF Aircraft."

The present report provides final documentation of the developments performed on Air Force Contract F33615-80-C-3403 between March, 1980 and December, 1982 for the Flight Dynamics Laboratory, Air Force Wright Aeronautical Laboratories, Wright-Patterson Air Force Base, Ohio. The project manager for this effort was Dr. Fred K. Bogner, and the Principal Investigator was Dr. Robert A. Brockman. Technical direction and support was provided by Mr. Robert E. McCarty (AFWAL/FIER) as the Air Force Project Engineer. The work described herein represents a continuation of previous developments performed in-house at the University of Dayton Research Institute, and on Air Force Contract F33615-76-C-3103.

The author wishes to express his appreciation for the contributions of several individuals and organizations whose efforts, support, and suggestions have resulted in significant improvements to the MAGNA program. Continuing support and many useful discussions have been provided by Dr. Fred K. Bogner; numerous improvements to both the program and its documentation have been suggested by Mr. Robert E. McCarty. The analytical development performed by Dr. H. C. Rhee and Dr. Mohan L. Soni, and the computer graphics support provided by Messrs. T. S. Bruner, C. S. King, M. P. Bouchard, M. J. Hecht, Ms. M. A. Dominic, and Ms. M. E. Wright are also

gratefully acknowledged. Mr. Thomas W. Held performed the conversion of MAGNA to the VAX 11/780. Computer resources and assistance in adapting the program to the CRAY-1 computer were provided by United Information Services; special thanks are due to Mr. Kent Griffith of UIS, who developed the necessary direct access file utilities. Finally, the efforts of Ms. Kathy Reineke in typing the manuscript of this manual are deeply appreciated.

This report (Parts I, II, III, and IV) supersedes AFWAL-TR-80-3152, AD A099454 dated January 1981; AFWAL-TR-80-3151, AD A099530 dated January 1981; AFWAL-TR-81-3180, AD A117544 dated February 1982; and AFWAL-TR-81-3181, AD A116541 dated February 1982.

TABLE OF CONTENTS

| <u>SECTION</u> | | <u>PAGE</u> |
|----------------|---|-------------|
| 1 | INTRODUCTION | 1.0.1 |
| 1.1 | OVERVIEW | 1.1.1 |
| 1.2 | MANUAL ORGANIZATION | 1.2.1 |
| 2 | THEORETICAL DEVELOPMENT | 2.0.1 |
| 2.1 | CONTINUUM EQUATIONS OF MOTION | 2.1.1 |
| 2.1.1 | Principle of Virtual Work | 2.1.1 |
| 2.1.2 | Incremental Principle of Virtual Work | 2.1.4 |
| 2.1.3 | Linearization of Equations of Motion | 2.1.7 |
| 2.1.4 | Equilibrium Corrections and Iteration | 2.1.8 |
| 2.2 | DISCRETE EQUATIONS OF MOTION | 2.2.1 |
| 2.2.1 | Element-Based Virtual Work Equations | 2.2.1 |
| 2.2.2 | Finite Element Discretization | 2.2.2 |
| 2.2.3 | Assembly of Finite Elements | 2.2.5 |
| 2.3 | MATERIAL CONSTITUTIVE DESCRIPTIONS | 2.3.1 |
| 2.3.1 | Isotropic Elastic Material | 2.3.1 |
| 2.3.2 | Initially Isotropic, Elastic-Plastic Material | 2.3.3 |
| 2.3.3 | Orthotropic Elastic Material | 2.3.14 |
| 2.4 | SURFACE CONTACT ANALYSIS | 2.4.1 |
| 2.4.1 | General Description of Contact Solution | 2.4.1 |
| 2.4.2 | Definition of Potential Contacting Surfaces | 2.4.4 |
| 2.4.3 | Screening of Possible Contact Conditions | 2.4.9 |
| 2.4.4 | Application of Constraints | 2.4.12 |
| 3 | FINITE ELEMENT LIBRARY | 3.0.1 |
| 3.1 | ONE-DIMENSIONAL CONTINUUM ELEMENTS | 3.1.1 |
| 3.2 | TWO-DIMENSIONAL AND AXISYMMETRIC CONTINUUM ELEMENTS | 3.2.1 |

TABLE OF CONTENTS (continued)

| <u>SECTION</u> | | <u>PAGE</u> |
|----------------|--|-------------|
| 3.3 | THREE-DIMENSIONAL CONTINUUM ELEMENTS | 3.3.1 |
| 3.4 | THREE-DIMENSIONAL PLATE AND SHELL ELEMENTS | 3.4.1 |
| 3.5. | THREE-DIMENSIONAL BEAM ELEMENTS | 3.5.1 |
| 4 | NUMERICAL SOLUTION OPTIONS | 4.0.1 |
| 4.1 | LINEAR STATIC ANALYSIS | 4.1.1 |
| 4.2 | LINEAR DYNAMIC ANALYSIS | 4.2.1 |
| 4.3 | NONLINEAR STATIC ANALYSIS (EQUILIBRIUM ITERATION) | 4.3.1 |
| 4.4 | NONLINEAR DYNAMIC ANALYSIS (IMPLICIT INTEGRATION) | 4.4.1 |
| 4.5 | NATURAL FREQUENCY AND NORMAL MODE ANALYSIS | 4.5.1 |
| 4.6 | STEADY-STATE HARMONIC ANALYSIS | 4.6.1 |
| 5 | SPECIAL PROGRAM FEATURES | 5.0.1 |
| 5.1 | CURVILINEAR COORDINATES | 5.1.1 |
| 5.2 | COORDINATE DATA GENERATION | 5.2.1 |
| 5.3 | ELEMENT GENERATION | 5.3.1 |
| 5.4 | INCREMENTAL LOADS | 5.4.1 |
| 5.5 | NONLINEAR MATERIAL STRESS-STRAIN DATA | 5.5.1 |
| 5.6 | LINEAR MULTIVARIABLE CONSTRAINTS | 5.6.1 |
| 5.7 | POSTPROCESSING INTERFACE | 5.7.1 |
| 5.8 | ANALYSIS RESTART UTILITIES | 5.8.1 |
| 5.9 | NATURAL FREQUENCY ANALYSIS WITH PRESTRESS EFFECTS | 5.9.1 |

TABLE OF CONTENTS (continued)

| <u>SECTION</u> | | <u>PAGE</u> |
|----------------|---|-------------|
| 6 | DEMONSTRATION PROBLEMS | 6.0.1 |
| 6.1 | ELASTIC-PLASTIC ANALYSIS OF A CIRCULAR PLATE | 6.1.1 |
| 6.2 | SHALLOW SPHERICAL SHELL UNDER CONCENTRATED LOAD | 6.2.1 |
| 6.3 | LARGE STRAIN ELASTIC ANALYSIS OF A BAR IN TENSION | 6.3.1 |
| 6.4 | ELASTIC DYNAMIC BUCKLING OF A CIRCULAR ARCH | 6.4.1 |
| 6.5 | LARGE DISPLACEMENT RESPONSE OF AN AIRCRAFT WINDSHIELD | 6.5.1 |
| 6.6 | STRESS CONCENTRATION IN A THIN PERFORATED SHEET | 6.6.1 |
| 6.7 | ELASTIC-PLASTIC, LARGE DISPLACEMENT ANALYSIS OF A TWO-BAY TRUSS | 6.7.1 |
| 6.8 | STRESS DISTRIBUTIONS IN A SINGLE-LAP BONDED JOINT | 6.8.1 |
| 6.9 | SANDWICH PLATE UNDER UNIFORM PRESSURE | 6.9.1 |
| 6.10 | LARGE DISPLACEMENTS AND ROTATIONS OF A DEEP ARCH | 6.10.1 |
| 6.11 | LARGE DISPLACEMENT, ELASTIC RESPONSE OF A THIN CIRCULAR PLATE | 6.11.1 |
| 6.12 | COMPRESSIVE BUCKLING OF A SIMPLY-SUPPORTED SANDWICH PLATE | 6.12.1 |
| 6.13 | CLAMPED PLATE UNDER UNIFORM PRESSURE LOADING | 6.13.1 |
| 6.14 | POSTBUCKLING RESPONSE OF A SIMPLY-SUPPORTED PLATE | 6.14.1 |
| 6.15 | ELASTIC-PLASTIC ANALYSIS OF A PERFORATED STRIP | 6.15.1 |
| 6.16 | NATURAL FREQUENCIES OF AN ORTHOTROPIC PLATE | 6.16.1 |

TABLE OF CONTENTS (continued)

| <u>SECTION</u> | | <u>PAGE</u> |
|----------------|--|-------------|
| 6.17 | PLASTIC COLLAPSE OF A RECESSED FASTENER | 6.17.1 |
| 6.18 | FREE VIBRATIONS OF A CLAMPED TRIANGULAR PLATE | 6.18.1 |
| 6.19 | COMPRESSION OF A DISK AGAINST A RIGID SURFACE | 6.19.1 |
| 6.20 | ELASTIC-PLASTIC ANALYSIS OF A CLAMPED BEAM | 6.20.1 |
| 6.21 | FORCED VIBRATIONS OF A JET ENGINE EXHAUST DUCT | 6.21.1 |
| 7 | PROGRAM OPERATION | 7.0.1 |
| 7.1 | CDC PROGRAM VERSION | 7.1.1 |
| | 7.1.1 Job Control Language | 7.1.1 |
| | 7.1.2 Modification of Storage Capacity | 7.1.13 |
| | 7.1.3 Reserved File Names | 7.1.16 |
| | 7.1.4 Typical Execution Times on CDC Computers | 7.1.18 |
| 7.2 | CRAY PROGRAM VERSION | 7.2.1 |
| | 7.2.1 Job Control Language | 7.2.1 |
| | 7.2.2 Modification of Storage Capacity | 7.2.8 |
| | 7.2.3 Execution Times on the CRAY-1 Computer | 7.2.12 |
| 7.3 | VAX PROGRAM VERSION | 7.3.1 |
| 8 | INPUT DATA | 8.0.1 |
| 8.1 | PROBLEM IDENTIFICATION | 8.1.1 |
| 8.2 | SOLUTION OPTIONS AND CONTROL PARAMETERS | 8.2.1 |
| 8.3 | ITERATIVE SOLUTION AND ANALYSIS RESTART DATA | 8.3.1 |
| | 8.3.1 Equilibrium Iteration Control Parameters | 8.3.2 |
| | 8.3.2 Eigenvalue Solution Control Parameters | 8.3.4 |
| | 8.3.3 Analysis Restart Data (CDC and CRAY versions only) | 8.3.7 |
| | 8.3.4 Analysis Restart Data (VAX version only) | 8.3.9 |
| | 8.3.5 Frequency Response Solution Control Parameters | 8.3.12 |

TABLE OF CONTENTS (continued)

| <u>SECTION</u> | | <u>PAGE</u> |
|----------------|---|-------------|
| 8.4 | NODAL COORDINATE DATA | 8.4.1 |
| 8.5 | ELEMENT PROPERTIES AND CONNECTIVITY | 8.5.1 |
| | 8.5.1 Data for Element Type 1 | 8.5.2 |
| | 8.5.2 Data for Element Type 2 | 8.5.16 |
| | 8.5.3 Data for Element Type 3 | 8.5.29 |
| | 8.5.4 Data for Element Type 4 | 8.5.38 |
| | 8.5.5 Data for Element Type 5 | 8.5.44 |
| | 8.5.6 Data for Element Type 6 | 8.5.48 |
| | 8.5.7 Data for Element Type 7 | 8.5.61 |
| | 8.5.8 Data for Element Type 8 | 8.5.74 |
| | 8.5.9 Data for Element Type 9 | 8.5.87 |
| | 8.5.10 Data for Element Type 10 | 8.5.95 |
| | 8.5.11 Data for Element Type 11 | 8.5.103 |
| | 8.5.12 Data for Element Type 12 | 8.5.114 |
| 8.6 | DATA FOR SURFACE CONTACT ANALYSIS | 8.6.1 |
| 8.7 | BOUNDARY CONDITIONS | 8.7.1 |
| 8.8 | LINEAR CONSTRAINT DATA | 8.8.1 |
| 8.9 | DATA CURVES FOR NONLINEAR AND/OR DYNAMIC ANALYSIS | 8.9.1 |
| 8.10 | EXTERNAL LOADS | |
| | 8.10.1 Concentrated Nodal Forces and Prescribed Displacements | 8.10.1 |
| | 8.10.2 Distributed Element Forces | 8.10.5 |
| | 8.10.3 Centrifugal Loading Data | 8.10.10 |
| 8.11 | HARMONIC FORCING FREQUENCIES | 8.11.1 |
| 9 | USER SUBROUTINES | 9.0.1 |
| 9.1 | MESHG (GENERATE COORDINATES) | 9.1.1 |
| 9.2 | CTYPE (COORDINATE TRANSFORMATIONS) | 9.2.1 |
| 9.3 | ULOAD, USRLD (INCREMENTAL LOADS) | 9.3.1 |
| 9.4 | VINIT (INITIAL VELOCITY CONDITIONS) | 9.4.1 |
| 9.5 | TEMG (GENERATE NODAL TEMPERATURES) | 9.5.1 |
| 9.6 | UOUT (SPECIFY OUTPUT PARAMETERS) | 9.6.1 |
| 9.7 | NELAS (NONLINEAR ELASTIC MATERIAL LAW) | 9.7.1 |

TABLE OF CONTENTS (continued)

| <u>SECTION</u> | | <u>PAGE</u> |
|----------------|--|-------------|
| 9.8 | USTOP (CONTROL POINT FOR JOB TERMINATION) | 9.8.1 |
| 9.9 | UPLASi (USER-DEFINED ELASTIC-PLASTIC MATERIAL LAW) | 9.9.1 |
| 9.10 | UDAMP (STEADY-STATE DAMPING PROPERTIES) | 9.10.1 |
| 9.11 | UPRESS (VARIABLE SURFACE PRESSURES) | 9.11.1 |
| 9.12 | UANIS2 (ANISOTROPIC MATERIAL PROPERTIES FOR 2-D ELEMENTS) | 9.12.1 |
| 10 | PROGRAM OUTPUT | 10.0.1 |
| 10.1 | STORAGE ALLOCATION MODULE (CDC MACHINE VERSION ONLY) | 10.1.1 |
| 10.2 | INPUT AND GENERATED DATA | 10.2.1 |
| 10.2.1 | Input Data Listing (CDC and VAX Versions) | 10.2.1 |
| 10.2.2 | Options and Solution Parameters | 10.2.1 |
| 10.2.3 | Nodal Coordinates | 10.2.1 |
| 10.2.4 | Element Definition Data | 10.2.2 |
| 10.2.5 | Boundary Conditions | 10.2.3 |
| 10.2.6 | Data Curves and Applied Loadings | 10.2.4 |
| 10.3 | MATRIX TOPOLOGY AND PARTITIONING DATA | 10.3.1 |
| 10.4 | ELEMENT GEOMETRIC PARAMETERS | 10.4.1 |
| 10.5 | ITERATIVE SOLUTION PARAMETERS | 10.5.1 |
| 10.6 | INCREMENTAL LOADS | 10.6.1 |
| 10.7 | DISPLACEMENT AND VELOCITY SOLUTIONS | 10.7.1 |
| 10.8 | ELEMENT STRESSES AND STRAINS | 10.8.1 |
| 10.8.1 | One-Dimensional Elements (Type 4) | 10.8.1 |
| 10.8.2 | Two-Dimensional and Axisymmetric Elements (Types 3, 9, and 10) | 10.8.2 |
| 10.8.3 | Three-Dimensional Elements (Types 1, 2, 6, 7, and 8) | 10.8.7 |
| 10.8.4 | Thin Plate/Shell Elements (Type 5) | 10.8.12 |
| 10.8.5 | Layered Shell Elements (Type 11) | 10.8.14 |
| 10.8.6 | Beam Elements (Type 12) | 10.8.16 |

TABLE OF CONTENTS (continued)

| <u>SECTION</u> | <u>PAGE</u> |
|--|-------------|
| 10.9 SOLUTION SUMMARY | 10.9.1 |
| 10.10 ERROR AND WARNING MESSAGES | 10.10.1 |
| 10.10.1 Model Definition Error Diagnostics | 10.10.2 |
| 10.10.2 Solution Error Diagnostics | 10.10.6 |
| 10.10.3 Central Memory and File Handling Errors | 10.10.9 |
| 10.10.4 System Errors and Abnormal Termination | 10.10.10 |
| 10.11 STRAVG OUTPUT | 10.11.1 |
| 10.11.1 Model Parts Definitions | 10.11.1 |
| 10.11.2 Nodal Strains and Stresses | 10.11.2 |
| 10.11.3 Error Messages | 10.11.2 |
| 11 PLOTTING UTILITIES | 11.0.1 |
| 11.1 GPLOT - DEFORMED AND UNDEFORMED GEOMETRY PLOTTING | 11.1.1 |
| 11.2 CPLOT - CONTOUR AND RELIEF PLOTTING | 11.2.1 |
| 11.3 XYPLOT - VARIABLE VERSUS VARIABLE PLOTTING | 11.3.1 |
| 11.4 PROCEDURES FOR ACCESSING GPLOT, CPLOT, AND XYPLOT | 11.4.1 |
| 12 GUIDELINES FOR EFFECTIVE MODELING | 12.0.1 |
| 12.1 ANALYSIS OPTIONS | 12.1.1 |
| 12.2 NODE POINT AND ELEMENT NUMBERING | 12.2.1 |
| 12.3 SELECTION OF ELEMENT TYPES AND OPTIONS | 12.3.1 |
| 12.4 USE OF EQUILIBRIUM ITERATION | 12.4.1 |
| APPENDIX | A.1 |
| REFERENCES | R.2.1 |

LIST OF FIGURES

| <u>NUMBER</u> | | <u>PAGE</u> |
|---------------|---|-------------|
| 2.1.1 | Successive States of Deformation of a Three-Dimensional Body. | 2.1.2 |
| 2.3.1 | Decomposition of Incremental Strains into Elastic and Plastic Components. | 2.3.6 |
| 2.3.2 | Isotropic and Kinematic Hardening Rules in a Two-Dimensional Stress Space. | 2.3.9 |
| 2.3.3 | Comparison of Isotropic, Kinematic, and Combined Hardening Rules for Elastic Unloading and Re-yielding. | 2.3.10 |
| 2.3.4 | Scaling of Stress Increments to the Yield Surface. | 2.3.13 |
| 2.4.1 | Contact between Three-Dimensional Bodies. | 2.4.2 |
| 2.4.2 | Typical Surface Contact Element. | 2.4.5 |
| 2.4.3 | Nodal Pattern of General Surface Contact Element. | 2.4.6 |
| 2.4.4 | Definition of Surface Element Sets for a Drawing Problem. | 2.4.7 |
| 2.4.5 | Solution for Relative Position of a Point and a Surface. | 2.4.11 |
| 3.1.1 | Three-Dimensional Truss Element. | 3.1.2 |
| 3.2.1 | Quadrilateral Plane Stress, Plane Strain, or Shear Panel Element. | 3.2.2 |
| 3.2.2 | Variable-Number-of-Nodes Plane Stress Element. | 3.2.5 |
| 3.2.3 | Quarter-Point Crack Tip Element. | 3.2.7 |
| 3.3.1 | Three-Dimensional Solid Element with Variable Number of Nodes. | 3.3.2 |
| 3.3.2 | Transitions Between Coarse and Fine Model Regions. | 3.3.3 |
| 3.3.3 | Three-Layered Sandwich Construction. | 3.3.7 |
| 3.4.1 | Three-Dimensional, Eight-Node Thin Shell Element. | 3.4.2 |

LIST OF FIGURES (continued)

| <u>NUMBER</u> | | <u>PAGE</u> |
|---------------|--|-------------|
| 3.4.2 | Modeling Capabilities of the Thin Shell Finite Element. | 3.4.3 |
| 3.4.3 | Nodal Connectivity for Sixteen-Node Layered Shell Element. | 3.4.5 |
| 3.4.4 | Layered Construction Using a Combination of Constant- and Variable-Thickness Layers. | 3.4.6 |
| 3.5.1 | Element Geometry and Node Numbering for Quadratic Beam Element. | 3.5.2 |
| 3.5.2 | Example of Beam Cross-Section Definition. | 3.5.3 |
| 3.5.3 | Use of Offsets in Stiffening Elements. | 3.5.4 |
| 5.1.1 | Cylindrical Coordinate System Definition. | 5.1.2 |
| 5.1.2 | Spherical Coordinate System Definition. | 5.1.3 |
| 5.2.1 | Incremental Node Point Coordinate Generation. | 5.2.2 |
| 5.5.1 | Reduction of Material Stress-Strain Data. | 5.5.5 |
| 5.6.1 | Enforcement of Displacement Constraint on a Skewed Boundary. | 5.6.3 |
| 6.1.1 | Circular Plate Loaded Through a Rigid Punch. | 6.1.2 |
| 6.1.2 | Finite Element Model of a Circular Plate. | 6.1.3 |
| 6.1.3 | Load-versus Displacement Solution for Elastic-Plastic Circular Plate. | 6.1.5 |
| 6.1.4 | Comparison of Displacement Solutions for Circular Plate. | 6.1.6 |
| 6.1.5 | Elastic-Plastic Boundary in Plate Cross-Section at Total Load $P = 1000$ Pounds. | 6.1.7 |
| 6.1.6 | Effective Stress Distribution at Total Load $P = 1000$ Pounds. | 6.1.8 |
| 6.1.7 | Elastic-Plastic Boundary in Plate Cross-Section at Total Load $P = 2000$ Pounds. | 6.1.10 |
| 6.1.8 | Radial Strain Distribution at $P = 2000$ Pounds. | 6.1.11 |
| 6.2.1 | Cross-Section of Shallow Spherical Shell Under Concentrated Loading. | 6.2.2 |

LIST OF FIGURES (continued)

| <u>NUMBER</u> | | <u>PAGE</u> |
|---------------|--|-------------|
| 6.2.2 | Shell Element Model of Spherical Cap Sector. | 6.2.3 |
| 6.2.3 | Five-Element Discretization of Spherical Cap Using Three-Dimensional, Twenty-Node Elements. | 6.2.4 |
| 6.2.4 | Nine-Element Discretization of Spherical Cap Using Three-Dimensional, Twenty-Node Elements. | 6.2.5 |
| 6.2.5 | Seven-Element Model of Spherical Cap Sector Using Three-Dimensional Solid Elements. | 6.2.6 |
| 6.2.6 | Static Nonlinear Solution for Shallow Cap (Fifteen Shell Elements). | 6.2.8 |
| 6.2.7 | Static Nonlinear Solution for Shallow Cap (Solid Element Models). | 6.2.9 |
| 6.2.8 | Shell Element Solution for Dynamic Response of Shallow Cap ($\Delta t = 2 \text{ } \mu\text{sec.}$). | 6.2.10 |
| 6.2.9 | Solid Element Solution for Dynamic Response of Shallow Cap ($\Delta t = 2 \text{ } \mu\text{sec.}$). | 6.2.11 |
| 6.2.10 | Solid Element Solution for Dynamic Response of Shallow Cap ($\Delta t = 4 \text{ } \mu\text{sec.}$). | 6.2.12 |
| 6.2.11 | Comparison of Dynamic Response Solutions With and Without Equilibrium Iterations. | 6.2.14 |
| 6.3.1 | Rectangular Bar Under Axial Load. | 6.3.2 |
| 6.3.2 | Finite Element Model of Axially Loaded Bar. | 6.3.3 |
| 6.3.3 | End Displacement Versus Load Solution for Axially Loaded Bar. | 6.3.6 |
| 6.4.1 | Shallow Arch Geometry and Loading. | 6.4.2 |
| 6.4.2 | Shell Element Model of Shallow Arch. | 6.4.4 |
| 6.4.3 | Dynamic Response of Shallow Arch for Selected Pressure Levels. | 6.4.5 |
| 6.5.1 | Three-Dimensional Solid Element Model of F-16 Windshield Canopy. | 6.5.2 |
| 6.5.2 | Shell Element Model of F-16 Windshield Canopy. | 6.5.3 |
| 6.5.3 | Nonlinear Static Response of Windshield Canopy (Solid Element Model). | 6.5.5 |

LIST OF FIGURES (continued)

| <u>NUMBER</u> | | <u>PAGE</u> |
|---------------|--|-------------|
| 6.5.4 | Nonlinear Static Response of Windshield Canopy (Shell Element Model). | 6.5.6 |
| 6.5.5 | Deformed Geometry of F-16 Windshield Under Static Loading. | 6.5.7 |
| 6.5.6 | Equivalent Stress Contours on Windshield Surface for 1100-Pound Static Load. | 6.5.8 |
| 6.5.7 | Solid Element Model of Windshield Canopy (189 Elements). | 6.5.9 |
| 6.6.1 | Thin Sheet with a Circular Hole. | 6.6.2 |
| 6.6.2 | Finite Element Model of Perforated Sheet. | 6.6.3 |
| 6.6.3 | Longitudinal Stress Distribution in Perforated Sheet at Edge of Symmetry. | 6.6.4 |
| 6.7.1 | Two-Bay Plane Truss Structure. | 6.7.2 |
| 6.7.2 | Nonlinear Elastic-Plastic Response of Two-Bay Plane Truss. | 6.7.3 |
| 6.8.1 | Single-Lap Bonded Joint Specimen. | 6.8.2 |
| 6.8.2 | Finite Element Discretization of Single Lap Joint. | 6.8.3 |
| 6.8.3 | Adhesive Shear Stress Distribution in Single-Lap Bonded Joint. | 6.8.4 |
| 6.8.4 | Adhesive Normal Stress Distribution in Single-Lap Bonded Joint. | 6.8.5 |
| 6.8.5 | Adhesive Stress Distributions for Free-End Bonded Joint Specimen. | 6.8.7 |
| 6.8.6 | Displaced Shape of Free-End Bonded Joint. | 6.8.8 |
| 6.9.1 | Three-Layer Sandwich Panel under Pressure Loading. | 6.9.2 |
| 6.9.2 | Load-Deflection Results for Uniformly Loaded Sandwich Plate. | 6.9.3 |
| 6.10.1 | Deep Arch with Asymmetric Boundary Conditions. | 6.10.2 |
| 6.10.2 | Deformed Geometry of Clamped-Hinged Arch at Maximum Loading. | 6.10.3 |

LIST OF FIGURES (continued)

| <u>NUMBER</u> | | <u>PAGE</u> |
|---------------|--|-------------|
| 6.10.3 | Comparison of MAGNA Solution with Analytical Results for Deep Arch. | 6.10.5 |
| 6.11.1 | Clamped Circular Plate. | 6.11.2 |
| 6.11.2 | Thin Shell Element Model of Circular Plate. | 6.11.3 |
| 6.11.3 | Radial Distribution of Circumferential Surface Stress in Clamped Circular Plate. | 6.11.4 |
| 6.11.4 | Load-versus-Deflection Solution for Large Displacements of a Circular Plate. | 6.11.6 |
| 6.11.5 | Midsurface Circumferential Stress Profiles in Clamped Circular Plate. | 6.11.7 |
| 6.12.1 | Simply-Supported Sandwich Plate Under Compression Load. | 6.12.2 |
| 6.13.1 | Finite Element Model of Clamped Plate. | 6.13.2 |
| 6.13.2 | Load-Displacement Solution for Clamped Plate Under Pressure. | 6.13.3 |
| 6.13.3 | Upper Surface Strains in Clamped Plate at Maximum Load. | 6.13.5 |
| 6.13.4 | Lower Surface Strains in Clamped Plate at Maximum Load. | 6.13.6 |
| 6.13.5 | Upper Surface Stresses in Clamped Plate at Maximum Load. | 6.13.7 |
| 6.13.6 | Lower Surface Stresses in Clamped Plate at Maximum Load. | 6.13.8 |
| 6.13.7 | Effective Stresses in Plate Upper Surface at Maximum Load. | 6.13.9 |
| 6.14.1 | Postbuckling Displacement History for Simply Supported Square Plate. | 6.14.2 |
| 6.15.1 | Perforated Sheet Subjected to Uniform Tension. | 6.15.2 |
| 6.15.2 | Finite Element Model of Tension Strip. | 6.15.3 |
| 6.15.3 | Longitudinal Strain History at Point of First Yielding. | 6.15.4 |
| 6.15.4 | Longitudinal Stresses in Tension Strip at $\sigma_{\text{mean}} = \sigma_{\text{yield}}$. | 6.15.5 |

LIST OF FIGURES (continued)

| <u>NUMBER</u> | | <u>PAGE</u> |
|---------------|--|-------------|
| 6.16.1 | Finite Element Model of Orthotropic Square Plate | 6.16.2 |
| 6.16.2 | First Mode ($m=1$, $n=1$) of Orthotropic Plate. | 6.16.4 |
| 6.16.3 | Second Mode ($m=2$, $n=2$) of Orthotropic Plate. | 6.16.5 |
| 6.16.4 | Third Mode ($m=1$, $n=3$) of Orthotropic Plate. | 6.16.6 |
| 6.16.5 | Fourth Mode ($m=2$, $n=1$) of Orthotropic Plate. | 6.16.7 |
| 6.17.1 | Idealized Recessed Fastener Geometry | 6.17.2 |
| 6.17.2 | Finite Element Model of Recessed Fastener. | 6.17.3 |
| 6.17.3 | Yield and Ultimate Stress Zones in Recessed Fastener at Load Levels of 2200, 2500 and 2800 Pounds. | 6.17.5 |
| 6.17.4 | Yield and Ultimate Stress Zones in Recessed Fastener at Load Levels of 4000, 4300 and 4600 Pounds. | 6.16.6 |
| 6.18.1 | Cantilevered Triangular Plate - Finite Element Model. | 6.18.2 |
| 6.19.1 | Finite Element Model of Disk in Contact with a Rigid Plane. | 6.19.2 |
| 6.19.2 | Undeformed and Deformed Geometries of Disk. | 6.19.3 |
| 6.19.3 | Three-Dimensional View of Disk Model with Contact Elements. | 6.19.4 |
| 6.19.4 | Displacement Histories for Individual Nodes along Lower Surface of Disk. | 6.19.5 |
| 6.20.1 | Central Deflection Histories for Clamped Beam, for Several Values of Yield Stress. | 6.20.2 |
| 6.20.2 | Cross-Sectional Stress Distribution in Clamped-Clamped Beam. | 6.20.3 |
| 6.21.1 | Engine Exhaust Duct. | 6.21.3 |
| 6.21.2 | Finite Element Model of Engine Exhaust Duct Shroud. | 6.21.4 |

LIST OF FIGURES (continued)

| <u>NUMBER</u> | | <u>PAGE</u> |
|---------------|--|-------------|
| 6.21.3 | Exhaust Duct Mode Shapes. | 6.21.5 |
| 6.21.4 | Engine Exhaust Duct: Effect of Damping Treatment on Amplitude-Frequency Response. | 6.21.6 |
| 7.3.1 | Typical Execution of VAX SETUP Control Procedure. | 7.3.2 |
| 7.3.2 | Batch Command Procedure MBATCH.COM. | 7.3.6 |
| 7.3.3 | Modification of Program Storage Capacity in SETUP. | 7.3.8 |
| 7.3.4 | Specification of New Executable Version of MAGNA. | 7.3.9 |
| 7.3.5 | Request for Restart Tape in SETUP. | 7.3.10 |
| 7.3.6 | Control Procedure MBATCH.COM, with Modification of Storage Capacity. | 7.3.11 |
| 7.3.7 | SETUP Sequence for Requesting Old and New Restart Files. | 7.3.15 |
| 7.3.8 | Introduction of User-Written Subroutines through SETUP. | 7.3.16 |
| 7.3.9 | Generated Control Procedure MBATCH.COM, with Storage Modifications and User-Written Subroutines. | 7.3.17 |
| 8.5.1 | Nodal Connectivity for Variable-Node Solid Element. | 8.5.7 |
| 8.5.2 | Definition of Orthotropic Material Axis Orientations. | 8.5.8 |
| 8.5.3 | Nodal Connectivity for Eight-Node Solid Element. | 8.5.21 |
| 8.5.4 | Definition of Orthotropic Material Axis Orientations. | 8.5.22 |
| 8.5.5 | Nodal Connectivity for Quadrilateral Plane Stress, Plane Strain, and Shear Panel Element. | 8.5.32 |
| 8.5.6 | Nodal Connectivity for Three-Dimensional Truss Element. | 8.5.41 |
| 8.5.7 | Nodal Connectivity for Three-Dimensional, Eight-Node Thin Shell Element. | 8.5.46 |

LIST OF FIGURES (continued)

| <u>NUMBER</u> | | <u>PAGE</u> |
|---------------|--|-------------|
| 8.5.8 | Nodal Connectivity for Twenty-Node Solid Element. | 8.5.53 |
| 8.5.9 | Definition of Orthotropic Material Axis Orientations. | 8.5.54 |
| 8.5.10 | Nodal Connectivity for Variable-Node Solid Element. | 8.5.66 |
| 8.5.11 | Definition of Orthotropic Material Axis Orientations | 8.5.67 |
| 8.5.12 | Nodal Connectivity for Sixteen Node Solid Element. | 8.5.79 |
| 8.5.13 | Definition of Orthotropic Material Axis Orientations. | 8.5.80 |
| 8.5.14 | Nodal Connectivity for Variable-Node Plane Stress Element. | 8.5.90 |
| 8.5.15 | Nodal Connectivity for Variable-Node Axisymmetric Element. | 8.5.98 |
| 8.5.16 | Layer Type Definitions for Multilayered Shell Finite Element. | 8.5.107 |
| 8.5.17 | Definition of Orthotropic Material Axis Orientation for a Shell Layer. | 8.5.108 |
| 8.5.18 | Nodal Connectivity for Sixteen-Node Layered Shell Element. | 8.5.110 |
| 8.5.19 | Some Typical Beam Sections Constructed from Rectangular Segments. | 8.5.116 |
| 8.5.20 | Beam Cross-Section Parameters. | 8.5.117 |
| 8.5.21 | Cross-Sectional Integration Stations in Curved Beam Element. | 8.5.118 |
| 8.5.22 | Connectivity and Local Axis Conventions for Beam Element. | 8.5.119 |
| 8.6.1 | Connectivity for Variable Node, Three-Dimensional Contact Element. | 8.6.3 |
| 8.10.1 | Example of Incremental Load Definition. | 8.10.4 |

LIST OF FIGURES (continued)

| <u>NUMBER</u> | | <u>PAGE</u> |
|---------------|---|-------------|
| 8.10.2 | Reference Surface Numbers for Pressure Loading on Three-Dimensional Solid and Shell Elements. | 8.10.7 |
| 8.10.3 | Edge Numbering for Two-Dimensional and Axisymmetric Distributed Loads. | 8.10.8 |
| 9.3.1 | Finite Element Model for ULOAD Follower Force Example. | 9.3.4 |
| 9.3.2 | Beam Supported by Nonlinear Spring Elements. | 9.3.8 |
| 10.1.1 | Output from Storage Allocation Module. | 10.1.2 |
| 10.3.1 | Matrix Profile Map Output. | 10.3.3 |
| 10.8.1 | Local Coordinate Directions for Two-Dimensional Elements. | 10.8.4 |
| 10.8.2 | Integration Point Locations (INT=1,2,3) for Two-Dimensional Elements. | 10.8.5 |
| 10.8.3 | Local Coordinate Directions for Thin Shell Elements. | 10.8.13 |
| 10.8.4 | Node Numbers and Natural Coordinate Directions for Layered Shell Element. | 10.8.15 |
| 10.8.5 | Local Coordinate Axes for Three-Dimensional, Curved Beam Element. | 10.8.17 |
| 10.8.6 | Typical Integration Point Locations in Beam Element Cross-Section. | 10.8.20 |
| 11.1.1 | Sample Terminal Session with GPLOT. | 11.1.4 |
| 11.2.1 | Sample Terminal Session with CPLOT. | 11.2.5 |
| 11.3.1 | X-Y Plot (Sample No. 1). | 11.3.4 |
| 11.3.2 | X-Y Plot (Sample No. 2). | 11.3.5 |
| 11.3.3 | X-Y Plot (Sample No. 3). | 11.3.6 |
| 12.2.1 | Variable Bandwidth Matrix Storage. | 12.2.2 |
| 12.2.2 | Effect of Node Point Numbering on Matrix Profile. | 12.2.3 |
| 12.3.1 | Approximation of Bending Deformation Using Eight-Node Solid Elements. | 12.3.3 |

LIST OF FIGURES (continued)

| <u>NUMBER</u> | | <u>PAGE</u> |
|---------------|--|-------------|
| 12.4.1 | Newton-Raphson and Modified Newton Iteration Schemes. | 12.4.2 |
| 12.4.2 | Combined Iteration Technique. | 12.4.3 |
| 12.4.3 | Effect of Large Loading Step upon Nonlinear Solution during Load Reversal. | 12.4.5 |
| 12.4.4 | Ratcheting Effect (due to Large Rotations) in Solution Without Equilibrium Iterations. | 12.4.7 |

LIST OF TABLES

| <u>TABLE</u> | | <u>PAGE</u> |
|--------------|--|-------------|
| 2.4.1 | Interaction Table for Drawing Example | 2.4.8 |
| 3.0.1 | MAGNA Finite Element Library | 3.0.2 |
| 3.0.2 | Summary of Available Options by Element Type | 3.0.3 |
| 3.3.1 | Spurious Zero-Strain-Energy Modes for Various Combinations of Nodal Pattern and Integration Rule | 3.3.5 |
| 5.7.1 | Header Records for Postprocessor File MPOST | 5.7.2 |
| 5.7.2 | Data Records for Postprocessor File MPOST | 5.7.3 |
| 5.7.3 | MAGNA Postprocessor File 'APOST' - General Description and Format | 5.7.6 |
| 6.3.1 | Linear Solution for Axially Loaded Bar | 6.3.5 |
| 6.3.2 | Nonlinear Load-Deflection Results for Rectangular Bar | 6.3.5 |
| 6.5.1 | Summary of Natural Frequency Calculations for Tactical Fighter Windshield (3-D Elements) | 6.5.10 |
| 6.7.1 | Summary of Results for Two-Bay Plane Truss at Applied Load of 10,000 Pounds | 6.7.4 |
| 6.7.2 | Truss Element Forces in Two-Bay Truss at Applied Load of 10 Kips | 6.7.6 |
| 6.7.3 | Comparison of Maximum Displacements of Two-Bay Truss at Load P = 10000 Pounds | 6.7.7 |
| 6.12.1 | Comparison of Buckling Loads for Simply-Supported Sandwich Panel | 6.12.3 |
| 6.16.1 | Comparison of Exact and Computed Natural Frequencies for Square Orthotropic Plate | 6.16.3 |
| 6.18.1 | Natural Frequencies of Triangular Cantilever Plate | 6.18.3 |
| 6.18.2 | Comparison of Natural Frequency Results for Cantilevered Triangular Plate | 6.18.4 |
| 7.1.1 | Default and Minimum COMMON Block Lengths (CDC Program Version) | 7.1.15 |
| 7.1.2 | Octal-Decimal Conversions | 1.17 |

LIST OF TABLES (continued)

| <u>TABLE</u> | | <u>PAGE</u> |
|--------------|--|-------------|
| 7.1.3 | Computing Time Factors for Individual Element Types (CDC 6600) | 7.1.19 |
| 7.1.4 | Typical Nonlinear Solution Times Using the MAGNA Program (CDC 6600 and CYBER Computers) | 7.1.20 |
| 7.2.1 | Default and Minimum COMMON Block Lengths (CRAY Program Version) | 7.2.10 |
| 7.2.2 | Computing Time Factors for Individual Element Types (CRAY-1) | 7.2.14 |
| 8.5.1 | Integration Point Locations for Variable-Node Solid Element with INT = 2 | 8.5.13 |
| 8.5.2 | Integration Point Locations for Variable-Node Solid Element with INT = 3 | 8.5.14 |
| 8.5.3 | Integration Point Locations for Variable-Node Solid Element with INT = 14 | 8.5.15 |
| 8.5.4 | Integration Point Locations for Eight Node Solid Element with INT = 2 | 8.5.26 |
| 8.5.5 | Integration Point Locations for Eight-Node Solid Element with INT = 3 | 8.5.27 |
| 8.5.6 | Integration Point Locations for Eight-Node Solid Element with INT = 6 | 8.5.28 |
| 8.5.7 | Integration Point Locations for Quadrilateral Plane Stress, Plane Strain, and Shear Panel Element with INT = 2 | 8.5.36 |
| 8.5.8 | Integration Point Locations for Four-Node Planar Element with INT = 3 | 8.5.37 |
| 8.5.9 | Integration Point Locations for Twenty-Node Solid Element with INT = 2 | 8.5.58 |
| 8.5.10 | Integration Point Locations for Twenty-Node Solid Element with INT = 3 | 8.5.59 |
| 8.5.11 | Integration Point Locations for Twenty-Node Solid Element with INT = 14 | 8.5.60 |
| 8.5.12 | Integration Point Locations for Variable 8-20 Node Solid Element with INT = 2 | 8.5.71 |

LIST OF TABLES (continued)

| <u>TABLE</u> | | <u>PAGE</u> |
|--------------|---|-------------|
| 8.5.13 | Integration Point Locations for Variable 8-20 Node Solid Element with INT = 3 | 8.5.72 |
| 8.5.14 | Integration Point Locations for Variable 8-20 Node Solid Element with INT = 14 | 8.5.73 |
| 8.5.15 | Integration Point Locations for Sixteen-Node Solid Element with INT = 2 | 8.5.84 |
| 8.5.16 | Integration Point Locations for Sixteen-Node Solid Element with INT = 3 | 8.5.85 |
| 8.5.17 | Integration Point Locations for Sixteen-Node Solid Element with INT = 14 | 8.5.86 |
| 8.5.18 | Integration Point Locations for Variable-Node Plane Stress Element with INT = 2 | 8.5.93 |
| 8.5.19 | Integration Point Locations for Variable-Node Plane Stress Element with INT = 3 | 8.5.94 |
| 8.5.20 | Integration Point Locations for Variable-Node Axisymmetric Element with INT = 2 | 8.5.101 |
| 8.5.21 | Integration Point Locations for Variable-Node Axisymmetric Element with INT = 3 | 8.5.102 |
| 8.5.22 | Integration Point Locations for Sixteen-Node Layered Shell Element | 8.5.113(a) |
| 8.10.1 | Loading Type and Direction Codes (LTYPE) | 8.10.6 |
| 10.8.1 | Integration Point Locations for Solid Elements (1 Integration Point) | 10.8.8 |
| 10.8.2 | Integration Point Locations for Solid Elements (6 Integration Points) | 10.8.8 |
| 10.8.3 | Integration Point Locations for Solid Elements (8 Integration Points) | 10.8.9 |
| 10.8.4 | Integration Point Locations for Solid Elements (14 Integration Points) | 10.8.10 |
| 10.8.5 | Integration Point Locations for Solid Elements (27 Integration Points) | 10.8.11 |
| 10.8.6 | Integration Point Locations for Sixteen-Node Layered Shell Element | 10.8.16 |

LIST OF TABLES (continued)

| <u>TABLE</u> | <u>PAGE</u> |
|-----------------------------------|-------------|
| 10.11.1 STRAVG Error Messages | 10.11.3 |
| 11.3.1 XYPLOT File Input Sequence | 11.3.3 |

CHAPTER 1

INTRODUCTION

The finite element method has emerged as a valuable tool for the design and performance qualification of complex engineering structures involving arbitrary geometry, boundary conditions, and applied loads. The mathematics of most types of linear finite element formulations are well understood, and effective numerical methods have been developed for the computation of linear solutions to large structural analysis problems.

The consideration of nonlinear effects (large displacements, finite strains, plasticity) in finite element structural analysis is often desirable for studying stability, crashworthiness, or collapse behavior. However, present capabilities for modeling nonlinear behavior in structures of practical size are largely limited to one- and two-dimensional (including axisymmetric) components. Although it is possible in principle to predict the nonlinear response of complex, three-dimensional bodies, the volume of calculation required to evaluate nonlinear effects on the elemental level often makes the required analysis prohibitively expensive.

This report describes the finite element program MAGNA (Materially And Geometrically Nonlinear Aalysis). MAGNA has been developed to perform nonlinear response solutions for general structures of practical size and complexity. In contrast to most existing nonlinear finite element systems, the code is oriented primarily toward the nonlinear analysis of three-dimensional structures, including solids, shells, and layered constructions. The emphasis on three-dimensional analysis is reflected in the history of the development of MAGNA: the three-dimensional continuum elements were developed and implemented first in the program, and the programming techniques used have been designed to function most efficiently for elements having many degrees of freedom and relatively

large bandwidth. The program also operates largely out of core, to remove most restrictions on the number of elements, number of degrees of freedom, and model topology. Elements are, of course, included in the program for the analysis of one- and two-dimensional problems; however, the major strengths of MAGNA lie in its three-dimensional nonlinear solution capabilities. It is hoped that in this respect the program will help to fill an important need in the current state of nonlinear analysis methodology.

1.1 OVERVIEW

MAGNA (Materially And Geometrically Nonlinear Aalysis) is a large-scale computer program for the static and dynamic analysis of complex, three-dimensional engineering structures. The program is based upon the finite element method of analysis to permit the simulation of practical structures composed of many different types of elements. MAGNA combines effective isoparametric modeling techniques with state-of-the-art numerical analysis and programming methods to provide accurate and efficient solutions for large problems involving highly nonlinear response.

The modeling capabilities of MAGNA include structural elements for truss members, plane stress and plane strain sections, "shear panels," axisymmetric solids, general three-dimensional solids, thin plates and shells, and beam/frame members. All finite elements are arbitrarily oriented and are fully compatible in three-dimensional space. Degrees of freedom can be coupled to represent skewed boundary conditions, rigid regions, and complex structural joints. Nonlinear boundary conditions due to surface contacts, including sliding, can also be considered. Uniform mass damping, as well as structural damping based upon the instantaneous stiffness, can be applied in the solution. Time history solutions are performed in MAGNA using an implicit scheme for direct integration of the equations of motion. Applied loading may consist of concentrated nodal forces, distributed surface pressures, body forces in line loads; "live" pressures such as fluid loading may be considered, as well as other deformation-dependent forces defined in user-written subroutines.

Each of the finite elements in MAGNA includes the effects of full geometrical nonlinearities (large displacements, large strains), using a Lagrangian (fixed reference) description of motion. In shell and beam analysis, arbitrarily large rotations can also be treated. Material nonlinearities, in the form of elastic-plastic behavior, are analyzed using a subincremental

solution strategy which minimizes the error in following the material stress-strain curve. Isotropic, kinematic, and combined strain-hardening rules are available for use in plastic analysis with MAGNA.

The MAGNA program includes numerous user convenience features to aid in the generation of finite element modeling data. Geometry data may be input in Cartesian, cylindrical, and spherical coordinates, or in arbitrary, user-defined systems. Incremental generation of nodal coordinates and element connections is also available to exploit repetitive patterns in the structural model. User-written subroutines, which provide for user intervention or specification of data at several stages of the analysis, can be supplied for defining mesh geometry, coordinate systems, initial conditions, and incremental applied loading.

Interactive plotting utilities are also available for use in checking data, and for interpreting analysis results obtained from MAGNA. Geometry plotting, including exploded views, is available for all finite elements. Postprocessing functions include stress and strain contours and stress relief plots. Scaled and exploded views or close-up plots of the deformed structural model can be generated, with the undeformed geometry optionally superimposed in the display.

A number of data generation and model editing facilities have also been developed for use with the MAGNA finite element code. These preprocessing utilities are described briefly in this report. Interfaces to existing pre- and postprocessing systems have been developed as well, to permit users of MAGNA to take full advantage of the many geometric modeling and graphical output packages currently used to support finite element structural analysis.

To facilitate the solution of complex nonlinear problems and to make effective use of computer resources, a restart capability is provided in MAGNA for all nonlinear and transient

analysis options. Restarts may be performed at any point during the solution, to perform dynamic analysis with a nonlinear equilibrium state as the initial condition, to modify solution parameters or strategy, or to continue an abnormally terminated run.

1.2 MANUAL ORGANIZATION

This report summarizes the theoretical basis of the MAGNA finite element program, the numerical procedures used, and information required for execution of the program. The documentation is divided into four parts:

- theoretical development (Chapter 2),
- finite element library, program options, and special features (Chapters 3, 4, and 5),
- demonstration problems (Chapter 6), and
- user information (Chapters 7-12).

Although the input data and control language described in Chapters 7 and 8 are sufficient to permit the definition and execution of many types of structural analysis problems, efficient usage of the program often requires a more thorough familiarity with the theoretical and numerical procedures used in MAGNA. The user is therefore encouraged to review the documentation as thoroughly as possible, particularly when large nonlinear applications are to be performed.

CHAPTER 2

THEORETICAL DEVELOPMENT

Theoretical aspects of the finite element analysis performed in MAGNA are outlined in the following sections. Governing equations, in both continuous and semidiscretized form, are developed for a general, three-dimensional body which undergoes large displacements, large strains, and nonlinear material behavior. The various analysis options and finite element types included in the program are all obtained from this mathematical basis, either directly or as special cases. The material constitutive laws included in MAGNA are also described in detail.

2.1 CONTINUUM EQUATIONS OF MOTION

The principle of virtual work is used in the following to obtain the governing incremental equations for a three-dimensional structure undergoing large elastic-plastic deformations. A Lagrangian description of motion, in which all kinematic quantities are referred to the initial configuration of the structure, is employed. The development, which is similar to that presented in References 1 and 2, accounts for the effects of materially nonlinear behavior as well as geometrical nonlinearities due to large displacements and large strains.

2.1.1 Principle of Virtual Work

Consider a body whose initial position and state are denoted by C_0 , and in which Cartesian coordinates X_i are assigned to a generic point P as shown in Figure 2.1.1. At an arbitrary time during the subsequent deformation of the body, denote the current configuration by C_1 and the position of P by x_i . The principle of virtual work³ in state C_1 is written as

$$\int_{0V} (\dot{1}\sigma_{ij} \delta \dot{1}\epsilon_{ij} + \dot{0}\rho \dot{1}\ddot{u}_i \delta u_i) dV = \int_{0V} \dot{1}\bar{f}_i \delta u_i dV + \int_{0\partial V} \dot{1}\bar{t}_i \delta u_i dA, \quad (2.1.1)$$

in which a left subscript denotes the configuration, and all kinematic variables are referred to the geometry in state C_0 . The integrals extend over the original material volume $0V$, and its traction boundary $0\partial V$. Differentiation with respect to time is indicated by an overdot. Inertial effects have been introduced in Equation 2.1.1 as body forces in the D'Alembert sense.

Some discussion of the force and deformation quantities in Equation 2.1.1 is in order, to identify the appropriate

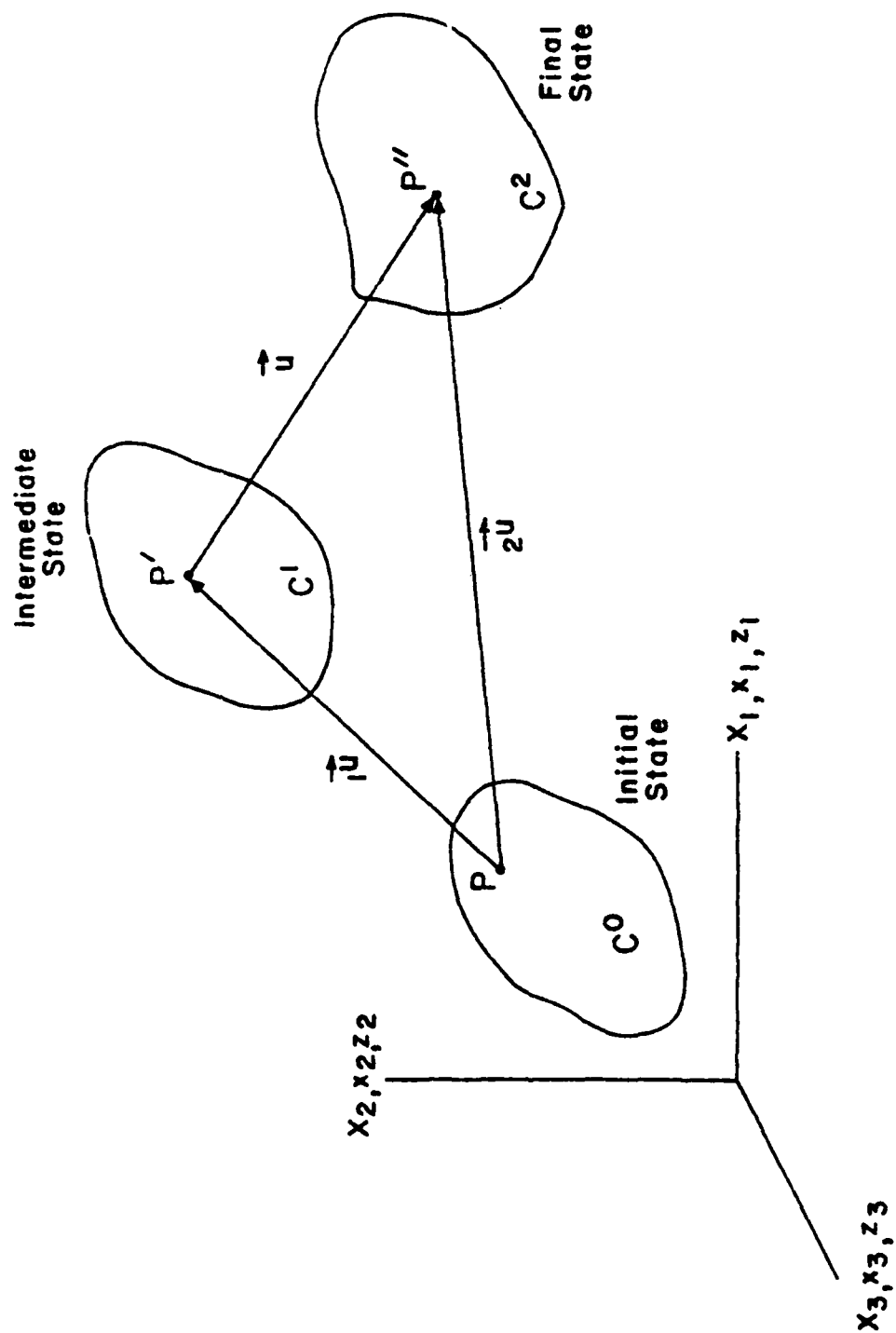


Figure 2.1.1 Successive States of Deformation of a Three-Dimensional Body.

measures for a Lagrangian description of motion. Displacements ${}_1u_i$ are resolved in the directions of X_i , and the corresponding strains are given by the Green-Saint Venant tensor,

$${}_1\epsilon_{ij} = \frac{1}{2} ({}_1u_{i,j} + {}_1u_{j,i} + {}_1u_{k,i} {}_1u_{k,j}) , \quad (2.1.2)$$

where differentiation is performed with respect to X_i . The stress measures ${}_1\sigma_{ij}$ are Cartesian components of the pseudo-stresses defined by⁴

$${}_1\sigma_{ij} = \sqrt{G} {}_1\Pi_{ij} \quad (2.1.3)$$

in which ${}_1\Pi_{ij}$ are the second (symmetric) Piola-Kirchhoff stresses⁵, and \sqrt{G} is the determinant of Green's deformation tensor, in state C_1 :

$$G = \left| \frac{\partial x_i}{\partial X_j} \right|^2 \quad (2.1.4)$$

The ${}_1\sigma_{ij}$ are interpreted as forces per unit of undeformed area, rotated by the local deformation, which occur in the deformed state. The foregoing stress and strain quantities are conjugate variables in the sense that the tensor product ${}_1\sigma_{ij} {}_1\epsilon_{ij}$ is a true measure of the internal work per unit of volume in the reference state⁴. The prescribed body forces ${}_1\bar{f}_i$ and surface tractions ${}_1\bar{t}_i$ represent the applied forces acting in state C_1 per unit initial volume and area, respectively.

Equation 2.1.1 can be recast in a more convenient form using the deformation gradients $\partial x_i / \partial X_j$, as¹

$$\int_V ({}_1\sigma_{ij} x_{k,i} \delta u_{k,j} + \rho {}_1\ddot{u}_i \delta u_i) dV = \int_V {}_1\bar{f}_i \delta u_i dV + \int_{\partial V} {}_1\bar{t}_i \delta u_i dA. \quad (2.1.5)$$

2.1.2 Incremental Principle of Virtual Work

For the purpose of obtaining an incremental form of the virtual work equality, it is necessary to compare two adjacent states of equilibrium whose difference corresponds to a small increment of time or loading. Consider a neighboring configuration C_2 , in which the virtual work expression is

$$\int_V ({}_2\sigma_{ij} z_{k,i} \delta u_{k,j} + {}_0\rho {}_2\ddot{u}_i \delta u_i) dV = \int_V {}_2\bar{f}_i \delta u_i dV + \int_{\partial V} {}_2\bar{t}_i \delta u_i dA, \quad (2.1.6)$$

and z_i are the new coordinates of the point P. As before, all quantities are referred to the initial state.

The increment of deformation between states C_1 and C_2 is characterized by the displacements

$$u_i = {}_2u_i - {}_1u_i. \quad (2.1.7)$$

Similarly, the incremental strains and stresses are denoted by ϵ_{ij} and σ_{ij} respectively; the internal virtual work per unit volume in state C_2 can therefore be restated as

$${}_2\sigma_{ij} z_{k,i} \delta u_{k,j} = ({}_1\sigma_{ij} + \sigma_{ij}) (x_{k,i} + u_{k,i}) \delta u_{k,j} \quad (2.1.8)$$

and Equation 2.1.6 becomes

$$\begin{aligned} \int_V [({}_1\sigma_{ij} + \sigma_{ij}) (x_{k,i} + u_{k,i}) \delta u_{k,j} + {}_0\rho ({}_1\ddot{u}_i + \ddot{u}_i) \delta u_i] dV \\ = \int_V {}_2\bar{f}_i \delta u_i dV + \int_{\partial V} {}_2\bar{t}_i \delta u_i dA. \end{aligned} \quad (2.1.9)$$

The incremental accelerations \ddot{u}_i have been obtained from the relations

$${}_2\ddot{u}_i = \ddot{z}_i = \ddot{x}_i + \ddot{u}_i = {}_1\ddot{u}_i + \ddot{u}_i . \quad (2.1.10)$$

Subtracting the virtual work equalities for the two neighboring configurations (Equations 2.1.5 and 2.1.9) yields

$$\int_V \{ [{}_1\sigma_{ij} u_{k,i} + \sigma_{ij}(x_{k,i} + u_{k,i})] \delta u_{k,j} + \rho \ddot{u}_i \delta u_i \} dV = \int_V \bar{f}_i \delta u_i dV + \int_{\partial V} \bar{t}_i \delta u_i dA , \quad (2.1.11)$$

where

$$\begin{aligned} \bar{f}_i &= {}_2\bar{f}_i - {}_1\bar{f}_i \\ \bar{t}_i &= {}_2\bar{t}_i - {}_1\bar{t}_i \end{aligned} \quad (2.1.12)$$

are increments of body force per unit reference volume and surface traction per unit reference area, respectively. Using the identity

$$\begin{aligned} \sigma_{ij} x_{k,i} \delta u_{k,j} &= \frac{1}{2} \sigma_{ij} \delta (u_{i,j} + u_{j,i}) \\ &+ \frac{1}{2} \sigma_{ij} ({}_1u_{k,i} \delta u_{k,j} + {}_1u_{k,j} \delta u_{k,i}) , \end{aligned} \quad (2.1.13)$$

which is true whenever the tensor σ_{ij} is symmetric, the incremental virtual work equality (Equation 2.1.11) is rearranged as follows:

$$\begin{aligned}
& \int_V \frac{1}{2} \left[{}_1\sigma_{ij} \delta(u_{k,i} u_{k,j}) + \frac{1}{2} \sigma_{ij} \delta(u_{i,j} + u_{j,i} + u_{k,i} u_{k,j}) \right] \\
& + \frac{1}{2} \left[\sigma_{ij} ({}_1u_{k,i} \delta u_{k,j} + {}_1u_{k,j} \delta u_{k,i}) + {}_0\rho \ddot{u}_i \delta u_i \right] dv = \\
& \int_V \bar{f}_i \delta u_i dv + \int_{\partial V} \bar{t}_i \delta u_i dA. \tag{2.1.1'}
\end{aligned}$$

The displacement terms occurring in the volume integral of Equation 2.1.14 can be identified as contributions to the incremental strains, ϵ_{ij} . Defining the total increment of strain between configurations C_1 and C_2 as

$$\epsilon_{ij} = {}_2\epsilon_{ij} - {}_1\epsilon_{ij} = e_{ij} + \eta_{ij} \tag{2.1.15}$$

with e_{ij} linear, and η_{ij} nonlinear, in the increments of displacement leads to the definitions⁶

$$\begin{aligned}
e_{ij} &= \frac{1}{2} (u_{i,j} + u_{j,i} + {}_1u_{k,i} u_{k,j} + {}_1u_{k,j} u_{k,i}) \\
\eta_{ij} &= \frac{1}{2} u_{k,i} u_{k,j} ; \tag{2.1.16}
\end{aligned}$$

Equation 2.1.14 is then simplified to

$$\begin{aligned}
& \int_V (\sigma_{ij} \delta \epsilon_{ij} + {}_1\sigma_{ij} \delta \eta_{ij} + {}_0\rho \ddot{u}_i \delta u_i) dv = \\
& \int_V \bar{f}_i \delta u_i dv + \int_{\partial V} \bar{t}_i \delta u_i dA. \tag{2.1.17}
\end{aligned}$$

The constitutive relation considered in the present development assumes that, at any instant, a linear

relationship exists between the increments of Lagrangian stresses and strains,

$$\sigma_{ij} = D_{ijkl} (\epsilon_{kl} - \alpha_{kl} T) . \quad (2.1.18)$$

Here α_{kl} represents the thermal expansion tensor, and T is the temperature change from the previous configuration. In general, the constitutive tensor D_{ijkl} depends upon the history of deformation and the temperature at a point. Specific forms of Equation 2.1.18 are considered in Section 2.3.

Introduction of the incremental constitutive equation, Equation 2.1.18, into the incremental principle of virtual work yields the incremental equations expressed solely in terms of displacement variables,

$$\int_V \left[D_{ijkl} (\epsilon_{kl} - \alpha_{kl} T) \delta \epsilon_{ij} + {}_1 \sigma_{ij} \delta \eta_{ij} + {}_0 \rho \ddot{u}_i \delta u_i \right] dV = \int_V \bar{f}_i \delta u_i dV + \int_{\partial V} \bar{t}_i \delta u_i dA, \quad (2.1.19)$$

in which ϵ_{ij} and η_{ij} are defined by Equations 2.1.15 and 2.1.16.

2.1.3 Linearization of Equations of Motion

The numerical solution of Equation 2.1.19 is complicated by the appearance of quadratic and cubic terms in the incremental displacements u_i . To obtain an efficient solution procedure for the incremental motion, it is useful to linearize the incremental virtual work equality. Linearization of Equation 2.1.19 involves the following considerations:

- expressions of higher order than linear in u_i are neglected; the nonlinear strains ϵ_{ij} in Equation 2.1.19 are therefore approximated by e_{ij} (Equation 2.1.16),

- the constitutive tensor D_{ijkl} is assumed to be constant for the increment,
- dependence of the body forces and surface tractions upon the incremental deformations for a single time or loading step is assumed to be negligible.

Under these assumptions, the linearized equation of virtual work becomes

$$\int_V \left[D_{ijkl} (e_{kl} - \alpha_{kl} T) \delta e_{ij} + {}_1\sigma_{ij} \delta \eta_{ij} + {}_0\rho \ddot{u}_i \delta u_i \right] dv = \int_V \bar{f}_i \delta u_i dv + \int_{\partial V} \bar{t}_i \delta u_i dA. \quad (2.1.20)$$

2.1.4 Equilibrium Corrections and Iteration

Using the linearized virtual work equality (Equation 2.1.20), a nonlinear solution can be performed as a sequence of linear subproblems; however, if no control is exercised over the accumulated truncation errors, the computed solution tends to drift rather quickly away from the true nonlinear solution. Consider, for example, a piecewise linear solution in which an approximate result has been obtained for an intermediate state C_1 . From Equation 2.1.1, the imbalance in virtual work in C_1 is simply

$$\begin{aligned} \delta_1 R = & \int_V {}_1\bar{f}_i \delta u_i dv + \int_{\partial V} {}_1\bar{t}_i \delta u_i dA \\ & - \int_V ({}_1\sigma_{ij} \delta_1 \epsilon_{ij} + {}_0\rho {}_1\ddot{u}_i \delta u_i) dv. \end{aligned} \quad (2.1.21)$$

Since $\delta_1 R = 0$ in an exact mathematical sense, Equation 2.1.21 provides a measure of error in the computed solution in configuration C_1 . As such, the residual $\delta_1 R$ can be employed as a means of a posteriori correction for the effects of linearization in the numerical analysis. To this end, the error $\delta_1 R$ (Equation 2.1.21) is appended to the linearized virtual work expression (Equation 2.1.20), as follows:

$$\begin{aligned} \int_V \left[D_{ijkl} (e_{kl} - \alpha_{kl} T) \delta e_{ij} + {}_1\sigma_{ij} \delta \eta_{ij} + {}_0\rho \ddot{u}_i \delta u_i \right] dV = \\ \int_V {}_2\bar{f}_i \delta u_i dV + \int_{\partial V} {}_2\bar{t}_i \delta u_i dA \\ - \int_V ({}_1\sigma_{ij} \delta {}_1\varepsilon_{ij} + {}_0\rho {}_1\ddot{u}_i \delta u_i) dV . \end{aligned} \quad (2.1.22)$$

The correction included in this augmented equation of virtual work may be viewed as an application of reactions to the out-of-balance forces observed in state C_1 , which tends to return the computed solution to the true conditions of nonlinear force equilibrium. By repeating this correction at a fixed value of time or loading, errors in the computed solution can be corrected to within a predetermined tolerance. This procedure, called equilibrium iteration, is discussed in detail in Section 4.3.

2.2 DISCRETE EQUATIONS OF MOTION

The incremental principle of virtual work as given by Equation 2.1.22 describes the static or transient behavior of a general, three-dimensional continuum experiencing both geometric and material nonlinearities. In the following, the construction of a finite element discretization of the virtual work equality, and the assembly of finite elements to form a complete structural model, are discussed.

2.2.1 Element-Based Virtual Work Equations

To obtain the appropriate continuum equations for a single finite element, the integrals in Equation 2.1.22 are expressed in terms of contributions from individual elements, as

$$\begin{aligned} \sum_e \int_{oV_e} \left[D_{ijkl} (e_{kl} - \alpha_{kl} T) \delta e_{ij} + {}_1\sigma_{ij} \delta \eta_{ij} + {}_0\rho \ddot{u}_i \delta u_i \right] dV = \\ \sum_e \int_{oV_e} {}_2\bar{t}_i \delta u_i dV + \sum_e \int_{o\partial V_e} {}_2\bar{t}_i \delta u_i dA \\ - \sum_e \int_{oV_e} ({}_1\sigma_{ij} \delta {}_1\varepsilon_{ij} + {}_0\rho {}_1\ddot{u}_i \delta u_i) dV . \end{aligned} \quad (2.2.1)$$

Such a decomposition into element contributions is valid, provided the displacement fields in adjoining elements are at least continuous¹. The interpretation of boundary integrals in Equation 2.2.1 is consistent with that of the global equation of virtual work (Equation 2.1.22). That is, the surface tractions ${}_2\bar{t}_i$ are understood to include prescribed external forces only, and the integrals on ${}_o\partial V_e$ are therefore nonzero only on the true external boundaries of the structure.

2.2.2 Finite Element Discretization

The discrete governing equations corresponding to Equations 2.2.1 are obtained by the assumption of an approximate state of displacement within each individual finite element. The displacement state for a single element has the form

$$\underline{u}(X_i, t) = \underline{N}^T(X_i) \underline{U}(t) , \quad (2.2.2)$$

in which $\underline{N}^T(X_i)$ represents a matrix of interpolation functions, and $\underline{U}(t)$ is the vector of nodal displacement parameters. In a particular state k , the total nodal displacement vector is denoted by ${}_k\underline{U}$, so that the increment in nodal displacements between states k and $k+1$ is

$$\underline{U} = (k+1)\underline{U} - {}_k\underline{U} \quad (2.2.3)$$

Strain-displacement equations can be written directly in matrix form for the linear part of the incremental strains (e_{ij} in Equation 2.1.16),

$$\underline{e} = {}_k\underline{B} \underline{\Delta} . \quad (2.2.4)$$

Here ${}_k\underline{B}$ is a function of the deformation gradients in state k , and $\underline{\Delta}$ is a vector containing the incremental displacement gradients. To fix ideas, consider the special case of plane deformation, for which

$$\underline{e}^T = [e_x \quad e_y \quad 2e_{xy}] , \quad (2.2.5)$$

$${}_k\underline{B} = \begin{bmatrix} (1+{}_k u_{,x}) & 0 & {}_k v_{,x} & 0 \\ 0 & {}_k u_{,y} & 0 & (1+{}_k v_{,y}) \\ {}_k u_{,y} & (1+{}_k u_{,x}) & (1+{}_k v_{,y}) & {}_k v_{,x} \end{bmatrix} \quad (2.2.6)$$

and

$$\underline{\Delta}^T = [u,_{x} \quad u,_{y} \quad v,_{x} \quad v,_{y}] \quad (2.2.7)$$

By virtue of Equation 2.2.2, the displacement gradients can be written as

$$\underline{\Delta} = \underline{\underline{C}}^T \underline{\underline{N}}^T \underline{U} , \quad (2.2.8)$$

in which $\underline{\underline{C}}^T$ is a matrix of linear, differential operators, and therefore

$$\underline{e} = {}_k \underline{\underline{B}} \underline{\underline{C}}^T \underline{\underline{N}}^T \underline{U} \quad (2.2.9)$$

for the increment from state k to state $(k+1)$.

Although the nonlinear contributions to the incremental strain tensor (η_{ij} in Equations 2.1.15 and 2.1.16) cannot be written explicitly in matrix form, the quadratic form ${}_k \sigma_{ij} \eta_{ij}$ appearing in the incremental virtual work equality is easily rewritten in a convenient matrix notation. Let ${}_k \underline{\underline{S}}$ denote the matrix of stresses in configuration k ,

$${}_k \underline{\underline{S}} = \begin{bmatrix} {}_k \sigma_{11} & {}_k \sigma_{12} & {}_k \sigma_{13} \\ {}_k \sigma_{12} & {}_k \sigma_{22} & {}_k \sigma_{23} \\ {}_k \sigma_{13} & {}_k \sigma_{23} & {}_k \sigma_{33} \end{bmatrix} , \quad (2.2.10)$$

and define

$${}_k \underline{\underline{S}}^* = \begin{bmatrix} {}_k \underline{\underline{S}} & \underline{\underline{0}} & \underline{\underline{0}} \\ \underline{\underline{0}} & {}_k \underline{\underline{S}} & \underline{\underline{0}} \\ \underline{\underline{0}} & \underline{\underline{0}} & {}_k \underline{\underline{S}} \end{bmatrix} . \quad (2.2.11)$$

Then,

$$2 \mathbf{k}^{\sigma}_{ij} \eta_{ij} = \underline{\Delta}^T \mathbf{k}^S \underline{\Delta} , \quad (2.2.12)$$

or, using Equation 2.2.8,

$$2 \mathbf{k}^{\sigma}_{ij} \eta_{ij} = \underline{\mathbf{U}}^T \underline{\mathbf{N}} \underline{\mathbf{C}} \mathbf{k}^S \underline{\mathbf{C}}^T \underline{\mathbf{N}}^T \underline{\mathbf{U}}. \quad (2.2.13)$$

With the foregoing definitions, the evaluation of the required element matrices and load vectors is straightforward. Corresponding to the terms in Equation 2.2.1, one can identify the tangent stiffness matrix,

$$\mathbf{k}^E_{KT} = \int_{V_e} (\underline{\mathbf{N}} \underline{\mathbf{C}} \mathbf{k}^B \mathbf{k}^D \underline{\mathbf{C}}^T \underline{\mathbf{N}}^T) dV, \quad (2.2.14)$$

and thermal load vector,

$$\mathbf{k}^e_{\theta} = \int_{V_e} (\underline{\mathbf{N}} \underline{\mathbf{C}} \mathbf{k}^B \mathbf{k}^D \underline{\alpha} \mathbf{k}^T) dV , \quad (2.2.15)$$

the geometric stiffness matrix,

$$\mathbf{k}^e_{KG} = \int_{V_e} (\underline{\mathbf{N}} \underline{\mathbf{C}} \mathbf{k}^S \underline{\mathbf{C}}^T \underline{\mathbf{N}}^T) dV , \quad (2.2.16)$$

and the element mass matrix

$$\underline{\mathbf{M}}^e = \int_{V_e} (\rho \underline{\mathbf{N}} \underline{\mathbf{N}}^T) dV . \quad (2.2.17)$$

The consistent loads due to prescribed body forces and surface tractions are given by

$${}_k \underline{F}^e = \int_{oV_e} (\underline{N} \quad {}_k \underline{\bar{f}}) \, dV \quad (2.2.18)$$

and

$${}_k \underline{T}^e = \int_{o\partial V_e} (\underline{N} \quad {}_k \underline{\bar{t}}) \, dA . \quad (2.2.19)$$

Equilibrium correction terms due to the internal forces become

$${}_k \underline{I}^e = \int_{oV_e} (\underline{N} \quad \underline{C}_k \underline{B}^T \quad {}_k \underline{S}) \, dV + \underline{M}^e \quad {}_k \underline{\ddot{U}} . \quad (2.2.20)$$

2.2.3 Assembly of Finite Elements

Using Equations 2.2.14 through 2.2.20, the incremental principle of virtual work (Equation 2.2.1) can be written in discrete form as

$$\sum_e \delta \underline{U}^T (\underline{K}_T^e + \underline{K}_G^e) \underline{U} + \delta \underline{U}^T \underline{M}^e \underline{\ddot{U}} = \sum_e \delta \underline{U}^T (\underline{F}^e + \underline{T}^e + \underline{\theta}^e - \underline{I}^e) , \quad (2.2.21)$$

where all terms are understood to be evaluated at the state k . The summation over the elements indicated in Equation 2.2.21 implies the enforcement of displacement compatibility on all interelement boundaries, as noted in Section 2.2.1. In practice, the enforcement of these conditions takes the form of an assembly of the element matrices, with the element

stiffness and loading terms at coincident nodes being summed in a consistent manner.

The nodal degrees of freedom \underline{U} for an element are related to the global vector of unknowns \underline{X} by

$$\underline{U} = \underline{A}\underline{X} , \quad (2.2.22)$$

in which \underline{A} is a Boolean matrix determined by the topology of the finite element model. Assembly of the individual finite elements to form the global discrete model is therefore represented formally by the equations

$$\sum_e \delta \underline{U}^T (\underline{K}_T^e + \underline{K}_G^e) \underline{U} = \delta \underline{X}^T (\underline{K}_T + \underline{K}_G) \underline{X} , \quad (2.2.23)$$

$$\sum_e \delta \underline{U}^T \underline{M}^e \ddot{\underline{U}} = \delta \underline{X}^T \underline{M} \ddot{\underline{X}} , \quad (2.2.24)$$

and

$$\sum_e \delta \underline{U}^T (\underline{F}^e + \underline{T}^e + \underline{\theta}^e - \underline{I}^e) = \delta \underline{X}^T (\underline{F} + \underline{T} + \underline{\theta} - \underline{I}) , \quad (2.2.25)$$

in which

$$\underline{K}_T = \sum_e \underline{A}^T \underline{K}_T^e \underline{A} , \quad (2.2.26)$$

and so on.*

The matrix equations of motion for the assembled finite element model are obtained from

*Note that the relationship stated in Equation 2.2.26 is only symbolic; the actual assembly of elements is performed using certain tables within the program, which accomplish this procedure much more efficiently.

$$\delta \underline{X}^T \left[(\underline{K}_T + \underline{K}_G) \underline{X} + \underline{M} \ddot{\underline{X}} - \underline{F} - \underline{T} - \underline{\theta} + \underline{I} \right] = 0 . \quad (2.2.27)$$

In view of the fact that the discrete virtual displacements $\delta \underline{X}^T$ are arbitrary and independent, their coefficients must vanish; the semidiscrete equations of motion are therefore

$$(\underline{K}_T + \underline{K}_G) \underline{X} + \underline{M} \ddot{\underline{X}} = \underline{F} + \underline{T} + \underline{\theta} - \underline{I} . \quad (2.2.28)$$

The discretization of Equation 2.2.28 in the time domain, as well as procedures for numerical solution of the equations for several classes of problems, are addressed in Chapter 4.

2.3 MATERIAL CONSTITUTIVE DESCRIPTIONS

The material stress-strain relationships used in MAGNA are incremental in nature, in keeping with the nonlinear analysis procedures described in Chapter 4. The constitutive descriptions are therefore of the hypoelastic type¹, in which increments of stress are linearly related to increments of strain,

$$\sigma_{ij} = k^{D_{ijmn}} \epsilon_{mn} , \quad (2.3.1)$$

where k denotes the current state. Stress-strain laws for specific classes of materials are discussed in the following sections.

2.3.1 Isotropic Elastic Material

For an ideally elastic material, the relationship between stress and strain is given by Hooke's Law²,

$$k^{\sigma_{ij}} = o^{D_{ijmn}} k^{\epsilon_{mn}} . \quad (2.3.2)$$

That is, the stress-strain law of Equation 2.3.1 may be interpreted either as a total or incremental equation, and the constitutive tensor $o^{D_{ijmn}}$ is unaffected by the history of deformation.

When the material is isotropic (does not exhibit direction-dependent behavior), the number of independent parameters which determine $o^{D_{ijmn}}$ reduces to two: the extensional modulus, E , and the Poisson's ratio, ν . In three dimensions, the isotropic elastic material law can be represented in matrix form by

$$\underline{\sigma} = \underline{D} \underline{\epsilon} , \quad (2.3.3)$$

in which

$$\underline{\sigma}^T = [\sigma_{11} \quad \sigma_{22} \quad \sigma_{33} \quad \sigma_{23} \quad \sigma_{13} \quad \sigma_{12}] , \quad (2.3.4)$$

$$\underline{\varepsilon}^T = [\varepsilon_{11} \quad \varepsilon_{22} \quad \varepsilon_{33} \quad 2\varepsilon_{23} \quad 2\varepsilon_{13} \quad 2\varepsilon_{12}] , \quad (2.3.5)$$

and

$$\underline{D} = \frac{E}{(1+\nu)(1-2\nu)} \begin{bmatrix} (1-\nu) & \nu & \nu & 0 & 0 & 0 \\ \nu & (1-\nu) & \nu & 0 & 0 & 0 \\ \nu & \nu & (1-\nu) & 0 & 0 & 0 \\ 0 & 0 & 0 & (\frac{1-2\nu}{2}) & 0 & 0 \\ 0 & 0 & 0 & 0 & (\frac{1-2\nu}{2}) & 0 \\ 0 & 0 & 0 & 0 & 0 & (\frac{1-2\nu}{2}) \end{bmatrix} \quad (2.3.6)$$

In the case of plane deformation, the number of stresses and strains which are independent is reduced to three,

$$\underline{\sigma}^T = [\sigma_{11} \quad \sigma_{22} \quad \sigma_{12}] \quad (2.3.7)$$

$$\underline{\varepsilon}^T = [\varepsilon_{11} \quad \varepsilon_{22} \quad 2\varepsilon_{12}] . \quad (2.3.8)$$

For the plane strain problem, the conditions $\varepsilon_{13} = \varepsilon_{23} = \varepsilon_{33} = 0$ are imposed, yielding the stress-strain matrix

$$\underline{D} = \frac{E}{(1+\nu)(1-2\nu)} \begin{bmatrix} (1-\nu) & \nu & 0 \\ \nu & (1-\nu) & 0 \\ 0 & 0 & (\frac{1-2\nu}{2}) \end{bmatrix} \quad (2.3.9)$$

In addition, the normal stress is determined by the condition $\epsilon_{33} = 0$,

$$\sigma_{33} = \nu(\sigma_{11} + \sigma_{22}) . \quad (2.3.10)$$

In plane stress analysis, the restrictions are $\sigma_{13} = \sigma_{23} = \sigma_{33} = 0$, and

$$\underline{\underline{D}} = \frac{E}{1-\nu^2} \begin{bmatrix} 1 & \nu & 0 \\ \nu & 1 & 0 \\ 0 & 0 & (\frac{1-\nu}{2}) \end{bmatrix} \quad (2.3.11)$$

2.3.2 Initially Isotropic, Elastic-Plastic Material

For most metals and a number of other homogeneous materials, nonlinear constitutive behavior (in the form of strain-hardening plastic deformation) can be described using a hypoelastic stress-strain relationship having the form of Equation 2.3.1. The elastic-plastic material law implemented in MAGNA is based upon an isothermal, time-independent theory of plasticity, using the von Mises yield criterion and its associated flow rule. Strain hardening is considered using isotropic, kinematic, and combined hardening rules.

To improve the computational efficiency of the elastic-plastic analysis, the formulation is based upon assumptions which are appropriate for large displacement, large rotation, and small strain problems³. In particular, the constitutive equations are written directly in terms of the second Piola-Kirchhoff stress and Green-St. Venant strain tensors, and an additive decomposition of the elastic and plastic Green's strains is assumed.

The general form of a yield criterion in which the yield locus is permitted to expand, contract, or translate is⁴

$$F(\sigma_{ij} - \alpha_{ij}) - k^2 = 0 . \quad (2.3.12)$$

Here σ_{ij} is the stress tensor*, α_{ij} describes the center of the yield surface in stress space, and k is a measure of the diameter of the yield surface. In general, both α_{ij} and k are dependent upon the history of inelastic deformation at a material point. The von Mises yield function is used in the present development, so that⁵

$$F = \frac{3}{2} (\sigma'_{ij} - \alpha'_{ij})(\sigma'_{ij} - \alpha'_{ij}) . \quad (2.3.13)$$

The notation $()'$ indicates deviatoric quantities, for example,

$$\sigma'_{ij} = \sigma_{ij} - \frac{1}{3} \sigma_{kk} \delta_{ij} \quad (2.3.14)$$

where δ_{ij} is the Kronecker delta. It is useful to note that, due to the form of Equation 2.3.13,

$$\frac{\partial F}{\partial \sigma_{ij}} = - \frac{\partial F}{\partial \alpha_{ij}} , \quad (2.3.15)$$

from which the differential of F can be written as

$$dF = \frac{\partial F}{\partial \sigma_{ij}} (d\sigma_{ij} - d\alpha_{ij}) . \quad (2.3.16)$$

The derivatives $\partial F / \partial \sigma_{ij}$ are given by

* For clarity, left subscripts indicating the current state are omitted throughout this section, and differential stresses and strains are simply denoted by $d\sigma_{ij}$ and $d\epsilon_{ij}$.

$$\frac{\partial F}{\partial \sigma_{ij}} = 3(\sigma'_{ij} - \alpha'_{ij}) . \quad (2.3.17)$$

The associated plastic flow rule corresponding to Equation 2.3.12 is

$$d\epsilon_{ij}^P = d\lambda \frac{\partial F}{\partial \sigma_{ij}} , \quad (2.3.18)$$

in which $d\lambda$ is as yet undetermined. Components of the incremental plastic strain are represented by $d\epsilon_{ij}^P$.

Consistent with Equation 2.3.18, the projection of a stress increment $d\sigma_{ij}$ onto the yield surface normal is proportional to the projection of the corresponding increment of plastic strain, $d\epsilon_{ij}^P$. Therefore⁴,

$$d\sigma_{ij} \frac{\partial F}{\partial \sigma_{ij}} = H d\epsilon_{ij}^P \frac{\partial F}{\partial \sigma_{ij}} \quad (2.3.19)$$

where H is a strain-hardening parameter determined from uniaxial stress-strain data. In particular, specialization of Equation 2.3.19 to the one-dimensional case gives

$$H = \frac{2}{3} \frac{d\sigma}{d\epsilon^P} = \frac{EE_t}{(E-E_t)} \quad (2.3.20)$$

where E_t is the instantaneous slope of the uniaxial stress-strain curve.

The increment of stress can be related to increments of strain by assuming the additive decomposition of elastic and plastic strain increments depicted in Figure 2.3.1; thus,

$$d\sigma_{ij} = E_{ijmn} (d\epsilon_{mn} - d\epsilon_{mn}^P) , \quad (2.3.21)$$

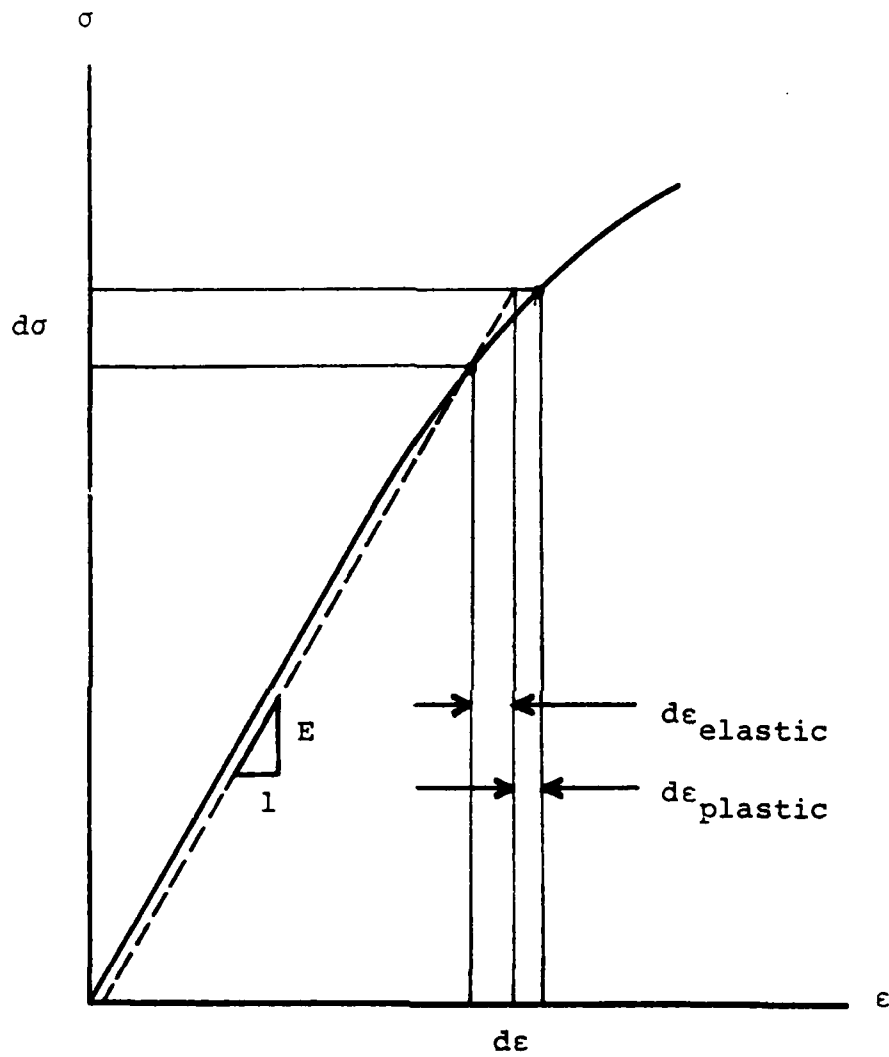


Figure 2.3.1 Decomposition of Incremental Strains into Elastic and Plastic Components.

where E_{ijmn} is the elastic constitutive tensor. With this assumption, it is now possible to determine the constant of proportionality $d\lambda$ in Equation 2.3.18. By multiplying Equation 2.3.21 by $\partial F / \partial \sigma_{ij}$, using Equation 2.3.19 to substitute for $d\sigma_{ij} \partial F / \partial \sigma_{ij}$, and eliminating $d\epsilon_{ij}^P$ by means of Equation 2.3.18, the final result is

$$d\lambda = \frac{E_{ijmn} d\epsilon_{mn} \frac{\partial F}{\partial \sigma_{ij}}}{(E_{ijmn} \frac{\partial F}{\partial \sigma_{mn}} + H \frac{\partial F}{\partial \sigma_{ij}}) \frac{\partial F}{\partial \sigma_{ij}}}, \quad (2.3.22)$$

Equations 2.3.18 and 2.3.22 are next used to eliminate the plastic strains, $d\epsilon_{mn}^P$, in Equation 2.3.21, yielding the required relationship between incremental stresses and strains,

$$d\sigma_{ij} = D_{ijmn} d\epsilon_{mn}^*, \quad (2.3.23)$$

in which

$$D_{ijmn} = E_{ijmn} - \frac{E_{ijkl} \frac{\partial F}{\partial \sigma_{kl}} \frac{\partial F}{\partial \sigma_{pq}} E_{pqmn}}{\frac{\partial F}{\partial \sigma_{kl}} E_{klpq} \frac{\partial F}{\partial \sigma_{pq}} + H \frac{\partial F}{\partial \sigma_{kl}} \frac{\partial F}{\partial \sigma_{kl}}}. \quad (2.3.24)$$

Equation 2.3.24 can be written in a more convenient form, as⁶

$$D_{ijmn} = E_{ijmn} - \beta (\sigma'_{ij} - \alpha'_{ij}) (\sigma'_{mn} - \alpha'_{mn}), \quad (2.3.25)$$

where β is defined by

$$\beta = \frac{3G}{(1 + H/2G)k^2} \quad (2.3.26)$$

* Note that, in the notation of the present section, this is the form corresponding to Equation 2.3.1.

for inelastic response ($\beta=0$ if the material behaves elastically). Here G is the elastic shear modulus, and H is the strain-hardening slope defined in Equation 2.3.20.

Equation 2.3.25 and 2.3.26 define the instantaneous material law corresponding to Equation 2.3.1. However, the parameters k , H , and α_{ij} , which describe the strain-hardening response of the material, must be determined separately in some manner. The hardening slope (H) is obtained from uniaxial test data, as indicated in Equation 2.3.20. In the present development the yield surface size (k) and components of translation (α_{ij}) are determined by one of three hardening rules:

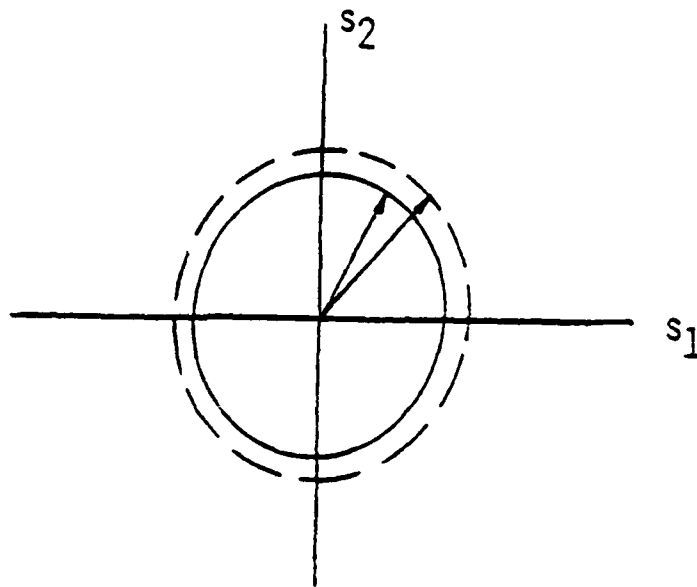
- isotropic hardening (uniform expansion of the yield surface),
- kinematic hardening (arbitrary translation of the yield surface), and
- combined hardening (both expansion and translation of the yield surface).

The isotropic and kinematic rules are shown in Figure 2.3.2, in a two-dimensional stress space. The above three descriptions of material strain hardening are equivalent when all components of stress are increased proportionally and monotonically, but produce quite different effects for problems involving non-proportional or reversed loading. A graphical comparison of the methods is shown in Figure 2.3.3, for the case of reversed loading in the plastic range.

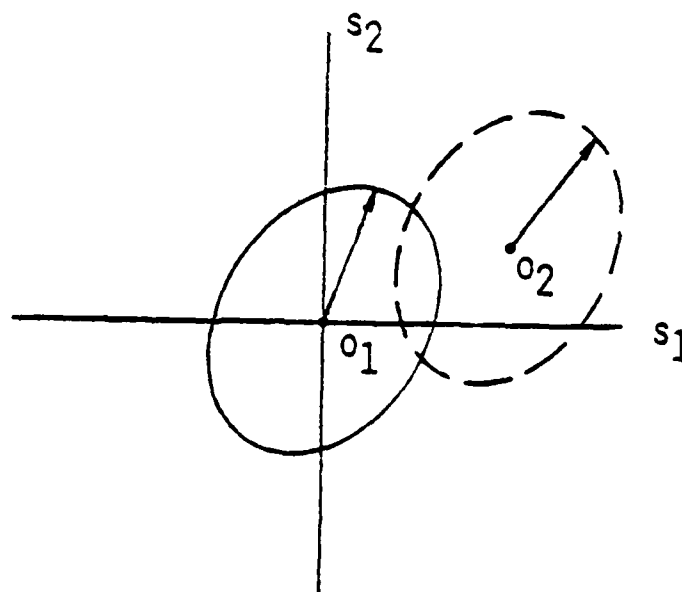
The kinematic hardening law is obtained from Ziegler's⁷ modification of Prager's kinematic rule⁸, in which the incremental components of yield surface translation are

$$d\alpha_{ij} = d\mu (\sigma_{ij} - \alpha_{ij}). \quad (2.3.27)$$

Noting that, since $k = \text{constant}$ (no expansion of the yield surface), the condition that the stress state remain exactly on the yield surface becomes



ISOTROPIC HARDENING



KINEMATIC HARDENING

Figure 2.3.2 Isotropic and Kinematic Hardening Rules in a Two-Dimensional Stress Space.

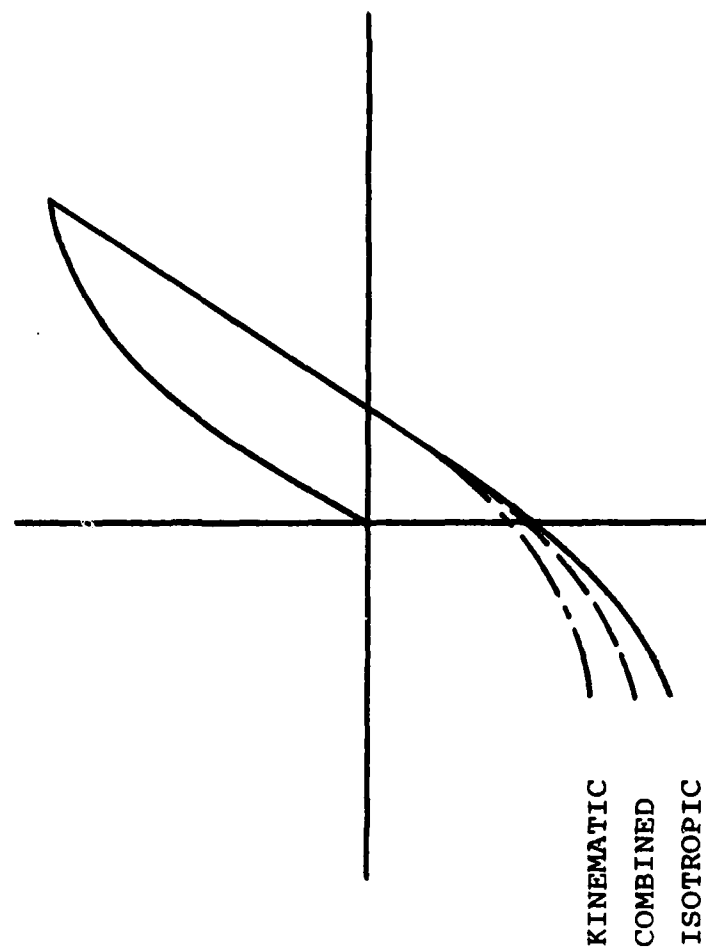


Figure 2.3.3 Comparison of Isotropic, Kinematic, and Combined Hardening Rules for Elastic Unloading and Re-yielding.

$$(d\sigma_{ij} - d\alpha_{ij}) \frac{\partial F}{\partial \sigma_{ij}} = 0 . \quad (2.3.28)$$

Combining these two equations, $d\mu$ is obtained from

$$d\mu = \frac{d\sigma_{ij} \frac{\partial F}{\partial \sigma_{ij}}}{(\sigma_{ij} - \alpha_{ij}) \frac{\partial F}{\partial \sigma_{ij}}} . \quad (2.3.29)$$

For purely isotropic hardening ($\alpha_{ij}=0$), the condition that the stress state lie on the yield surface becomes

$$\frac{\partial F}{\partial \sigma_{ij}} d\sigma_{ij} = 2k dk , \quad (2.3.30)$$

and the uniform yield surface expansion is therefore

$$dk = \frac{1}{2k} \frac{\partial F}{\partial \sigma_{ij}} d\sigma_{ij} . \quad (2.3.31)$$

A combined isotropic/kinematic hardening rule, as suggested by Tanaka⁹, is also used for elastic-plastic analysis. With this method, both translation and expansion of the yield surface is permitted. The relative magnitudes of the translation and expansion are determined by a parameter γ , such that $\gamma=0$ corresponds to ideal kinematic hardening, and $\gamma=1$ to fully isotropic hardening. In this case, the yield surface expansion is given by

$$dk = \frac{\gamma}{2k} \frac{\partial F}{\partial \sigma_{ij}} d\sigma_{ij} , \quad (2.3.32)$$

and the translation is obtained from Equation 2.3.27, with

$$d\mu = \frac{(1-\gamma)}{2k^2} \frac{\partial F}{\partial \sigma_{ij}} d\sigma_{ij} . \quad (2.3.33)$$

Negative values of γ can also be used in the combined hardening law, to model the yield surface as simultaneously translating and contracting.

During an incremental analysis, yielding of a material point may occur in the middle of an increment of loading. It is therefore desirable to account for the rapid change in constitutive behavior by analyzing the elastic and elastic-plastic portions of the increment separately. To accomplish this, it is necessary to adopt a scaling algorithm which determines that fraction of the current increment which is sufficient to cause initial yielding at a point. The procedure suggested by Yamada⁶ is used here, and is outlined briefly below.

Consider a single increment of loading, for which the initial elastic stress state at a point is denoted by P. The state at first yielding is represented by Q, and the final stress state by R, as shown in Figure 2.3.4. The equivalent stress at P, $\bar{\sigma}$, is assumed to be known. Consider next a point S, which falls on the radial path \overrightarrow{OP} , and lies on the same yield locus as point R. Then, the equivalent stresses at R and S are equal, and given by

$$\bar{\sigma} + d\bar{\sigma} = \sqrt{\frac{3}{2} (\sigma'_{ij} + d\sigma'_{ij})(\sigma'_{ij} + d\sigma'_{ij})} \quad (2.3.34)$$

The stress increment required to cause yielding is represented by \overrightarrow{PQ} , letting

$$\frac{|\overrightarrow{PQ}|}{|\overrightarrow{PR}|} = r , \quad (2.3.35)$$

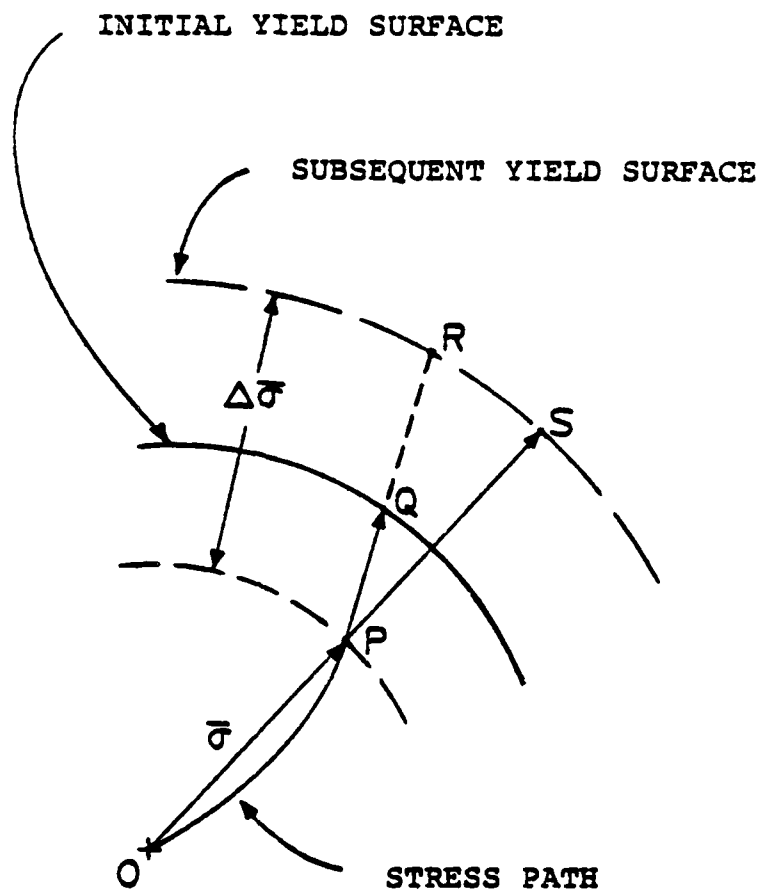


Figure 2.3.4 Scaling of Stress Increments to the Yield Surface.

the associated components of stress are simply $(\sigma_{ij} + r d\sigma_{ij})$. The value of r to cause initial yielding can therefore be determined by solving

$$k^2 = \frac{3}{2} (\sigma'_{ij} + r d\sigma'_{ij})(\sigma'_{ij} + r d\sigma'_{ij}) \quad (2.3.36)$$

for r on the interval $[0,1]$.

The above formulation of initially isotropic, elastic-plastic material behavior is implemented in MAGNA using a subincremental method,^{4,10} which permits a very accurate determination of the material behavior even for large increments of loading. Each load increment is divided into a number of smaller intervals for treating the calculation of material nonlinearities, with this interval size chosen so that a specified increment of strain is never exceeded. Since the subincrement sizes are chosen independently at each integration point of the finite element model, regions of rapidly increasing strain are automatically treated in finer detail in the analysis.

2.3.3 Orthotropic Elastic Material

The elastic constitutive properties of an orthotropic material are completely specified by nine independent constants:

- Young's moduli E_1, E_2, E_3 ,
- shear moduli G_{12}, G_{13}, G_{23} , and
- Poisson's ratios $\nu_{12}, \nu_{13}, \nu_{23}$.

These properties are defined with respect to the preferential axes of the material (denoted 1,2,3), which in general do not coincide with the reference coordinate axes of the structure under consideration (referred to here as x,y,z). The notation for the basic orthotropic properties used above follows that of Jones¹¹; that is, E_i refers to the extensional stiffness

along direction i , G_{ij} describes the engineering measure of shear stiffness in the plane (i,j) , and ν_{ij} is the lateral contraction in direction j due to a unit longitudinal extension in direction i .

Conditions upon the orthotropic material constants, which are useful in verifying that material properties have been specified correctly, can be summarized as follows. From the symmetry of the compliance matrix (inverse of stiffness), it is required that

$$\frac{\nu_{ij}}{E_i} = \frac{\nu_{ji}}{E_j} \quad ; \quad i, j = 1, 2, 3. \quad (2.3.37)$$

The positive definiteness of the stiffness and compliance matrices leads to the conditions

$$\begin{aligned} E_i &> 0 & ; \quad i = 1, 2, 3 \\ G_{ij} &> 0 & ; \quad i, j = 1, 2, 3 \end{aligned} \quad (2.3.38)$$

and

$$\begin{aligned} (1 - \nu_{ij}\nu_{ji}) &> 0 & ; \quad i, j = 1, 2, 3 \\ \Delta = 1 - \nu_{12}\nu_{21} - \nu_{23}\nu_{32} - \nu_{31}\nu_{13} - 2\nu_{21}\nu_{32}\nu_{13} &> 0. \end{aligned} \quad (2.3.39)$$

The complete stress-strain relation of an orthotropic material can be written with respect to the principal axes of the material as

$$\begin{Bmatrix} \sigma_1 \\ \sigma_2 \\ \sigma_3 \\ \tau_{23} \\ \tau_{13} \\ \tau_{12} \end{Bmatrix} = \begin{bmatrix} D_{11} & D_{12} & D_{13} & 0 & 0 & 0 \\ D_{12} & D_{22} & D_{23} & 0 & 0 & 0 \\ D_{13} & D_{23} & D_{33} & 0 & 0 & 0 \\ 0 & 0 & 0 & D_{44} & 0 & 0 \\ 0 & 0 & 0 & 0 & D_{55} & 0 \\ 0 & 0 & 0 & 0 & 0 & D_{66} \end{bmatrix} \begin{Bmatrix} \epsilon_1 \\ \epsilon_2 \\ \epsilon_3 \\ \gamma_{23} \\ \gamma_{13} \\ \gamma_{12} \end{Bmatrix} \quad (2.3.40)$$

The constants D_{ij} are defined by

$$\begin{aligned} D_{11} &= (1 - \nu_{23}\nu_{32})E_1/\Delta \\ D_{12} &= (\nu_{12} + \nu_{32}\nu_{13})E_2/\Delta \\ D_{13} &= (\nu_{13} + \nu_{12}\nu_{23})E_3/\Delta \\ D_{22} &= (1 - \nu_{13}\nu_{31})E_2/\Delta \\ D_{23} &= (\nu_{23} + \nu_{21}\nu_{13})E_3/\Delta \\ D_{33} &= (1 - \nu_{12}\nu_{21})E_3/\Delta \\ D_{44} &= G_{23} \\ D_{55} &= G_{13} \\ D_{66} &= G_{12} \end{aligned} \quad (2.3.41)$$

and Δ is as defined previously.

The above stress-strain relation is used in linear and geometrically nonlinear analysis with MAGNA. In nonlinear analysis, the given constitutive equation is presumed to hold between the second Piola-Kirchhoff stress and the Green-St. Venant strains in Cartesian coordinates. This description is consistent for small strain situations, in which the Piola-Kirchhoff stress corresponds closely to the nominal (engineering) stress.

In general, the principal axes of an orthotropic material do not coincide with the reference axes defined for the total structure under consideration. Thus, it is necessary

to transform the orthotropic stress-strain relation to the analysis reference coordinates prior to assembly of the finite element approximation.

Consider a material having principal axes x_i , oriented arbitrarily with respect to reference coordinates X_j . Let the relationship between these two sets of coordinate axes be

$$x_i = a_{ij} X_j . \quad (2.3.42)$$

That is, a_{ij} are the direction cosines of the direction x_i with respect to X_j . The tensorial values of stress and strain in the two systems are therefore related by

$$\begin{aligned} \sigma_{ij} &= a_{ik} a_{jl} \sigma'_{kl} \\ \epsilon_{ij} &= a_{ik} a_{jl} \epsilon'_{kl} \end{aligned} \quad (2.3.43)$$

where primed quantities refer to the principal material directions. These can be expressed in matrix form as

$$\begin{aligned} \underline{\sigma} &= \underline{T} \underline{\sigma'} \\ \underline{\epsilon} &= \underline{T} \underline{\epsilon'} \end{aligned} \quad (2.3.44)$$

Since the stress and strain vectors used for computational purposes include the shear terms only once each, the right half of matrix \underline{T} is modified to provide the correct transformation of the shear stress and strain quantities.

Write the stress-strain relation of Equation 2.3.40 as

$$\underline{\sigma'} = \underline{D} \underline{\gamma'} \quad (2.3.45)$$

where $\underline{\gamma}'$ refers to the engineering strains. Note that the engineering strains are related to the tensorial strains by

$$\underline{\gamma}' = \underline{\beta} \underline{\epsilon}' \quad (2.3.46)$$

in which

$$\underline{\beta} = \begin{bmatrix} \underline{I} & 0 \\ 0 & 2\underline{I} \end{bmatrix} . \quad (2.3.47)$$

Thus the stress-strain relation may be written in terms of the tensors $\underline{\sigma}'$, $\underline{\epsilon}'$ as

$$\underline{\sigma}' = \underline{D} \underline{\beta} \underline{\epsilon}' . \quad (2.3.48)$$

Transforming the stress-strain vectors to global coordinates gives

$$\underline{T}^{-1} \underline{\sigma} = \underline{D}' \underline{\beta} \underline{T}^{-1} \underline{\epsilon} \quad (2.3.49)$$

or

$$\underline{\sigma} = \underline{T} \underline{D}' \underline{\beta} \underline{T}^{-1} \underline{\beta}^{-1} \underline{\gamma} = \underline{D} \underline{\gamma} . \quad (2.3.50)$$

Therefore, the engineering stress-strain coefficients must be transformed by

$$\underline{D} = \underline{T} \underline{D}' \underline{\beta} \underline{T}^{-1} \underline{\beta}^{-1} . \quad (2.3.51)$$

However, it is straightforward to show that¹¹

$$\underline{\beta} \underline{T}^{-1} \underline{\beta}^{-1} = \underline{T}^t \quad (2.3.52)$$

so that the transformation of \underline{D} to the analysis coordinates has the simple form

$$\underline{D} = \underline{T} \underline{D}' \underline{T}^t . \quad (2.3.53)$$

2.4 SURFACE CONTACT ANALYSIS

In many structural analyses, support conditions and applied loading distributions can be specified a priori with sufficient accuracy for engineering purposes. However, in some cases boundary conditions may involve appreciable relative motion between the structure and supports, or a loading distribution may be the result of mechanical contact between objects. Still other situations may involve constraints which are applied only after a certain (finite) displacement has occurred. For each of these situations, the details of the support conditions and/or the loading involve nonlinearities, which are best taken into account as a part of the finite element solution.

Such situations can be considered with MAGNA using the surface contact analysis option, which includes the nonlinear effects arising from mechanical contact between two or more portions of a finite element mesh. By defining one of the contacting bodies as a rigid surface, a variety of other nonlinear support situations can likewise be included in the numerical solution.

2.4.1 General Description of Contact Solution

Consider two bodies which, in their current configurations, occupy the regions V_1 and V_2 ; the corresponding boundaries are denoted by ∂V_1 and ∂V_2 (Figure 2.4.1). If the two bodies are in contact with one another, their common boundary is

$$\Gamma = \partial V_1 \cap \partial V_2. \quad (2.4.1)$$

When $\Gamma = \emptyset$, the usual displacement and stress boundary conditions apply. If frictionless contact occurs, however, the displacements and tractions on the surfaces of the two bodies are related by

$$\underline{T}_1 \cdot \underline{n}_1 = \underline{T}_2 \cdot \underline{n}_2 \leq 0 \quad \text{on } \Gamma \quad (2.4.2)$$

$$\underline{u}_1 \cdot \underline{n}_1 + \underline{u}_2 \cdot \underline{n}_2 = 0 \quad \text{on } \Gamma \quad (2.4.3)$$

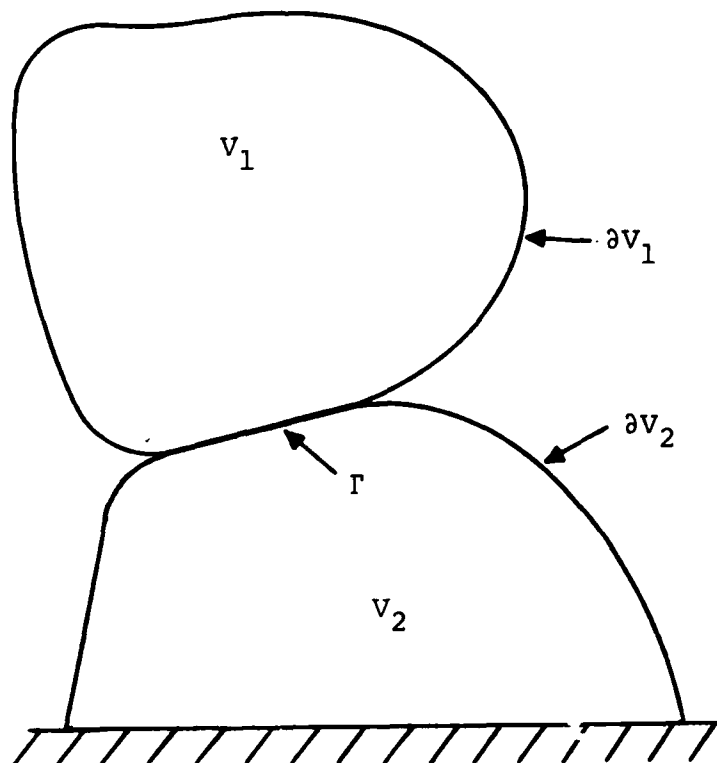


Figure 2.4.1. Contact between Three-Dimensional Bodies.

Here T_i represents the Cauchy surface traction vector on ∂V_i , u_i the corresponding displacement, and n_i the outward unit normal to surface i .

In the numerical solution, the region of contact Γ is not determined explicitly; only the condition

$$(V_1 - \partial V_1) \cap \partial V_2 = \emptyset \quad (2.4.4)$$

which states that interpenetration of the two bodies is not permitted, is used in the analysis. Relevant portions of the surfaces ∂V_1 and ∂V_2 (and others as necessary) are represented in a piecewise, isoparametric form, and the regions V_i are defined implicitly by these surface definitions. Note that, since ∂V_i is defined in a piecewise fashion, situations in which two portions of a singly-connected body come into contact can also be considered.

Since the analysis is performed using a displacement formulation of the finite element method, the essential constraints for the contact problem are those of Equation (2.4.3), and only these conditions are imposed directly. The force equilibrium condition on common surfaces, Equation (2.4.2), is to be satisfied as a consequence of the iterative solution method in which all unbalanced forces are systematically eliminated. Equation (2.4.2) is considered explicitly only as a condition for releasing contact constraints when load reversal or rebounding occur in the solution.

The essential elements of the numerical analysis of contact used in MAGNA are as follows. First, surface regions which represent potential areas of contact are defined. At each iteration cycle, each possible combination of surface segments is screened using simple, conservative tests to eliminate those pairs which are obviously not in contact. For remaining pairs of surface segments, a more precise determination of the relative positions is then made. Finally, when a contact

condition is detected, constraint equations are formulated which suppress all relative motions normal to the contact surface, or restore the displacement condition of Equation (2.4.3) in the event penetration has already occurred. Each of these steps is discussed in detail below.

2.4.2 Definition of Potential Contacting Surfaces

The first step in the contact analysis is the identification of those surfaces between which contact might occur during the course of the numerical solution. Each such surface is defined by a grid of special surface elements, which for the boundaries of flexible bodies simply correspond to external faces of three dimensional structural elements (Figure 2.4.2). A completely rigid surface is represented by surface elements alone, connected to node points whose motions are suppressed or otherwise prescribed.

A typical surface element configuration is shown in Figure 2.4.3. The element may have from four to nine connected nodes, depending upon the type of structural element to which it is connected. For rigid boundaries, the number of nodes depends upon the geometry of the surface to be defined. A rigid half-space, for instance, can always be defined using a single surface element having four nodal points.

Once the surface element geometry has been defined, surface element sets are defined, each of which consists of a specified range of elements. Combinations of surface element sets which represent potential pairs of contacting surfaces are identified in an interaction table. All possible combinations of nodes and elements corresponding to nonzero entries in the interaction table are to be examined for possible contact at each iteration cycle of the solution. As an example, consider the drawing problem shown in Figure 2.4.4. Four sets of surface elements are defined, and the interaction table is defined as in Table 2.4.1. By convention, the higher-numbered surface of a pair is always considered the master surface, while node points

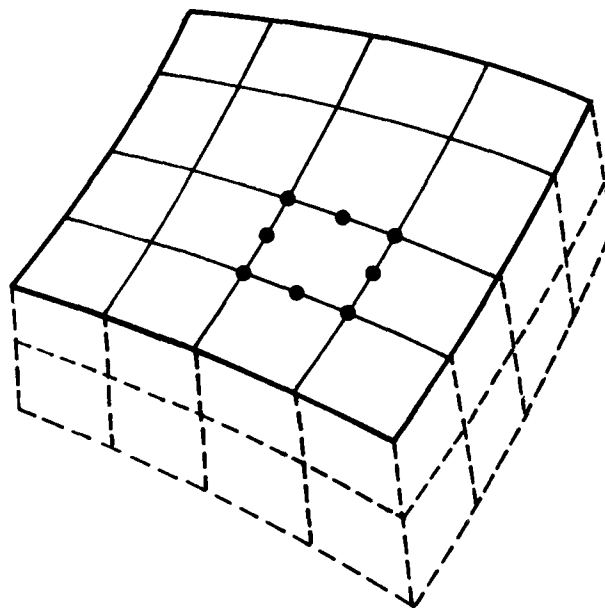
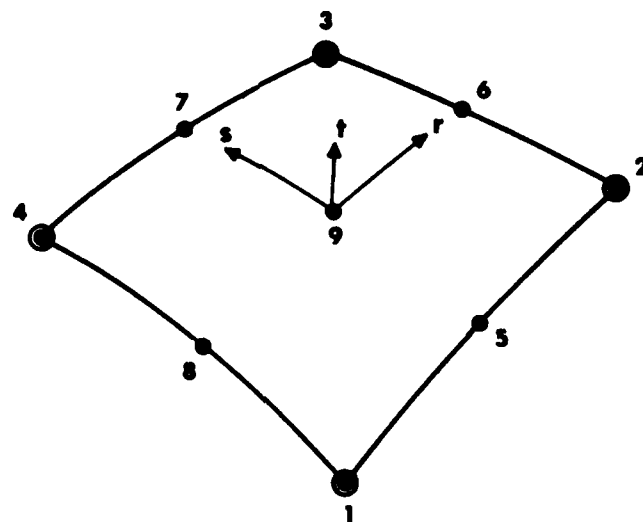
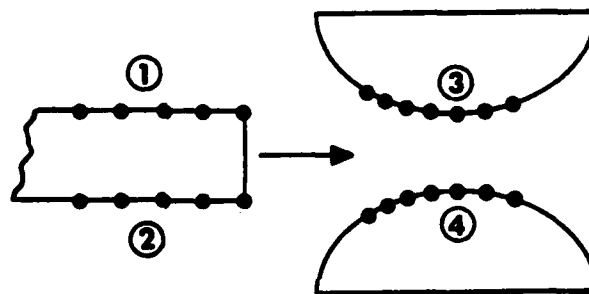


Figure 2.4.2. Typical Surface Contact Element.



- midside / center nodes (optional)
- corner nodes (required)

Figure 2.4.3. Nodal Pattern of General Surface Contact Element.



① = surface element set

Figure 2.4.4. Definition of Surface Element Sets for a Drawing Problem.

TABLE 2.4.1
INTERACTION TABLE FOR DRAWING EXAMPLE

| | | Master Surface | | | |
|---------------|---|----------------|---|---|---|
| | | 1 | 2 | 3 | 4 |
| Slave Surface | 1 | - | 0 | 1 | 0 |
| | 2 | - | - | 0 | 1 |
| | 3 | - | - | - | 0 |
| | 4 | - | - | - | - |

- = Entry Not Possible

0 = No Contact Considered

1 = Potential Contacting Surface Pair

in the lower-numbered set are considered slave nodes in the formulation of displacement constraints. Generally, the boundary of the stiffer of two bodies is defined as a master surface, although this is not essential. Note also that a given surface may represent a master surface in one interaction table entry, and a slave node surface in another.

2.4.3 Screening of Possible Contact Conditions

The effectiveness of the contact analysis depends, at least in part, upon the ability to eliminate all but a few possible combinations of nodes and elements from consideration with a relatively small amount of computation. In practical analyses, it may be necessary to examine hundreds of potential contact conditions before isolating the few which are truly active. For this reason, an approximate screening procedure is used to eliminate those node/element combinations which obviously need not be considered in detail. When this procedure fails, a more accurate determination of the relative positions of the surfaces in question is undertaken.

In each iteration cycle, all possible slave node/master surface element combinations, as defined in the interaction table, are examined for contact. In each master element, a local rectangular coordinate system x_i is constructed which is approximately aligned with the natural coordinates (r,s,t) of the element shown in Figure 2.4.3. The current position of each node of the element is determined in this system, as well as the maximum and minimum values of x_i ; $i=1,2,3$. The current location of each slave node, denoted by X_i , is also computed in the local coordinates. As an initial check, any master/slave pair for which one of

$$x_i^P > \max(x_i) + \epsilon_1 [\max(x_i) - \min(x_i)]; i=1,2,3 \quad (2.4.5)$$

$$x_i^P < \min(x_i) - \epsilon_1 [\max(x_i) - \min(x_i)]; i=1,2 \quad (2.4.6)$$

is satisfied is rejected unconditionally. Typically, $\epsilon_1 \approx 0.1$. This simple test eliminates most of the potential slave nodes which are obviously out of range of the master element. If neither of Equations 2.4.5 or 2.4.6 are satisfied, the coordinate values in the local coordinate system are used to estimate the natural coordinate values (r,s) at which the normal to the surface passes through the slave node in question.

Using the initial estimate so obtained, a Newton-Raphson solution is performed to determine the position $\tilde{R}(r,s)$ whose surface normal vector

$$\tilde{n} = \frac{\frac{\partial \tilde{R}}{\partial r} \times \frac{\partial \tilde{R}}{\partial s}}{\left| \frac{\partial \tilde{R}}{\partial r} \times \frac{\partial \tilde{R}}{\partial s} \right|} \quad (2.4.7)$$

intersects the given slave point. The condition to be satisfied is

$$\tilde{R}_p = \tilde{R}(r,s) + d\tilde{n} \quad (2.4.8)$$

in which r and s are to be determined. Figure 2.4.5 shows the geometry of Equation 2.4.8 for the simple case of a planar master surface and an initial trial point $r=0, s=0$.

From the solution of Equation 2.4.8, the orientation of a potential slave point with respect to the master surface element is known precisely. The slave point is rejected on the basis of this solution if the inequality

$$\max [|r|-1, |s|-1] > \epsilon_2 \quad (2.4.9)$$

is satisfied, in which $\epsilon_2 \approx 0.001$. Points for which r,s are very slightly beyond the boundaries of the master element are retained, since discontinuities in the slope of adjacent elements might otherwise permit a node to penetrate the master surface without being detected.

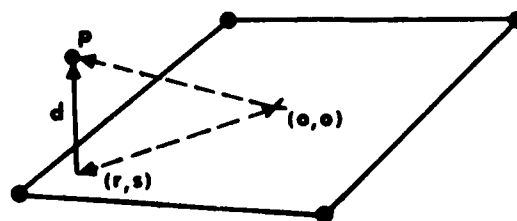


Figure 2.4.5. Solution for Relative Position of a Point and a Surface.

The remaining checks for determining whether or not contact occurs are straightforward, since Equations 2.4.2 and 2.4.4 may be applied directly. In particular, if $d \leq 0$ in Equation 2.4.8, interpenetration occurs and the appropriate contact constraints must be applied. During iteration, previously active constraints for which d becomes slightly positive are also retained if the corresponding normal forces are compressive in order to suppress artificial oscillations in the solution. For similar reasons, previously active constraints for which $d \leq 0$ and the normal forces are very small and positive are also permitted to remain active. Small fractions of the existing element internal forces and of the current surface element size are used to provide a measure of scale for force and displacement quantities.

2.4.4 Application of Constraints

Consider next the case in which a slave/master element combination has been found for which contact occurs. Let d be the distance of the slave point from the surface element along its normal at the point (r,s) as in Equation 2.4.8. For the constraint equation, a generalization of Equation 2.4.3 is used which returns the slave node to the master surface in the event that $d < 0$:

$$[\underline{u}_p - \underline{u}(r,s)] \cdot \underline{n} + d = 0 \quad (2.4.10)$$

In Equation 2.4.10, \underline{u}_p is the incremental displacement vector of the slave point, and $\underline{u}(r,s)$ is the incremental displacement of the element at the position (r,s)

$$\underline{u}(r,s) = \sum_{i=1}^9 N_i(r,s) \underline{u}_i \quad (2.4.11)$$

where $N_i(r,s)$ are the surface element shape functions. In the present development, the above constraint is introduced into the system-level equations via the penalty function

$$\frac{\kappa}{2} [\underline{u}_p \cdot \underline{n} - \underline{u}(r,s) \cdot \underline{n}]^2 = \kappa d^2 - d[\underline{u}_p - \underline{u}(r,s)] \cdot \underline{n} \quad (2.4.12)$$

The left side of Equation 2.4.12 is quadratic in the incremental nodal displacements \underline{u}_p and \underline{u}_i and therefore represents a contribution to the stiffness matrix. The remaining terms are linear in \underline{u}_p and \underline{u}_i and enter the incremental equilibrium equations as additional "incremental force" terms. The penalty factor κ is made sufficiently large to enforce the required constraint, while maintaining reasonably good conditioning of the system of equations. In the current implementation of the procedure, the value

$$\kappa = 100 \max(K_{ii}) ; i=1,2,\dots,N \quad (2.4.13)$$

is used, in which K is the most recently computed tangent stiffness matrix and N is the number of degrees of freedom in the finite element model.

CHAPTER 3

FINITE ELEMENT LIBRARY

The MAGNA program contains a variety of finite element types to permit the effective modeling of complex structures. The element library currently consists of twelve element types, which are summarized in Table 3.0.1. These elements are fully compatible with one another, and can have arbitrary orientation in three-dimensional space.* Thus, any two elements having similar nodal patterns may be joined directly, with the compatibility of displacements on common boundaries being enforced automatically. Layered or sandwich structures, as well as tangential joints between shells and solids, can therefore be considered without the use of constraints or other special joining techniques.

Each element in the MAGNA finite element library is available for both linear and nonlinear analysis. A summary of the major analysis options available with each element type appears in Table 3.0.2. Since the computations for nonlinear elements are considerably more involved than for linearized elements, MAGNA contains separately-programmed linear and nonlinear versions of each element type. Therefore, no penalty is paid when using the program for linear analysis.

The finite element library is discussed in the following sections. Particular attention is devoted to the specific strong points and/or limitations of each element type, and to the proper selection of numerical integration rules.

*The single exception is the axisymmetric solid element (Type 10), which is required to lie in the global X-Y coordinate plane.

TABLE 3.0.1
MAGNA FINITE ELEMENT LIBRARY

| ELEMENT TYPE | DESCRIPTION | NUMBER OF NODES | DEGREES OF FREEDOM |
|-----------------|------------------------------|--------------------|-----------------------|
| 1 | 3-D Solid | 8-27 | 24-81 |
| 2 | 3-D Solid | 8 | 24 |
| 3 | Plane Stress/ Shear Panel | 4 | 12 |
| 4 | Truss | 2 | 6 |
| 5 | Thin Plate or Shell | 8 | 24 |
| 6 | 3-D Solid | 20 | 60 |
| 7 | 3-D Solid | 8-20 | 24-60 |
| 8 | 3-D Solid/ Thick Shell | 16 | 48 |
| 9 | Plane Stress | 4-9 | 12-27 |
| 10 | Axisymmetric Solid | 4-9 | 12-27 |
| 11 | Layered Plate or Shell | 16 | 48 |
| 12 | 3-D Curved Beam | 2-3 | 12-18 |

TABLE 3.0.2
SUMMARY OF AVAILABLE OPTIONS BY ELEMENT TYPE

| | ELEMENT TYPE | | | | | | | | | | | |
|---------------------------|--------------|---|---|---|---|---|---|---|---|----|----|----|
| | 1 | 2 | 3 | 4 | 5 | 6 | 7 | 8 | 9 | 10 | 11 | 12 |
| Linear Analysis | X | X | X | X | X | X | X | X | X | X | X | X |
| Lumped Mass | X | X | X | X | X | X | X | X | X | X | X | |
| Consistent Mass | X | X | X | | X | X | X | X | X | X | X | X |
| Thermal Stress | X | X | X | X | X | X | X | X | X | | | |
| Distributed Loads | X | X | X | X | X | X | X | X | X | X | X | |
| Large Displacements | X | X | X | X | X | X | X | X | X | X | X | X |
| Plasticity | X | X | X | X | | X | X | X | X | X | X | X |
| NELASi User Routine | X | X | X | X | | X | X | X | X | X | | |
| UPLASi User Routine | X | X | X | | | X | X | X | X | X | | |
| Orthotropic Material | X | X | | | | X | X | X | | | X | |
| Averaged Stiffness Option | X | | | | | X | X | X | | | | |
| Steady-state Harmonic | X | X | X | X | X | X | X | X | X | X | | |

3.1 ONE-DIMENSIONAL CONTINUUM ELEMENTS

The one-dimensional bar or truss element (Element Type 4) is a prismatic, axial-force member with arbitrary orientation in space. Figure 3.1.1 shows the truss element, which is defined by the two connected nodes at its end points.

Both the geometry and the displacements of the bar are represented by linear interpolation between the two nodes of the element. Consequently, the axial strain and stress are constant within an element, and all integrations of the element properties (stiffness, mass, residual forces) are evaluated exactly.

The truss element formulation includes full geometrical and material nonlinearities, using the original configuration as a reference state. Three-dimensional inertial effects are included in the mass matrix formulation, to ensure correct results in dynamic analysis with arbitrary orientations. A lumped mass matrix is used in all dynamics problems with the bar element.

Typical applications of the truss element include the following:

- one-dimensional problems,
- cable structures,
- pin-jointed plane or space trusses, and
- modeling of spar/rib caps and posts in wing-like aerospace structures.

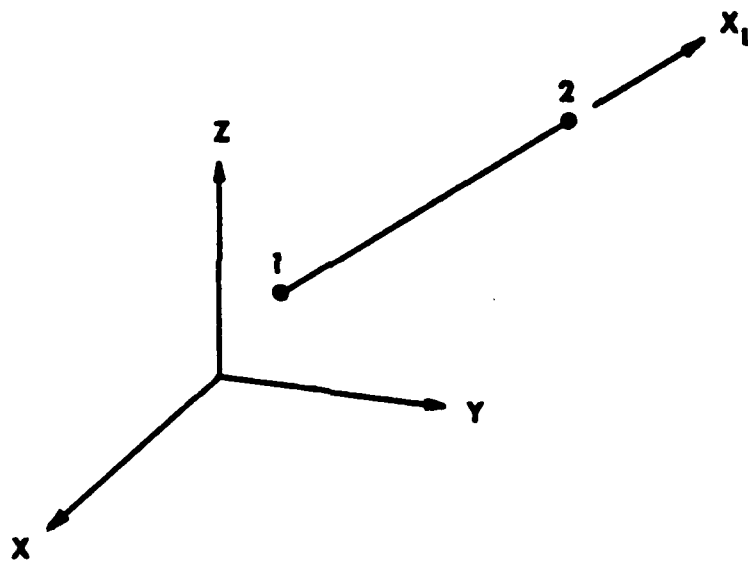


Figure 3.1.1 Three-Dimensional Truss Element.

3.2 TWO-DIMENSIONAL AND AXISYMMETRIC CONTINUUM ELEMENTS

Two-dimensional elements contained in MAGNA include Element Type 3 (four node, plane stress, plane strain or shear panel element), Element Type 9 (variable-node plane stress element), and Element Type 10 (variable-node axisymmetric solid element). These elements are planar (i.e., not warped) but may assume an arbitrary orientation in space. Axisymmetric elements must lie in the x-y plane, with x being the radial coordinate. Geometrical (large-displacement) nonlinearities, including warping and other out-of-plane deformations, are included, as well as material nonlinearities (plasticity). Elements 3, 9, and 10 may be used with either a lumped or consistent mass formulation. Out-of-plane inertial effects are included in Element Types 3 and 9.

The three/four node plane element (Type 3) is shown in Figure 3.2.1. Its geometry and displacement field are approximated by linear polynomials in each natural coordinate direction. Since certain components of stress or strain in the direction transverse to the element are assumed to vanish, an auxiliary local coordinate system (X_L , Y_L in the figure) is used to describe the element properties; all output is given in this system of coordinates to facilitate the interpretation of results. The X_L axis is directed from node 1 to node 2, and the Y_L axis is perpendicular to X_L and in the plane determined by nodes 1, 2, and 3. The fourth node is optional; however, the three-node element is suggested only when mesh geometry dictates that it be used.

Element Type 3 can be used for plane stress analysis, plane strain analysis, and in specialized application as a shear panel element. The primary difference in these three element subtypes is in the material stress-strain law employed. Constitutive equations for the plane stress and plane strain forms of the element are given in Section 2.3; for the shear

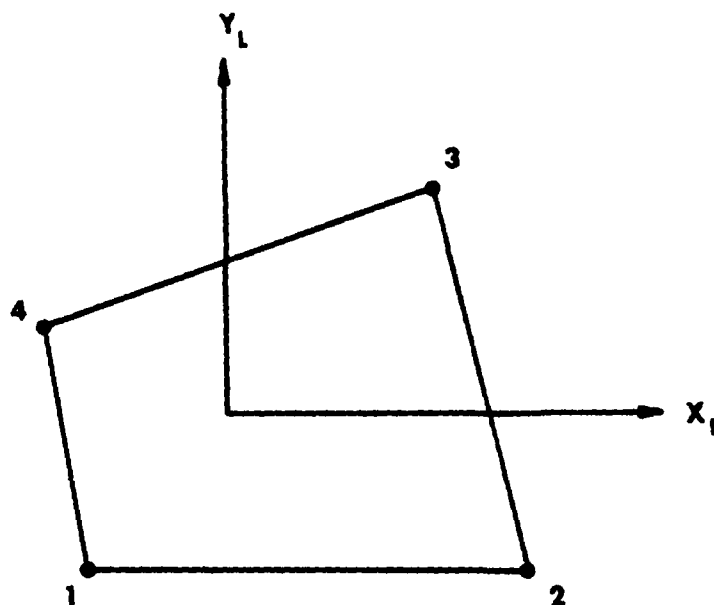


Figure 3.2.1 Quadrilateral Plane Stress, Plane Strain,
or Shear Panel Element.

panel (usually used to model vertical rib and spar sections in aerospace structures), the element is assumed to carry only shear stresses, $\tau_{xy} = G\gamma_{xy}$. Consistent formulations of the elastic-plastic stress-strain law are provided for the plane stress and shear panel element. *At present, the plane strain formulation uses the relation*

$$\sigma_z = \nu(\sigma_x + \sigma_y)$$

which is only approximate when plastic deformations occur.

Numerical integration of the four-node planar element may be performed using 1, 2, or 3 point Gaussian quadrature (1, 4, or 9 integration stations), or by a selective integration technique. A 2-point integration is sufficient for virtually all applications. The triangular version of the element is integrated using one-point integration in all cases. The one-point integration and selective (2x2 rule with one-point shear integral) integration options are provided for use in the analysis of planar beams and other situations involving large element length-to-thickness ratios. *The performance of the four node element in representing in-plane bending is poor unless an extremely fine mesh is used; the reduced and selective integration options help to relieve this deficiency.*

The most common application of the Type 3 element is in the analysis of airplane wings and similar box-type structures, using the plane stress formulation for skin elements, the shear web element for spar/rib sections, and bars (Element Type 4) as caps and posts. Another specialized application is in the analysis of crack-tip stresses in perfectly plastic materials; here one edge of the elements at the crack tip can be degenerated to zero length to provide the needed $1/r$ - type singularity in the shear strains. Notice that in such applications, either edge 3-4 or edge 4-1 must be degenerated, since the first three nodes must be non-collinear. In most plane stress applications, Element Type 9 is considerably more effective.

Element Type 9 (Figure 3.2.2) is a plane stress element which can possess from three to nine nodes per element. The first three (corner) nodes are always required, but *each* of nodes 4 through 9 are optional. The absence or presence of each optional node is automatically taken into account by the program. Node 4 *must* be present whenever any of the midside nodes are used. Thus, Element 9 may be used as a nine-node Lagrangian element, as the popular eight-node serendipity element (node 9 omitted), or as a transition from lower-order to higher-order elements. The eight-node and nine-node forms are particularly effective for general plane stress analysis, but lower-order versions of the element can often be used to advantage. For example, in analyzing planar beam structures, a six-node element (with linear interpolation through the thickness) is often effective.

The variable-node plane stress element can be integrated with 1, 2, or 3 point Gaussian quadrature in each direction. One-point integration is provided for use when only three or four nodes per element are specified; in such cases, the use of Element Type 3 will be slightly more efficient. *The higher-order versions of the element generally require the use of 3x3 quadrature (nine integration stations) for exact evaluation, particularly when all nine nodes are present.* In bending problems, the six and eight-node elements can sometimes be integrated with a 2x2 rule to improve element flexibility, provided the number of boundary conditions is sufficient to eliminate all singularities in the assembled mesh.

Although the Type 9 element may have a general orientation in space, the primary use of this element is in plane stress analysis. Therefore, element properties are computed in global coordinates if possible, and output is referred to the global (x,y) axes for all elements which are oriented parallel to the (x,y) plane. When a more general orientation is specified, output is given with respect to local axis directions defined in the same manner as for Element Type 3.

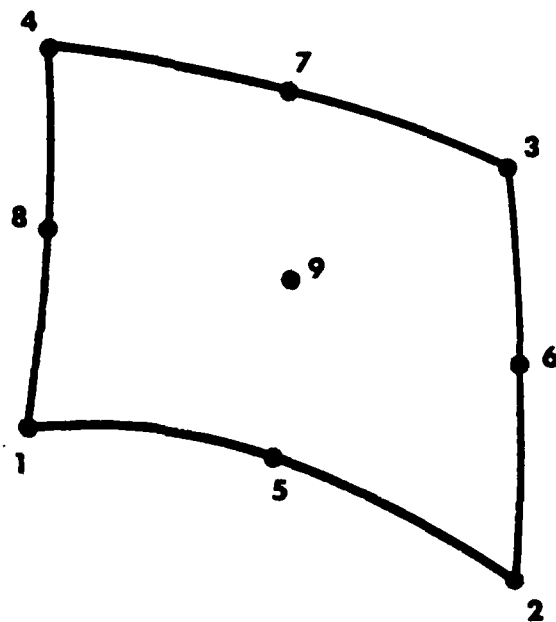


Figure 3.2.2 Variable-Number-of-Nodes Plane Stress Element.

The usual applications of the variable-node plane stress element are in general plane stress analysis and in the analysis of planar beam or frame structures. Another more specialized application is the analysis of crack problems in two dimensions. The simple device of positioning midside nodes (and the centroidal node) at the $1/4$ -points in elements located at the tip of a crack yields the $1/\sqrt{r}$ singularity in strains predicted by linear fracture mechanics, permitting such problems to be modeled using relatively few elements. This technique is illustrated in Figure 3.2.3.

The axisymmetric solid element (Type 10) in MAGNA is a variable-number-of-nodes element, whose appearance is exactly the same as the 3-9 node plane stress element (Figure 3.2.2). The first three vertex nodes (nodes 1-3) are always required. For quadrilateral elements (nodes 1-4 present), each of the remaining five nodes may be included or omitted as appropriate. The eight- and nine-node configurations are particularly effective for general axisymmetric stress analysis, although a linear interpolation in the thickness direction is often acceptable for axisymmetric plate and shell analysis.

Axisymmetric solid elements are assumed to be situated in the global x-y coordinate plane. The x-direction corresponds to the radial coordinate, and y is parallel to the axis of revolution of the model.

One, two, or three Gaussian integration points may be used in each element coordinate direction to evaluate the element stiffness and mass properties. While the choice of integration rules follows the same reasoning as the Type 9 plane stress element, the use of a 3×3 integration is advisable in most applications.

Either a consistent or lumped mass formulation may be chosen for inertial properties of the axisymmetric element; the use of consistent masses for the Type 10 element is recommended. *Thermal stress analysis is currently not available with the axisymmetric solid element.*

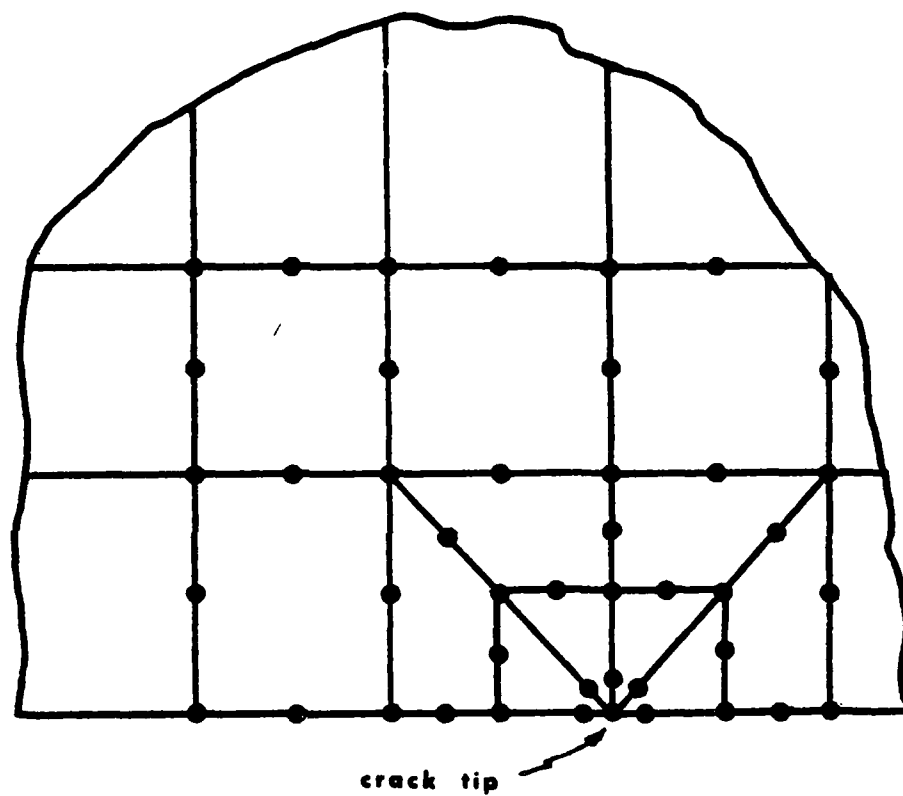


Figure 3.2.3 Quarter-Point Crack Tip Element.

3.3 THREE--DIMENSIONAL CONTINUUM ELEMENTS

MAGNA contains a number of three-dimensional solid elements for linear and nonlinear analysis:

Element Type 1 - 8-27 Variable-Node Solid

Element Type 2 - Eight-Node Brick

Element Type 6 - Twenty-Node Brick

Element Type 7 - 8-20 Variable Node Solid

Element Type 8 - Sixteen-Node Solid or Thick Shell.

All of the above elements contain full geometrical nonlinearities (large displacements and finite strains) and material nonlinearities (metal plasticity), and may be used either in static or dynamic analysis. Orthotropic materials can be considered for *elastic* analysis, whether linear or nonlinear. *Elastic-plastic materials must be initially isotropic.*

The 8-27 node solid (Element Type 1) is shown in Figure 3.3.1. The remaining solid elements (Types 2, 6, 7 and 8) have similar nodal patterns, with node points numbered higher than the maximum for a specific element type simply being omitted. Element Types 1 and 7 are variable-number-of-nodes elements; with each of these types, nodes 1 through 8 are always required, but *each* of the remaining nodes is optional and may simply be omitted if not needed. The absence or presence of each optional node is accounted for automatically in the program. The variable-node elements are particularly useful in transitioning between coarse and fine regions within the mesh (Figure 3.3.2), and for blending regions modeled using Element Types 2, 6 and 8. Alternatively, the variable-number-of-nodes elements can be used to construct standard element types not included explicitly in the program (e.g., eighteen-node thick shell elements with nine nodes per surface).

This variety of solid elements is included in MAGNA primarily for reasons of efficiency. In nonlinear analysis the

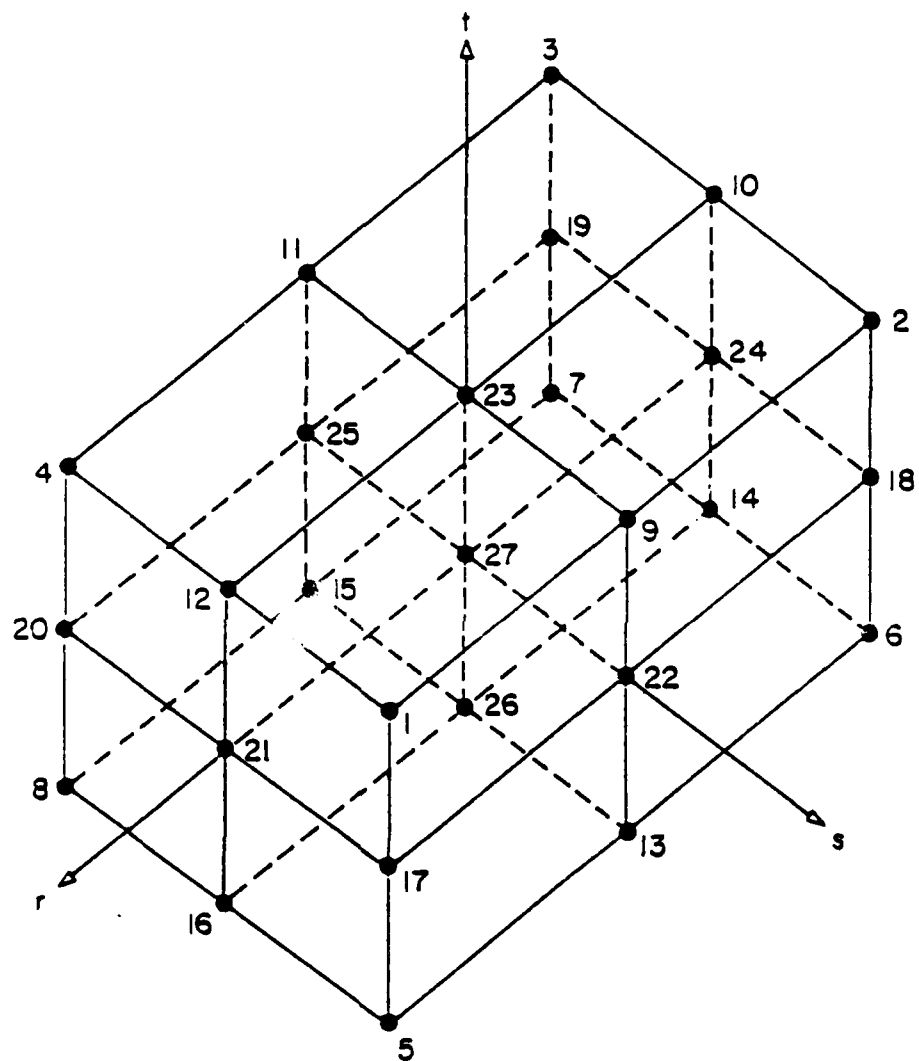


Figure 3.3.1 Three-Dimensional Solid Element with Variable Number of Nodes.

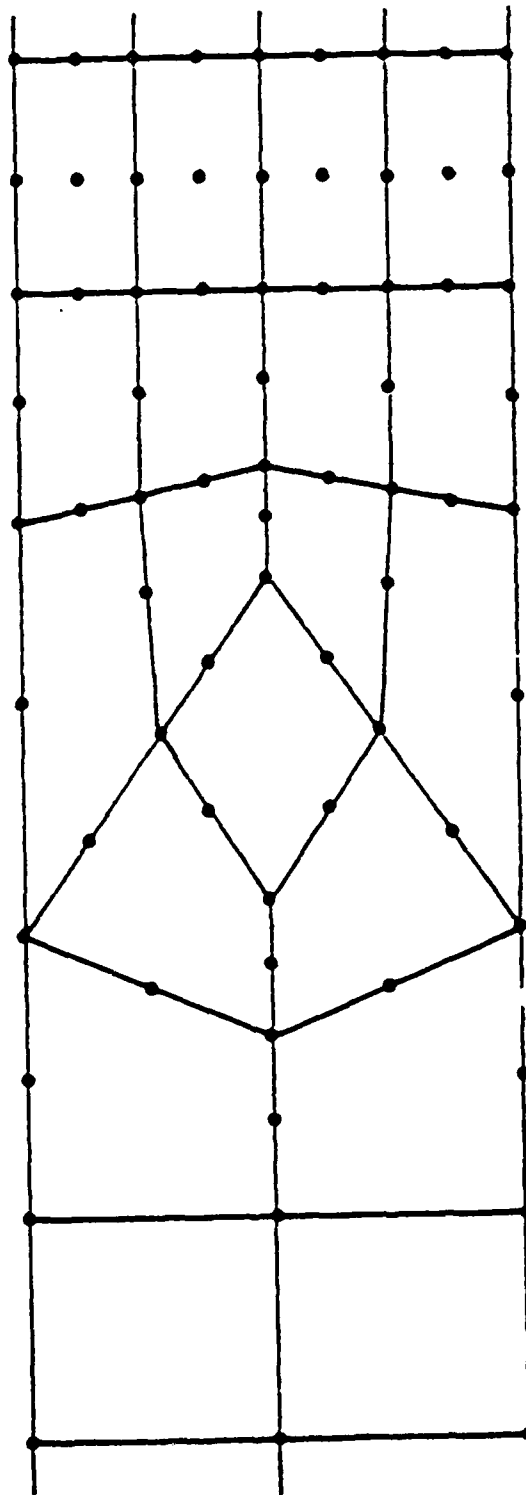


Figure 3.3.2 Transitions Between Coarse and Fine Model Regions.

AD-A129 773

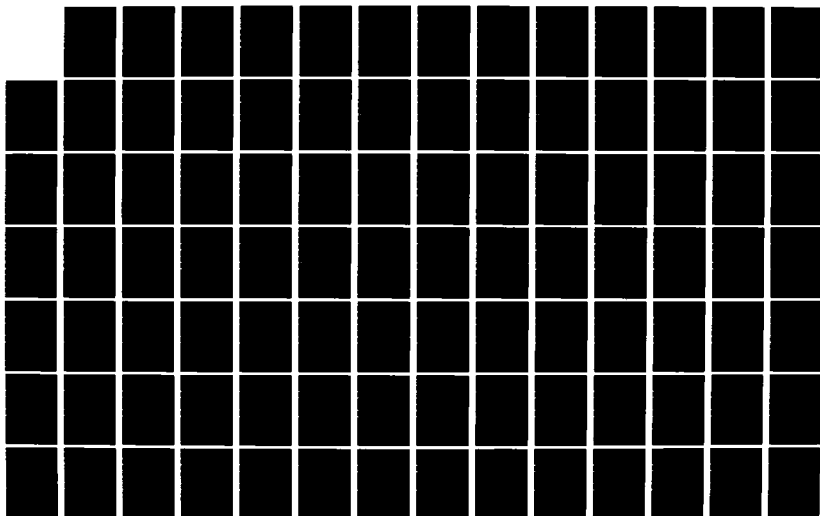
MAGNA (MATERIALLY AND GEOMETRICALLY NONLINEAR ANALYSIS)
PART I FINITE ELE. (U) DAYTON UNIV OH RESEARCH INST
R A BROCKMAN DEC 82 UDR-TR-82-111 AFWL-TR-82-3098-PT-1
F33615-80-C-3403

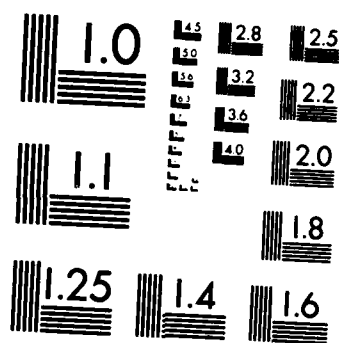
2/8

UNCLASSIFIED

F/G 12/1

NL





MICROCOPY RESOLUTION TEST CHART
NATIONAL BUREAU OF STANDARDS-1963-A

computing time per element for a single increment will vary approximately as the square of the maximum number of nodes for that Element Type. Therefore, Element Type 8 requires about 35 percent as much CPU time per element as Element Type 1, since $(16/27)^2 = 0.351$. In general, then, it is advisable to select the Element Type with the least "excess" nodes for a specific application.

Numerical integration of the higher-order solid elements (Types 1, 6, 7 and 8) can be performed using 2 or 3 point Gaussian quadrature in each coordinate direction (i.e., 8 or 27 integration stations). Also available is the 14-point integration rule introduced by Irons¹. For general application, the 14-point rule is recommended; this rule possesses similar accuracy to the 3x3x3 Gaussian integration, does not permit artificial "zero-energy" modes in most solid elements and involves only half as many sampling points as the Gaussian rule. The moderate increase in element flexibility using the 14-point rule leads to improved results with coarse meshes, while the reduction in number of integration stations over 3x3x3 integration reduces computing times considerably. For elements with 20 nodes or less (no mid-face or centroid nodes), a 2x2x2 Gaussian rule can often be used, provided the boundary conditions are sufficient to remove all singularities from the final system of equations. This integration scheme is particularly useful in problems of moderately thin plates or shells. For the sixteen-node element (Type 8), which is commonly used for such applications, the 2x2x2 integration rule is generally reliable.

The effect of the choice of integration rule for various three-dimensional solid elements is illustrated in Table 3.3.1. For each combination of element nodal pattern and integration scheme, the Table gives the number of zero-frequency modes present in the linear element stiffness matrix (less the normal six rigid body modes). Thus, a zero entry indicates that the element is fully integrated and, therefore, completely reliable. For the reduced integration orders shown, the application of

TABLE 3.3.1
SPURIOUS ZERO-STRAIN-ENERGY MODES FOR VARIOUS COMBINATIONS
OF NODAL PATTERN AND INTEGRATION RULE

| Integration Rule | Number of Nodes Per Element | | | |
|-------------------|-----------------------------|--------|------|------|
| | 8 | 16 | 20 | 27 |
| 1 x 1 x 1 Gauss | 12* | N.A.** | N.A. | N.A. |
| 6 Point Rule | 3 | N.A. | N.A. | N.A. |
| 9 Point Selective | 3 | N.A. | N.A. | N.A. |
| 2 x 2 x 2 Gauss | 0 | 2 | 6 | 27 |
| 14 Point Rule | N.A. | 0 | 0 | 4 |
| 3 x 3 x 3 Gauss | 0 | 0 | 0 | 0 |

* - Number of spurious mechanisms in unconstrained stiffness matrix of a single element. Zero entries denote full-integrated elements.

** - N.A. appears when a particular combination of element type and integration rule is not available in MAGNA.

boundary conditions is often sufficient to eliminate the unwanted zero-energy modes. For models involving high aspect ratios, very light constraints or large disparities in material modulus, however, the use of fully-integrated elements is always indicated.

Element Type 2 (eight-node brick) can be numerically integrated using 1, 2 or 3 point Gaussian quadrature (1, 8 or 27 integration stations). A non-Gaussian, 6-point rule is also provided; this integration rule gives similar performance to 2x2x2 Gauss integration, at a slightly lower cost. A special selective integration option, which uses nine integrating points, is also available. The 2x2x2 and the 6-point rules are generally sufficient, and the use of a larger number of elements is generally preferred over an increase in integration order. The nine-point, selective rule is appropriate for use when the eight-node brick must be used to represent bending-type response. An example of an application of this type is the sandwich construction pictured in Figure 3.3.3. Here the core layers are represented by Type 2 elements with nine-point integration, and Type 5 shell elements are used in the face sheet layers. For the analysis of general continua, the quadratic solid elements are usually more effective than the eight-node brick. In particular, *the use of the eight-node brick in problems involving bending-type response is not advisable, except with the use of the selective integration option.*

Three-dimensional nonlinear analyses can involve a great deal of computing effort, in spite of the fact that highly nonlinear effects may be concentrated in relatively small portions of the finite element model. In view of this, a number of stiffness formulation options are provided in MAGNA for the quadratic solid elements (Types 1, 6, 7 and 8). Normally all elements are formulated using the "tangent" stiffness method, in which the element stiffness matrices are recomputed exactly at user-controlled intervals within an analysis. However, a

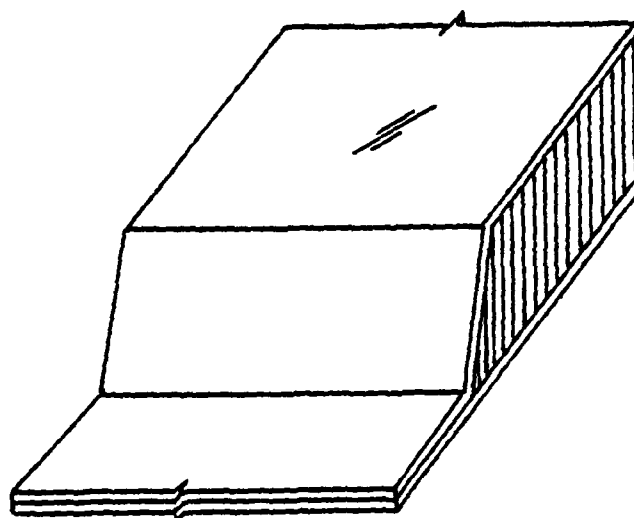
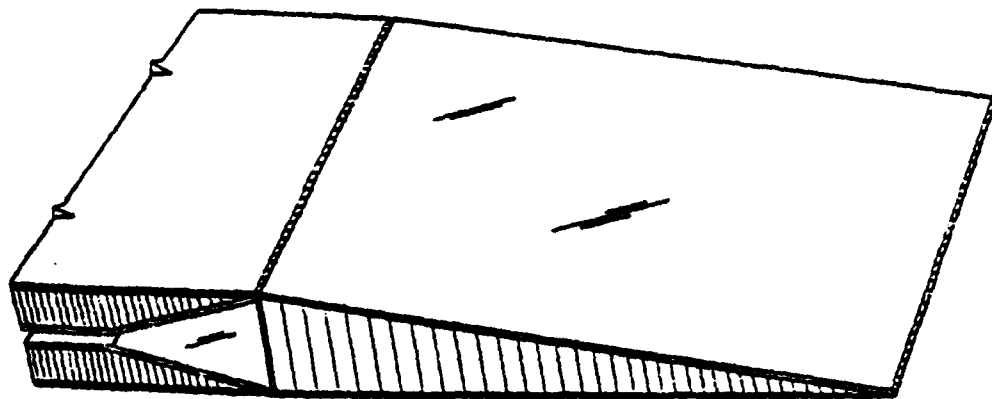


Figure 3.3.3 Three-Layered Sandwich Construction.

"pseudo-force" formulation may also be specified for selected elements, causing the original (linear elastic) stiffness matrix to be used in these elements throughout the analysis. This option, which merely accounts for nonlinear effects in a different manner from the tangent stiffness approach, is suitable for use in elements for which nonlinearities are expected to be rather mild. Alternatively, the analyst may specify a special "averaged" stiffness formulation for selected elements, in which the element tangent stiffness is computed in an approximate manner by averaging nonlinear effects in an individual element. Nonlinearities are still represented with full accuracy in the averaged stiffness method, since the element residuals (i.e., out-of-balance forces) are always computed exactly. *Both the averaged stiffness and constant stiffness formulations can drastically reduce computing times in nonlinear analysis, but should always be used with equilibrium iterations to maintain stability of the solution.* In highly nonlinear portions of a model, the use of the standard tangent stiffness formulation is generally superior because of its improved numerical stability characteristics.

3.4 THREE-DIMENSIONAL PLATE AND SHELL ELEMENTS

MAGNA contains two types of shell elements: a monolithic, linear-displacement thin shell (Element Type 5) and a layered, quadratic-displacement shell element (Element Type 11). Both of these element types are described briefly below.

The eight-node thin plate or shell element (Element Type 5) is an isoparametric finite element, based upon a penalty function formulation. Full geometrical nonlinearities can be considered, including both large displacements and arbitrary rotations. *Materially nonlinear analysis is currently not available with the Type 5 shell element.* Both static and dynamic formulations of the element are included in the program.

Element geometry and local node numbering for the eight-node shell are shown in Figure 3.4.1. Note that the element has nodes at the upper and lower surfaces, not at the shell midsurface. Each node point is permitted three translational degrees of freedom, in the global coordinate directions (rotational degrees of freedom are not used). With this choice of nodal locations and degrees of freedom, the shell element is fully compatible on *all* exterior surfaces with other shells and with conventional solid isoparametric elements. Layered shells, sandwich constructions, transitions between shells and solids, or joined shells are thus easily modeled without special constraints (Figure 3.4.2). The shell element can be of variable thickness, and the lateral boundaries of the element need not lie along the normal to the shell midsurface.

The nonlinear capabilities of the Type 5 shell element include the analysis of arbitrarily large displacements and rotations. Full coupling between the bending and extensional strains is retained, and nonlinearities are included in the stretching strains as well. Details of the theoretical formulation of the shell element can be found in Reference 1.

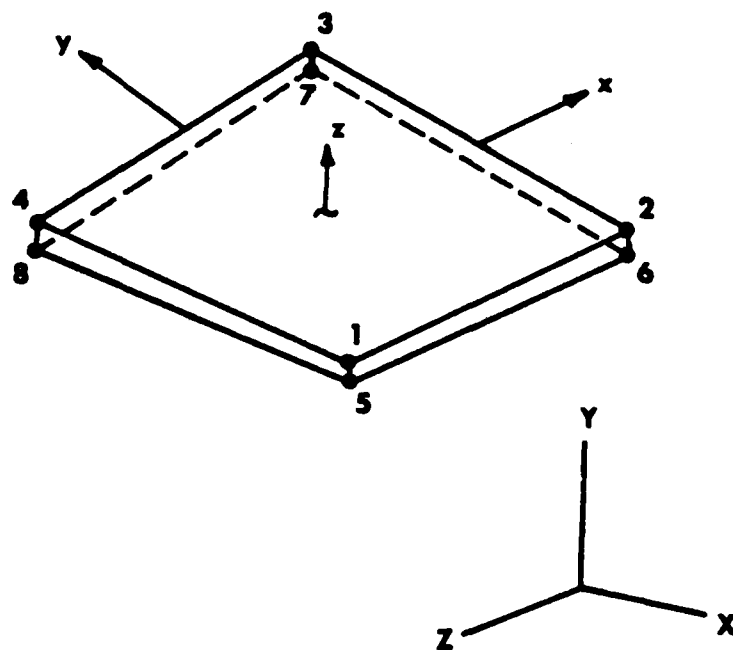
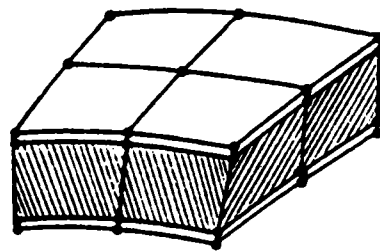
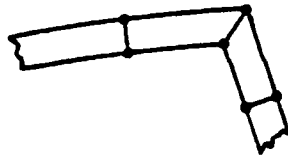


Figure 3.4.1 Three-Dimensional, Eight-Node Thin Shell Element.

GEOMETRIC MODELLING CAPABILITIES



LAYERED/SANDWICH STRUCTURES

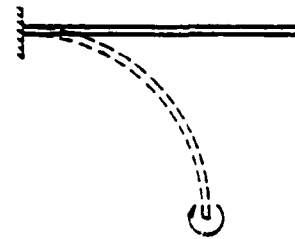


GENERAL SHELL JOINTS/BOUNDARIES

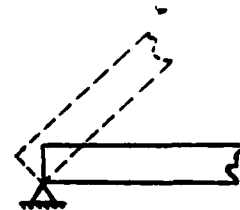


FULL COMPATIBILITY WITH SOLIDS

RESPONSE MODELLING CAPABILITIES



LARGE DISPLACEMENT, ROTATION



NONSTANDARD SHELL EDGE CONDITIONS



FULL COUPLING BETWEEN STRETCHING
AND BENDING STRAINS

Figure 3.4.2 Modeling Capabilities of the Thin Shell Finite Element.

Element Type 11 is a specialized element intended for use in analyzing multilayered, moderately thin shell structures. Like the Type 5 element, Element Type 11 contains full nonlinearities and may be joined to isoparametric solid elements without the use of special constraints. However, the Type 11 shell element may be composed of multiple layers of different materials, each of which may have variable thickness within an element.

The element geometry and local node numbering for the sixteen-node layered shell (Type 11) are shown in Figure 3.4.3. This element is identical in appearance to Element Type 8 (16-node solid/thick shell), and uses the same quadratic displacement approximation. Each node possesses three translational degrees of freedom in the global coordinate directions. The element may have a variable total thickness (defined by the nodal positions), and lateral boundaries of the element need not be normal to the shell midsurface.

The composition of the Type 11 shell element through its thickness is defined by *laminate cross-section* definitions, each one referring to a different combination of layer materials and relative thicknesses. Materials may be of two types, initially-isotropic, elastic-plastic material, with bilinear stress-strain curve, or orthotropic, elastic material. These may be combined arbitrarily within the shell cross-section. Individual layers of the cross-section may be classified as *variable-thickness layers* or as *constant-thickness layers*. This type of classification is useful in modeling layered constructions such as the one shown in Figure 3.4.4. Constant-thickness layers are defined by specifying the material and the actual thickness of the layer; variable thickness layers are defined by specifying the material and a *thickness fraction* f_T . At any point within an element, the thickness of a variable-thickness layer is simply

$$t_{\text{layer}} = f_T \left[t_{\text{total}} - \sum_i t_{(\text{constant thickness})}^{(i)} \right]$$

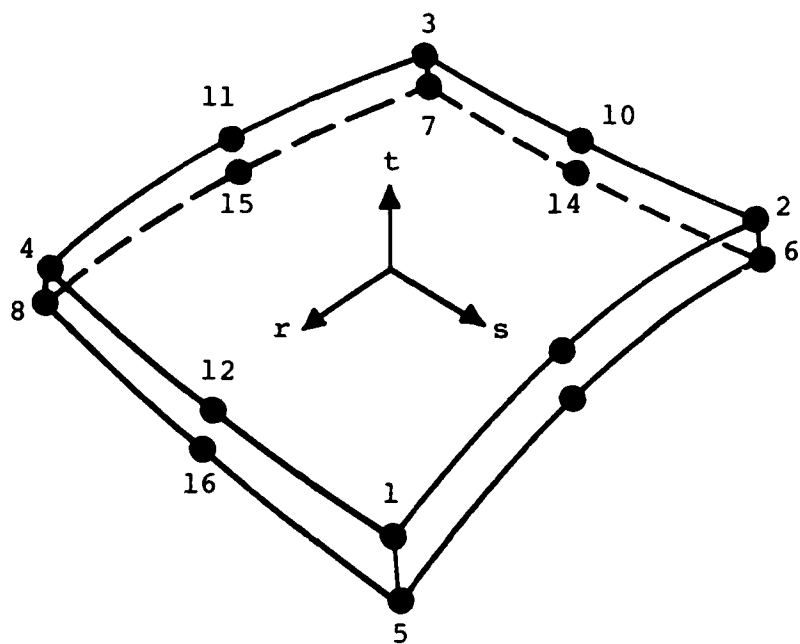


Figure 3.4.3. Nodal Connectivity for Sixteen-Node Layered Shell Element.

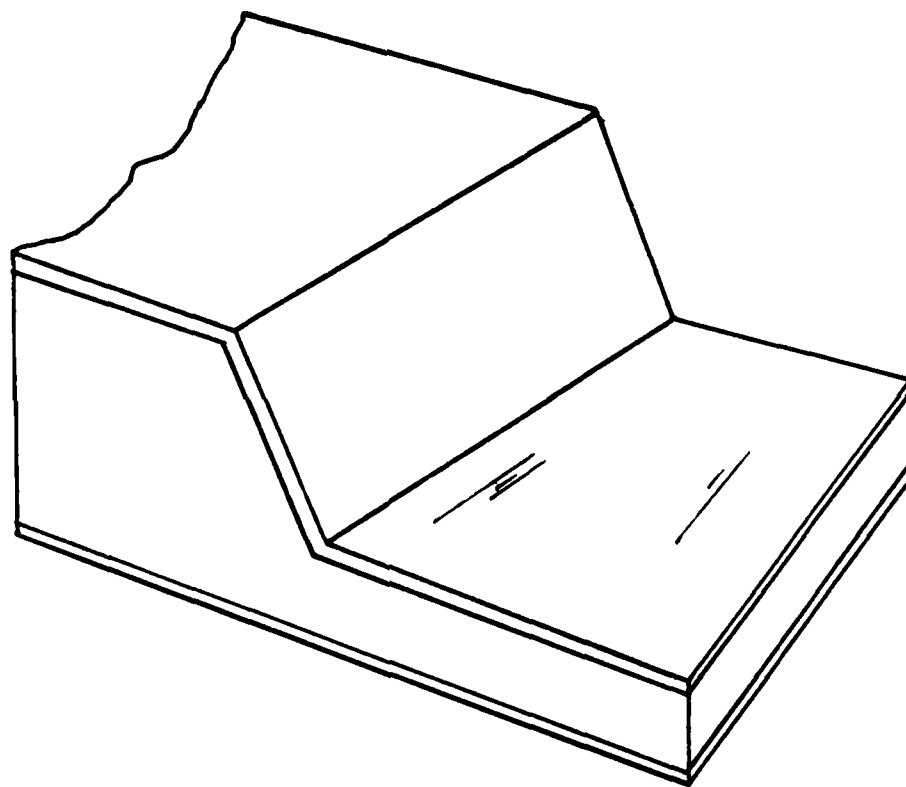


Figure 3.4.4. Layered Construction Using a Combination of Constant- and Variable-Thickness Layers.

At least one layer of each laminate cross-section must have variable thickness, to avoid ambiguous geometry for the element. The total number of layers in any Type 11 shell element may be between two and eleven.

Either 2x2 or 3x3 Gaussian integration may be used in the Type 11 shell element; the 2x2 integration rule is advisable in most situations for good element performance. The thickness integration for Element Type 11 is performed analytically, using two integration points per layer. Note that in materially nonlinear situations, resolution of yielded zones through the element thickness may be increased by simply defining more layers in the element cross-section.

3.5 THREE-DIMENSIONAL BEAM ELEMENTS

The three-dimensional beam element (Element Type 12) in MAGNA is a curved, quadratic-displacement element which may be used in static or dynamic analysis. Nonlinear effects included in the beam element formulation include large displacements, large rotations, and plasticity, the only restriction being that of small strains.

Element geometry and node numbering for the Type 12 beam element are shown in Figure 3.5.1. Nodes 1-3 define the reference axis of the element, and each possess six degrees of freedom: three nodal translations and three rotations, all referred to global coordinate directions. Node 3 (the mid-length node) may be omitted if desired; however, element performance will be improved substantially in most problems if all three of these nodes are retained. Node 4 is an auxiliary node, which may be used optionally for the definition of local coordinate directions within the beam cross-section.

The cross-section of a beam element is defined using from one to four rectangular "segments." Each segment is defined by its dimensions in the two local coordinate directions, and by the offset distances from the reference axis of the element. Examples of cross-section definitions are shown in Figure 3.5.2.

An important consideration is the use of beam elements as stiffening members on shell or solid finite elements. The Type 12 beam element is based upon the *independent approximation of displacements and rotations*, so that compatibility of displacements between the beam and other elements is easily accomplished by correct specification of the beam offset parameters (Figure 3.5.3). When stiffener torsion is important, linear constraints can be used to relate the axial rotation of the beam to the appropriate displacements in neighboring elements.

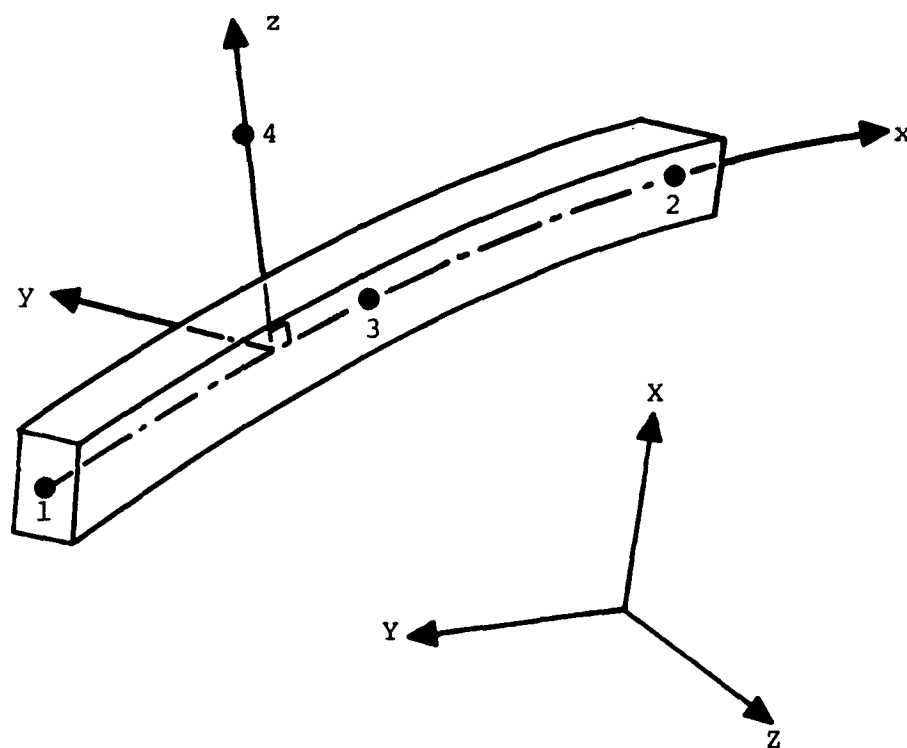
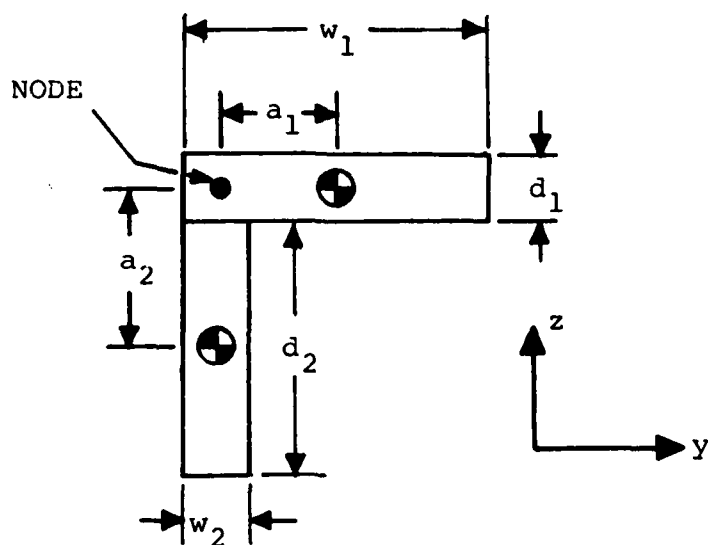


Figure 3.5.1. Element Geometry and Node Numbering for Quadratic Beam Element.



| | <u>Segment 1</u> | <u>Segment 2</u> |
|-------------|------------------|------------------|
| Y-dimension | w_1 | w_2 |
| Z-dimension | d_1 | d_2 |
| Y-offset | a_1 | 0 |
| Z-offset | 0 | a_2 |

Figure 3.5.2. Example of Beam Cross-Section Definition.

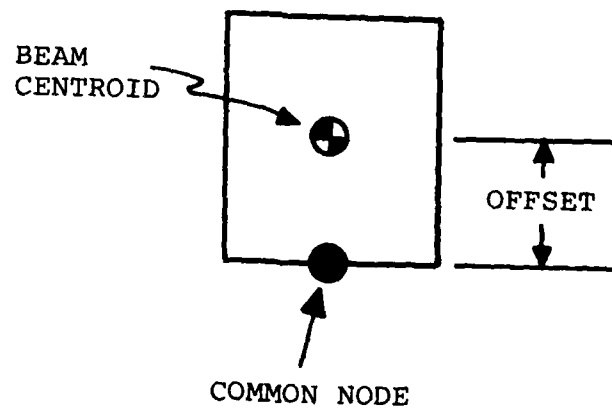
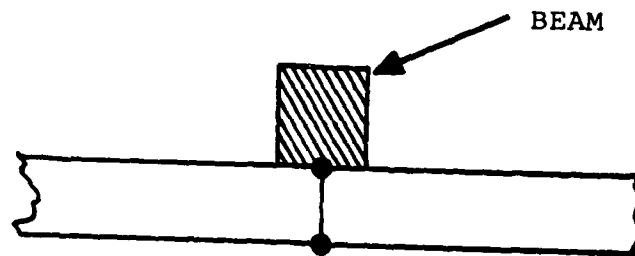


Figure 3.5.3. Use of Offsets in Stiffening Elements.

Integration of the beam element is always performed using a three-point Gaussian quadrature along the element length. In linear analysis, integration over the beam cross-section is performed analytically. For nonlinear problems, cross-section integration is performed by separate, three-point Newton-Cotes integrations (Simpson's rule) over each of the segments comprising the beam cross-section.

CHAPTER 4

NUMERICAL SOLUTION OPTIONS

Analysis procedures which are currently available in the MAGNA computer program include linear and nonlinear, static and transient dynamic solutions, natural frequency/normal mode analysis, and steady-state forced vibration analysis. The nonlinear analysis options include all effects due to geometric and material nonlinearities, as well as error control measures to prevent drifting during the incremental solution. Specially-programmed linear versions of each element type are provided to eliminate unneeded calculations wherever possible; in this way, no penalty is paid in computation time when performing linear analysis with a program which is primarily designed for nonlinear analysis.

In this chapter, specialization of the discrete governing equations of Section 2.2 to each of the possible analysis options is discussed, and the numerical algorithms used in the solutions are presented. Special features available for use with a particular solution option are noted where appropriate.

4.1 LINEAR STATIC ANALYSIS

In a linear static analysis, all loadings are assumed to be carefully applied, so that inertial effects may be neglected. Further, the resulting displacements are taken to be small enough that nonlinearities in the strain displacement equations are negligibly small. Material nonlinearities are not considered.

With these assumptions, the discrete equations governing response of the finite element model are

$$\underline{\underline{K}}_E \underline{X} = \underline{F} + \underline{T} + \underline{\theta} , \quad (4.1.1)$$

in which

$\underline{\underline{K}}_E$ = linear stiffness matrix

\underline{X} = nodal displacement vector

\underline{F} = body force vector

\underline{T} = external loads vector

$\underline{\theta}$ = thermal force vector.

A solution is obtained by the following steps:

$$\text{Decomposition: } \underline{\underline{K}}_E = \underline{\underline{L}} \underline{\underline{D}} \underline{\underline{L}}^T \quad (4.1.2)$$

$$\text{Forward Substitution: } \underline{\underline{L}} \underline{Z} = \underline{F} + \underline{T} + \underline{\theta} \quad (4.1.3)$$

$$\text{Scaling: } \underline{\underline{D}} \underline{Y} = \underline{Z} \quad (4.1.4)$$

$$\text{Back Substitution: } \underline{\underline{L}} \underline{X} = \underline{Y} . \quad (4.1.5)$$

Nodal loads are specified directly in the program by input of a load case number, node, component (direction), and load magnitude. The number of static load cases which can be solved in a single analysis is limited only by the available storage. Nonzero, imposed values of displacements can also be analyzed as a separate loading case.

4.2 LINEAR DYNAMIC ANALYSIS

In the linear dynamic analysis, inertial effects are included, but displacements and strains are assumed to be sufficiently small that neither geometric nor material nonlinearities are significant. It should be noted that, although the structural response is assumed to be linear, certain types of nonlinearities can be considered in such an analysis; an example is the presence of external loads which depend upon velocity or displacement (follower forces, etc.).

The semidiscrete equations of motion for a linear, dynamic problem are

$$\underline{\underline{K}}_E \underline{X} + \underline{\underline{M}} \ddot{\underline{X}} = \underline{F}' + \underline{T} + \underline{\theta} \quad (4.2.1)$$

where

$\underline{\underline{K}}_E$ = linear stiffness matrix

$\underline{\underline{M}}$ = consistent mass matrix

\underline{X} = nodal displacement vector

\underline{F}' = body force vector

\underline{T} = traction vector

$\underline{\theta}$ = thermal force vector,

and $(\dot{})$ denotes the differentiation with respect to time. In the general case, the body force \underline{F}' may be considered to include dissipative forces due to damping, which are assumed to be of the form

$$\underline{F}' = \underline{F} + \underline{F}_D \quad (4.2.2)$$

$$\underline{F}_D = -(\beta \underline{\underline{K}}_E + \gamma \underline{\underline{M}}) \dot{\underline{X}} = -\underline{\underline{C}} \dot{\underline{X}} \quad , \quad (4.2.3)$$

where β, γ are arbitrary constants. Selection of β and γ typically depends upon known or estimated values of modal or structural damping for the particular structure to be analyzed. Substitution of Equation 4.2.3 into Equation 4.2.1 gives

$$\underline{\underline{K}}_E \underline{X} + \underline{\underline{C}} \dot{\underline{X}} + \underline{\underline{M}} \ddot{\underline{X}} = \underline{F} + \underline{T} + \underline{\theta} . \quad (4.2.4)$$

In a linear dynamic analysis, implicit integration of Equation 4.2.4 in time uses Newmark's generalized operator^{1,2}, which is based upon the following finite difference approximations in time:

$$\dot{\underline{X}}_2 = \dot{\underline{X}}_1 + \left[(1-\delta)\ddot{\underline{X}}_1 + \delta\ddot{\underline{X}}_2 \right] \Delta t \quad (4.2.5)$$

$$\underline{X}_2 = \underline{X}_1 + \dot{\underline{X}}_1 \Delta t + \left[\left(\frac{1}{2}-\alpha\right)\ddot{\underline{X}}_1 + \alpha\ddot{\underline{X}}_2 \right] (\Delta t)^2 . \quad (4.2.6)$$

Here subscripts 1, 2 denote the state; that is,

$$\underline{X}_i = \underline{X} (t_i) \quad (4.2.7)$$

$$t_{i+1} = t_i + \Delta t . \quad (4.2.8)$$

The parameters α, δ are free parameters which can be chosen in such a way as to obtain desirable numerical properties with the algorithm. In particular, it can be shown that the conditions

$$\delta > 1/2 \quad (4.2.9)$$

$$\alpha > (\delta + 1/2)^2/4 \quad (4.2.10)$$

are sufficient to ensure unconditional stability of the numerical integration for linear problems. The values

$\delta=1/2$ and $\alpha=1/4$ yield the so-called "constant average acceleration" operator, a commonly used form of the Newmark algorithm.

Combining Equations 4.2.4 through 4.2.6, the current velocity and acceleration are eliminated as unknowns in the integration; the result is

$$\begin{aligned} \left[\underline{\underline{K}}_E + \frac{1}{\alpha \Delta t^2} \underline{\underline{M}} + \frac{\delta}{\alpha \Delta t} \underline{\underline{C}} \right] \underline{X}_2 = \underline{F}_2 + \underline{T}_2 + \underline{\theta}_2 \\ + \underline{\underline{M}} \left[\frac{1}{\alpha \Delta t^2} \underline{X}_1 + \frac{1}{\alpha \Delta t} \dot{\underline{X}}_1 + \left(\frac{1}{2\alpha} - 1 \right) \ddot{\underline{X}}_1 \right] \\ + \underline{\underline{C}} \left[\frac{\delta}{\alpha \Delta t} \underline{X}_1 + \left(\frac{\delta}{\alpha} - 1 \right) \dot{\underline{X}}_1 + \frac{\Delta t}{2} \left(\frac{\delta}{\alpha} - 2 \right) \ddot{\underline{X}}_1 \right] \end{aligned} \quad (4.2.11)$$

A somewhat simpler form is obtained in terms of incremental displacement unknowns $\underline{X} = \underline{X}_2 - \underline{X}_1$. Assuming Equations 4.2.11 to be satisfied at time t_1 gives the incremental form

$$\begin{aligned} \left[\underline{\underline{K}}_E + \frac{1}{\alpha \Delta t^2} \underline{\underline{M}} + \frac{\delta}{\alpha \Delta t} \underline{\underline{C}} \right] \underline{X} = \underline{F}_{12} + \underline{T}_{12} + \underline{\theta}_{12} \\ + \underline{\underline{M}} \left[\frac{1}{\alpha \Delta t} \dot{\underline{X}}_1 + \frac{1}{2\alpha} \ddot{\underline{X}}_1 \right] \\ + \underline{\underline{C}} \left[\frac{\delta}{\alpha} \dot{\underline{X}}_1 + \frac{\Delta t}{2} \left(\frac{\delta}{\alpha} - 2 \right) \ddot{\underline{X}}_1 \right] \end{aligned} \quad (4.2.12)$$

where

$$\underline{F}_{12} = \underline{F}_2 - \underline{F}_1 \quad (4.2.13)$$

$$\underline{T}_{12} = \underline{T}_2 - \underline{T}_1 \quad (4.2.14)$$

$$\underline{\theta}_{12} = \underline{\theta}_2 - \underline{\theta}_1 \quad (4.2.15)$$

Equation 4.2.12 is written symbolically as

$$\underline{K}_e \underline{X} = \underline{P}_e . \quad (4.2.16)$$

The "effective stiffness" \underline{K}_e is constant over any part of the solution during which the time step Δt remains constant; the "effective loads" \underline{P}_e at a particular time depend not only upon the increment in external forces, but also upon the velocities and accelerations computed at the previous increment of time.

Solution of Equation 4.2.16 is obtained using the Gauss-Doolittle decomposition

$$\underline{K}_e = \underline{L} \underline{D} \underline{L}^T , \quad (4.2.17)$$

followed by the forward- and back-substitutions

$$\underline{L} \underline{Z} = \underline{P}_e \quad (4.2.18)$$

$$\underline{D} \underline{Y} = \underline{Z} \quad (4.2.19)$$

$$\underline{L} \underline{X} = \underline{Y} \quad (4.2.20)$$

to obtain the current displacement increment \underline{X} . It is important to note that, when $\Delta t = \text{constant}$, \underline{K}_e is the same for any increment; the process of matrix decomposition (Equation 4.2.17) therefore must be performed only once to obtain the factors \underline{L} and \underline{D} . The solution procedure of a typical increment of time then consists only of

- calculation of effective loads \underline{P}_e
- forward/back substitution for \underline{X}
- updating the solution $\underline{X}_{i+1} = \underline{X}_i + \underline{X}$.

Calculations for element stresses and strains are performed only at the particular increments in which output is required, since this part of the solution is not necessary to advance integration in time.

4.3 NONLINEAR STATIC ANALYSIS (EQUILIBRIUM ITERATION)

The discrete governing equations for a nonlinear structure with inertial effects neglected are, from Section 2.2,

$$(\underline{K}_T + \underline{K}_G)\underline{X} = \underline{F} + \underline{T} + \underline{\theta} - \underline{I} , \quad (4.3.1)$$

in which

\underline{K}_T = tangent stiffness matrix

\underline{K}_G = geometric stiffness

\underline{X} = nodal displacement increments

\underline{F} = body force vector

\underline{T} = surface traction vector

$\underline{\theta}$ = thermal loads vector

\underline{I} = vector of internal forces

In the application of Equation 4.3.1, all loadings are assumed to be gradually applied; the resulting displacements and strains may be arbitrarily large, and material response may be nonlinear. If the response is geometrically nonlinear, \underline{K}_T , \underline{K}_G , and \underline{I} are functions of the solution \underline{X} by virtue of the nonlinear relationships existing between strains and displacements; in the case of material nonlinearity (stress a nonlinear function of strain), \underline{K}_T and \underline{I} are dependent upon the displacement increments \underline{X} .

In view of the nonlinear nature of Equation 4.3.1, the numerical solution must either permit the use of iteration to any desired accuracy, or provide a means of correction for errors due to linearization. In practice, nonlinearities are accounted for in the solution by four different methods: equilibrium correction, "constant stiffness" equilibrium iteration, full Newton-Raphson iterations, and a combined strategy using Newton iterations followed by constant stiffness iterations.

The contents of \underline{I} , as defined in Sections 2.1 and 2.2, provide a step-by-step correction to the solution of Equation 4.3.1 in an incremental form; that is, within the increment from state C_i to state C_{i+1} , imbalances in virtual work observed in the state C_i are automatically corrected in an approximate way. This procedure, called "equilibrium correction," tends to prevent the incremental solution from drifting from the true solution, provided the displacement steps are sufficiently small. Equilibrium correction is an intrinsic part of the numerical solution, and is applied automatically whether or not equilibrium iterations are used. The use of such a correction leads to substantial improvement over direct step-by-step integration.

Equilibrium iteration by the constant stiffness method involves repeated application of Equation 4.3.1 at a single increment of loading. However, the expensive operations of element stiffness computation and matrix decomposition are not repeated at each iteration. At a particular loading level, the tangent stiffness matrices are formed, and an initial solution is performed. Using the initial tangent stiffness, iterations are then performed, consisting of the following steps:

- (a) compute out-of-balance forces, $(\underline{F} + \underline{T} + \underline{\theta} - \underline{I})$
- (b) test for convergence or divergence, and exit the cycle if either occurs
- (c) using the original tangent stiffness, solve for a new estimate of the displacements \underline{X}
- (d) compute element strains and stresses
- (e) return to step (a).

Note that errors incurred in this procedure due to use of the initial tangent stiffness at all iterations are compensated by the continual updating of the vector \underline{I} , which accounts for imbalance in internal and external forces. That is, as the internal forces in the element assemblage approach true equilibrium with the applied forces,

$$(\underline{F} + \underline{T} + \underline{\theta} - \underline{I}) \rightarrow \underline{0}$$

(4.3.2)

regardless of the coefficient matrix used. The constant stiffness form of iteration corresponds exactly to the modified Newton iteration for solution of nonlinear systems¹.

Full Newton-Raphson iterations at a given loading level proceed in the same manner as the constant stiffness iteration described above; however, the coefficient matrix ($\underline{K}_T + \underline{K}_G$) is continually updated using the latest estimates of the true solution. The advantage of the full Newton iteration is faster convergence at the expense of increased computational effort per iteration. Computation of new element stiffness, as well as reassembly and complete resolution, are required at every iteration.

The nonlinear static analysis performed in MAGNA permits a variety of types of solutions to be carried out:

- (a) solution with equilibrium corrections only, without iteration (one-step Newton method),
- (b) solution with constant stiffness (modified Newton) iterations, using the tangent stiffness from the beginning of the step,
- (c) solution with continuously-updated stiffness during iteration (Newton-Raphson iteration), and
- (d) solution with a combined iteration strategy, in which the tangent stiffness is updated in the first two iterations of a step, and then held constant.

Convergence of an iterative solution is determined in terms of the unbalanced forces and the differences in successive estimates of the nodal displacement vector, with user-defined tolerances placed upon both of these quantities. It is also possible to direct the program to use the same stiffness matrix for several loading increments in succession; with this option, a mildly nonlinear problem may be solved with stiffness matrices

being recomputed and resolved only a few times during the analysis. Alternatively, a "pseudo-force" solution can be performed using the original linear stiffness for the entire analysis, with nonlinearities accounted for by equilibrium corrections and iterations exclusively.

With the higher-order solid elements in MAGNA (types 1, 6, 7 and 8), still further flexibility is possible in a nonlinear analysis. Each element independently is assigned a stiffness formulation parameter, causing it to be treated as a constant stiffness element, a tangent stiffness element, or an "averaged stiffness" element. With the averaged stiffness formulation, nonlinear effects are averaged over the element before forming the stiffness matrix, thus saving considerable computing time. Unbalanced forces are *always* computed exactly, however, to ensure correct results with iteration. If only a few elements of the finite element model experience significant nonlinearity, these can be analyzed with the tangent stiffness approach while the remainder employ either constant or averaged stiffness matrices.

The finite element solution of Equation 4.3.1 is applicable to geometrical nonlinearities, in the form of large displacements, large rotations and finite strains. Material nonlinearities, in the form of elastic-plastic, strain-hardening material behavior, are analyzed by a subincremental method to follow the material stress-strain curve as closely as possible. Each increment of loading is divided into several (up to 500) strain subincrements, whose size is user controlled. Elastic-plastic constitutive matrices, strain-hardening slopes, and states of stress are updated at each subincrement in an attempt to minimize the accumulated error. The number of subincrements is controlled by the size of the total strain increment at a point, so that points experiencing the most rapidly increasing strains are automatically treated in the greatest detail. The states of strain and stress within an element are permanently updated only after all iterations are converged, to prevent artificial

oscillations (e.g., unloading and reyielding) from occurring during equilibrium iterations.

External loads are specified for nonlinear analysis in the form of piecewise linear data curves, which define the magnitude of a force versus an arbitrary independent variable. Several such curves may be input to describe non-proportional loading systems. Both concentrated nodal forces and distributed surface pressure loads may be specified in this fashion. Pressure loads may be "dead loads," which act in a constant direction, or "live loads," which act in the direction normal to deformed element surfaces. Applied forces can alternatively be defined in user-written subroutines which are accessed at each increment of the nonlinear solution. This option is useful in defining deformation-dependent loads (or velocity-dependent loads in dynamic analysis) which cannot be estimated prior to performing the nonlinear analysis. The use of user-written routines for the specification of loading in nonlinear problems is described in Section 9.3.

4.4 NONLINEAR DYNAMIC ANALYSIS (IMPLICIT INTEGRATION)

In a nonlinear dynamic analysis, the response is governed by the semidiscrete equations of motion

$$(\underline{K}_T + \underline{K}_G)\underline{X} + \underline{M} \ddot{\underline{X}} = \underline{F}' + \underline{T} + \underline{\theta} - \underline{I} , \quad (4.4.1)$$

in which

\underline{K}_T = tangent stiffness matrix

\underline{K}_G = geometric stiffness

\underline{M} = consistent mass matrix

\underline{X} = nodal displacement increments

\underline{F}' = body force vector

\underline{T} = surface traction vector

$\underline{\theta}$ = thermal loads vector

\underline{I} = vector of internal forces

and an overdot denotes the temporal derivative. Equation 4.4.1 is appropriate for large displacement and large strain response; material behavior may be nonlinear as well. As in the linear dynamic analysis (Section 4.2), the body force \underline{F}' is considered to include dissipative forces of the general form

$$\underline{F}' = \underline{F} + \underline{F}_D , \quad (4.4.2)$$

$$\underline{F}_D = - \left[\beta (\underline{K}_T + \underline{K}_G) + \gamma \underline{M} \right] \dot{\underline{X}} = -\underline{C} \dot{\underline{X}} , \quad (4.4.3)$$

where β and γ are arbitrarily selected constants. With these definitions, Equation 4.4.1 can be rewritten as

$$(\underline{K}_T + \underline{K}_G)\underline{X} + \underline{C}\dot{\underline{X}} + \underline{M}\ddot{\underline{X}} = \underline{F} + \underline{T} + \underline{\theta} - \underline{I} . \quad (4.4.4)$$

Implicit integration of Equation 4.4.4 with respect to time is performed using Newmark's generalized operator (see

Section 4.2). For a nonlinear analysis, general conditions of numerical stability of the integration operator cannot be proved; choice of time increments for the dynamic solution will, however, generally be made on the basis of accuracy (rather than stability) considerations.

Use of the finite difference formulas

$$\dot{\underline{X}} = \left[(1 - \delta) \ddot{\underline{X}}_1 + \delta \ddot{\underline{X}}_2 \right] \Delta t \quad (4.4.5)$$

$$\underline{X} = \dot{\underline{X}}_1 \Delta t + \left[\left(\frac{1}{2} - \alpha \right) \ddot{\underline{X}}_1 + \alpha \ddot{\underline{X}}_2 \right] (\Delta t)^2 \quad (4.4.6)$$

in Equation 4.4.4 yields the discrete system

$$\underline{\underline{K}}_e \underline{X} = \underline{P}_e, \quad (4.4.7)$$

in which the "effective" stiffness and loads are

$$\underline{\underline{K}}_e = \left[1 + \frac{\delta \beta}{\alpha \Delta t} \right] (\underline{\underline{K}}_T + \underline{\underline{K}}_G) + \frac{1 + \gamma \delta \Delta t}{\alpha \Delta t^2} \underline{M} \quad (4.4.8)$$

and

$$\begin{aligned} \underline{P}_e = & \underline{F} + \underline{T} + \underline{\theta} - \underline{I} \\ & + (\underline{\underline{K}}_T + \underline{\underline{K}}_G) \left[\frac{\beta}{\alpha} \dot{\underline{X}}_1 + \beta \Delta t \left(\frac{\delta}{2\alpha} - 1 \right) \ddot{\underline{X}}_1 \right] \\ & + \underline{M} \left[\frac{1 + \gamma \delta \Delta t}{\alpha \Delta t} \dot{\underline{X}}_1 + \frac{1 - \delta \gamma \Delta t - 2\alpha \gamma \Delta t}{2\alpha} \ddot{\underline{X}}_1 \right]. \end{aligned} \quad (4.4.9)$$

The incremental solution of Equation 4.4.7 is performed in the same manner as a nonlinear static analysis (Section 4.3), since the dependence of $\underline{\underline{K}}_e$ upon both geometric and material nonlinearities dictates that the effective stiffness matrix be reformulated and solved at frequent intervals in the solution. Full, modified or combined Newton-Raphson iterations can be

performed at a fixed value of time in the nonlinear dynamic analysis, with convergence measured in terms of tolerances upon both the unbalanced residual forces and the displacement corrections at any iteration. A more complete description of the equilibrium iteration options is given in Section 4.3.

Nonlinear dynamic solutions obtained with the program are valid for large displacements and large strains. Nonlinear material response under dynamic loading is analyzed by a subincremental strategy (see Sections 2.3 and 4.3), which automatically treats regions of rapidly increasing strains in the greatest detail.

Incremental loads which are known a priori in the dynamic analysis are specified in load versus time curves, and may include suddenly-applied forces, live or dead distributed loads, and nonproportional or cyclic loading. User-written subroutine interfaces are also supplied to permit the calculation of concentrated loads whose magnitude and direction are functions of the displacements or velocities.

4.5 NATURAL FREQUENCY AND NORMAL MODE ANALYSIS

For the natural frequency analysis in MAGNA, linear behavior (small displacements and linear elastic material response) is assumed, and external forces are not considered. For harmonic motions, then, the nodal displacement vector is

$$\underline{X} = \underline{U} \sin \omega t \quad (4.5.1)$$

and the equation of motion becomes

$$\underline{K}_E \underline{U} = \omega^2 \underline{M} \underline{U} = \underline{0} . \quad (4.5.2)$$

Here

\underline{K}_E = linear stiffness matrix

\underline{M} = consistent mass matrix

\underline{U} = vector of relative nodal displacements

ω = circular frequency of vibration.

Optionally, nonlinear effects such as membrane stiffening can be considered in the equation of motion, in which case \underline{K}_E is replaced by $(\underline{K}_E + \underline{K}_G)$, \underline{K}_G being the geometric stiffness matrix. Equation 4.5.2 is an eigenvalue problem of standard form, in which both ω and \underline{U} are unknowns. If the order of \underline{K}_E and \underline{M} is n , there are n solutions $\omega_i, U_k; i=1,2,\dots,n$.

Generally, the order of the finite element system is large, which only a relative few of the natural frequencies (ω) and normal mode shapes (\underline{U}) are of interest. Therefore, the free vibration solution is based upon a vector iteration method which permits a specified number of the lowest (or highest) frequencies to be solved, along with their corresponding mode shapes. The particular method employed is the simultaneous iteration algorithm of Jennings¹ and Rutishauser²; further details and a sample implementation of the method can be found in Reference 3.

Beginning with Equation 4.5.2, a Choleski factorization of \underline{K}_E is carried out,

$$\underline{K}_E = \underline{L} \underline{L}^T , \quad (4.5.3)$$

giving

$$\underline{\underline{L}} \underline{\underline{L}}^T \underline{U} = \omega^2 \underline{\underline{M}} \underline{U} . \quad (4.5.4)$$

Defining

$$\underline{P} = \underline{\underline{L}}^T \underline{U} , \quad (4.5.5)$$

and premultiplying Equation (4.5.4) by the inverse of $\underline{\underline{L}}$ yields

$$(\underline{\underline{L}}^{-1} \underline{\underline{M}} \underline{\underline{L}}^{-T}) \underline{P} = \frac{1}{\omega^2} \underline{P} \quad (4.5.6)$$

or

$$\underline{\underline{A}} \underline{P} = \frac{1}{\omega^2} \underline{P} . \quad (4.5.7)$$

Equation 4.5.7 is the form of the eigenvalue problem on which the simultaneous iteration is based, although matrix $\underline{\underline{A}}$ is never computed explicitly. Instead, multiplication of a vector by $\underline{\underline{A}}$ (the major computational step in the iteration) is accomplished by backsubstitution using $\underline{\underline{L}}^T$, multiplication by $\underline{\underline{M}}$, and then forward substitution using $\underline{\underline{L}}$. Thus, sparsity of both $\underline{\underline{L}}$ and $\underline{\underline{M}}$ can be used to advantage both to reduce storage requirements and to eliminate unnecessary operations.

The actual iteration is carried out using m trial vectors, where $m \ll n$. If r represents the number of frequencies and mode shapes to be extracted, m is usually slightly larger than r ;

$$m = \min (2r, r + 5) \quad (4.5.8)$$

has been found to provide a suitable balance between rate of convergence and storage requirements. The matrix whose columns consist of the trial vectors, \underline{P}_i ; $i=1,2,\dots,m$ is denoted by $\underline{\Phi}$,

$$\underline{\Phi} = [\underline{P}_1, \underline{P}_2, \dots, \underline{P}_m] . \quad (4.5.9)$$

The first step in the iteration is an interaction analysis, in which the $m \times m$ interaction matrix

$$\underline{B} = \underline{\Phi}^T \underline{A} \underline{\Phi} \quad (4.5.10)$$

is formed. If the columns of $\underline{\Phi}$ are indeed eigenvectors, \underline{B} should be a diagonal matrix. If the trial vectors are suitably normalized, the diagonal entries of \underline{B} are estimates of the eigenvalues,

$$b_{ii} \approx \omega_i^2 \quad (\text{no sum}) \quad (4.5.11)$$

Since \underline{B} is in general not diagonal, an approximate solution for the eigenvectors of \underline{B} is next used to uncouple the trial vectors. Define the $m \times m$ matrix \underline{T} by

$$t_{ij} = \begin{cases} -1 & i=j \\ -2b_{ij} & \\ r_{ij} + \text{sign}(r_{ij}) \sqrt{r_{ij}^2 + 16b_{ij}^2} & i \neq j \end{cases} \quad (4.5.12)$$

in which

$$r_{ij} = b_{ii} - b_{jj} \quad (\text{no sum}) \quad (4.5.13)$$

A set of decoupled trial vectors \underline{W} is then constructed from

$$\underline{W} = \underline{A} \underline{\Phi} \underline{T} , \quad (4.5.14)$$

in which

$$\underline{W} = [\underline{w}_1, \underline{w}_2, \dots, \underline{w}_m] . \quad (4.5.15)$$

Finally, Schmidt orthogonalization is used to obtain a new set of trial vectors,

$$\underline{p}_i = \underline{w}_i - \sum_{j=1}^{i-1} \alpha_{ji} \underline{w}_j, \quad (4.5.16)$$

in which

$$\alpha_{ji} = \underline{w}_j^T \underline{w}_i. \quad (4.5.17)$$

The above sequence of calculations is repeated until the norm of the change in the first r eigenvectors is less than a specified tolerance. Generally the convergence of the eigenvalues (frequencies) is much quicker than that of the eigenvectors, and the entire procedure typically converges in very few iterations. Since only a single factorization of \underline{K}_E is performed, the simultaneous iteration solution is quite economical, and its effectiveness relative to other solution techniques tends to increase with the size of the problem under consideration.

Generalized mass and stiffness information is also generated by MAGNA upon completion of the natural frequency solution. The generalized mass associated with vibration mode "k" is defined by

$$M_k = \underline{U}_k^T \underline{M} \underline{U}_k \quad (4.5.18)$$

Where the mode shapes \underline{U} are orthonormalized, such that

$$\underline{U}_i^T \underline{U}_j = \delta_{ij} \quad (4.5.19)$$

the corresponding generalized stiffness is

$$K_k = \underline{U}_k^T \underline{K} \underline{U}_k = \omega_k^2 M_k \quad (4.5.20)$$

4.6 STEADY-STATE HARMONIC ANALYSIS

The steady-state, harmonic response solution is a specialized case of linear dynamic analysis (Section 4.2). When the external forces are sinusoidal functions of time with given frequency ω , the linear solution for the system displacements is sinusoidal at the same frequency, provided sufficient time has elapsed for transient motions (due to initial conditions) to have "died out."

If the amplitude of the nodal forces is \underline{P} , the applied loading is

$$\underline{F}(t) = \text{Re}[\underline{P} e^{i\omega t}] \quad (4.6.1)$$

The corresponding steady-state displacements are of the form

$$\underline{X}(t) = \underline{U} e^{i\omega t} \quad (4.6.2)$$

in which \underline{U} is the vector of nodal displacement amplitudes. If the motion is undamped, \underline{U} is real-valued since the response is exactly in phase with the harmonic forcing function. When dissipative effects are present \underline{U} may be complex-valued, reflecting the phase differences between input (forces) and output (displacements).

In the steady-state solution, material structural damping may be included by means of the "complex modulus" description. That is, the modulus of any material may be expressed as

$$E^* = E(1 + i\eta) \quad (4.6.3)$$

in which E is the elastic modulus and η is the material loss factor. Loss factors may be different for each material in the model.

The stiffness matrix used for steady-state vibration analysis is, in general, complex-valued,

$$\underline{K} = \underline{K}_R + i\underline{K}_I \quad (4.6.4)$$

The complete equation of motion for the unknown displacement amplitudes is then

$$(\underline{K}_R + i\underline{K}_I - \omega^2 \underline{M}) \underline{U} = \underline{P} \quad (4.6.5)$$

which is a set of simultaneous equations with complex-valued coefficients.

Solution of Equation 4.6.5 is accomplished in much the same way as for linear static analysis (Section 4.1), except that the equation-solving process involves complex variables. Note also that a separate solution is required for each forcing frequency (ω) to be considered; many such solutions may be performed within a single analysis run, to provide amplitude-versus-frequency data for each of the nodal displacements in the model.

Many commonly-used materials exhibit elastic and damping properties which vary strongly with frequency and/or temperature. The user-supplied subroutine UDAMP (Section 9.10), which is required for the specification of material damping properties in the steady-state solution, can also be used to define these properties as arbitrary functions of forcing frequency and temperature. When frequency dependent properties are used, the damping matrix \underline{K}_I is reformulated at each new forcing frequency based upon the material properties specified in UDAMP.

CHAPTER 5

SPECIAL PROGRAM FEATURES

The MAGNA finite element program contains several special analysis features designed to improve analysis flexibility and ease of use for a wide variety of problems. These features include capabilities for incremental generation of analysis data, creation of data files for postprocessing functions, analysis restart options, and provisions for intervention by user-written subroutines at appropriate stages of an analysis. Additional program features which are not described elsewhere in the manual are also introduced in this chapter.

5.1 CURVILINEAR COORDINATES

In many applications, it is convenient to define all or part of a finite element model in terms of coordinates other than the global Cartesian system. Geometry data for the program may be entered in any desired coordinate system(s), and transformed internally to the global axis system. Coordinate transformations for circular cylindrical and spherical systems are available in the code, and additional transformations can be defined in a user subroutine CTYPE (see Section 9.2). The built-in coordinate systems (cylindrical and spherical) are shown in Figures 5.1.1 and 5.1.2.

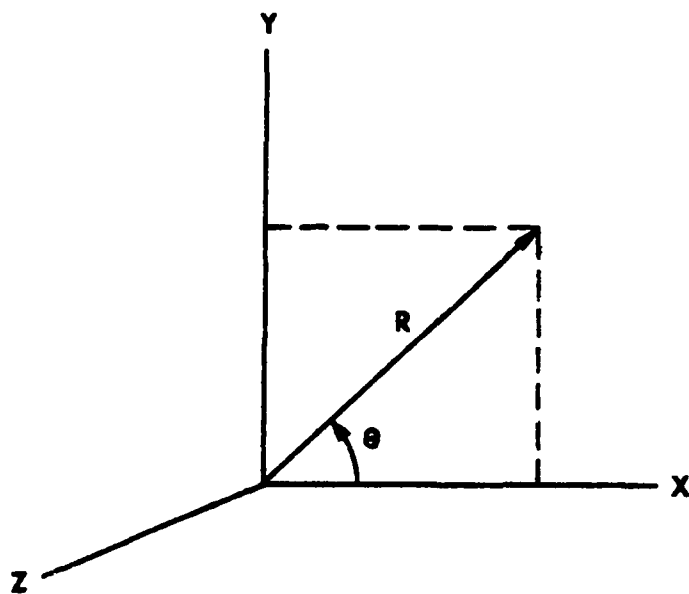


Figure 5.1.1 Cylindrical Coordinate System Definition.

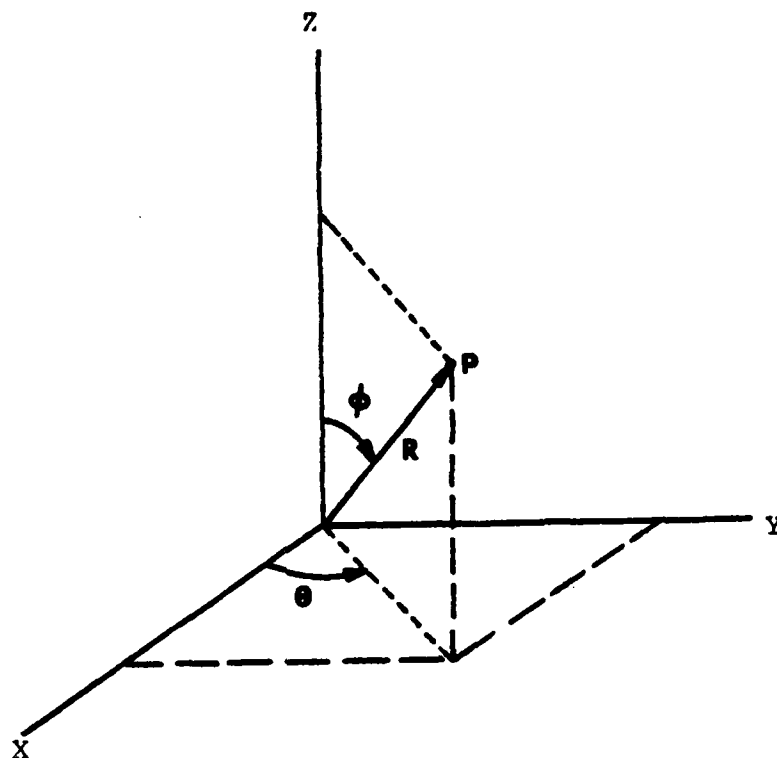


Figure 5.1.2 Spherical Coordinate System Definition.

5.2 COORDINATE DATA GENERATION

The MAGNA program contains utilities for incremental coordinate generation which are useful in describing geometrically regular portions of the finite element nodal mesh. Given two node positions, the program will generate equally spaced nodal points with specified numbering increment on a straight line between the given points, as shown in Figure 5.2.1. Nodes 23 and 35 in the figure are defined explicitly, and the increment specified for generation is INCR=3; node points 26, 29, and 32 are then defined automatically within the program. The node numbering increment must be positive, and generation of node points is performed in the global Cartesian coordinate system.

Coordinate data generation can also be performed in a user-written subroutine MESHG, described in Section 9.1. Such a routine can be created to automatically generate all nodal data, or to read coordinate input in non-standard card formats.

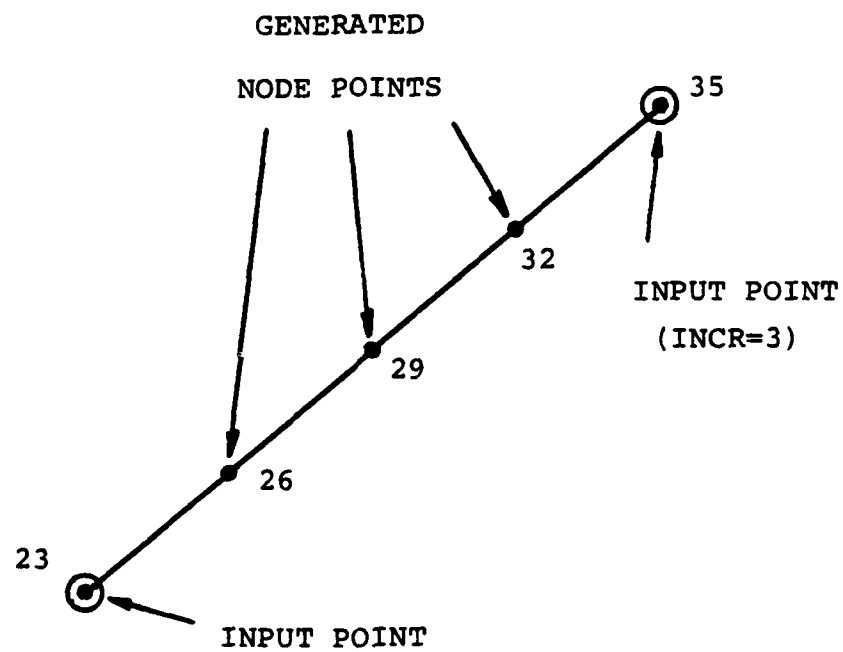


Figure 5.2.1 Incremental Node Point Coordinate Generation.

5.3 ELEMENT GENERATION

Element connectivity data, which describes the connection of individual elements to nodal points of the finite element model, can be generated incrementally within the program in many cases. Sequences of elements whose connectivities are different by a constant are defined simply by inputting the first element of the sequence, the ending element number, and a node generation parameter (KGEN). This utility is available for all element types; for the variable-node elements, in which some connected nodes may be absent (i.e., zero), generation is performed only on nonzero node numbers, so that all elements in a generator sequence have an identical number of nodes. Finite elements generated in a given sequence are assigned the same material properties, but need not have similar geometries. The node generation parameter KGEN, which specifies the difference in connected node numbers between successive elements, must be a positive integer value.

5.4 INCREMENTAL LOADS

Nonlinear and dynamic solutions are performed in MAGNA by considering a number of successive increments of time or loading. In dynamic analysis, external loads applied to a finite element model are defined directly in terms of time. For nonlinear static analysis, where inertial effects are neglected, loadings are also defined as functions of time; however, in the static case, "time" is simply used as a loading parameter (i.e., independent variable) which increases continually throughout the solution.

Applied forces whose magnitude is known in advance are specified by defining loading curves which describe the forces as functions of time (or loading parameter). External forces defined in this manner may include nodal forces in a given direction, or distributed surface pressures. In the case of pressure loading, surface pressures can be specified to act in the direction normal to the element in its initial state ("dead" load), or to act along the current (deformed) surface of an element ("live" load, e.g., fluid pressure). Concentrated nodal follower forces, and concentrated or pressure loads whose magnitude depends upon the structural response, can be defined in the user-written subroutines ULOAD and USRLOD (see Section 9.3) which are called during each time or load increment of the solution.

5.5 NONLINEAR MATERIAL STRESS-STRAIN DATA

The analysis of elastic-plastic, strain hardening materials in MAGNA is performed using a "subincremental" method, which allows the stress state at integrating points in the finite element model to follow the material stress-strain curve as closely as possible (see Section 2.3). Determination of the work hardening behavior of the material uses known, uniaxial stress-strain data, from which the instantaneous hardening slopes (i.e., tangent moduli) are found. These uniaxial data are supplied to the program in the form of piecewise linear data curves which define stress as a function of plastic strain in the Lagrangian description.

Typically, material stress-strain data are obtained in the form of total stress versus total strain, where the stresses and strains recorded are either "true" or "engineering" values. Reduction of the data to the form required by the program therefore consists of two steps:

(1) Conversion of total stress/strain values to the appropriate measures for a Lagrangian description (namely, Piola-Kirchhoff stresses and Green-St. Venant strains), and

(2) Reduction of the data to give total stress in terms of *plastic* strains.

For raw data given in terms of engineering values σ_E, ϵ_E ,

$$\sigma_E = \frac{\text{applied force}}{\text{original area}} = \frac{P}{A_0} \quad (5.5.1)$$

$$\epsilon_E = \frac{\text{elongation}}{\text{original length}} = \frac{u}{L_0} \quad (5.5.2)$$

The Lagrangian measures of stress and strain (σ_L, ϵ_L) can be obtained from

$$\sigma_L = \frac{\sigma_E}{(1+\epsilon_E)} \quad (5.5.3)$$

$$\epsilon_L = \epsilon_E \left(1 + \frac{1}{2}\epsilon_E\right) . \quad (5.5.4)$$

True stress and true strain values σ_T, ϵ_T are defined by

$$\sigma_T = \frac{\text{applied force}}{\text{current area}} = \frac{P}{A} \quad (5.5.5)$$

and

$$\epsilon_T = \ln \left[\frac{\text{current length}}{\text{original length}} \right] = \int_{L_0}^L \frac{dL}{L} , \quad (5.5.6)$$

and can be converted to the Lagrangian values (σ_L, ϵ_L) using

$$\sigma_L = \frac{\sigma_T}{\exp(\epsilon_T)} \frac{A}{A_0} \quad (5.5.7)$$

$$\epsilon_L = \frac{1}{2} [\exp(2\epsilon_T) - 1] . \quad (5.5.8)$$

The ratio of current to original areas in Equation 5.5.7 is normally not available as part of the data for a material, but can be estimated from the following:

$$\frac{A_0}{A} = \frac{1 + \epsilon_E}{1 + (1-2\nu)\epsilon_E} \quad (\text{Elastic Range}) \quad (5.5.9)$$

$$\frac{A_0}{A} = \frac{1 + \epsilon_E}{1 + (1-2\nu)\epsilon_E^Y} \quad (\text{Plastic Range}) \quad (5.5.10)$$

in which ϵ_E is the engineering strain

$$\epsilon_E = \exp(\epsilon_T) - 1, \quad (5.5.11)$$

ϵ_E^Y denotes the engineering strain at first yielding, and ν is the Poisson's ratio of the material. Equations 5.5.9 and 5.5.10 are valid provided

- (1) the elastic strains at first yield are small
(much less than unity)
- (2) the material is incompressible during *plastic* deformation
- (3) necking instability of the specimen has not occurred.

The final step in preparing the stress-strain data is the reduction to the form of stress versus plastic strain. The required plastic strains are obtained from

$$\epsilon_L^P = \epsilon_L - \frac{\sigma_L}{E}. \quad (5.5.12)$$

As an example, consider a material whose engineering stress-strain behavior is defined by the table of values below:

| ϵ_E | σ_E |
|--------------|------------|
| 0. | 0. |
| 0.0030 | 30000. |
| 0.0045 | 35000. |
| 0.0060 | 37500. |
| 0.0090 | 40000. |
| 0.0150 | 41000. |
| 0.1000 | 45000. |

From Equations 5.5.3 and 5.5.4, the Lagrangian measures of stress and strain are found to be

| ϵ_L | σ_L |
|--------------|------------|
| 0. | 0. |
| 0.003005 | 29910.3 |
| 0.004510 | 34843.2 |
| 0.006018 | 37276.3 |
| 0.009041 | 39643.2 |
| 0.015113 | 40394.1 |
| 0.105000 | 40909.1 |

Next, Equation 5.5.12 is used to obtain stress as a function of the plastic strain

| ϵ_L^P | σ_L |
|----------------|------------|
| 0. | 29910.3 |
| 0.001026 | 34843.2 |
| 0.002290 | 37276.3 |
| 0.005077 | 39643.2 |
| 0.011074 | 40394.1 |
| 0.100909 | 40909.1 |

The original (engineering) data and the stress-versus-plastic strain input data are shown in Figure 5.5.1.

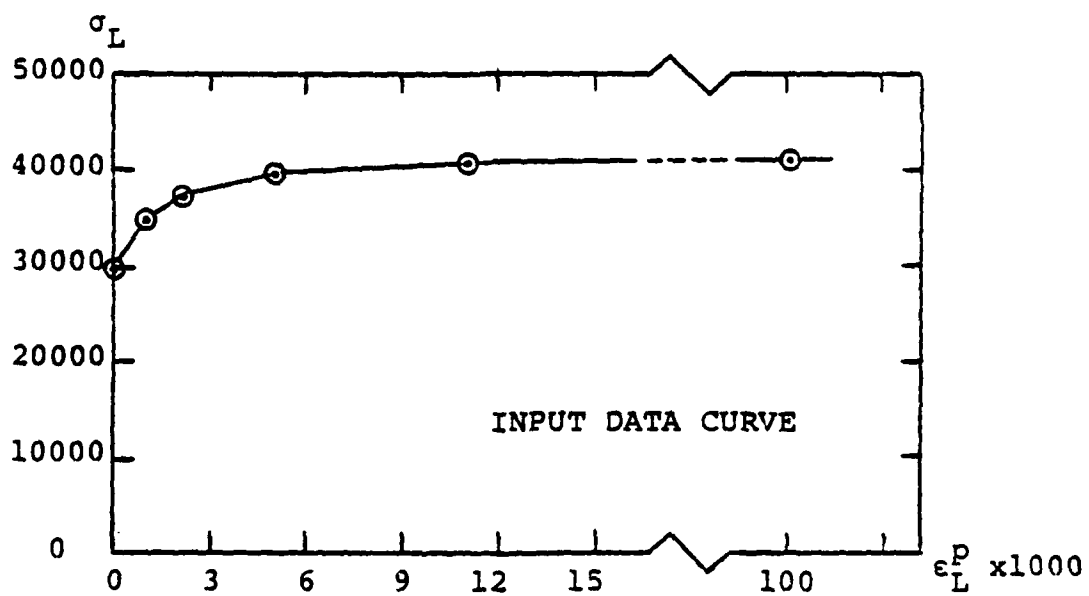
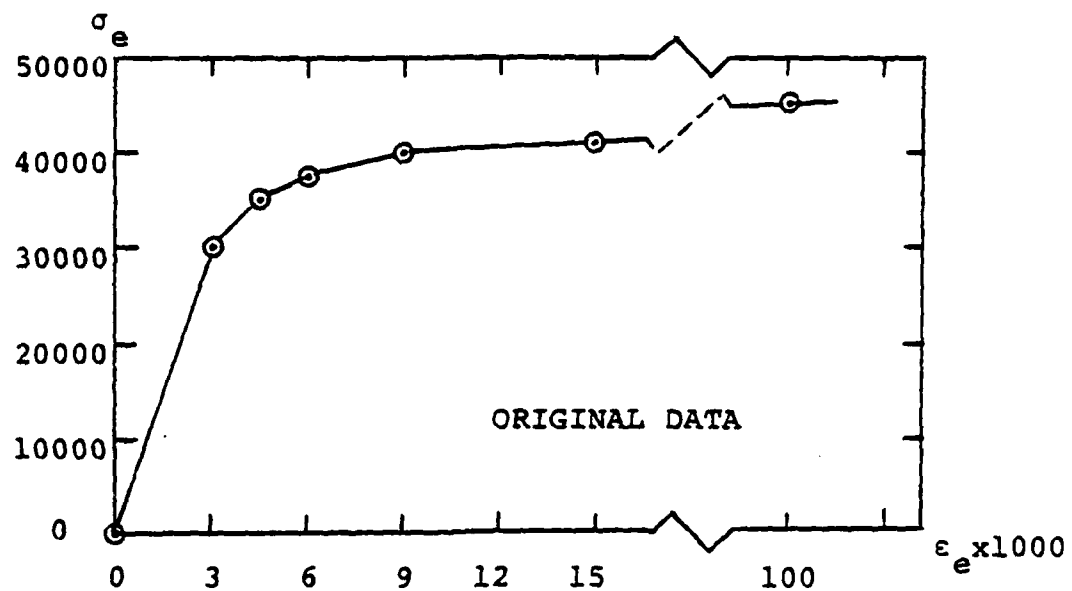


Figure 5.5.1 Reduction of Material Stress-Strain Data.

5.6 LINEAR MULTIVARIABLE CONSTRAINTS

Linear constraints are a special type of boundary condition which may be used in MAGNA to represent fixed relationships between a number of degrees of freedom of a finite element model. Examples include nodal constraints (due to fixity or symmetry) in skewed coordinate directions, and rigid links between nodes of a model.

A single linear constraint equation has the form

$$\sum_{i=1}^n C_i U_{(n_i)}^{(d_i)} = 0 \quad (5.6.1)$$

in which n is the number of individual terms in the constraint. Each term is defined by a coefficient (C_i), a node number (n_i) and a direction (d_i); the node number and direction together define a single unique degree-of-freedom of the model. A simple example is shown in Figure 5.6.1, in which a node is constrained to move along an inclined surface in the (X,Y) plane. If θ is the angle between the surface and the X-axis, displacements perpendicular to it may be suppressed using the linear constraint

$$(-\sin\theta)u + (\cos\theta)v = 0. \quad (5.6.2)$$

Here $n = 2$, and

$$\begin{aligned} C_1 &= -\sin\theta & C_2 &= \cos\theta \\ d_1 &= 1 & d_2 &= 2 \\ n_1 &= (\text{node number}) & n_2 &= (\text{node number}) \end{aligned}$$

Equations of linear constraint are introduced into the global equations of the finite element model using a penalty function technique. Expressing a single constraint in the form

$$\tilde{C}^T \tilde{X} = 0, \quad (5.6.3)$$

the penalty function is constructed by squaring the constraint and assigning an associated penalty factor α ,

$$\frac{\alpha}{2} \tilde{X}^T \tilde{C} \tilde{C}^T \tilde{X} = 0 \quad (5.6.4)$$

The left-hand side of Equation 5.6.4 may be interpreted as a "strain energy penalty" associated with the violation of the original constraint. When Equation 5.6.4 is added to the strain energy of the finite element model, this error may be forced to arbitrarily small values as the penalty factor (α) takes on a very large value. In practice, the magnitude of α is based upon the magnitude of existing coefficients in the stiffness matrix, so that constraints are enforced properly while the system of equations remains well-conditioned.

In non-linear and dynamic analysis, repeated solution of the system may lead to accumulated errors in the satisfaction of the linear constraint equations. To avoid this potential source of error, each linear constraint is evaluated at each iteration or time step in the solution to obtain the error

$$\tilde{C}^T \tilde{X}^{(i)} = \epsilon \quad (5.6.5)$$

During the next time step (or iteration), a corrected constraint is applied, requiring

$$\tilde{C}^T \tilde{X}^{(i+1)} = \tilde{C}^T \Delta \tilde{X} + \epsilon = 0 \quad (5.6.6)$$

The error in satisfying the linear constraints is, therefore, limited to very small values by the displacement convergence tolerance normally used within MAGNA.

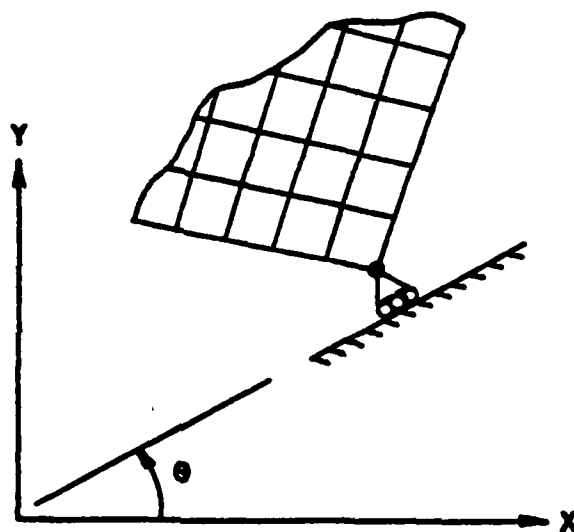


Figure 5.6.1 Enforcement of Displacement Constraint on a Skewed Boundary.

5.7 POSTPROCESSING INTERFACE

Interpretation of the results of a finite element solution can be greatly facilitated by the use of postprocessing programs which provide tabular and/or graphical display of the computed response. In addition to printed output, MAGNA optionally produces a summary of analysis results which is suitable for use as input to special-purpose postprocessing programs. The analysis summary is output from the program in the form of a formatted file on disc or magnetic tape, with the local (temporary) file name MPOST. The MAGNA geometry plotter (GPLOT, see Chapter 11) accepts the MPOST file as input for the preparation of deformed mesh plots in an interactive mode. Contents of the MPOST file include the following:

1. Nodal coordinate (input and generated values)
2. Element connectivities (input and generated)
3. Nodal displacements for each solution increment
4. Element strains, stresses, and equivalent stress levels at integration points for each increment.

Logical blocks of data are separated by formatted header records; the contents of the data headers are indicated in Table 5.7.1. A description of individual data records, in their approximate order of appearance on the file*, is given in Table 5.7.2. The maximum record length on file MPOST is 130 characters, so that the file can be copied to a high-speed printer to provide a concise printed summary of the analysis if required.

An additional postprocessing file is produced by the stress extrapolation and smoothing program STRAVG (Section 10.11), which is normally executed as part of a MAGNA batch analysis run. STRAVG, which generates smoothed nodal stress values

*The exact ordering of the postprocessor file data is dependent upon the type of analysis being performed.

TABLE 5.7.1
HEADER RECORDS FOR POSTPROCESSOR FILE MPOST

| Item | | Data Type | Format |
|------|--|-----------|--------|
| COOR | Keyword for Nodal Coordinates Data | A | A4,11X |
| I1 | Number of Node Points | I | I5 |
| CONN | Keyword for Element Connectivity Data | A | A4,1X |
| I1 | Element Type | I | I5 |
| I2 | Maximum Number of Nodes per Element | I | I5 |
| I3 | Number of Elements of this Type | I | I5 |
| ENDD | Keyword for End of Data | A | A4 |
| DISP | Keyword for Nodal Displacement Data | A | A4,1X |
| I1 | Increment or Load Case Number | I | I5 |
| I2 | Number of Nodes | I | I5 |
| R1 | Time (or Load Parameter) Value | R | E15.8 |
| ELSS | Keyword for Element Stress/Strain Data | A | A4,1X |
| I1 | Number of Element Types Used | I | I5 |
| I1 | Increment or Load Case Number | I | I5 |
| R1 | Time (or Load Parameter) Value | R | E15.8 |
| ETYP | Element Type Header for Stress/Strain Data | A | A4,1X |
| I1 | Element Type | I | I5 |
| I2 | Element Dimensionality | I | I5 |
| I3 | Interpolation Type Code | I | I5 |
| I4 | Number of Elements of this Type | I | I5 |
| ELEM | Element Header for Stress/Strain Data | A | A4,1X |
| I1 | Element Number | I | I5 |
| I2 | Maximum Number of Nodes per Element | I | I5 |
| I3 | Number of Numerical Integration Points | I | I5 |
| ENDP | End-of-Problem Trailer | A | A4 |

TABLE 5.7.2
DATA RECORDS FOR POSTPROCESSOR FILE MPOST

| DATA TYPE | DATA DESCRIPTION | FORMAT |
|----------------------------------|--|-----------------|
| COOR Header | (1) | A4,11X,I5 |
| Coordinates | 1. Node Number 2. Coordinates X,Y,Z (one record per node point) | I5,5X,3E10.3 |
| CONN Header (2) | (1) | A4,1X,3I5 |
| Connectivity (2) | 1. Element Number 2. Connected Nodes (one record per element) | 28I4 |
| ENDD Trailer | (1) | A4 |
| DISP Header (3) | (1) | A4,1X,2I5,E15.8 |
| Displacements (3) | 1. Node Number 2. Displacement Components (one record per node point) | I5,5X,3E10.3 |
| ELSS Header (3) | (1) | A4,1X,2I5,E15.8 |
| ETYP Header (4) | (1) | A4,1X,4I5 |
| ELEM Header (5) | (1) | A4,1X,3I5 |
| Element Strain and Stress (6) | 1. Strain Components (6) 2. Stress Components (6) 3. Equivalent Stress | 13E10.3 |
| ENDP Trailer | (1) | A4 |

Notes:

- (1) See Table 5.7.1 for header and trailer record descriptions
- (2) Repeated for each element type used
- (3) Repeated for each solution time step or loading case
- (4) Repeated for each element type at each time step or loading case
- (5) Repeated for each element at each time step or loading case
- (6) Repeated for each integration point at each time step or loading case; for Element Type 11 (layered shell), integration point values are output for each layer of an element.

(and individual layer stresses for Element Type 11) as printed output, also creates an "averaged-stress" postprocessor file (APOST) which is used as input to contour plotters and other special purpose data presentation programs. The contour/relief plotter CPLOT (Chapter 11) developed for use with MAGNA accepts the APOST file as input to generate a variety of stress, strain, and displacement plots under interactive control.

The header information and data contained on the APOST postprocessing file is summarized in Table 5.7.3. This data is always arranged in the exact order shown in the Table. It should be noted that the individual increments (or loading conditions, or mode numbers) appearing on the APOST file are the same as those contained in the MPOST file.

Normally, no input is required for execution of STRAVG. However, input can be supplied to control the amount of printed output, and/or the increment numbers to be processed. When input is supplied to STRAVG, the first input line contains a printing specification

or PRINT=YES (normal printed output)
 PRINT=NO (minimal printed output)

beginning in column 1, with no embedded blanks. Additional input lines should contain numbers or ranges of increments to be processed by STRAVG; increment ranges are distinguished by a negative sign on the second number of a pair. The increment number data are read in 16I5 format, on as many lines as necessary, with blank fields being ignored.

The following example of STRAVG input requests minimal printing, with increments 5, 7, and 10 through 14 to be processed:

```
PRINT=NO
^^^^5^^^^7
^^^10^^-14
```

Requested increments which do not appear on the input MPOST file are simply ignored. For example, if the MPOST file contained increments 6 through 12, the above input stream would cause increments 7, 10, 11, and 12 to be processed and written to the APOST postprocessing file.

TABLE 5.7.3

MAGNA POSTPROCESSOR FILE 'APOST' - GENERAL DESCRIPTION AND FORMAT

| <u>Record</u> | <u>Columns</u> | <u>Format</u> | <u>Description</u> |
|---------------|---|--|--|
| 1 | 1-80 | 20A4 | Problem Title (Line 1 of 3) |
| 2 | 1-80 | 20A4 | Problem Title (Line 2 of 3) |
| 3 | 1-80 | 20A4 | Problem Title (Line 3 of 3) |
| 4 | 1-4 5 6-10 | A4 1X 15 | 'INCS' - Increment List Header (Blank) Number of Solution Increments, Modes or Loading Conditions to appear on file |
| 5 | 1-100 | 20I5 | List of Increments in ascending order. (Additional records are used as needed) |
| 6 | 1-10 | 10I1 | Flags for Element Types Appearing in the Model. |
| 7 | 1-4 5 6-20 21-35 36-50 51-65 66-80 81-95 | A4 1X E15.8 E15.8 E15.8 E15.8 E15.8 E15.8 | 'LIMC' - Coordinate Limits Header (Blank) X - Maximum Value Y - Maximum Value Z - Maximum Value X - Minimum Value Y - Minimum Value Z - Minimum Value |

```

<<<<< Records 8-17 (described on the next page) each >>>>>
<<<<< include data computed at each increment of the >>>>>
<<<<< finite element solution. Each of these records >>>>>
<<<<< is repeated (in the same order) for each solu- >>>>>
<<<<< tion increment, mode shape or loading case >>>>>
<<<<< listed in Record 5. >>>>>

```

TABLE 5.7.3 (continued)

| <u>Record</u> | <u>Columns</u> | <u>Format</u> | <u>Description</u> |
|---------------|----------------|---------------|--|
| 8 | 1-4 | A4 | 'INCT' - Increment Header. |
| | 5 | 1X | (Blank) |
| | 6-10 | I5 | Increment Number |
| | 11-15 | I5 | Total Number of Elements |
| | 16-30 | E15.8 | Time Value at this Increment |
| 9 | 1-4 | A4 | 'LIMC' - Displacement Limits Header |
| | 5 | 1X | (Blank) |
| | 6-20 | E15.8 | X - Maximum Displacement |
| | 21-35 | E15.8 | Y - Maximum Displacement |
| | 36-50 | E15.8 | Z - Maximum Displacement |
| | 51-65 | E15.8 | X - Minimum Displacement |
| | 66-80 | E15.8 | Y - Minimum Displacement |
| | 81-05 | E15.8 | Z - Minimum Displacement |
| 10 | 1-4 | A4 | 'ELMT' - Element Header |
| | 5 | 1X | (Blank) |
| | 6-10 | I5 | Part Number (A 'part' is any distinct combination of element type and material property code; elements appearing in the file are sorted by parts). |
| | 11-15 | I5 | Global Element Sequence Number (numbers are secondary sort key) |
| | 16-20 | I5 | Element Type (as defined in MAGNA) |
| | 21-25 | I5 | Element Sequence Number (within type) |
| | 26-30 | I5 | Material Property Code |
| | 31-35 | I5 | Maximum Number of Nodes |
| | 36-40 | I5 | Length of Coordinate Records (3*Nodes) |
| | 41-45 | I5 | Number of Layers (Element Type 11 only) |
| 11 | 1-108 | 27I4 | List of Connected Nodes (up to 27) |
| 12 | 1-120 | 10E12.5 | (Xcoor(i),i=1,maxnodes), (Ycoor(i),i=1,maxnodes), (Zcoor(i),i=1,maxnodes). Nodal coordinates are written up to 10 entries per line, over as many lines as needed (up to 9, for 27-node elements). |
| 13 | 1-120 | 10E12.5 | (Xdisp(i),i=1,maxnodes), (Ydisp(i),i=1,maxnodes), (Zdisp(i),i=1,maxnodes). |

TABLE 5.7.3 (concluded)

| <u>Record</u> | <u>Columns</u> | <u>Format</u> | <u>Description</u> |
|---|----------------|---------------|--|
| 14 | 1-10 | E10.3 | XX - Strain at Local Node #1 |
| | 11-20 | E10.3 | YY - Strain at Local Node #1 |
| | 21-30 | E10.3 | ZZ - Strain at Local Node #1 |
| | 31-40 | E10.3 | YZ - Strain at Local Node #1 |
| | 41-50 | E10.3 | XZ - Strain at Local Node #1 |
| | 51-60 | E10.3 | XY - Strain at Local Node #1 |
| | 61-70 | E10.3 | XX - Stress at Local Node #1 |
| | 71-80 | E10.3 | YY - Stress at Local Node #1 |
| | 81-90 | E10.3 | ZZ - Stress at Local Node #1 |
| | 91-100 | E10.3 | YZ - Stress at Local Node #1 |
| | 101-110 | E10.3 | XZ - Stress at Local Node #1 |
| | 111-120 | E10.3 | XY - Stress at Local Node #1 |
| | 121-130 | E10.3 | Von Mises Stress for Node #1 |
| <<<< Record 14 is repeated for each node point >>>> | | | |
| <<<< connected to the element. Omitted points >>>> | | | |
| <<<< in variable-node elements assigned zeros. >>>> | | | |
| <<<< For the layered shell element (Type 11), >>>> | | | |
| <<<< a complete set of nodal values is output >>>> | | | |
| <<<< for each layer of the element. >>>> | | | |
| 15 | 1-4 | A4 | 'LIMS' - Stress/Strain Limits Header |
| 16 | 1-10 | E10.3 | Maximum XX - Strain for this Increment |
| | 11-20 | E10.3 | Maximum YY - Strain for this Increment |
| | 21-30 | E10.3 | Maximum ZZ - Strain for this Increment |
| | 31-40 | E10.3 | Maximum YZ - Strain for this Increment |
| | 41-50 | E10.3 | Maximum XZ - Strain for this Increment |
| | 51-60 | E10.3 | Maximum XY - Strain for this Increment |
| | 61-70 | E10.3 | Maximum XX - Stress for this Increment |
| | 71-80 | E10.3 | Maximum YY - Stress for this Increment |
| | 81-90 | E10.3 | Maximum ZZ - Stress for this Increment |
| | 91-100 | E10.3 | Maximum YZ - Stress for this Increment |
| | 101-110 | E10.3 | Maximum XZ - Stress for this Increment |
| | 111-120 | E10.3 | Maximum XY - Stress for this Increment |
| | 121-130 | E10.3 | Maximum von Mises Stress for Increment |
| 17 | 1-10 | E10.3 | Minimum XX - Strain for this Increment |
| | 11-20 | E10.3 | Minimum YY - Strain for this Increment |
| | 21-30 | E10.3 | Minimum ZZ - Strain for this Increment |
| | 31-40 | E10.3 | Minimum YZ - Strain for this Increment |
| | 41-50 | E10.3 | Minimum XZ - Strain for this Increment |
| | 51-60 | E10.3 | Minimum XY - Strain for this Increment |
| | 61-70 | E10.3 | Minimum XX - Stress for this Increment |
| | 71-80 | E10.3 | Minimum YY - Stress for this Increment |
| | 81-90 | E10.3 | Minimum ZZ - Stress for this Increment |
| | 91-100 | E10.3 | Minimum YZ - Stress for this Increment |
| | 101-110 | E10.3 | Minimum XZ - Stress for this Increment |
| | 111-120 | E10.3 | Minimum XY - Stress for this Increment |
| | 121-130 | E10.3 | Minimum von Mises Stress for Increment |

5.8 ANALYSIS RESTART UTILITIES

In practical situations, very little may be known about the characteristics of the solution prior to performing an analysis. When a large nonlinear or dynamic analysis is to be performed, it is therefore desirable in many instances for the analyst to intervene at certain points within the solution to monitor progress and to make decisions concerning solution strategy, analysis options or modifications to the input data. In other cases, it may be convenient to perform the solution in several steps to safeguard against job failure or to improve turnaround time.

MAGNA provides utilities to permit the interruption and subsequent restarting of any nonlinear analysis, with the frequency of checkpointing and the point of restart controlled by the user. The same restart facilities may be used in linear, transient dynamic solutions. Input or output restart files, or both, may be used, depending upon whether a new analysis, an intermediate analysis, or a run to completion is being made. Job control procedures necessary for using the restart facilities are described in Chapter 7.

During a restart analysis, a number of options and data items may be changed from those specified in the original solution. Examples of data which may be redefined freely during a restart include:

- analysis type (static or transient),
- output options, including postprocessing files,
- time or load increments, integration parameters or system damping coefficients,
- iteration parameters,
- stiffness formulation options or recompute frequencies, and
- nodal/element loads and corresponding time functions.

During a restart job, a *complete* input deck (Chapter 8) is supplied to the program. It should be noted that nonlinear analyses may *only* be restarted as nonlinear, and linear dynamic analyses must be restarted as linear. In nonlinear analysis, however, the solution type (static, transient) may be changed when restarting. *The following data should not be modified in a restart analysis:*

- nodal coordinates,
- material properties and axis definitions,
- element connectivities (connected nodes),
- element integration order, and
- homogeneous boundary conditions.

Furthermore, those nonlinear elements using constant (linear) stiffness matrices (ISUP=1 for Element Types 1, 6, 7, and 8) should generally remain unchanged from the original analysis; all other stiffness computation options and frequencies of reformulation may, however, be modified as desired. If elements using the constant stiffness option (ISUP=1) are modified to use the averaged or tangent stiffness formulation (ISUP=-1 or 0), all such elements must be changed to one of the non-constant stiffness options. Such a change in stiffness formulation method is usual following non-convergence using the constant stiffness approach in nonlinear analysis.

Input data which defines the actual restart parameters is described in Section 8.3. Any analysis which creates a restart tape is identified by a four-character identification code, and each increment written to the tape is identified by the number of the increment. When a restart analysis is performed, both the identification code and the increment value are verified prior to the restart, to detect any inconsistency which might lead to erroneous results.

5.9 NATURAL FREQUENCY ANALYSIS WITH PRESTRESS EFFECTS

The tendency of gross structural response to change markedly in the presence of nonlinear effects is important in determining both static and dynamic behavior of a structure. In addition to the modification of static and transient response to loading, geometrical or material nonlinearities may bring about changes in the nature of small, superimposed motions (such as free vibration). A simple example is the increase in fundamental frequency which accompanies the "stiffening" effect in a beam experiencing large displacements.

MAGNA contains an option to compute the influence of nonlinearities upon superimposed free vibrations within the natural frequency branch of the problem. The solution is a two-step procedure. First a nonlinear analysis must be performed, to compute the equilibrium state corresponding to the prestressed position. Secondly, the stiffness coefficients in the prestressed state are included in a free vibration analysis, which solves for the superimposed small harmonic motions about this equilibrium position.

For purposes of plotting, the MPOST postprocessor file (Section 5.7) from the preliminary nonlinear solution may also be communicated to the natural frequency analysis. When this option is exercised, the final geometry in the prestressed state will be copied to the MPOST file for the frequency solution; after completion of the entire analysis, geometry plots can be generated showing the true mode shape(s), superimposed on the prestressed shape of the model.

The following points should be noted concerning the eigenvalue solution with prestress:

- the nonlinear portion of the analysis is best performed with equilibrium iterations;
- strain and stress information generated in the natural frequency solution is the superimposed strain and stress state due to small vibration, and is assumed to be elastic; and

- the plotting scheme described in the previous paragraph is optional, and may be omitted without affecting the solution.

CHAPTER 6

DEMONSTRATION PROBLEMS

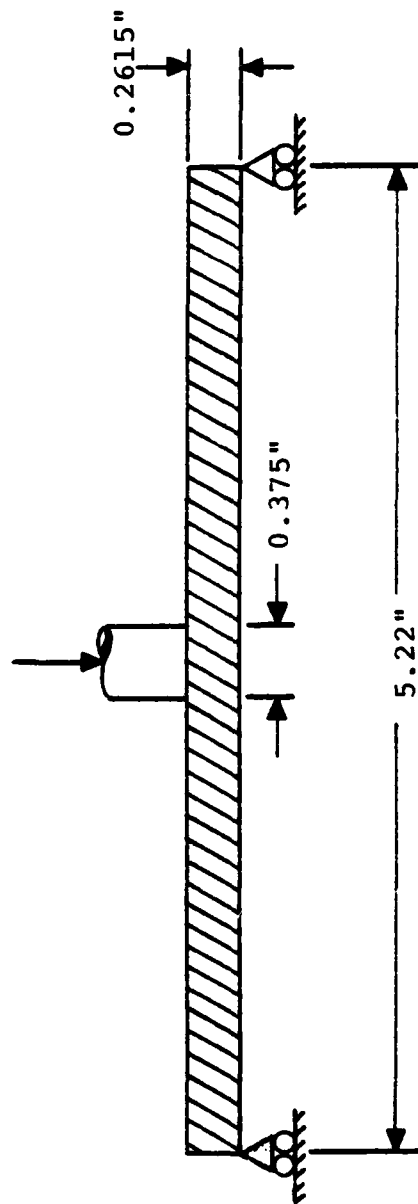
A number of sample analyses are presented in this chapter to demonstrate the linear and nonlinear solution capabilities of the MAGNA program. The problems described include both small structures having well-known or documented solutions, and larger models corresponding to practical applications of the program. In some cases, solutions to two-dimensional or axisymmetric problems are obtained using three-dimensional finite element models; this reflects the emphasis during the early program development stage on efficient three-dimensional analysis techniques, as well as the scarcity of well-documented benchmark problems for nonlinear response in three dimensions. The more practical applications described in this chapter (many of which are truly three-dimensional) demonstrate the capabilities of the MAGNA program for performing nonlinear analyses of structures of practical size and complexity.

6.1 ELASTIC-PLASTIC ANALYSIS OF A CIRCULAR PLATE

The circular plate shown in Figure 6.1.1 is subjected to a transverse load applied through a rigid punch. Dimensions of the specimen are given in the Figure. Experimental load-displacement curves for this plate have been presented by Winter and Levine (Reference 1, Plate 4A250), together with an axisymmetric shell solution obtained with the PLANS finite element code. Analytical results obtained using axisymmetric solid finite elements are reported by Hunsaker, Haisler and Stricklin².

Although this problem is axisymmetric, a MAGNA solution has been performed using solid twenty-node elements (Element Type 6) to demonstrate the three-dimensional large displacement plastic analysis capabilities of the program. The finite element model of one quarter of the plate, consisting of 14 solid elements, is shown in Figure 6.1.2. Two elements are used through the plate thickness, since the specimen is rather thick ($R/t = 9.98$) and considerable material nonlinearity can be expected to occur before large displacement effects become significant.

Two different sets of integration rules and stiffness options have been employed in performing nonlinear analysis of the plate. In the first model, which uses the tangent stiffness option in all elements, 3x3x3 Gaussian integration is used for the innermost six elements ($R \leq 0.995$) and 2x2x2 quadrature is specified elsewhere. The second model uses a tangent stiffness option and 14-point numerical integration for the six elements closest to the center of the plate, while 2x2x2 quadrature and an averaged stiffness option is used for the remaining eight elements. The averaged stiffness approach is appropriate due to the relatively simple strain and stress distributions which are expected near the supported edge. Model 1 is used without equilibrium iteration, while Model 2 is solved by combined Newton-Raphson iterations to maintain solution stability.



$$E = 10.05 \times 10^6 \text{ psi}$$

$$\nu = 0.325$$

$$\sigma_y = 10000. \text{ psi}$$

Figure 6.1.1.1 Circular Plate Loaded Through a Rigid Punch.

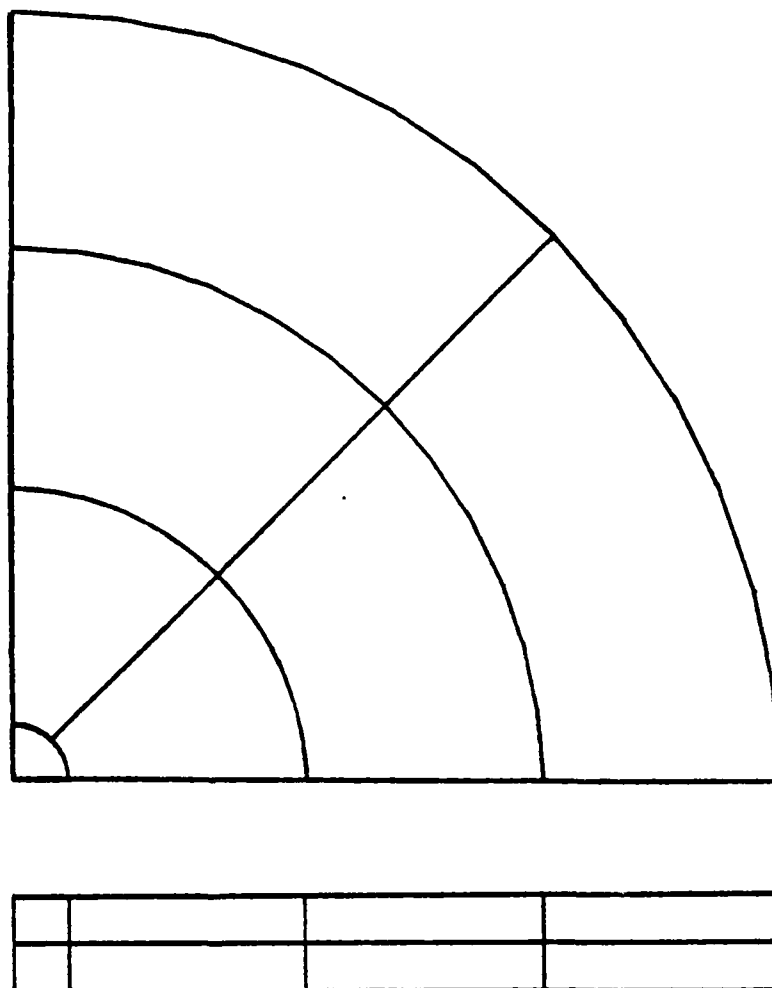


Figure 6.1.2 Finite Element Model of a Circular Plate.

The stress-strain curve of the material, a strain-hardening aluminum alloy, are defined by the engineering stress and strain values listed below.

| ϵ_E | σ_E |
|--------------|-----------------------|
| 0. | 0. |
| 0.009950 | 10000. (yield stress) |
| 0.013100 | 20000. |
| 0.045020 | 28000. |
| 0.118000 | 36000. |
| 0.363110 | 48000. |

The MAGNA solution for the central displacement of the plate versus the total applied load is compared with the experimental results in Figure 6.1.3. Forty equal increments of 100 pounds each have been used in the solution. The particular solution pictured, which is obtained from Model 1, uses a kinematic strain-hardening description: in fact, the type of strain-hardening rule selected is rather unimportant for the present solution². Solution accuracy is quite good for the entire range of loading, during which the Green's strains attain maximum values in excess of 30 percent.

Displacement solutions at the center of the plate corresponding to Models 1 and 2 are compared in Figure 6.1.4. Model 2 predicts slightly larger displacements throughout the loading history, but the agreement between the two results is reasonably good. It should be noted that the most significant reason for the differences in computed displacements between the two models is the use of equilibrium iteration in Model 2, rather than in the use of different integration schemes and stiffness options.

Figures 6.1.5 and 6.1.6 show selected stress results, in the form of contour plots, corresponding to an applied load of

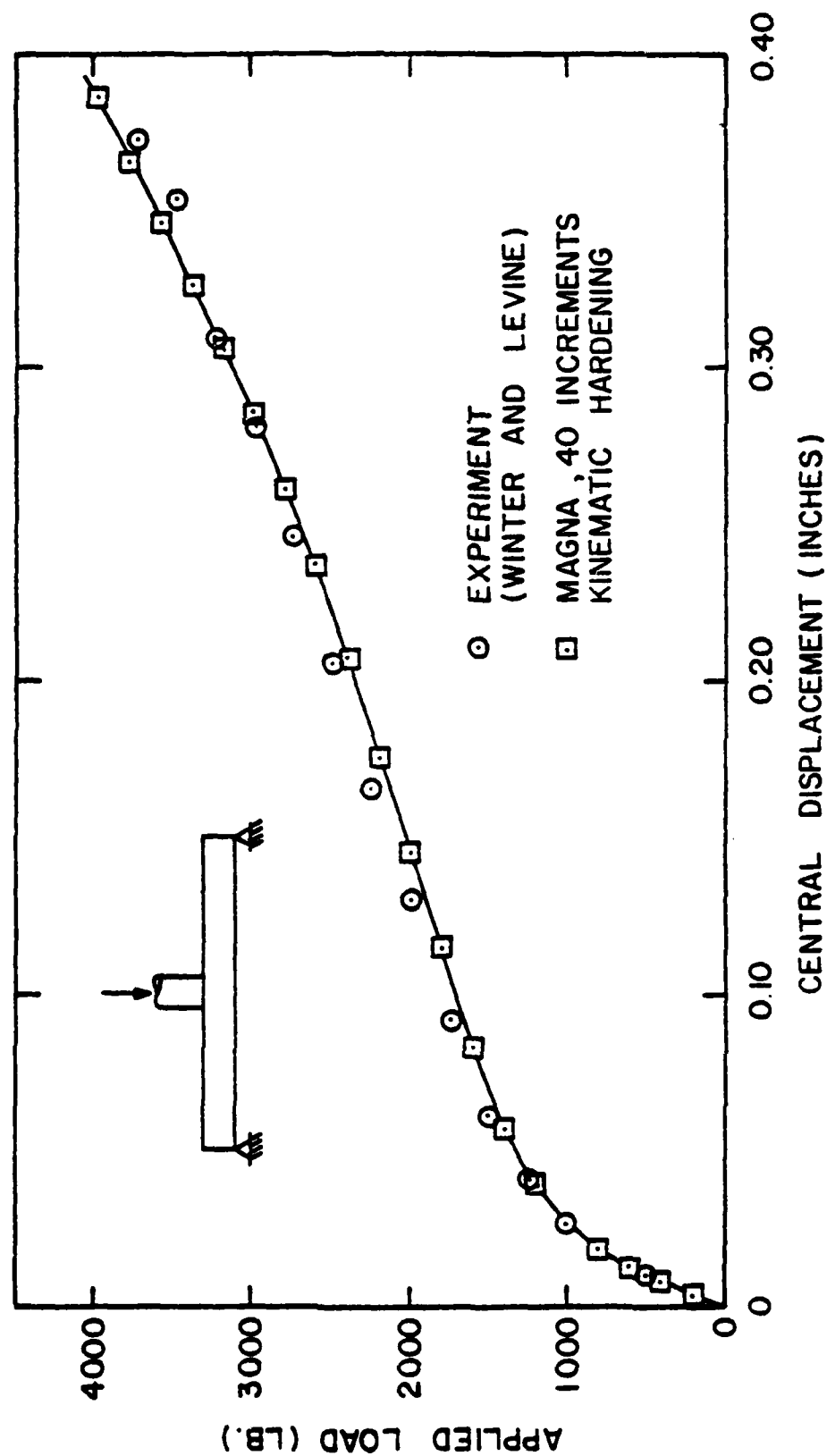


Figure 6.1.3 Load-versus Displacement Solution for Elastic-Plastic Circular Plate.

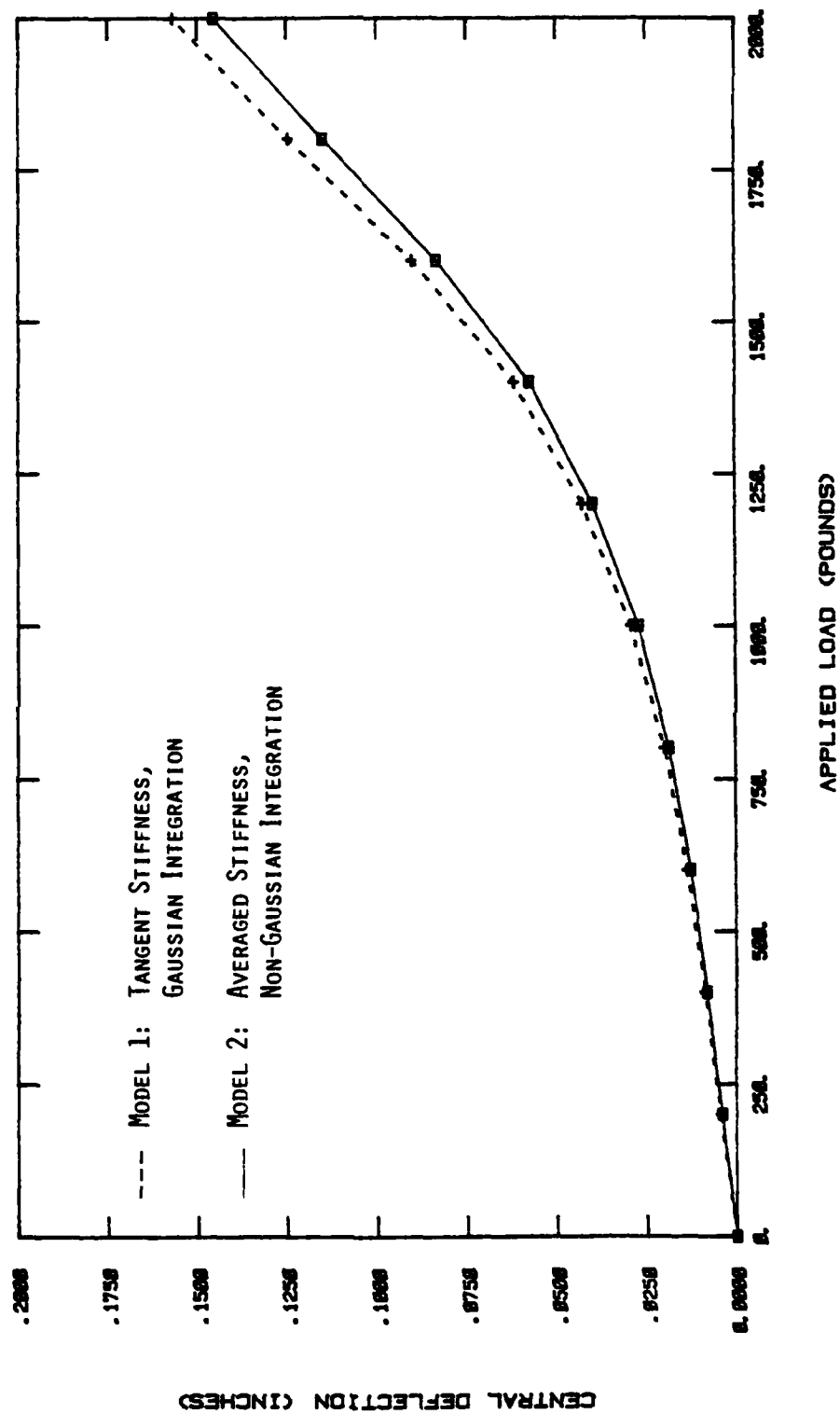
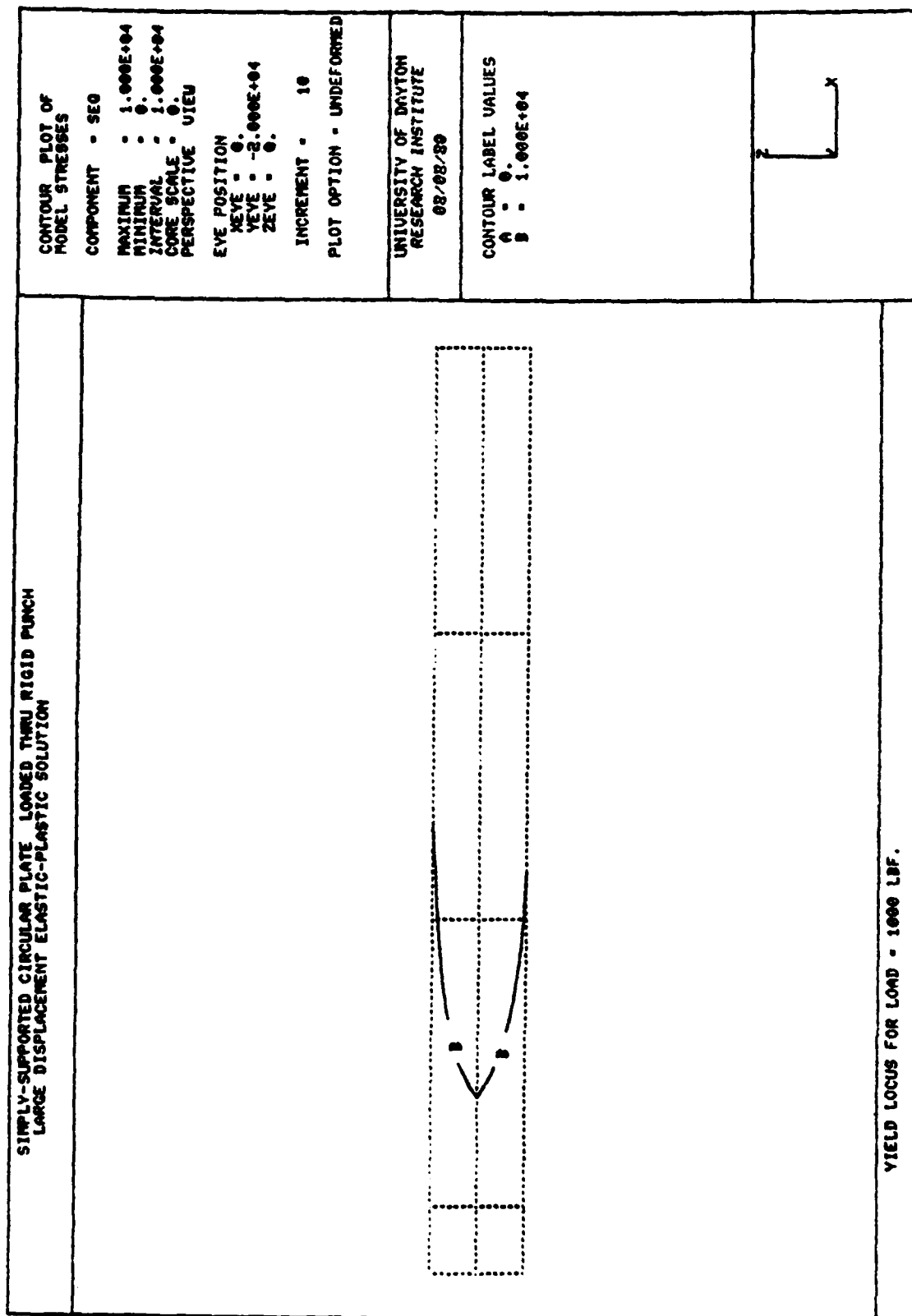


Figure 6.1.4 Comparison of Displacement Solutions for Circular Plate.



6.1.7

Figure 6.1.5 Elastic-Plastic Boundary in Plate Cross-Section at Total Load $P = 1000$ Pounds.

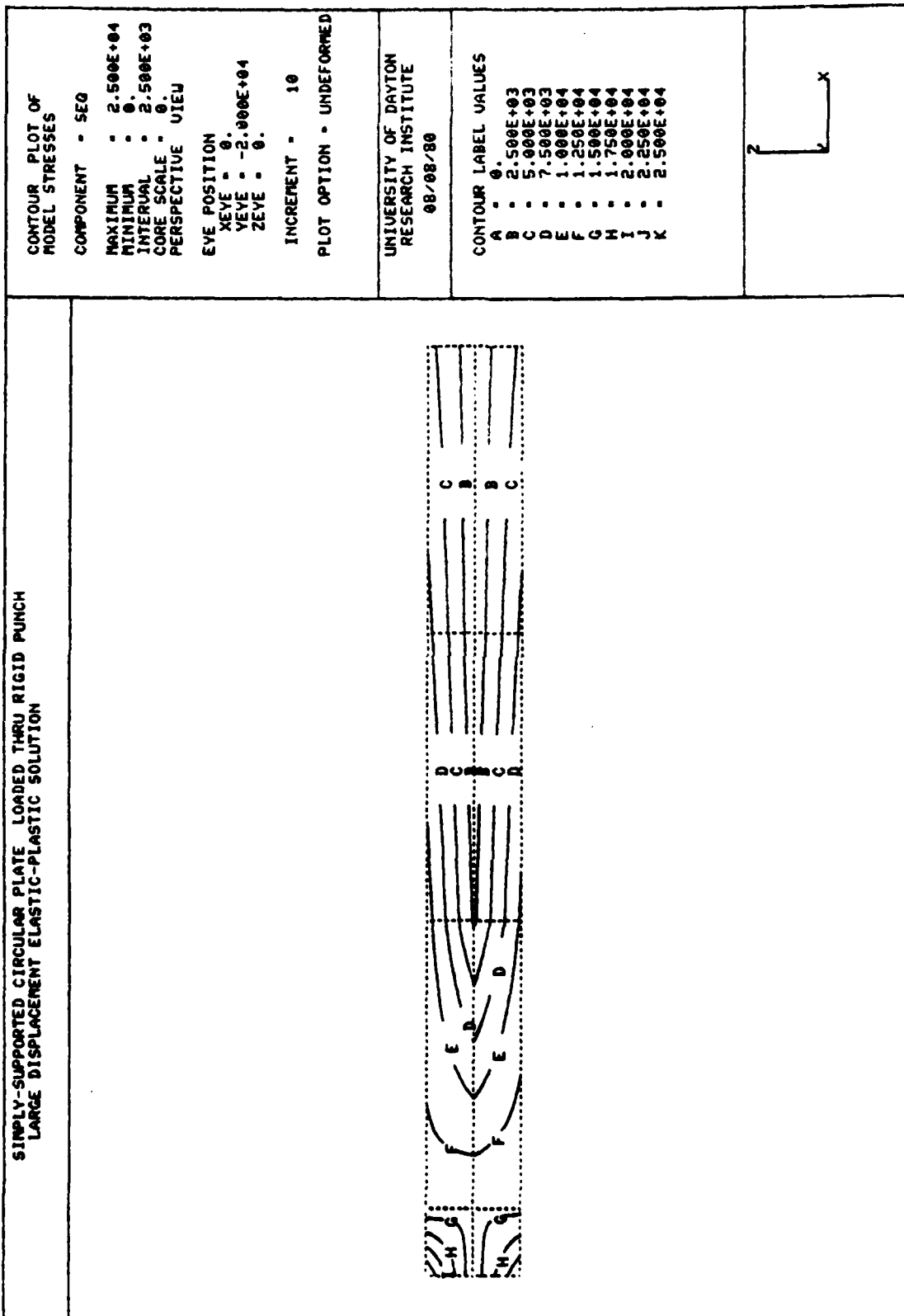


Figure 6.1.6 Effective Stress Distribution at Total Load $P = 1000$ Pounds.

1000 pounds. At this stage yielding is confined to a small region near the center of the plate, as shown in the yield locus plot of Figure 6.1.5. The distribution of von Mises effective stress is nearly midplane-symmetric (Figure 6.1.6).

Similar contour maps for the 2000 pound loading level are presented in Figures 6.1.7 and 6.1.8. Figure 6.1.7 shows the yield locus, which is interpreted as a series of straight lines due to the 2x2x2 integration rule used in the outermost elements; only a small region near the boundary and the midsurface remains elastic. The radial strain distributions of Figure 6.1.8 already show the influence of geometric nonlinearities, although the maximum strains are still rather small (6 percent).

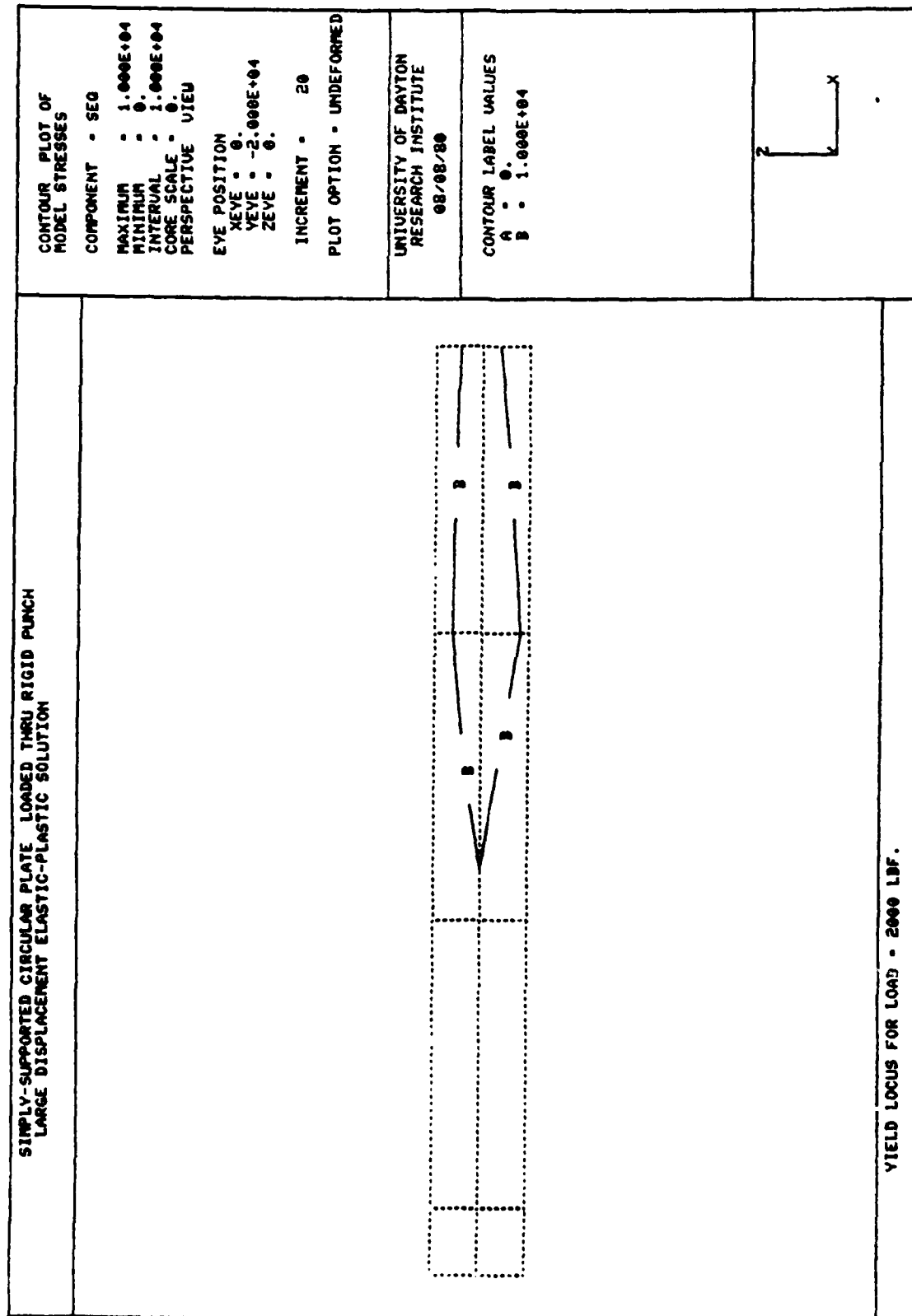


Figure 6.1.7 Elastic-Plastic Boundary in Plate Cross-Section at Total Load $P = 2000$ Pounds.

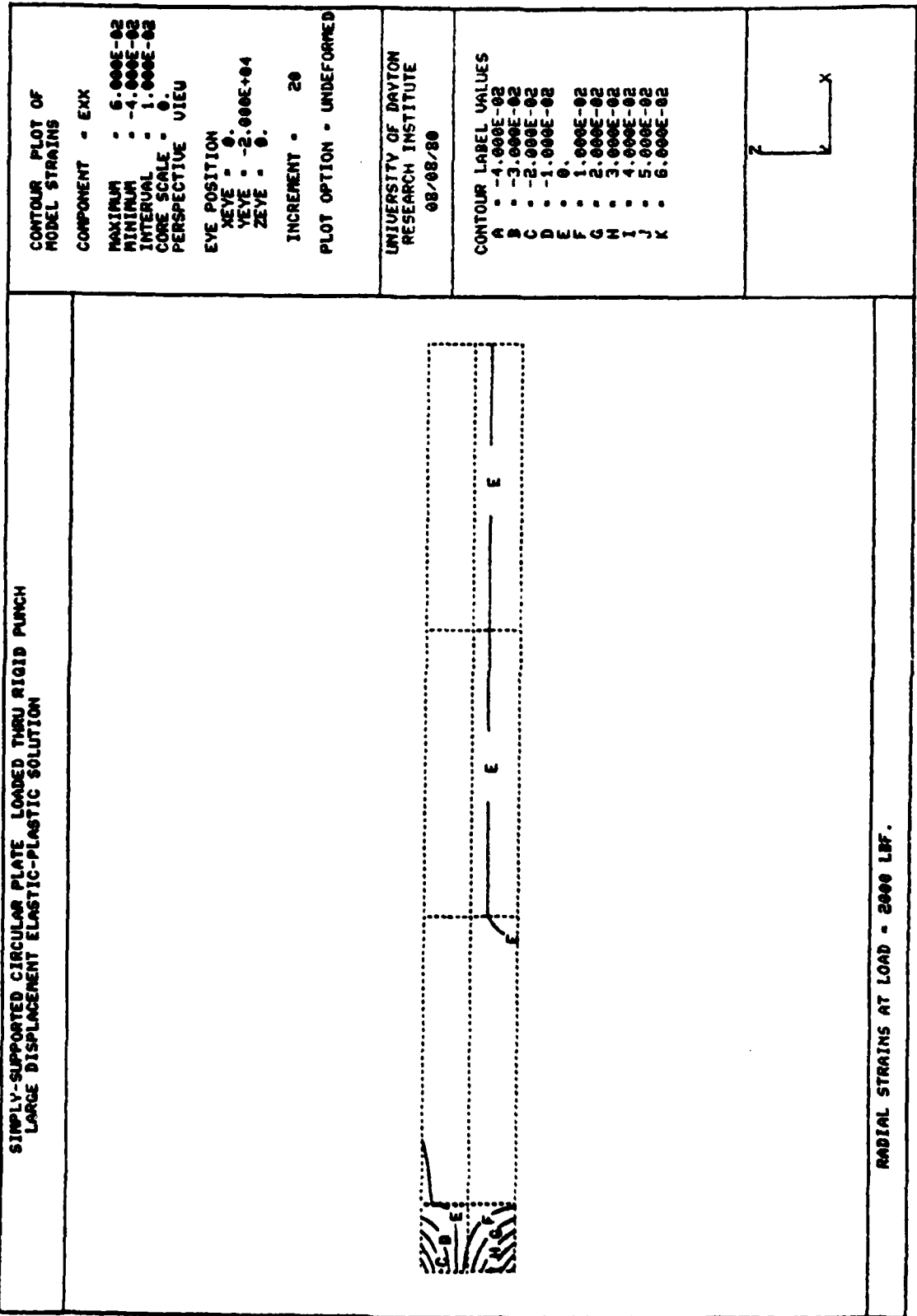


Figure 6.1.8 Radial Strain Distribution at P = 2000 Pounds.

6.2 SHALLOW SPHERICAL SHELL UNDER CONCENTRATED LOAD

The large displacement, elastic response of a shallow spherical cap, subjected to a point force at the apex, is considered. Figure 6.2.1 shows a cross-section of the undeformed shell geometry: the included angle of the cap (from the apex to the boundary) is 10.9 degrees. The shell material is assumed to be linear and elastic, but nonlinear effects due to large displacements are considered in the solution. The static solution of this problem has been studied by several investigators¹⁻³; in Reference 3, Mondkar and Powell also presented nonlinear dynamic solutions for the case of a constant, suddenly applied load.

Several three-dimensional finite element models of the cap are shown in Figures 6.2.2 through 6.2.5. The model of Figure 6.2.2 consists of fifteen shell elements (Element Type 5), forming a ten-degree sector of the cap. Since the response is axisymmetric, displacements normal to the lateral boundary have been suppressed using linear constraints (see Section 5.6). In Figures 6.2.3 and 6.2.4, the discretization consists of three-dimensional solid elements (Element Type 1), using twenty nodes per element and a 2x2x2 integration rule. Five and nine elements, respectively, are used to represent a ninety-degree sector of the shell. The last model (Figure 6.2.5) consists of seven solid elements (Element Type 1) on a fifteen-degree sector of the cap: linear constraints are again used to suppress the circumferential displacements on the skewed boundary. In each case, the outer edge of the shell is assumed to be completely clamped.

The nonlinear, static behavior of the spherical cap has been studied for the loading range of 0-100 pounds. At low load levels, the shell gradually becomes more flexible until the curvature of the deformed shell begins to generate midsurface tension stresses, causing a rapidly stiffening response. The static behavior is highly nonlinear, involving displacements which are twice the initial rise of the cap.

$$\begin{array}{ll}
 R = 4.7600 \text{ in.} & E = 10 \times 10^6 \text{ psi} \\
 t = 0.01576 \text{ in.} & \nu = 0.30 \\
 h = 0.0859 \text{ in.} & \rho = 2.45 \times 10^{-4} \text{ lb-sec}^2/\text{in}^4
 \end{array}$$

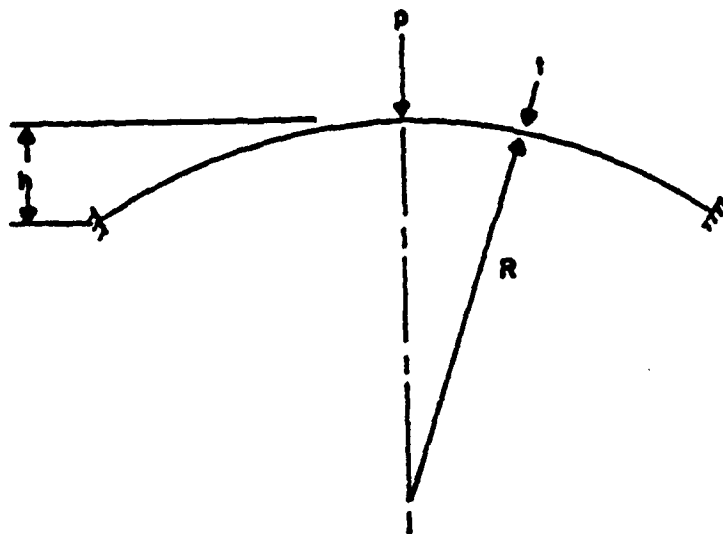


Figure 6.2.1 Cross-Section of Shallow Spherical Shell Under Concentrated Loading.

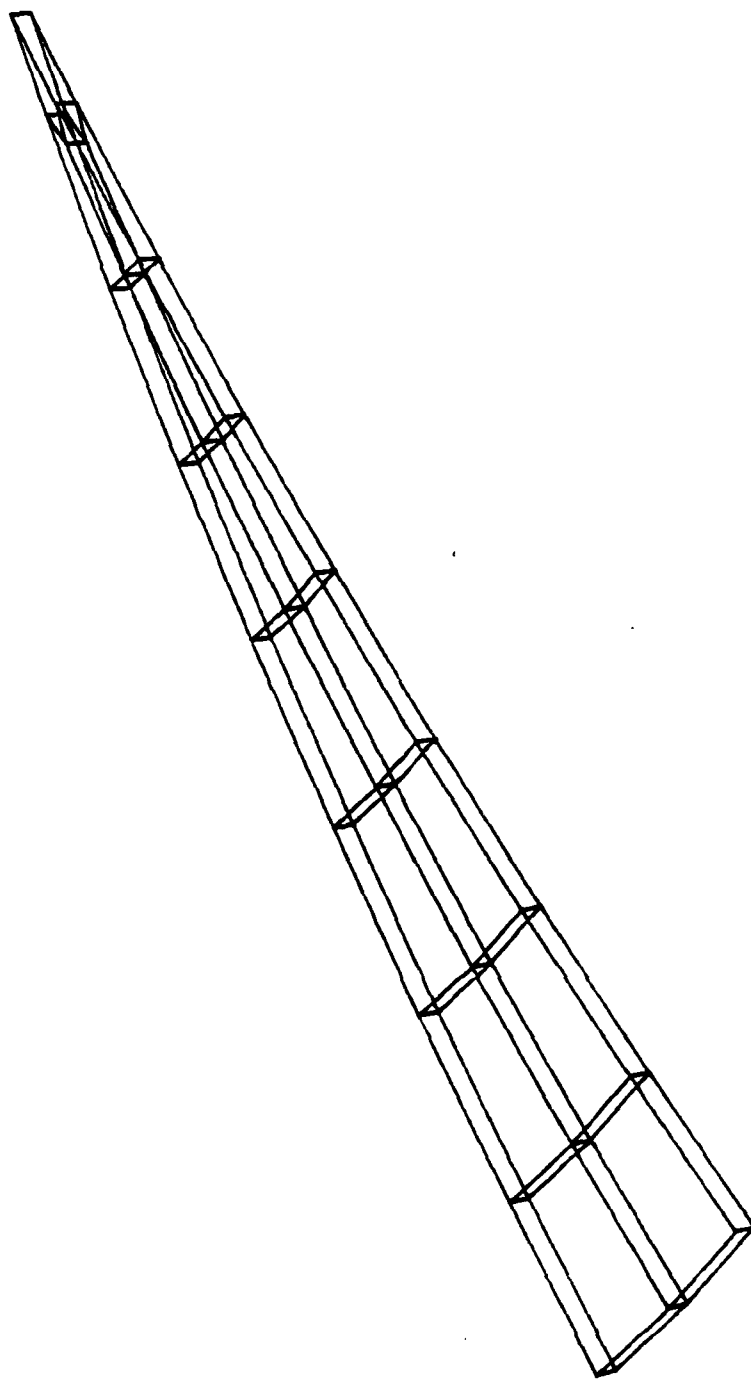


Figure 6.2.2 Shell Element Model of Spherical Cap Sector.

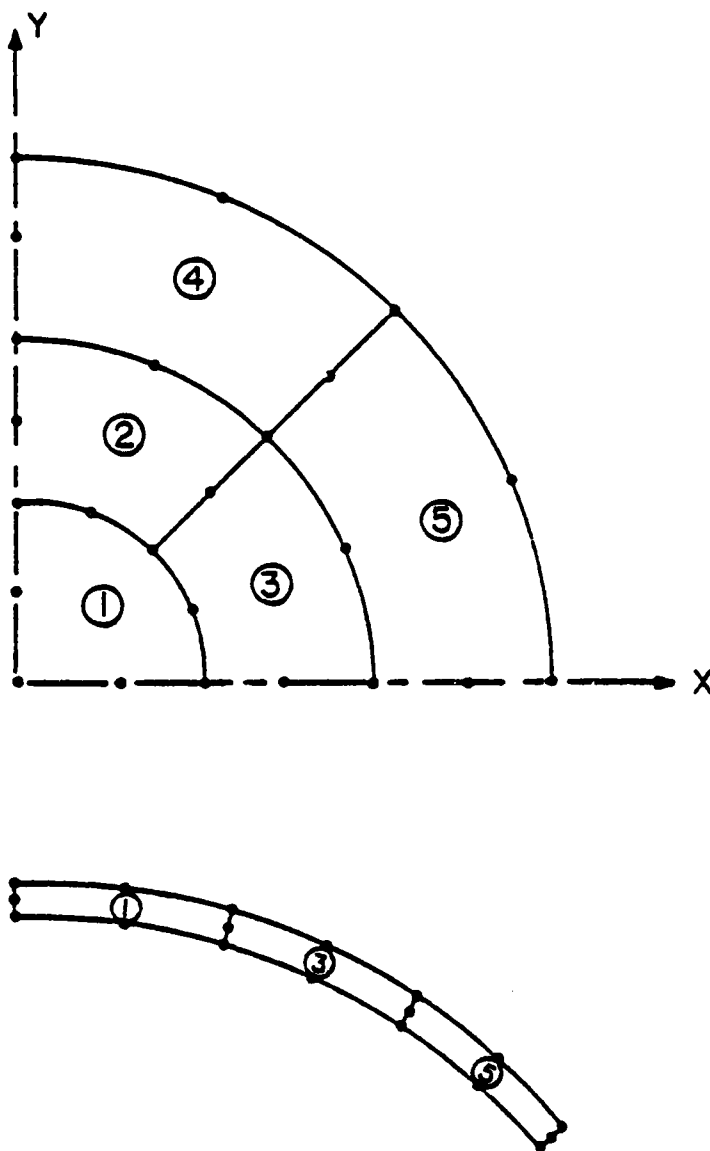


Figure 6.2.3 Five-Element Discretization of Spherical Cap Using Three-Dimensional, Twenty-Node Elements.

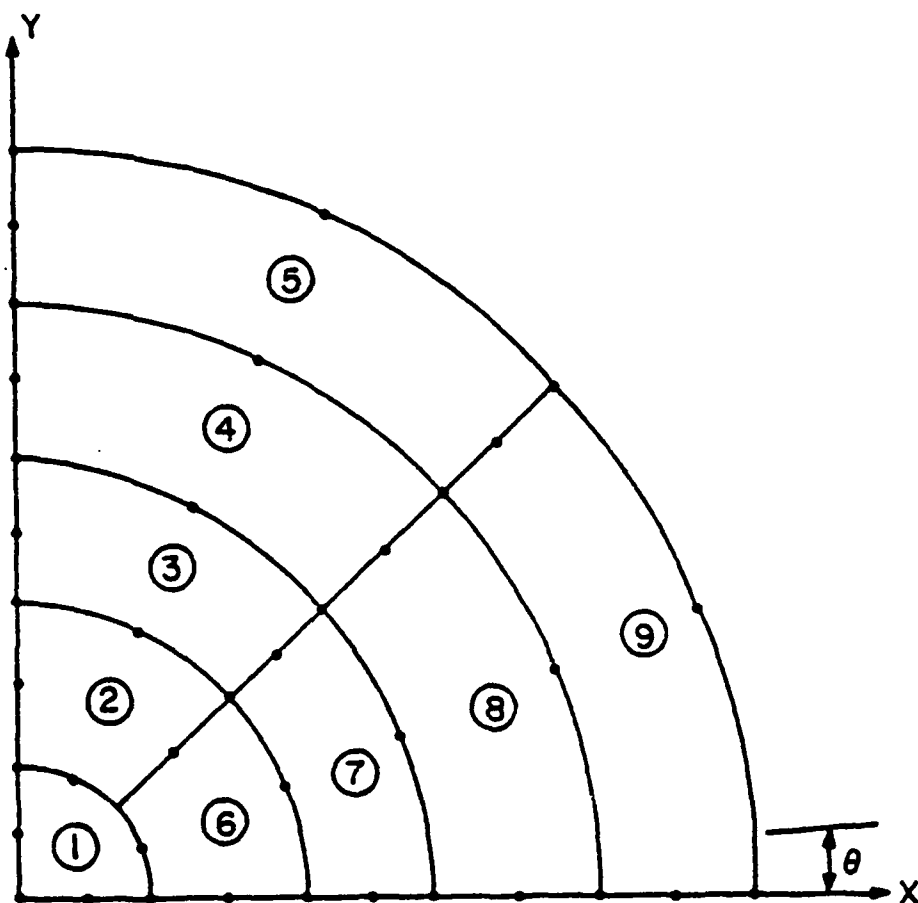


Figure 6.2.4 Nine-Element Discretization of Spherical Cap Using Three-Dimensional, Twenty-Node Elements.

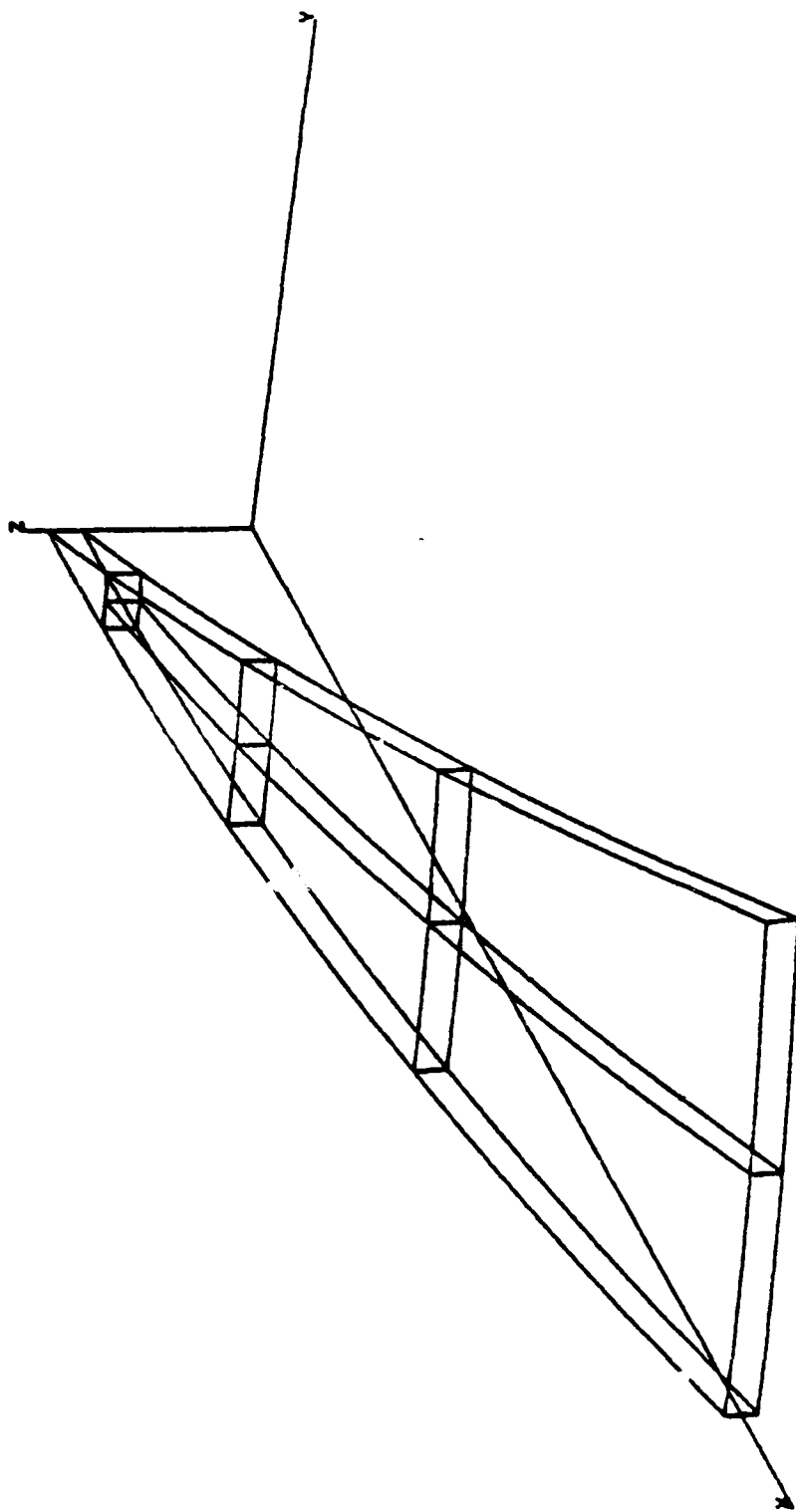


Figure 6.2.5 Seven-Element Model of Spherical Cap Sector Using Three-Dimensional Solid Elements.

A load-displacement solution obtained with the fifteen shell element model and two-pound loading increments is given in Figure 6.2.6. The results reported by Mondkar and Powell³ using ten axisymmetric quadratic continuum elements, and a MARC² solution performed with twenty axisymmetric shell elements, are shown for comparison. Agreement among the three solutions is quite good.

Static solutions using the five and seven-element three-dimensional solid models are plotted in Figure 6.2.7. The prediction by Mondkar and Powell is again shown for purposes of comparison. The seven-element model gives displacement results which are in good qualitative agreement with the solution of Reference 3; the displacement values at maximum load are different by approximately four percent. The five-element result is surprisingly good, and demonstrates that relatively few solid elements can be used to represent a fairly complex nonlinear response to within engineering accuracy. It should be emphasized, however, that such a coarse discretization is generally not sufficient for good stress accuracy.

The initial nonlinear dynamic response of the cap to a suddenly applied load of 100 pounds has also been predicted using MAGNA. In each case, the solution is obtained using the Newmark constant-average-acceleration operator ($\delta = 1/2$, $d = 1/4$; see Section 4.2). Figure 6.2.8 shows the transient response computed with the shell element model (fifteen elements), using a time step of two microseconds. Similar results due to Mondkar and Powell³ are shown for comparison. The solutions show good agreement, while the difference in superimposed high-frequency oscillations reflects the difference in the two methods of discretization. Nonlinear dynamic solutions obtained using the nine-solid-element model (Figure 6.2.4) are given in Figures 6.2.9 and 6.2.10, for solution time steps of two and four microseconds. The solid element results

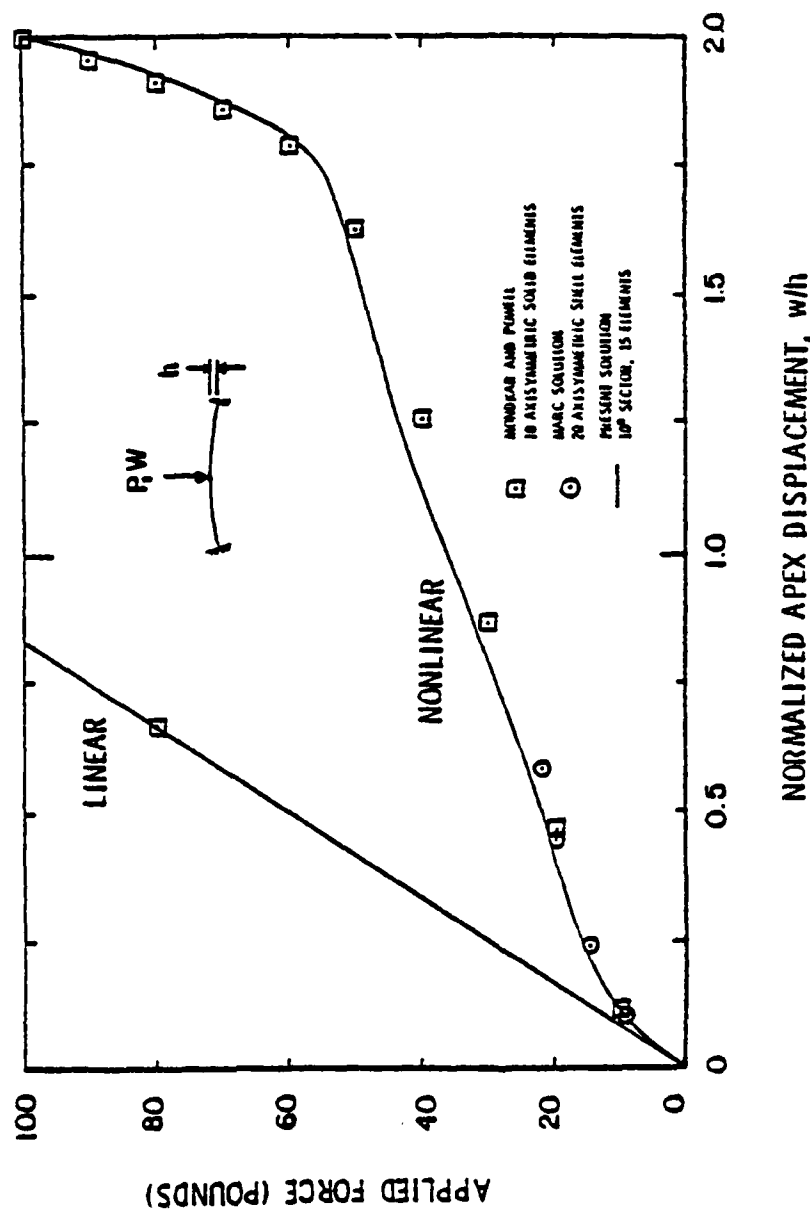


Figure 6.2.6 Static Nonlinear Solution for Shallow Cap (Fifteen Shell Elements).

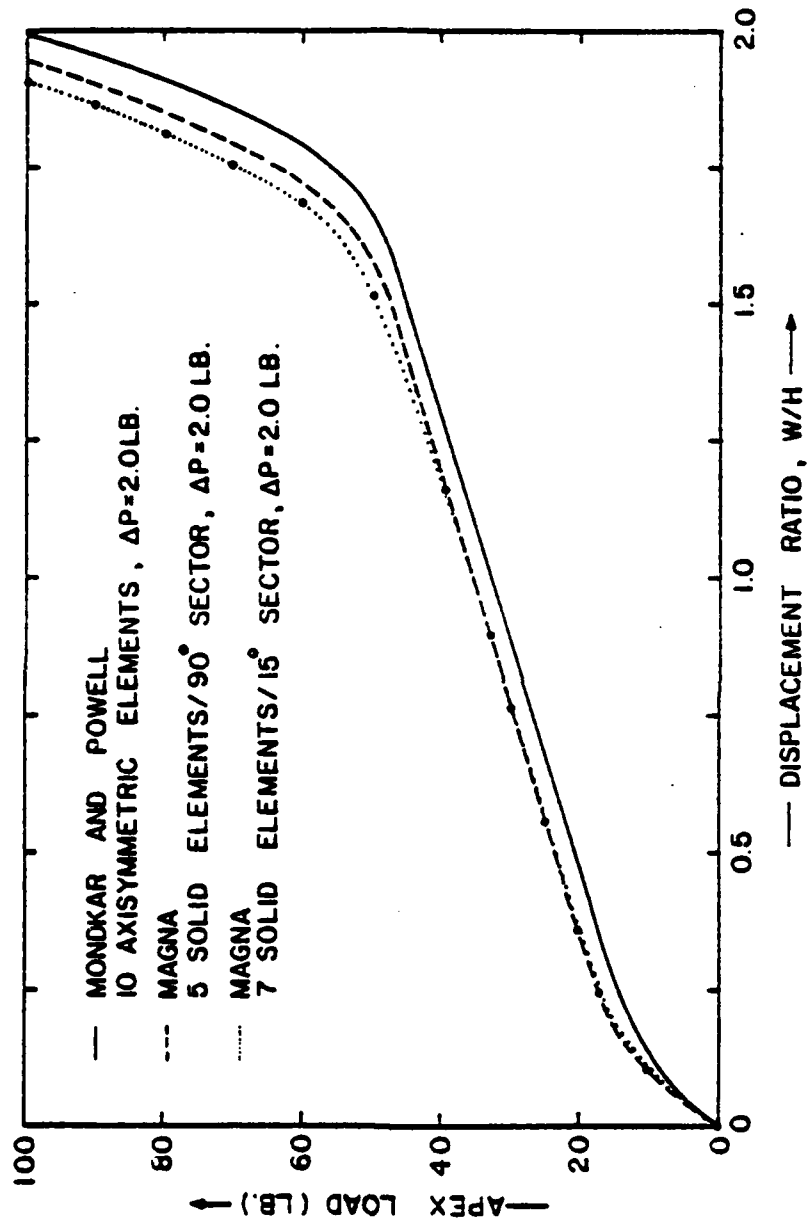


Figure 6.2.7 Static Nonlinear Solution for Shallow Cap (Solid Element Models).

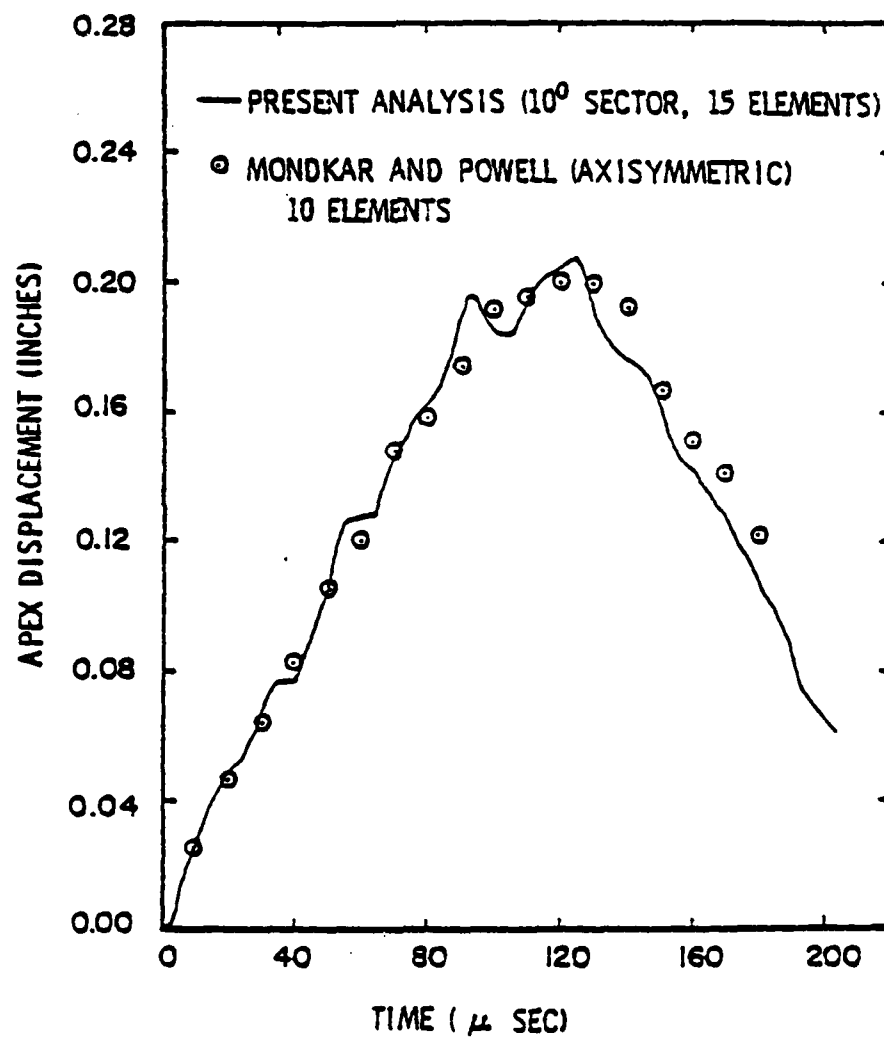


Figure 6.2.8 Shell Element Solution for Dynamic Response of Shallow Cap ($\Delta t = 2 \mu\text{sec.}$).

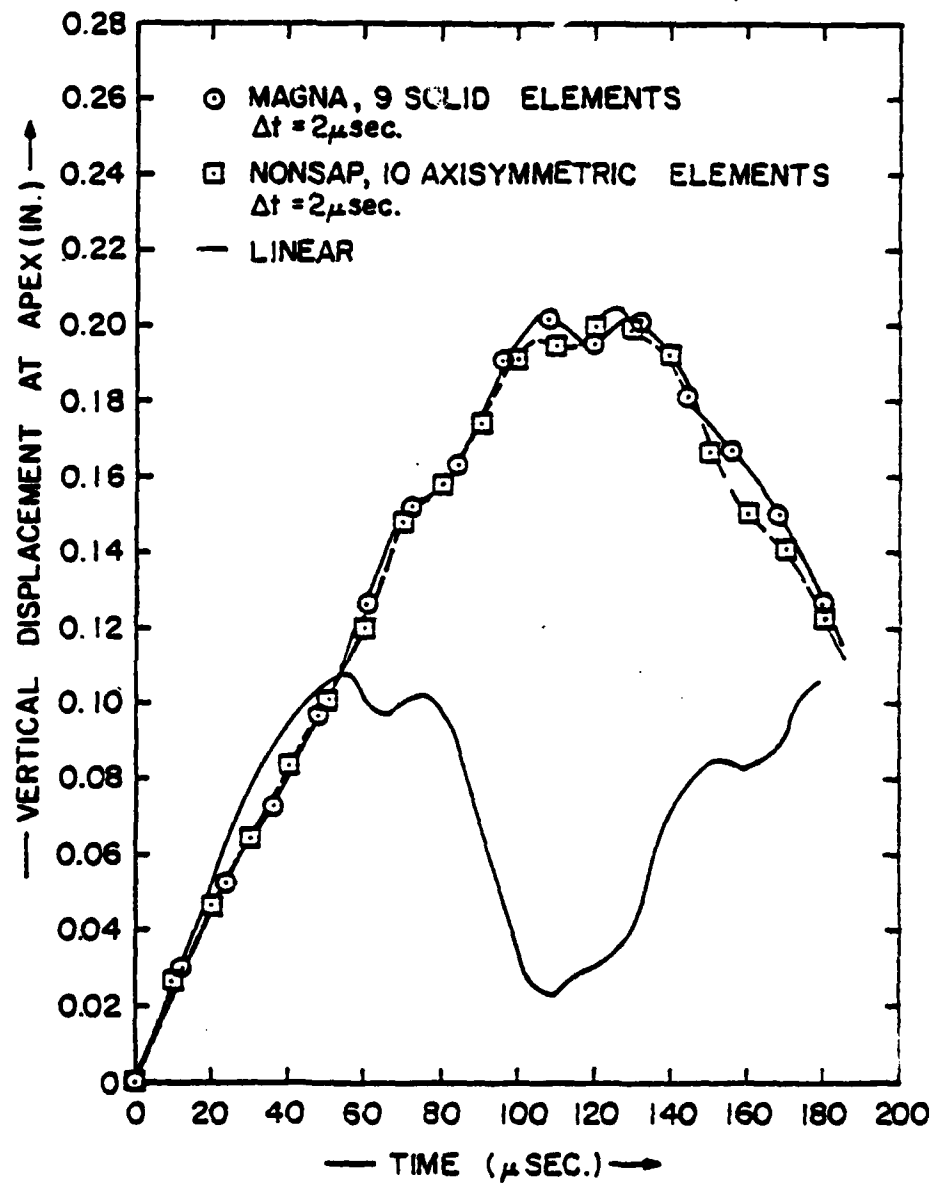


Figure 6.2.9 Solid Element Solution for Dynamic Response of Shallow Cap ($\Delta t = 2 \mu\text{sec.}$).

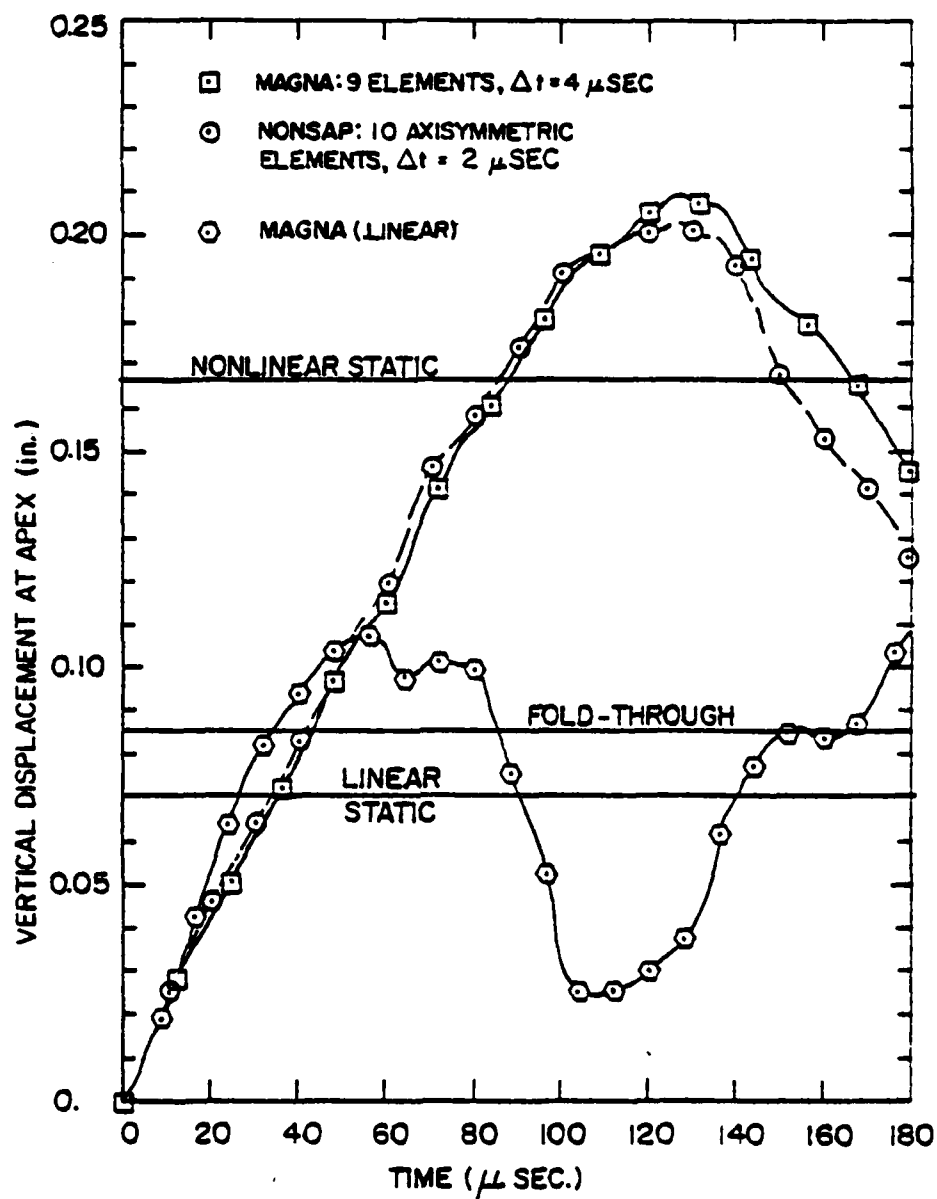


Figure 6.2.10 Solid Element Solution for Dynamic Response of Shallow Cap ($\Delta t = 4 \mu$ sec.).

are plotted with a NONSAP⁴ solution, which is virtually identical to the results of Reference 3. For the smaller increment size, the solution is quite good. At $\Delta t = 4 \text{ } \mu\text{sec.}$, the maximum displacement is well represented but the period of oscillation is overestimated; this error is typical of the Newmark integration operator at large time steps. A similar effect can be observed to a lesser degree even in the solution for $\Delta t = 2 \text{ } \mu\text{sec.}$, as shown in Figure 6.2.11. In this case, Newton-Raphson iterations have been used at each increment of the solution for a 4 μsec time step, and can be seen to control the period distortion in the integration quite effectively. It is worthy of mention that the total cost of the two solutions shown in Figure 6.2.11 is nearly the same, since relatively few Newton iteration cycles are required at each time increment to stabilize the solution.

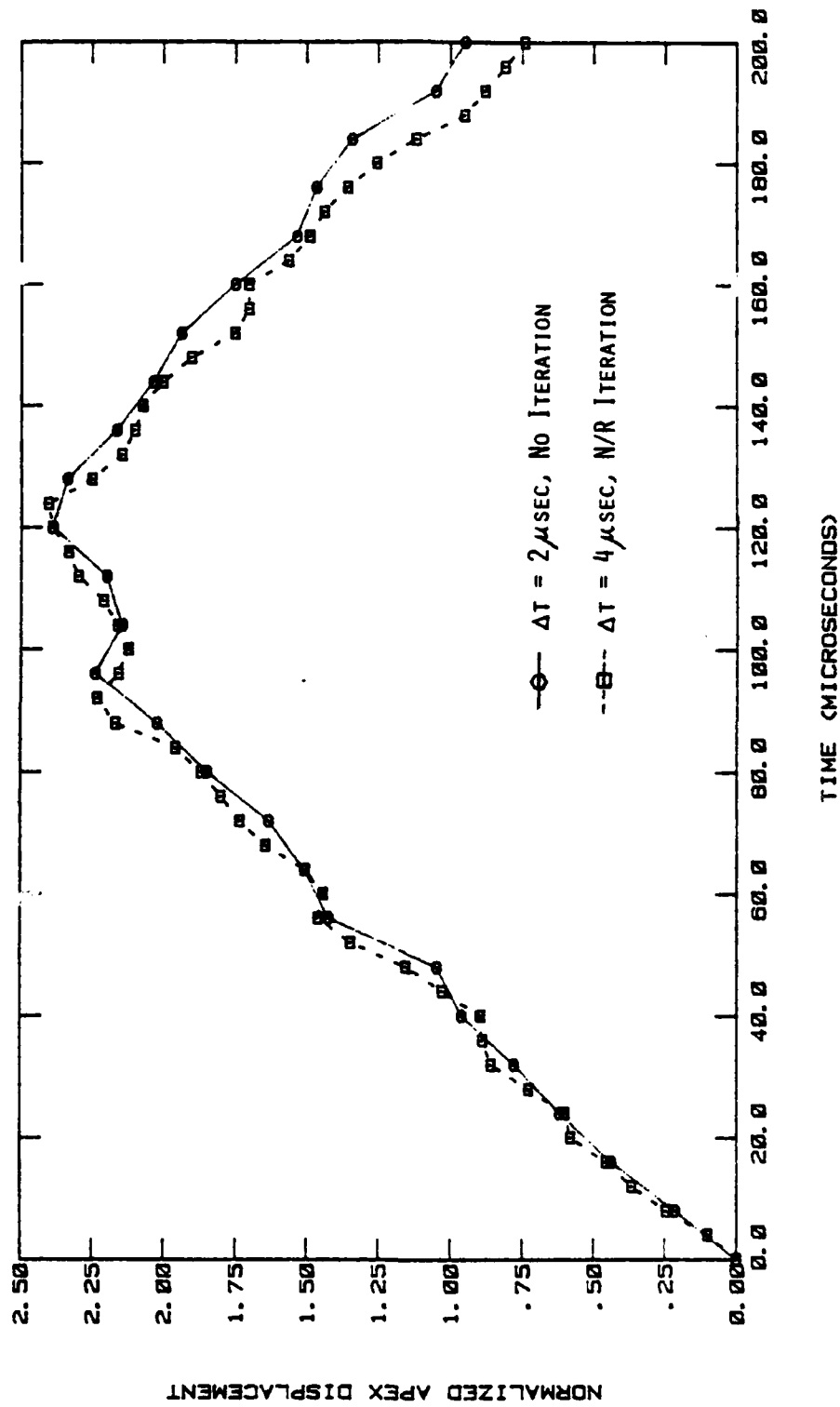


Figure 6.2.11 Comparison of Dynamic Response Solutions With and Without Equilibrium Iterations.

6.3 LARGE STRAIN ELASTIC ANALYSIS OF A BAR IN TENSION

The problem of a rectangular, elastic bar under axial load is considered, to test the large displacement and large strain analysis in MAGNA. Figure 6.3.1 shows the geometry of the bar; the material properties used are those of aluminum ($E = 1.0 \times 10^7$ psi; $\nu = 0.30$). Only axial displacements are permitted in the solution, so that the only nonzero component of strain is longitudinal (ϵ_{xx}).

The linear response of the bar has the following three-dimensional solution:

$$u = \frac{P_x}{A_0(\lambda + 2\mu)}$$

$$\epsilon_{xx} = \frac{P}{A_0(\lambda + 2\mu)}$$

$$\epsilon_{yy} = \epsilon_{zz} = 0$$

$$\sigma_x = \frac{P}{A_0}$$

$$\sigma_y = \sigma_z = \frac{P}{A_0(\lambda + 2\mu)},$$

in which P denotes the total load, A_0 is the initial area of the bar, and λ, μ are the Lamé constants of the material. In the geometrically nonlinear range, the load-deflection curve can easily be obtained as

$$P = A_0(\lambda + 2\mu) \nu (1 + \nu)(1 + \nu/2)$$

where ν is the end deflection of the bar divided by the original length.

The three-dimensional finite element discretization of the bar (Figure 6.3.2) consists of twenty eight-node solid elements (Element Type 2). A large number of elements has

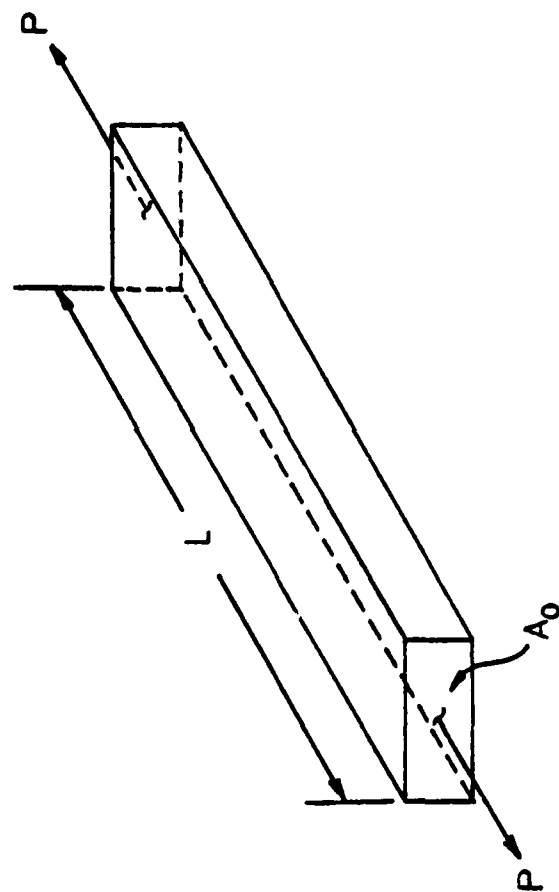


Figure 6.3.1 Rectangular Bar Under Axial Load.

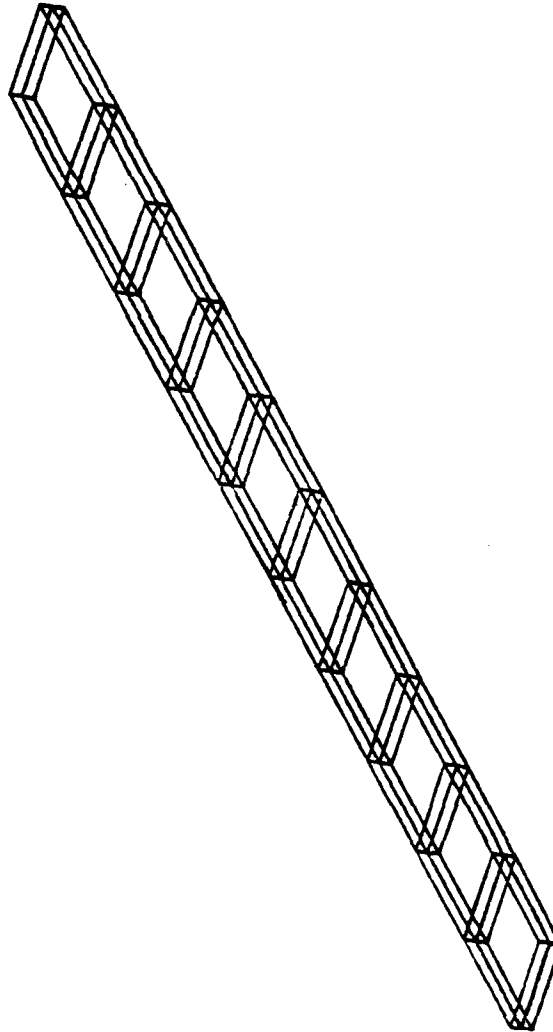


Figure 6.3.2 Finite Element Model of Axially Loaded Bar.

been used here to provide a check of the uniformity of the stress and strain solutions; one element would, in fact, provide correct results.

A linear solution has been performed for the bar, using the data

$$A_0 = 0.0625 \text{ in.}^2$$

$$L = 10.0 \text{ in}$$

$$\lambda = 5.7693 \times 10^6 \text{ lb./in.}^2$$

$$\mu = 3.8462 \times 10^6 \text{ lb./in.}^2$$

$$P = 6,000 \text{ lb.}$$

Numerical results for the problem are compared with the exact solution in Table 6.3.1; computed values of the end displacement, stresses, and strains agree with the analytical values to the same accuracy as the data (above).

Load-deflection response obtained from the geometrically nonlinear solution are compared with the analytical solution in Figure 6.3.3, and tabulated in increments of 40,000 pounds in Table 6.3.2. The maximum load level considered is 2.4×10^5 lb., corresponding to Green's strains of approximately 25%. Load increments of 10,000 pounds have been used, without iteration. Table 6.3.2 shows that the error in the numerical solution actually tends to decrease as the load is increased; errors in the computed response at all load levels are quite small.

TABLE 6.3.1
LINEAR SOLUTION FOR AXIALLY LOADED BAR

| Quantity | Exact | Computed | Error (%) |
|--|----------|----------|-----------|
| End Deflection | 0.07131 | 0.07132 | 0.01 |
| Strain ϵ_{xx} | 0.007131 | 0.007131 | 0.00 |
| Strains $\epsilon_{yy}, \epsilon_{zz}$ | 0. | 0. | 0.00 |
| Stress σ_{xx} | 96000. | 96000. | 0.00 |
| Stresses σ_{yy}, σ_{zz} | 41140. | 41143. | 0.01 |

TABLE 6.3.2
NONLINEAR LOAD-DEFLECTION RESULTS FOR RECTANGULAR BAR

| Load | Displacement | Exact Load | Error (%) |
|---------|--------------|------------|-----------|
| 40000. | 0.446839 | 40152. | 0.38 |
| 80000. | 0.842871 | 80153. | 0.17 |
| 120000. | 1.202215 | 120120. | 0.10 |
| 160000. | 1.532662 | 160111. | 0.07 |
| 200000. | 1.839616 | 200104. | 0.05 |
| 240000. | 2.127008 | 240100. | 0.04 |

AD-A129 773

MAGNA (MATERIALLY AND GEOMETRICALLY NONLINEAR ANALYSIS)

3/8

PART I FINITE ELE. (U) DAYTON UNIV OH RESEARCH INST

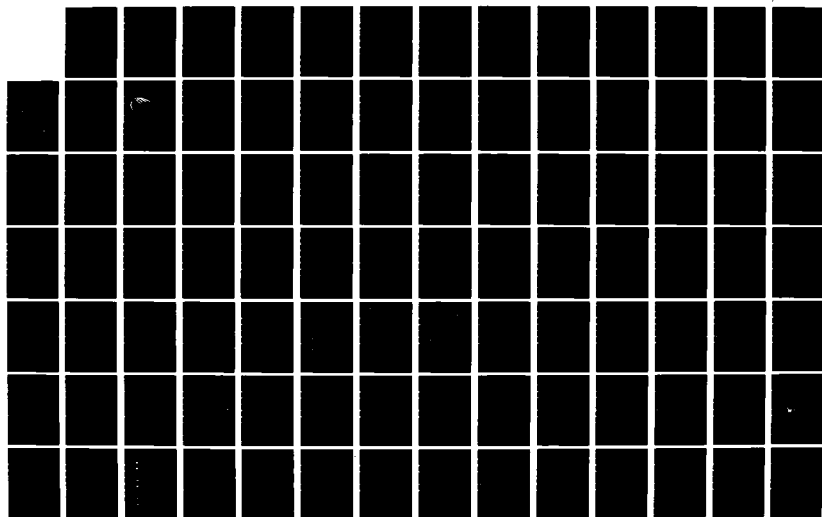
R A BROCKMAN DEC 82 UDR-TR-82-111 AFMRL-TR-82-3098-PT-1

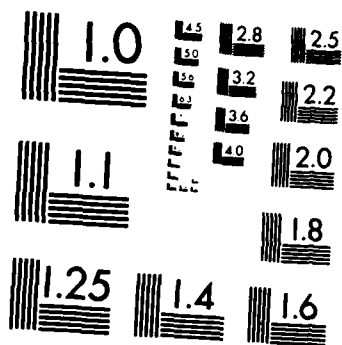
UNCLASSIFIED

F33615-88-C-3403

F/G 12/1

NL





MICROCOPY RESOLUTION TEST CHART
NATIONAL BUREAU OF STANDARDS-1963-A

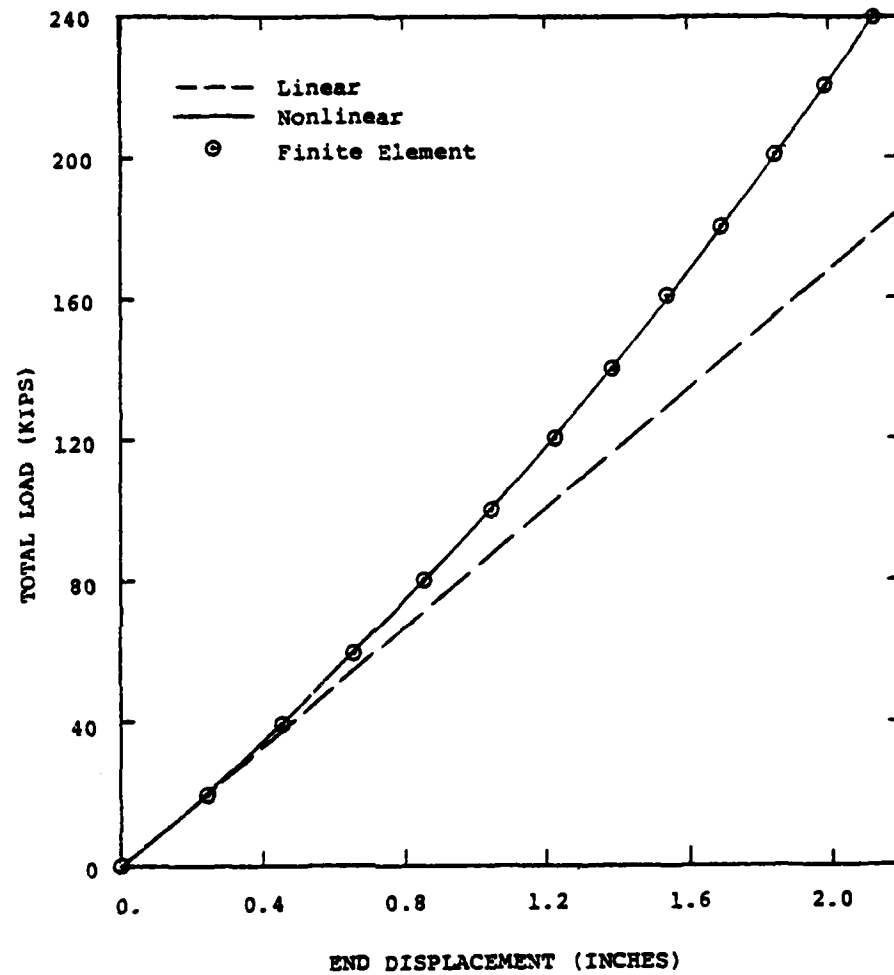


Figure 6.3.3 End Displacement Versus Load Solution for Axially Loaded Bar.

6.4 ELASTIC DYNAMIC BUCKLING OF A CIRCULAR ARCH

The dynamic stability of a shallow arch is considered, to demonstrate the capabilities of the MAGNA program in performing dynamic solutions involving both large displacements and large rotations. A circular arch, pinned at each end, is subjected to a rapid pressure loading, as indicated in Figure 6.4.1. The geometry and material properties of the structure are as follows:

$$R = 67.115 \text{ inches}$$

$$\alpha = 15.0 \text{ degrees}$$

$$h = b = 1.0 \text{ inch}$$

$$E = 10.0 \times 10^6 \text{ psi}$$

$$\nu = 0.20$$

$$\rho = 2.44 \times 10^{-4} \text{ lb. sec}^2/\text{in.}^4$$

The initial height of the arch is $H = 2.87$ inches.

The pressure loading applied to the arch increases linearly with time for 331.5 microseconds; after this time, the distributed load remains constant at P_0 pounds per square inch. At small values of the maximum pressure P_0 , small vibrations are observed which do not exceed the initial height of the arch. However, for pressures greater than a certain critical value P_{cr} (which is to be determined), the arch snaps through and oscillates about an inverted position.

The stability of the arch has been studied using analog methods by Humphreys¹, who showed that asymmetric buckling cannot occur for the particular case under consideration; symmetry can, therefore, be used in the finite element discretization. A finite element solution of the problem has been presented by Bathe, Ozdemir and Wilson², using six eight-node plane stress continuum elements to represent one-half of the arch. In Reference 2, the critical pressure is estimated to be between 420 and 440 psi.

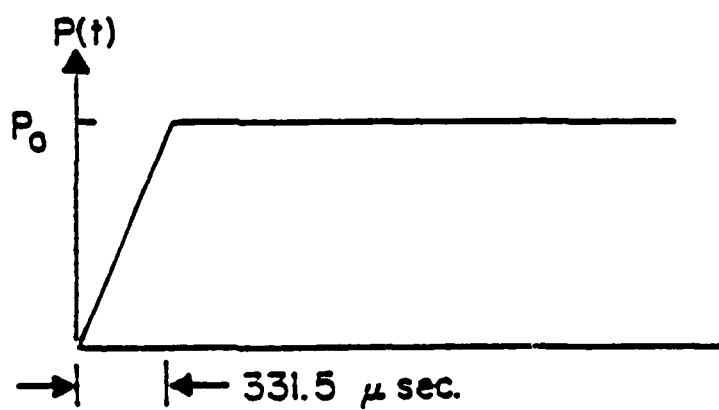
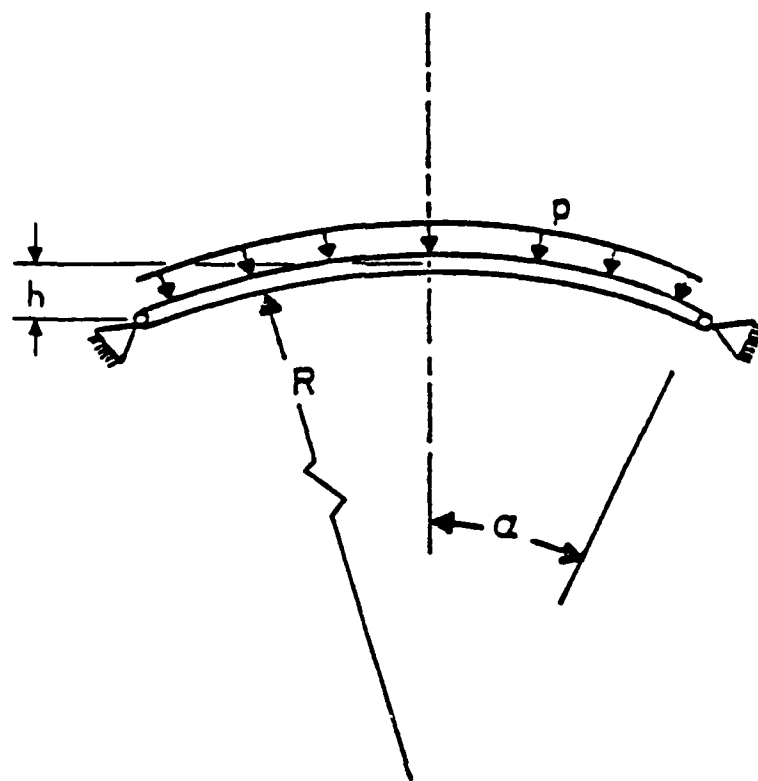


Figure 6.4.1 Shallow Arch Geometry and Loading.

A finite element model of the arch using six trilinear thin shell elements (Element Type 5) is shown in Figure 6.4.2. Note that the solution could be performed more economically using quadratic plane stress elements (Element Type 9); however, use of the thin shell element is made to demonstrate the dynamic and large rotation capabilities of the element. Half of the arch is considered, taking advantage of symmetry, and displacements normal to the plane of the arch are suppressed. The dynamic response of the arch is obtained with MAGNA using Newmark integration, with a constant time increment of 55.25 μ sec. Transverse displacements at the crown of the arch are plotted versus time in Figure 6.4.3, for several values of the pressure P_0 . For an applied pressure of $P_0 = 420$ psi, relatively small oscillations are observed about the initial position of the arch. At $P_0 = 430$ psi, the arch snaps completely through; the critical pressure is, therefore, in the range $420 \leq P_{cr} \leq 430$ psi. This conclusion is in agreement with the solution of Bathe, Ozdemir and Wilson.

The solutions shown in Figure 6.4.3 indicate that, for pressures greater than the critical value, the amplitude of vibration is insensitive to the exact magnitude of the load; a subsequent solution for $P_0 = 800$ psi has confirmed this fact, producing maximum displacements of slightly less than eight inches. While membrane stiffening effects control the displacement amplitude at large pressures, the influence of softening behavior is apparent at load levels which are less than the critical level. For example, the period of oscillation for $P_0 = 420$ psi is considerably larger than that for $P_0 = 380$ psi; this difference is due to the diminishing gross stiffness of the arch at displacements which approach the flat position.

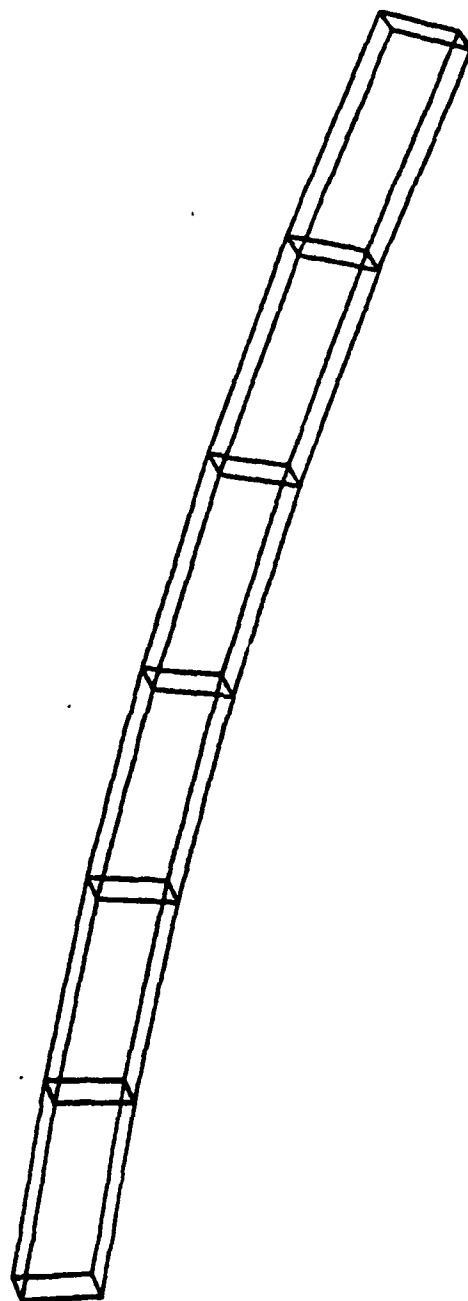


Figure 6.4.2 Shell Element Model of Shallow Arch.

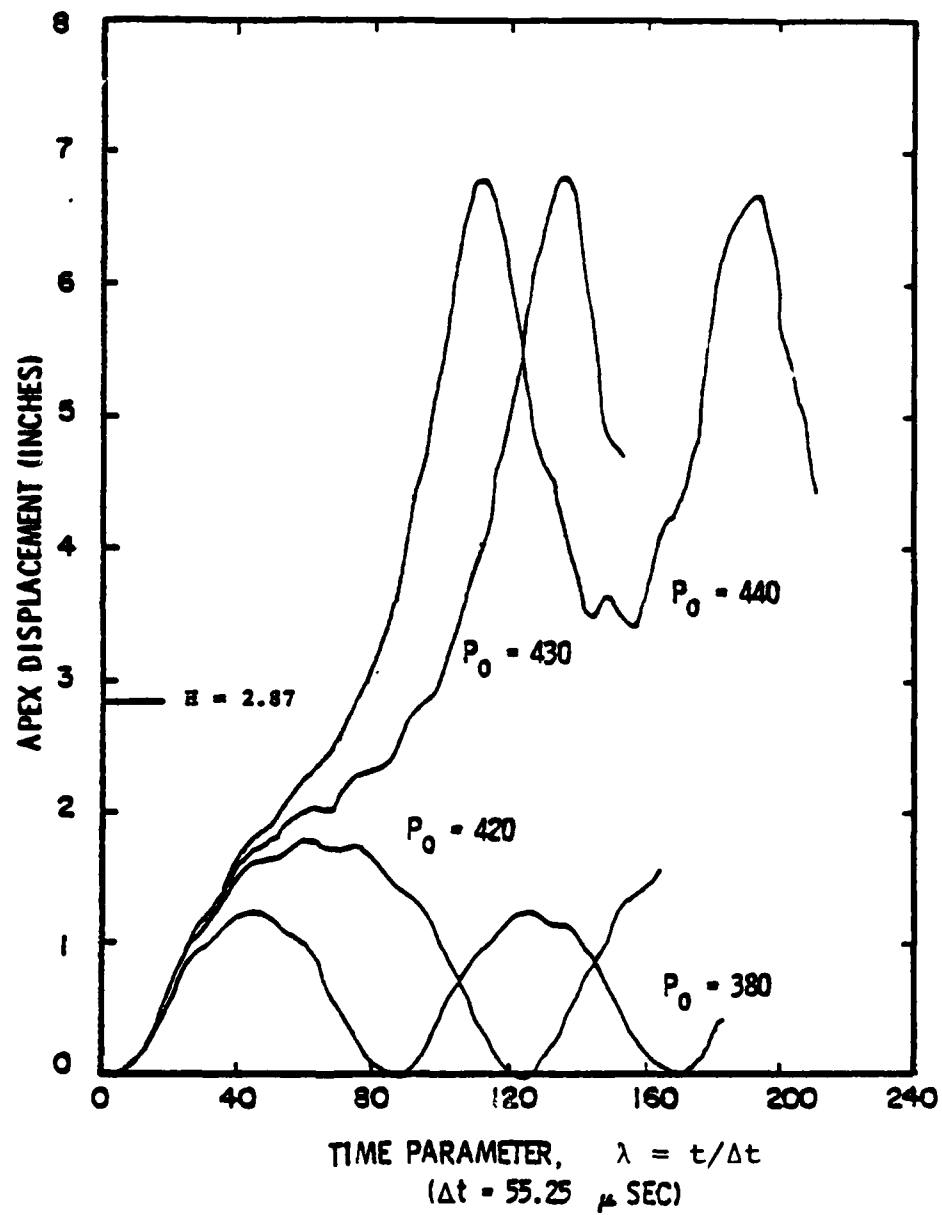


Figure 6.4.3 Dynamic Response of Shallow Arch for Selected Pressure Levels.

6.5 LARGE DISPLACEMENT RESPONSE OF AN AIRCRAFT WINDSHIELD

The windshield transparency of the F-16 tactical fighter is a monolithic, moderately thick shell made of polycarbonate material. Static calibration tests of the windshield, performed as part of a series of impact studies¹, have been modeled numerically using MAGNA. This particular example demonstrates the application of the program to a nonlinear problem of practical size and complexity.

Figures 6.5.1 and 6.5.2 show two finite element discretizations used for nonlinear analysis of the canopy. The fifty-element model of Figure 6.5.1 is composed of three-dimensional twenty-node solid elements (Element Type 6); stiffness properties are evaluated using 3x3x3 Gaussian quadrature and with 14-point integration, in two different versions of the model. This mesh contains 428 nodes and 1110 active degrees of freedom. The shell (Element Type 5) model of Figure 6.5.2 contains 100 elements, 242 nodes and 613 degrees of freedom.

In each case, symmetry is assumed along the fuselage center line. Adjacent support structure is not considered in the numerical analysis, since the boundary reaction forces are rather small for the range of loading considered. Rigid line supports are assumed instead on the three external boundaries of the model.

The material properties of the windshield material are not well defined, as the available data for the elastic modulus vary between 211000 and 300000 psi. Analyses have been performed for three values of the elastic modulus (211000, 235000 and 285000 psi) using the solid element model, while for the shell model a single value $E = 250000$ psi is used. Poisson's ratio is taken to be $\nu = 0.325$.

A concentrated load is applied to the canopy through a small circular pad, approximately two feet from the forward

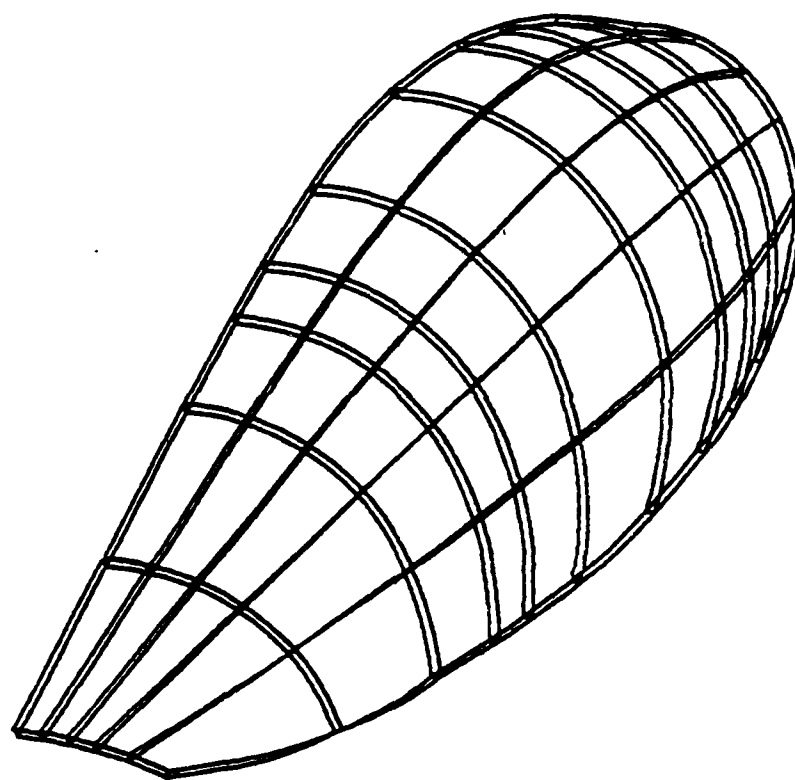


Figure 6.5.1 Three-Dimensional Solid Element Model of F-16 Windshield Canopy.

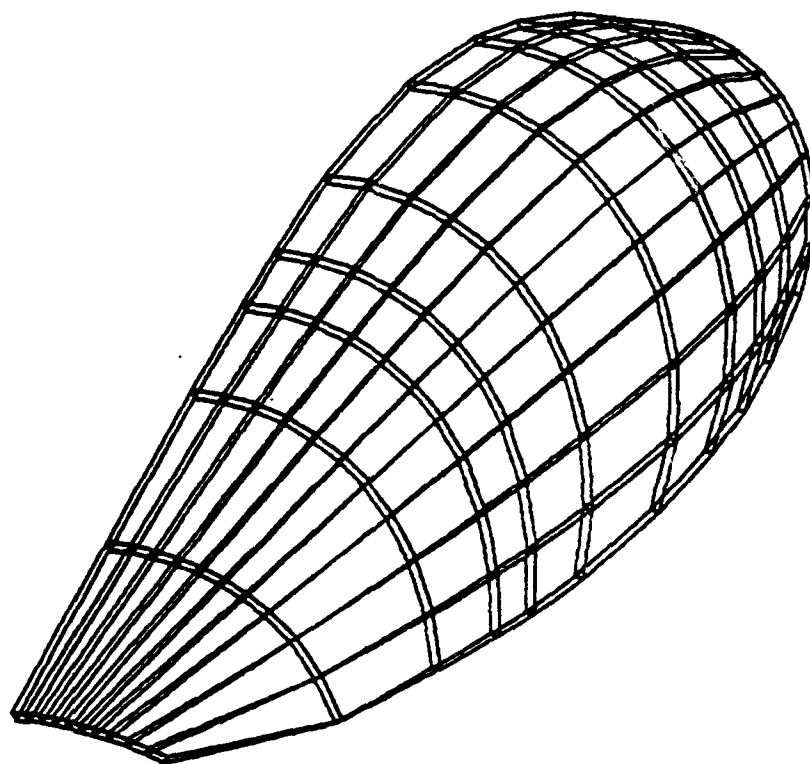


Figure 6.5.2 Shell Element Model of F-16 Windshield Canopy.

edge on the windshield center line. Experimental values of the deflection normal to the canopy at the point of loading have been measured with deflectometers mounted inside the shell.

Experimental and computed values of the canopy deflections, for the loading range 0-2200 pounds, are compared in Figures 6.5.3 and 6.5.4 for the solid and shell models, respectively. In view of the uncertainties in material properties, boundary conditions and local load distribution, the agreement between measured and calculated deflections is excellent. A plot of the deformed windshield geometry is shown in Figure 6.5.5. In each analysis, the response has been computed in ten equal loading steps of 220 pounds. For the solid element model, best agreement with the experimental results is obtained using an intermediate value of the elastic modulus ($E = 235000$ psi). However, no conclusions should be drawn from this comparison regarding the true value of the polycarbonate material modulus. Typical stress results, obtained at the 1100 pound load level, are pictured in the contour plot of Figure 6.5.6.

Natural frequency calculations have also been performed for the F-16 windshield, using the fifty element model and a finer solid element model which has been prepared for dynamic stress studies under impact conditions. The finer mesh, shown in Figure 6.5.7 consists of 189 sixteen-node elements (Element Type 8), 1256 nodes, and 3450 active degrees of freedom. Results for the two lowest frequencies using the solid element models and the associated computing times are compared in Table 6.5.1. The slightly higher frequencies obtained with the 189-element model are due to a slightly higher value of the modulus having been used.

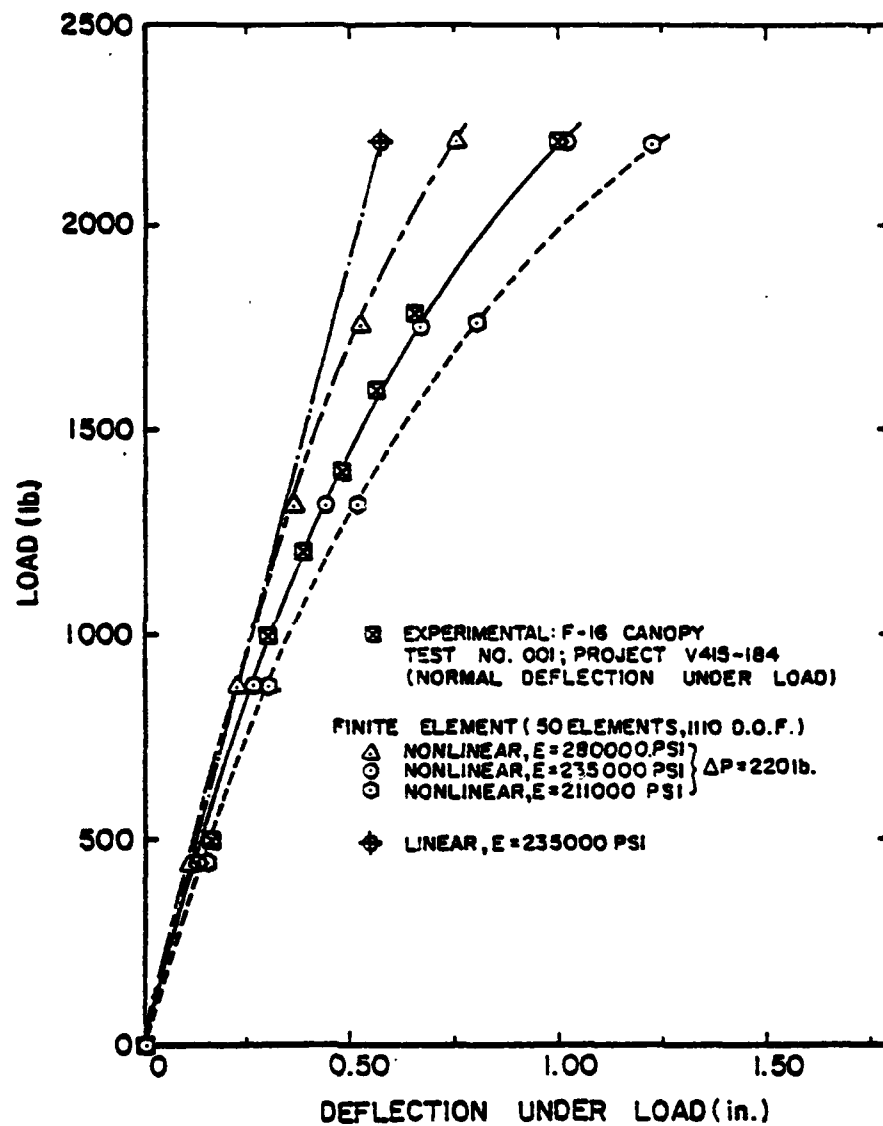


Figure 6.5.3 Nonlinear Static Response of Windshield Canopy (Solid Element Model).

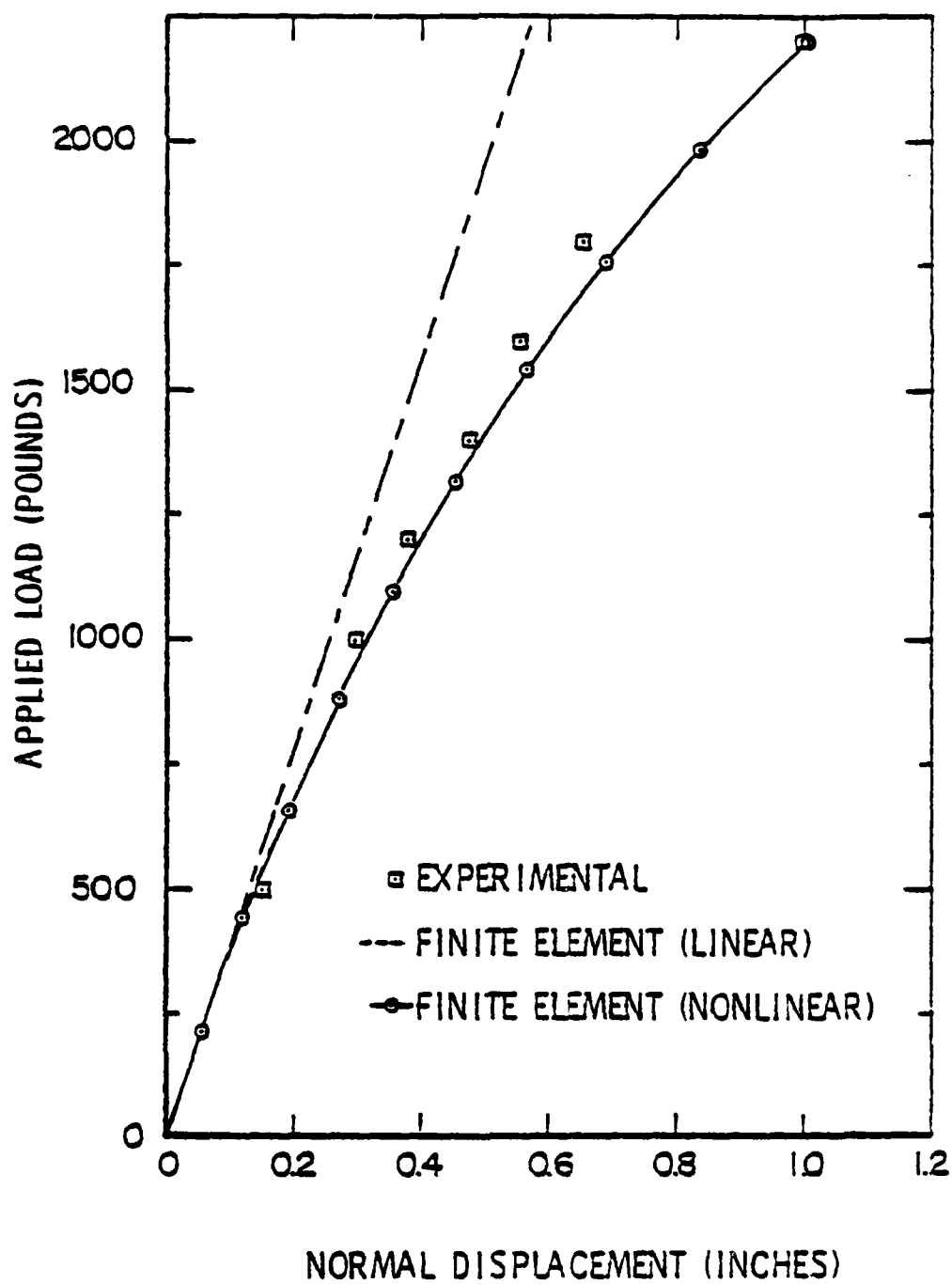


Figure 6.5.4 Nonlinear Static Response of Windshield Canopy (Shell Element Model).

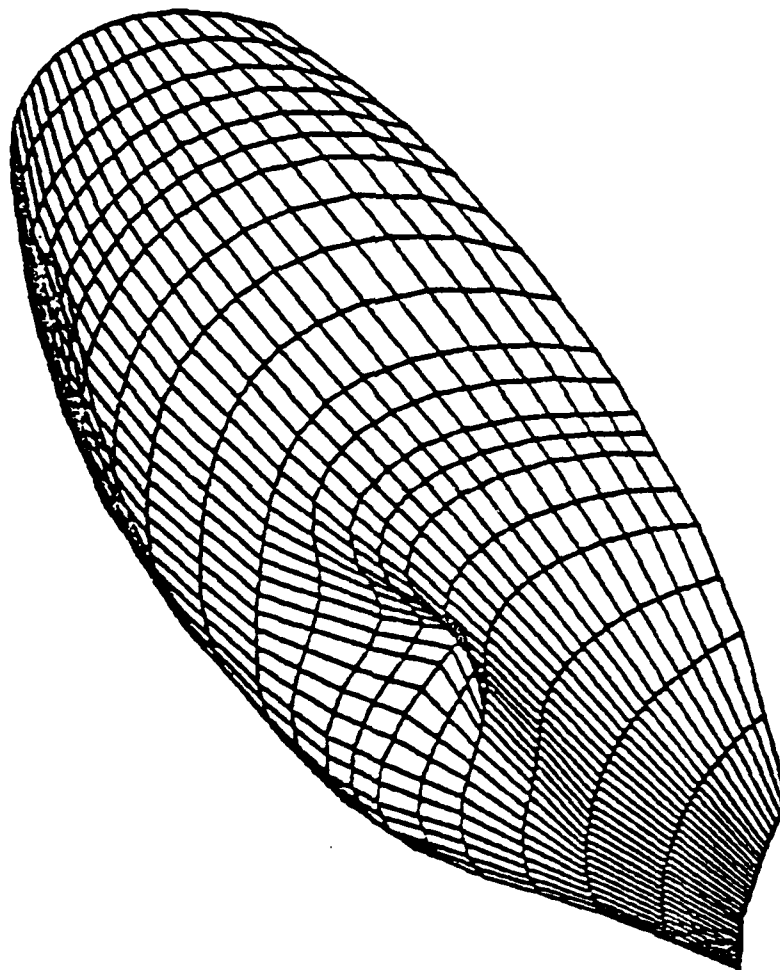


Figure 6.5.5 Deformed Geometry of F-16 Windshield Under Static Loading.

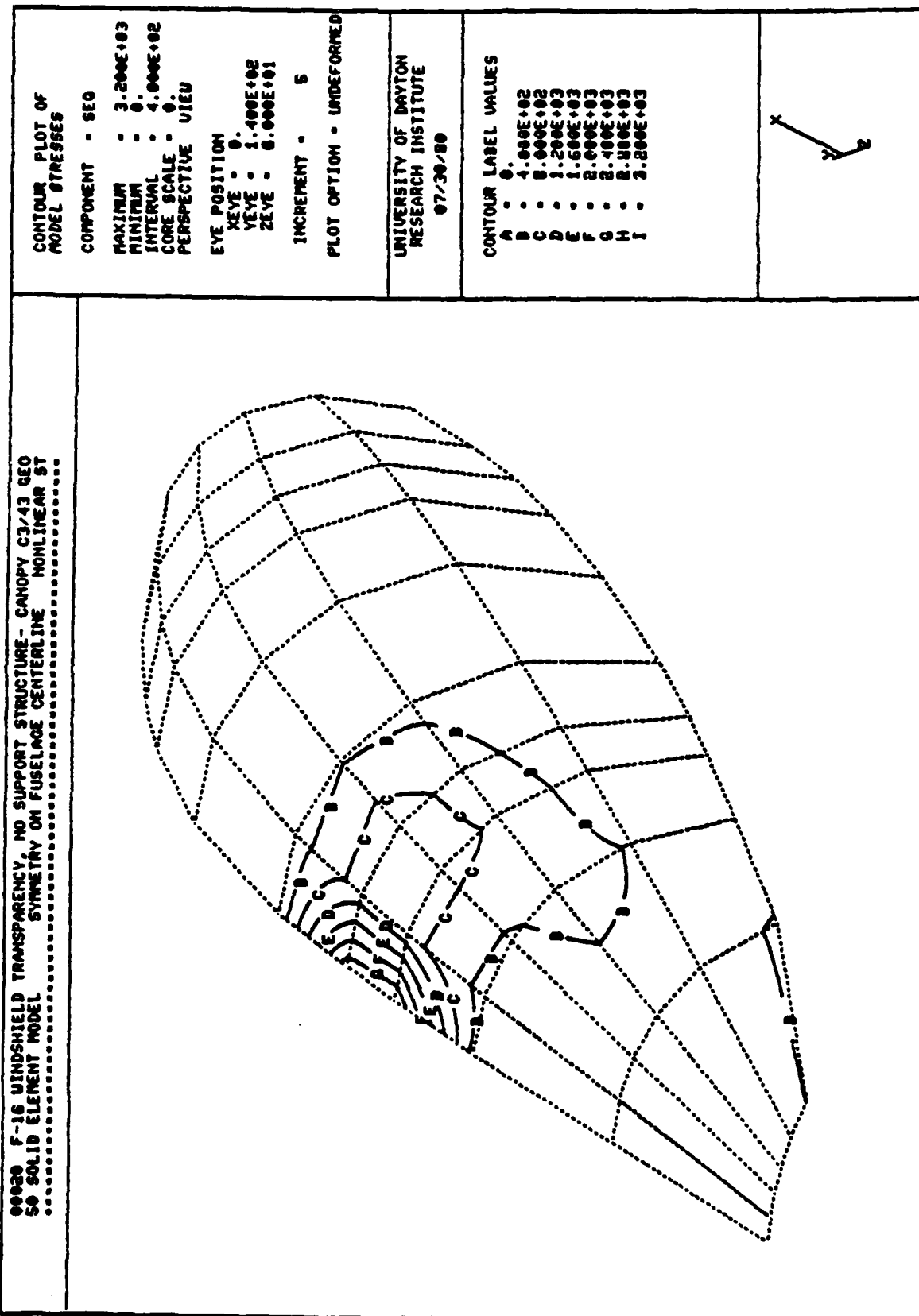


Figure 6.5.6 Equivalent Stress Contours on Windshield Surface for 1100-Pound Static Load.

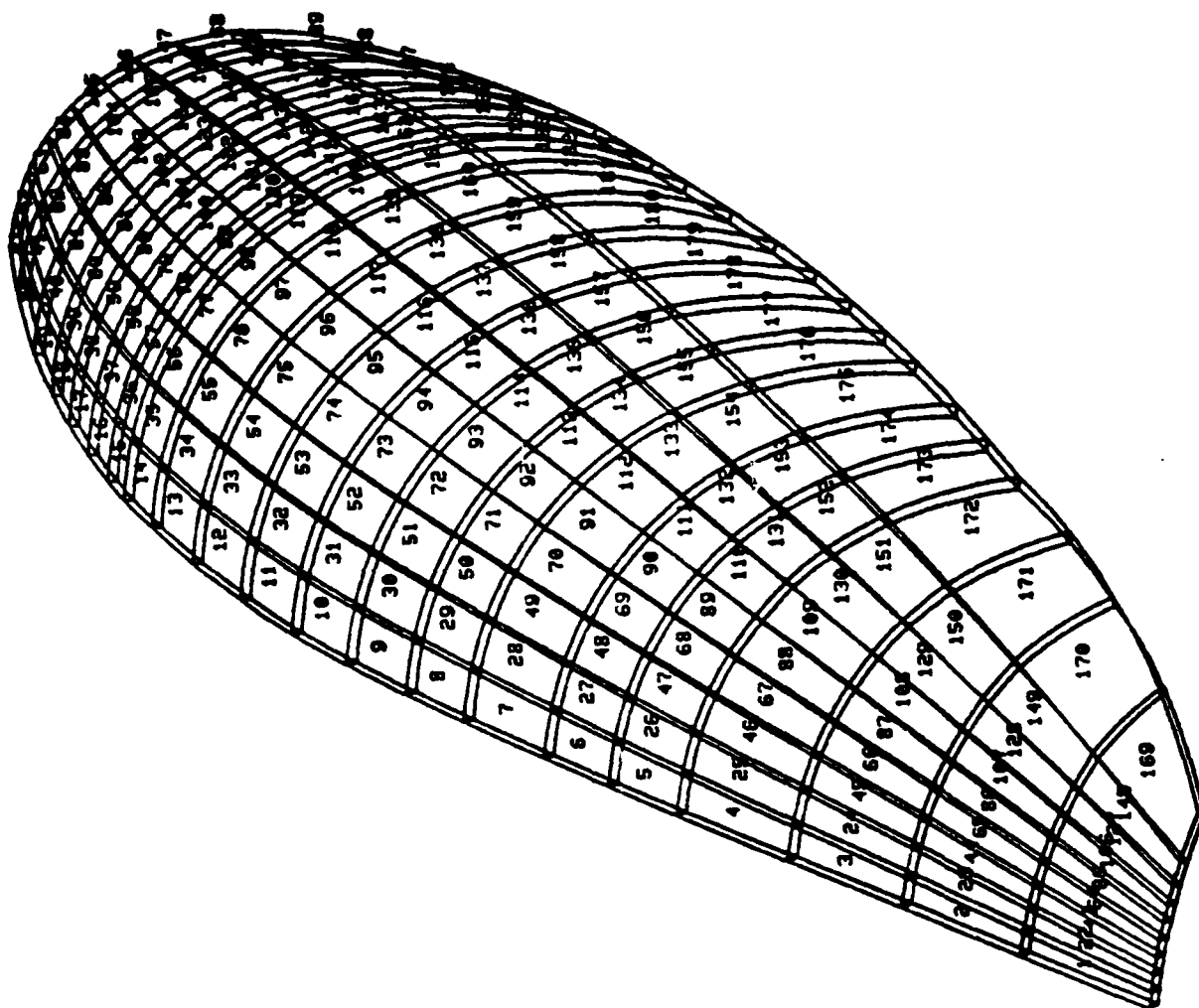


Figure 6.5.7 Solid Element Model of Windshield Canopy (189 Elements).

TABLE 6.5.1
SUMMARY OF NATURAL FREQUENCY CALCULATIONS
FOR TACTICAL FIGHTER WINDSHIELD (3-D ELEMENTS)

| Model No. | 1 | 2 | 3 |
|---------------------|-------|--------|-------|
| Nodes | 428 | 1256 | 1256 |
| Degrees of Freedom | 1110 | 3450 | 3450 |
| Elements | 50 | 189 | 189 |
| Integration | 3x3x3 | 14 pt. | 2x2x2 |
| ω_1 (Hz.) | 51.0 | 55.3 | 55.2 |
| ω_2 (Hz.) | 70.4 | 73.3 | 73.9 |
| CPU Sec (CYBER 175) | 49. | 182. | 173. |

6.6 STRESS CONCENTRATION IN A THIN PERFORATED SHEET

A thin plate with a circular hole is subjected to a uniform axial tension load, as shown in Figure 6.6.1. The ratio of plate width to hole diameter is 2:1. For small elastic deformations, the analytical solution for longitudinal stresses at the hole edge and the outer edge of the plate are given by Timoshenko¹:

$$\sigma_y = 4.30 S, \text{ at point A (edge of hole)}$$

$$\sigma_y = 0.75 S, \text{ at point B (edge of plate)}$$

where S is the applied average stress.

The finite element discretization, consisting of 56 four-node plane stress elements (Element Type 3), is indicated in Figure 6.6.2. Only one quadrant of the plate is modeled, taking advantage of symmetry. The hole diameter is two inches, and the total length of the plate is 20 inches. Material properties typical of aluminum ($E = 10^7$ psi, $\nu = 0.30$) are used in the numerical solution.

Longitudinal stresses computed at the centerline \overline{AB} (i.e., $y = 0$.) are plotted in Figure 6.6.3, for an applied stress $S = 50$ psi. Linear extrapolation of the integration point stresses to the inner and outer edges of the sheet yields

$$\sigma_y = 4.19 S \text{ at point A}$$

$$\sigma_y = 0.75 S \text{ at point B}$$

which are in good agreement with the analytical solution.

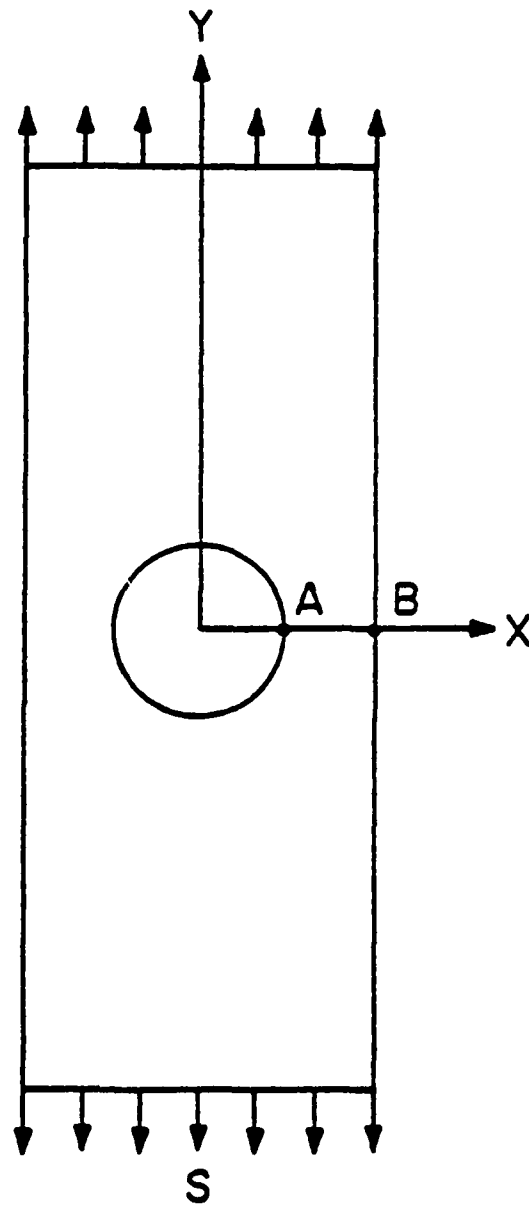


Figure 6.6.1 Thin Sheet with a Circular Hole.

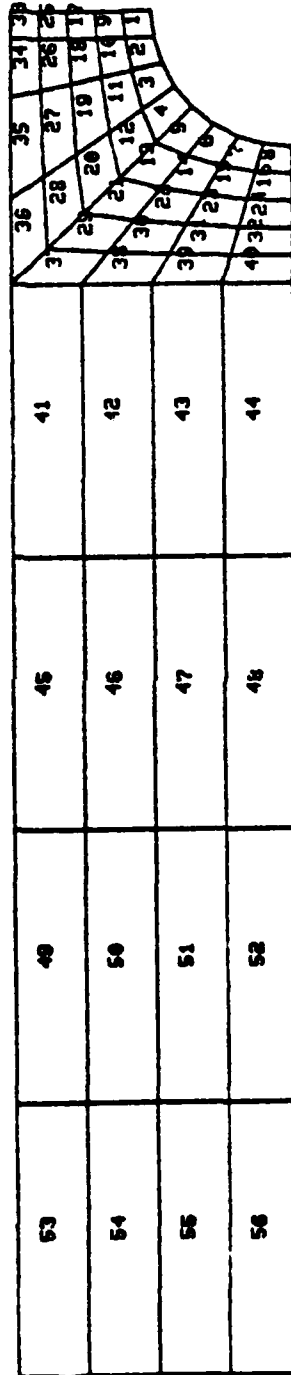


Figure 6.6.2 Finite Element Model of Perforated Sheet.

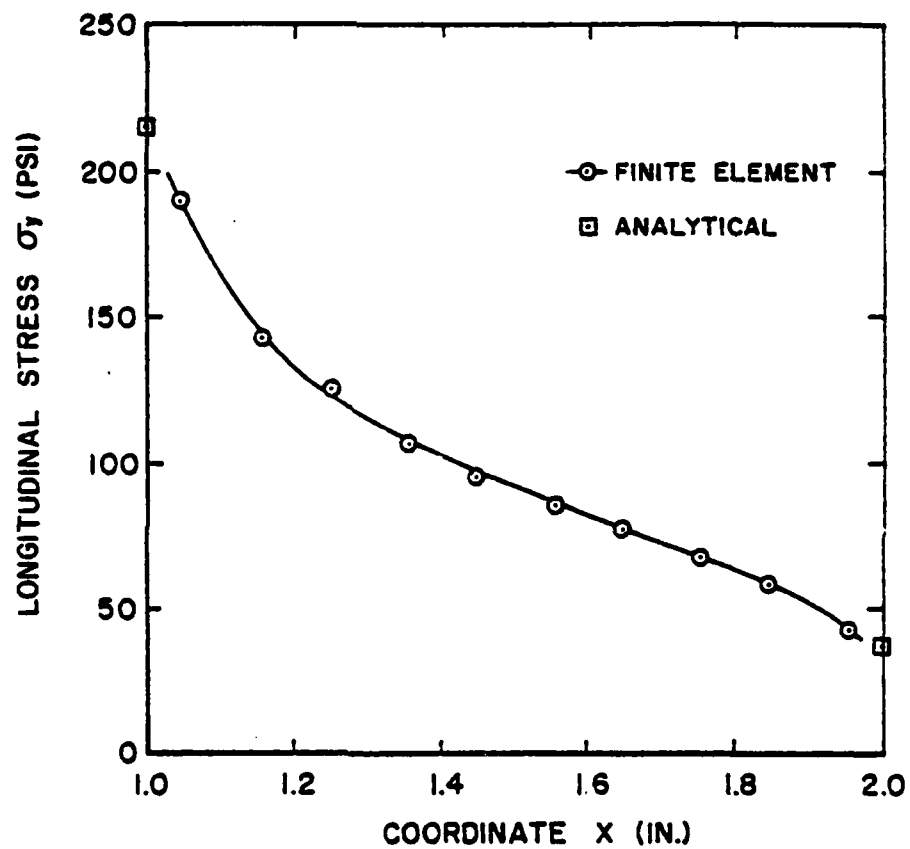


Figure 6.6.3 Longitudinal Stress Distribution in Perforated Sheet at Edge of Symmetry.

6.7 ELASTIC-PLASTIC, LARGE DISPLACEMENT ANALYSIS OF A TWO-BAY TRUSS

The ten member truss shown in Figure 6.7.1 has been analyzed for its static response due to a single concentrated load. Both material and geometric nonlinearities are considered in the solution. The same truss has been analyzed by Mondkar and Powell¹ and Goldberg and Richard², using the displacement method, and by Noor³ using a mixed force and displacement approximation.

Horizontal members of the truss are assigned areas of 0.25 square inches; the vertical and diagonal elements are 0.20 square inches. The truss material is defined by a Ramberg-Osgood stress-strain relation of the form

$$\frac{\epsilon}{\epsilon_0} = \frac{\sigma}{\sigma_0} \left[1 + a \left(\frac{\sigma}{\sigma_0} \right)^n \right]$$

in which $a = 3/7$, $n = 6$, the yield stress $\sigma_0 = 40520$ psi, and the corresponding strain is $\epsilon_0 = 0.004052$ in./in. Young's modulus for the material is, therefore, $E = 1.0 \times 10^7$ psi. In the numerical solution, the Ramberg-Osgood curve has been approximated by a piecewise linear stress-strain path with ten segments, and an isotropic strain hardening law.

The load-deflection curve predicted using MAGNA for a range of applied loads between 0 and 15,200 pounds is shown in Figure 6.7.2. A load increment of 400 pounds has been used in this solution. First yielding in the structure occurs in element 1 at a load of about 5500 pounds, below which the response is very nearly linear. Nonlinearities due to large displacements appear to be minor for the entire range of loading considered.

Complete results of the analysis at an applied load of 10,000 pounds are presented in Table 6.7.1. Computed values shown in the table have been obtained using two load incrementation

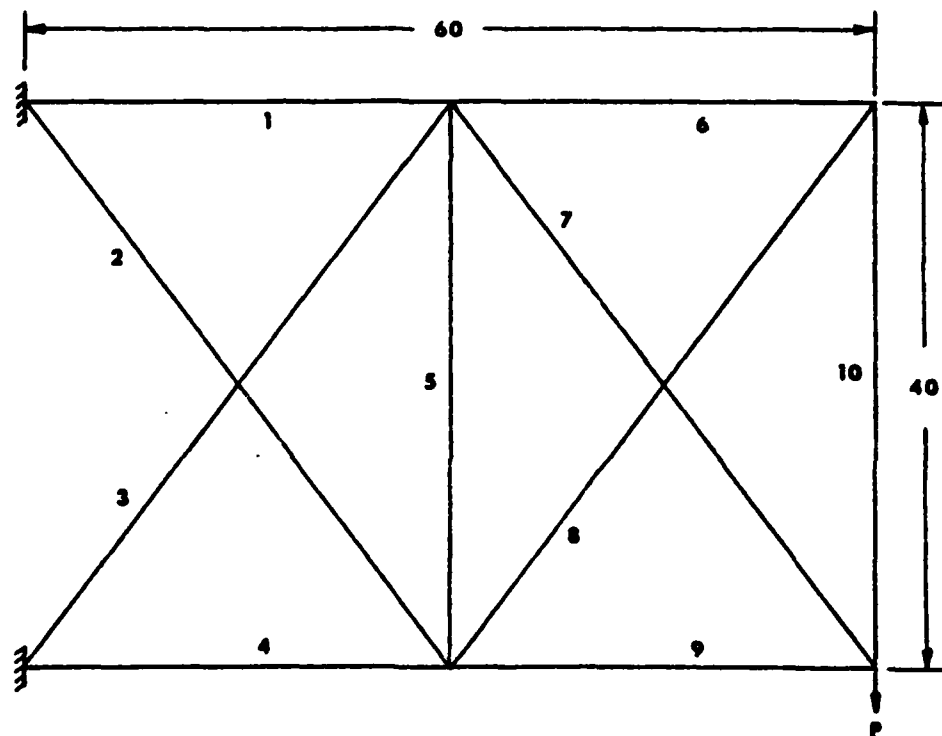


Figure 6.7.1 Two-Bay Plane Truss Structure.

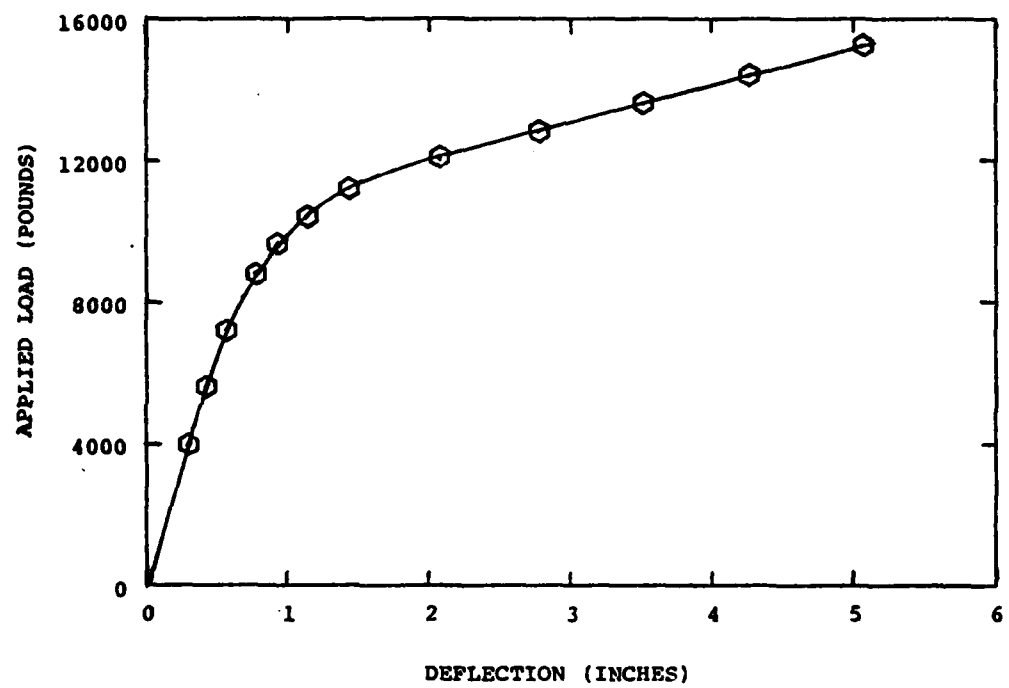


Figure 6.7.2 Nonlinear Elastic-Plastic Response of Two-Bay Plane Truss.

TABLE 6.7.1
SUMMARY OF RESULTS FOR TWO-BAY PLANE TRUSS
AT APPLIED LOAD OF 10,000 POUNDS

| Element | Area | Length | Strain | Plastic Strain | Stress | Force |
|---------|------|--------|----------|----------------|---------|---------|
| 1 | 0.25 | 30. | 0.00791 | 0.00344 | 44702. | 11176. |
| 2 | 0.20 | 50. | 0.00332 | 0.00025 | 30690. | 6138. |
| 3 | 0.20 | 50. | -0.00352 | -0.00035 | -31703. | -6341. |
| 4 | 0.25 | 30. | -0.00786 | -0.00339 | -44723. | -11181. |
| 5 | 0.20 | 40. | -0.00026 | 0. | -2621. | -524. |
| 6 | 0.25 | 30. | 0.00133 | 0. | 13341. | 3335. |
| 7 | 0.20 | 50. | 0.00405 | 0.00059 | 34669. | 6934. |
| 8 | 0.20 | 50. | -0.00290 | -0.00012 | -27834. | -5567. |
| 9 | 0.25 | 30. | -0.00161 | 0. | -16108. | -4027. |
| 10 | 0.20 | 40. | 0.00222 | 0. | 22230. | -446. |

Note: Dimensions in inches, pounds, and pounds per square inch;
strains are in inches per inch.

schemes: (1) 25 equal increments of 400 pounds each, and (2) a single 10,000 pound step, followed by Newton-Raphson iterations. Results of the two analyses are in agreement to within less than one percent. At this point, all elements in the truss have yielded except for the vertical posts and the two outermost horizontal members. Individual member forces predicted by MAGNA are compared with those reported in References 1-3 in Table 6.7.2, and the corresponding deflection results are given in Table 6.7.3. The four solutions are in excellent qualitative agreement; most of the numerical differences noted are attributable to the details of analyzing material nonlinearities in each analysis. For example, the solution of Reference 1 simulates the nonlinear Ramberg-Osgood material curve using a series of elastic, perfectly plastic parallel material elements, while the present analysis employs a piecewise linear stress-strain curve and isotropic strain hardening.

TABLE 6.7.2
TRUSS ELEMENT FORCES IN TWO-RAY TRUSS
AT APPLIED LOAD OF 10 KIPS

| Element | Total Force in kips, at P = 10.0 kip | | | |
|---------|--------------------------------------|------------------|----------|--------|
| | MAGNA | Mondkar & Powell | Goldberg | Noor |
| 1 | 11.18 | 11.27 | 11.26 | 11.28 |
| 2 | 6.14 | 6.19 | 6.18 | 6.19 |
| 3 | -6.34 | -6.30 | -6.31 | -6.31 |
| 4 | -11.18 | -11.20 | -11.19 | -11.21 |
| 5 | -0.52 | -0.50 | -0.58 | -0.51 |
| 6 | 3.34 | 3.34 | 3.27 | 3.33 |
| 7 | 6.93 | 6.92 | 7.04 | 6.94 |
| 8 | -5.57 | -5.57 | -5.46 | -5.56 |
| 9 | -4.03 | -4.16 | -4.22 | -4.17 |
| 10 | 4.45 | 4.46 | 4.37 | 4.45 |

TABLE 6.7.3
COMPARISON OF MAXIMUM DISPLACEMENTS OF TWO-BAY TRUSS
AT LOAD P = 10000 POUNDS

| | |
|-------------------|------------|
| MAGNA* | 1.0388 in. |
| Mondkar & Powell* | 1.0511 in. |
| Goldberg* | 0.923 in. |
| Noor** | 1.0574 in. |

* Displacement Method

** Mixed Force and Displacement Method

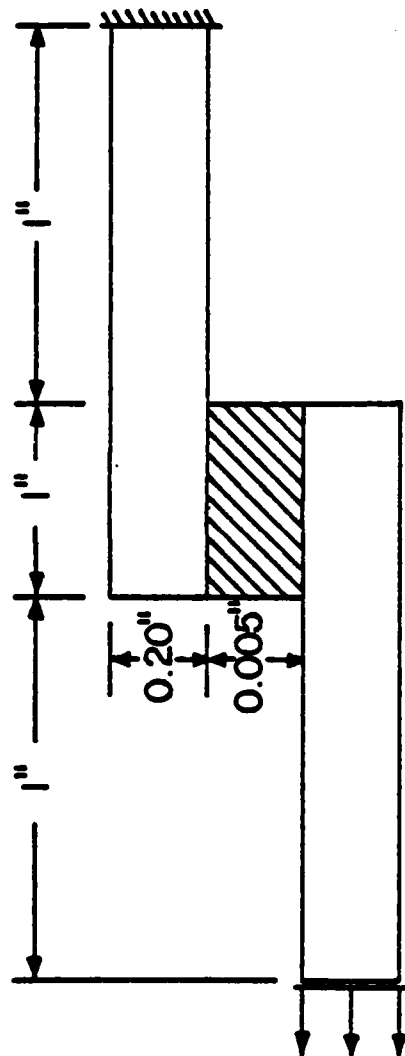
6.8 STRESS DISTRIBUTIONS IN A SINGLE-LAP BONDED JOINT

The elastic, small-displacement response of a single lap adhesive joint is considered, to determine the shear and normal stress distributions within the adhesive layer. The particular joint considered, shown in Figure 6.8.1, consists of 0.020 inch aluminum adherends joined by a 0.005 inch layer of HYSOL EA 9601 adhesive. Material properties are listed in the figure. This problem has been studied previously by Dickson¹, using the special-purpose computer program BONJO²; Reference 1 also presents an analytical solution obtained by the method of Goland and Reissner³.

The solution for the adhesive stresses has been performed using 144 Type 3 (Plane Stress) elements in MAGNA; each adherend is modeled with 52 four-node elements, while 40 elements are used in the adhesive layer. One end of the joint is completely fixed, while the loaded end is constrained to move only in the direction parallel to the applied forces. The finite element grid for the problem is shown in Figure 6.8.2.

Adhesive stress profiles corresponding to an applied load of 1000 pounds are indicated in Figures 6.8.3 and 6.8.4. Both the shear and normal stress are nearly constant through the thickness of the joint, but vary rapidly along the bond line direction. Agreement between the MAGNA and BONJO analyses is reasonably good, but the finite element grid is too coarse to resolve the shear stress distribution at the extreme ends of the bond line, where a sharp peak is observed before the shear stress vanishes at the free boundary. The MAGNA analysis also predicts a lower maximum normal stress at the joint edge, and hence a lower compressive stress near the center of the joint.

It is interesting to note the sensitivity of the computed stress distributions to the boundary conditions applied at the loaded end of the specimen. When transverse displacements of the loaded edge are permitted, the peak shear and normal stresses



ADHERENDS (ALUMINUM) ADHESIVE (HYSOL EA-9601)

$E = 10.5 \times 10^6$
 $\nu = 0.3125$

$E = 2600000$
 $\nu = 0.30$

Figure 6.8.1 Single-Lap Bonded Joint Specimen.

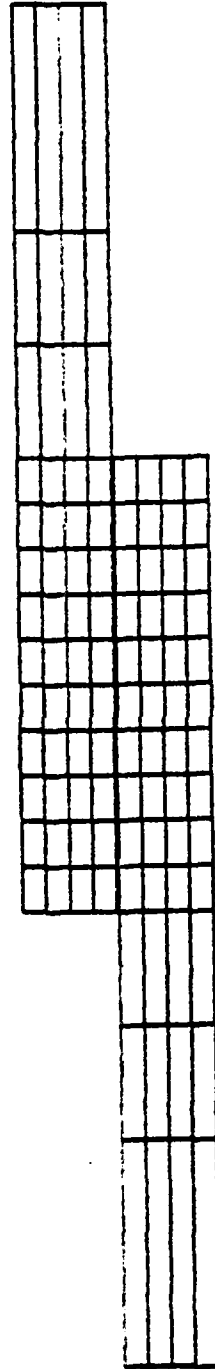


Figure 6.8.2 Finite Element Discretization of Single Lap Joint.

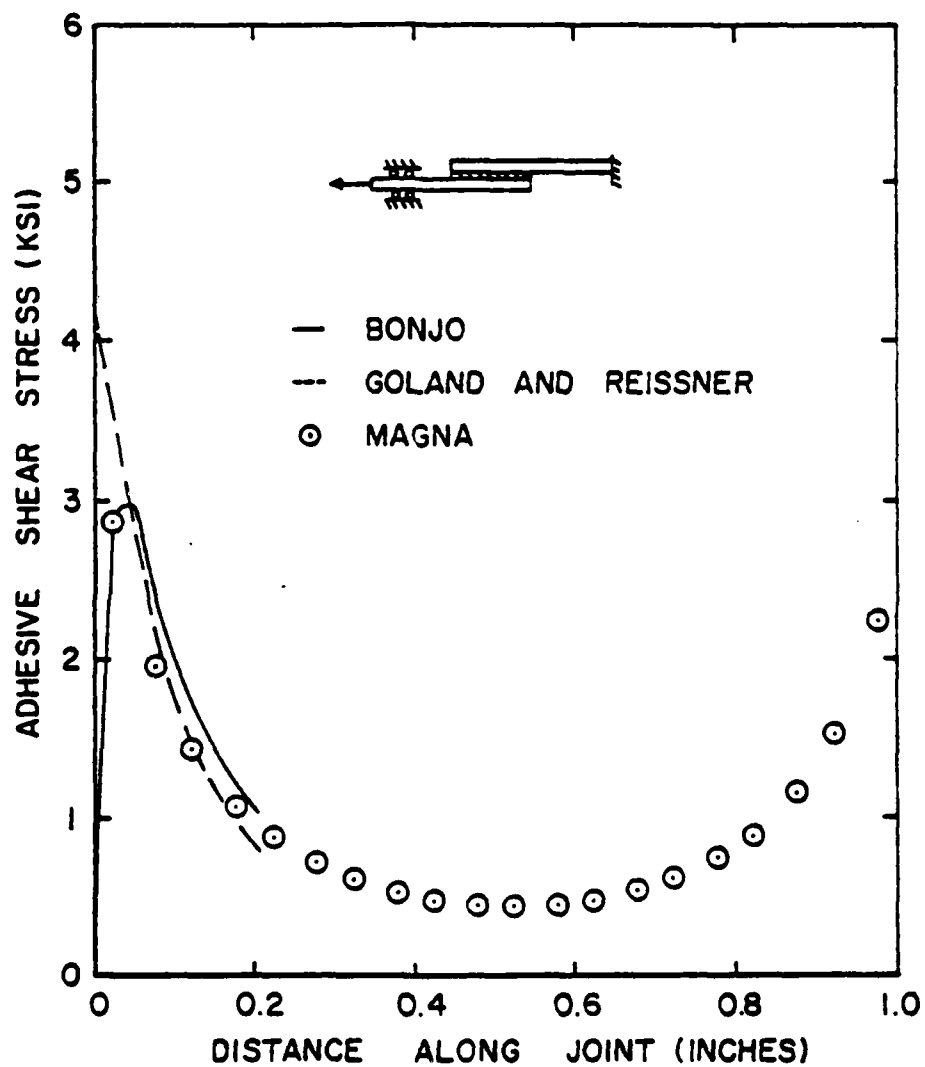


Figure 6.8.3 Adhesive Shear Stress Distribution in Single-Lap Bonded Joint.

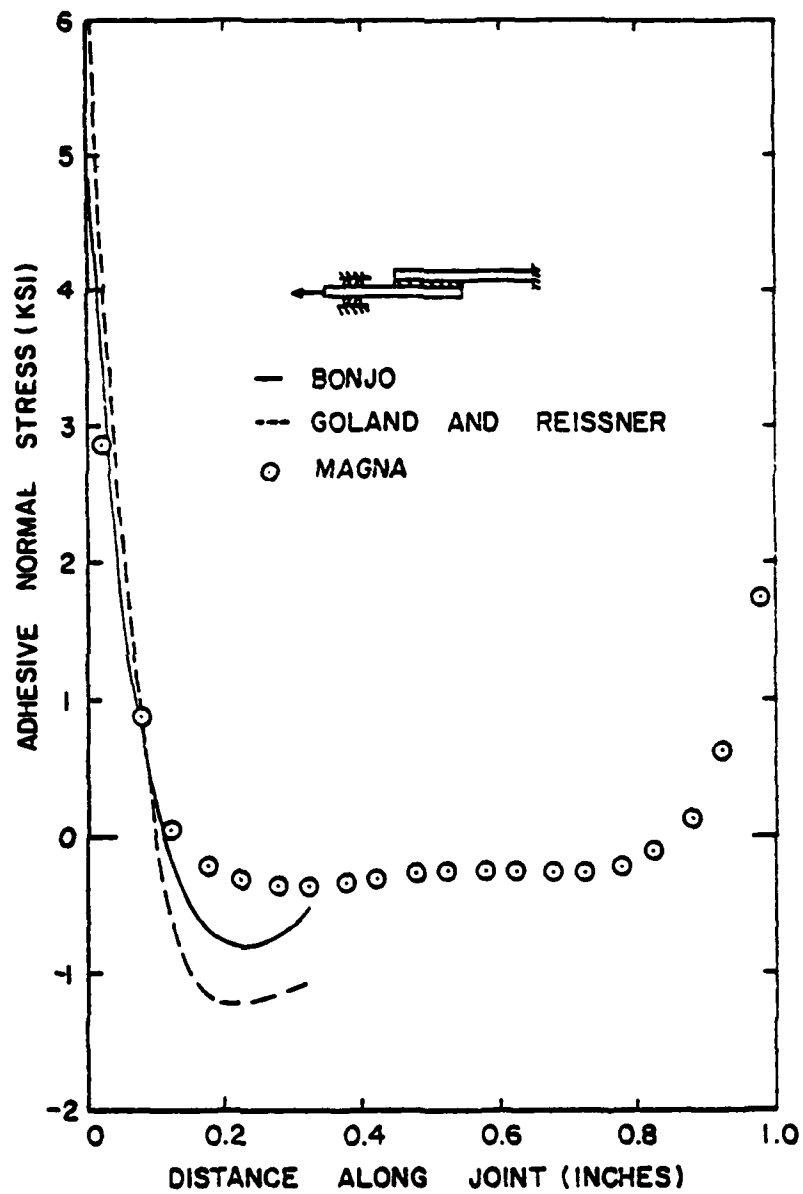


Figure 6.8.4 Adhesive Normal Stress Distribution in Single-Lap Bonded Joint.

become considerably greater, and the largest adhesive stresses are redistributed toward the opposite end of the bond line, as shown in Figure 6.8.5. Figure 6.8.6 shows the displaced geometry of the free-end specimen, with displacements magnified by a factor of ten. Transverse bending is, in this instance, the predominant mode of deformation, due to the eccentricity of the applied loads.

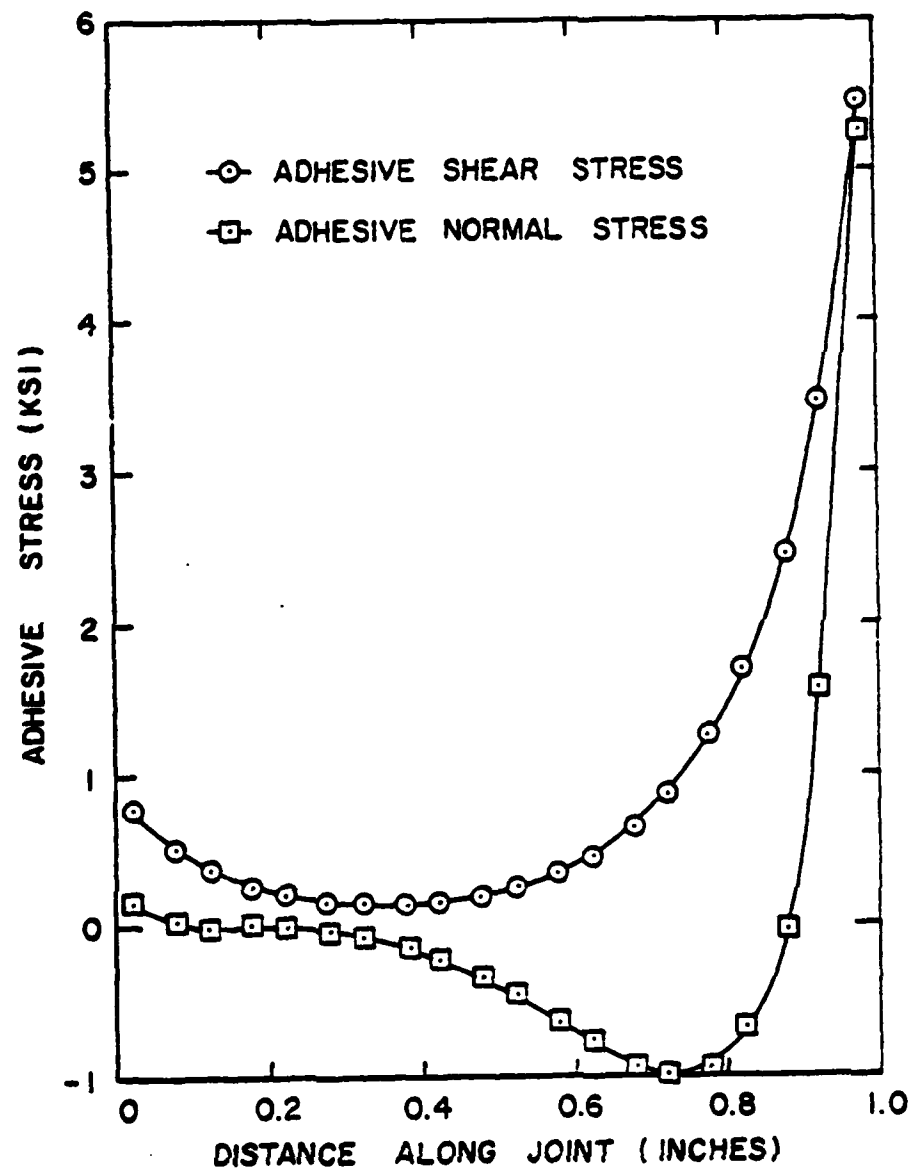


Figure 6.8.5 Adhesive Stress Distributions for Free-End Bonded Joint Specimen.

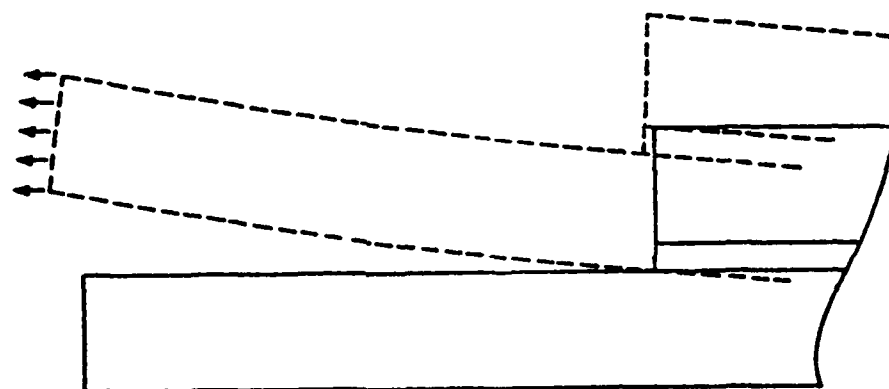


Figure 6.8.6 Displaced Shape of Free-End Bonded Joint.

6.9 SANDWICH PLATE UNDER UNIFORM PRESSURE

A square sandwich panel, 50 inches on each side, is subjected to a uniform lateral pressure loading. The three-layer plate (Figure 6.9.1) has identical aluminum face sheets ($E = 10.5 \times 10^6$ psi; $\nu = 0.3$), 0.015 inches in thickness, bonded to an aluminum honeycomb core one inch thick. The core is assumed to be isotropic, with shear modulus $G = 50,000$ psi. All lateral boundaries of the sandwich are fully clamped.

Due to the symmetry of the geometry and applied loading, one quarter of the panel is considered in solution. The finite element discretization consists of a total of 75 finite elements, 25 in each layer. The two face sheets are modeled using eight-node, thin shell elements (Element Type 5). Three-dimensional, eight-node solid elements (Element Type 2), with a single integration point per element, are used for the sandwich core. Note that these element types are fully compatible, so that no special constraints are necessary for joining the shell and solid layers. The nonlinear solution has been obtained in load increments of one psi to a total pressure of 20 psi, followed by two psi increments to 30 psi.

The nonlinear central displacement of the sandwich is plotted versus load in Figure 6.9.2. Nonlinear finite element results obtained by Monforton¹, using sixteen specially formulated bicubic sandwich elements, are shown for comparison. Agreement between the two finite element solutions is quite good. Figure 6.9.2 also shows the perturbation solution of Kan and Huang², given by

$$q = 10.5299w_c + 4.8550w_c^3 \quad (6.9.1)$$

in which q is the applied pressure and w_c the transverse center displacement. The analytical solution of Reference 2 is valid for deflections which are smaller than the core thickness, and reasonable agreement with the two numerical

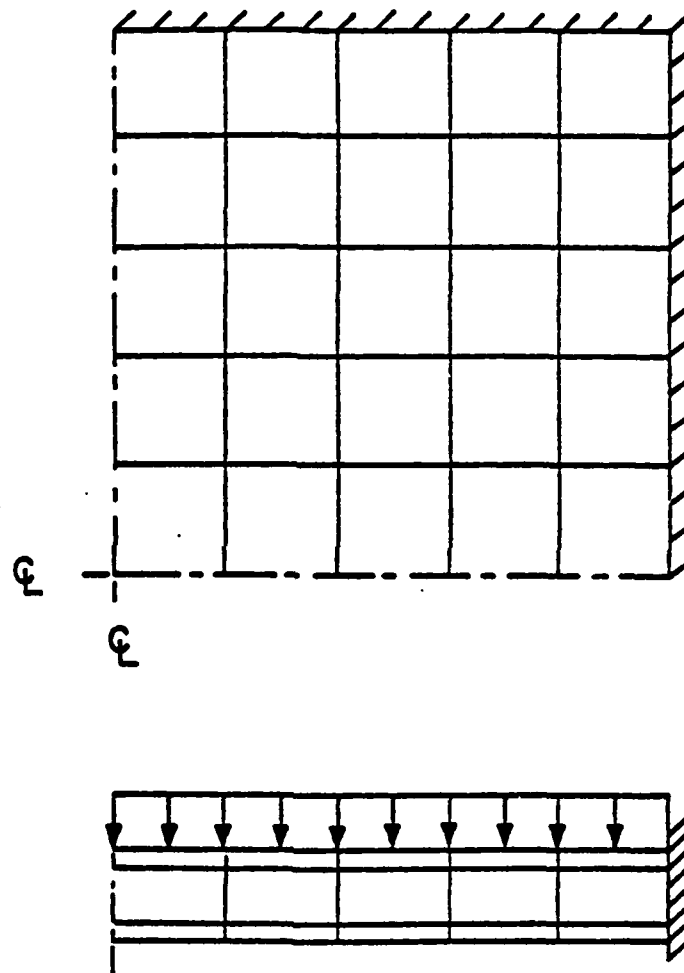


Figure 6.9.1 Three-Layer Sandwich Panel under Pressure Loading.

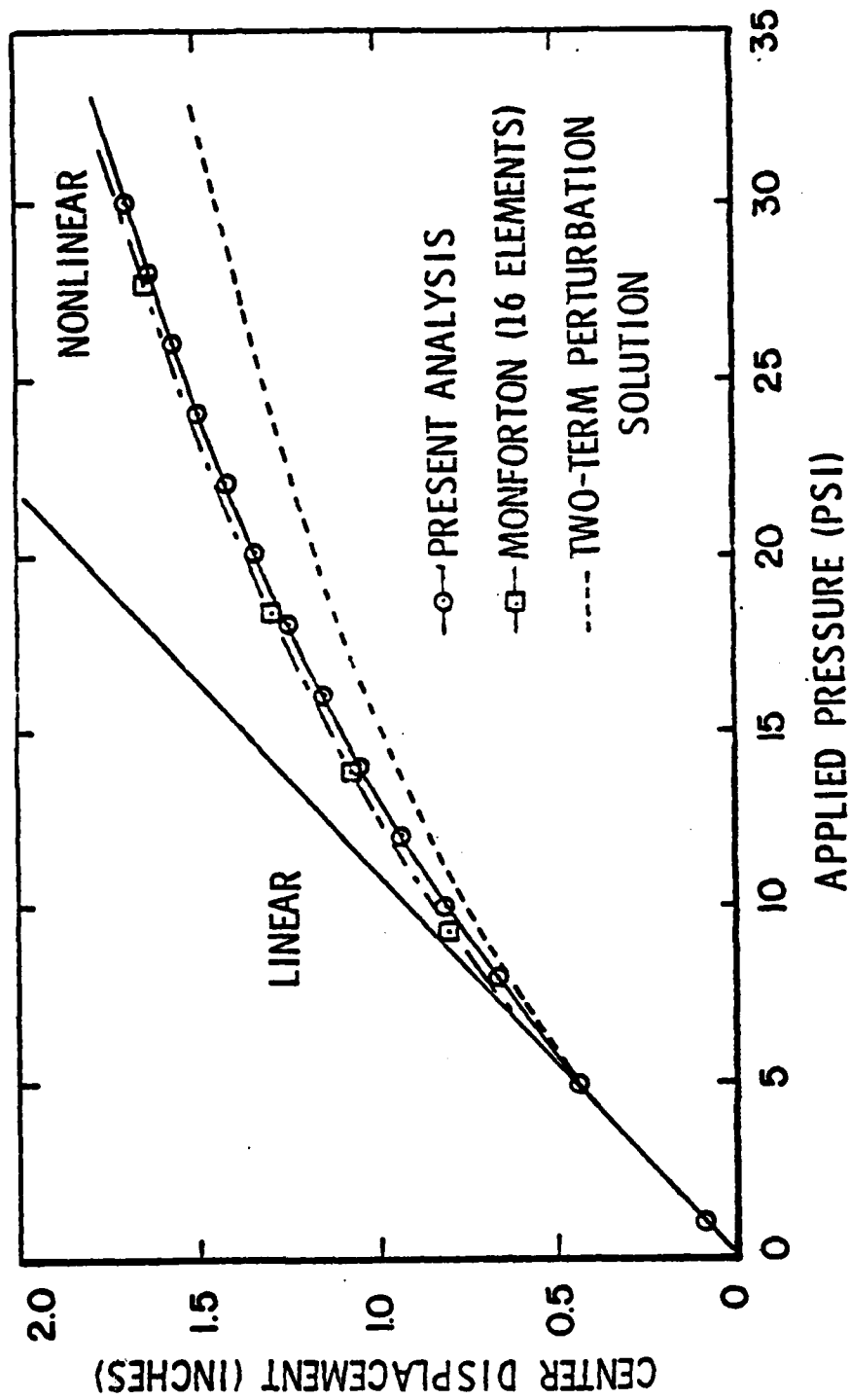


Figure 6.9.2 Load-Deflection Results for Uniformly Loaded Sandwich Plate.

solutions is observed in this region. For larger deflections, the perturbation analysis requires more terms for acceptable accuracy; the two-term solution gives results which overestimate the influence of membrane stiffening upon the panel deflection.

6.10 LARGE DISPLACEMENTS AND ROTATIONS OF A DEEP ARCH

A deep, clamped-hinged arch (Figure 6.10.1) is subjected to a concentrated vertical load at the crown. Due to the asymmetry of the edge conditions, the arch is capable of executing extremely large, stable deflections prior to the onset of buckling. This behavior has been studied experimentally by Deutsch¹, and an analytical solution based upon Euler's inextensional theory (the elastica) has been presented by DaDeppo and Schmidt². The prebuckling displacements, which can be similar in magnitude to the radius of curvature, are accompanied by very large rotations; thus, the prediction of the arch response presents a demanding test of a finite element solution using thin shell elements.

The particular arch under consideration has radius of curvature $R = 100$ inches, thickness $t = 1.0$ inches, and a flexural rigidity of $EI = 1.0 \times 10^6$ lb.-in². The included angle is 215 degrees. For this set of properties, the analysis of Reference 2 indicates that stable behavior occurs up to a load of 897 pounds, at which time the vertical displacement is 113.7 inches. Only prebuckling displacements are considered in the present analysis.

For the MAGNA finite element solution, the entire arch is represented by 43 thin shell elements (Element Type 5), each subtending a sector of five degrees. Displacements normal to the plane of the arch are completely suppressed to permit comparison with the analytical results, which do not account for finite width of the structure. The range of loading considered is 0-870 pounds, applied in six equal increments. Full Newton-Raphson iterations are used to maintain equilibrium, due to the large loading increments and the relatively large incremental rotations expected.

The deformed shape of the arch at maximum loading is shown in Figure 6.10.2. The vertical displacement of the

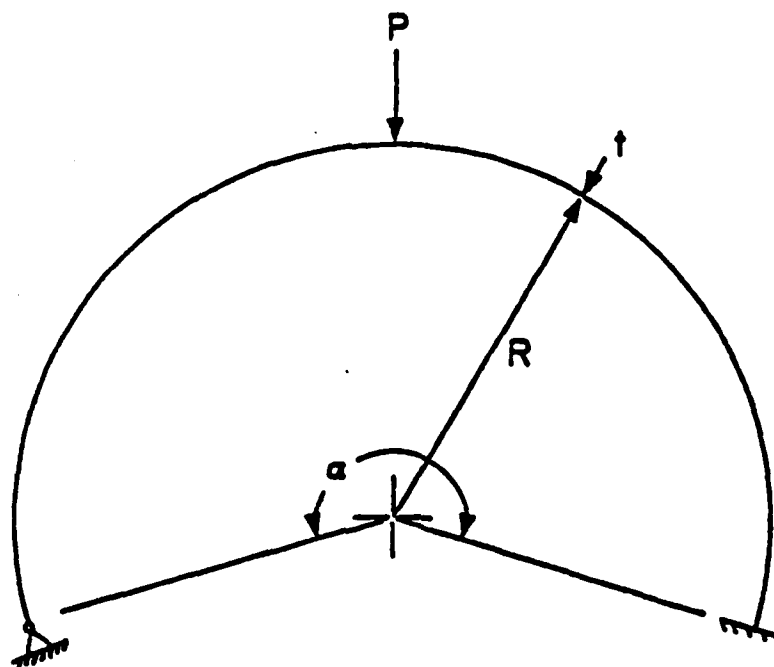


Figure 6.10.1 Deep Arch with Asymmetric Boundary Conditions.

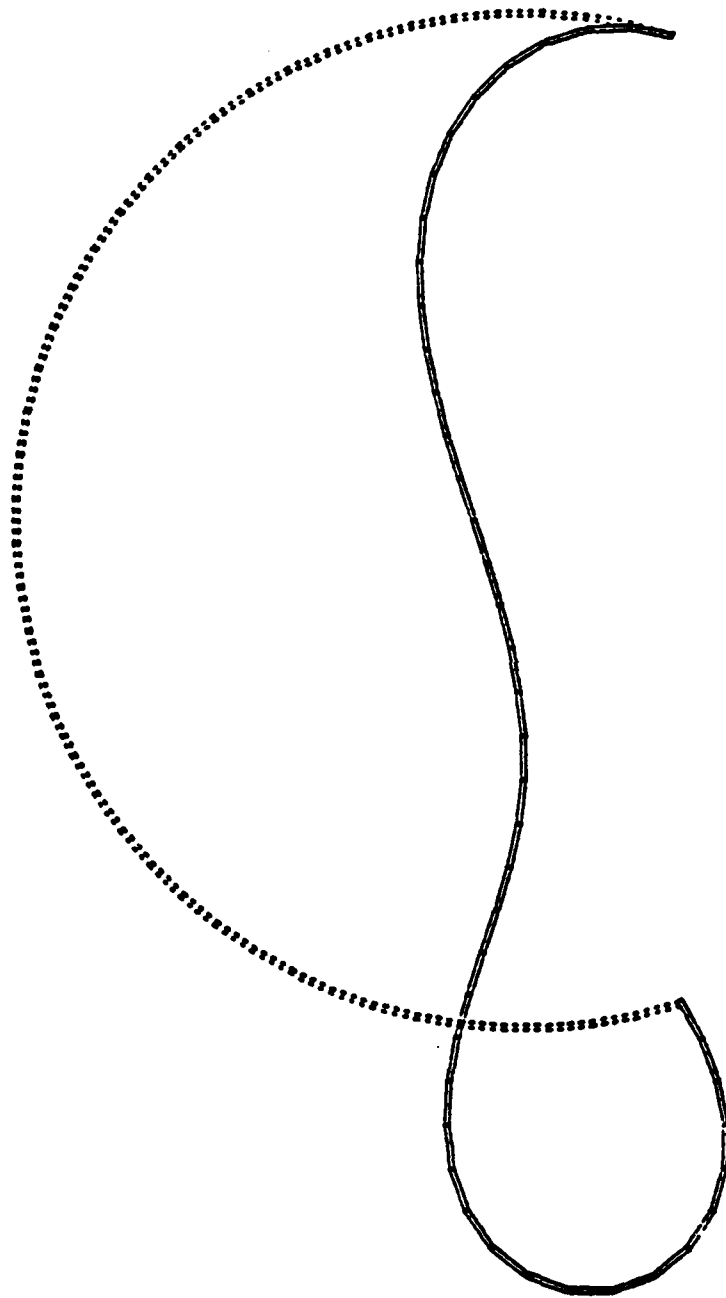


Figure 6.10.2 Deformed Geometry of Clamped-Hinged Arch at Maximum Loading.

arch crown is slightly larger than the radius, and very large rotations (in excess of 120 degrees) are observed near the hinged support. An average of nine Newton iterations per step is required for convergence, with a tolerance of 0.1 on the residual force errors. Finite element results for the entire load-deflection history, obtained using 10-pound increments, are compared with the solution of DaDeppo and Schmidt in Figure 6.10.3. Agreement between the two predictions is quite good. The accuracy of the finite element solution does not diminish, even when predicting rotations which are approximately eight times as large as those which can be considered by the best available shell theories.

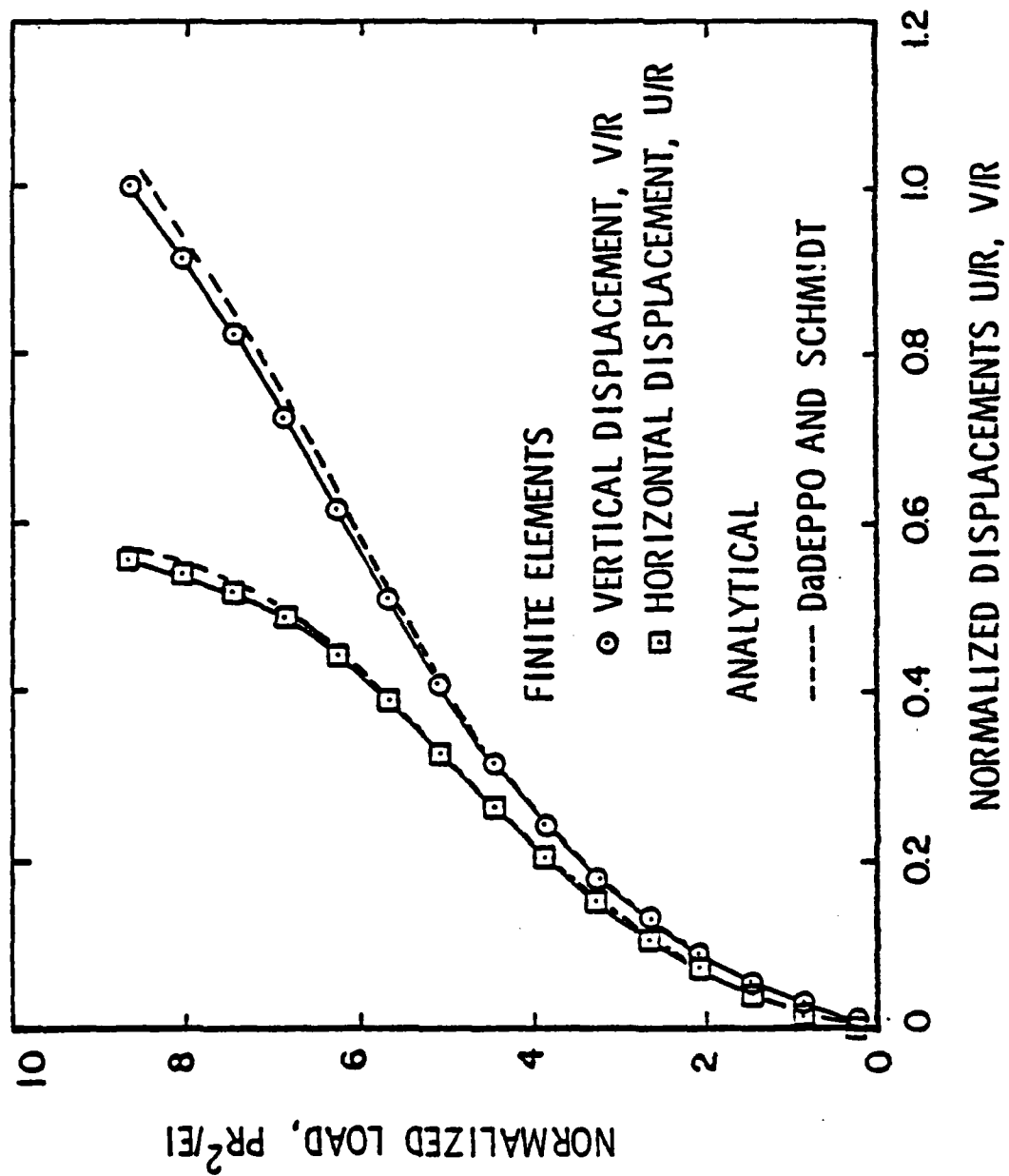


Figure 6.10.3 Comparison of MAGNA Solution with Analytical Results for Deep Arch.

6.11 LARGE DISPLACEMENT, ELASTIC RESPONSE OF A THIN CIRCULAR PLATE

The problem of a circular flat plate under transverse loading provides an example of purely stiffening behavior for increasing load levels. In particular, the clamped plate pictured in Figure 6.11.1, subjected to a concentrated force at the center, is considered. The plate is five inches in radius, and the thickness is $t = 0.1$ inches. Material properties used in the analysis are roughly characteristic of aluminum ($E = 10.92 \times 10^6$ psi, $\nu = 0.30$).

Timoshenko¹ has presented a solution for the linear displacement of the center of the plate as $w_c = Pa^2/16\pi D$, where a is the radius of the plate, P is the applied force, and D is the flexural rigidity, $Et^3/12(1 - \nu^2)$. Using twelve thin shell finite elements (Element Type 5) to model a single quadrant of the plate (Figure 6.11.2), a central deflection of 0.4923 inches is obtained for $P = 1000$ pounds. Compared with the exact value of $w_c = 0.49736$, this displacement is approximately one percent in error. The principal bending stresses (which are largest in the circumferential direction) are computed with a similar degree of accuracy. The exact solution¹ gives for the tangential surface stress

$$\sigma_\theta = \frac{3P}{2\pi t^2} \left[(1 + \nu) \ln \frac{a}{r} - \nu \right], \quad (6.11.1)$$

in which r is the radial coordinate. The computed stress profile (Figure 6.11.3) shows a maximum error of about seven percent, which occurs in the element nearest the center of the plate. It should be noted that the stress distribution is particularly difficult to resolve in this region, since the moments predicted by thin plate theory become infinite at the point of loading. Although the finite element mesh is not refined in the area near the singularity, the stress accuracy of the MAGNA solution is extremely good.

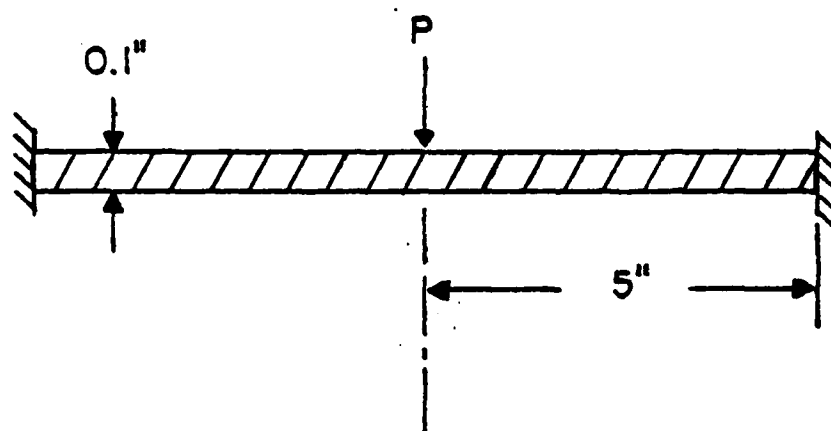


Figure 6.11.1 Clamped Circular Plate.

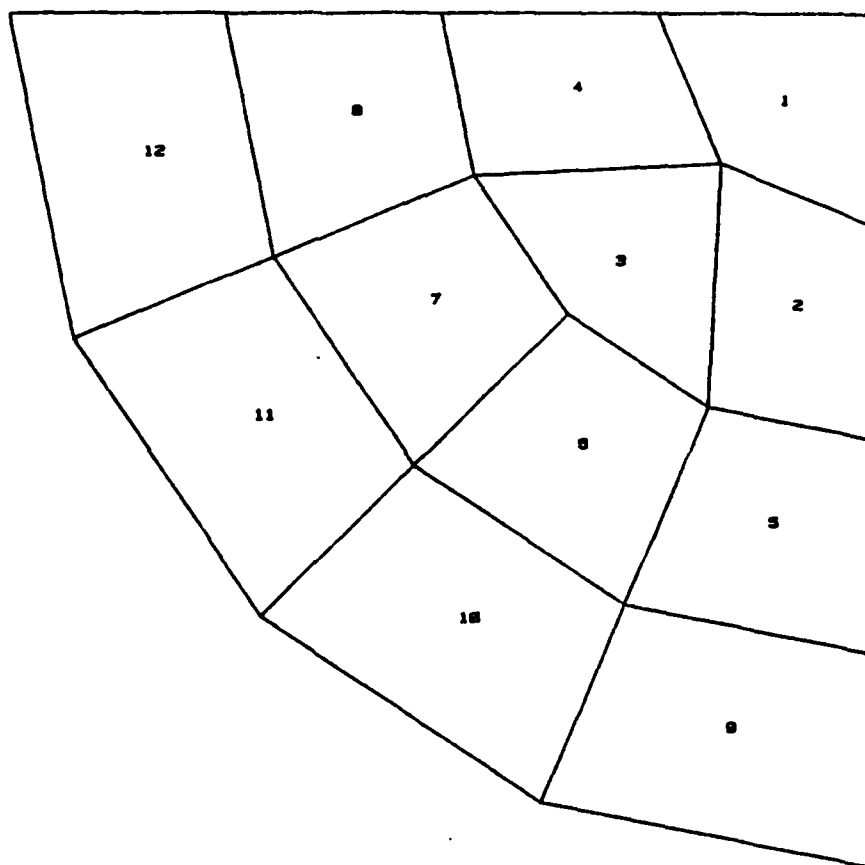


Figure 6.11.2 Thin Shell Element Model of Circular Plate.

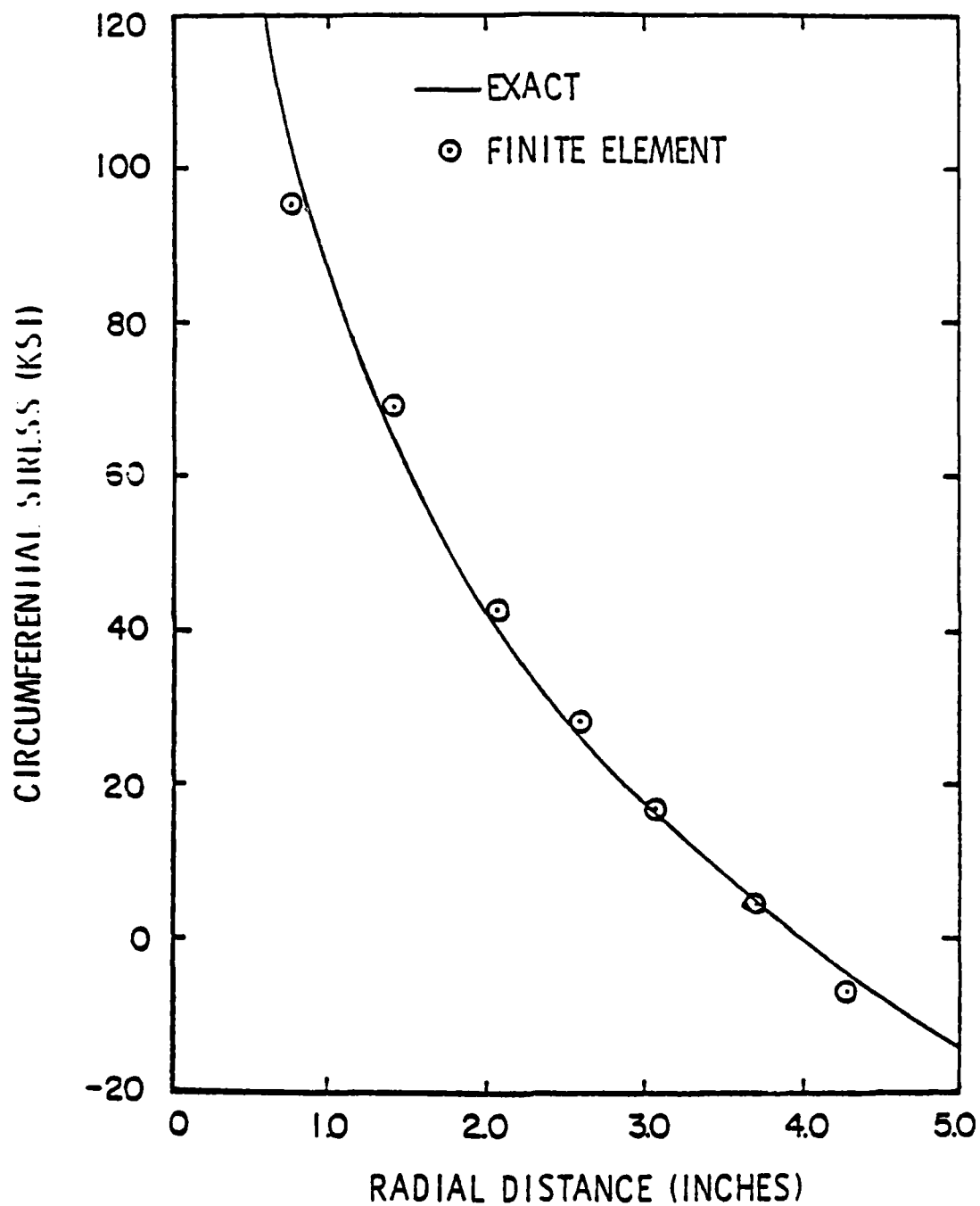


Figure 6.11.3 Radial Distribution of Circumferential Surface Stress in Clamped Circular Plate.

The nonlinear solution for the central displacement of the plate is also given in Reference 1, in the form

$$\frac{w_c}{t} + 0.443 \left(\frac{w_c}{t} \right)^3 = 0.217 \frac{Pa^2}{Et^4} . \quad (6.11.2)$$

This solution corresponds to the case in which inplane displacements at the boundary are prevented, and is valid for deflections which are similar in magnitude to the plate thickness. Using the same twelve-element discretization, a finite element solution has been performed for the range of loading $0 \leq P \leq 3000$ pounds. The numerical results are compared with the analytical solution (Equation 6.11.2) in Figure 6.11.4. Exceptionally good agreement between the two predictions is observed up to deflections which are twice the plate thickness. Beyond this point, Equation 6.11.2 does not apply, and the finite element solution shows a response which is slightly more flexible than the analytical result. Figure 6.11.5 shows the distributions of midplane circumferential stress predicted at selected load levels with the nonlinear finite element model.

It is interesting to note the effect of the midplane tensile stresses in redistributing the internal loading. Surface stresses for a load of 1000 pounds, obtained from the nonlinear solution, are plotted in Figure 6.11.3 for comparison with the linear solution; the relatively small net tension stress in the plate is sufficient to reduce the computed peak bending stresses by approximately a factor of two. Since the applied forces are resisted more efficiently by tensile (rather than bending) stresses, a significant increase in load-carrying capacity is apparent which is not reflected in the linear solution.

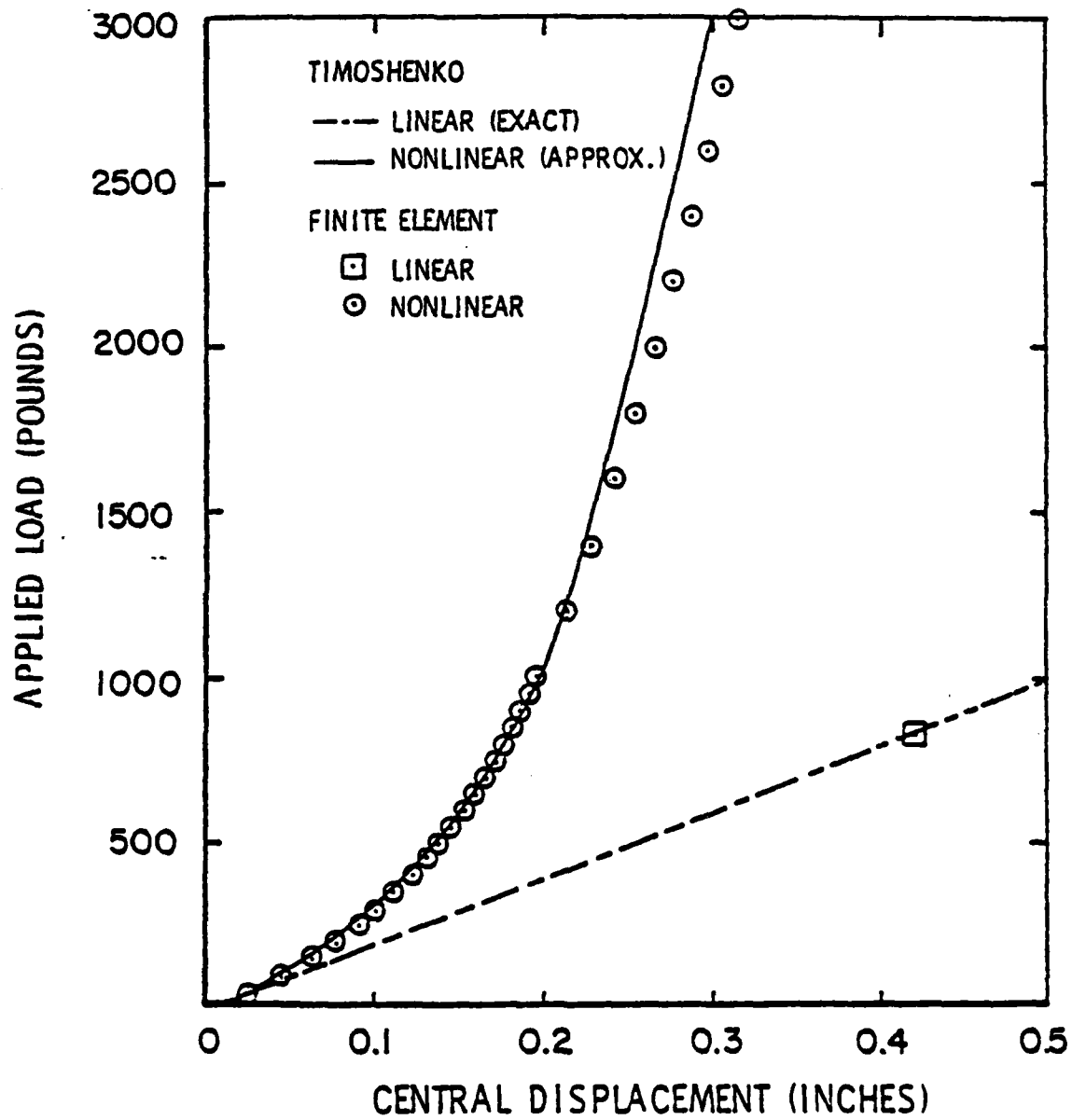


Figure 6.11.4 Load-versus-Deflection Solution for Large Displacements of a Circular Plate.

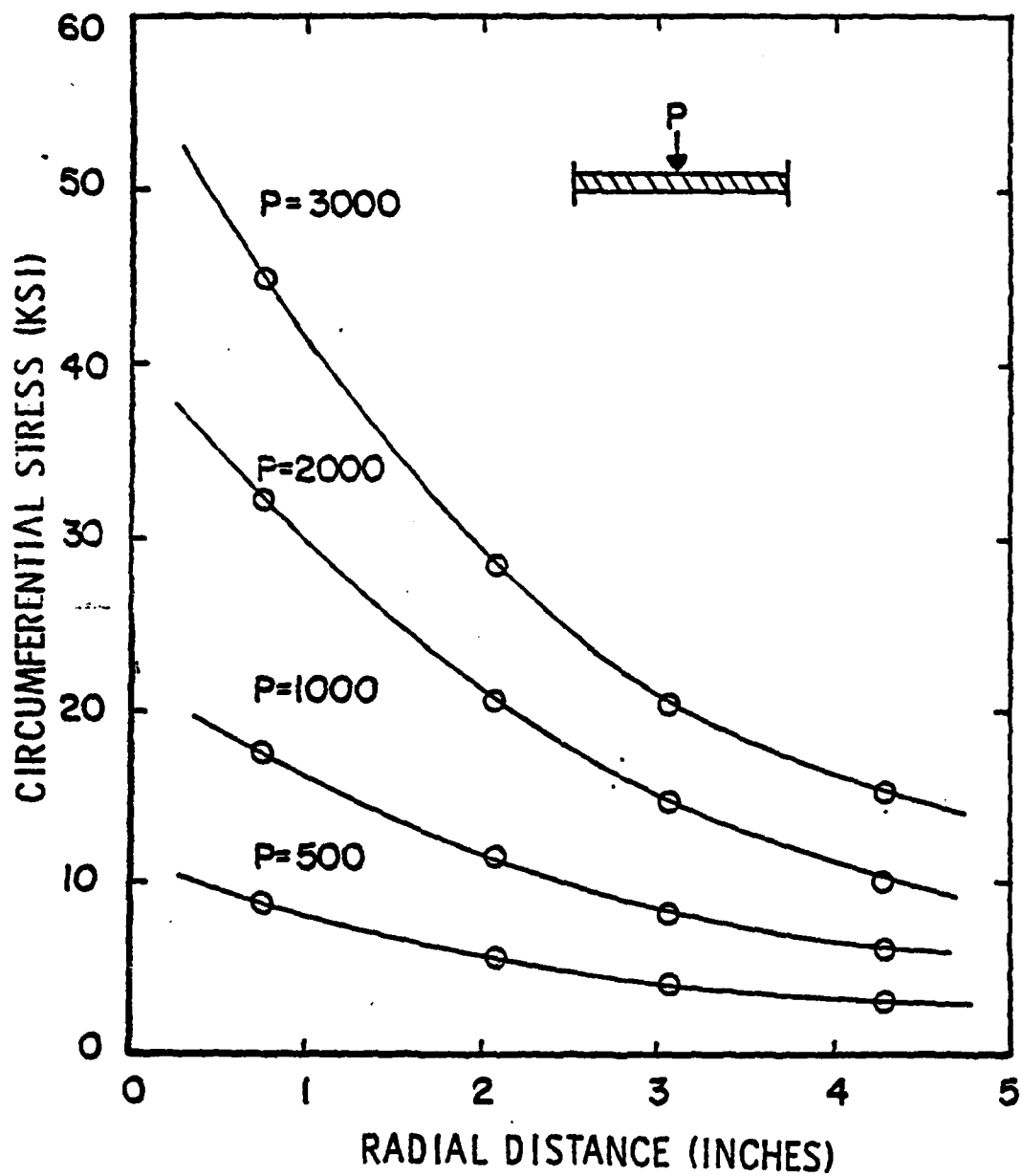


Figure 6.11.5 Midsurface Circumferential Stress Profiles in Clamped Circular Plate.

6.12 COMPRESSIVE BUCKLING OF A SIMPLY-SUPPORTED SANDWICH PLATE

The stability of a plate of sandwich construction is considered to demonstrate the use of the thin shell element (Element Type 5) in the same model with standard isoparametric three-dimensional finite elements (Element Type 2). A square, three-layer panel (Figure 6.12.1) is subjected to a uniform compressive load of \bar{N}_x pounds per inch. The panel is 23.5 inches on each side, and supported at each face of the sandwich on all four edges (vertical displacements only are prevented).

The outer face sheets of the panel, which are represented by thin shell finite elements, are each 0.021 inches in thickness, with isotropic material properties $E = 9.5 \times 10^6$ psi, $\nu = 0.3$. The core layer, 0.181 inches thick, has a transverse shear rigidity $G = 19000$ psi. In the finite element solution, the sandwich core is modeled using three-dimensional, eight-node solid elements (Type 2). Each layer of the model contains sixteen elements of equal planform dimensions. Only one quadrant of the panel is considered in the numerical solution, due to symmetry of the geometry and loading. On the lateral boundaries, the tangential transverse shear strains within the core are suppressed by making the upper and lower face sheet displacements equal in the direction parallel to each edge.

A solution for the buckling load \bar{N}_{CR} has been obtained by applying the inplane forces incrementally until a sudden increase in transverse displacement is observed. Out of plane deflections are triggered by a small (one pound) transverse load applied at the center of the plate. Buckling is found to occur for an applied load of $\bar{N}_x = 305$ pounds per inch; this computed value compares well with previous analytical and experimental results¹⁻⁵, as shown in Table 6.12.1. It is noted that all of the analytical results give estimates of the critical load which are about nine percent too high; it is likely that the assumption of zero transverse shear strains at the panel

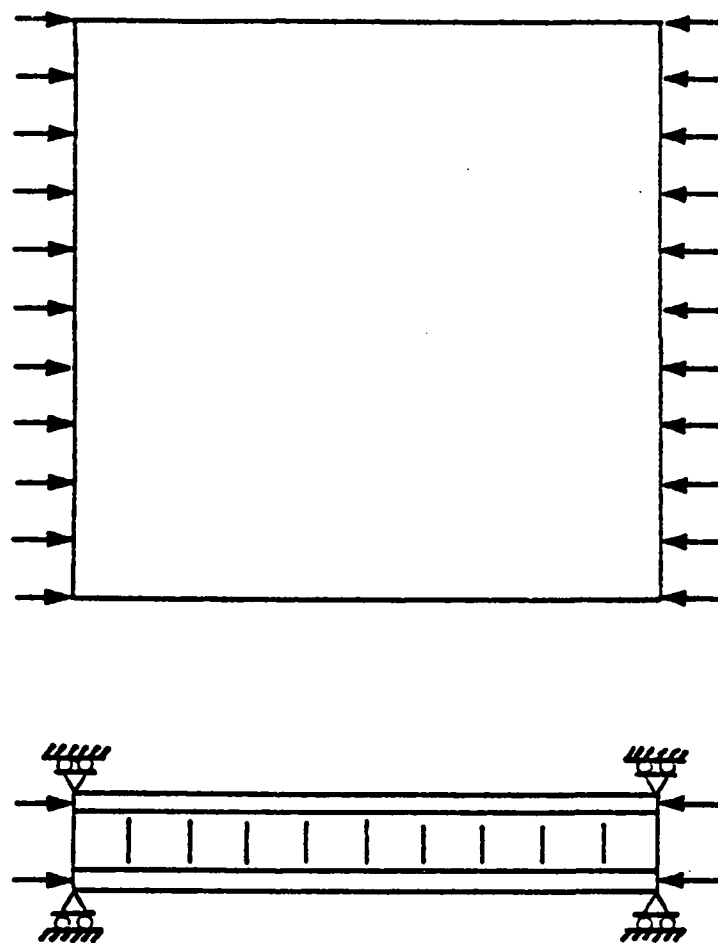


Figure 6.12.1 Simply-Supported Sandwich Plate Under Compression Load.

TABLE 6.12.1
COMPARISON OF BUCKLING LOADS FOR SIMPLY-SUPPORTED SANDWICH PANEL

| Reference | Method | N_{cr} (pounds/inch) |
|------------------------|-----------------|------------------------|
| Hoff ¹ | Series Solution | 303.0 |
| Plantema ² | Series Solution | 308.0 |
| Brockman ³ | Series Solution | 309.4 |
| Boller ⁴ | Experimental | 266. - 300. |
| Monforton ⁵ | Finite Element | 307.5 |
| MAGNA | Finite Element | 305.0 |

boundaries is largely responsible for this error. The transverse shear constraint has been used in the MAGNA solution to provide a fair comparison with previous analytical solutions.

6.13 CLAMPED PLATE UNDER UNIFORM PRESSURE LOADING

A moderately thin square plate is analyzed in this example for geometrically nonlinear response to a uniform pressure loading. Such a problem has been considered by Pica, Wood and Hinton¹, as part of their evaluation of plate-bending elements.

Physical properties of the particular plate considered are:

| | |
|-----------------|--|
| Width | $a = 508.0 \text{ mm (20.0 in.)}$ |
| Thickness | $t = 1.27 \text{ mm (0.05 in.)}$ |
| Modulus | $E = 68.9 \text{ GPa (1. x 10}^7 \text{ psi)}$ |
| Poisson's Ratio | $\nu = 0.30$ |

The boundaries of the plate are fully clamped. A uniform pressure q is applied to the upper surface of the plate.

Figure 6.13.1 shows a finite element model of one quadrant of the plate, using 16 three-dimensional, 16-node thick shell elements (Element Type 8). Element properties are evaluated using a 2x2x2 Gaussian integration. Pressure loading is applied incrementally in increments of $\Delta P = 51.2$, where P is the normalized pressure

$$P = qa^4/Et^4.$$

The maximum normalized pressure considered is $P = 512$.

A load-versus-displacement history for the nonlinear solution is shown in Figure 6.13.2. The central displacement is normalized with respect to the plate thickness. The problem is only mildly nonlinear, since the maximum displacement is only about twice the plate thickness. However, the linear and nonlinear displacement solutions at $P = 512$ are significantly different (5.520 and 1.992, respectively). Combined Newton-Raphson iterations have been used in the solution, with an average of four iterations per load increment being required to maintain equilibrium.

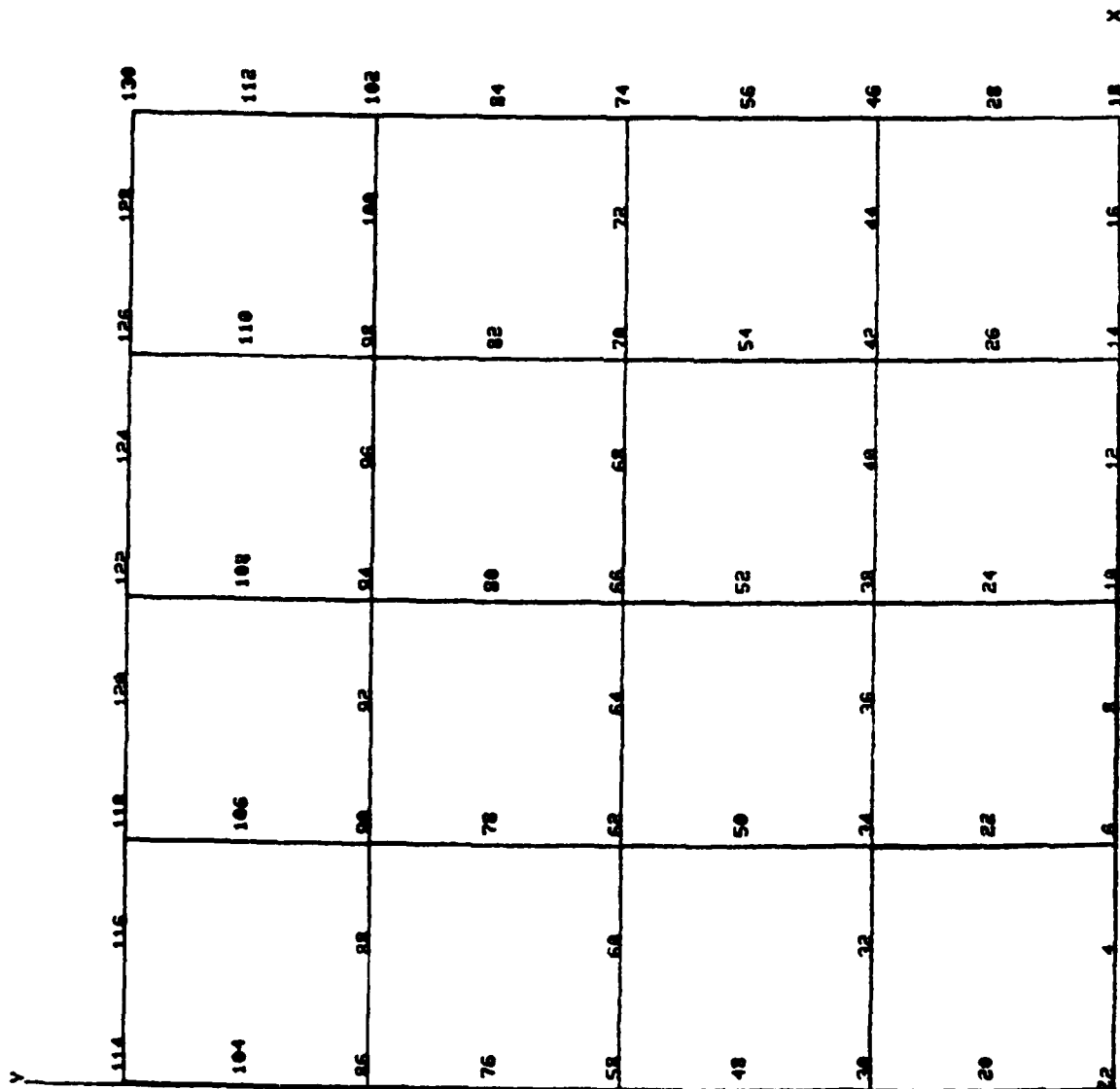


Figure 6.13.1 Finite Element Model of Clamped Plate.

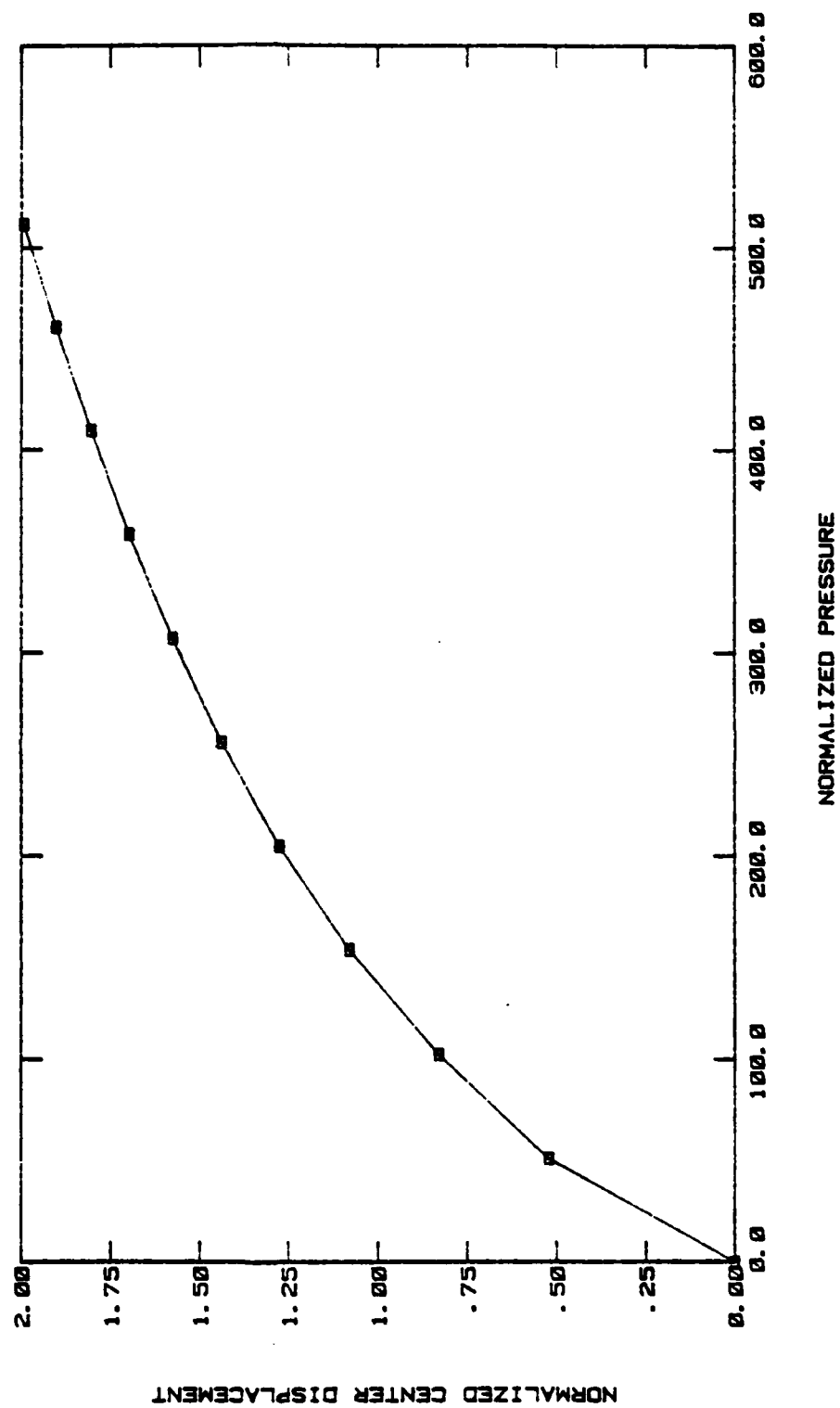


Figure 6.13.2 Load-Displacement Solution for Clamped Plate Under Pressure.

Selected strain and stress results for the plate at maximum loading are given in the form of contour plots in Figures 6.13.3 through 6.13.7. Figures 6.13.3 and 6.13.4, which show the strain E_{xx} on the lower and upper surfaces (labeled surfaces 3 and 6, respectively), illustrate the asymmetry caused by geometric nonlinearity. Similarly in Figures 6.13.5 and 6.13.6, geometric stiffening is evident in the x-direction stresses; the maximum compression at the upper surface is about 4000 psi, while the lower (tension) surface stresses exceed 5000 psi. The upper surface von Mises equivalent stress is shown in Figure 6.13.7.

The efficiency of the 16-node thick shell (Element Type 8) in nonlinear analysis is apparent from the computing times for this solution. On the CYBER 175 computer, an average of 3.75 CPU seconds is required per iteration for a 16-element mesh.

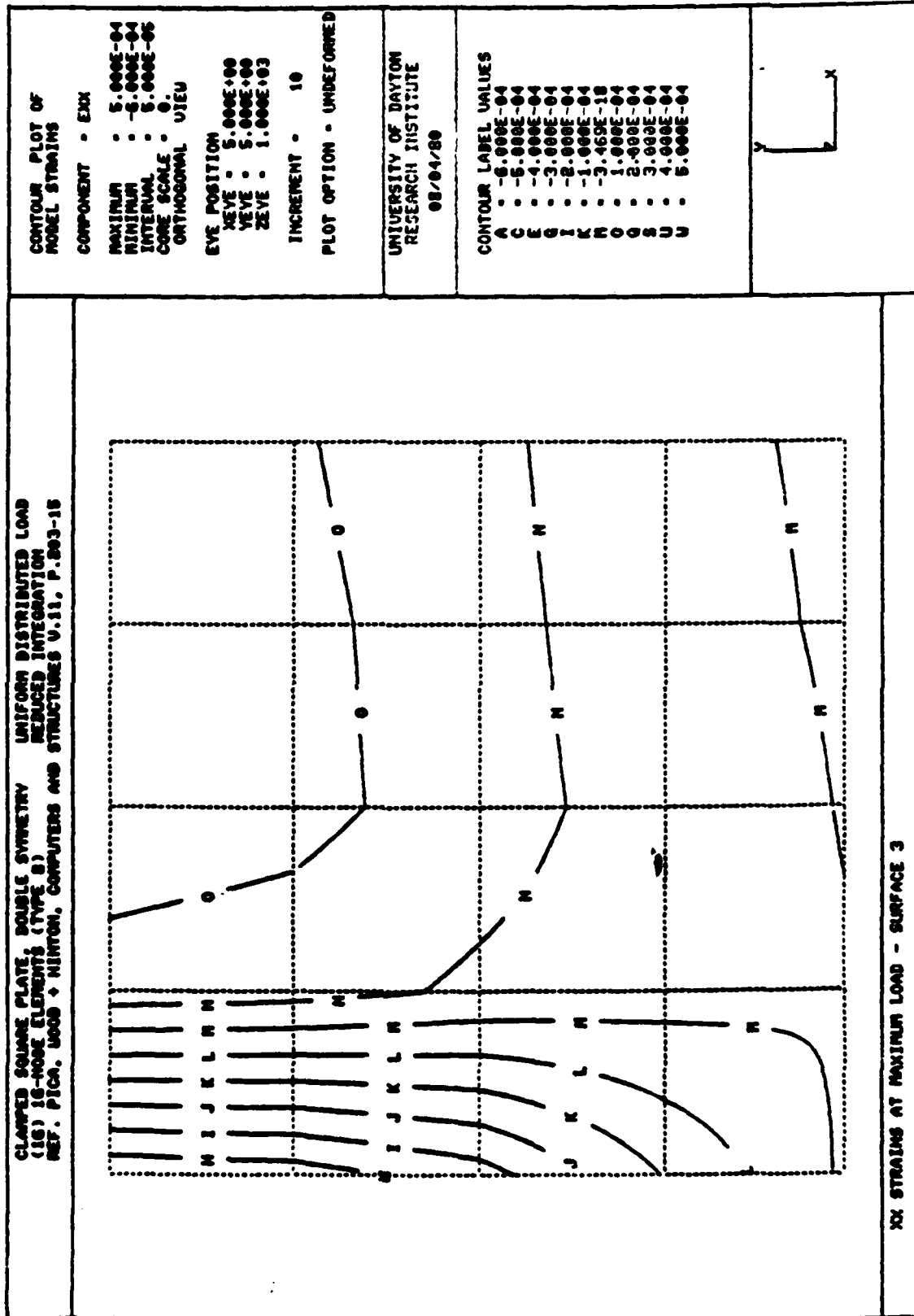


Figure 6.13.3 Upper Surface Strains in Clamped Plate at Maximum Load.

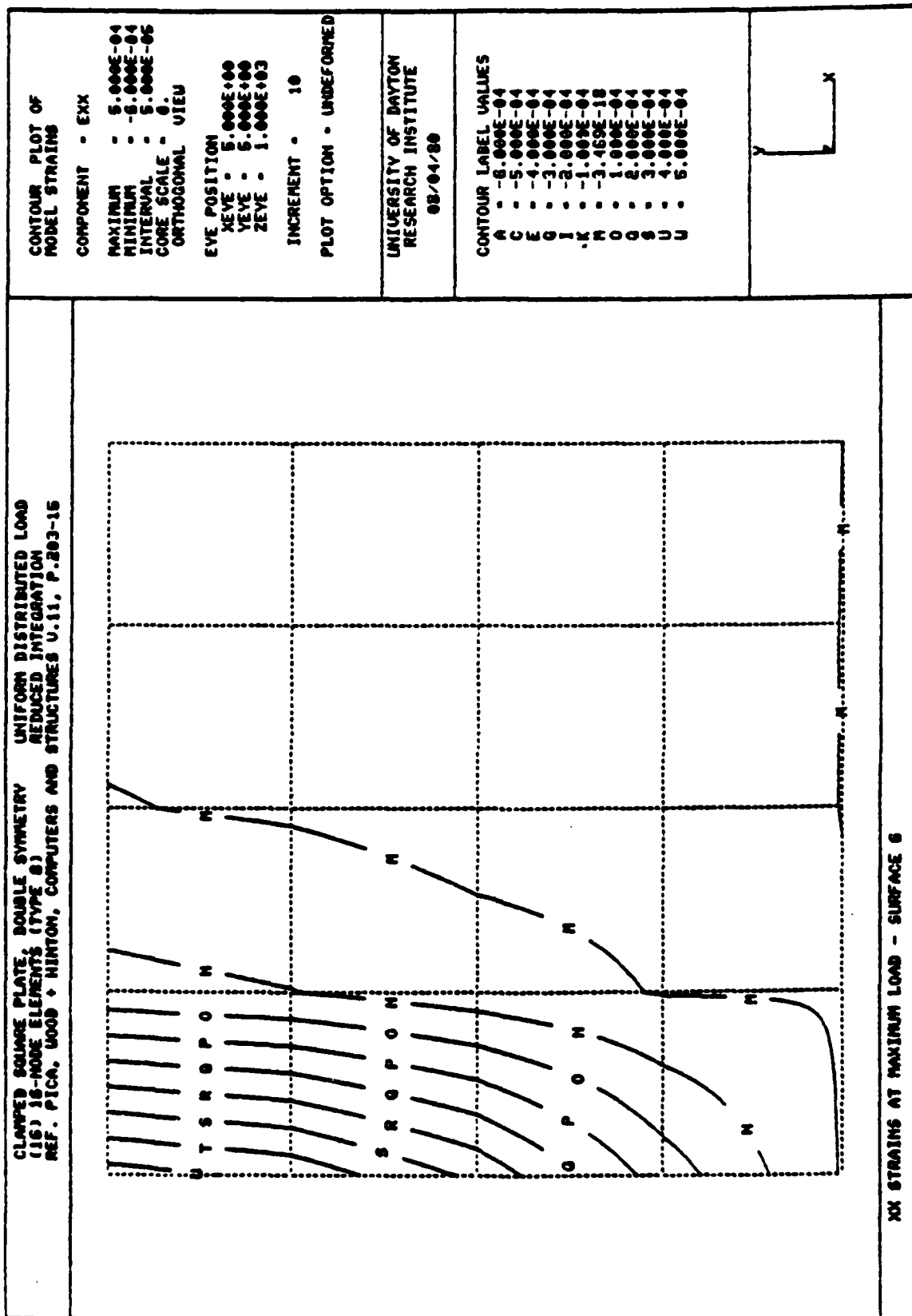


Figure 6.13.4 Lower Surface Strains in Clamped Plate at Maximum Load.

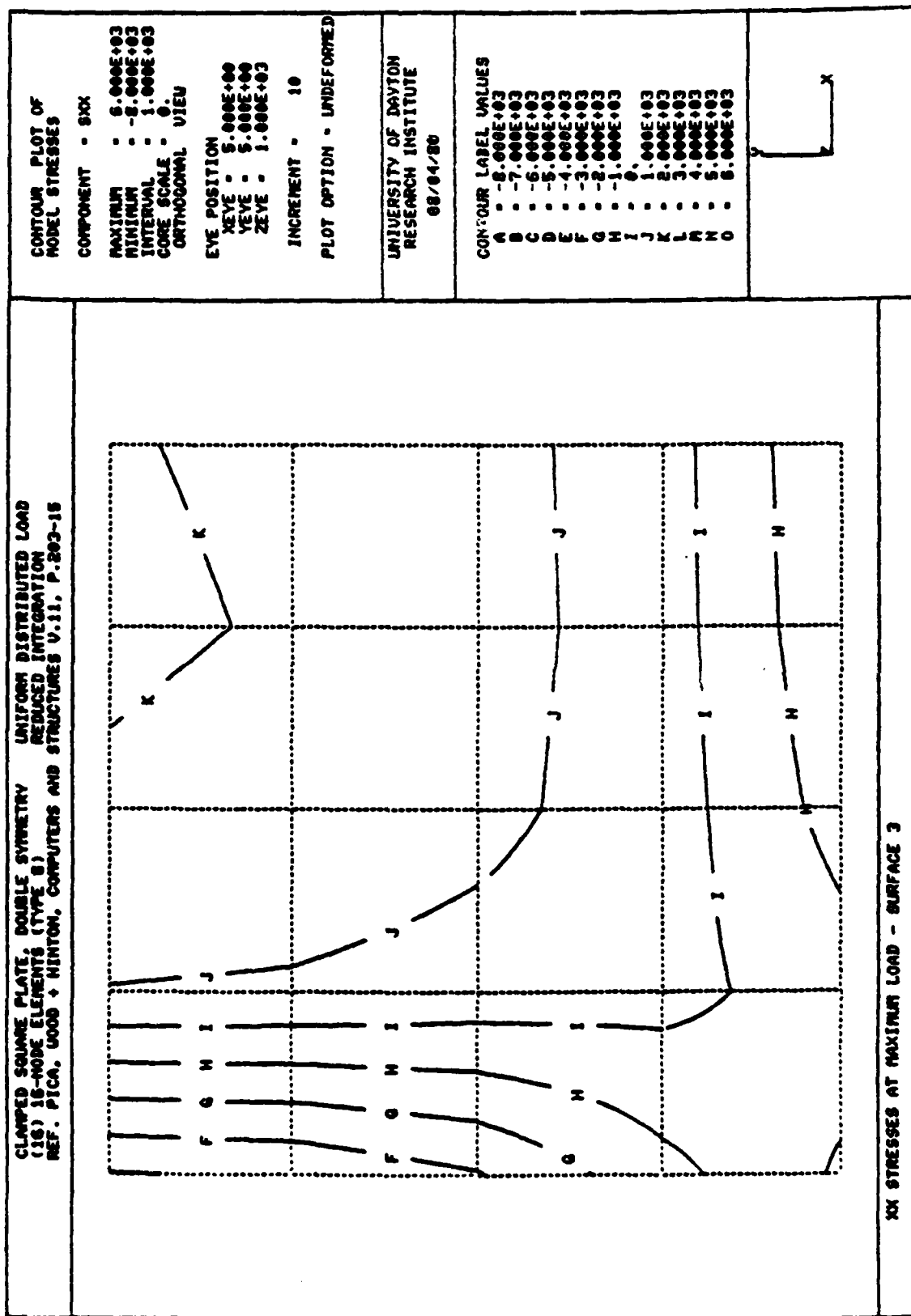


Figure 6.13.5 Upper Surface Stresses in Clamped Plate at Maximum Load.

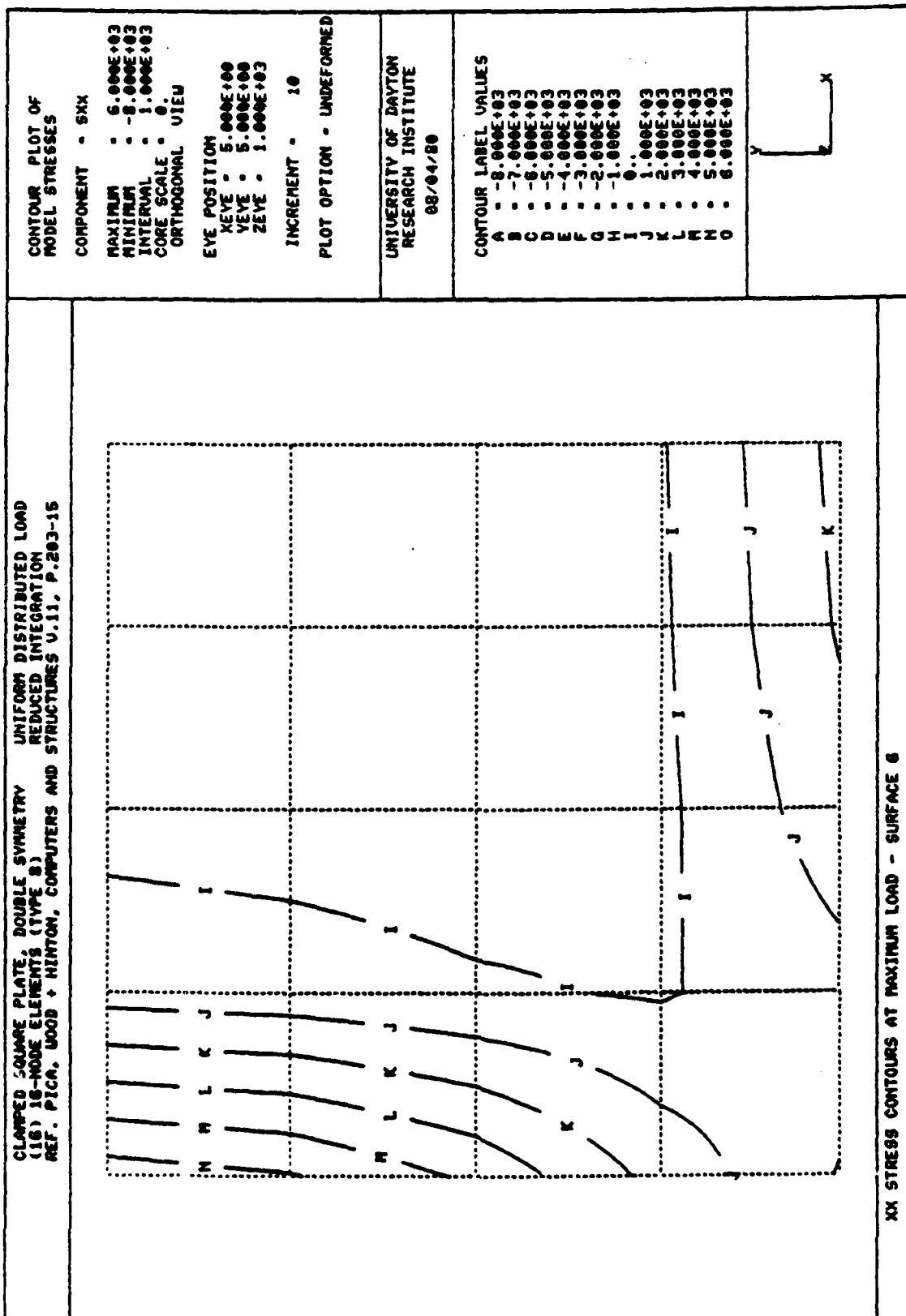


Figure 6.13.6 Lower Surface Stresses in Clamped Plate at Maximum Load.

CLAMPED SQUARE PLATE, DOUBLE SYMMETRY
 (16) 16-NODE ELEMENTS (TYPE 8)
 REF. PICA, WOOD & HINTON, COMPUTERS AND STRUCTURES V.11, P.803-15

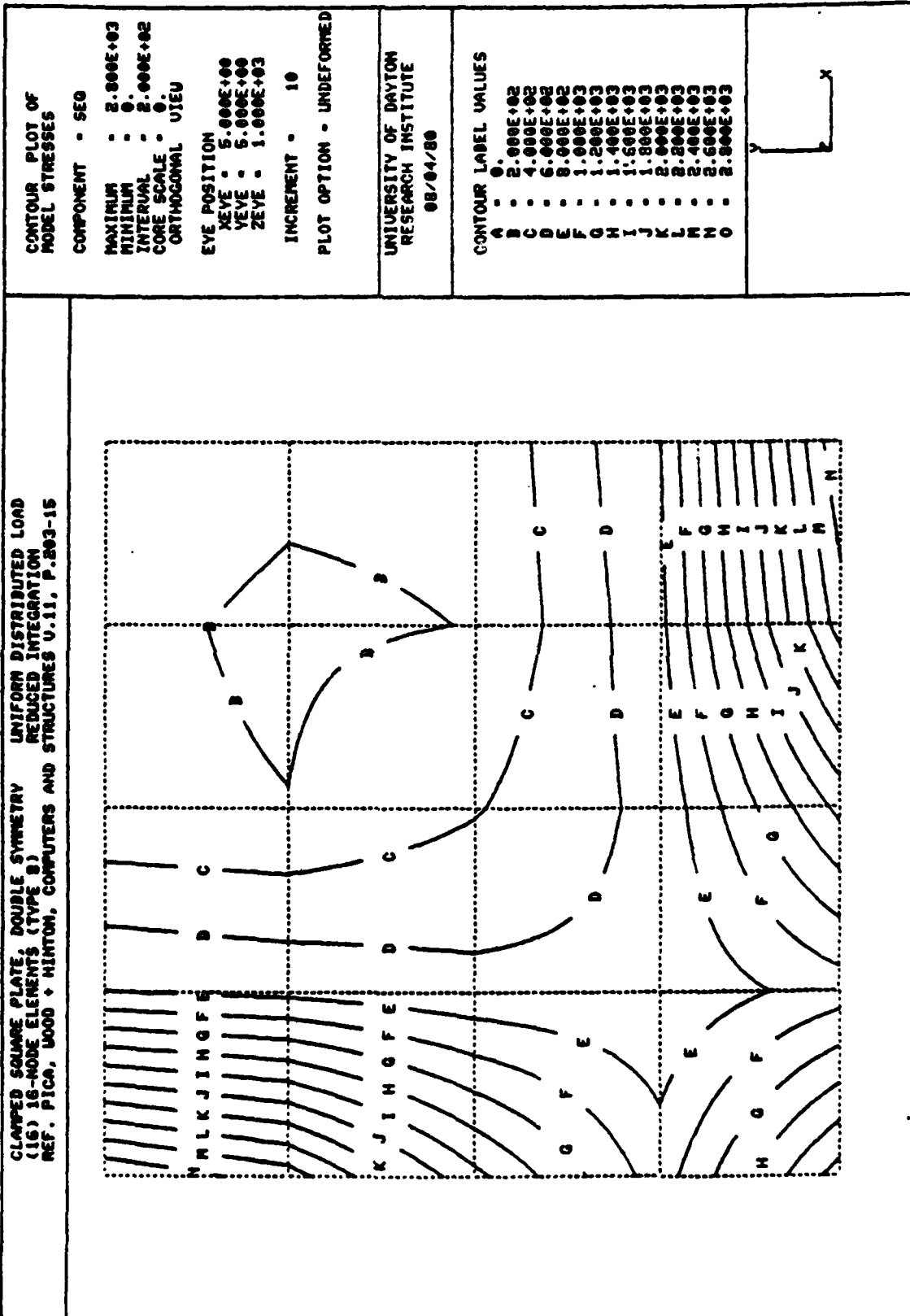


Figure 6.13.7 Effective Stresses in Plate Upper Surface at Maximum Load.

6.14 POSTBUCKLING RESPONSE OF A SIMPLY-SUPPORTED PLATE

A simply-supported square plate is considered, to determine its static buckling and postbuckling response under compressive loading. The plate geometry and properties are identical to those used in the previous example,

Width $a = 508.0$ mm (20.0 in.)
Thickness $t = 1.27$ mm (0.05 in.)
Modulus $E = 68.9$ GPa ($1. \times 10^7$ psi)
Poisson's Ratio $\nu = 0.30$.

In this case, the boundaries of the plate are simply supported, with inplane motions permitted at all points. A uniform compressive stress is applied to opposite edges of the plate.

Since the buckling response is known to be doubly symmetric, one quarter of the plate is modeled. Sixteen solid elements (Element Type 8) are used in the discretization, with all integrations performed using the 2x2x2 Gauss rule. To follow the response past the point of bifurcation, the solution is performed using the nonlinear dynamic option and a large time step ($\Delta t = 1000$. sec.). Equilibrium iteration is used at each increment, in the form of combined Newton-Raphson iteration.

A solution for the central displacement of the plate as a function of the compressive edge load is shown in Figure 6.14.1. The theoretical buckling load¹ of $\sigma_{cr} = 1558$ kPa (226 psi) is predicted with accuracy. In the analysis, a very small concentrated force is applied at the center point of the panel to trigger the out-of-plane displacement, and thus a slight nonzero deflection appears on the plot prior to the actual onset of buckling.

At the maximum applied loading of 3500 kPa (510 psi), the predicted central displacement is 3.594 mm (0.1415 in.), and the average end-shortening over half of the plate is about 0.0044 mm. For the case of *uniform* end-shortening, the central deflection predicted by Timoshenko¹ using an effective width

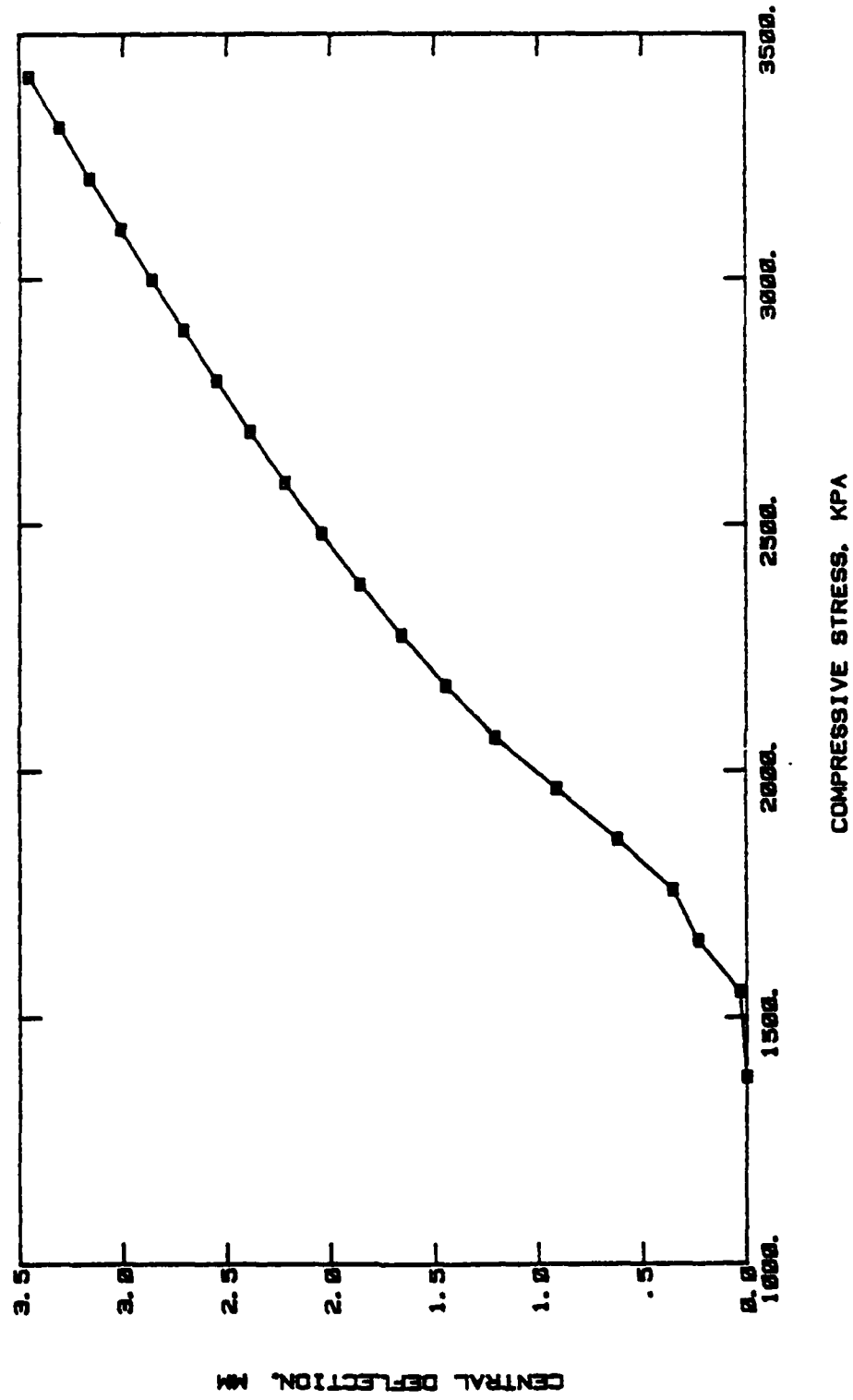


Figure 6.14.1 Postbuckling Displacement History for Simply Supported Square Plate.

formula is 3.663 mm, so that the postbuckled solutions are in reasonable agreement.

6.15 ELASTIC-PLASTIC ANALYSIS OF A PERFORATED STRIP

The thin metal sheet shown in Figure 6.15.1 is subjected to a uniform applied tension parallel to its longitudinal axis. Overall dimensions of the plate are 36 mm by 20 mm, with a hole diameter of 10 mm. Material properties of the strip are $E = 7000 \text{ kgf/mm}^2$, $\nu = 0.20$, and the yield stress is $\sigma_y = 24.3 \text{ kgf/mm}^2$.

This particular problem has been considered by Bathe, Ozdemir and Wilson¹, and experimental results are available from the work of Theocaris and Marketos². As in the analysis of Reference 1, plane stress conditions are assumed, and the plate material is taken to have the strain hardening slope $H = 0.032 E$.

The finite element model of one-quarter of the plate (Figure 6.15.2) consists of 24 eight-node plane stress elements (Element Type 9). Stiffness properties are evaluated in all elements using a 3x3 Gaussian quadrature. The model contains 95 node points and 174 unconstrained degrees of freedom.

Strain results obtained at the point of first yielding are presented in Figure 6.15.3. The point for which results are plotted is located nearest the center of the plate, in element 1 (see Figure 6.15.2); the normalized strain is defined by $E\varepsilon_y/\sigma_y$. The measure of applied loading is the mean stress at the root section of the plate. Note that the applied stress at the ends of the plate are one-half this value, since the hole diameter is one-half the plate width. The range of loading considered is $0 \leq \sigma_{\text{mean}} \leq \sigma_y$. Two solutions are shown in the Figure; one uses a load increment of $0.125\sigma_y$ and combined Newton-Raphson iterations at each step, while the other consists of two increments of $0.4\sigma_y$ with full Newton-Raphson iterations used to maintain equilibrium. In this instance, the elastic-plastic behavior is not highly path dependent, since the two solutions agree quite well. Longitudinal stresses in the plate at maximum loading ($\sigma_{\text{mean}} = \sigma_y$) are shown in Figure 6.15.4 in the form of a contour map.

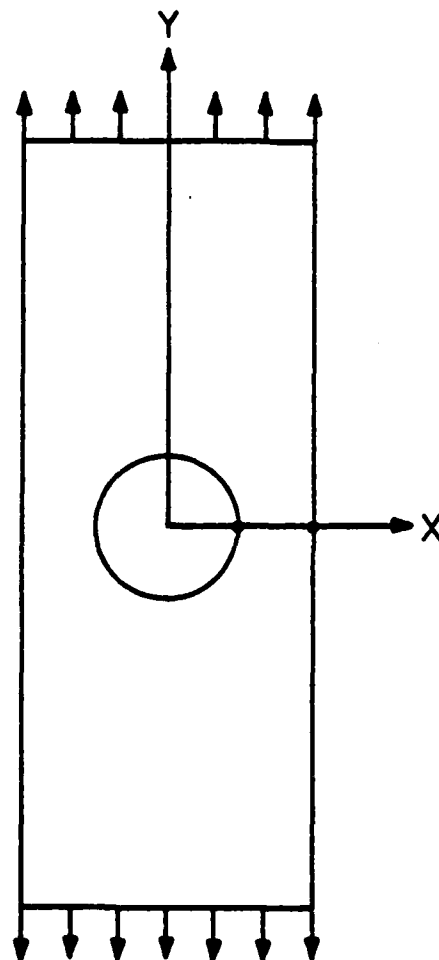


Figure 6.15.1 Perforated Sheet Subjected to Uniform Tension.

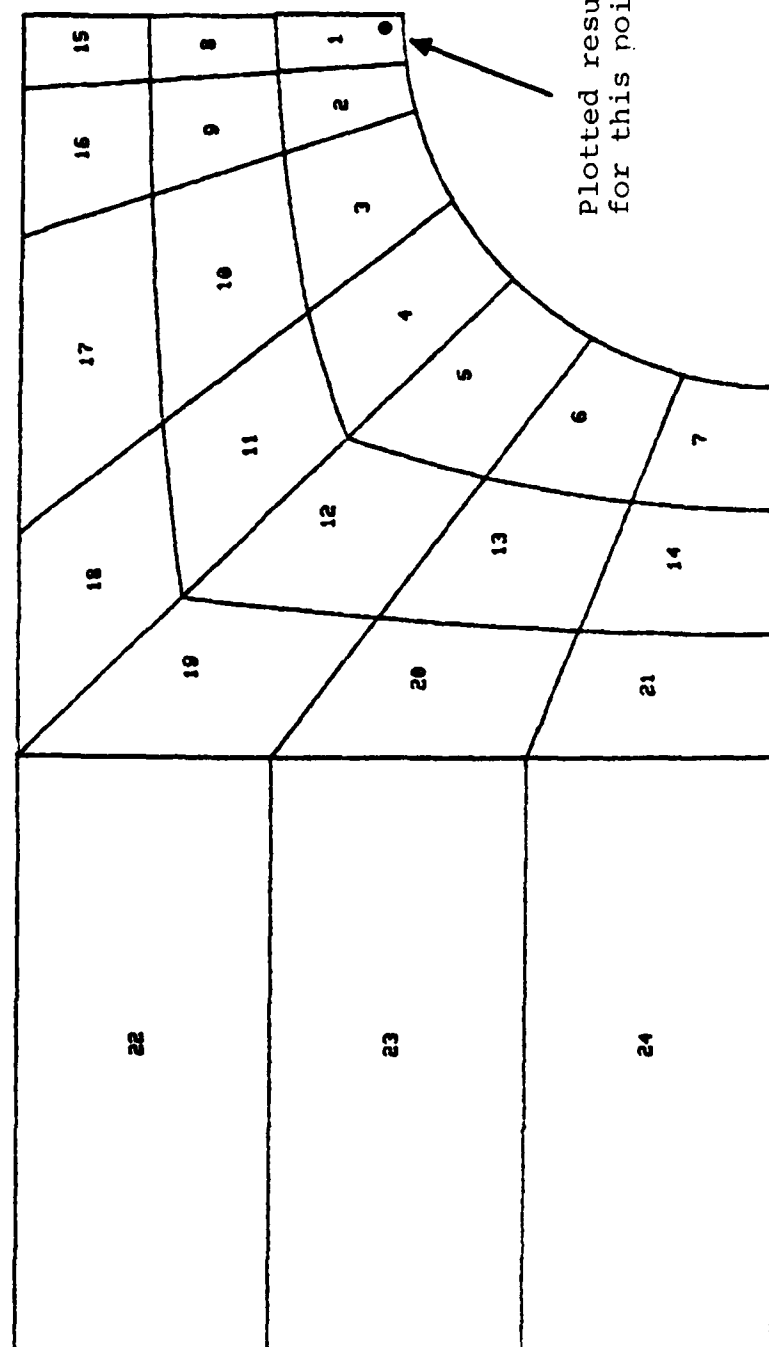
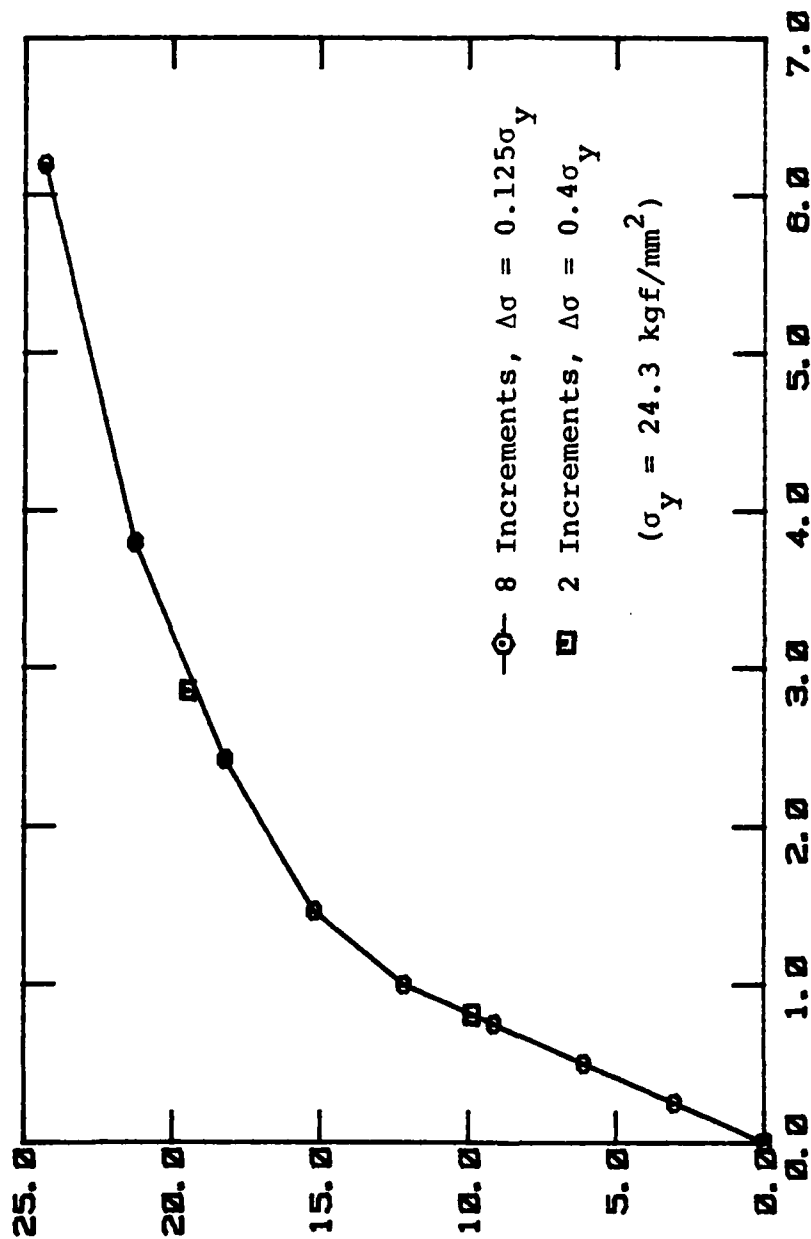


Figure 6.15.2 Finite Element Model of Tension Strip.

MEAN STRESS AT ROOT SECTION (KGF/SQ. MM)



NORMALIZED LONGITUDINAL STRAIN

Figure 6.15.3 Longitudinal Strain History at Point of First Yielding.

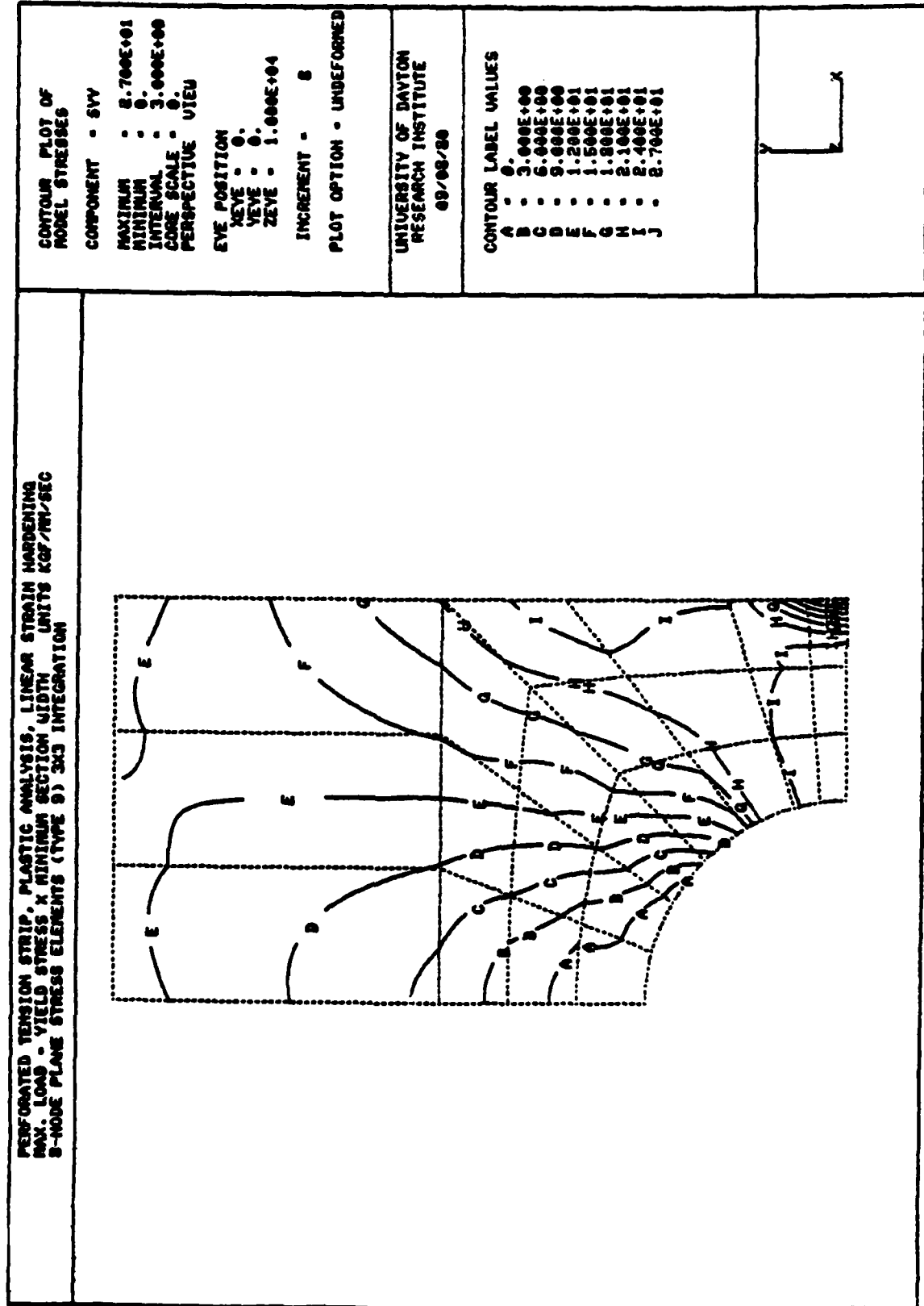


Figure 6.15.4 Longitudinal Stresses in Tension Strip at $\sigma_{\text{mean}} = \sigma_{\text{yield}}$

6.16 NATURAL FREQUENCIES OF AN ORTHOTROPIC PLATE

A simply-supported, one-layer orthotropic plate is considered, to determine its natural vibration response. The 12-inch square plate is specially orthotropic; that is, the principal material axes (1,2,3) are aligned with the reference axes (x,y,z) of the structure. The specific material properties considered are:

$$\begin{aligned}\text{Moduli} \quad E_1 &= 1.0 \times 10^7 \text{ psi} \\ E_2 &= E_3 = 1.0 \times 10^6 \text{ psi} \\ G_{12} &= G_{13} = G_{23} = 48000. \text{ psi}\end{aligned}$$

$$\begin{aligned}\text{Poisson's Ratio} \quad \nu_{12} &= 0.03 \\ \nu_{13} &= \nu_{23} = 0.0\end{aligned}$$

$$\text{Thickness} \quad t = 0.050 \text{ in.}$$

$$\text{Density} \quad \rho = 7.764 \times 10^{-5} \text{ lb-sec}^2/\text{in}^4$$

In the finite element solution, 36 twenty-node elements (Element Type 6) are used to represent the entire plate (Figure 6.16.1). The model contains 315 nodes and 727 unconstrained degrees of freedom.

The exact and computed frequencies for the first four vibration modes of the plate are compared in Table 6.16.1. In the table, m represents the number of waves in the fiber (high-modulus) direction, and n the wave number for the lower-modulus direction. Note that the 1,3 mode corresponds to a lower frequency than the 2,1 mode, due to the strong orthotropy of the plate. Deformed geometry plots for the first four modes are pictured in Figure 6.16.2 through 6.16.5.

The eigenvalue solution was performed using six trial iteration vectors, with four frequencies required to converge (NREQD = 4). Convergence was obtained in 11 iterations, to a vector tolerance of 0.001. The entire solution required 39.6 CPU seconds on the CYBER-175 computer.

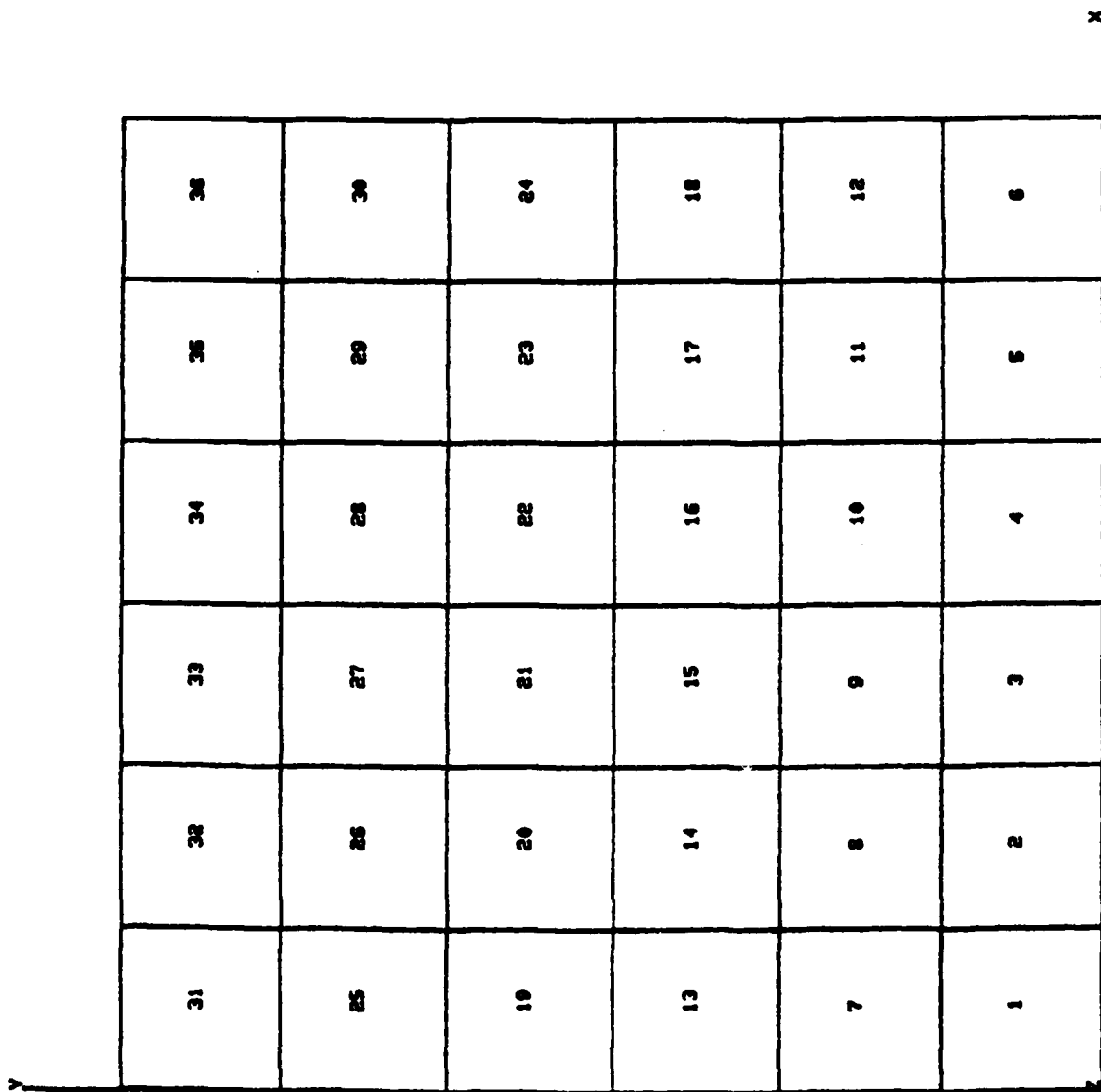


Figure 6.16.1 Finite Element Model of Orthotropic Square Plate.

TABLE 6.16.1
COMPARISON OF EXACT AND COMPUTED NATURAL FREQUENCIES
FOR SQUARE ORTHOTROPIC PLATE

| Mode Number | ω_{exact} (Hz.) | $\omega_{\text{comp.}}$ (Hz.) |
|--------------|-------------------------------|-------------------------------|
| m = 1, n = 1 | 59.6 | 59.9 |
| m = 1, n = 2 | 92.0 | 93.1 |
| m = 1, n = 3 | 171.5 | 175.3 |
| m = 2, n = 1 | 225.7 | 226.9 |

m = number of half-waves in high-modulus direction

n = number of half-waves in low-modulus direction

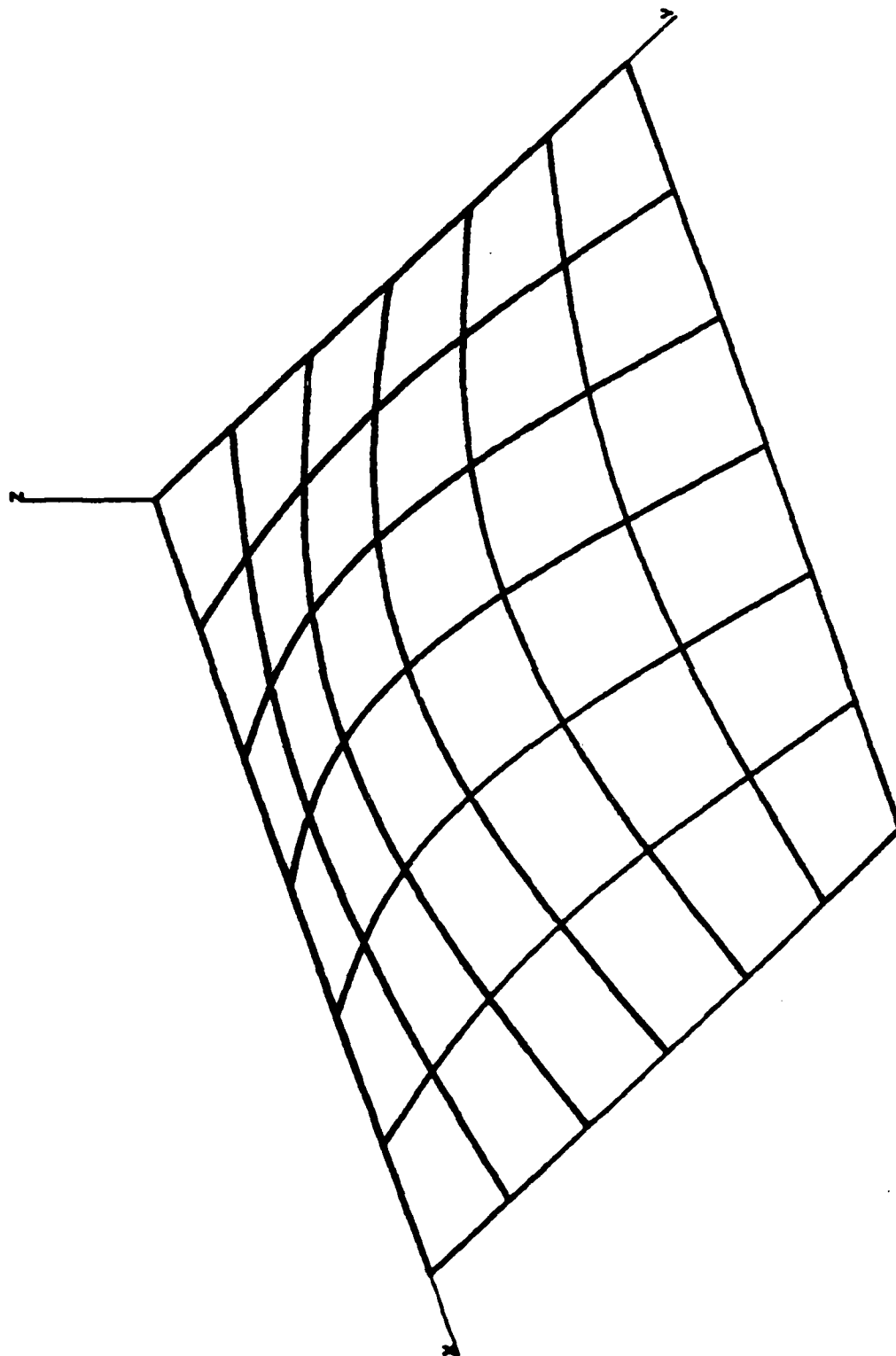


Figure 6.16.2 First Mode ($m=1$, $n=1$) of Orthotropic Plate.

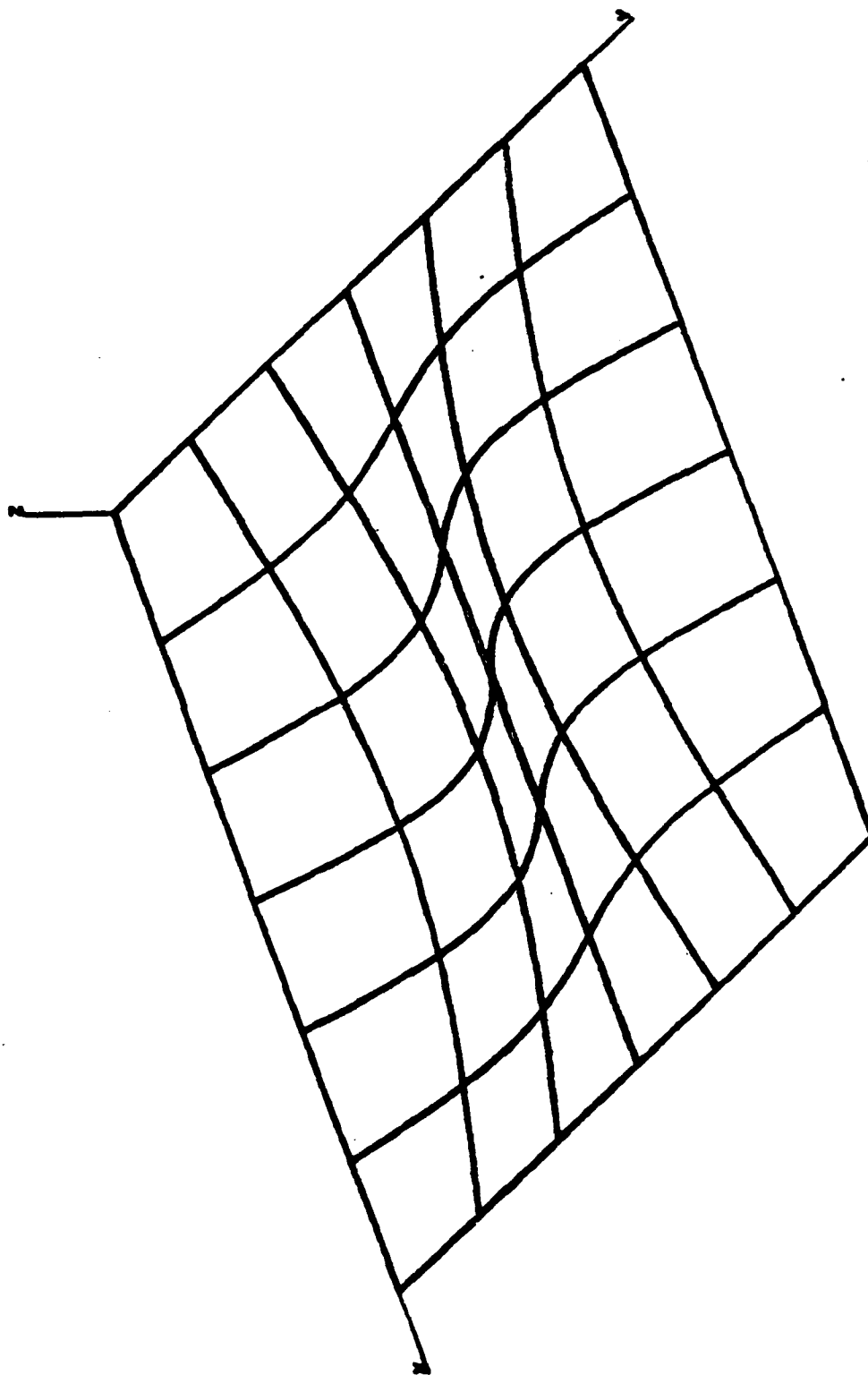


Figure 6.16.3 Second Mode ($m=1$, $n=2$) of Orthotropic Plate.

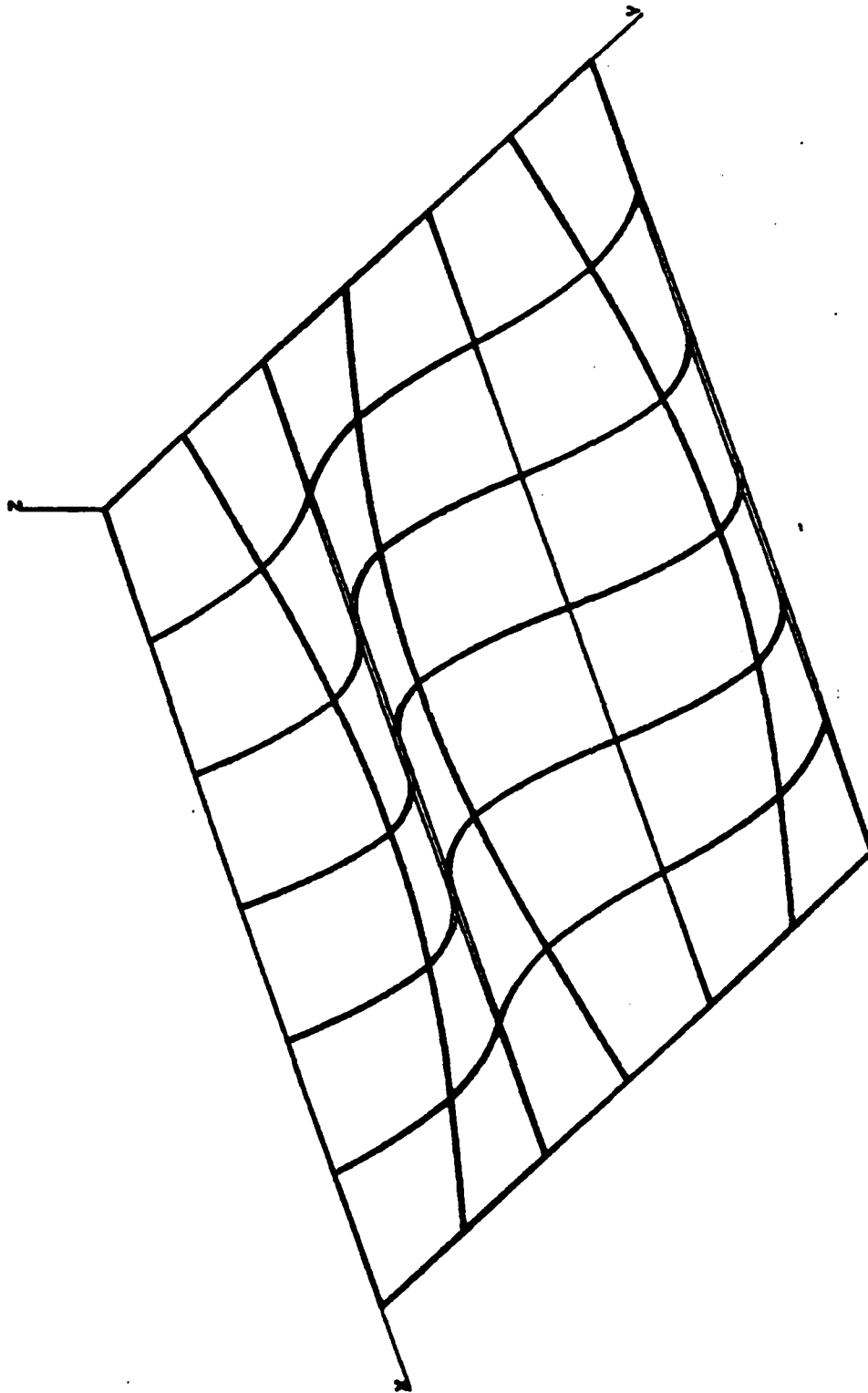


Figure 6.16.4 Third Mode ($m=1$, $n=3$) of Orthotropic Plate.

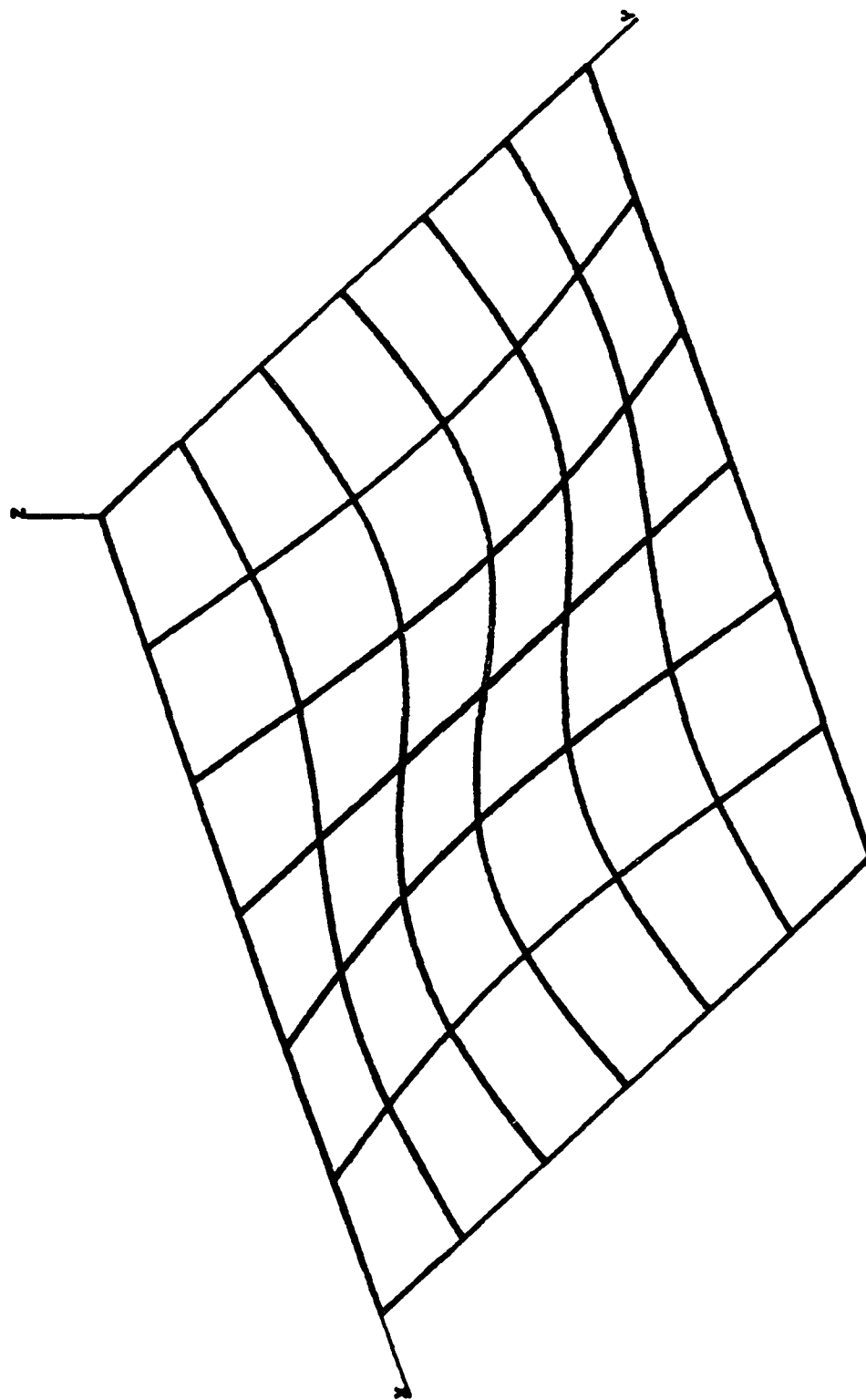


Figure 6.16.5 Fourth Mode ($m=2$, $n=1$) of Orthotropic Plate.

6.17 PLASTIC COLLAPSE OF A RECESSED FASTENER

The elastic-plastic failure analysis of a recessed-head mechanical fastener has been performed, as a part of an evaluation of the simplified design/analysis method introduced by Venkayya and Eimermacher¹. The failure estimates of Reference 1 are based upon an approximate axisymmetric fastener geometry, as indicated in Figure 6.17.1, and the assumption of a failure surface located as shown in the figure. Limited test results on actual hardware are also available; see, for example, Reference 2.

Since the idealized geometry of the fastener is rotationally symmetric, a representative one-degree sector has been modeled in the MAGNA analysis. The finite element grid, shown in Figure 6.17.2, consists of 100 eight-node solid elements (Type 2). The elements nearest the axis of revolution are triangular prisms, having two coplanar faces on the rear edge of the model. The eight-node element is used in this case because the load paths are relatively simple, no bending deformation is anticipated, and material nonlinearities are the predominant effect in the nonlinear response. Normal displacements on the rear face of the model are prevented using linear constraints, and rigid supports along the inclined edge of the fastener head are applied in a similar manner. The applied loading is purely axial, in the form of a uniform stress over the bottom surface of the part. The fastener material is high-strength steel, with the properties

$$E = 30. \times 10^6 \text{ psi}$$

$$\nu = 0.30$$

$$\sigma_y = 155000. \text{ psi}$$

$$\sigma_{ult} = 170000. \text{ psi}$$

The incremental solution is performed using a single 1000 pound step to the approximate point of first yielding, followed by 300 pound increments up to the collapse load. The early progression of yielding, which proceeds along the expected

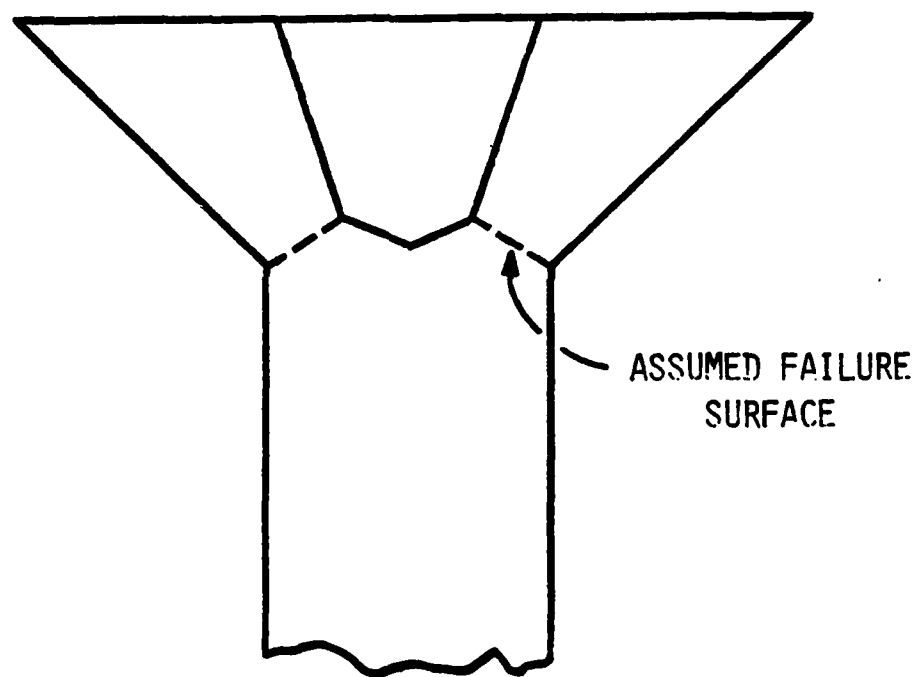


Figure 6.17.1 Idealized Recessed Fastener Geometry.

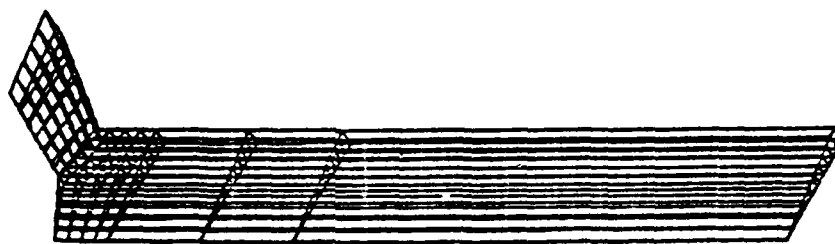


Figure 6.17.2 Finite Element Model of Recessed Fastener.

failure surface, is shown in Figure 6.17.3 for load levels of 2200, 2500 and 2800 pounds. In the figure, the completely darkened region represents the zone throughout which the ultimate stress has been attained, while a single contour line shows the boundary of the plastic region. Figure 6.17.4 presents similar results at the highest loading levels considered (4000, 4300, 4600 pounds, respectively). As the part nears collapse, the failure surface gradually shifts upward, away from the base of the recess; thus, the ultimate collapse mode is somewhat different from that assumed in the simplified analysis. This effect is also observed in the experimental results. The collapse load of approximately 4600 pounds predicted by the analysis is substantially higher than the experimental failure load of 3732 pounds. This discrepancy is likely the result of the simplified geometry used in the analysis, which produces a uniform stress distribution in the circumferential direction, and the fact that no cracking and/or material removal has been considered in the numerical solution.

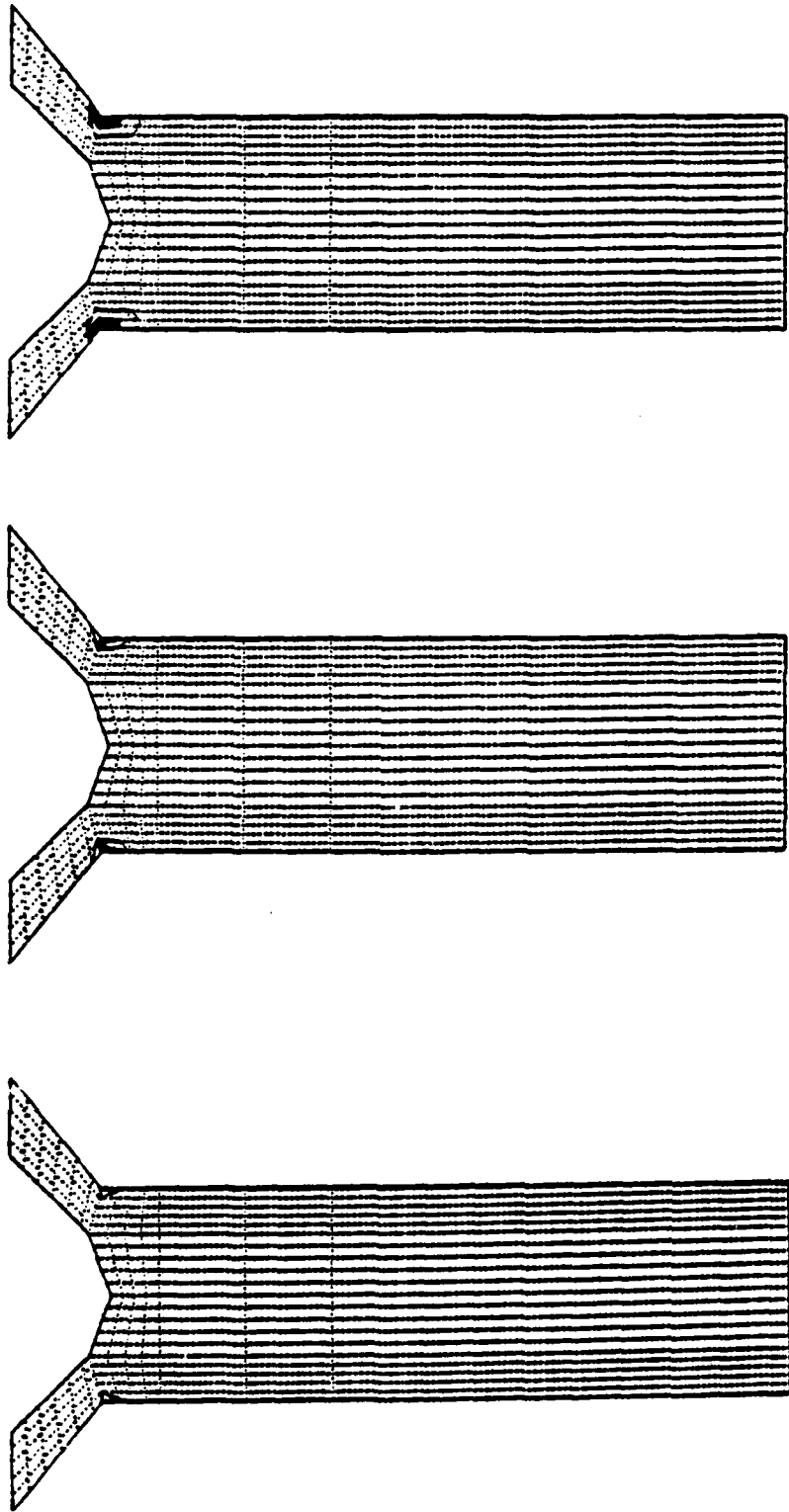


Figure 6.17.3 Yield and Ultimate Stress Zones in Recessed Fastener at Load Levels of 2200, 2500 and 2800 Pounds.

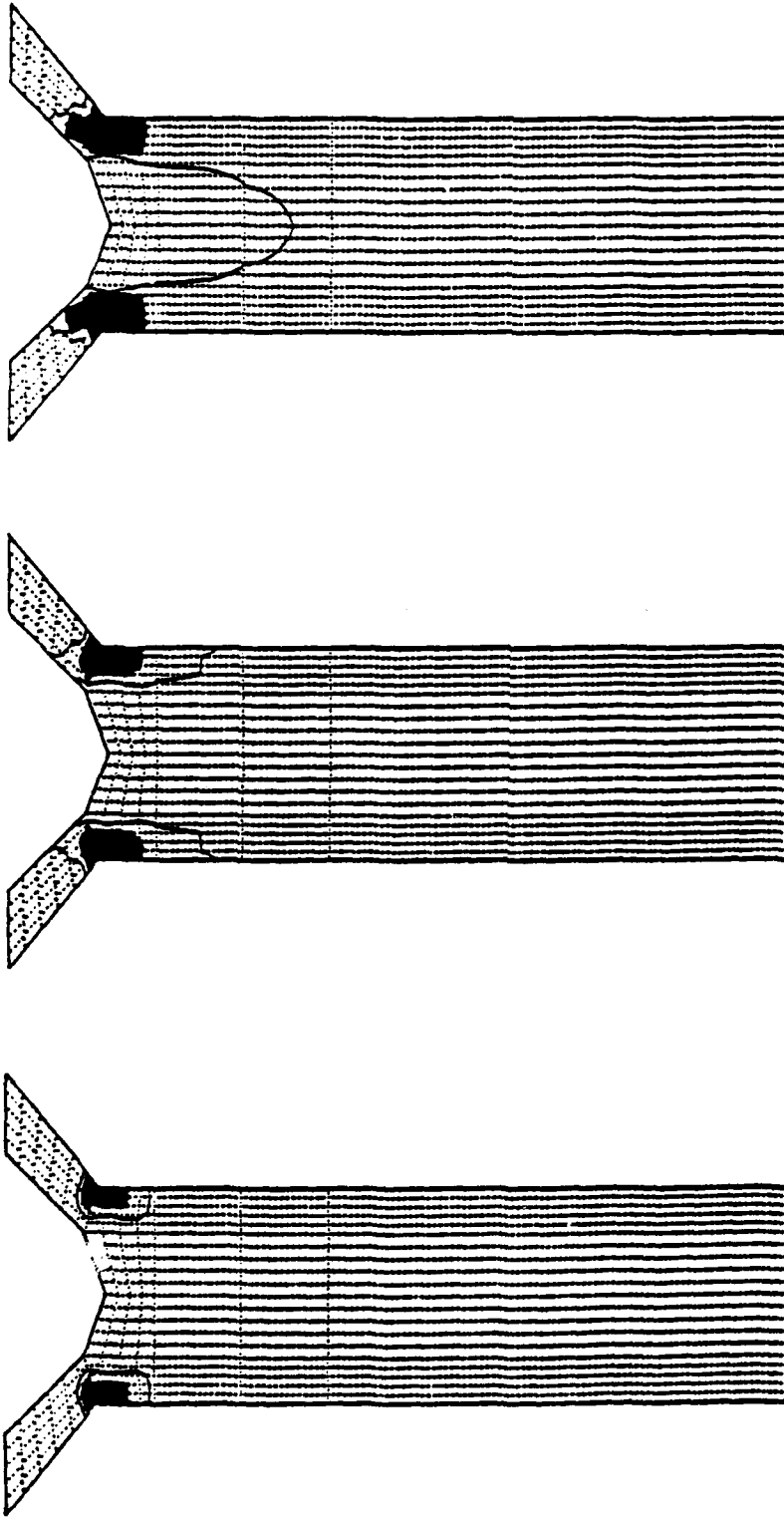


Figure 6.17.4 Yield and Ultimate Stress Zones in Recessed Fastener at Load Levels of 4000, 4300 and 4600 Pounds.

6.18 FREE VIBRATIONS OF A CLAMPED TRIANGULAR PLATE

A cantilevered right-triangular flat plate is analyzed for its natural vibration response. In this example, a very coarse finite element mesh is used, both to illustrate the effectiveness of the thin shell element (Type 5) and to contrast the behavior of lumped and consistent mass formulations where relatively crude element divisions are used.

Physical properties of the plate, which is made of magnesium, are as follows:

| | |
|-----------------|---|
| Side Length | $a = 6.0$ in. |
| Thickness | $t = 0.034$ in. |
| Modulus | $E = 6.5 \times 10^6$ psi |
| Poisson's Ratio | $\nu = 0.3541$ |
| Density | $\rho = 1.66 \times 10^{-4}$ lb-sec ² /in ⁴ |

The finite element discretization of the plate (Figure 6.18.1) consists of three linear-displacement shell elements, and contains 24 active degrees of freedom. The boundary containing nodes 2, 4, and 6 is completely fixed. Numerical solutions have been performed for the first three vibration modes using both lumped and consistent mass formulations; the frequency results are given in Table 6.18.1.

The lumped mass calculations are in reasonable agreement with solutions obtained from the NASTRAN¹ and ANSYS² programs using very fine meshes, and compare quite well with results obtained from NISA³ using three quadratic-displacement shell elements (Table 6.18.2).

The consistent mass results, however, are reasonable only for the lowest natural frequency, even though the mode shapes are only slightly different from those predicted using lumped masses. The source of the difficulty in the consistent mass solution is the coarseness of the finite element mesh,

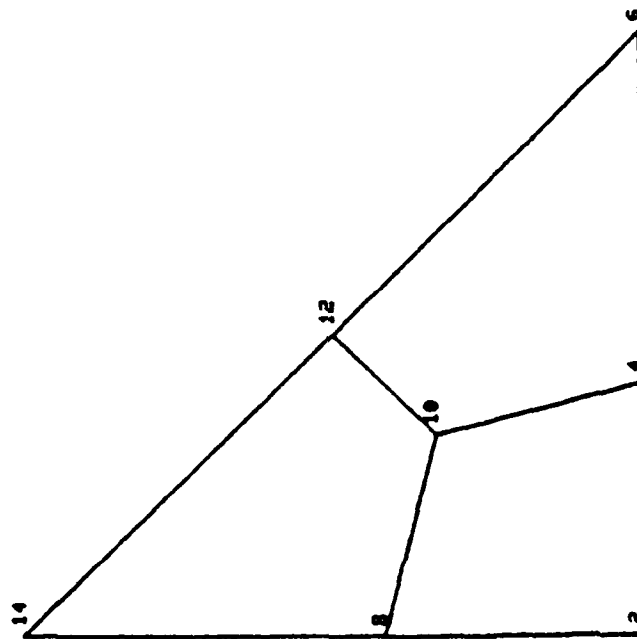


Figure 6.18.1 Cantilevered Triangular Plate - Finite Element Model.

TABLE 6.18.1
NATURAL FREQUENCIES OF TRIANGULAR CANTILEVER PLATE

| Mode | Frequency (Lumped Mass) | Frequency (Consistent Mass) |
|------|-------------------------|-----------------------------|
| 1 | 53.3 | 59.7 |
| 2 | 201.8 | 324.0 |
| 3 | 248.1 | 476.7 |

(All frequencies are given in Hertz)

TABLE 6.18.2
COMPARISON OF NATURAL FREQUENCY RESULTS FOR
CANTILEVERED TRIANGULAR PLATE

| Program | NASTRAN | ANSYS | NISA | MAGNA* |
|------------------|---------|-------|-------|--------|
| No. of Nodes | 496 | 66 | 16 | 14 |
| No. of Elements | 900 | 100 | 3 | 3 |
| Mode 1 Frequency | 55.9 | 55.9 | 54.3 | 53.3 |
| Mode 2 Frequency | 210.8 | 210.9 | 215.4 | 201.8 |
| Mode 3 Frequency | 292.1 | 293.5 | 303.7 | 248.1 |

*Lumped Mass Results

which is extremely crude when one recalls that the shell element (Element Type 5) uses only *linear* functions for all of the shell displacement.

If one were to perform an analysis of this plate alone, a finer mesh of elements would normally be employed. However, in the modeling of more complex structures, the element division used in this example is rather typical of the degree of model refinement used in relatively small components of the total structure. The above problem illustrates the fact that, when relatively coarse modeling is necessary, the lumped mass approach is likely to yield results far superior to those obtained using consistent masses. Naturally, as the model is progressively refined, the distinction between the two mass representations tends to become less and less crucial.

6.19 COMPRESSION OF A DISK AGAINST A RIGID SURFACE

The analysis of a disk compressed against a rigid plane provides a simple example of the surface contact feature in MAGNA. The particular problem considered involves a disk of unit thickness and radius 4.0 inches, assumed to behave elastically in plane stress. Material properties of the part are $E = 1000. \text{ lb./in}^2$, $\nu = 0.3$. The range of loading considered is 0-150 pounds, distributed over a small area at the top of the disk.

The undeformed and deformed geometries for a coarse model of the disk are shown in Figures 6.19.1 and 6.19.2. Here the rigid surface is constructed using a single contact element, with all nodes fixed. Figure 6.19.3 shows the geometry of the master (rigid) surface in three dimensions, with a somewhat finer finite element model.

Vertical displacements for a series of nodes at successively larger distances from the rigid surface are plotted versus a normalized load factor in Figure 6.19.4, for the model of Figure 6.19.3. Since the load is monotonically increasing, nodes along the circumference of the disk gradually come into contact with the master surface and are thereafter constrained to move only in the horizontal direction.

Notice that the displacement accuracy of the contact solution is determined by the mesh refinement in the region of contact, since the elements may be quadratic while contact constraints are imposed only at discrete node points. The coarse solution of Figure 6.19.2 illustrates this very well. When two of the three nodes defining an element edge are in contact, minor amounts of interpenetration can occur, though the constraints at the nodes are satisfied quite well. Therefore, the mesh in the contact region is best prepared with an eye toward the degree of resolution required in defining the contact area and the associated local stress field. When the contact analysis is expected only to reproduce overall load transfer characteristics, a coarse mesh may be appropriate.

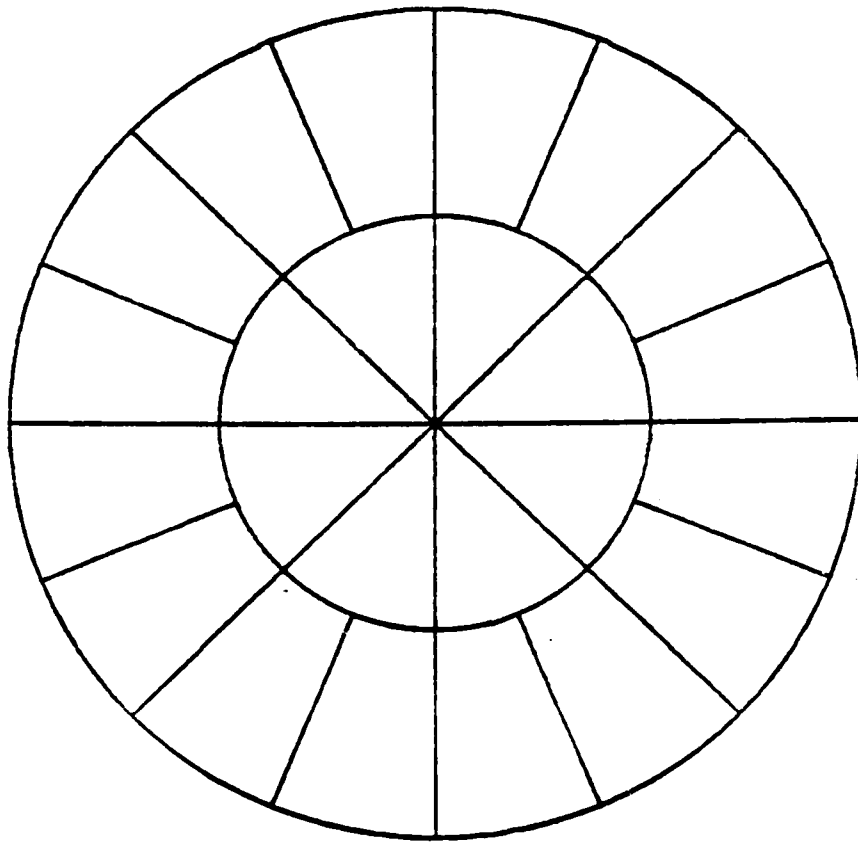


Figure 6.19.1. Finite Element Model of Disk in Contact with a Rigid Plane.

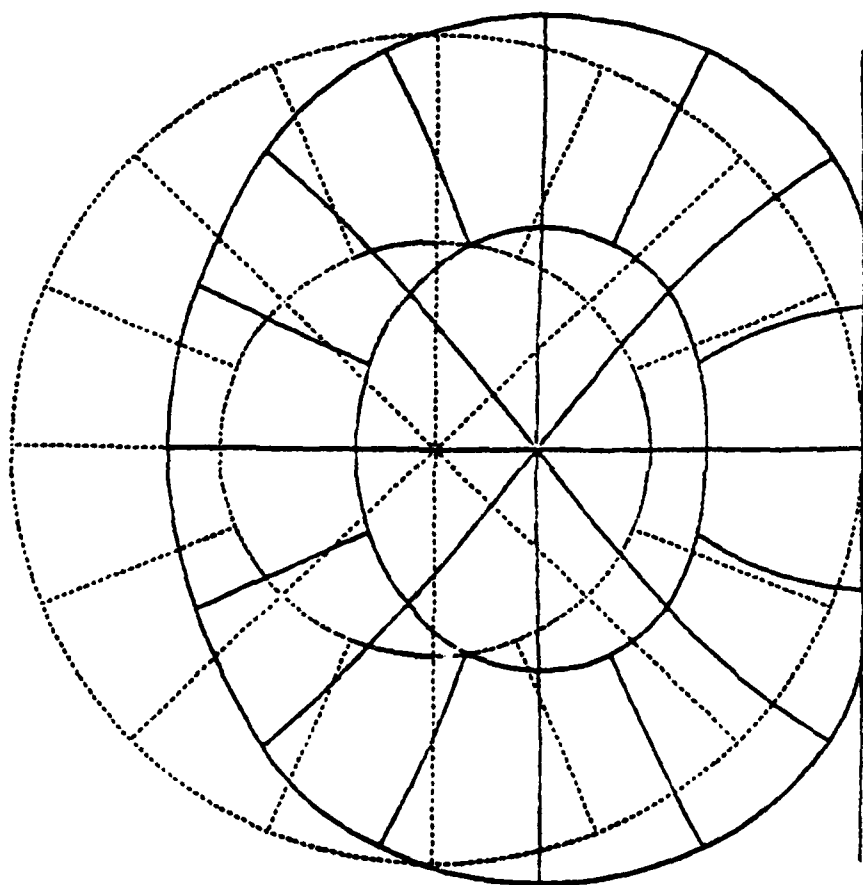


Figure 6.19.2. Undeformed and Deformed Geometries of Disk.

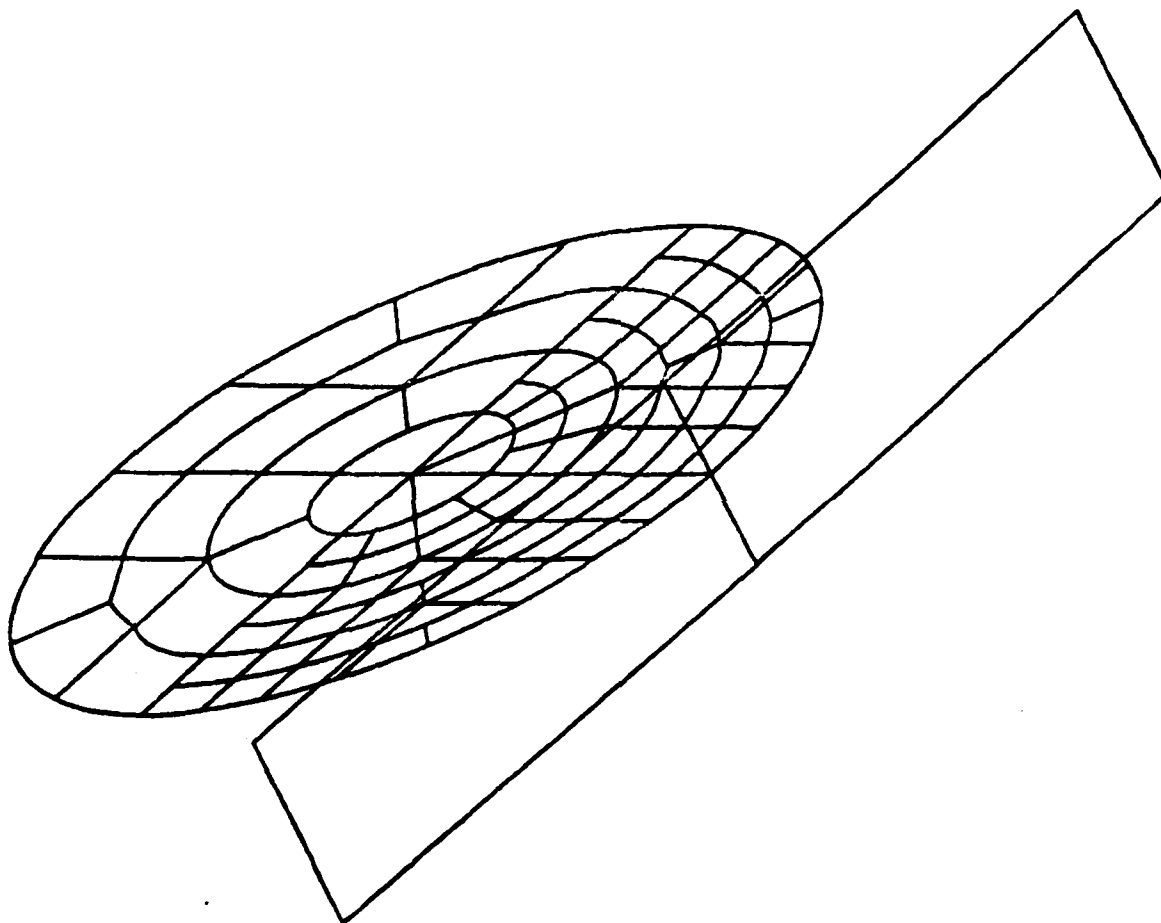


Figure 6.19.3. Three-Dimensional View of Disk Model with Contact Elements.

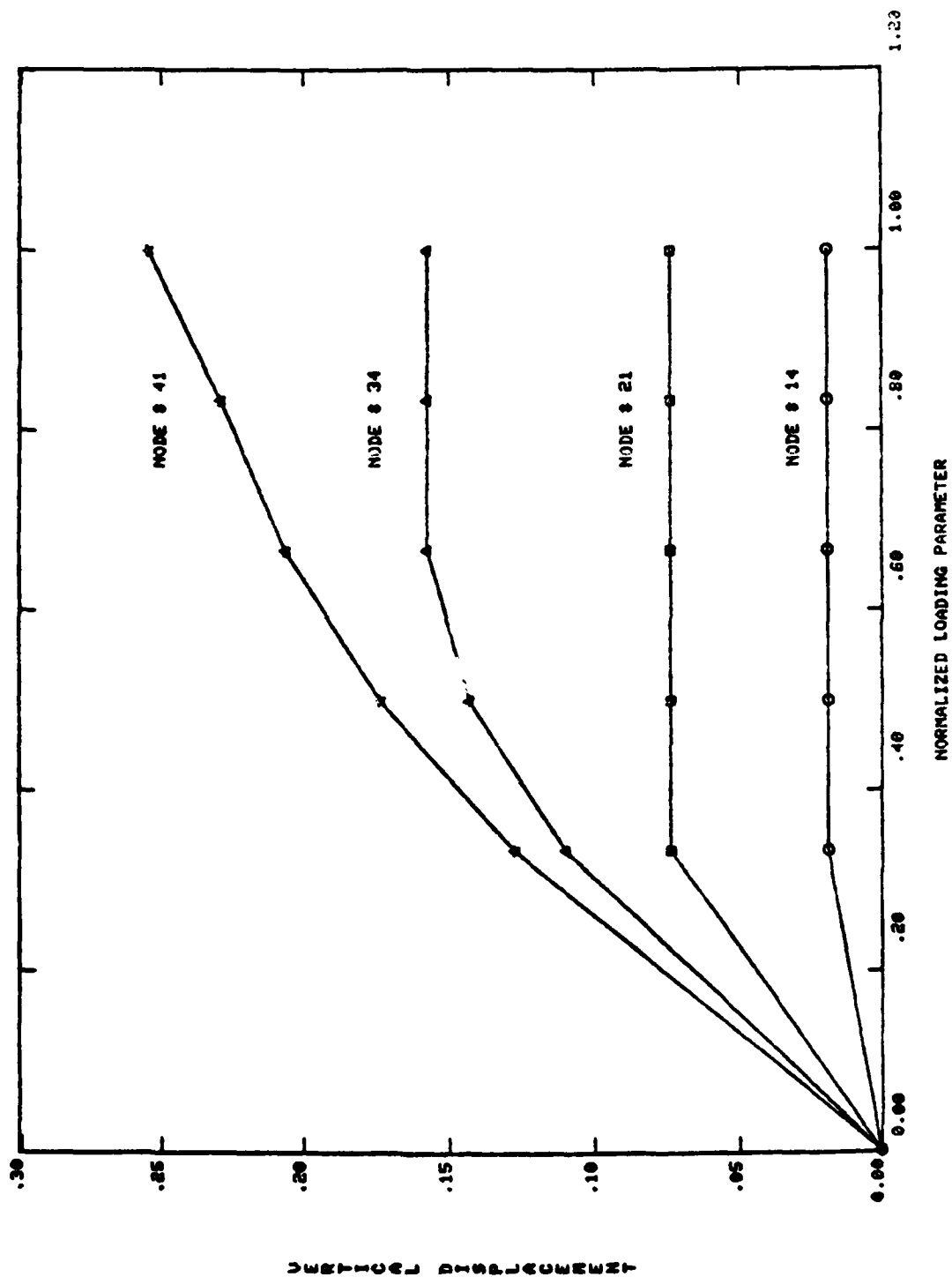


Figure 6.19.4. Displacement Histories for Individual Nodes Along Lower Surface of Disk.

6.20 ELASTIC-PLASTIC ANALYSIS OF A CLAMPED BEAM

A clamped-clamped beam subjected to a central transverse load is analyzed using the three-node, quadratic beam finite element (Element Type 12). The elastic, large displacement solution for such a problem is considered in References 1 and 2.

The following physical data has been used for analysis of the beam:

| | |
|-----------------|----------------|
| Total length | - 20.0 inches |
| Section width | - 1.0 inches |
| Section depth | - 0.125 inches |
| Young's modulus | - 1.E7 psi |
| Poisson's ratio | - 0.0 |

Half of the beam is modeled in the solution due to symmetry. Ten beam elements are used, giving a total of 21 node points and 59 degrees of freedom.

Solutions for the static load vs. central deflection response of the beam are shown in Figure 6.20.1, for several values of the material yield stress. In all cases elastic, perfectly plastic behavior has been assumed. For lower values of the yield stress, relatively little geometric stiffening occurs prior to yielding, and yielding occurs initially in bending. When the yield stress is relatively high, yielding occurs at the upper surface due to combined tension and bending, and yielding of the lower surface does not occur until near the point of collapse.

Figure 6.20.2 shows profiles of direct stress through the beam cross-section at the integration station nearest the clamped end at various load levels, for a yield stress value of 15,000 psi. For this particular case, the lower surface stress reaches a minimum value, near compressive yielding, at the same time that geometric stiffening begins to dominate the state of stress; thereafter, the lower surface stress increases continuously until yielding (and collapse) occurs in tension over the entire section.

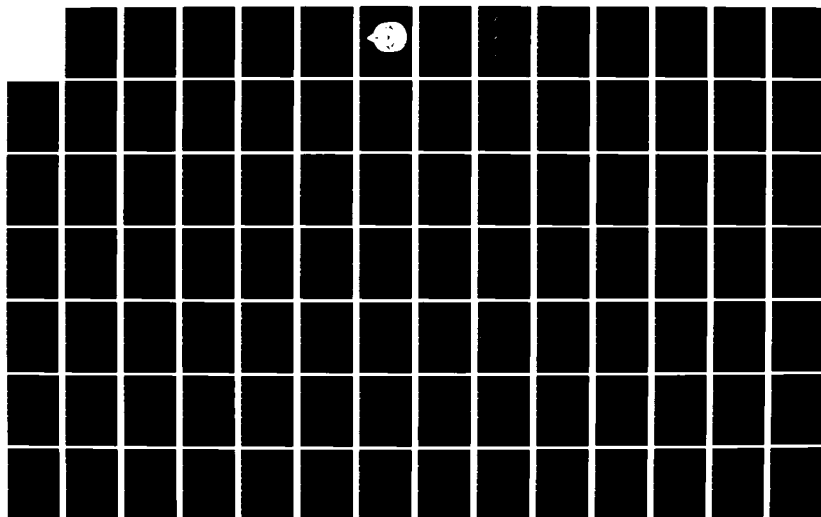
AD-A129 773

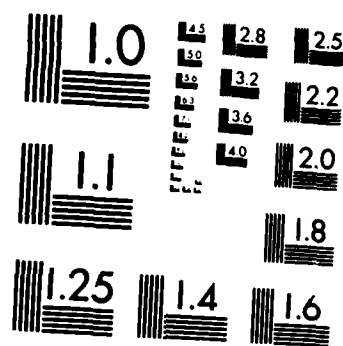
MAGNA (MATERIALLY AND GEOMETRICALLY NONLINEAR ANALYSIS)
PART I FINITE ELE. (U) DAYTON UNIV OH RESEARCH INST
R A BROCKMAN DEC 82 UDR-TR-82-111 AFWAL-TR-82-3098-PT-1
F33615-80-C-3403 F/G 12/1

4/8

UNCLASSIFIED

NL





MICROCOPY RESOLUTION TEST CHART
NATIONAL BUREAU OF STANDARDS-1963-A

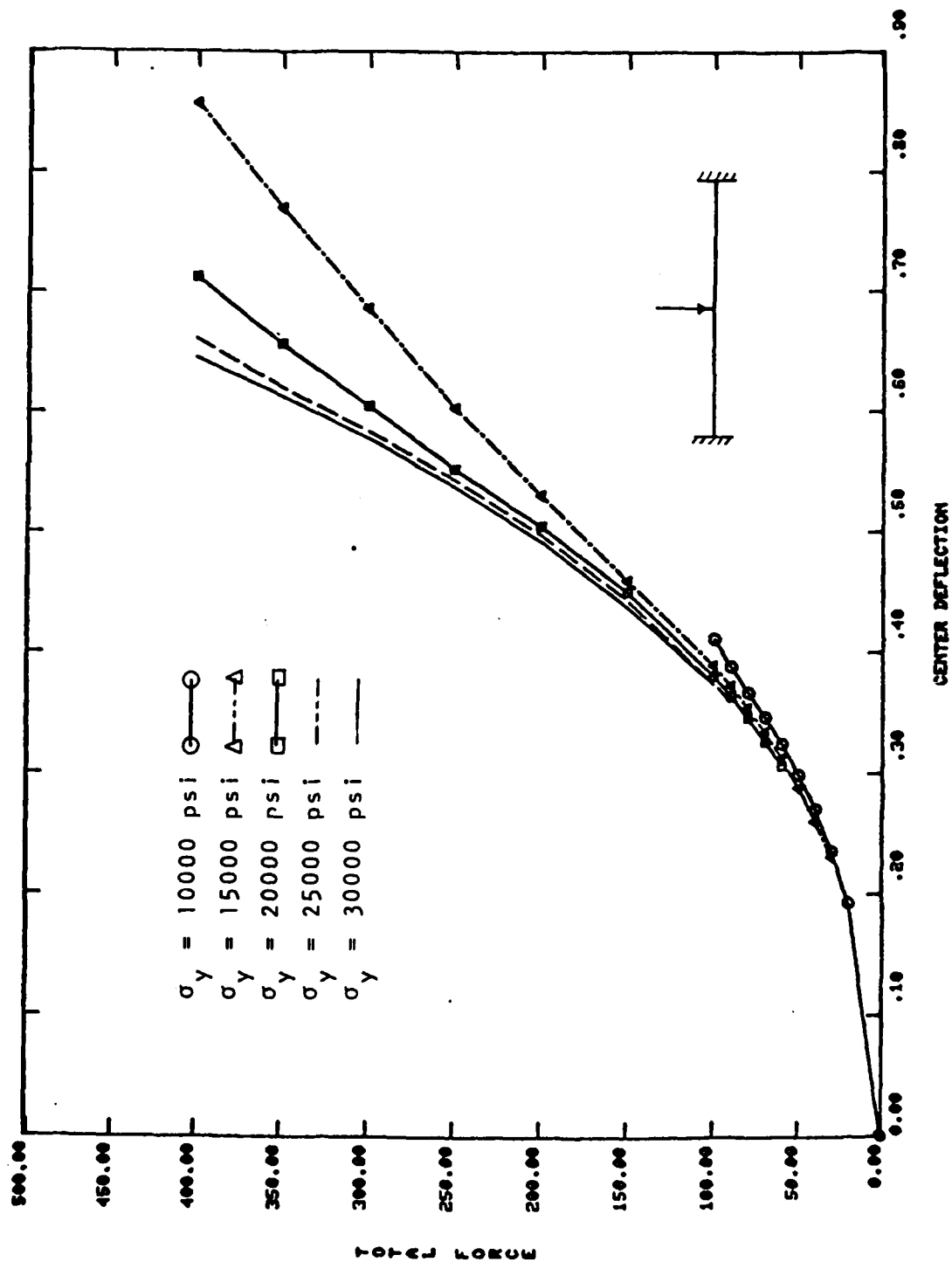


Figure 6.20.1 Central Deflection Histories for Clamped Beam, for Several Values of Yield Stress.

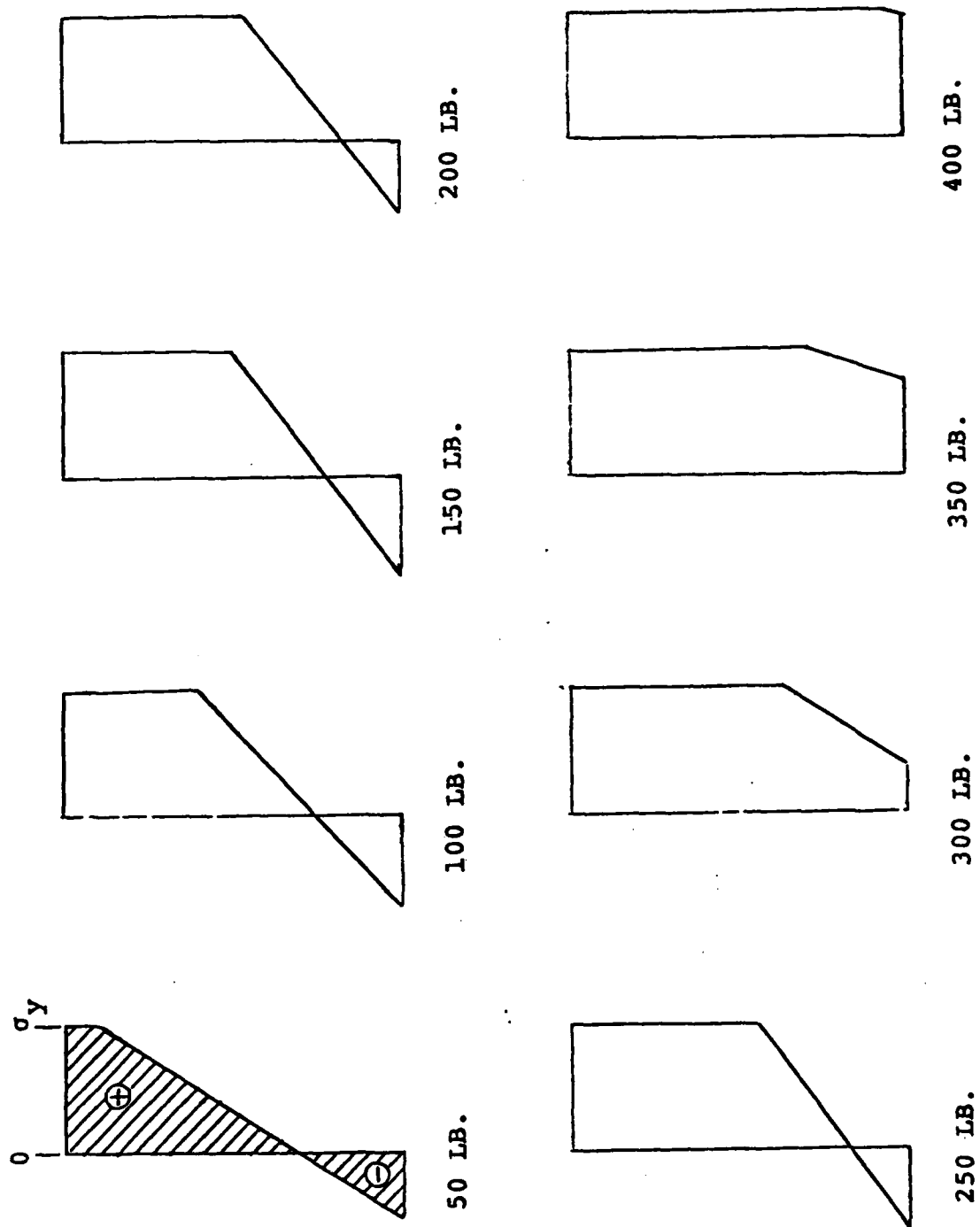


Figure 6.20.2 Cross-Sectional Stress Distribution in Clamped-Clamped Beam.

6.21 FORCED VIBRATIONS OF A JET ENGINE EXHAUST DUCT

The jet engine exhaust duct pictured in Figure 6.21.1 has been analyzed to determine the effect of damping treatment upon its forced vibration response. For a preliminary analysis, a highly idealized model of the cylindrical shroud and vanes is used, as shown in Figure 6.21.2. The model is constructed from variable-node solid elements (Element Type 7), and contains 414 degrees of freedom for one-half of the structure.

The vane and shroud are both made of steel. The primary geometric parameters are listed below.

| <u>Shroud</u> | <u>Vanes</u> |
|----------------|-----------------|
| 10.0 in. I.D. | 2.50 in. length |
| 0.05 in. thick | 0.10 in. thick |
| 3.0 in. wide | 1.0 in. wide |

The boundary conditions are indicated in Figure 6.22.2; each of the vane inner ends is fully clamped, as is the rearward edge of the shroud.

A natural frequency analysis has been performed for the shroud model, for the undamped case. The first three (symmetric) mode shapes are shown in Figure 6.21.3.

For forced vibration analysis, the exciting force is a single nodal force applied in the radial direction, at the top of the free edge of the shroud (see Figure 6.21.2). Although multiple-layer damping treatments could be modeled in detail, the present analysis uses internally damped elements to reduce the problem size. Four different cases are considered:

- (1) No damping;
- (2) Vane elements damped;
- (3) Shroud elements damped;
- (4) Vane and shroud elements damped.

In each damped case, a nominal value of five percent damping is used.

The variation of steady-state amplitude and phase angle versus frequency, at the point of load application, is shown for each of the four cases in Figure 6.21.4. For each case, frequency sweeps have been made over 20 forcing frequencies near the first undamped natural frequency, a total of 80 separate solutions. The results include both amplitude and phase angle information (similar to that shown in Figure 6.21.4) for each degree of freedom in the model. Each curve (20 solutions) required approximately 1.1 minutes of CPU time on the CYBER 175 computer.

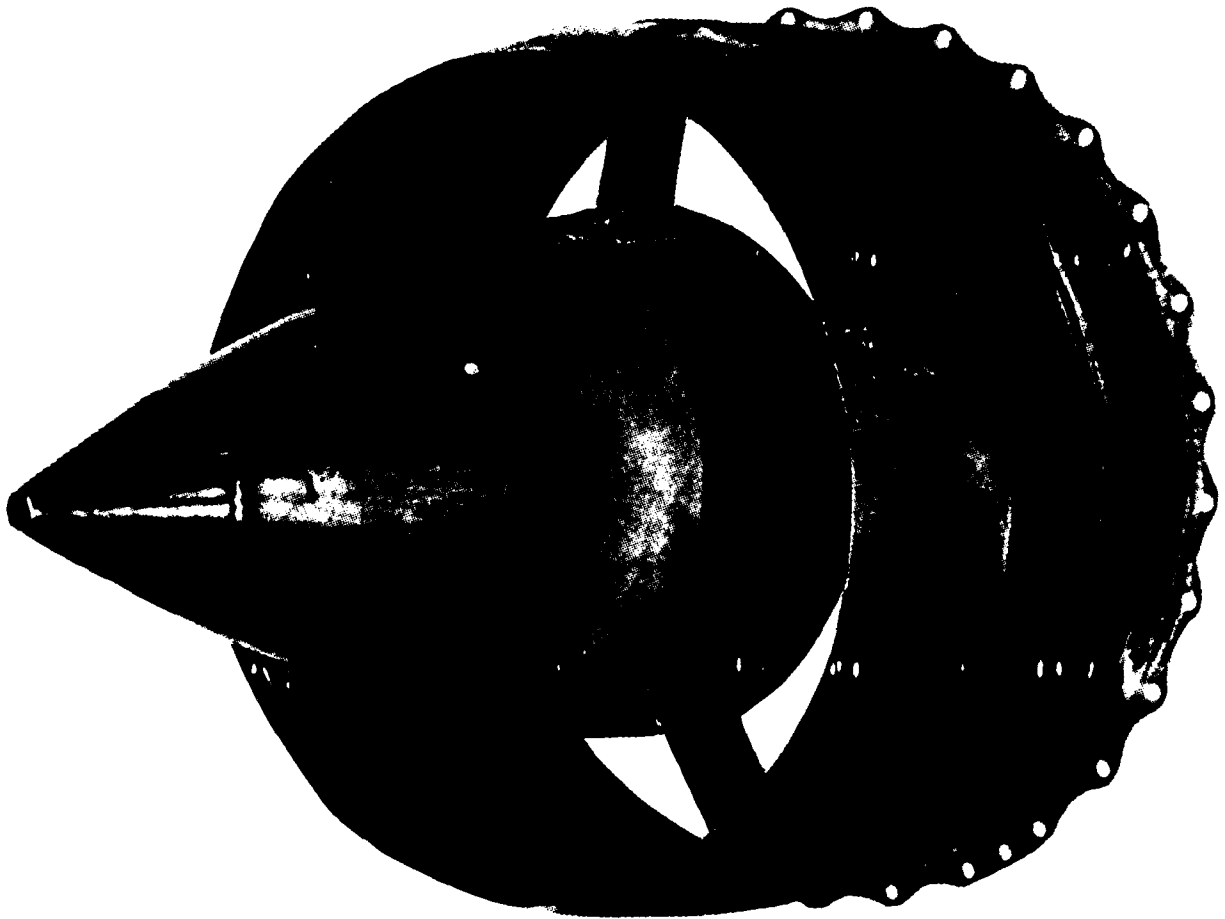


Figure 6.21.1 Engine Exhaust Duct.

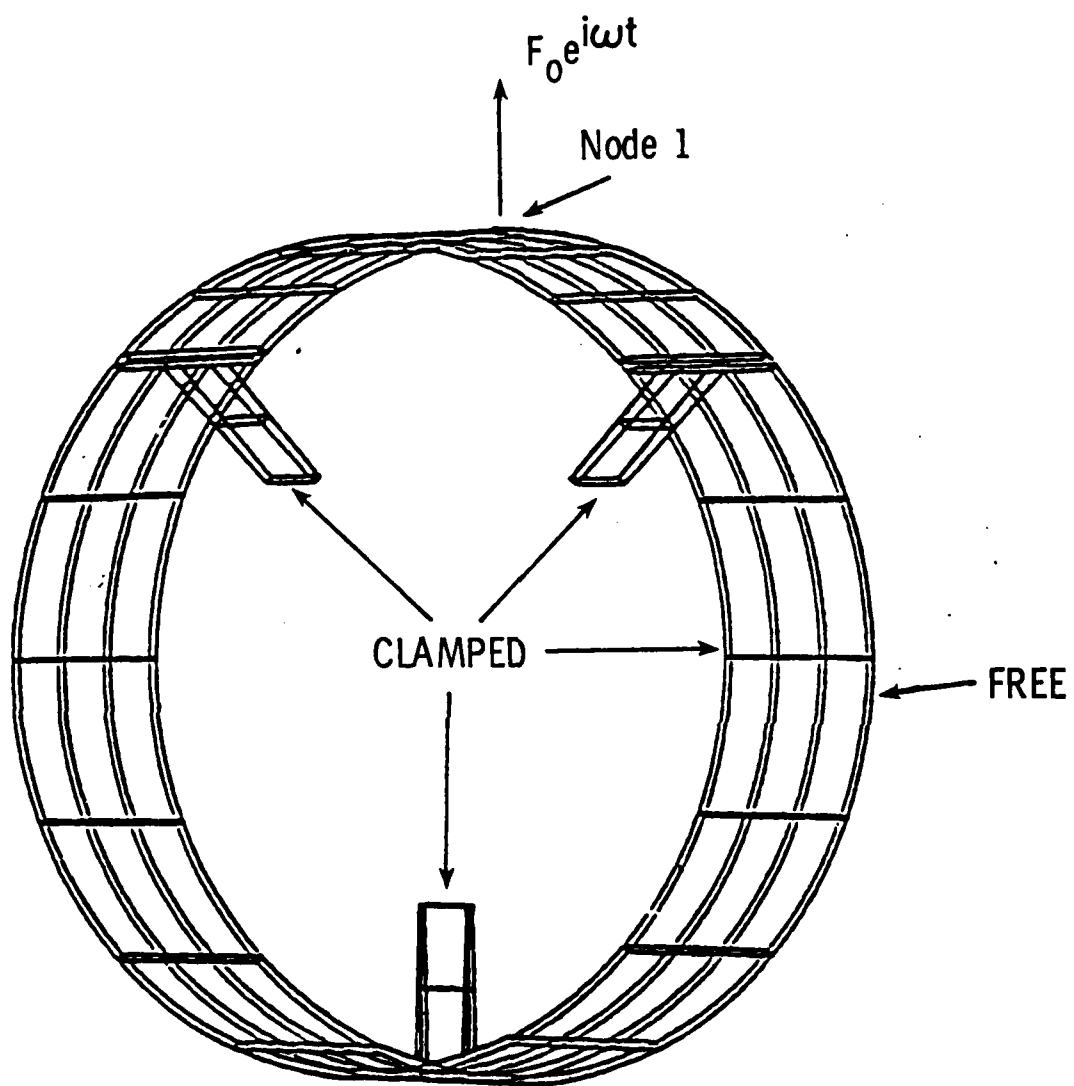


Figure 6.21.2 Finite Element Model of Engine Exhaust Duct Shroud.

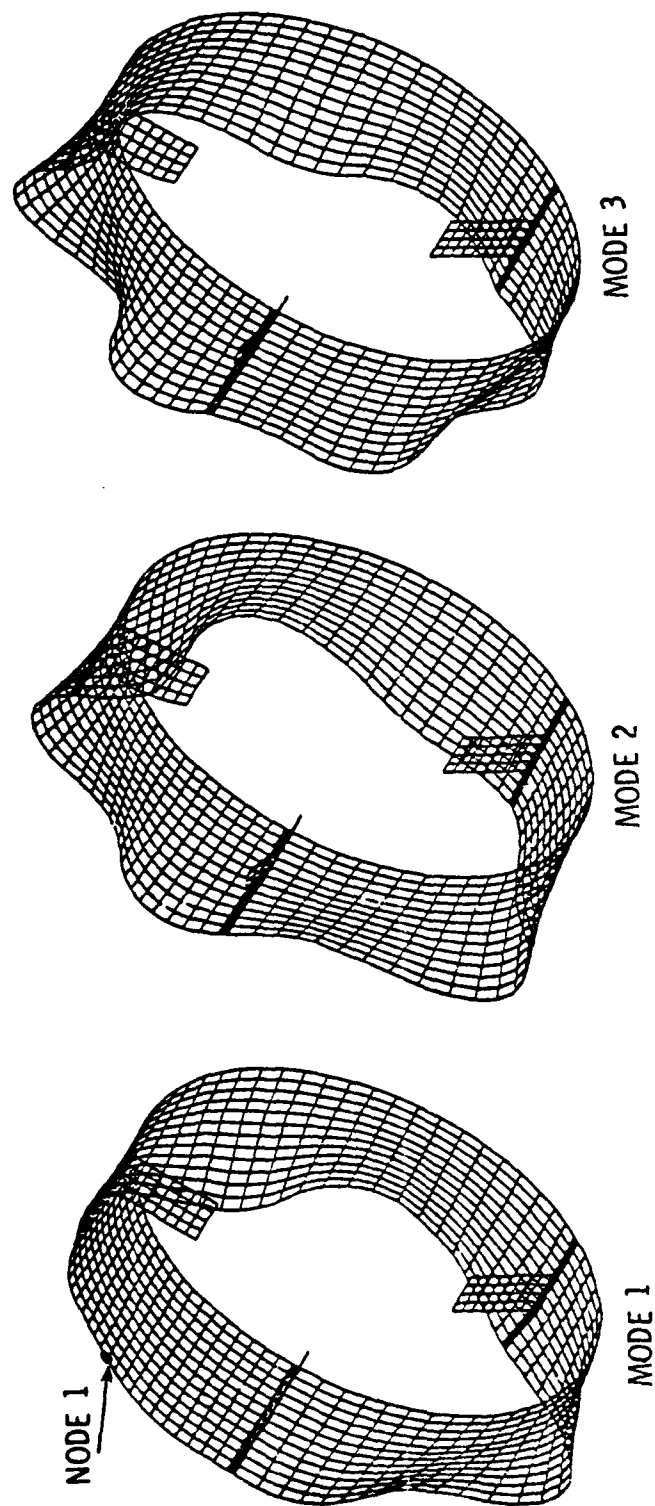
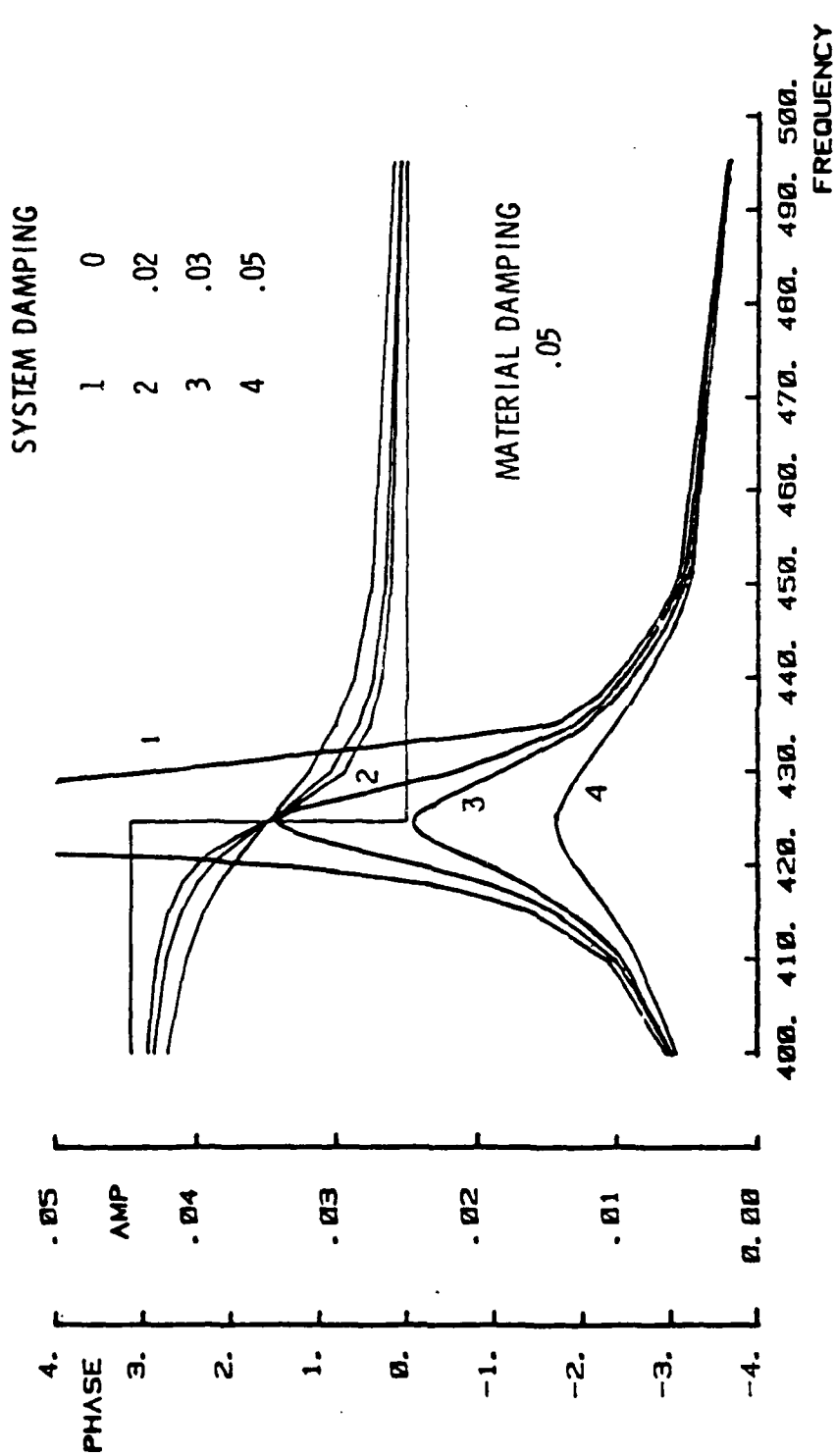


Figure 6.21.3 Exhaust Duct Mode Shapes.



Legend: 1 = no damping; 2 = vanes only; 3 = shroud only; 4 = shroud and vanes

Figure 6.21.4 Engine Exhaust Duct: Effect of Damping Treatment on Amplitude-Frequency Response.

CHAPTER 7

PROGRAM OPERATION

The MAGNA finite element program is currently operational on the following computer systems:

- CDC 6000 and CYBER series, under NOS/BE operating system;
- CRAY-1/S under COS 1.08; and
- Digital Equipment VAX 11/780 under VAX/VMS operating system.

Operation of the program on each of these computer systems is outlined in detail in this Chapter. Information to be used in estimating execution times for the various analysis options are also presented for each machine version.

7.1 CDC PROGRAM VERSION

The CDC version of MAGNA, excluding pre- and post-processing utility programs, consists of the following program files:

- MAGNAJCL - CDC Procedure for MAGNA Execution
- MAGNALGØ - Relocatable Object Version of MAGNA
- SEGLØD - Segmentation Loader Directives
- RABDRIVER - Main Program Source, in UPDATE Old Program Library Format
- MAGNAUPDGEN - Update Input Generator for Storage Capacity Modification
- STRAVG - CCL Procedure for STRAVG Execution
- STRAVGLGØ - Executable Version of STRAVG

While all of these programs and control procedures may be accessed during a typical MAGNA run, all but two, MAGNAJCL and STRAVG, are transparent to the user of the program. The execution of MAGNA is accomplished by simple commands which BEGIN execution of stored control language procedures which reside on these two files; in some instances, where postprocessing or restart files are to be used or saved, the needed files must be supplied as local (temporary) files before initiating the control procedures.

In subsequent sections, the use of these stored control procedures in conjunction with a variety of program options is discussed in some detail. Typical execution times on CDC machines are also tabulated for reference.

7.1.1 Job Control Language

The MAGNA program is normally executed on CDC machines under the control of the CCL (CYBER Control Language) procedure XMAGNA. This procedure automatically generates the command sequences required to attach and modify program files, compile and insert user-written subroutines, and load and execute the program.

The general form of the MAGNA job deck is as follows*:

1. JØB,T500,IØ500,CM165000.
2. SET,R1=MFL.
3. ATTACH,TAPE5,USERDATAFILE.
4. ATTACH,USRSUB,USERSUBROUTINEFILE.
5. REQUEST,MPØST,*PF.
6. ATTACH,P,MAGNAJCL,ID=BRØCKMAN,MR=1.
7. BEGIN,XMAGNA,P,MAIN,USRSUB,R1+B.
8. CATALOG,MPØST,PØSTPROCESSØRFILE.
9. ATTACH,STRAVG,ID=BROCKMAN,MR=1.
10. REQUEST,APØST,*PF.
11. BEGIN,STRAVG,STRAVG.
12. CATALOG,APØST,APØSTFILE.
13. 7/8/9 (end of record)
14. (STORAGE ALLOCATION card)
15. 7/8/9 (end of record)
16. 6/7/8/9 (end of job)

In the above deck, several options are used which are not always exercised in a typical analysis:

- user written subroutines
- modifications to storage capacity,
- execution of the stress smoothing utility STRAVG,
and
- cataloging of postprocessor files MPØST and APØST.

*Control statements required for analysis restarts can take on a number of different forms; for this reason, use of the restart functions is described separately at the end of this section.

For the simplest case, in which the above options are not needed, the deck setup has the much simpler form:

1. JØB,T500,IØ500,CM165000.
2. SET,R1=MFL.
3. ATTACH,TAPE5,USERDATAFILE.
6. ATTACH,P,MAGNAJCL,ID=BRØCKMAN,MR=1.
7. BEGIN,XMAGNA,P,,,R1+B.
8. 7/8/9 (end of record)
9. 6/7/8/9 (end of job)

The function of each card in the MAGNA execution deck is described in detail below.

CARD 1: JOB CONTROL CARD. The job control card requests system resources and identifies the job to the system. Estimates of execution times (T and IØ specifications) are discussed in Section 7.1.4. The default central memory (165000 octal words) is shown in the above examples; if user subroutines are supplied, or the storage capacity of the program is modified, the central memory requested should be modified accordingly (see Section 7.1.2). Note that if the postprocessor file MPØST is to be saved on magnetic tape, a single tape drive (i.e., MT1, NT1, PE1 or GE1) must be requested on the job card.

CARD 2: SET COMMAND. This control card places the amount of central memory requested in a machine register which is assessed by the procedure XMAGNA. The format of the SET command is always the same.

CARD 3: ATTACH, TAPE5. This command attaches the problem data (see Chapter 8) to the job as local file TAPE5. The data can also be copied directly from the input file (see the examples at the end of this Section).

CARD 4: ATTACH, user-written subroutines. This command is *optional*, and should be used to attach the source code of user-written subroutines on a named local file. User subroutines are then compiled and loaded automatically by XMAGNA. User-written subroutines can also be copied directly from the input file (see the examples at the end of this Section).

CARD 5: REQUEST,MPØST. If a postprocessor (MPØST) file is to be saved following the MAGNA analysis, the file must be assigned to a permanent storage device prior to the program execution. The command REQUEST, MPOST,*PF indicates that MPØST is to be saved as a permanent file on disc following the analysis. To record the file MPØST on magnetic tape, the request command is of the form REQUEST,MPØST,VSN=X01234.

CARD 6: ATTACH,P,MAGNAJCL. This command attaches the control language procedure XMAGNA as local file P. This card is always required, and its format is always the same. The required filename (MAGNAJCL,ID=BRØCKMAN is used above) may be installation dependent.

CARD 7: BEGIN command. The BEGIN statement initiates execution of the MAGNA program. The keyword MAIN is used only if the program storage capacity is to be modified (see Section 7.1.2); if this keyword appears in the BEGIN command, a STORAGE ALLOCATION card (Card 14, below) must be supplied. The second keyword (USRSUB in the above sample) is the name of the local file on which user-written subroutines are stored (this file is defined in Card 4); if user subroutines are not supplied, the second keyword is simply omitted. The last argument (R1+B) of the BEGIN command always has the same format.

CARD 8: CATALØG,MPØST. If the postprocessor file MPØST is to be saved on disc as a permanent file, the CATALØG statement is used to accomplish this. When MPØST is written directly to magnetic tape, the command UNLOAD,MPØST can be used

at this point, unless the STRAVG procedure is to be executed. If the postprocessor file is not to be saved, this command is simply omitted.

CARD 9: ATTACH,STRAVG. This command accesses the control procedure for the stress-smoothing utility program STRAVG. This job step is optional (and in fact may be performed in a separate background job). If smoothed nodal stress output is desired, an MPOST file must be created, since STRAVG uses the MPOST file as input. If no stress smoothing is done, lines 9-12 of the job deck should be omitted.

CARD 10: REQUEST,APOST. A request is issued at this point to associate the local file APOST (Averaged-stress POSTprocessor file) with either a permanent file device or a magnetic tape volume. The REQUEST command is of the same format as that described under Card 5.

CARD 11: BEGIN,STRAVG. The BEGIN command initiates execution of the STRAVG processor, described in Section 5.7. STRAVG accepts the MAGNA MPOST file as input, and generates the output file APOST. During this job step, it is advisable to have the MPOST file attached as a local disk file (rather than a tape file). The APOST file is written sequentially in one pass, and may be written directly to tape if desired.

CARD 12: CATALOG,APOST. The CATALOG statement writes the newly created APOST file to permanent storage on disk. If APOST has been written directly to tape, the UNLOAD command can be substituted for CATALOG.

CARD 13: (end of record). This card signifies the end of the control commands for the job, and is always required.

CARD 14: STORAGE ALLOCATION card. The STORAGE ALLOCATION card is required whenever the program storage capacity is to be modified. The keyword MAIN in the BEGIN statement (Card 7) causes the card to be read. The format of the

allocation card is (5I5); that is, five integer numbers of five digits each. Contents of the data fields, and the default and minimum values of each, are described in Section 7.1.2.

CARD 15: (end of record). This end of record card should be added whenever the STORAGE ALLOCATION card is present in a MAGNA job deck.

CARD 16: (end of job). The end of job (end of file) card is always required as the last card of the deck.

Other forms of the MAGNA job deck are possible. The most common alternate format consists of control cards and data together in the input stream. In this case, the input deck is arranged as shown below.

```
JØB,T500,IØ500,CM165000.  
SET,R1=MFL.  
CØPYCR,INPUT,TAPE5.  
ATTACH,P,MAGNAJCL,ID=BRØCKMAN,MR=1.  
BEGIN,XMAGNA,P,,,R1+B.  
7/8/9 (end of record)
```

|
input data
|

```
7/8/9 (end of record)  
6/7/8/9 (end of job)
```

When the postprocessor file MPØST is to be saved from the analysis, the needed REQUEST and CATALØG (or UNLØAD) commands are simply inserted before and after the BEGIN statement as before. The additional input deck sample below illustrates the user of user subroutines, the MPØST option, the use of STRAVG, and the STORAGE ALLOCATION card, with all data and user-written routines supplied in the job deck. The MPØST file is copied to seven-track magnetic tape prior to the execution of STRAVG. The APOST file is written directly to disk.

```

JØB, T500, IØ500, CM145000, MT1.
SET, R1=MFL.
CØPYCR, INPUT, TAPE5.
CØPYCR, INPUT, USRSUB.
REWIND, USRSUB.
ATTACH, P, MAGNAJCL, ID=BRØCKMAN, MR=1.
BEGIN, XMAGNA, P, MAIN, USRSUB, R1+B.
REQUEST, TEMP, MT, RING, VSN=X01234.
REWIND, MPØST, TEMP.
CØPYBF, MPØST, TEMP.
RETURN, TEMP.
ATTACH, STRAVG, ID=BRØCKMAN, MR=1.
REQUEST, APØST, *PF.
BEGIN, STRAVG, STRAVG.
CATALØG, APØST, MYAPØST.
7/8/9 (end of record)

```

input data

7/8/9 (end of record)

user-written subroutines

7/8/9 (end of record)

12000^^200

7/8/9 (end of record)

6/7/8/9 (end of job)

STORAGE ALLOCATION CARD

Many nonlinear solutions are best performed in more than one submission of the program, in order to

- permit monitoring of the progress of the solution,
- reduce computer resource requests and safeguard against "time limit" errors, and
- modify the analysis data or solution type at intervals during the solution.

When requested, MAGNA will create a checkpoint file at the conclusion of specified increments during the solution, permitting the analysis to be restarted from any of these points in a subsequent job. The necessary input data is described in Sections 5.8 and 8.3. A new restart tape always has the local (temporary) file name NRSTAP, while old restart tapes (i.e., those to be read in to restart the analysis) are expected to reside on local file TAPE23. Both NRSTAP and TAPE23 can reside physically on the same tape, as illustrated in the examples below. Each solution increment which is written to the restart tape constitutes one system logical record on the tape; this rule is used to position the restart tape correctly prior to executing MAGNA. Several example cases are given below to illustrate the use of the nonlinear restart function.

Case 1: New Analysis, and Creation of Restart Tape

In this case, a new restart tape is to be written directly to magnetic tape. No input tape is used, since this is the beginning of a new analysis. Problem data is included in the job deck, and the program storage area is modified using a STORAGE ALLOCATION card.

JØB,T300,IØ450,CM145000,GE1.

SET,R1=MFL.

COPYCR,INPUT,TAPE5.

REQUEST,NRSTAP,GE,RING,VSN=XØ1234.

ATTACH,P,MAGNAJCL,ID=BRØCKMAN,MR=1.

BEGIN,XMAGNA,P,MAIN,,R1+B.

RETURN,NRSTAP.

7/8/9 (end of record)

input data

7/8/9 (end of record)

12000^^400

7/8/9 (end of record)

6/7/8/9 (end of job)

Case 2: Analysis Restart, with no New Restart Tape

This example illustrates a restart analysis in which the solution is to be continued from the ninth increment written to tape (i.e., the old restart tape must be positioned after the end of the eighth checkpoint file). No new restart tape is to be written. Also, in this analysis a postprocessing file (MPØST) is copied to tape upon completion of the run. Note in particular that the old restart tape is requested, and then the needed file is copied to a local file TAPE23. The file TAPE23 need not be rewound prior to execution. This procedure should *always* be followed, rather than requesting the magnetic tape directly as TAPE23. Failure to do so will result in an error.

```
JØB,T1000,IØ1500,CØ165000,GE1.  
SET,R1=MFL.  
CØPYCR,INPUT,TAPE5.  
REQUEST,ØLDTAP,GE,NØRING,VSN=XØ1234.  
SKIPF,ØLDTAP,8,0,B.  
CØPYBR,ØLDTAP,TAPE23.  
UNLØAD,ØLDTAP.  
ATTACH,P,MAGNAJCL,ID=BRØCKMAN,MR=1.  
BEGIN,XMAGNA,P,,,R1+B.  
REWIND,MPØST.  
REQUEST,PØSTAP,GE,RING,VSN=X12345.  
CØPYBR,MPØST,PØSTAP.  
RETURN,PØSTAP.  
7/8/9 (end of record)
```

input data

```
7/8/9 (end of record)  
6/7/8/9 (end of job)
```

Case 3: Intermediate Analysis, with Both Old and
New Restart Tapes Used

In the job below, a solution is restarted from the sixth (and last) stored increment of an existing restart tape. Results of the current analysis are to be added to the end of the previous restart tape for later use.

```
JØB,T600,IØ600,CM165000,GE1.  
SET,R1=MFL.  
ATTACH,TAPE5,MYDATA,CY=3.  
REQUEST,NRSTAP,GE,RING,VSN=X23456.  
SKIPF,NRSTAP,5,0,B.  
CØPYBR,NRSTAP,TAPE23.  
REWIND,NRSTAP.  
SKIPF,NRSTAP,6,0,B.  
ATTACH,P,MAGNAJCL,ID=BRØCKMAN,MR=1.  
BEGIN,XMAGNA,P,,,R1+B.  
RETURN,NRSTAP.  
7/8/9 (end of record)  
6/7/8/9 (end of job)
```

Note that the old and new restart tapes need not be the same; the use of multiple tapes may be desirable when one analysis is to be restarted from one (or more) intermediate points. The above case is modified below to demonstrate the use of different tapes for the old and new restart files.

```
JØB,T600,IØ600,CM165000,3E1.  
SET,R1=MFL.  
ATTACH,TAPE5,MYDATA,CY=3.  
REQUEST,ØLDTAP,GE,NØRING,VSN=X01234.  
SKIPF,ØLDTAP,5,0,B.  
CØPYBR,ØLDTAP,TAPE23.  
UNLØAD,ØLDTAP.  
REQUEST,NRSTAP,GE,RING,VSN=X12345.  
ATTACH,P,MAGNAJCL,ID=BRØCKMAN,MR=1.  
BEGIN,XMAGNA,P,,,R1+B.  
RETURN,NRSTAP.  
7/8/9 (end of record)  
6/7/8/9 (end of job)
```


The second type of restart function performed by MAGNA is the eigenvalue solution with prestress effects (Sections 4.5, 5.9, and 8.3.). With this option, a nonlinear solution is performed first to determine an equilibrium state, in which large deflections and plastic deformation may be present. The element stiffnesses computed from the nonlinear solution are then incorporated into the natural frequency analysis, which represents a small, superimposed vibratory motion.

The following example demonstrates the use of the eigenvalue-with-prestress option. In the example, the MPOST file from the nonlinear analysis is also used to provide the reference geometry to the frequency solution; the MPOST file generated in the natural frequency analysis will then contain (a) the prestressed state geometry as the "undeformed" geometry, and (b) the superimposed vibration modes as the displacements.

Run No. 1: Nonlinear Analysis for Prestressed State

```
JØB,T800,IØ1000,CM165000.  
SET,R1=MFL.  
ATTACH,TAPE5,NØNLINDATA.  
ATTACH,P,MAGNAJCL,ID=BRØCKMAN,MR=1.  
REQUEST,MPØST,*PF.  
BEGIN,XMAGNA,P,,,R1+B.  
CATALØG,MPØST,NØNLINMPØST.  
REQUEST,DUMMY,*PF.  
REWIND,STIFF,DUMMY.  
CØPYBF,STIFF,DUMMY.  
CATALØG,DUMMY,NLSTIFF.  
7/8/9 (end of record)  
6/7/8/9 (end of job)
```

Run No. 2: Frequency Analysis with Prestress

```
JØB,T400,IØ600,CM165000.  
SET,R1=MFL.  
ATTACH,TAPE5,FREQDATA.  
ATTACH,TAPE22,NLSTIFF.
```

```

ATTACH,TAPE23,NØNLINMPØST.
ATTACH,P,MAGNAJCL,ID=BRØCKMAN,MR=1.
REQUEST,MPØST*PF.
BEGIN,XMAGNA,P,,,R1+B.
CATALØG,MPØST,FREQMPØST.
7/8/9 (end of record)
6/7/8/9 (end of job)

```

7.1.2 Modification of Storage Capacity

The MAGNA finite element program allocates array storage dynamically for all matrices and internal tables whose size is problem-dependent. Although analyses of rather large size can be accomplished using only a small amount of array space, computational and input-output efficiencies on CDC computers can be improved dramatically by allocating additional storage for larger problems. Modification of the program capacity is quite simple, since only one additional data card is needed in the input deck (see Section 7.1.1, Card 14, STORAGE ALLOCATION card).

Program storage capacity is controlled by the lengths of five labeled COMMON blocks declared in the main program:

1. /BLANK/* - major arrays and internal tables, including assembled stiffness, mass, or effective stiffness matrix partitions.
2. /IDENT/ - tables describing the envelope of active nonzero coefficients in the system matrix.
3. /BLOX/ - tables containing matrix partitioning data for out-of-core solutions.
4. /BLEQ/ - additional partitioning data for out-of-core matrix storage.

*Labeled COMMON is used to replace blank COMMON in the program for compatibility with the CDC segmentation loader.

5. /INDXK/ - record key tables for random-access disc files.

This ordering corresponds to the integer data fields appearing on the STORAGE MODIFICATION card. The minimum and default lengths of these blocks are summarized in Table 7.1.1.

The COMMON areas /BLANK/ and /IDENT/ determine the *in-core* storage capacity of the program, while the remaining blocks are directly related to limits on *out-of-core* storage used in the solution. In general, the most effective use of the program for large-scale analysis results from increasing the blocks /BLANK/ and /IDENT/. The default lengths of COMMON blocks /BLOX/, and /BLEQ/, and /INDXK/ are normally sufficient for all but the largest three-dimensional problems.

The largest array areas allocated in /BLANK/ correspond to partitions of the system stiffness (or effective stiffness) matrices. Therefore, the length of this block is determined largely by the number of unknowns in the model and the density of the stiffness matrix. For models consisting primarily of one- and two-dimensional elements, the default length of 20000 words in COMMON/BLANK/ is often sufficient for problems of a few thousand degrees of freedom. In three-dimensional nonlinear and/or dynamic analysis, input-output efficiency can be substantially improved by extending /BLANK/ for discretization involving more than about 2000 degrees of freedom or very large matrix bandwidth.

The length of COMMON/IDENT/ must be greater than the total number of unknowns in the final system of equations to be solved. The total number of unknowns is the sum of the number of unconstrained nodal degrees of freedom and the number of linear constraints specified in the problems.

Lengths of the COMMON blocks /BLOX/, /BLEQ/, and /INDXK/, which determine the out-of-core storage capacity of MAGNA, can generally remain at their default values for all but the largest three-dimensional analyses. A possible exception

TABLE 7.1.1
 DEFAULT AND MINIMUM COMMON BLOCK LENGTHS
 (CDC Program Version)

| <u>BLOCK</u> | <u>DEFAULT LENGTH</u> | <u>MINIMUM LENGTH</u> |
|--------------|-----------------------|-----------------------|
| /BLANK/ | 20000 | 12000 |
| /IDENT/ | 2500 | 100 |
| /BLOX/ | 150 | 150 |
| /BLEQ/ | 150 | 150 |
| /INDXK/ | 170 | 170 |

is the case of a linear static analysis in which many load cases are to be solved. For the purpose of increasing problem size capacity, increasing the available in-core storage (by extending /BLANK/ and /IDENT/) is *always* preferred.

It should be noted that, when the program storage capacity is modified, the central memory (CM on the job card, see Section 7.1.1) requested for the job must be adjusted accordingly. The default central memory requirement for execution of MAGNA is approximately 165000 octal (60000 decimal) words. Table 7.1.2 provides a list of octal-decimal conversions for use in determining the number of octal words of memory to be requested when the program storage space is changed.

Additional increases in central memory may be necessary when user-written subroutines (Chapter 9) are supplied to the program, if lengthy code or large amounts of data are involved. For storage of smaller amounts of data which is defined and used in these subroutines, a reserved COMMON block, COMMON/USERC/, is provided, with a default length of 20 words. This area, which is saved and reloaded whenever user subroutines are called, is included in the stated values for central memory.

7.1.3 Reserved File Names

Since the MAGNA program is executed through control language procedures which automatically attach, return, and create the proper files for use in the analysis, certain local file names are reserved for use in the CDC control procedure XMAGNA. The following names are *reserved file names*, and should not be in use at the time the BEGIN command is issued.

| | |
|---------|--------|
| ABS | NEWPL |
| COMPILE | OLDPL |
| ERRORS | SEGLD |
| MAGNA | TEMP |
| MAIN | UPDGEN |
| MODS | UPDIN |
| NEWB | USUB |

TABLE 7.1.2
OCTAL-DECIMAL CONVERSIONS

| Decimal | Octal | Octal | Decimal |
|---------|--------|--------|---------|
| 1000 | 1750 | 1000 | 512 |
| 5000 | 11610 | 10000 | 4096 |
| 10000 | 23420 | 60000 | 24576 |
| 20000 | 47040 | 100000 | 32768 |
| 30000 | 72460 | 120000 | 40960 |
| 40000 | 116100 | 140000 | 49152 |
| 50000 | 141520 | 160000 | 57344 |
| 60000 | 165140 | 200000 | 65536 |
| 70000 | 210560 | 220000 | 73728 |
| 80000 | 234200 | 240000 | 81920 |
| 90000 | 257620 | 260000 | 90112 |
| 100000 | 303240 | 300000 | 98304 |

7.1.4 Typical Execution Times on CDC Computers

Data are presented in this section to aid in the estimation of computer run times on CDC machines using MAGNA. The times, formulas, and data given are based upon observed computer times on the CDC 6600 computer. For the CYBER 74 machine, run times are nearly identical; on the CYBER 170 series machines, CPU times should be approximately one-half the CDC 6600 requirement, and I/O times may be slightly less.

In nonlinear analysis, computing times are typically dominated by the *number of elements* rather than by the time to solve the system equations. This observation is particularly true in three-dimensional problems, due to the computational effort involved in evaluating nonlinear effects on the element level. Computing time factors for each of the MAGNA elements are listed in Table 7.1.3; for most nonlinear solutions, the CPU time requirement can be estimated conservatively using the formula:

$$\begin{aligned} \text{CPU time} = & (\text{CPU Time Factor}) \times (\text{Number of Elements}) \\ & \times (\text{Number of Integration Points/Element}) \\ & \times (\text{Number of Increments}) \end{aligned}$$

where CPU time factor is read from the table. A small amount of overhead (typically 10-15 percent) should be added to this estimate to account for additional calculations (e.g., solution of equations). The IO-to-CPU ratios given in the table are next used to estimate the IO time requirement. For nonlinear analyses using equilibrium iteration, each cycle of iteration should be counted as an "increment" in estimating computing time requirements. However, since iteration cycles generally require less time than an incremental step, the resulting estimates will generally be quite conservative.

Typical solution times for selected linear and nonlinear analyses are given in Table 7.1.4. As an example of the estimation of CPU times, consider the F-16 windshield

TABLE 7.1.3
COMPUTING TIME FACTORS FOR INDIVIDUAL ELEMENT TYPES (CDC 6600)

| Element Type | CPU Sec/Integration Point/Increment | | IO/CPU Time Ratio | |
|--------------|-------------------------------------|-----------|-------------------|-----------|
| | Linear | Nonlinear | Linear | Nonlinear |
| 1 | 0.04 | 0.20 | 2.0-6.0 | 1.0-1.4 |
| 2 | 0.01 | 0.04 | 2.0-6.0 | 2.0-4.0 |
| 3 | 0.04 | 0.01 | 4.0-7.0 | 4.0-10.0 |
| 4 | 0.01 | 0.01 | 4.0-10.0 | 4.0-10.0 |
| 5 | 0.02 | 0.08 | 1.0-6.0 | 2.0-4.0 |
| 6 | 0.03 | 0.11 | 2.0-8.0 | 1.5-3.5 |
| 7 | 0.03 | 0.11 | 2.0-8.0 | 1.5-3.5 |
| 8 | 0.02 | 0.07 | 2.0-10.0 | 2.0-5.0 |
| 9 | .01 | .01 | 3.0-7.0 | 4.0-8.0 |
| 10 | .01 | .01 | 3.0-7.0 | 4.0-8.0 |

TABLE 7.1.1.4
TYPICAL NONLINEAR SOLUTION TIMES USING THE MAGNA PROGRAM
(CDC 6600 and CYBER Computers)

| Structure Description | Number of Nodes | Degrees of Freedom | Number of Elements | Element Types | Nonlinearities /Solution Type | Number of Solution Increments | Total Number of Iterations | Computer and Memory Requirements | CPU Time (sec.) | I/O Time (sec.) |
|---------------------------|-----------------|--------------------|--------------------|----------------------------|----------------------------------|-------------------------------|----------------------------|----------------------------------|-----------------|-----------------|
| Plane, 2 bay Truss | 6 | 8 | 10 | Truss | Large Displacement, Plasticity | 25 | 25 | CDC CYBER 175 135K (8) | 12 | 96 |
| Aircraft Wing | 56 | 144 | 166 | Membrane Shear Panel Truss | Large Displacement, Plasticity | 20 | 20 | CDC CYBER 74 135K (8) | 187 | 305 |
| Perforated Strip | 95 | 174 | 24 | Eight-Node Plane Stress | Large Displacement, Plasticity | 8 | 23 | CDC CYBER 175 135K (8) | 54 | 222 |
| Clamped Beam | 20 | 36 | 4 | Three-Dimensional Shell | Large Displacement | 16 | 16 | CDC CYBER 74 135K (8) | 60 | 88 |
| Aircraft Windshield | 242 | 613 | 100 | Three-Dimensional Shell | Large Displacement | 10 | 10 | CDC CYBER 175 156K (8) | 382 | 309 |
| Deep Arch, Clamped/Hinged | 176 | 340 | 43 | Three-Dimensional Shell | Large Displacement | 6 | 56 | CDC CYBER 175 156K (8) | 652 | 426 |
| Circular Plate | 122 | 287 | 14 | 20-Node Solid | Large Displacement, Plasticity | 20 | 20 | CDC CYBER 175 135K (8) | 895 | 572 |
| Square Plate | 130 | 328 | 16 | 16-Node Solid | Large Displacement, Postbuckling | 20 | 47 | CDC CYBER 175 140K (8) | 268 | 1082 |
| Recessed Fastener | 248 | 756 | 100 | Eight-Node Solid | Large Displacement, Plasticity | 13 | 13 | CDC CYBER 175 156K (8) | 475 | 1762 |
| Aircraft Windshield | 483 | 1110 | 50 | 20-Node Solid | Large Displacement | 10 | 10 | CDC CYBER 175 156K (8) | 420 | 980 |

analysis using solid isoparametric elements (Type 6), with a 3x3x3 integration rule for each element. From Table 7.1.3, the CPU time factor is 0.11 for nonlinear analysis with Element Type 6. Thus,

$$\text{CPU Time} \approx (0.11) \times (50 \text{ elements}) \times (27 \text{ points/element}) \\ \times (10 \text{ increments}),$$

giving 1485 seconds. Allowing a 10 percent overhead for equation solving and other calculations gives an estimate of 1630 CPU seconds (for the CDC 6600). Actual execution time on the CYBER 175 is 673 seconds. The actual IO time required for the above example is 1136 seconds, so that the IO/CPU factor of 1.5 gives a conservative estimate.

Computation time for nonlinear dynamic analysis are only slightly higher than for nonlinear static analysis, and the above estimating procedure can be used with confidence. It should be noted that, in elastic-plastic analysis, the computing time cannot be predicted quite as accurately, since the amount of calculation per element may vary considerably. For strongly materially nonlinear analysis, it is suggested that 30-50 percent overhead be allowed with the estimates obtained using the table. IO times are *not* affected in materially nonlinear analysis.

For linear analysis with MAGNA, the estimation of computer resources is much more difficult, since solution times are dominated by the assembly and equation solving steps. Values of the CPU time factor given in Table 7.1.3 refer to element calculations *only*, and are not reliable for estimating computer times in linear analysis. The IO/CPU time ratios which appear in the table are fairly accurate, if a reasonable value of the CPU time can be predicted. The higher values of the IO/CPU ratio in Table 7.1.3 are applicable primarily in linear dynamic analysis, where CPU times are typically very modest.

7.2 CRAY PROGRAM VERSION

The CRAY-1 version of MAGNA offers the highest capacity and computational speed of all the machine versions available. The usual CRAY batch analysis run consists of executing MAGNA and the STRAVG utility, as described in the subsequent sections.

Since the CRAY-1 computer does not support interactive operation, job streams and data files will generally be prepared on a "front-end" computer and then submitted to the CRAY system through remote batch input utility. For this reason, the exact procedures to be used in executing the CRAY version of MAGNA can be highly installation-dependent. Some typical procedures, which conform to the conventions of the United Computing Systems, Inc. APEX/SL time sharing service, are outlined in this section. For information concerning job control language and job submission at particular installations, users should contact the installation representative, or look for system information files outlining the correct procedures to be followed.

7.2.1 Job Control Language

The CRAY computer version of MAGNA is typically executed using a job stream of the form shown below.

1. JØB,T20
2. ACCOUNT, username, password.
3. GET,FT05=data filename.
4. REWIND,FT05.
5. ASSIGN,DN=FT10,BS=10.
6. GET,MAGNA/CRYLBRY.
7. MAGNA.
8. RETURN,FT10,FT12,FT14,FT20,FT98.
9. PUT,FT99=MPØST/D.
10. GET,STRAVG/CRYLBRY.
11. STRAVG.

12. PUT,FT98=APØST/D.
EØR (end-of-record)
EØF (end-of-job)

An input file such as the one listed above is submitted to the CRAY computer using an RJE (Remote Job Entry) command:

RJE,F=filename,D=CRAY,CI=TTY

Here "filename" defines the file on which the job stream resides; D=CRAY gives the job destination; CI=TTY defines the character set under which the input file was created (in this case, 6- or 12-bit characters, 60 bits per word).

The function of each entry in the MAGNA input file is explained in detail below.

CARD 1: JOB CARD. The JOB card identifies the start of the job stream and requests system resources for the run. Note that the central memory (CM) parameter may be necessary if storage capacity is changed (see Section 7.2.2) or if user subroutines are used.

CARD 2: ACCOUNT CARD. This entry defines the user number under which the job is to be executed, and a password entry which is verified to prevent unauthorized access.

CARD 3: GET,FT05. This control card accesses the problem data from permanent disk storage. It should be noted that the data file must be converted to CRAY ASCII format, as follows:

GET,TEMP=originaldatafile.
REFØRM,I=TEMP,Ø=DATA,CI=TTY,CØ=CAS.
PUT,DATA=datafilename.

CARD 4: REWIND,FT05. The REWIND command positions the input data file at the beginning of information.

CARD 5: ASSIGN,DN=FT10. This ASSIGN command allocates memory buffer space to the main random access file used by MAGNA. While the use of this command is optional, its use is suggested for all moderate to large size problems to maximize input/output efficiency.

CARD 6: GET,MAGNA. This command is used to access the MAGNA executable program. The exact filename may vary with the installation.

CARD 7: MAGNA. This control statement initiates execution of the MAGNA program.

CARD 8: RETURN. Following execution, several scratch files created by MAGNA must be RETURNed to the system before succeeding job steps, to avoid conflicting usage.

CARD 9: PUT,FT99. This command is used immediately following the execution of MAGNA, to save the MPØST postprocessor file created during the run. The MPØST file must be saved if deformed geometry plotting is to be done (see Section 5.7 and Chapter 11). If no MPOST file is created during the analysis, this and the three control statements following should be omitted.

CARD 10: GET,STRAVG. The STRAVG utility program, which performs element stress extrapolation and smoothing operations, is accessed in this job step. Note that the MPOST postprocessor file is needed for execution of STRAVG (see Section 5.7); if no postprocessor file has been written, this and the remaining two control statements should be omitted.

CARD 11: STRAVG. This command initiates execution of STRAVG.

CARD 12: PUT,FT98. The PUT command is used to save (or replace) the APØST postprocessing file created by STRAVG. The APØST file is used interactively following the analysis to generate contour plots and a variety of variable-versus-variable plots.

Alternatively, MPØST and APØST files may be archived on magnetic tape using the TAPEØUT control command. To write the MPØST file to tape, for example, Card 10 is replaced by:

TAPEØUT,DN=FT99,VSN=XXXXXX,PE,NT.

It should be noted that the MPØST and/or APØST files, having been written in CRAY ASCII format, must be converted at some point for use in plotting on the front-end computer. The needed data conversion may be performed as a part of the batch analysis run (preceding the corresponding PUT commands) or at a later time.

The use of user-written subroutines with the CRAY version of MAGNA is straightforward, although the program must be accessed in a somewhat different manner than before. The following example demonstrates the required procedure, assuming that the source version of all user subroutines resides on the permanent file USUBS, in CRAY ASCII format.

```

JOB,T10
ACCOUNT,USERID,PASSWD.
GET,FT05=MYDATA.
REWIND,FT05.
GET,USUBS.
CFT,I=USUBS,E=2,ØN=A.
RETURN,USUBS.
REWIND,$BLD.
GET,$ØBL-MAGØBJ/CRYLBRY.
BUILD,I=0,NØDIR.
LDR,DN=$NBL.
RETURN,FT10,FT12,FT14,FT20,FT98.
GET,STRAVG/CRYLBRY.
STRAVG.
EØR
EØF

```

The analysis restart facilities in MAGNA are useful in monitoring the progress of a solution, changing the solution strategy if necessary, and safeguarding against time limits or other causes of premature termination. Use of the restart option is discussed in Sections 5.8 and 8.3, and job control procedures for restart with the CRAY version of MAGNA are outlined below.

Due to the rather limited tape processing capabilities available on the CRAY-1 computer, the restart facility for the CRAY version of the program works with permanent disk files. These files can be transferred to and from magnetic tape at the beginning and end of a job as necessary. During

execution, MAGNA will access existing restart files directly from permanent file storage, and will save new restart files as permanent files automatically during the analysis.

The only additional job control statements which are needed in using restart are those which retrieve existing files from tape, or write newly created files to tape. The following rules should be noted concerning restart files stored on disk:

- the file label IDOLD input in Section 8.3.3 is also assumed to be the permanent file name of an existing restart file;
- if the file IDOLD is not found, the program will attempt to read restart data from the local data set FT23;
- new restart files will be written to a permanent file whose name is defined by IDNEW (Section 8.3.3), with each completed restart checkpoint replacing the last one; and
- if either of IDOLD, IDNEW are blank strings, a file name of "REST" is assumed.

The following example shows a typical job control stream in which an input restart file is transferred from tape, and the newly created restart file is copied to tape at the end of the job. It is assumed that the RESTART card in Section 8.3.3 defines IDOLD=RES1 and IDNEW=RES2. The input data file resides on the permanent disk file NLDATA.

```
JOB,T40
ACCOUNT,MYID,MYPASS.
GET,FT05=NLDATA.
REWIND,FT05.
TAPEIN,DN=TEMP,VSN=10325,PE,NT.
PUT,TEMP=RES1/D.
```



```

RETURN,TEMP.
ASSIGN,DN=FT10,BS=10.
GET,MAGNA/CRYLBRY.
MAGNA.
UNSAVE,RES1.
GET,RES2.
TAPEØUT,DN=RES2,VSN=12486,PE,NT.
UNSAVE,RES2.
RETURN,FT10,FT12,FT14,FT20,FT98.
GET,STRAVG/CRYLBRY.
STRAVG.
PUT,FT98=APØST2/D.
EØR
EØF

```

The use of the eigenvalue-with-prestress restart function (Sections 4.5, 5.9 and 8.3) requires two job submissions. First, a nonlinear solution is performed to determine the prestressed equilibrium state, in which large deflections and material yielding may occur. The element stiffness file obtained from the nonlinear analysis is supplied to the natural frequency analysis to compute the frequencies and mode shapes associated with small superimposed vibrations. Optionally, the MPØST file from the nonlinear solution can also be read into the eigenvalue analysis. This permits post-plotting to be done with the computed mode shapes superimposed on the deformed geometry in the prestressed state.

The following example illustrates the use of this option, in which both the nonlinear stiffness file and the MPØST file are passed from one solution to the other.

Run No. 1: Nonlinear Analysis for Prestressed State

```

JØB,T20.
ACCØUNT,USERID,PASSWD.
GET,FT05=NLDATA.

```

REWIND, FT05.
ASSIGN, DN=FT10, BS=10.
GET, MAGNA/CRYLBRY.
MAGNA.
PUT, FT12=NLSTIF/D.
PUT, FT99=NLPØST/D.
EØR
EØR

Run No. 2: Frequency Analysis with Prestress

JØB, T10.
ACCØUNT, USERID, PASSWD.
GET, FT05=EIGDAT.
REWIND, FT05.
GET, FT22=NLSTIF.
GET, FT23=NLPØST.
ASSIGN, DN=FT10, BS=10.
GET, MAGNA/CRYLBRY.
MAGNA.
PUT, FT99=MPØST/D.
EØR
EØF

7.2.2 Modification of Storage Capacity

The CRAY-1 version of MAGNA takes advantage of the large amount of main memory available on the CRAY computer (typically 1-4 million decimal 64-bit words), and the default storage allocations should generally be sufficient for nonlinear problems involving several thousand degrees of freedom. For extremely large problems the program capacity can be modified using the procedures outlined below.

The storage capacity of MAGNA is controlled by the lengths of five labeled COMMON blocks declared in the main program:

1. /BLANK/ - major arrays and internal tables, including assembled stiffness, mass, or effective stiffness matrix partitions.
2. /IDENT/ - tables describing the envelope of active nonzero coefficients in the system matrices.
3. /BLOX/ - tables containing matrix partitioning data for out-of-core solutions.
4. /BLEQ/ - additional partitioning data for out-of-core matrix storage.
5. /INDXK/ - record key tables for random-access disc files.

Table 7.2.1 shows both the minimum and the default lengths of each block.

COMMON areas /BLANK/ and /IDENT/ control the *in-core* storage capacity of the program, while the remaining blocks are related to limits on *out-of-core* storage available during a solution. It is generally most effective to extend the storage capacity of MAGNA by adjusting the in-core blocks /BLANK/ and /IDENT/, since input/output operations are relatively expensive on the CRAY machine. The default lengths of the remaining three COMMON areas should be sufficient even for large three-dimensional problems.

Situations in which the main storage block, /BLANK/, can be profitably increased include larger problems (10000 degrees of freedom or more), models with very large average bandwidth, and natural frequency solutions in which a number of frequencies and modes are to be extracted.

The array area declared in COMMON block /IDENT/ must be greater than the total number of unknowns in the final system of equations (including linear constraint equations).

TABLE 7.2.1
 DEFAULT AND MINIMUM COMMON BLOCK LENGTHS
 (CRAY Program Version)

| <u>BLOCK</u> | <u>DEFAULT LENGTH</u> | <u>MINIMUM LENGTH</u> |
|--------------|-----------------------|-----------------------|
| /BLANK/ | 80000 | 12000 |
| /IDENT/ | 15000 | 100 |
| /BLOX/ | 150 | 150 |
| /BLEQ/ | 150 | 150 |
| /INDXK/ | 170 | 170 |

To implement changes in storage capacity on the CRAY system, it is necessary to edit the main program (MAGNA) on the front-end computer. For each COMMON block described above, an associated variable is also defined which gives the length of the block. The pertinent COMMON and assignment statements are listed below.

```

PROGRAM MAGNA

.
.
.
COMMON/BLANK/A(n1)
COMMON/IDENT/ID(n2)
COMMON/BLØX/NSHFT(n3)
COMMON/BLEQ/NEQLIM(n3)
COMMON/INDXK/INDK(n4)
.
.
.
NWØRK  = n1
NID    = n2
NNS    = n3
NINDXK = n4
.
.
.
END

```

Once the main program has been edited, the run procedure is similar to that used with user-written subroutines (see Section 7.2.1). The following example illustrates the necessary control language, assuming that the edited main program (and any user-written subroutines) are contained on the permanent file MYMAIN in CRAY ASCII file format.

```

JØB,T15
ACCØUNT,MYID,MYPASS.
GET,FT05=MYDATA.

```

```

GET,MYMAIN.
REWIND,MYMAIN.
CFT,I=MYMAIN,E=2,ØN=A.
RETURN,MYMAIN.
REWIND,$BLD.
GET,$ØBL=MAGØBJ/CRYLBRY.
BUILD,I=0,NØDIR.
LDR,DN=$NBL.
RETURN,FT10,FT12,FT14,FT20,FT98.
GET,STRAVG/CRYLBRY.
STRAVG.
PUT,FT98=APØST/D.
EØR
EØF

```

7.2.3 Execution Times on the CRAY-1 Computer

Data collected from observed solution times on the CRAY-1 system are summarized briefly in this section, to aid in the estimation of computer run times for MAGNA. Although the CRAY-1 computer is a vector processor, near-maximum CPU speed is attained even for relatively short vector operations; this virtue permits computing times to be estimated with reasonable accuracy, at least for nonlinear problems.

In nonlinear analysis, computing times are typically dominated by the *number of elements* rather than by the time to solve the system equations. This observation is particularly true in three-dimensional problems, due to the computational effort involved in evaluating nonlinear effects

on the element level. Computing time factors on the CRAY-1 for each of the MAGNA elements are listed in Table 7.2.2; for most nonlinear solutions, the CPU time requirement can be estimated using the formula

$$\begin{aligned} \text{CPU time} = & (\text{CPU Time Factor}) \times (\text{Number of Elements}) \\ & \times (\text{Number of Integration Points/Element}) \\ & \times (\text{Number of Increments}) \end{aligned}$$

where the CPU time factor is read from the table. Additional processing time (typically 15-20 percent) should be added to this estimate to account for additional calculations (e.g., solution of equations). When equilibrium iterations are used in the nonlinear analysis, each cycle of iteration should be counted as an "increment" when estimating computer time requirements. Since iteration cycles consume less time than a full incremental solution step, the resulting estimates will be quite conservative in general.

Computation times for nonlinear dynamic analysis are only slightly higher than for nonlinear static analysis, and the above estimating procedure can be used with confidence. It should be noted that, in elastic-plastic analysis, the computing time cannot be predicted quite as accurately, since the amount of calculation per element may vary considerably. For materially nonlinear analysis, it is suggested that 30-50 percent overhead be allowed with the estimates obtained using the table.

For linear analysis with MAGNA, the estimation of computer resources is much more difficult, since solution times are dominated by the assembly and equation solving steps. Values of the CPU time factor given in the Table refer to element calculations *only*; typically, the assembly and solution steps in a linear analysis will require an equal (or slightly greater) amount of processing time.

TABLE 7.2.2

COMPUTING TIME FACTORS FOR INDIVIDUAL ELEMENT TYPES (CRAY-1)

| Element Type | CPU Second/Integration Point/Increment | |
|--------------|--|-----------|
| | Linear | Nonlinear |
| 1 | 0.002 | 0.021 |
| 2 | 0.001 | 0.002 |
| 3 | 0.001 | 0.001 |
| 4 | 0.001 | 0.001 |
| 5 | 0.002 | 0.005 |
| 6 | 0.002 | 0.011 |
| 7 | 0.002 | 0.011 |
| 8 | 0.002 | 0.007 |
| 9 | 0.001 | 0.001 |
| 10 | 0.001 | 0.001 |

7.3 VAX PROGRAM VERSION

The VAX 11/780 minicomputer version of MAGNA, although slowest in execution of the machine versions available, is by far the most convenient to use. All necessary job control procedures are generated interactively in response to simple prompts, including assignment of data files, modification of program storage capacity and linking of user-written subroutines. Several examples are included in this section to indicate the general procedures involved.

Generation of the MAGNA batch command sequence is initiated by executing an interactive procedure from the VAX command mode:

```
$@[MAGNA.RAB]SETUP*
```

The SETUP procedure requests the needed information for processing the analysis run, and writes the completed command file to disk under the name MBATCH.COM. The MBATCH command file is then entered for execution using the VAX/VMS SUBMIT command; for example,

```
$SUBMIT/AFTER=time MBATCH
```

An example of the execution of SETUP is shown in Figure 7.3.1, for an analysis which uses no special features of MAGNA (e.g., user subroutines, restart). Data describing the options and resources needed for the job are segregated into three *data modules*:

- (1) User-Written Subroutines
- (2) Storage Allocation Modification
- (3) Process File Names and Devices

For the example shown, the input is limited to module (3), in which the input data file (MYDATA.DAT) is defined, and the

*Directory and file names may be installation dependent.

\$ plmagna.rablssetup

```
*****
*
*           MAGNA BATCH INPUT PROCEDURE
*           -----
*   TERMINAL SESSION :      28-OCT-1981 19:00
*           -----
*   DO MODIFY/CORRECT/ABORT SESSION, TYPE <CTRL> Y .
*
*****
```

1. USER SUBROUTINES.

.....ANY USER SUPPLIED SUBROUTINES?(Y/N).....: n

END SPECIFICATIONS FOR MODULE : 1

2. STORAGE ALLOCATION MODIFICATION.

.....CHANGE DEFAULT STORAGE ALLOCATION?(Y/N).....: n

END SPECIFICATIONS FOR MODULE : 2

3. INPUT OF PROCESS FILE NAMES AND DEVICES.

.....SHOW DIRECTORY?(Y/N).....: y

.....TYPE DIRECTORY NAME (DEF=<RET>).....:

Figure 7.3.1. Typical Execution of VAX SETUP Control Procedure.

Directory _DRA1:[MAGNA.TEST]

APOST.DAT:1 MYDATA.DAT:1

Total of 2 files.

3(A)...DEFINE INPUT JOB STREAM (UNIT 5 - ALL CASES).

. . . .TYPE INPUT DATA FILE_NAME.TYPE.....: mydata.dat

3(B)...DEFINE OUTPUT JOB STREAM (UNIT 6 - ALL CASES).

. . . .DEFAULT OUTPUT IS TO BATCH PRINTER...OK?(Y/N).....: y

3(C)...EXEC FILE SPECIFICATION:

. . . .DEFAULT EXE FILE NAME IS [MAGNA.RAB]MAGNA...OK?(Y/N).....: y

3(D)...POST-PROCESSOR FILE MANAGEMENT.

. . . .WILL A POST-PROCESSOR FILE BE WRITTEN?(Y/N).....: y

. . . .P-P FILE WILL BE WRITTEN TO DISK...OK?(Y/N).....: y

3(E)...RESTART FILE MANAGEMENT.

. . . .INPUT FROM OLD RESTART FILE?(Y/N).....: n

. . . .OUTPUT TO NEW RESTART FILE?(Y/N).....: n

END SPECIFICATIONS FOR MODULE : 3

BATCH INPUT SPECIFICATIONS COMPLETED.

. . . .DISPLAY TABLE OF COMPLETED MODULES?(Y/N).....: n

Figure 7.3.1 (continued).

ANY INITIAL OR FURTHER MODIFICATIONS?(Y/N).....: n

WRITING COMMAND PROCEDURE...

PROCEDURE WRITTEN. DISPLAY HERE TO USER?(Y/N).....: n

%PURGE-I-NOFILPURG, no files purged for _DRA1:[MAGNA.TEST]MBATCH.COM;

SESSION TERMINATED.

MAGNA BATCH RUN PROCEDURE WRITTEN TO FILE MBATCH.COM

‡ dir/size/date

Directory _DRA1:[MAGNA.TEST]

| | | |
|--------------|-----|-------------------|
| APOST.DAT;1 | 246 | 15-OCT-1981 14:23 |
| MBATCH.COM;1 | 6 | 28-OCT-1981 19:02 |
| MYDATA.DAT;1 | 11 | 13-OCT-1981 14:59 |

Total of 3 files, 263 blocks.

\$

Figure 7.3.1 (concluded).

disposition of the output and postprocessing files is declared. The resulting job procedure MBATCH.COM is listed in Figure 7.3.2.

When the program storage capacity is to be modified for larger problems (see Section 7.1.2, for example), additional input must be entered in module (2). This procedure is illustrated in Figure 7.3.3; here the default lengths of work areas /BLANK/ and /IDENT/ are modified from 20000 to 40000 and from 2500 to 4000 , respectively. Note that, when the storage capacity is changed, a new executable file must be created. The name of the new executable file is input as part of the module (3) data as shown in the Figure.

The executable version of MAGNA which is created when storage modifications are made is written to disk and may be reused without repeating the procedure. To reuse the modified executable version, it is necessary to override the use of the default executable file, as shown in Figure 7.3.4. For the case shown, the previously created file MYEXE.EXE (created in Figure 7.3.3) is reused, with the previous storage allocations retained.

Restart analyses on the VAX computer require input regarding the disposition of newly-created checkpoint files (tape or disk); the necessary file names are input as part of the problem data (see Section 8.3). Figure 7.3.5 shows the necessary input to SETUP for writing a new restart file to magnetic tape*. Figure 7.3.6 contains a listing of the MBATCH procedure generated when both the restart option and storage modifications are used in a single job.

When old restart files are to be read during an analysis, the present control procedure requires that the old restart

*Tape mounting procedures and device names may vary between installations, and therefore minor modifications of the generated control procedure may be necessary.

```

$ type mbatch.com
$ SET VERIFY
$ SET DEF [MAGNA.TEST]
$!
$! MAGNA BATCH INPUT PROCEDURE.
$! USER : [MAGNA.TEST]
$! SESSION : 28-OCT-1981 19:00
$!
$! ON ERROR THEN GOTO TERMINUS
$!-----RUN MAGNA.
$ ASSIGN/USER_MODE [MAGNA.TEST]MYDATA.DAT FOR005
$ ASSIGN/USER_MODE SYS$OUTPUT FOR006
$ RUN [MAGNA.RAB]MAGNA
$!-----COMPLETED RUN.
$ RUN DRA1:[MAGNA.RAB]COST
$ DEL MAGNEM.DAT;*
$ RUN DRA1:[MAGNA.RAB]PAGER
$!-----STRESS_AVERAGING AND NODAL_STRESS OUTPUT
$ RUN DRA1:[MAGNA.RAB]STRAVG
$ RUN DRA1:[MAGNA.RAB]PAGER
$ SET NOVERIFY
$!-----DETERMINE EXEC_FILE.
$ DIR := DIR/DATE/OUTPUT=SCRATCH.TXT/VERSION=1
$ DIR [MAGNA.RAB]MAGNA
$ OPEN/READ SCR SCRATCH.TXT
$ READ SCR ABC
$ READ SCR ABC
$ READ SCR ABC
$ READ SCR EXEC_FILE
$ CLOSE SCR
$ DELETE SCRATCH.TXT;0
$ COPY SYS$INPUT: SYS$OUTPUT

*****
* INPUT SPECIFICATIONS USED BY MAGNA BATCH INPUT PROCEDURE *
* USER DIRECTORY : [MAGNA.TEST] *
* ----- *
* PROC FILE USED : MBATCH.COM;1 28-OCT-1981 19:02 *
* ----- *
$ WRITE SYS$OUTPUT "* EXEC FILE USED : ", EXEC_FILE, " *"
$ COPY SYS$INPUT: SYS$OUTPUT
* ----- *
*
*****

```

Figure 7.3.2. Batch Command Procedure MBATCH.COM.

1. USER SPECIFIED SUBROUTINES :

FORTTRAN FILES INPUT :
NONE INPUT
OBJECT FILES INPUT :
NONE INPUT

2. STORAGE ALLOCATION MODIFICATIONS :

NO NEW MODIFICATIONS. ALLOCATIONS
ARE SET IN NAMED EXECUTABLE FILE.

3. PROCESS FILE NAMES AND DEVICES :

INPUT DATA FILE (UNIT 5)...: CMAGNA.TESTIMYDATA.DAT
OUTPUT FILE (UNIT 6).....: SYS\$OUTPUT
EXEC FILE (NEW OR OLD)....: CMAGNA.RABIMAGNA

POST-PROCESSOR FILE.....: WRITE TO DISK
RESTART INPUT FILE.....: NONE INPUT
RESTART OUTPUT FILES...: NONE OUTPUT
TAPE LOGICAL NAME.....: NONE USED

***** TABLE COMPLETE *****

\$ TERMINUS:
\$ SET NOVERIFY
\$ LOGOUT
\$ EXIT
\$

Figure 7.3.2. (concluded).

2. STORAGE ALLOCATION MODIFICATION.

. . . .CHANGE DEFAULT STORAGE ALLOCATION?(Y/N).....: y

. . . .DEFAULT /BLANK/ LENGTH = 20000 ...OK?(Y/N)....: n

. . . .NEW /BLANK/ LENGTH?.....: 40000

. . . .DEFAULT /IDENT/ LENGTH = 2500 ...OK?(Y/N)....: n

. . . .NEW /IDENT/ LENGTH?.....: 4000

END SPECIFICATIONS FOR MODULE : 2

3. INPUT OF PROCESS FILE NAMES AND DEVICES.

. . . .SHOW DIRECTORY?(Y/N).....: n

3(A)...DEFINE INPUT JOB STREAM (UNIT 5 - ALL CASES).

. . . .TYPE INPUT DATA FILE_NAME.TYPE.....: metadata.dat

3(B)...DEFINE OUTPUT JOB STREAM (UNIT 6 - ALL CASES).

. . . .DEFAULT OUTPUT IS TO BATCH PRINTER...OK?(Y/N).....: y

3(C)...NAME OF EXEC FILE TO BE CREATED:

. . . .TYPE NEW EXEC FILE_NAME.....: mvexe.exe

Figure 7.3.3. Modification of Program Storage Capacity in SETUP.

3. INPUT OF PROCESS FILE NAMES AND DEVICES.

. . . .SHOW DIRECTORY?(Y/N).....: n

3(A)...DEFINE INPUT JOB STREAM (UNIT 5 - ALL CASES).

. . . .TYPE INPUT DATA FILE_NAME,TYPE.....: mydata.dat

3(B)...DEFINE OUTPUT JOB STREAM (UNIT 6 - ALL CASES).

. . . .DEFAULT OUTPUT IS TO BATCH PRINTER...OK?(Y/N).....: y

3(C)...EXEC FILE SPECIFICATION:

. . . .DEFAULT EXE FILE NAME IS CMAGNA.RABIMAGNA...OK?(Y/N).....: n

. . . .TYPE EXE FILE_NAME.....: myexe.exe

Figure 7.3.4. Specification of New Executable Version of MAGNA.

3(D)...POST-PROCESSOR FILE MANAGEMENT.

. . . .WILL A POST-PROCESSOR FILE BE WRITTEN?(Y/N).....: y

. . . .P-P FILE WILL BE WRITTEN TO DISK...OK?(Y/N).....: y

3(E)...RESTART FILE MANAGEMENT.

. . . .INPUT FROM OLD RESTART FILE?(Y/N).....: n

. . . .OUTPUT TO NEW RESTART FILE?(Y/N).....: y

. . . .RESTART FILE WILL BE WRITTEN TO DISK...OK?(Y/N).....: n

RESTART FILE WILL BE WRITTEN TO TAPE.

3(F)...TAPE OUTPUT DEFINITIONS.

WHEN MOUNTING TAPE USER MUST DEFINE A
LOGICAL NAME FOR THE VOLUME MOUNTED.

. . . .TYPE LOGICAL NAME TO BE USED ABOVE.....: rf

END SPECIFICATIONS FOR MODULE : 3

Figure 7.3.5. Request for Restart Tape in SETUP.

```

$ type mbatch.com
$ SET VERIFY
$ SET DEF [MAGNA.TEST]
$!
$!  MAGNA BATCH INPUT PROCEDURE.
$!    USER : [MAGNA.TEST]
$!    SESSION : 28-OCT-1981 19:07
$!
$ ON ERROR THEN GOTO TERMINUS
$!----CREATE/RUN EDIT PROCEDURE
$!----TO ALTER STORAGE ALLOCATION.
$ COPY DRA1:[MAGNA.RAB]MAINDUMMY.FOR MAGNDUMMY.FOR
$ OPEN/WRITE ED MAINEDT.COM
$ WRITE ED "$ SET VERIFY"
$ WRITE ED "$ EDIT/EDT -"
$ WRITE ED " MAGNDUMMY.FOR/OUTPUT=MAINMOD.FOR"
$ WRITE ED " S/**BLANK**/40000/ BEGIN THRU END"
$ WRITE ED " S/**IDENT**/4000/ BEGIN THRU END"
$ WRITE ED " S/**BLOX**/150/ BEGIN THRU END"
$ WRITE ED " S/**BLEQ**/150/ BEGIN THRU END"
$ WRITE ED " S/**INDXK**/170/ BEGIN THRU END"
$ WRITE ED " S/**NNS**/150/ BEGIN THRU END"
$ WRITE ED " EXIT"
$ WRITE ED "$ SET NOVERIFY"
$ WRITE ED "$ EXIT"
$ CLOSE ED
$ @ MAINEDT
$ DELETE MAGNDUMMY.FOR;0
$ DELETE MAINEDT.COM;0
$!----COMPILE FORTRAN FILES.
$ FORTRAN/NOLIST MAINMOD.FOR
$!----LINK NEW ROUTINES.
$ LINK/NOMAP/EXECUTABLE=[MAGNA.TEST]MYEXE.EXE-
  MAINMOD,-
  [MAGNA.RAB]MAGNALIB/INCLUDE=MAINX,-
  [MAGNA.RAB]MAGNALIB/LIBRARY

```

Figure 7.3.6. Control Procedure MBATCH.COM, with Modification of Storage Capacity.

```

$!-----RUN MAGNA.
$ ASSIGN/USER_MODE [MAGNA.TEST]MYDATA.DAT FOR005
$ ASSIGN/USER_MODE SYS$OUTPUT FOR006
$ ASSIGN/USER_MODE RF FOR098
$ RUN [MAGNA.TEST]MYEXE.EXE
$!-----COMPLETED RUN.
$ RUN DRA1:[MAGNA.RAB]ICOST
$ DEL MAGNEM.DAT;*
$ RUN DRA1:[MAGNA.RAB]PAGER
$!-----STRESS_AVERAGING AND NODAL_STRESS OUTPUT
$ RUN DRA1:[MAGNA.RAB]STRAVG
$ RUN DRA1:[MAGNA.RAB]PAGER
$ SET NOVERIFY
$!-----DETERMINE EXEC_FILE.
$ DIR := DIR/DATE/OUTPUT=SCRATCH.TXT/VERSION=1
$ DIR [MAGNA.TEST]MYEXE.EXE
$ OPEN/READ SCR SCRATCH.TXT
$ READ SCR ABC
$ READ SCR ABC
$ READ SCR ABC
$ READ SCR EXEC_FILE
$ CLOSE SCR
$ DELETE SCRATCH.TXT;0
$ COPY SYS$INPUT: SYS$OUTPUT

```

```

*****
*
* INPUT SPECIFICATIONS USED BY MAGNA BATCH INPUT PROCEDURE *
*
* USER DIRECTORY : [MAGNA.TEST] *
* ----- *
* PROC FILE USED : MBATCH.COM;2 28-OCT-1981 19:10 *
* ----- *
$ WRITE SYS$OUTPUT '* EXEC FILE USED : ', EXEC_FILE, ' *'
$ COPY SYS$INPUT: SYS$OUTPUT
* ----- *
*
*****

```

Figure 7.3.6. (continued).

1. USER SPECIFIED SUBROUTINES :

FORTTRAN FILES INPUT :
NONE INPUT
OBJECT FILES INPUT :
NONE INPUT

2. STORAGE ALLOCATION MODIFICATIONS :

/BLANK/ LENGTH = 40000
/IDENT/ LENGTH = 4000
/BLOX/ LENGTH = 150
/BLEQ/ LENGTH = 150
/INDXK/ LENGTH = 170

3. PROCESS FILE NAMES AND DEVICES :

INPUT DATA FILE (UNIT 5)...: CMAGNA.TESTJMYDATA.DAT
OUTPUT FILE (UNIT 6).....: SYS\$OUTPUT
EXEC FILE (NEW OR OLD)....: CMAGNA.TESTJMYEXE.EXE

POST-PROCESSOR FILE.....: WRITE TO DISK
RESTART INPUT FILE.....: NONE INPUT
RESTART OUTPUT FILES...: WRITE TO TAPE
TAPE LOGICAL NAME.....: RF

***** TABLE COMPLETE *****

\$ TERMINUS:
\$ SET NOVERIFY
\$ LOGOUT
\$ EXIT
\$

Figure 7.3.6. (concluded).

file reside on disk rather than tape, although a new restart file may be written to tape during the same job. A typical input sequence in SETUP, in which both old and new restart files are used, is given in Figure 7.3.7.

User subroutines may be supplied to the VAX version of MAGNA either in FORTRAN source or object (already compiled) form. FORTRAN source files must have the file type .FOR, and all user routines should reside on files having the same name as the user subroutine itself. Thus, the user routine TEMGEN (see Chapter 9), for example, must reside on file TEMGEN.FOR or TEMGEN.OBJ. Figure 7.3.8 demonstrates the declaration of user-written subroutines within the SETUP procedure. As with storage modification, the introduction of user subroutines will result in a new executable program, which can be used repeatedly without reentering the same user-written routines. Figure 7.3.9 shows the MBATCH procedure generated from the input of Figure 7.3.8; the new executable file MODVER.EXE, can be used again by simply overriding the default executable file name in SETUP (Figure 7.3.4).

At present, there exists only one instance in which the generated MBATCH procedure must be modified manually. This exception occurs in the nonlinear run used to obtain the prestressed state prior to a natural frequency solution with prestress included. In this situation, the statement

```
$DEL MAGNEM.DAT;*
```

must be modified to read

```
$RENAME MAGNEM.DAT MAGNST.DAT
```

This modification, together with the appropriate input parameters for the frequency analysis in Section 8.3, will supply the proper nonlinear stiffness coefficients to the eigenvalue solution. If the geometry file from the nonlinear analysis is to be passed to the frequency solution (for plotting only), the MPOST file should be renamed prior to the natural frequency run, by entering

```
$RENAME MAGNPO.DAT MAGNRO.DAT
```

3(D)...POST-PROCESSOR FILE MANAGEMENT.

. . . .WILL A POST-PROCESSOR FILE BE WRITTEN?(Y/N).....: y

. . . .P-P FILE WILL BE WRITTEN TO DISK...OK?(Y/N).....: y

3(E)...RESTART FILE MANAGEMENT.

. . . .INPUT FROM OLD RESTART FILE?(Y/N).....: y

. . . .TYPE OLD RESTART FILE_NAME.TYPE (DISK ONLY).....: myrest.dat

. . . .OUTPUT TO NEW RESTART FILE?(Y/N).....: y

. . . .RESTART FILE WILL BE WRITTEN TO DISK...OK?(Y/N).....: n

RESTART FILE WILL BE WRITTEN TO TAPE.

3(F)...TAPE OUTPUT DEFINITIONS.

WHEN MOUNTING TAPE USER MUST DEFINE A
LOGICAL NAME FOR THE VOLUME MOUNTED.

. . . .TYPE LOGICAL NAME TO BE USED ABOVE.....: rf2

END SPECIFICATIONS FOR MODULE : 3

Figure 7.3.7. SETUP Sequence for Requesting Old and New Restart Files.

\$ @[magna.rab]setup

```
*****
*
*              MAGNA BATCH INPUT PROCEDURE
*
*      -----
*      TERMINAL SESSION :      28-OCT-1981 19:21
*      -----
*
*      TO MODIFY/CORRECT/ABORT SESSION, TYPE <CTRL> Y .
*
*****
```

1. USER SUBROUTINES.

```

. . . .ANY USER SUPPLIED SUBROUTINES?(Y/N).....: y
1(A)...FILES WITH USER SUBROUTINES.
. . . .TYPE NUMBER OF USER FORTRAN FILES.....: 2
. . . .TYPE FORTRAN FILE NAME ( *OMIT* .FOR).....: uout
. . . .TYPE FORTRAN FILE NAME ( *OMIT* .FOR).....: vinit
1(B)...FILES WITH USER SUBROUTINES.
. . . .TYPE NUMBER OF USER OBJECT FILES.....: 1
. . . .TYPE OBJECT FILE NAME.....: nelas3.obj

END SPECIFICATIONS FOR MODULE : 1
-----
```

Figure 7.3.8. Introduction of User-Written Subroutines through SETUP.


```

$ type mbatch.com
$ SET VERIFY
$ SET DEF [MAGNA.TEST]
$!
$! MAGNA BATCH INPUT PROCEDURE.
$! USER : [MAGNA.TEST]
$! SESSION : 28-OCT-1981 19:21
$!
$ ON ERROR THEN GOTO TERMINUS
$!-----CREATE/RUN EDIT PROCEDURE
$!-----TO ALTER STORAGE ALLOCATION.
$ COPY DRA1:[MAGNA.RAB]MAINDUMMY.FOR MAGNDUMMY.FOR
$ OPEN/WRITE ED MAINEDT.COM
$ WRITE ED "$ SET VERIFY"
$ WRITE ED "$ EDIT/EDT -"
$ WRITE ED " MAGNDUMMY.FOR/OUTPUT=MAINMOD.FOR"
$ WRITE ED " S/**BLANK**/30000/ BEGIN THRU END"
$ WRITE ED " S/**IDENT**/3200/ BEGIN THRU END"
$ WRITE ED " S/**BLOX**/150/ BEGIN THRU END"
$ WRITE ED " S/**BLEQ**/150/ BEGIN THRU END"
$ WRITE ED " S/**INDXK**/170/ BEGIN THRU END"
$ WRITE ED " S/**NNS**/150/ BEGIN THRU END"
$ WRITE ED " EXIT"
$ WRITE ED "$ SET NOVERIFY"
$ WRITE ED "$ EXIT"
$ CLOSE ED
$ @ MAINEDT
$ DELETE MAGNDUMMY.FOR;0
$ DELETE MAINEDT.COM;0
$!-----COMPILE FORTRAN FILES.
$ FORTRAN/NOLIST MAINMOD.FOR
$ FORTRAN/LIST=SYS$OUTPUT -
    [MAGNA.TEST]UOUT,-
    [MAGNA.TEST]VINIT
$!-----LINK NEW ROUTINES.
$ LINK/NOMAP/EXECUTABLE=[MAGNA.TEST]MODVER.EXE-
    MAINMOD,-
    [MAGNA.TEST]UOUT,-
    [MAGNA.TEST]VINIT,-
    [MAGNA.TEST]NELAS3.OBJ,-
    [MAGNA.RAB]MAGNALIB/INCLUDE=MAINX,-
    [MAGNA.RAB]MAGNALIB/LIBRARY

```

Figure 7.3.9. Generated Control Procedure MBATCH.COM, with Storage Modifications and User-Written Subroutines.

```

$!-----RUN MAGNA.
$ ASSIGN/USER_MODE [MAGNA.TEST]PROBLEM2.DAT FOR005
$ ASSIGN/USER_MODE SYS$OUTPUT FOR006
$ RUN [MAGNA.TEST]MODVER.EXE
$!-----COMPLETED RUN.
$ RUN DRA1:[MAGNA.RAB]COST
$ DEL MAGNEM.DAT;*
$ RUN DRA1:[MAGNA.RAB]PAGER
$!-----STRESS_AVERAGING AND NODAL_STRESS OUTPUT
$ RUN DRA1:[MAGNA.RAB]STRAVG
$ RUN DRA1:[MAGNA.RAB]PAGER
$ SET NOVERIFY
$!-----DETERMINE EXEC_FILE.
$ DIR := DIR/DATE/OUTPUT=SCRATCH.TXT/VERSION=1
$ DIR [MAGNA.TEST]MODVER.EXE
$ OPEN/READ SCR SCRATCH.TXT
$ READ SCR ABC
$ READ SCR ABC
$ READ SCR ABC
$ READ SCR EXEC_FILE
$ CLOSE SCR
$ DELETE SCRATCH.TXT;0
$ COPY SYS$INPUT: SYS$OUTPUT

```

```

*****
* INPUT SPECIFICATIONS USED BY MAGNA BATCH INPUT PROCEDURE *
* USER DIRECTORY : [MAGNA.TEST] *
* ----- *
* PROC FILE USED : MBATCH.COM;1 28-OCT-1981 19:28 *
* ----- *
$ WRITE SYS$OUTPUT "* EXEC FILE USED : ", EXEC_FILE, " *"
$ COPY SYS$INPUT: SYS$OUTPUT
* ----- *
*
*****

```

Figure 7.3.9. (continued).

1. USER SPECIFIED SUBROUTINES :

FORTRAN FILES INPUT :
 UOUT
 VINIT
OBJECT FILES INPUT :
 NELAS3.OBJ

2. STORAGE ALLOCATION MODIFICATIONS :

/BLANK/ LENGTH = 30000
/IDENT/ LENGTH = 3200
/BLOX/ LENGTH = 150
/BLEQ/ LENGTH = 150
/INDXK/ LENGTH = 170

3. PROCESS FILE NAMES AND DEVICES :

INPUT DATA FILE (UNIT 5)...: CMAGNA.TESTJPROBLEM2.DAT
OUTPUT FILE (UNIT 6).....: SYS\$OUTPUT
EXEC FILE (NEW OR OLD)....: CMAGNA.TESTJMODVER.EXE

POST-PROCESSOR FILE....: WRITE TO DISK
RESTART INPUT FILE.....: NONE INPUT
RESTART OUTPUT FILES...: NONE OUTPUT
TAPE LOGICAL NAME.....: NONE USED

***** TABLE COMPLETE *****

\$ TERMINUS:
\$ SET NOVERIFY
 LOGOUT
\$ EXIT
\$

Figure 7.3.9. (concluded).

CHAPTER 8

INPUT DATA

The following sections describe the preparation of card input data for the MAGNA finite element analysis program. Input is divided into ten sets of data:

1. Problem Identification
2. Solution Options and Control Parameters
3. Iteration and Restart Parameters
4. Nodal Coordinate Data
5. Element Properties and Connectivity
6. Surface Contact Analysis Data
7. Boundary Conditions
8. Linear Constraint Data
9. Data Curves for Nonlinear and/or Dynamic Analysis
10. External Loads.

For each item of input, a corresponding FORTRAN variable name is listed. Unless otherwise noted, the type of the input variable corresponds to the standard FORTRAN naming conventions (names beginning with letters I through N are integer; all others are floating point numbers). All floating point data may be input with or without exponents in the data field provided. Integers and exponents must be right-justified in the data field.

Default values and other information about each item of input data are given in the form of notes which appear at the end of each section in this Chapter. Further examples of the input data formats can be found in the Appendix to this manual.

8.1 PROBLEM IDENTIFICATION

(Required)

| CARD | COL | DATA | DESCRIPTION | NOTES |
|------|------|-------|----------------------------------|-------|
| 1-3 | 1-80 | TITLE | Alphanumeric Problem Description | - |

8.2 SOLUTION OPTIONS AND CONTROL PARAMETERS

(Required)

| CARD | COL | DATA | DESCRIPTION | NOTES |
|------|-------|---------|---|-------|
| 1 | 1-4 | IOPT(1) | Solution Variable Set Code =1: Displacement U,V,W =2: Displacements and Rotations | (1) |
| | 5-8 | IOPT(2) | Analysis Type =1: Static =2: Transient Dynamic =3: Natural Frequencies =6: Steady-State Harmonic | - |
| | 9-12 | IOPT(3) | Material Nonlinearities Flag =1: Elastic Analysis =2: Materially Nonlinear Analysis | (2) |
| | 13-16 | IOPT(4) | Geometric Nonlinearities Flag =1: Small Displacement Analysis =2: Large Displacement Analysis | - |
| | 17-20 | IOPT(5) | Dynamic Solution Option =1: Newmark Integration (Implicit) =2: (Inactive) | (3) |
| | 21-24 | IOPT(6) | Matrix Reformation Interval for Nonlinear Analysis | (4) |
| | 25-28 | IOPT(7) | Matrix Profile Map Flag =0: No Map =1: Print Map of Matrix Topology | - |
| | 29-32 | IOPT(8) | Random File Write-in-Place Flag =0: No Write-in-Place =1: Rewrite All Random File Records Directly in Place | (5) |
| | 33-36 | IOPT(9) | Flag for Element Distributed Loads =0: No Distributed Loads =1: Read Distributed Loading Data | - |

| CARD | COL | DATA | DESCRIPTION | NOTES |
|-------------|-------|-----------|---|-------|
| 1 (cont) | 37-40 | IOPT(10) | Flag for User Loads Subroutine =0: Normal Loads Input =1: User Subroutine(s) Provided | - |
| | 41-44 | IOPT(11) | Flag for Postprocessor File Option =0: No Postprocessor File Written >1: Postprocessor File is to be Written on Local File MPOST at every IOPT (11)th Increment | - |
| | 45-48 | IOPT(12) | Number of Time Increment Changes in Nonlinear Solution | (6) |
| | 49-52 | IOPT(13) | Variable Time Step Flag =0: Fixed Time or Loading Increments =1: Automatic Variable Time Step to be Used in Solution | (7) |
| | 53-56 | IOPT(14) | Thermal Stress Analysis Flag =0: Neglect Thermal Effects =1: Include Thermal Effects | (8) |
| | 57-60 | IOPT(15) | Contact Analysis Flag =0: No Surface Contact =1: Include Surface Contact Analysis | (9) |
| 2 | 1-4 | NSTEP | Number of Solution Time Steps | (10) |
| | 5-8 | IPRF | Printing Frequency (in Increments) | (11) |
| | 9-12 | NRANGE | Number of Nodal Ranges for Printed Output (Default=Print all Nodes) | (12) |
| | 13-16 | IVPRNT | Velocity Printing Flag =0: Velocity Output Suppressed =1: Print Velocities | |
| | 17-20 | ISTART(1) | Beginning Node Number for Output Range No. 1. | (12) |
| | 21-24 | IEND(1) | Final Node Number for Output Range No. 1. | (12) |

| CARD | COL | DATA | DESCRIPTION | NOTES |
|-------------|-------|-----------|--|-------|
| 2 (cont) | 25-28 | ISTART(2) | Beginning Node for Range No. 2. | (12) |
| | 29-32 | IEND(2) | Final Node for Range No. 2. | (12) |
| | . | . | . | |
| | . | . | . | |
| | . | . | . | |
| | 73-76 | ISTART(8) | Beginning Node for Range No. 8. | (12) |
| | 77-80 | IEND(8) | Final Node for Range No. 8. | (12) |
| 3 | 1-10 | DT | Time (or Load Parameter) Step Size | (13) |
| | 11-20 | TZERO | Time at Start of Solution | (13) |
| | 21-30 | TMAX | Maximum Time Value | (13) |
| | 31-40 | DTMIN | Minimum Time Step Size (Variable Time-Step Option Only) | (14) |
| | 41-50 | DTMAX | Maximum Time Step Size (Variable Time-Step Option Only) | (14) |
| 4 | 1-10 | ALPHA | Time Integration Parameter, α | (15) |
| | 11-20 | DELTA | Time Integration Parameter, δ | (15) |
| 5 | 1-10 | BETA | Stiffness Matrix Coefficient for Proportional Damping, β | (16) |
| | 11-20 | GAMMA | Mass Matrix Coefficient for Proportional Damping, γ | (16) |
| 6* | 1-5 | INCR(1) | Increment Number for First Time Increment Change | (17) |
| | 6-15 | TIME(1) | Time Increment Value | |
| | 16-20 | INCR(2) | Increment Number for Second Time Increment Change | |

*NOTE: Card 6 is required only if IOPT(12)>0; that is, if the solution time increment is to be modified during a nonlinear analysis.

| CARD | COL | DATA | DESCRIPTION | NOTES |
|-------------|-------|---------|--|-------|
| 6 (cont) | 21-30 | TIME(2) | Time Increment Value | |
| | 31-35 | INCR(3) | Increment Number for Third Time Increment Change | |
| | 36-45 | TIME(3) | Time Increment Value | |
| | 46-50 | INCR(4) | Increment Number for Fourth Time Increment Change | |
| | 51-60 | TIME(4) | Time Increment Value | |

NOTES:

- (1) Rotational degrees of freedom are permitted only when $IOPT(1) = 2$; when beam elements (Element Type 12) are used, $IOPT(1) = 2$ is required. $IOPT(1) = 1$ is sufficient for all other element types, which use only displacement variables.
- (2) In the current version of the program, a value of 2 for the material nonlinearity flag automatically invokes the large-displacement (geometric nonlinearity) option.
- (3) Required only for transient dynamic analysis.
- (4) $IOPT(6)$ determines the interval at which both element and system stiffness matrices are reformulated in a nonlinear analysis. Default value = 1.
- (5) The write-in-place option causes random file record (including global stiffness and mass matrices, load vectors, and displacement, velocity, and acceleration vectors) to be rewritten directly in place to reduce the total amount of disc storage used by the program in a nonlinear analysis. This option is appropriate for large nonlinear problems (many degrees of freedom, many time or load steps, or both). I/O times may be increased 25-30 percent when using the write-in-place utility.
- (6) In any nonlinear (static or dynamic) analysis, the solution time step may be increased or decreased at predetermined stages of the solution. A maximum of four time step changes are permitted.
- (7) If $IOPT(13) = 0$, user-defined time or loading increment values will be used throughout the solution. When $IOPT(13) = 1$, the program will increase or reduce solution increment sizes based upon the rate of convergence in previous steps. When variable time stepping is used, equilibrium iterations must be performed at frequent intervals in the solution to maintain numerical stability. The solution terminates whenever $NSTEP$ increments have been performed or when $T \geq TMAX$.

- (8) IOPT(14) must be set to 1 to perform thermal stress analysis (linear or nonlinear). If the input data contains nodal temperatures, thermal expansion coefficients, etc., these data can be suppressed if desired by setting IOPT(14) = 0.
- (9) Contact between three-dimensional surfaces may be considered in nonlinear static and dynamic analysis only. Contact analysis data is entered as shown in Section 3.6 if IOPT(15) > 0. At present, surface contact and thermal stress may not be analyzed simultaneously.
- (10) NSTEP is applicable in all nonlinear and/or transient dynamic solutions. The analysis is continued until NSTEP increments have been performed, or until the time value exceeds TMAX (Card 3). In a restart run, NSTEP is interpreted as the last increment to be performed (including those completed in the preceding run(s)).
- (11) Solutions will be printed every IPRF time or load steps. It should be noted that, in linear dynamic analysis, stress and strain calculations are performed only when output is required, so that use of a small printing frequency can significantly increase solution time. Choice of an output frequency in nonlinear analysis affects solution time only slightly.
- (12) If NRANGE is zero or blank, nodal solution quantities (e.g., displacements, velocities, reactions) will be output for all nodes in the model. When NRANGE > 0, output will be generated for all nodes contained in any of the point ranges ISTART(i) - IEND(i), for $i=1,2,\dots, NRANGE$. Up to eight ranges of nodes may be specified for selective nodal output.
- (13) Solutions are performed at times $(TZERO + I*DT)$, for $I = 1,2,\dots, NSTEP$, or until the value of time exceeds TMAX. In a transient dynamic solution, DT and TZERO represent actual values of time. For nonlinear static analysis, "time" is used as a load parameter; that is, all loads are specified in the form $P = P(t)$ (see Section 8.9), and values of $t_i = TZERO + I*DT$ are used to determine the successive load levels at which increments of the solution begin and end. As an example, a 1000 lb. load applied in increments of 100 lb. could be specified using $DT = 1.0$, $TZERO = 0.0$, and specifying (in Section 8.9) that $P(t) = 100 \cdot t$.

- (14) *DTMIN and DTMAX are used as limiting time (or load parameter) step sizes in solutions based upon the variable time step option (IOPT(13)=1). In dynamic analysis, it is advisable to specify at least a maximum time step (DTMAX), as the automatic time step feature may, in some cases, select a time step which is too large for high accuracy. In plasticity and/or contact analysis, the time step may tend to become quite small; in these circumstances, a minimum step size should always be specified.*
- (15) *Parameters α , δ are relevant for transient dynamic analysis by Newmark's operator (implicit integration). A linear dynamic solution is unconditionally stable provided $\delta \geq 1/2$ and $\alpha \geq (1/4)(1/2 + \delta)^2$. Default values are $\alpha = 1/4$, $\delta = 1/2$ ("constant-average-acceleration" operator).*
- (16) *In transient dynamic analyses, a damping matrix is permitted, of the form $C = BK + \gamma M$ (Rayleigh damping). For an undamped solution, $\beta = \gamma = 0$.*
- (17) *IOPT(12) determines the number of pairs (increment, time step) to be entered in this section. The initial time step, DT, is entered on card 3 (see note 13); at increment INCR(1), the time step will be changed to the value of TIME(1), and so on. Increment values INCR(1) must be entered in ascending order. If IOPT(12) ≤ 0 , do not enter this line of data. Note that time step changes are permitted only in nonlinear analysis, and that a maximum of four such changes is permitted.*

8.3 ITERATIVE SOLUTION AND ANALYSIS RESTART DATA

- Enter data in Section 8.3.1 for all nonlinear analyses
- Enter data in Section 8.3.2 for natural frequency analyses
- Enter data in Section 8.3.3 or 8.3.4 for all nonlinear analyses in which restart data is to be read or written
- Enter data in Section 8.3.5 for steady-state harmonic analysis

8.3.1 Equilibrium Iteration Control Parameters

(Required for nonlinear, static and dynamic analysis only)

| CARD | COL | DATA | DESCRIPTION | NOTES |
|------|-------|--------|---|-------|
| 1 | 1-5 | ITFLAG | Equilibrium Iteration Flag =0: No Iteration =1: Modified Newton-Raphson (constant stiffness) Iteration =2: Full Newton-Raphson Iteration =3: Combined Full and Modified Newton-Raphson Iterations | (1) |
| | 6-10 | INTRVL | Number of Solution Increments Between Equilibrium Iterations (Default = 5) | - |
| | 11-15 | MAXIT | Maximum Number of Iterations per Solution Increment (Default = 10) | - |
| | 16-25 | EQTOL | Relative Convergence Tolerance on Residual Forces (Default = 0.10) | (2) |
| | 26-35 | DISTOL | Absolute Convergence Tolerance on Displacement Corrections (Default = 0.0005) | (3) |
| | 36-40 | LRGRDT | Large Rotations Flag =0: Normal Iteration Used =1: Modified Iteration for Large Rotation Problem | (4) |

NOTES:

- (1) ITFLAG determines the type of equilibrium iteration (if any) to be performed at specified intervals in the solution to restore the nonlinear conditions of equilibrium (i.e., internal forces = external forces). Modified Newton-Raphson iteration (ITFLAG = 1) involves no reformulation of the system stiffness matrix; internal forces are computed at each iteration, and the resulting out-of-balance forces are applied to obtain displacement corrections to improve the solution. With full Newton-Raphson iteration (ITFLAG = 2), the stiffness is formed and resolved at each iteration; this procedure is, therefore, more expensive than the modified iteration, but is normally quicker to converge. For ITFLAG = 3, two full Newton iterations are performed, followed by modified Newton iterations until convergence is achieved. Convergence is achieved when either the out-of-balance force tolerance or the displacement correction tolerance is satisfied. The only exception occurs in contact analysis, where both criteria must be satisfied for convergence.
- (2) EQTOL defines the convergence tolerance on out-of-balance forces \tilde{R} , as a fraction of the applied load, \tilde{F} , during equilibrium iteration. The iteration is considered converged when

$$\frac{\|\tilde{R}\|}{\|\tilde{F}\|} \leq \text{EQTOL} ,$$

where $\|\tilde{V}\|$ denotes the Euclidean norm, $\sqrt{\tilde{V}^T \tilde{V}}$.

- (3) DISTOL is an absolute tolerance on the displacement corrections computed during an equilibrium iteration. If \tilde{u} is the displacement correction vector, the iteration is considered converged if $\sqrt{\tilde{u}^T \tilde{u}} \leq \text{DISTOL}$. If convergence is to be measured only on the basis of out-of-balance forces (EQTOL), the DISTOL should be set to a very small value (e.g., $\text{DISTOL} = 1.0 \times 10^{-20}$).
- (4) LRGRCT = 1 causes the normal equilibrium iteration methods to be modified to improve convergence in problems involving large incremental rotations (e.g., a cantilever beam). The use of full or combined Newton iteration (ITFLAG = 2 or 3) is suggested when the large rotations flag is switched on.

8.3.2 Eigenvalue Solution Control Parameters

(Required *only* for natural frequency analyses)

| CARD | COL | DATA | DESCRIPTION | NOTES |
|------|-------|--------|--|-------|
| 1 | 1-5 | NTRIAL | Number of Iteration Trial Vectors (Default = 2, Maximum = 50) | (1) |
| | 6-10 | NREQD | Number of Natural Frequencies to be Determined (Default = 1) | (2) |
| | 11-15 | MAXIT | Maximum Number of Iterations (Default = 3) | (3) |
| | 16-25 | TOLVEC | Vector Tolerance for Convergence of Frequency Solution (Default = 0.001) | (4) |
| | 26-30 | MFLAG | Mass Matrix Type =0: Consistent Mass =1: Lumped Mass | |
| | 31-35 | ITYPE | Frequency Range Flag =0: Lowest =1: Highest | (5) |
| | 36-40 | IPREST | Flag for Prestress Effects =0: No Prestressing Considered =1: Include Nonlinear Prestress Effect | (6) |
| | 41-45 | INCPRE | Flag for Initial Geometry File =0: No Geometry File >0: Increment Number on Initial Geometry File corresponding to Nonlinear, Prestressed State | (7) |
| | 46-55 | ESHIFT | Eigenvalue Shift | (8) |

NOTES:

- (1) The natural frequency/normal mode problem is solved by the vector iteration procedure described in Section 4.5. In general, the greater the number of trial iteration vectors, N_{TRIAL} , the better the convergence and accuracy characteristics of the solution. However, the use of an excessive number of iteration vectors is costly and inefficient in terms of central memory requirements. The use of the $N_{TRIAL} = \min(2*N, N+5)$, where N is the number of frequencies to be solved, has been found to provide a good balance between rate of convergence and storage requirements.
- (2) The program will determine the first $NREQD$ natural frequencies and normal modes of the linear system $\underline{K}\underline{X} = \omega^2 \underline{M}\underline{X}$, where \underline{K} is the system stiffness matrix and \underline{M} the mass matrix. Note that, since the solution is performed by a vector iteration method, $NREQD$ is limited to values which are relatively small for large finite element models.
- (3) $MAXIT$ controls the total number of iteration cycles performed during the solution. A value of $MAXIT = 15$ to 20 is sufficient for nearly all problems, unless the number of frequencies to be computed ($NREQD$) is quite large.
- (4) $TOLVEC$ defines the convergence tolerance on successive approximations to each eigenvector requested. If \underline{V}_i and \underline{V}_{i+1} are successive iterates to a single eigenvector, that eigenvector is considered converged if

$$\|\underline{V}_{i+1} - \underline{V}_i\| < TOLVEC ,$$

where $\|\underline{V}\|$ denotes the Euclidean norm, $\sqrt{\underline{V}^T \underline{V}}$. The solution is terminated when the first $NREQD$ eigenvectors have converged.

- (5) For most problems, $ITYPE = 0$ is appropriate, causing the lowest $NREQD$ frequencies of the finite element model to be determined. $ITYPE = 1$ specifies that the $NREQD$ highest frequencies are to be computed; the normal usage of this option would be to determine the highest natural frequency to determine critical time step values for dynamic analysis. For this purpose, one would specify $NREQD = 1$ and $ITYPE = 1$.

- (6) The option $IPREST = 1$ can be used in computing the natural frequency of the model about an existing deformation state. A nonlinear solution must be performed to obtain the nonlinear equilibrium state; in addition, the file of element stiffness matrices from the nonlinear solution must be saved for use in the natural frequency solution. In the nonlinear solution, the element stiffness file is file *STIFF* (CDC version), dataset *FT12* (CRAY version), or file *MAGNEM.DAT* (VAX version). If $IPREST = 1$, MAGNA will use the nonlinear stiffness coefficients stored on this file in the eigenvalue solution. For the eigenvalue solution, the saved stiffnesses must be supplied to MAGNA as file *TAPE22* (CDC), *FT22* (CRAY), or *MAGNST.DAT* (VAX).
- (7) The initial geometry file is used in conjunction with the prestressed natural frequency option (see Note 6). If $INCPRE > 0$, MAGNA will read the *MPOST* postprocessor file from the previous (nonlinear) solution, and record the geometry in the prestressed state on the current postprocessor file. Mode shape plots of the computed vibration modes superimposed on the geometry in the prestressed state can then be obtained using *GPLOT*. If $INCPRE > 0$, the *MPOST* file created during the nonlinear solution should be supplied to the eigenvalue analysis as logical unit 23 (*TAPE23* on CDC, *FT23* on CRAY, and *MAGNRO.DAT* on VAX machines).
- (8) When $ESHIFT = 0$, the usual natural frequency analysis $\underline{K}\underline{X} = \omega^2 \underline{M}\underline{X}$ is performed. If $ESHIFT = p$ ($p > 0$), the modified system $(\underline{K} + p\underline{M})\underline{X} = (\omega^2 + p)\underline{M}\underline{X}$ is considered. If the model is unconstrained, rigid body modes have zero frequencies ($\omega^2 = 0$) associated with them, while the modified system has only positive eigenvalues $\omega^2 + p > 0$.

8.3.3 Analysis Restart Data (CDC and CRAY versions only)

(Required for all nonlinear or dynamic analyses which read or write a restart tape)

| CARD | COL | DATA | DESCRIPTION | NOTES |
|------|-------|--------|---|-------|
| 1 | 1-7 | - | Literal "RESTART" | |
| | 8-10 | - | (blank) | |
| | 11-15 | IREAD | Analysis Restart Flag =0: New Analysis (no Restart) =1: Read Restart File from Previous Analysis | (1) |
| | 16 | - | (blank) | |
| | 17-20 | IDOLD | Restart File Label | (2) |
| | 21-25 | INCOLD | Increment at Which Analysis is to be Restarted | (2) |
| | 26-30 | IWRITE | Checkpoint Flag =0: No Restart File to be Written =1: Restart File to be Written During Current Job | (3) |
| | 31 | - | (blank) | |
| | 32-35 | IDNEW | Label for New Restart File | (4) |
| | 36-40 | IRFREQ | Number of Increments between Checkpoints on New Restart File | (5) |

IMPORTANT: In the CRAY-1 version of MAGNA, IDOLD defines the *permanent file name* of an existing restart file, as well as its label. IDNEW similarly provides the *permanent file name* for new restart files created during the run.

NOTES:

- (1) *IREAD = 1* indicates that a previous analysis is to be continued in the current job. The restart file written by the previous analysis must be supplied to the program on unit 23; the necessary job control language is described in Chapter 7.
- (2) *IDOLD* is the four-character alphanumeric label written to the restart file in a previous analysis. *INCOLD* is the increment of the previous analysis at which the solution is to be continued. The current analysis begins at increment $INCOLD + 1$. Prior to executing an analysis restart, both *IDOLD* and *INCOLD* are compared with the values written on the restart file to verify that it is properly positioned.
- (3) *IWRITE = 1* indicates that a restart file is to be written during the current job. The new restart file (usually written directly on magnetic tape in case of job failure) may be written to the same tape as the old restart file (if *IREAD = 1*), or to a different tape. In either case, the new restart tape is written to file *NRSTAP*. The necessary job control language is described in Chapter 7.
- (4) *IDNEW* is any alphanumeric string of four characters, which is used to identify the restart file created during the current job. Subsequent jobs which access the restart file must supply this string as *IDOLD* (Note 2) for identification. If no verification of the file is desired on subsequent runs, *IDNEW* may simply be left blank.
- (5) When *IWRITE = 1*, a restart checkpoint is written to *NRSTAP* whenever the last complete increment is an integral multiple of *IRFREQ*. Note that each increment written to *NRSTAP* corresponds to a single system logical record (i.e., an end-of-record mark is recorded at the end of each checkpoint).

8.3.4 Analysis Restart Data (Vax version only)

Required for all nonlinear or dynamic analyses
which read or write a restart file (tape or disk)

| CARD | COL | DATA | DESCRIPTION | NOTES |
|------|-------|--------|--|-------|
| 1 | 1-9 | - | Literal "RESTARTVX" | (1) |
| | 10 | - | (blank) | |
| | 11-15 | IREAD | Analysis Restart Flag =0: New Analysis =1: Read Restart File from Previous Analysis | |
| | 16-20 | - | (blank) | (1) |
| | 21-25 | INCOLD | Increment (number) at which analysis is to be restarted | |
| | 26-30 | IWRITE | Checkpoint Flag =0: No New Restart File to be Written =1: New Restart File to be written during current job. | (2) |
| | 31-35 | - | (blank) | (3) |
| | 36-40 | IRFREQ | Number of Increments Between Checkpoints on New Restart File | |
| 2 | 1-9 | - | Literal "RESTARTVX" | (4) |
| | 10 | - | (blank) | |
| | 11-60 | IDOLDX | Old (input) Restart File Name and Version Number (e.g., REST.DAT:10) | |
| 3 | 1-9 | - | Literal "RESTARTVX" | (5) |
| | 10 | - | (blank) | |
| | 11-56 | IDNEWX | New Restart File Name (Name Only) | |
| | 57 | - | (blank) | (6) |
| | 58-67 | INITVN | Initial Version Number for New Restart File | |

NOTES:

- (1) *IREAD = 1 indicates that a previous analysis is to be continued in the current job. The restart file written by the previous analysis is identified by name in IDOLDX. The first increment in the current analysis will be numbered (INCOLD + 1).*
- (2) *IWRITE = 1 indicates that a new restart file is to be written during the current job. The initial restart file name is defined by IDNEWX; the initial version number is defined by INITVN.*
- (3) *When IWRITE = 1, a restart checkpoint is written whenever the last complete increment is an integral multiple of IRFREQ. Each checkpoint is contained in a separate file, with successive checkpoints each being assigned unique (and increasing) version numbers.*
- (4) *IDOLDX is the complete VAX file specification for the old (input) restart file, including a file version number.*
 - (a) *IDOLDX must include the device name (e.g., MTIA0:) if the file is to be read from tape. Default device specification is allowed (for disk) but it is advisable to specify the device explicitly whenever possible.*
 - (b) *The usual VAX/VMS rules for file specification must be followed, e.g., no blanks are allowed in the file name. Within the card field, the file name need not be left - or right - justified.*

For a new analysis with no restart file, card 2 is still required. Columns 1-9 must contain the literal "RESTARTVX". The remainder of the card is ignored.
- (5) *For the new restart file name IDNEWX, the user must specify the complete file name, including the device name. No file version number should be specified in the input field for INDNEWX.*

If the new file is to have the same name as the old restart file (except for version number), this field may be left blank. A blank field encountered where a new name is required will not cause termination of the job. Data will be written to the disk file MAGNRST.DAT.

- (6) *INITVN is the initial version number for the new restart file. An integer is required, in the range $1 \leq \text{INITVN} \leq 999$. Any other numbers read will cause the initial version number to be set to 1.*

8.3.5 Frequency Response Solution Control Parameters

(Required *only* for steady-state harmonic solution)

| CARD | COL | DATA | DESCRIPTION | NOTES |
|------|-------|--------|--|-------|
| 1 | 1-5 | NFREQ | Number of Excitation Frequencies | (1) |
| | 6-10 | IMASS | Mass Matrix Type =0: Consistent Mass =1: Lumped Mass | - |
| | 11-15 | IFDEP | Frequency-Dependent Materials Flag =0: Constant Properties =1: Frequency-Dependent Material Properties | (2) |
| | 16-20 | - | (blank - Inactive Option) | - |
| | 21-25 | - | (blank - Inactive Option) | - |
| | 26-30 | - | (blank - Inactive Option) | - |
| | 31-35 | ILOSSF | Flag for Loss Factor Calculation =0: No Loss Factor Calculation =1: Compute System Loss Factors | (3) |
| | 36-40 | ISTRES | Flag for Stress Calculation =0: No Stress Calculation =1: Compute Stress Data | (4) |

NOTES:

- (1) *The maximum number of forcing frequencies per analysis is 50. Values of the excitation frequencies are entered as data in Section 8.11. Note that the magnitudes of the harmonic forces are entered in Section 8.10.*
- (2) *When IFDEP = 0, identical stiffness and damping properties are assumed at all excitation frequencies. Frequency-dependent data (modulus, loss factor) may be used by setting IFDEP = 1 and supplying the user-written subroutine UDAMP described in Chapter 9.*
- (3) *ILOSSF = 1 causes the overall system loss factor (the ratio of dissipated energy to stored energy) to be computed for each forcing frequency considered. This option is useful in obtaining information on the variation in energy dissipation for a range of frequency values.*
- (4) *When ISTRES = 1, harmonic stresses are computed at each excitation frequency considered in the analysis.*

8.4 NODAL COORDINATE DATA

(Required)

The number of cards entered in this Section is determined by the number of nodal points to be defined in the model. *Nodal input is terminated by a single blank card (i.e., NODE = 0).*

| CARD | COL | DATA | DESCRIPTION | NOTES |
|------|-------|---------|---|-------|
| 1 | 1-15 | | Literal "COORDINATES" | - |
| | 16-20 | NODES | Total Number of Node Points | - |
| | 21-25 | MGEN | Mesh Generator Flag | (1) |
| | | | .LE.0: Read Coordinates | |
| | | | .GT.0: Coordinates to be Read or Generated in User Subroutine MESHG | |
| | 26-35 | TDFLT | Default Nodal Temperature Value | (2) |
| | 36-40 | ITDATA | Data Curve Index for Time Variation of Nodal Temperatures | (3) |
| 2-n | 1-5 | NODE | Node Point Number | (4) |
| | 6 | ISYS | Reference Coordinate System | (5) |
| | | | = : Cartesian X,Y,Z | |
| | | | =A: Cylindrical R, θ ,Z | |
| | | | =B: Spherical R, ϕ , θ | |
| | | | =C: (user-defined) | |
| | | | =D: (user-defined) | |
| | | | =E: (user-deinfed) | |
| | 7-10 | NINCR | Increment for Node Point Generation | (6) |
| | 11-20 | X(NODE) | Coordinate X_1 | |
| | 21-30 | Y(NODE) | Coordinate X_2 | |
| | 31-40 | Z(NODE) | Coordinate X_3 | |
| | 41-50 | T(NODE) | Nodal Temperature | (7) |

NOTES:

- (1) Coordinate data may, optionally, be read and/or generated in a user-written subroutine MESHG. User subroutines are described in Chapter 9.
- (2) TDFLT is a default temperature value which will be assigned to any node point whose input temperature value is zero. This parameter is commonly used in problems of uniform heating, etc., in which temperature data may be absent from the original input data.
- (3) ITDATA refers to a user-defined data curve (i.e., function of time) which is input in Section 8.3. Data curve ITDATA describes the time variation of temperature at all nodes in the model, and is used in all nonlinear analyses and all dynamic analyses.
- (4) Acceptable nodal point numbers are between 1 and NODES. Not every node need be connected to an active element in the model, but inactive nodes must be fully constrained (through boundary condition input). Coordinate data is read until a blank (i.e., NODE = 0) is encountered.
- (5) Nodes may be defined in circular cylindrical coordinates by setting ISYS=A and providing as input the R, θ , Z coordinates of the point, where θ is measured in degrees. In this case, the node coordinates are converted internally to Cartesian coordinates defined by:

$$X = R \cos \theta$$

$$Y = R \sin \theta$$

$$Z = Z.$$

When ISYS=B, the program interprets coordinate data as spherical coordinate values R, ϕ , and θ , where both ϕ and θ are measured in degrees. Spherical coordinates are then converted to Cartesian coordinates by the formulas:

$$X = R \sin \phi \cos \theta$$

$$Y = R \sin \phi \sin \theta$$

$$Z = R \cos \phi.$$

Alternate systems of coordinates can be defined to facilitate input data preparation. Transformations for user-defined systems are performed in the user subroutine CTYPE, described in Chapter 9.

- (6) Node generation increments *NINCR* are entered on the second card of a pair, causing nodes to be equally spaced between the last and current nodes, with numbering increment *NINCR*. As an example, the data

| | | | | |
|----|---|-----|------|----|
| 10 | | 0. | 0. | 5. |
| 20 | 2 | 35. | -25. | 0. |

is equivalent to

| | | | |
|----|-----|------|----|
| 10 | 0. | 0. | 5. |
| 12 | 7. | -5. | 4. |
| 14 | 14. | -10. | 3. |
| 16 | 21. | -15. | 2. |
| 18 | 28. | -20. | 1. |
| 20 | 35. | -25. | 0. |

Note that incremental node generation is performed in the Cartesian system only.

- (7) Nodal temperatures are understood to be the differences in temperature from the (unstressed) reference state of the structure (usually "room temperature").

8.5 ELEMENT PROPERTIES AND CONNECTIVITY

(Required)

Element input data is entered by element types. For each element type requested, the following sequence of data is required:

- A. ELEMENT TYPE HEADER CARD
- B. MATERIAL PROPERTIES DATA
- C. ELEMENT DEFINITION DATA.

Element types should be entered in ascending order (all Type 1 elements first, followed by Type 2, etc.). For any given element type, elements are numbered continuously from 1 to NELEM, where NELEM is the number of elements of this type (given on the header card).

IMPORTANT: *Following the last block of element data, a single blank card is required to terminate element input (i.e., ITYPE = 0 is read by the program).*

8.5.1 Data for Element Type 1

(Three-Dimensional, Isoparametric Solid with
Variable Number of Nodes)

A. HEADER CARD, ELEMENT TYPE 1

| CARD | COL | DATA | DESCRIPTION | NOTES |
|------|-------|-------|---|-------|
| 1 | 1-5 | ITYPE | Element Type; Enter the Number "1" | - |
| | 6-10 | NMAT | Number of Material Property Sets | - |
| | 11-15 | NELEM | Number of Elements of this Element Type | - |
| | 16-20 | NAXIS | Number of Orthotropic Axis Definitions | - |

B. MATERIAL PROPERTIES DATA, ELEMENT TYPE 1

- For each initially isotropic material, enter properties data from Section B-1, below (one card/material).
- For each elastic orthotropic material, enter properties data from Section B-2, below (two cards/material).
- NMAT material property sets should be defined in this data block.

B-1. Isotropic Material Properties

| CARD | COL | DATA | DESCRIPTION | NOTES |
|------|-------|----------|--|-------|
| 1 | 1-10 | EE(I) | Elastic Modulus | (1) |
| | 11-20 | PR(I) | Poisson's Ratio | - |
| | 21-30 | DNS(I) | Mass Density | (2) |
| | 31-40 | YLD(I) | Equivalent Stress at First Yield | (3) |
| | 41-50 | DEMAX(I) | Maximum Strain Subincrement | (4) |
| | 51-60 | GAMMA(I) | Ratio of Yield Surface Expansion to Translation for Combined Isotropic and Kinematic Strain Hardening | (5) |
| | 61-65 | IHARD(I) | Strain Hardening Type Code =1: Isotropic Hardening =2: Kinematic Hardening =3: Combined Isotropic and Kinematic Hardening, with Constant Proportions of Yield Surface Expansion and Translation | (6) |
| | 66-70 | ISSC(I) | Number of Data Curve Containing Uniaxial Stress-Strain Data for this Material | (7) |
| | 71-80 | ALPHA(I) | Coefficient of Thermal Expansion | - |

B-2. Orthotropic Material Properties

| CARD | COL | DATA | DESCRIPTION | NOTES |
|------|-------|-----------|---|-------|
| 1 | 1 | MTYPE | Literal "A" - Flag for Orthotropic Materials Data | - |
| | 2-10 | E1(I) | Elastic Modulus in Direction 1 | (8) |
| | 11-20 | E2(I) | Elastic Modulus in Direction 2 | - |
| | 21-30 | E3(I) | Elastic Modulus in Direction 3 | - |
| | 31-40 | G12(I) | Shear Modulus in Plane 1-2 | - |
| | 41-50 | G13(I) | Shear Modulus in Plane 1-3 | - |
| | 51-60 | G23(I) | Shear Modulus in Plane 2-3 | - |
| 2 | 1-10 | PR12(I) | Poisson's Ratio in Plane 1-2 | (9) |
| | 11-20 | PR13(I) | Poisson's Ratio in Plane 1-3 | - |
| | 21-30 | PR23(I) | Poisson's Ratio in Plane 2-3 | - |
| | 31-40 | DNS(I) | Mass Density | (2) |
| | 41-50 | ALPHA1(I) | Coefficient of Thermal Expansion in Direction 1 | - |
| | 51-60 | ALPHA2(I) | Coefficient of Thermal Expansion in Direction 2 | - |
| | 61-70 | ALPHA3(I) | Coefficient of Thermal Expansion in Direction 3 | - |

C. ORTHOTROPIC MATERIAL AXIS DATA, ELEMENT TYPE 1

- Enter NAXIS sets of orthotropic axis data in this section
- If NAXIS \leq 0, skip this data block.

| CARD | COL | DATA | DESCRIPTION | NOTES |
|------|-------|----------|--|-------|
| 1 | 1-5 | NODE1(I) | Node Number Defining Origin of Coordinates | (10) |
| | 6-10 | NODE2(I) | Node Number Defining Material Direction 1 | |
| | 11-15 | NODE3(I) | Node Number Defining one Additional Point in the 1-2 Plane of the Material | |

D. ELEMENT DEFINITION DATA, ELEMENT TYPE 1

(A single blank card terminates input)

| CARD | COL | DATA | DESCRIPTION | NOTES |
|------|-------|-------|--|-------|
| 1 | 1-5 | IEL | Element Number | (11) |
| | 6 | IOUT | Output Code (Blank or "N") | (12) |
| | 7-10 | IPR | Material Property Set for this Element | - |
| | 11-13 | IAX | Orthotropic Axis Set | - |
| | 14-15 | INT | Order of Numerical Integration | (13) |
| | 16-20 | KGEN | Node Increment for Element Generation | (14) |
| | 21-25 | ISUP | Stiffness Generation Code | (15) |
| | 26-30 | N(1) | Local Node Number 1 | (16) |
| | 31-35 | N(2) | Local Node Number 2 | - |
| | . | . | . | . |
| | . | . | . | . |
| | . | . | . | . |
| 2 | 75-80 | N(11) | Local Node Number 11 | - |
| | 1-5 | N(12) | Local Node Number 12 | (17) |
| | 6-10 | N(13) | Local Node Number 13 | - |
| | . | . | . | . |
| | . | . | . | . |
| | . | . | . | . |
| | 75-80 | N(27) | Local Node Number 27 | - |

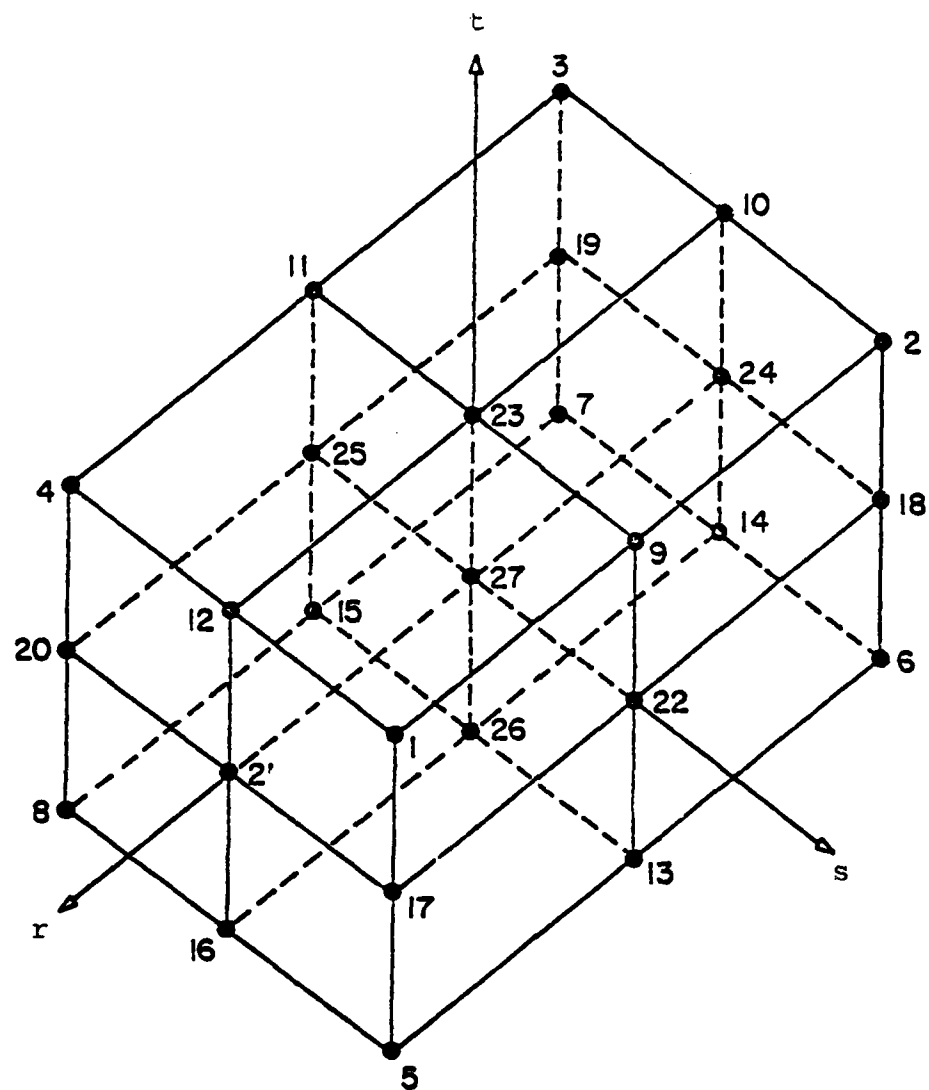


Figure 8.5.1 Nodal Connectivity for Variable-Node Solid Element.

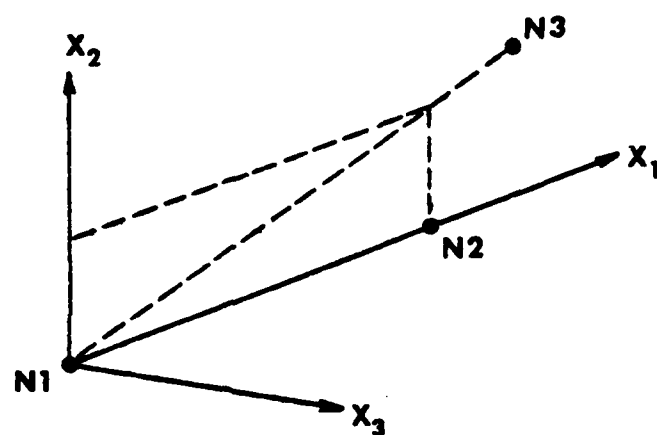


Figure 8.5.2. Definition of Orthotropic Material Axis Orientations.

AD-A129 773

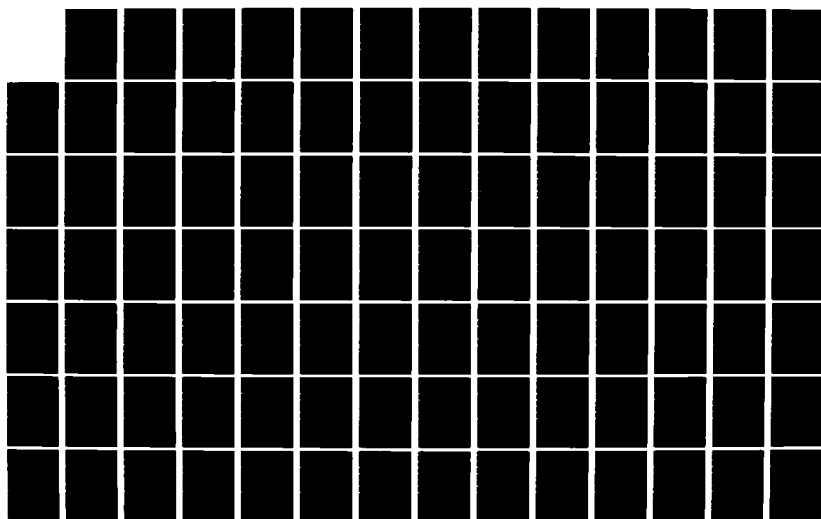
MAGNA (MATERIALLY AND GEOMETRICALLY NONLINEAR ANALYSIS)
PART 1 FINITE ELE. (U) DAYTON UNIV OH RESEARCH INST
R A BROCKMAN DEC 82 UDR-TR-82-111 AFWAL-TR-82-3098-PT-1
F33615-88-C-3483

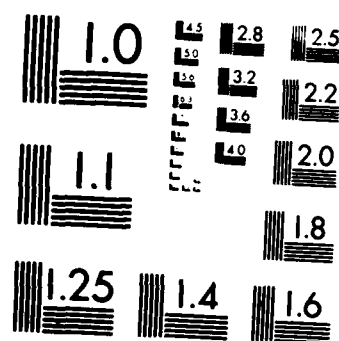
5/8

UNCLASSIFIED

F/G 12/1

NL





MICROCOPY RESOLUTION TEST CHART
NATIONAL BUREAU OF STANDARDS-1963-A

NOTES:

- (1) Repeat card set B-1 (or B-2) for each material property set to be defined. The n^{th} card set entered in this section defines material property set n for $n = 1, 2, \dots, \text{NMAT}$.
- (2) Mass densities are entered in a Force-Length-Time system of units consistent with those used elsewhere in the data. For example, in British units, mass density is entered in units of $\text{lb-f-sec}^2/\text{in}^4$. The mass density of aluminum, for instance, would be entered as $\rho = (0.1 \text{ lb/in}^3) / (386.4 \text{ in/sec}^2) = 0.000259 \text{ lb-f-sec}^2/\text{in}^4$.
- (3) Omit yield stress as input if material nonlinearities are to be neglected. Default value set to 1.0×10^{12} .
- (4) The program attempts to follow the material stress-strain curve as closely as possible, using a subincremental method of analyzing plastic flow. Each increment of time or load is divided into several "strain subincrements" at which material behavior is analyzed. $\text{DEMAX}(I)$ is the largest value of any incremental strain component which is permitted before stresses, strains, and the constitutive law are reevaluated. Default value set to 0.00020.
- (5) Applies only when $\text{IHARD}(I) = 3$ (combined hardening rule). Definition of γ is discussed in Chapter 2.
- (6) Isotropic hardening permits a uniform expansion of the yield locus in stress space; it predicts no Bauschinger effect, and is generally applicable in elastic-plastic problems involving nearly proportional systems of loading. Kinematic hardening allows the yield locus to translate in stress space, giving an "ideal" Bauschinger effect. The combined hardening rule, which permits both expansion and translation of the yield surface, is sometimes preferable for unloading and cyclic plasticity problems. Default hardening type is isotropic.
- (7) Uniaxial stress-strain data for a material are entered in Section 8.9, DATA CURVES. $\text{ISSC}(I)$ is the index of a particular data curve describing the uniaxial stress-strain behavior of the current material. Note that uniaxial material curves are represented as piecewise

linear functions, giving equivalent stress versus plastic strain; that is, the required data in Section 8.9 defines

$$\sigma_{eq} \text{ vs. } (\epsilon - \sigma/E) \text{ for } \sigma_{eq} \geq \sigma_{yield}$$

- (8) Orthotropic material properties must be defined with respect to the principal directions of the material (e.g., parallel and perpendicular to the fiber directions, for a filamentary material). Elements in which the principal material directions are not aligned with the global coordinate axes are transformed to global coordinates using the orthotropic axis data entered in part C (see Note 10).
- (9) The Poisson's ratio $PR_{ij}(I)$ defines the lateral contraction in direction j due to a unit extension in direction i . Care should be taken to ensure that these values satisfy the symmetry conditions and other restrictions summarized in Chapter 2.
- (10) The definition of material axis direction is depicted in Figure 8.5.2. NODE1 defines an "origin of coordinates," located arbitrarily in space; NODE2 locates the first principal direction of the material by specifying any point on the 1-axis. NODE3 is any third point, which, together with NODE1 and NODE2, uniquely defines the 1-2 plane (i.e., the three nodes should not be collinear). Repeat card C-1 as required to define all orthotropic axis systems for this element type. The n^{th} line entered in this section defines material axis set n , for $n = 1, 2, \dots, NAXIS$.
- (11) Valid element numbers are 1, 2, ..., NELEM. Elements must be defined sequentially, but intermediate elements can be generated automatically (see Note 14, below). Cards D-1 and D-2 are repeated as needed to define all Type 1 elements in the model. Following the last element, a single blank card (setting IEL = 0) is entered to terminate input for element Type 1.
- (12) The output code determines whether or not integration point stress output will be printed for element IEL. A blank field causes full printing for the element; an "N" in column 6 suppresses stress output.

- (13) Integration orders available for the variable-node solid elements are 2 and 3 point Gaussian rules, corresponding to 8 and 27 integration points per element, respectively. The non-Gaussian 14-point integration rule is selected by setting $INT = 14$. Locations of integration points for $INT = 2, 3$, and 14 are listed in Tables 8.5.1 through 8.5.3, respectively.
- (14) A nonzero value of $KGEN$ on the second card of a pair causes elements between the last and current elements to be generated automatically. With the exception of node numbers, all elements generated are assigned the same data as the current element. Local node numbers for the previous element are incremented by $KGEN$ to generate each succeeding element. Only nonzero local node numbers are incremented, and node numbers for the current element need not be given. More than one element must be generated to use this feature. If element cards are omitted but $KGEN = 0$, a default value of 1 is used.
- (15) $ISUP$ should be set to zero for linear analysis. In a nonlinear solution, $ISUP = 0$ permits full nonlinearities to be included in the stiffness calculation for an element. If $ISUP = 1$ for a nonlinear element, the original (linear) stiffness matrix is used throughout the solution for the element in question. Nonlinearities in elements having $ISUP = 1$ are taken into account by means of equilibrium correction, as in constant stiffness iteration. The use of $ISUP = 1$ is appropriate for regions in a structure which experience very mild nonlinearities. If $ISUP = -1$ for a nonlinear element, the nonlinear stiffness is reformulated at each increment using an approximate calculation based upon the average values of the nonlinear terms over the element. For $ISUP = -1$, internal forces are still evaluated exactly at all times, to avoid erroneous results. The use of $ISUP = -1$ can result in considerable savings of computer time in nonlinear analysis, but should not be used without equilibrium iteration (Section 8.3).
- (16) Local node numbering proceeds as shown in Figure 8.5.1. Nodes 1 through 8 (vertices) are required for all elements. Nodes 9 through 27 are each optional, and element interpolation functions generated

by the program automatically account for the absence or presence of each local node.

- (17) Card D-2 must be entered, even if local nodes 12 through 27 are not used in a particular element.*

TABLE 8.5.1

INTEGRATION POINT LOCATIONS FOR VARIABLE-NODE
SOLID ELEMENT WITH INT = 2

| Point | Nearest Node | r | s | t |
|-------|-----------------|--------|------|------|
| 1 | 7 | $-h^*$ | $-h$ | $-h$ |
| 2 | 3 | $-h$ | $-h$ | h |
| 3 | 6 | $-h$ | h | $-h$ |
| 4 | 2 | $-h$ | h | h |
| 5 | 8 | h | $-h$ | $-h$ |
| 6 | 4 | h | $-h$ | h |
| 7 | 5 | h | h | $-h$ |
| 8 | 1 | h | h | h |

* $h = 0.5773502691896$

TABLE 8.5.2
INTEGRATION POINT LOCATIONS FOR VARIABLE-NODE
SOLID ELEMENT WITH INT = 3

| Point | Nearest Node | r | s | t |
|-------|--------------|-----|----|----|
| 1 | 7 | -h* | -h | -h |
| 2 | 19 | -h | -h | 0 |
| 3 | 3 | -h | -h | h |
| 4 | 14 | -h | 0 | -h |
| 5 | 24 | -h | 0 | 0 |
| 6 | 10 | -h | 0 | h |
| 7 | 6 | -h | h | -h |
| 8 | 18 | -h | h | 0 |
| 9 | 2 | -h | h | h |
| 10 | 15 | 0 | -h | -h |
| 11 | 25 | 0 | -h | 0 |
| 12 | 11 | 0 | -h | h |
| 13 | 26 | 0 | 0 | -h |
| 14 | 27 | 0 | 0 | 0 |
| 15 | 23 | 0 | 0 | h |
| 16 | 13 | 0 | h | -h |
| 17 | 22 | 0 | h | 0 |
| 18 | 9 | 0 | h | h |
| 19 | 8 | h | -h | -h |
| 20 | 20 | h | -h | 0 |
| 21 | 4 | h | -h | h |
| 22 | 16 | h | 0 | -h |
| 23 | 21 | h | 0 | 0 |
| 24 | 12 | h | 0 | h |
| 25 | 5 | h | h | -h |
| 26 | 17 | h | h | 0 |
| 27 | 1 | h | h | h |

*h = 0.7745966692415

TABLE 8.5.3

INTEGRATION POINT LOCATIONS FOR VARIABLE-NODE
SOLID ELEMENT WITH INT = 14

| Point | r | s | t |
|-------|-------|----|----|
| 1 | *-a | 0 | 0 |
| 2 | a | 0 | 0 |
| 3 | 0 | -a | 0 |
| 4 | 0 | a | 0 |
| 5 | 0 | 0 | -a |
| 6 | 0 | 0 | a |
| 7 | ** -b | -b | -b |
| 8 | -b | b | -b |
| 9 | -b | -b | b |
| 10 | -b | b | b |
| 11 | b | -b | -b |
| 12 | b | b | -b |
| 13 | b | -b | b |
| 14 | b | b | b |

* a = 0.795822426

** b = 0.758786911

8.5.2 Data for Element Type 2

(Three-Dimensional, Isoparametric Eight-Node Brick)

A. HEADER CARD, ELEMENT TYPE 2

| CARD | COL | DATA | DESCRIPTION | NOTES |
|------|-------|-------|---|-------|
| 1 | 1-5 | ITYPE | Element Type; Enter the number "2" | - |
| | 6-10 | NMAT | Number of Material Property Sets | - |
| | 11-15 | NELEM | Number of Elements of this Element Type | - |
| | 16-20 | NAXIS | Number of Orthotropic Axis Definitions | - |

B. MATERIAL PROPERTIES DATA, ELEMENT TYPE 2

- For each initially isotropic material, enter properties data from Section B-1, below (one card/material)
- For each elastic orthotropic material, enter properties data from Section B-2, below (two cards/material)
- NMAT material property sets should be defined in this data block.

B-1. Isotropic Material Properties

| CARD | COL | DATA | DESCRIPTION | NOTES |
|------|-------|----------|--|-------|
| 1 | 1-10 | EE(I) | Elastic Modulus | (1) |
| | 11-20 | PR(I) | Poisson's Ratio | - |
| | 21-30 | DNS(I) | Mass Density | (2) |
| | 31-40 | YLD(I) | Equivalent Stress at First Yield | (3) |
| | 41-50 | DEMAX(I) | Maximum Strain Subincrement | (4) |
| | 51-60 | GAMMA(I) | Ratio of Yield Surface Expansion to Translation for Combined Isotropic and Kinematic Strain Hardening | (5) |
| | 61-65 | IHARD(I) | Strain-Hardening Type Code =1: Isotropic Hardening =2: Kinematic Hardening =3: Combined Isotropic and Kinematic Hardening, with Constant Proportions of Yield Surface Expansion and Translation | (6) |
| | 66-70 | ISSC(I) | Number of Data Curve Containing Uniaxial Stress-Strain Data for this Material | (7) |
| | 71-80 | ALPHA(I) | Coefficient of Thermal Expansion | - |

B-2. Orthotropic Material Properties

| CARD | COL | DATA | DESCRIPTION | NOTES |
|------|-------|-----------|---|-------|
| 1 | 1 | MTYPE | Literal "A" - Flag for Orthotropic Materials Data | - |
| | 2-10 | E1(I) | Elastic Modulus in Direction 1 | (8) |
| | 11-20 | E2(I) | Elastic Modulus in Direction 2 | - |
| | 21-30 | E3(I) | Elastic Modulus in Direction 3 | - |
| | 31-40 | G12(I) | Shear Modulus in Plane 1-2 | - |
| | 41-50 | G13(I) | Shear Modulus in Plane 1-3 | - |
| | 51-60 | G23(I) | Shear Modulus in Plane 2-3 | - |
| 2 | 1-10 | PR12(I) | Poisson's Ratio in Plane 1-2 | (9) |
| | 11-20 | PR13(I) | Poisson's Ratio in Plane 1-3 | - |
| | 21-30 | PR23(I) | Poisson's Ratio in Plane 2-3 | - |
| | 31-40 | DNS(I) | Mass Density | (2) |
| | 41-50 | ALPHA1(I) | Coefficient of Thermal Expansion in Direction 1 | - |
| | 51-60 | ALPHA2(I) | Coefficient of Thermal Expansion in Direction 2 | - |
| | 61-70 | ALPHA3(I) | Coefficient of Thermal Expansion in Direction 3 | - |

C. ORTHOTROPIC MATERIAL AXIS DATA, ELEMENT TYPE 2

- Enter NAXIS sets of orthotropic axis data in this section
- If $NAXIS \leq 0$, skip this data block.

| CARD | COL | DATA | DESCRIPTION | NOTES |
|------|-------|----------|--|-------|
| 1 | 1-5 | NODE1(I) | Node Number Defining Origin of Coordinates | (10) |
| | 6-10 | NODE2(I) | Node Number Defining Material Direction 1 | |
| | 11-15 | NODE3(I) | Node Number Defining one Additional Point in the 1-2 Plane of the Material | |

D. ELEMENT DEFINITION DATA, ELEMENT TYPE 2

(A single blank card terminates input)

| CARD | COL | DATA | DESCRIPTION | NOTES |
|------|-------|------|--|-------|
| 1 | 1-5 | IEL | Element Number | (11) |
| | 6 | IOUT | Output Flag (Blank or "N") | (12) |
| | 7-10 | IPR | Material Property Set for this Element | - |
| | 11-13 | IAX | Orthotropic Axis Set | - |
| | 14-15 | INT | Order of Numerical Integration | (13) |
| | 16-20 | KGEN | Node Increment for Element Generation | (14) |
| | 21-25 | | (Blank - Inactive Option) | |
| | 26-30 | N(1) | Local Node Number 1 | (15) |
| | 31-35 | N(2) | Local Node Number 2 | - |
| | . | . | . | . |
| | . | . | . | . |
| | . | . | . | . |
| | 61-65 | N(8) | Local Node Number 8 | - |

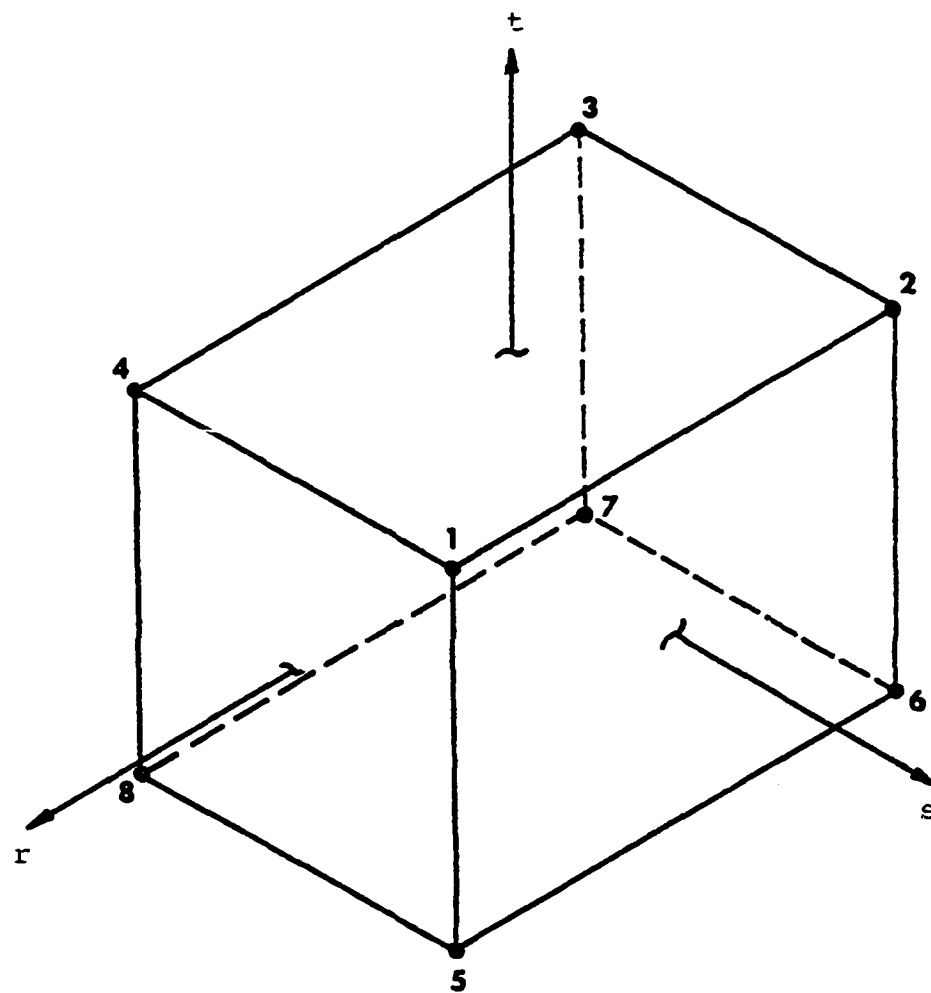


Figure 8.5.3 Nodal Connectivity for Eight-Node Solid Element.

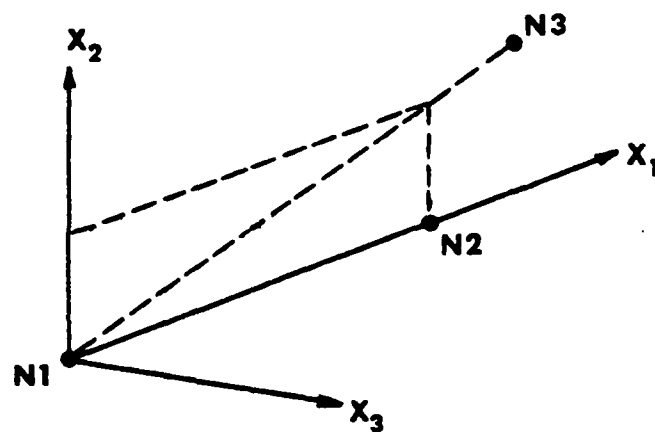


Figure 8.5.4. Definition of Orthotropic Material Axis Orientations.

NOTES:

- (1) Repeat card set B-1 or B-2 for each material property set to be defined. The n^{th} card set entered in this section defines material property set n for $n = 1, 2, \dots, \text{NMAT}$.
- (2) Mass densities are entered in a Force-Length-Time system of units consistent with those used elsewhere in the data. For example, in British units, mass density is entered in units of $\text{lb-f-sec}^2/\text{in}^4$. The mass density of aluminum, for instance, would be entered as $\rho = (0.1 \text{ lb/in}^3)/(386.4 \text{ in/sec}^2) = 0.000259 \text{ lb-f-sec}^2/\text{in}^4$.
- (3) Omit yield stress as input if material nonlinearities are to be neglected. Default value set to 1.0×10^{12} .
- (4) The program attempts to follow the material stress-strain curve as closely as possible, using a subincremental method of analyzing plastic flow. Each increment of time or load is divided into several "strain subincrements" at which material behavior is analyzed. $\text{DEMAX}(I)$ is the largest value of any incremental strain component which is permitted before stresses, strains, and the constitutive law are reevaluated. Default value set to 0.00020.
- (5) Applies only when $\text{IHARD}(I) = 3$ (combined hardening rule). Definition of γ is discussed in Chapter 2.
- (6) Isotropic hardening permits a uniform expansion of the yield locus in stress space; it predicts no Bauschinger effect, and is generally applicable in elastic-plastic problems involving nearly proportional systems of loading. Kinematic hardening allows the yield locus to translate in stress space, giving an "ideal" Bauschinger effect. The combined hardening rule, which permits both expansion and translation of the yield surface, is sometimes preferable for unloading and cyclic plasticity problems. Default hardening type is isotropic.
- (7) Uniaxial stress-strain data for a material are entered in Section 8.9 DATA CURVES. $\text{ISSC}(I)$ is the index of a particular data curve describing the uniaxial stress-strain behavior of the current material. Note that uniaxial material curves are represented as piecewise linear functions, giving equivalent stress versus plastic strain; that is, the required data in Section 8.9 defines

$$\sigma_{eq} \text{ vs. } (\epsilon - \sigma/E) \text{ for } \sigma_{eq} \geq \sigma_{yield}$$

- (8) Orthotropic material properties must be defined with respect to the principal directions of the material (e.g., parallel and perpendicular to the fiber directions, for a filamentary material). Elements in which the principal material directions are not aligned with the global coordinate axes are transformed to global coordinates using the orthotropic axis data entered in part C (see Note 10).
- (9) The Poisson's ratio $PR_{ij}(I)$ defines the lateral contraction in direction j due to a unit extension in direction i . Care should be taken to ensure that these values satisfy the symmetry conditions and other restrictions summarized in Chapter 2.
- (10) The definitions of material axis directions is depicted in Figure 8.5.4. NODE1 defines an "origin of coordinates," located arbitrarily in space; NODE2 locates the first principal direction of the material by specifying any point on the 1-axis. NODE3 is any third point which, together with NODE1 and NODE2, uniquely defines the 1-2 plane (i.e., the three nodes should not be collinear). Repeat card C-1 as required to define all orthotropic axis systems for this element type. The n^{th} line entered in this section defines material axis set n , for $n = 1, 2, \dots, NAXIS$.
- (11) Valid element numbers are 1, 2, ..., NELEM. Elements must be defined sequentially, but intermediate elements can be generated automatically (see Note 14, below). Card D-1 is repeated as needed to define all Type 2 elements in the model. Following the last element, a blank card setting (IEL = 0) is entered to terminate input for Element Type 2.
- (12) The output code determines whether or not integration point stress output will be printed for element IEL. A blank field causes full printing for the element; an "N" in column 6 suppresses stress output.
- (13) Integration orders available for the eight-node solid element are 1, 2, and 3 point Gaussian rules, corresponding to 1, 8 or 27 integration

points per element, respectively. A non-Gaussian rule using six integration points is also available ($INT = 6$), as well as a selective, nine-point integration rule ($INT = 9$). Locations of integration points for $INT = 2, 3$, and 6 are listed in Tables 8.5.4 through 8.5.6, respectively.

- (14) A nonzero value of $KGEN$ on the second card of a pair causes elements between the last and current elements to be generated automatically. With the exception of node numbers, all elements generated are assigned the same data as the current element. Local node numbers for the previous element are incremented by $KGEN$ to generate each succeeding element. Node numbers for the current element need not be given. More than one element must be generated to use this feature. If element cards are omitted but $KGEN = 0$, a default value of 1 is used.
- (15) Local node numbering proceeds as shown in Figure 8.5.4.

TABLE 8.5.4

INTEGRATION POINT LOCATIONS FOR EIGHT NODE
SOLID ELEMENT WITH INT = 2

| Point | Nearest Node | r | s | t |
|-------|--------------|-----|----|----|
| 1 | 7 | -h* | -h | -h |
| 2 | 3 | -h | -h | h |
| 3 | 6 | -h | h | -h |
| 4 | 2 | -h | h | h |
| 5 | 8 | h | -h | -h |
| 6 | 4 | h | -h | h |
| 7 | 5 | h | h | -h |
| 8 | 1 | h | h | h |

* $h = 0.5773502691896$

TABLE 8.5.5
INTEGRATION POINT LOCATIONS FOR EIGHT-NODE
SOLID ELEMENT WITH INT = 3

| Point | Nearest Node | r | s | t |
|-------|--------------|-----|----|----|
| 1 | 7 | -h* | -h | -h |
| 2 | 19 | -h | -h | 0 |
| 3 | 3 | -h | -h | h |
| 4 | 14 | -h | 0 | -h |
| 5 | 24 | -h | 0 | 0 |
| 6 | 10 | -h | 0 | h |
| 7 | 6 | -h | h | -h |
| 8 | 18 | -h | h | 0 |
| 9 | 2 | -h | h | h |
| 10 | 15 | 0 | -h | -h |
| 11 | 25 | 0 | -h | 0 |
| 12 | 11 | 0 | -h | h |
| 13 | 26 | 0 | 0 | -h |
| 14 | 27 | 0 | 0 | 0 |
| 15 | 23 | 0 | 0 | h |
| 16 | 13 | 0 | h | -h |
| 17 | 22 | 0 | h | 0 |
| 18 | 9 | 0 | h | h |
| 19 | 8 | h | -h | -h |
| 20 | 20 | h | -h | 0 |
| 21 | 4 | h | -h | h |
| 22 | 16 | h | 0 | -h |
| 23 | 21 | h | 0 | 0 |
| 24 | 12 | h | 0 | h |
| 25 | 5 | h | h | -h |
| 26 | 17 | h | h | 0 |
| 27 | 1 | h | h | h |

*h = 0.77459666924

TABLE 8.5.6

INTEGRATION POINT LOCATIONS FOR EIGHT-NODE
SOLID ELEMENT WITH INT = 6

| Point | r | s | t |
|-------|----|----|----|
| 1 | -1 | 0 | 0 |
| 2 | 0 | -1 | 0 |
| 3 | 0 | 0 | -1 |
| 4 | 1 | 0 | 0 |
| 5 | 0 | 1 | 0 |
| 6 | 0 | 0 | 1 |

8.5.3 Data for Element Type 3

(Quadrilateral Plane Stress, Plane Strain, or
Shear Panel Element in Three Dimensions)

A. HEADER CARD, ELEMENT TYPE 3

| CARD | COL | DATA | DESCRIPTION | NOTES |
|------|-------|-------|---|-------|
| 1 | 1-5 | ITYPE | Element Type; Enter the Number "3" | - |
| | 6-10 | NMAT | Number of Material Property Sets (Maximum of 20) | - |
| | 11-15 | NELEM | Number of Elements of this Element Type | - |

B. MATERIAL PROPERTY DATA, ELEMENT TYPE 3

(NMAT Cards are Required in this Section)

| CARD | COL | DATA | DESCRIPTION | NOTES |
|------|-------|----------|---|----------|
| 1 | 1-10 | EE(I) | Elastic Modulus | (1), (2) |
| | 11-20 | PR(I) | Poisson's Ratio | (3) |
| | 21-30 | DNS(I) | Mass Density | (4) |
| | 31-40 | YLD(I) | Equivalent Stress at First Yield | (5) |
| | 41-50 | DEMAX(I) | Maximum Strain Subincrement | (6) |
| | 51-60 | GAMMA(I) | Ratio of Yield Surface Expansion to Translation, for Combined Isotropic and Kinematic Strain Hardening | (7) |
| | 61-65 | IHARD(I) | Strain Hardening Type Code =1: Isotropic Hardening =2: Kinematic Hardening =3: Combined Isotropic and Kinematic Hardening with Constant Proportions of Yield Translation | (8) |
| | 66-70 | ISSC(I) | Number of Data Curve Containing Uniaxial Stress-Strain Data for this Material | (9) |
| | 71-80 | ALPHA(I) | Thermal Expansion Coefficient | |

C. ELEMENT DEFINITION DATA, ELEMENT TYPE 3

(A single blank card terminates input)

| CARD | COL | DATA | DESCRIPTION | NOTES |
|------|-------|-------|---|-------|
| 1 | 1-5 | IEL | Element Number | (10) |
| | 6 | IOUT | Output Flag (Blank or "N") | (11) |
| | 7-10 | ITYP | Element Subtype =1: Plane Stress (Membrane) =2: Plane Strain =3: Shear Panel | (12) |
| | 11-15 | IPR | Material Property Set for this Element | - |
| | 16-20 | INT | Order of Numerical Integration | (13) |
| | 21-25 | KGEN | Node Increment for Element Generation | (14) |
| | 26-30 | N(1) | Local Node Number 1 | (15) |
| | 31-35 | N(2) | Local Node Number 2 | |
| | 36-40 | N(3) | Local Node Number 3 | |
| | 41-45 | N(4) | Local Node Number 4 | |
| | 46-55 | THICK | Element Thickness | (16) |
| | 56-60 | ISEL | Selective Integration Flag | (17) |

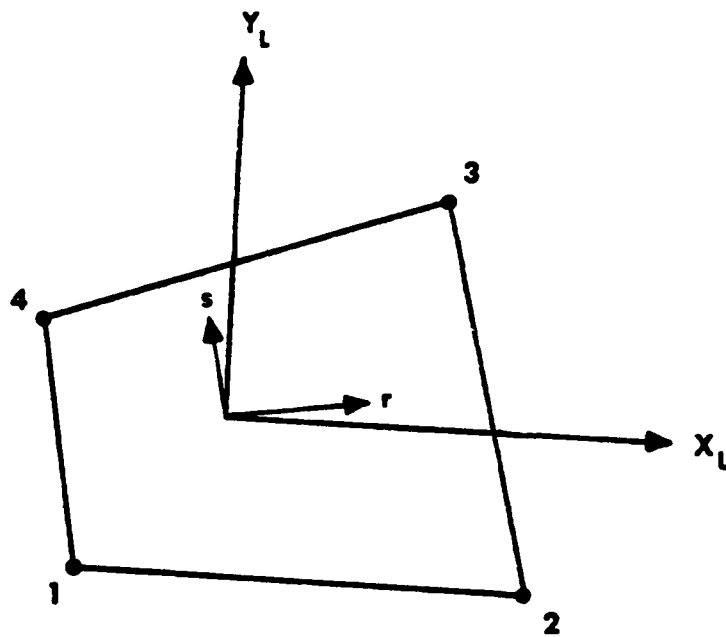


Figure 8.5.5 Nodal Connectivity for Quadrilateral Plane Stress, Plane Strain, and Shear Panel Element.

NOTES:

- (1) Repeat Card B-1 for each material property set to be defined. The n^{th} card entered in this section defines material property set n , for $n = 1, 2, \dots, \text{NMAT}$.
- (2) For plane stress or plane strain analysis, $EE(I)$ is the Young's modulus (i.e., extensional modulus) of the material. When shear elements are used, $EE(I)$ is interpreted as the shear modulus.
- (3) $PR(I)$ is ignored in shear panel elements.
- (4) Mass densities are entered in a Force-Length-Time system of units consistent with those used elsewhere in the data. For example, in British units, mass density is entered in units of $\text{lbf-sec}^2/\text{in}^4$. The mass density of aluminum, for instance, would be entered as $\rho = (0.1 \text{ lb/in}^3)/(386.4 \text{ in/sec}^2) = 0.000259 \text{ lbf-sec}^2/\text{in}^4$.
- (5) If material nonlinearities are to be neglected, omit the yield stress as input. Default value set to 1.0×10^{12} .
- (6) The program attempts to follow the material stress strain curve as closely as possible, using a subincremental method of analyzing plastic flow. Each increment of time or load is divided into several "strain subincrements" at which material behavior is analyzed. $DEMAX(I)$ is the largest value of any incremental strain component which is permitted before stresses, strains, and the constitutive law are reevaluated. Default value set to 0.00020.
- (7) Applies only when $I\text{HARD}(I) = 3$ (combined hardening rule). Definition of γ is discussed in Chapter 2.
- (8) Isotropic hardening permits a uniform expansion of the yield locus in stress space; it predicts no Bauschinger effect, and is generally applicable in elastic-plastic problems involving nearly proportional systems of loading. Kinematic hardening allows the yield locus to translate in stress space, giving an "ideal" Bauschinger effect. The combined hardening rule, which permits both expansion and translation of the yield surface, is sometimes preferable for unloading and cyclic plasticity problems. Default hardening type is isotropic.

- (9) Uniaxial stress-strain data for a material are defined in Section 8.9, DATA CURVES. ISSC(I) is the index of the particular data curve describing the uniaxial stress-strain behavior of the current material. Note that uniaxial material curves are represented as piecewise linear functions, giving equivalent stress versus plastic strain; that is, the required data in Section 8.9 defines

$$\sigma_{eq} \text{ vs. } (\epsilon - \sigma/E) \text{ for } \sigma_{eq} \geq \sigma_{yield}$$

- (10) Valid element numbers are 1, 2, ..., NELEM. Elements must be defined sequentially, but intermediate elements can be generated automatically (see Note 14, below). Card C-1 is repeated as needed to define all Type 3 elements in the model. Following the last element, a single blank card (setting IEL = 0) is entered to terminate input for Element Type 3.
- (11) The output code determines whether or not integration point stress output will be printed for element IEL. A blank field causes full printing for the element; an "N" in column 6 suppresses stress output.
- (12) All element subtypes are based upon the same theoretical formulation, but the stress-strain descriptions for the three possible subtypes are different. Subtypes 1 and 2 use the usual plane stress/strain assumptions; generalized plane strain (in which the transverse strain is uniform, but nonzero) is not available with Element Type 3 but may be analyzed using the three-dimensional elements (Types 1, 2, 6, 7 and 8) and the LINEAR CONSTRAINT utility (Section 8.8). Shear panel elements are assumed to sustain only shear stresses in the plane of the element; a shear web element may experience strain in tension or compression, but such direct strains produce no stress, and no strain energy.
- (13) Integration orders available for Element Type 3 are 2 and 3 point Gaussian rules, corresponding to 4 and 9 integration points per element, respectively. Locations for the integration points for INT = 2 and 3 are listed in Tables 8.5.7 and 8.5.8, respectively.

- (14) A nonzero value of KGEN on the second card of a pair causes elements between the last and current elements to be generated automatically. With the exception of node numbers, all elements generated are assigned the same data as the current element. Local node numbers for the previous element are incremented by KGEN to generate each succeeding element. Node numbers for the current element (second card of the pair) need not be given. More than one element must be generated to use this feature. If element cards are omitted but KGEN = 0, a default value of 1 is used.
- (15) Local node numbers are given in counterclockwise order around the element, as shown in Figure 8.5.5. Nodes 1 and 2 determine the local x-axis of the element, and nodes 1, 2, and 3 define the reference plane for an element (computed stresses and strains for Type 3 elements are output in this local system of coordinates).
- (16) For plane strain elements (ITYP = 2), the thickness is automatically set to 1.0, and need not be input.
- (17) Normally, ISEL = 0, and the element is integrated using the order of Gaussian quadrature specified by INT. When ISEL > 0, shear strain contributions to the element stiffness are evaluated by a single-point integration, to alleviate excessive element stiffness when the element is extremely long and thin. Generally, the use of ISEL > 0 is advantageous in modeling plane bending of slender beams, whose length-to-thickness ratio is sufficiently large that transverse shear stresses would be expected to vanish.

TABLE 8.5.7

INTEGRATION POINT LOCATIONS FOR QUADRILATERAL PLANE STRESS,
PLANE STRAIN, AND SHEAR PANEL ELEMENT WITH INT = 2

| Point | Nearest Node | r | s |
|-------|-----------------|--------|------|
| 1 | 1 | $-h^*$ | $-h$ |
| 2 | 4 | $-h$ | h |
| 3 | 2 | h | $-h$ |
| 4 | 3 | h | h |

$$^*h = 0.5773502691896$$

TABLE 8.5.8
 INTEGRATION POINT LOCATIONS FOR FOUR-NODE
 PLANAR ELEMENT WITH INT = 3

| Point | r | s |
|-------|--------|------|
| 1 | $-h^*$ | $-h$ |
| 2 | $-h$ | 0 |
| 3 | $-h$ | h |
| 4 | 0 | $-h$ |
| 5 | 0 | 0 |
| 6 | 0 | h |
| 7 | h | $-h$ |
| 8 | h | 0 |
| 9 | h | h |

* $h = 0.7745966692415$

8.5.4 Data for Element Type 4

(Truss Element in Three Dimensions)

A. HEADER CARD, ELEMENT TYPE 4

| CARD | COL | DATA | DESCRIPTION | NOTES |
|------|-------|-------|---|-------|
| 1 | 1-5 | ITYPE | Element Type; Enter the Number "4" | - |
| | 6-10 | NMAT | Number of Material Property Sets (Maximum of 20) | |
| | 11-15 | NELEM | Number of Elements of this Element Type | |

B. MATERIAL PROPERTY DATA, ELEMENT TYPE 4

(NMAT Cards are Required in this Section)

| CARD | COL | DATA | DESCRIPTION | NOTES |
|------|-------|----------|--|-------|
| 1 | 1-10 | EE(I) | Elastic Modulus | (1) |
| | 11-20 | DNS(I) | Mass Density | (2) |
| | 21-30 | YLD(I) | Equivalent Stress at First Yield | (3) |
| | 31-40 | DEMAX(I) | Maximum Strain Subincrement | (4) |
| | 41-50 | GAMMA(I) | Ratio of Yield Surface Expansion to Translation, for Combined Isotropic and Kinematic Strain Hardening | (5) |
| | 51-55 | IHARD(I) | Strain Hardening Type Code =1: Isotropic Hardening =2: Kinematic Hardening =3: Combined Isotropic and Kinematic Hardening, with Constant Proportions of Yield Surface Expansion and Translation | (6) |
| | 56-60 | ISSC(I) | Number of Data Curve Containing Uniaxial Stress-Strain Data for this Material | (7) |
| | 61-70 | ALPHA(I) | Coefficient of Thermal Expansion | - |

C. ELEMENT DEFINITION DATA, ELEMENT TYPE 4

(A single blank card terminates input)

| CARD | COL | DATA | DESCRIPTION | NOTES |
|------|-------|------|--|-------|
| 1 | 1-5 | IEL | Element Number | (8) |
| | 6 | IOUT | Output Flag (Blank or "N") | (9) |
| | 7-10 | IPR | Material Property Set for this Element | - |
| | 11-15 | KGEN | Node Increment for Element Generation | (10) |
| | 16-20 | N(1) | Local Node Number 1 | (11) |
| | 21-25 | N(2) | Local Node Number 2 | |
| | 26-35 | AREA | Element Cross-Sectional Area | |

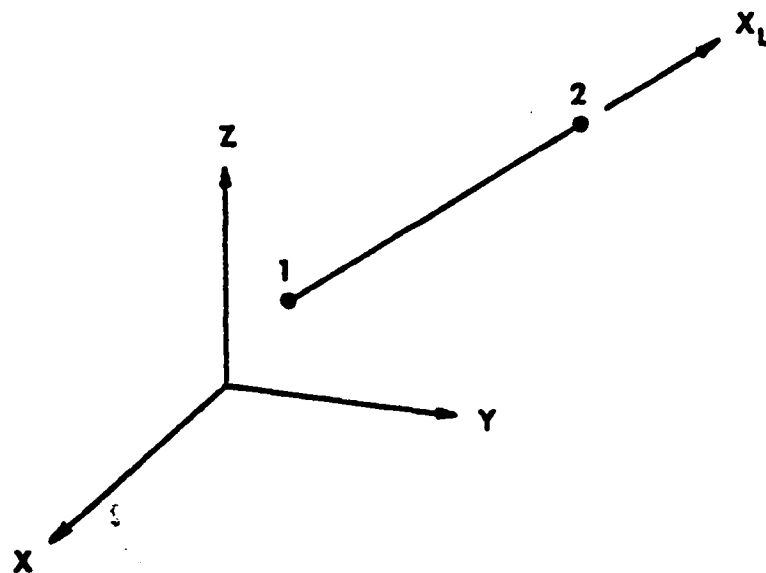


Figure 8.5.6 Nodal Connectivity for Three-Dimensional Truss Element.

NOTES:

- (1) Repeat card B-1 for each material property set to be defined. The n^{th} card entered in this section defines material property set n , for $n = 1, 2, \dots, \text{NMAT}$.
- (2) Mass densities are entered in a Force-Length-Time system of units consistent with those used elsewhere in the data. For example, in British units, mass density is entered in units of $\text{lbf-sec}^2/\text{in}^4$. The mass density of aluminum, for instance, would be entered as $\rho = (0.1 \text{ lb/in}^3)/(386.4 \text{ in/sec}^2) = 0.000259 \text{ lbf-sec}^2/\text{in}^4$.
- (3) If material nonlinearities are to be neglected, omit the yield stress as input. Default value set to 1.0×10^{12} .
- (4) The program attempts to follow the material stress strain curve as closely as possible, using a subincremental method of analyzing plastic flow. Each increment of time or load is divided into several "strain subincrements" at which material behavior is analyzed. $\text{DEMAX}(I)$ is the largest value of any incremental strain component which is permitted before stresses, strains, and the constitutive law are reevaluated. Default value set to 0.00020.
- (5) Applies only when $\text{IHARD}(I) = 3$ (combined hardening rule). Definition of γ is discussed in Chapter 2.
- (6) Isotropic hardening permits a uniform expansion of the yield locus in stress space; it predicts no Bauschinger effect, and is generally applicable in elastic-plastic problems involving nearly proportional systems of loading. Kinematic hardening allows the yield locus to translate in stress space, giving an "ideal" Bauschinger effect. The combined hardening rule, which permits both expansion and translation of the yield surface, is sometimes preferable for unloading and cyclic plasticity problems. Default hardening type is isotropic.
- (7) Uniaxial stress-strain data for a material are defined in Section 8.9, DATA CURVES. $\text{ISSC}(I)$ is the index of the particular data curve describing the uniaxial stress-strain behavior of the current material. Note that uniaxial material curves are represented as piecewise linear

functions, giving equivalent stress versus equivalent plastic strain; that is, the required data in Section 8.9 defines

$$\sigma_{eq} \text{ vs. } (\epsilon - \sigma/E) \text{ for } \sigma_{eq} \geq \sigma_{yield}$$

- (8) Valid element numbers are 1, 2, ..., NELEM. Elements must be defined sequentially, but intermediate elements can be generated automatically (see Note 10, below). Card C-1 is repeated as needed to define all Type 4 elements in the model. Following the last element, a single blank card (setting IEL = 0) is entered to terminate input for element Type 4.
- (9) The output code determines whether or not integration point stress output will be printed for element IEL. A blank field causes full printing for the element; an "N" in column 6 suppresses stress output.
- (10) A nonzero value of KGEN on the second card of a pair causes elements between the last and current elements to be generated automatically. With the exception of node numbers, all elements generated are assigned the same data as the current element. Local node numbers for the previous element are incremented by KGEN to generate each succeeding element. Node numbers for the current element (second card of a pair) need not be given. More than one element must be generated to use this feature. If element cards are omitted but KGEN = 0, a default value of 1 is used.
- (11) Local node numbers for Element Type 4 are shown in Figure 8.5.6.

8.5.5 Data for Element Type 5

(Three-Dimensional Thin Shell Element)

A. HEADER CARD, ELEMENT TYPE 5

| CARD | COL | DATA | DESCRIPTION | NOTES |
|------|-------|-------|---|-------|
| 1 | 1-5 | ITYPE | Element Type; Enter the Number "5" | - |
| | 6-10 | NMAT | Number of Material Property Sets (Maximum of 20) | - |
| | 11-15 | NELEM | Number of Elements of this Element Type | - |

B. MATERIAL PROPERTY DATA, ELEMENT TYPE 5

(NMAT Cards are Required in this Section)

| CARD | COL | DATA | DESCRIPTION | NOTES |
|------|-------|----------|----------------------------------|-------|
| 1 | 1-10 | EE(I) | Elastic Modulus | (1) |
| | 11-20 | PR(I) | Poisson's Ratio | - |
| | 21-30 | DNS(I) | Mass Density | (2) |
| | 31-40 | ALPHA(I) | Coefficient of Thermal Expansion | - |

C. ELEMENT DEFINITION DATA, ELEMENT TYPE 5

(A single blank card terminates input)

| CARD | COL | DATA | DESCRIPTION | NOTES |
|------|-------|------|--|-------|
| 1 | 1-5 | IEL | Element Number | (3) |
| | 6 | IOUT | Output Flag (Blank or "N") | (4) |
| | 7-10 | IPR | Material Property Set for this Element | - |
| | 11-15 | KGEN | Node Increment for Element Generation | (5) |
| | 16-20 | N(1) | Local Node Number 1 | (6) |
| | 21-25 | N(2) | Local Node Number 2 | |
| | . | . | . | |
| | . | . | . | |
| | 51-55 | N(8) | Local Node Number 8 | - |

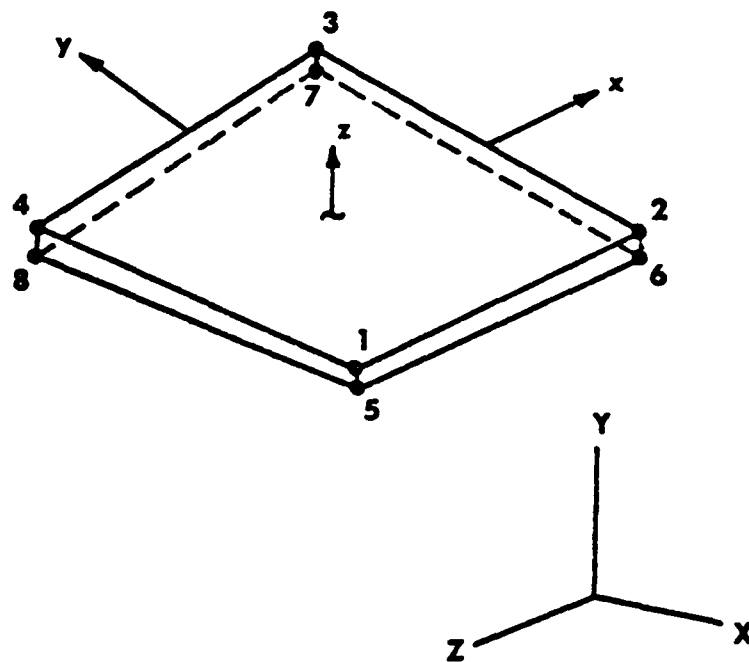


Figure 8.5.7 Nodal Connectivity for Three-Dimensional, Eight-Node Thin Shell Element.

NOTES:

- (1) Repeat card B-1 for each material property set to be defined. The n^{th} card entered in this section defines material property set n for $n = 1, 2, \dots, \text{NMAT}$.
- (2) Mass densities are entered in a Force-Length-Time system of units consistent with those used elsewhere in the data. For example, in British units, mass density is entered in units of $\text{lbf-sec}^2/\text{in}^4$. The mass density of aluminum, for instance, would be entered as $\rho = (0.1 \text{ lb/in}^3) / (386.4 \text{ in/sec}^2) = 0.000259 \text{ lbf-sec}^2/\text{in}^4$.
- (3) Valid element numbers are $1, 2, \dots, \text{NELEM}$. Elements must be defined sequentially, but intermediate elements can be generated automatically (see Note 5, below). Card C-1 is repeated as needed to define all Type 5 elements in the model). Following the last element, a single blank card (setting $\text{IEL} = 0$) is entered to terminate input for Element Type 5.
- (4) The output code determines whether or not integration point stress output will be printed for element IEL . A blank field causes full printing for the element; an "N" in column 6 suppresses stress output.
- (5) A nonzero value of KGEN on the second card of a pair causes elements between the last and current elements to be automatically generated. With the exception of node numbers, all elements generated are assigned the same data as the current element. Local node numbers for the previous element are incremented by KGEN to generate each succeeding element. More than one element must be generated to use this feature; node numbers for the current element need not be given. If element cards are omitted but $\text{KGEN} = 0$, a default value of 1 is used.
- (6) Local node numbering proceeds as shown in Figure 8.5.7.

8.5.6 Data for Element Type 6

(Three-Dimensional, Isoparametric Solid Twenty Node Brick)

A. HEADER CARD, ELEMENT TYPE 6

| CARD | COL | DATA | DESCRIPTION | NOTES |
|------|-------|-------|---|-------|
| 1 | 1-5 | ITYPE | Element Type; Enter the Number "6" | - |
| | 6-10 | NMAT | Number of Material Property Sets | - |
| | 11-15 | NELEM | Number of Elements of this Element Type | - |
| | 16-20 | NAXIS | Number of Orthotropic Axis Definitions | - |

B. MATERIAL PROPERTIES DATA, ELEMENT TYPE 6

- For each initially isotropic material, enter properties data from Section B-1, below (one card/material)
- For each elastic orthotropic material, enter properties data from Section B-2, below (two cards/material)
- NMAT material property sets should be defined in this data block.

B-1. Isotropic Material Properties

| CARD | COL | DATA | DESCRIPTION | NOTES |
|------|-------|----------|--|-------|
| 1 | 1-10 | EE(I) | Elastic Modulus | (1) |
| | 11-20 | PR(I) | Poisson's Ratio | - |
| | 21-30 | DNS(I) | Mass Density | (2) |
| | 31-40 | YLD(I) | Equivalent Stress at First Yield | (3) |
| | 41-50 | DEMAX(I) | Maximum Strain Subincrement | (4) |
| | 51-60 | GAMMA(I) | Ratio of Yield Surface Expansion to Translation for Combined Isotropic and Kinematic Strain Hardening | (5) |
| | 61-65 | IHARD(I) | Strain-Hardening Type Code =1: Isotropic Hardening =2: Kinematic Hardening =3: Combined Isotropic and Kinematic Hardening, with Constant Proportions of Yield Surface Expansion and Translation | (6) |
| | 66-70 | ISSC(I) | Number of Data Curve Containing Uniaxial Stress-Strain Data for this Material | (7) |
| | 71-80 | ALPHA(I) | Coefficient of Thermal Expansion | - |

B-2. Orthotropic Material Properties

| CARD | COL | DATA | DESCRIPTION | NOTES |
|------|-------|-----------|---|-------|
| 1 | 1 | MTYPE | Literal "A" - Flag for Orthotropic Materials Data | - |
| | 2-10 | E1(I) | Elastic Modulus in Direction 1 | (8) |
| | 11-20 | E2(I) | Elastic Modulus in Direction 2 | - |
| | 21-30 | E3(I) | Elastic Modulus in Direction 3 | - |
| | 31-40 | G12(I) | Shear Modulus in Plane 1-2 | - |
| | 41-50 | G13(I) | Shear Modulus in Plane 1-3 | - |
| | 51-60 | G23(I) | Shear Modulus in Plane 2-3 | - |
| 2 | 1-10 | PR12(I) | Poisson's Ratio in Plane 1-2 | (9) |
| | 11-20 | PR13(I) | Poisson's Ratio in Plane 1-3 | - |
| | 21-30 | PR23(I) | Poisson's Ratio in Plane 2-3 | - |
| | 31-40 | DNS(I) | Mass Density | (2) |
| | 41-50 | ALPHA1(I) | Coefficient of Thermal Expansion in Direction 1 | - |
| | 51-60 | ALPHA2(I) | Coefficient of Thermal Expansion in Direction 2 | - |
| | 61-70 | ALPHA3(I) | Coefficient of Thermal Expansion in Direction 3 | - |

C. ORTHOTROPIC MATERIAL AXIS DATA, ELEMENT TYPE 6

- Enter NAXIS sets of orthotropic axis data in this section
- If $NAXIS \leq 0$, skip this data block.

| CARD | COL | DATA | DESCRIPTION | NOTES |
|------|-------|----------|--|-------|
| 1 | 1-5 | NODE1(I) | Node Number Defining Origin of Coordinates | (10) |
| | 6-10 | NODE2(I) | Node Number Defining Material Direction 1 | |
| | 11-15 | NODE3(I) | Node Number Defining one Additional Point in the 1-2 Plane of the Material | |

D. ELEMENT DEFINITION DATA, ELEMENT TYPE 6

(A single blank card terminates input)

| CARD | COL | DATA | DESCRIPTION | NOTES |
|------|-------|-------|--|-------|
| 1 | 1-5 | IEL | Element Number | (11) |
| | 6 | IOUT | Output Code (Blank or "N") | (12) |
| | 7-10 | IPR | Material Property Set for this Element | - |
| | 11-13 | IAX | Orthotropic Axis Set | - |
| | 14-15 | INT | Order of Numerical Integration | (13) |
| | 16-20 | KGEN | Node Increment for Element Generation | (14) |
| | 21-25 | ISUP | Stiffness Generation Code | (15) |
| | 26-30 | N(1) | Local Node Number 1 | (16) |
| | 31-35 | N(2) | Local Node Number 2 | - |
| | . | . | . | . |
| | . | . | . | . |
| 2 | 78-80 | N(11) | Local Node Number 11 | - |
| | 1-5 | N(12) | Local Node Number 12 | - |
| | 6-10 | N(13) | Local Node Number 13 | - |
| | . | . | . | . |
| | . | . | . | . |
| | . | . | . | . |
| | 41-45 | N(20) | Local Node Number 20 | - |

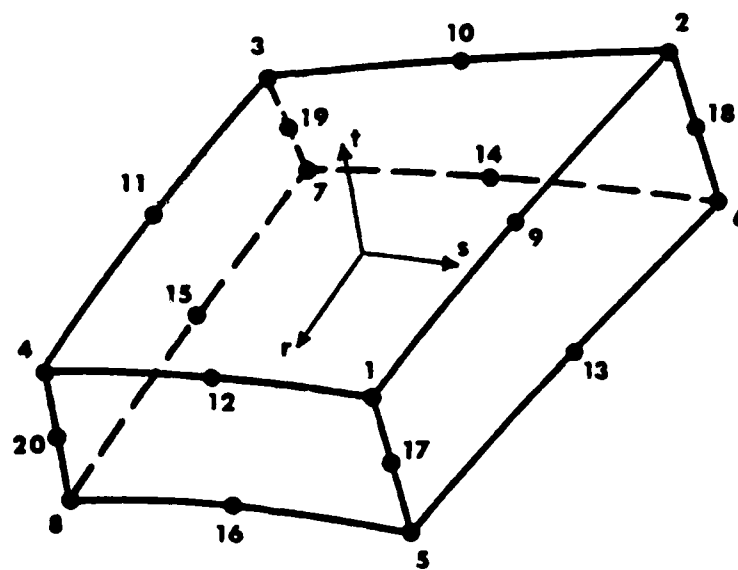


Figure 8.5.8 Nodal Connectivity for Twenty-Node Solid Element.

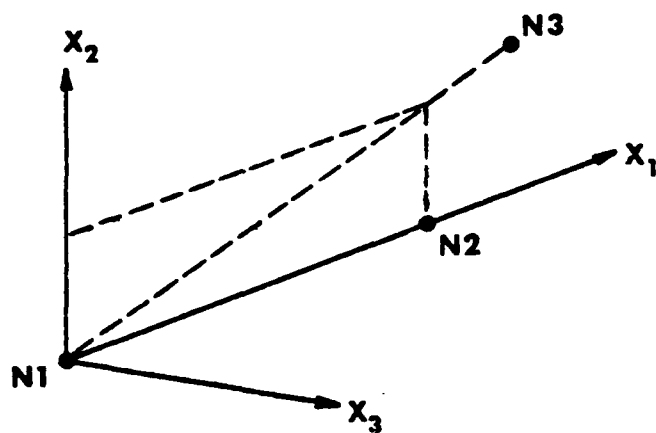


Figure 8.5.9 Definition of Orthotropic Material Axis Orientation.

NOTES:

- (1) Repeat card set B-1 or B-2 for each material property set to be defined. The n^{th} card set entered in this section defines material property set n for $n = 1, 2, \dots, \text{NMAT}$.
- (2) Mass densities are entered in a Force-Length-Time system of units consistent with those used elsewhere in the data. For example, in British units, mass density is entered in units of $\text{lbf-sec}^2/\text{in}^4$. The mass density of aluminum, for instance, would be entered as $\rho = (0.1 \text{ lb/in}^3) / (386.4 \text{ in/sec}^2) = 0.000259 \text{ lbf-sec}^2/\text{in}^4$.
- (3) Omit yield stress as input if material nonlinearities are to be neglected. Default value set to 1.0×10^{12} .
- (4) The program attempts to follow the material stress-strain curve as closely as possible, using a subincremental method of analyzing plastic flow. Each increment of time or load is divided into several "strain subincrements" at which material behavior is analyzed. $\text{DEMAX}(I)$ is the largest value of any incremental strain component which is permitted before stresses, strains, and the constitutive law are reevaluated. Default value set to 0.00020.
- (5) Applies only when $\text{IHARD}(I) = 3$ (combined hardening rule). Definition of γ is discussed in Chapter 2.
- (6) Isotropic hardening permits a uniform expansion of the yield locus in stress space; it predicts no Bauschinger effect, and is generally applicable in elastic-plastic problems involving nearly proportional systems of loading. Kinematic hardening allows the yield locus to translate in stress space, giving an "ideal" Bauschinger effect. The combined hardening rule, which permits both expansion and translation of the yield surface, is sometimes preferable for unloading and cyclic plasticity problems. Default hardening type is isotropic.
- (7) Uniaxial stress-strain data for a material are entered in Section 8.9, DATA CURVES. $\text{ISSC}(I)$ is the index of a particular data curve describing the uniaxial stress-strain behavior of the current material. Note that uniaxial material curves are represented as piecewise

linear functions, giving equivalent stress versus equivalent plastic strain; that is, the required data in Section 8.9 defines

$$\sigma_{eq} \text{ vs. } (\epsilon - \sigma/E) \text{ for } \sigma_{eq} \geq \sigma_{yield}$$

- (8) Orthotropic material properties must be defined with respect to the principal directions of the material (e.g., parallel and perpendicular to the fiber directions, for a filamentary material). Elements in which the principal material directions are not aligned with the global coordinate axes are transformed to global coordinates using the orthotropic axis data entered in part C (see Note 10).
- (9) The Poisson's ratio $PR_{ij}(I)$ defines the lateral contraction in direction j due to a unit extension in direction i . Care should be taken to ensure that these values satisfy the symmetry conditions and other restrictions summarized in Chapter 2.
- (10) The definition of material axis direction is depicted in Figure 8.5.9. NODE1 defines an "origin of coordinates," located arbitrarily in space; NODE2 locates the first principal direction of the material by specifying any point on the 1-axis. NODE3 is any third point which, together with NODE1 and NODE2, uniquely defines the 1-2 plane (i.e., the three nodes should not be collinear). Repeat Card C-1 as required to define all orthotropic axis systems for this element type. The n^{th} line entered in this section defines material axis set n , for $n = 1, 2, \dots, NAXIS$.
- (11) Valid element numbers are 1, 2, ..., NELEM. Elements must be defined sequentially, but intermediate elements can be generated automatically (see Note 14, below). Cards D-1 and D-2 are repeated as needed to define all Type 6 elements in the model. Following the last element, a single blank card (setting IEL = 0) is entered to terminate input for element Type 6.
- (12) The output code determines whether or not integration point stress output will be printed for element IEL. A blank field causes full printing for the element; an "N" in column 6 suppresses stress output.
- (13) Integration orders available for the twenty-node solid element are 2 and 3 point Gaussian rules, corresponding to 8 and 27 integration

points per element, respectively. The non-Gaussian 14-point integration rule is selected by setting $INT = 14$. Locations of integration points for $INT = 2, 3$, and 14 are listed in Tables 8.5.9 through 8.5.11, respectively.

- (14) A nonzero value of $KGEN$ on the second card of a pair causes elements between the last and current elements to be generated automatically. With the exception of node numbers, all elements generated are assigned the same data as the current element. Local node numbers for the previous element are incremented by $KGEN$ to generate each succeeding element. Node numbers for the current element need not be given. More than one element must be generated to use this feature. If element cards are omitted but $KGEN = 0$, a default value of 1 is used.
- (15) $ISUP$ should be set to zero for linear analysis. In a nonlinear solution, $ISUP = 0$ permits full nonlinearities to be included in the stiffness calculation for an element. If $ISUP = 1$ for a nonlinear element, the original (linear) stiffness matrix is used throughout the solution for the element in question. Nonlinearities in elements having $ISUP = 1$ are taken into account by means of equilibrium correction, as in constant stiffness iteration. The use of $ISUP = 1$ is appropriate for regions in a structure which experience very mild nonlinearities. If $ISUP = -1$ for a nonlinear element, the nonlinear stiffness is reformulated at each increment using an appropriate calculation based upon the average values of the nonlinear terms over the element. For $ISUP = 1$, internal forces are still evaluated exactly at all times, to avoid erroneous results. The use of $ISUP = -1$ can result in considerable savings of computer time in nonlinear analysis, but should not be used without equilibrium iteration (Section 8.3).
- (16) Local node numbering proceeds as shown in Figure 8.5.8.

TABLE 8.5.9

INTEGRATION POINT LOCATIONS FOR TWENTY-NODE
SOLID ELEMENT WITH INT = 2

| Point | Nearest Node | r | s | t |
|-------|-----------------|--------|------|------|
| 1 | 7 | $-h^*$ | $-h$ | $-h$ |
| 2 | 3 | $-h$ | $-h$ | h |
| 3 | 6 | $-h$ | h | $-h$ |
| 4 | 2 | $-h$ | h | h |
| 5 | 8 | h | $-h$ | $-h$ |
| 6 | 4 | h | $-h$ | h |
| 7 | 5 | h | h | $-h$ |
| 8 | 1 | h | h | h |

* $h = 0.5773502691896$

TABLE 8.5.10

INTEGRATION POINT LOCATIONS FOR TWENTY-NODE
SOLID ELEMENT WITH INT = 3

| Point | Nearest Node | r | s | t |
|-------|--------------|-----|----|----|
| 1 | 7 | -h* | -h | -h |
| 2 | 19 | -h | -h | 0 |
| 3 | 3 | -h | -h | h |
| 4 | 14 | -h | 0 | -h |
| 5 | 24 | -h | 0 | 0 |
| 6 | 10 | -h | 0 | h |
| 7 | 6 | -h | h | -h |
| 8 | 18 | -h | h | 0 |
| 9 | 2 | -h | h | h |
| 10 | 15 | 0 | -h | -h |
| 11 | 25 | 0 | -h | 0 |
| 12 | 11 | 0 | -h | h |
| 13 | 26 | 0 | 0 | -h |
| 14 | 27 | 0 | 0 | 0 |
| 15 | 23 | 0 | 0 | h |
| 16 | 13 | 0 | h | -h |
| 17 | 22 | 0 | h | 0 |
| 18 | 9 | 0 | h | h |
| 19 | 8 | h | -h | -h |
| 20 | 20 | h | -h | 0 |
| 21 | 4 | h | -h | h |
| 22 | 16 | h | 0 | -h |
| 23 | 21 | h | 0 | 0 |
| 24 | 12 | h | 0 | h |
| 25 | 5 | h | h | -h |
| 26 | 17 | h | h | 0 |
| 27 | 1 | h | h | h |

* $h = 0.7745966692415$

TABLE 8.5.11

INTEGRATION POINTS FOR TWENTY NODE
SOLID ELEMENT WITH INT = 14

| Point | r | s | t |
|-------|-------|----|----|
| 1 | *-a | 0 | 0 |
| 2 | a | 0 | 0 |
| 3 | 0 | -a | 0 |
| 4 | 0 | a | 0 |
| 5 | 0 | 0 | -a |
| 6 | 0 | 0 | a |
| 7 | ** -b | -b | -b |
| 8 | -b | b | -b |
| 9 | -b | -b | b |
| 10 | -b | b | b |
| 11 | b | -b | -b |
| 12 | b | b | -b |
| 13 | b | -b | b |
| 14 | b | b | b |

* a = 0.795822426

** b = 0.758786911

8.5.7 Data for Element Type 7

(Three-Dimensional, Isoparametric Solid with
8-20 Nodes)

A. HEADER CARD, ELEMENT TYPE 7

| CARD | COL | DATA | DESCRIPTION | NOTES |
|------|-------|-------|---|-------|
| 1 | 1-5 | ITYPE | Element Type; Enter the Number "7" | - |
| | 6-10 | NMAT | Number of Material Property Sets | - |
| | 11-15 | NELEM | Number of Elements of this Element Type | - |
| | 16-20 | NAXIS | Number of Orthotropic Axis Definitions | - |

B. MATERIAL PROPERTIES DATA, ELEMENT TYPE 7

- For each initially isotropic material, enter properties data from Section B-1, below (one card/material)
- For each elastic orthotropic material, enter properties data from Section B-2, below (two cards/material)
- NMAT material property sets should be defined in this data block.

B-1. Isotropic Material Properties

| CARD | COL | DATA | DESCRIPTION | NOTES |
|------|-------|----------|--|-------|
| 1 | 1-10 | EE(I) | Elastic Modulus | (1) |
| | 11-20 | PR(I) | Poisson's Ratio | - |
| | 21-30 | DNS(I) | Mass Density | (2) |
| | 31-40 | YLD(I) | Equivalent Stress at First Yield | (3) |
| | 41-50 | DEMAX(I) | Maximum Strain Subincrement | (4) |
| | 51-60 | GAMMA(I) | Ratio of Yield Surface Expansion to Translation for Combined Isotropic and Kinematic Strain Hardening | (5) |
| | 61-65 | IHARD(I) | Strain-Hardening Type Code =1: Isotropic Hardening =2: Kinematic Hardening =3: Combined Isotropic and Kinematic Hardening, with Constant Proportions of Yield Surface Expansion and Translation | (6) |
| | 66-70 | ISSC(I) | Number of Data Curve Containing Uniaxial Stress-Strain Data for this Material | (7) |
| | 71-80 | ALPHA(I) | Coefficient of Thermal Expansion | - |

B-2. Orthotropic Material Properties

| CARD | COL | DATA | DESCRIPTION | NOTES |
|------|-------|-----------|---|-------|
| 1 | 1 | MTYPE | Literal "A" - Flag for Orthotropic Materials Data | - |
| | 2-10 | E1(I) | Elastic Modulus in Direction 1 | (8) |
| | 11-20 | E2(I) | Elastic Modulus in Direction 2 | - |
| | 21-30 | E3(I) | Elastic Modulus in Direction 3 | - |
| | 31-40 | G12(I) | Shear Modulus in Plane 1-2 | - |
| | 41-50 | G13(I) | Shear Modulus in Plane 1-3 | - |
| | 51-60 | G23(I) | Shear Modulus in Plane 2-3 | - |
| 2 | 1-10 | PR12(I) | Poisson's Ratio in Plane 1-2 | (9) |
| | 11-20 | PR13(I) | Poisson's Ratio in Plane 1-3 | - |
| | 21-30 | PR23(I) | Poisson's Ratio in Plane 2-3 | - |
| | 31-40 | DNS(I) | Mass Density | (2) |
| | 41-50 | ALPHA1(I) | Coefficient of Thermal Expansion in Direction 1 | - |
| | 51-60 | ALPHA2(I) | Coefficient of Thermal Expansion in Direction 2 | - |
| | 61-70 | ALPHA3(I) | Coefficient of Thermal Expansion in Direction 3 | - |

C. ORTHOTROPIC MATERIAL AXIS DATA, ELEMENT TYPE 7

- Enter NAXIS sets of orthotropic axis data in this section
- If $NAXIS \leq 0$, skip this data block.

| CARD | COL | DATA | DESCRIPTION | NOTES |
|------|-------|----------|--|-------|
| 1 | 1-5 | NODE1(I) | Node Number Defining Origin of Coordinates | (10) |
| | 6-10 | NODE2(I) | Node Number Defining Material Direction 1 | |
| | 11-15 | NODE3(I) | Node Number Defining one Additional Point in the 1-2 Plane of the Material | |

D. ELEMENT DEFINITION DATA, ELEMENT TYPE 7

(A single blank card terminates input)

| CARD | COL | DATA | DESCRIPTION | NOTES |
|------|-------|-------|--|-------|
| 1 | 1-5 | IEL | Element Number | (11) |
| | 6 | IOUT | Output Code (Blank or "N") | (12) |
| | 7-10 | IPR | Material Property Set for this Element | - |
| | 11-13 | IAX | Orthotropic Axis Set | - |
| | 14-15 | INT | Order of Numerical Integration | (13) |
| | 16-20 | KGEN | Node Increment for Element Generation | (14) |
| | 21-25 | ISUP | Stiffness Generation Code | (15) |
| | 26-30 | N(1) | Local Node Number 1 | (16) |
| | 31-35 | N(2) | Local Node Number 2 | - |
| | . | . | . | . |
| | . | . | . | . |
| 2 | 75-80 | N(11) | Local Node Number 11 | - |
| | 1-5 | N(12) | Local Node Number 12 | (17) |
| | 6-10 | N(13) | Local Node Number 13 | - |
| | . | . | . | . |
| | . | . | . | . |
| | 41-45 | N(20) | Local Node Number 20 | - |

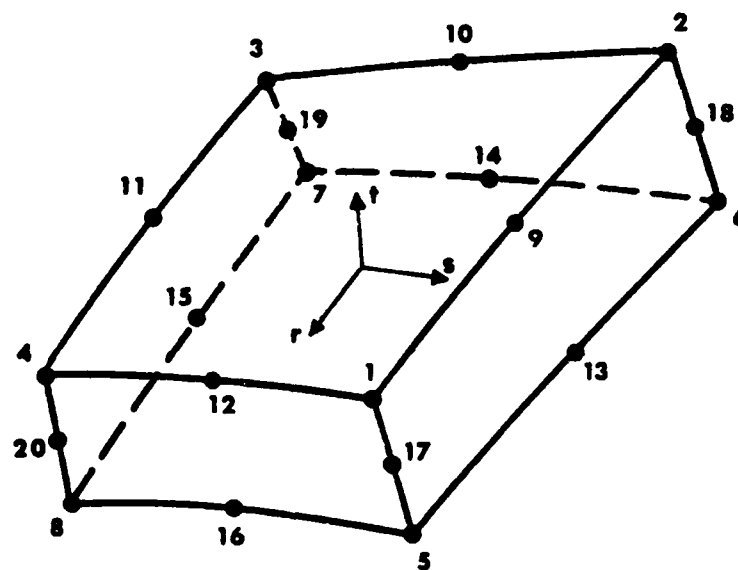


Figure 8.5.10 Nodal Connectivity for Variable-Node Solid Element.

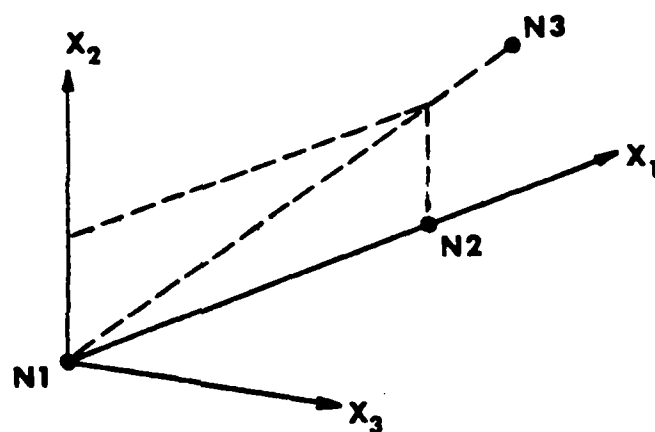


Figure 8.5.11 Definition of Orthotropic Material Axis Orientations.

NOTES:

- (1) Repeat card set B-1 or B-2 for each material property set to be defined. The n^{th} card set entered in this section defines material property set n for $n = 1, 2, \dots, \text{NMAT}$.
- (2) Mass densities are entered in a Force-Length-Time system of units consistent with those used elsewhere in the data. For example, in British units, mass density is entered in units of $\text{lbf-sec}^2/\text{in}^4$. The mass density of aluminum, for instance, would be entered as $\rho = (0.1 \text{ lb/in}^3)/(386.4 \text{ in/sec}^2) = 0.000259 \text{ lbf-sec}^2/\text{in}^4$.
- (3) Omit yield stress as input if material nonlinearities are to be neglected. Default value set to 1.0×10^{12} .
- (4) The program attempts to follow the material stress-strain curve as closely as possible, using a subincremental method of analyzing plastic flow. Each increment of time or load is divided into several "strain subincrements" at which material behavior is analyzed. $\text{DEMAX}(I)$ is the largest value of any incremental strain component which is permitted before stresses, strains, and the constitutive law are reevaluated. Default value set to 0.00020.
- (5) Applies only when $\text{IHARD}(I) = 3$ (combined hardening rule). Definition of γ is discussed in Chapter 2.
- (6) Isotropic hardening permits a uniform expansion of the yield locus in stress space; it predicts no Bauschinger effect, and is generally applicable in elastic-plastic problems involving nearly proportional systems of loading. Kinematic hardening allows the yield locus to translate in stress space, giving an "ideal" Bauschinger effect. The combined hardening rule, which permits both expansion and translation of the yield surface, is sometimes preferable for unloading and cyclic plasticity problems. Default hardening type is isotropic.
- (7) Uniaxial stress-strain data for a material are entered in Section 8.9, DATA CURVES. $\text{ISSC}(I)$ is the index of a particular data curve describing the uniaxial stress-strain behavior of the current material. Note that uniaxial material curves are represented as piecewise

linear functions, giving equivalent stress versus equivalent plastic strain; that is, the required data in Section 8.9 defines

$$\sigma_{eq} \text{ vs. } (\epsilon - \sigma/E) \text{ for } \sigma_{eq} \geq \sigma_{yield}.$$

- (8) Orthotropic material properties must be defined with respect to the principal directions of the material (e.g., parallel and perpendicular to the fiber directions, for a filamentary material). Elements in which the principal material directions are not aligned with the global coordinate axes are transformed to global coordinates using the orthotropic axis data entered in part C (see Note 10).
- (9) The Poisson's ratio $PR_{ij}(I)$ defines the lateral contraction in direction j due to a unit extension in direction i . Care should be taken to ensure that these values satisfy the symmetry conditions and other restrictions summarized in Chapter 2.
- (10) The definitions of material axis directions is depicted in Figure 8.5.11. NODE1 defines an "origin of coordinates," located arbitrarily in space; NODE2 locates the first principal direction of the material by specifying any point on the 1-axis. NODE3 is any third point which, together with NODE 1 and NODE2, uniquely defines the 1-2 plane (i.e., the three nodes should not be collinear). Repeat card C-1 as required to define all orthotropic axis systems for this element type. The n^{th} line entered in this section defines material axis set n , for $n = 1, 2, \dots, NAXIS$.
- (11) Valid element numbers are 1, 2, ..., NELEM. Elements must be defined sequentially, but intermediate elements can be generated automatically (see Note 14, below). Cards D-1 and D-2 are repeated as needed to define all Type 7 elements in the model. Following the last element, a single blank card (setting IEL = 0) is entered to terminate input for element Type 7.
- (12) The output code determines whether or not integration point stress output will be printed for element IEL. A blank field causes full printing for the element; an "N" in column 6 suppresses stress output.
- (13) Integration orders available for the variable-node solid element are 2 and 3 point Gaussian rules, corresponding to 8 and 27 integration

points per element, respectively. The non-Gaussian 14-point integration rule is selected by setting $INT = 14$. Locations of integration points for $INT = 2, 3$, and 14 are listed in Tables 8.5.12 through 8.5.14, respectively.

- (14) A nonzero value of $KGEN$ on the second card of a pair causes elements between the last and current elements to be generated automatically. With the exception of node numbers, all elements generated are assigned the same data as the current element. Local node numbers for the previous element are incremented by $KGEN$ to generate each succeeding element. Only nonzero local node numbers are incremented, and node numbers for the current element need not be given. More than one element must be generated to use this feature. If element cards are omitted but $KGEN = 0$, a default value of 1 is used.
- (15) $ISUP$ should be set to zero for linear analysis. In a nonlinear solution $ISUP = 0$ permits full nonlinearities to be included in the stiffness calculation for an element. If $ISUP = 1$ for a nonlinear element, the original (linear) stiffness matrix is used throughout the solution for the element in question. Nonlinearities in elements having $ISUP = 1$ are taken into account by means of equilibrium correction, as in constant stiffness iteration. The use of $ISUP = 1$ is appropriate for regions in a structure which experience very mild nonlinearities. If $ISUP = -1$ for a nonlinear element, the nonlinear stiffness is reformulated at each increment using an approximate calculation based upon the average values of the nonlinear terms over the element. For $ISUP = -1$, internal forces are still evaluated exactly at all times, to avoid erroneous results. The use of $ISUP = -1$ results in considerable savings of computer time in nonlinear analysis, but should not be used without equilibrium iteration (Section 8.3).
- (16) Local node numbering proceeds as shown in Figure 8.5.10. Nodes 1 through 8 (vertices) are required for all elements. Nodes 9 through 20 are each optional, and element interpolation functions generated by the program automatically account for the absence or presence of each local node.
- (17) Card D-2 must be entered, even if local nodes 12 through 20 are not used in a particular element.

TABLE 8.5.12

INTEGRATION POINT LOCATIONS FOR VARIABLE 8-20 NODE
SOLID ELEMENT WITH INT = 2

| Point | Nearest Node | r | s | t |
|-------|-----------------|-----|----|----|
| 1 | 7 | -h* | -h | -h |
| 2 | 3 | -h | -h | h |
| 3 | 6 | -h | h | -h |
| 4 | 2 | -h | h | h |
| 5 | 8 | h | -h | -h |
| 6 | 4 | h | -h | h |
| 7 | 6 | h | h | -h |
| 8 | 1 | h | h | h |

* $h = 0.5773502691896$

TABLE 8.5.13

INTEGRATION POINT LOCATIONS FOR VARIABLE 8-20 NODE
SOLID ELEMENT WITH INT = 3

| Point | Nearest Node | r | s | t |
|-------|--------------|-----|----|----|
| 1 | 7 | -h* | -h | -h |
| 2 | 19 | -h | -h | 0 |
| 3 | 3 | -h | -h | h |
| 4 | 14 | -h | 0 | -h |
| 5 | 24 | -h | 0 | 0 |
| 6 | 10 | -h | 0 | h |
| 7 | 6 | -h | h | -h |
| 8 | 18 | -h | h | 0 |
| 9 | 2 | -h | h | h |
| 10 | 15 | 0 | -h | -h |
| 11 | 25 | 0 | -h | 0 |
| 12 | 11 | 0 | -h | h |
| 13 | 26 | 0 | 0 | -h |
| 14 | 27 | 0 | 0 | 0 |
| 15 | 23 | 0 | 0 | h |
| 16 | 13 | 0 | h | -h |
| 17 | 22 | 0 | h | 0 |
| 18 | 9 | 0 | h | h |
| 19 | 8 | h | -h | -h |
| 20 | 20 | h | -h | 0 |
| 21 | 4 | h | -h | h |
| 22 | 16 | h | 0 | -h |
| 23 | 21 | h | 0 | 0 |
| 24 | 12 | h | 0 | h |
| 25 | 5 | h | h | -h |
| 26 | 17 | h | h | 0 |
| 27 | 1 | h | h | h |

* $h = 0.7745966692415$

TABLE 8.5.14
INTEGRATION POINT LOCATIONS FOR VARIABLE 8-20 NODE
SOLID ELEMENT WITH INT = 14

| Point | r | s | t |
|-------|-------|----|----|
| 1 | *-a | 0 | 0 |
| 2 | a | 0 | 0 |
| 3 | 0 | -a | 0 |
| 4 | 0 | a | 0 |
| 5 | 0 | 0 | -a |
| 6 | 0 | 0 | a |
| 7 | ** -b | -b | -b |
| 8 | -b | b | -b |
| 9 | -b | -b | b |
| 10 | -b | b | b |
| 11 | b | -b | -b |
| 12 | b | b | -b |
| 13 | b | -b | b |
| 14 | b | b | b |

* $a = 0.795822426$

** $b = 0.758786911$

8.5.8 Data for Element Type 8

(Three-Dimensional, Isoparametric Sixteen-Node
Solid/Thick Shell)

A. HEADER CARD, ELEMENT TYPE 8

| CARD | COL | DATA | DESCRIPTION | NOTES |
|------|-------|-------|---|-------|
| 1 | 1-5 | ITYPE | Element Type; Enter the Number "8" | - |
| | 6-10 | NMAT | Number of Material Property Sets | - |
| | 11-15 | NELEM | Number of Elements of this Element Type | - |
| | 16-20 | NAXIS | Number of Orthotropic Axis Definitions | - |

B. MATERIAL PROPERTIES DATA, ELEMENT TYPE 8

- For each initially isotropic material, enter properties data from Section B-1, below (one card/material)
- For each elastic orthotropic material, enter properties data from Section B-2, below (two cards/material)
- NMAT material property sets should be defined in this data block.

B-1. Isotropic Material Properties

| CARD | COL | DATA | DESCRIPTION | NOTES |
|------|-------|----------|--|-------|
| 1 | 1-10 | EE(I) | Elastic Modulus | (1) |
| | 11-20 | PR(I) | Poisson's Ratio | - |
| | 21-30 | DNS(I) | Mass Density | (2) |
| | 31-40 | YLD(I) | Equivalent Stress at First Yield | (3) |
| | 41-50 | DEMAX(I) | Maximum Strain Subincrement | (4) |
| | 51-60 | GAMMA(I) | Ratio of Yield Surface Expansion to Translation for Combined Isotropic and Kinematic Strain Hardening | (5) |
| | 61-65 | IHARD(I) | Strain-Hardening Type Code =1: Isotropic Hardening =2: Kinematic Hardening =3: Combined Isotropic and Kinematic Hardening, with Constant Proportions of Yield Surface Expansion and Translation | (6) |
| | 66-70 | ISSC(I) | Number of Data Curve Containing Uniaxial Stress Strain Data for this Material | (7) |
| | 71-80 | ALPHA(I) | Coefficient of Thermal Expansion | - |

B-2. Orthotropic Material Properties

| CARD | COL | DATA | DESCRIPTION | NOTES |
|------|-------|-----------|---|-------|
| 1 | 1 | MTYPE | Literal "A" - Flag for Orthotropic Materials Data | - |
| | 2-10 | E1(I) | Elastic Modulus in Direction 1 | (8) |
| | 11-20 | E2(I) | Elastic Modulus in Direction 2 | - |
| | 21-30 | E3(I) | Elastic Modulus in Direction 3 | - |
| | 31-40 | G12(I) | Shear Modulus in Plane 1-2 | - |
| | 41-50 | G13(I) | Shear Modulus in Plane 1-3 | - |
| | 51-60 | G23(I) | Shear Modulus in Plane 2-3 | - |
| 2 | 1-10 | PR12(I) | Poisson's Ratio in Plane 1-2 | (9) |
| | 11-20 | PR13(I) | Poisson's Ratio in Plane 1-3 | - |
| | 21-30 | PR23(I) | Poisson's Ratio in Plane 2-3 | - |
| | 31-40 | DNS(I) | Mass Density | (2) |
| | 41-50 | ALPHA1(I) | Coefficient of Thermal Expansion in Direction 1 | - |
| | 51-60 | ALPHA2(I) | Coefficient of Thermal Expansion in Direction 2 | - |
| | 61-70 | ALPHA3(I) | Coefficient of Thermal Expansion in Direction 3 | - |

C. ORTHOTROPIC MATERIAL AXIS DATA, ELEMENT TYPE 8

- Enter NAXIS sets of orthotropic axis data in this section
- If NAXIS \leq 0, skip this data block.

| CARD | COL | DATA | DESCRIPTION | NOTES |
|------|-------|----------|--|-------|
| 1 | 1-5 | NODE1(I) | Node Number Defining Origin of Coordinates | (10) |
| | 6-10 | NODE2(I) | Node Number Defining Material Direction 1 | |
| | 11-15 | NODE3(I) | Node Number Defining one Additional Point in the 1-2 Plane of the Material | |

D. ELEMENT DEFINITION DATA, ELEMENT TYPE 8

(A single blank card terminates input)

| CARD | COL | DATA | DESCRIPTION | NOTES |
|------|-------|-------|--|-------|
| 1 | 1-5 | IEL | Element Number | (11) |
| | 6 | IOUT | Output Code (Blank or "N") | (12) |
| | 7-10 | IPR | Material Property Set for this Element | - |
| | 11-13 | IAX | Orthotropic Axis Set | - |
| | 14-15 | INT | Order of Numerical Integration | (13) |
| | 16-20 | KGEN | Node Increment for Element Generation | (14) |
| | 21-25 | ISUP | Stiffness Generation Code | (15) |
| | 26-30 | N(1) | Local Node Number 1 | (16) |
| | 31-35 | N(2) | Local Node Number 2 | - |
| | . | . | . | . |
| | . | . | . | . |
| 2 | 75-80 | N(11) | Local Node Number 11 | - |
| | 1-5 | N(12) | Local Node Number 12 | - |
| | 6-10 | N(13) | Local Node Number 13 | - |
| | . | . | . | . |
| | . | . | . | . |
| | . | . | . | . |
| | 21-25 | N(16) | Local Node Number 16 | - |

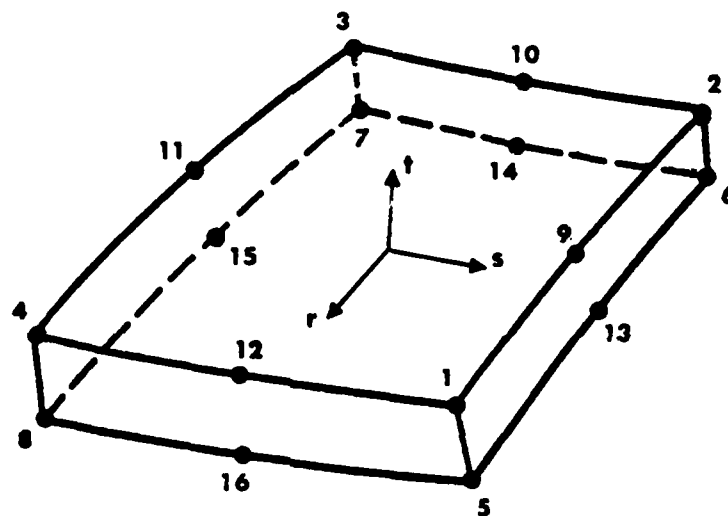


Figure 8.5.12 Nodal Connectivity for Sixteen Node Solid Element.

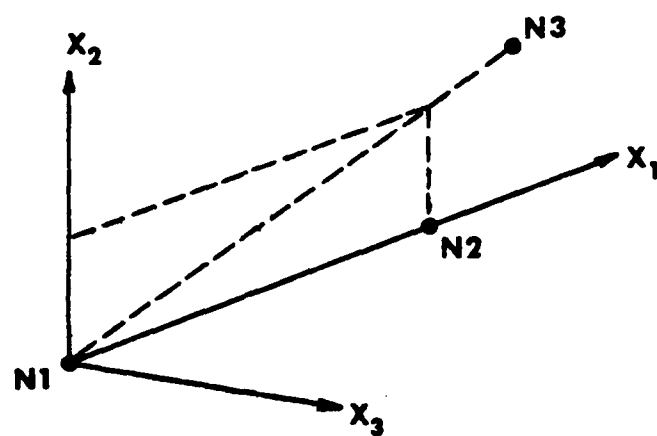


Figure 8.5.13 Definition of Orthotropic Material Axis Orientations.

NOTES:

- (1) Repeat card set B-1 or B-2 for each material property set to be defined. The n^{th} card set entered in this section defines material property set n for $n = 1, 2, \dots, \text{NMAT}$.
- (2) Mass densities are entered in a Force-Length-Time system of units consistent with those used elsewhere in the data. For example, in British units, mass density is entered in units of $\text{lbf-sec}^2/\text{in}^4$. The mass density of aluminum, for instance, would be entered as $\rho = (0.1 \text{ lb/in}^3) / (386.4 \text{ in/sec}^2) = 0.000259 \text{ lbf-sec}^2/\text{in}^4$.
- (3) Omit yield stress as input if material nonlinearities are to be neglected. Default value set to 1.0×10^{12} .
- (4) The program attempts to follow the material stress-strain curve as closely as possible, using a subincremental method of analyzing plastic flow. Each increment of time or load is divided into several "strain subincrements" at which material behavior is analyzed. $\text{DEMAX}(I)$ is the largest value of any incremental strain component which is permitted before stresses, strains, and the constitutive law are reevaluated. Default value set to 0.00020.
- (5) Applies only when $\text{IHARD}(I) = 3$ (combined hardening rule). Definition of γ is discussed in Chapter 2.
- (6) Isotropic hardening permits a uniform expansion of the yield locus in stress space; it predicts no Bauschinger effect, and is generally applicable in elastic-plastic problems involving nearly proportional systems of loading. Kinematic hardening allows the yield locus to translate in stress space, giving an "ideal" Bauschinger effect. The combined hardening rule, which permits both expansion and translation of the yield surface, is sometimes preferable for unloading and cyclic plasticity problems. Default hardening type is isotropic.
- (7) Uniaxial stress-strain data for a material are entered in Section 8.9, DATA CURVES. $\text{ISSC}(I)$ is the index of a particular data curve describing the uniaxial stress-strain behavior of the current material. Note that uniaxial material curves are represented as piecewise

linear functions, giving equivalent stress versus equivalent plastic strain; that is, the required data in Section 8.9 defines

$$\sigma_{eq} \text{ vs. } (\epsilon - \sigma/E) \text{ for } \sigma_{eq} \geq \sigma_{yield}$$

- (8) Orthotropic material properties must be defined with respect to the principal directions of the material (e.g., parallel and perpendicular to the fiber directions, for a filamentary material). Elements in which the principal material directions are not aligned with the global coordinate axes are transformed to global coordinates using the orthotropic axis data entered in part C (see Note 10).
- (9) The Poisson's ratio $PR_{ij}(I)$ defines the lateral contraction in direction j due to a unit extension in direction i . Care should be taken to ensure that these values satisfy the symmetry conditions and other restrictions summarized in Chapter 2.
- (10) The definition of material axis directions is depicted in Figure 8.5.13. NODE1 defines an "origin of coordinates," located arbitrarily in space; NODE 2 locates the first principal direction of the material by specifying any point on the 1-axis. NODE3 is any third point which, together with NODE1 and NODE2, uniquely defines the 1-2 plane (i.e., the three nodes should not be collinear). Repeat card C-1 as required to define all orthotropic axis systems for this element type. The n^{th} line entered in this section defines material axis set n , for $n = 1, 2, \dots, NAXIS$.
- (11) Valid element numbers are 1, 2, ..., NELEM. Elements must be defined sequentially but intermediate elements can be generated automatically (see Note 14, below). Cards D-1 and D-2 are repeated as needed to define all Type 8 elements in the model. Following the last element, a single blank card (setting IEL = 0) is entered to terminate input for element Type 8.
- (12) The output code determines whether or not integration point stress output will be printed for element IEL. A blank field causes full printing for the element; an "N" in column 6 suppresses stress output.
- (13) Integration orders available for the sixteen-node solid element are 2 and 3 point Gaussian rules, corresponding to 8 and 27 integration

points per element, respectively. The non-Gaussian 14-point integration rule is selected by setting $INT = 14$. Locations of integration points for $INT = 2, 3$, and 14 are listed in Tables 8.5.15 through 8.5.17, respectively.

- (14) A nonzero value of $KGEN$ on the second card of a pair causes elements between the last and current elements to be generated automatically. With the exception of node numbers, all elements generated are assigned the same data as the current element. Local node numbers for the previous element are incremented by $KGEN$ to generate each succeeding element. Node numbers for the current element need not be given. More than one element must be generated to use this feature. If element cards are omitted by $KGEN = 0$, a default value of 1 is used.
- (15) $ISUP$ should be set to zero for linear analysis. In a nonlinear solution $ISUP = 0$ permits full nonlinearities to be included in the stiffness calculation for an element. If $ISUP = 1$ for a nonlinear element, the original (linear) stiffness matrix is used throughout the solution for the element in question. Nonlinearities in elements have $ISUP = 1$ are taken into account by means of equilibrium correction, as in constant stiffness iteration. The use of $ISUP = 1$ is appropriate for regions in a structure which experience very mild nonlinearities. If $ISUP = -1$ for a nonlinear element, the nonlinear stiffness is reformulated at each increment using an approximate calculation based upon the average values of the nonlinear terms over the element. For $ISUP = -1$, internal forces are still evaluated exactly at all times, to avoid erroneous results. The use of $ISUP = -1$ results in considerable savings of computer time in nonlinear analysis, but should not be used without equilibrium iteration (Section 8.3.).
- (16) Local node numbering proceeds as shown in Figure 8.5.12.

TABLE 8.5.15

INTEGRATION POINT LOCATIONS FOR SIXTEEN-NODE
SOLID ELEMENT WITH INT = 2

| Point | Nearest Node | r | s | t |
|-------|-----------------|-----|----|----|
| 1 | 7 | -h* | -h | -h |
| 2 | 3 | -h | -h | h |
| 3 | 6 | -h | h | -h |
| 4 | 2 | -h | h | h |
| 5 | 8 | h | -h | -h |
| 6 | 4 | h | -h | h |
| 7 | 5 | h | h | -h |
| 8 | 1 | h | h | h |

* $h = 0.5773506291896$

TABLE 8.5.16

INTEGRATION POINT LOCATIONS FOR SIXTEEN-NODE
SOLID ELEMENT WITH INT = 3

| Point | Nearest Node | r | s | t |
|-------|--------------|-----|----|----|
| 1 | 7 | -h* | -h | -h |
| 2 | 19 | -h | -h | 0 |
| 3 | 3 | -h | -h | h |
| 4 | 14 | -h | 0 | -h |
| 5 | 24 | -h | 0 | 0 |
| 6 | 10 | -h | 0 | h |
| 7 | 6 | -h | h | -h |
| 8 | 18 | -h | h | 0 |
| 9 | 2 | -h | h | h |
| 10 | 15 | 0 | -h | -h |
| 11 | 25 | 0 | -h | 0 |
| 12 | 11 | 0 | -h | h |
| 13 | 26 | 0 | 0 | -h |
| 14 | 27 | 0 | 0 | 0 |
| 15 | 23 | 0 | 0 | h |
| 16 | 13 | 0 | h | -h |
| 17 | 22 | 0 | h | 0 |
| 18 | 9 | 0 | h | h |
| 19 | 8 | h | -h | -h |
| 20 | 20 | h | -h | 0 |
| 21 | 4 | h | -h | h |
| 22 | 16 | h | 0 | -h |
| 23 | 21 | h | 0 | 0 |
| 24 | 12 | h | 0 | h |
| 25 | 5 | h | h | -h |
| 26 | 17 | h | h | 0 |
| 27 | 1 | h | h | h |

* $h = 0.7745966692415$

TABLE 8.5.17
INTEGRATION POINT LOCATIONS FOR SIXTEEN-NODE
SOLID ELEMENT WITH INT = 14

| Point | r | s | t |
|-------|-------|----|----|
| 1 | *-a | 0 | 0 |
| 2 | a | 0 | 0 |
| 3 | 0 | -a | 0 |
| 4 | 0 | a | 0 |
| 5 | 0 | 0 | -a |
| 6 | 0 | 0 | a |
| 7 | ** -b | -b | -b |
| 8 | -b | b | -b |
| 9 | -b | -b | b |
| 10 | -b | b | b |
| 11 | b | -b | -b |
| 12 | b | b | -b |
| 13 | b | -b | b |
| 14 | b | b | b |

* $a = 0.795822426$

** $b = 0.758786911$

8.5.9 Data for Element Type 9

(Isoparametric Plane-Stress Element with 4-9 Nodes)

A. HEADER CARD, ELEMENT TYPE 9

| CARD | COL | DATA | DESCRIPTION | NOTES |
|------|-------|-------|---|-------|
| 1 | 1-5 | ITYPE | Element Type; Enter the Number "9" | - |
| | 6-10 | NMAT | Number of Material Property Sets (Maximum of 20) | - |
| | 11-15 | NELEM | Number of Elements of this Element Type | - |

B. MATERIAL PROPERTIES DATA, ELEMENT TYPE 9

(NMAT Cards are Required in this Section)

| CARD | COL | DATA | DESCRIPTION | NOTES |
|------|-------|----------|--|-------|
| 1 | 1-10 | EE(I) | Elastic Modulus | (1) |
| | 11-20 | PR(I) | Poisson's Ratio | - |
| | 21-30 | DNS(I) | Mass Density | (2) |
| | 31-40 | YLD(I) | Equivalent Stress at First Yield | (3) |
| | 41-50 | DEMAX(I) | Maximum Strain Subincrement | (4) |
| | 51-60 | GAMMA(I) | Ratio of Yield Surface Expansion to Translation, for Combined Strain Hardening Rule | (5) |
| | 61-65 | IHARD(I) | Strain Hardening Type Code =1: Isotropic Hardening =2: Kinematic Hardening =3: Combined Isotropic and Kinematic Hardening | (6) |
| | 66-70 | ISSC(I) | Number of Data Curve Containing Uniaxial Stress-Strain Data for this Material | (7) |
| | 71-80 | ALPHA(I) | Coefficient of Thermal Expansion | - |

C. ELEMENT DEFINITION DATA, ELEMENT TYPE 9

(A single blank card terminates input)

| CARD | COL | DATA | DESCRIPTION | NOTES |
|------|-------|-------|--|-------|
| 1 | 1-5 | IEL | Element Number | (8) |
| | 6 | IOUT | Output Code (Blank or "N") | (9) |
| | 7-10 | IPR | Material Property Set for this Element | - |
| | 11-15 | INT | Order of Numerical Integration | (10) |
| | 16-20 | KGEN | Node Increment for Element Generation | (11) |
| | 21-25 | N(1) | Local Node Number 1 | (12) |
| | 26-30 | N(2) | Local Node Number 2 | |
| | 31-35 | N(3) | Local Node Number 3 | |
| | . | . | . | . |
| | . | . | . | . |
| | . | . | . | . |
| | . | . | . | . |
| | 61-65 | N(9) | Local Node Number 9 | |
| | 66-75 | THICK | Element Thickness (Default = 1.0) | |

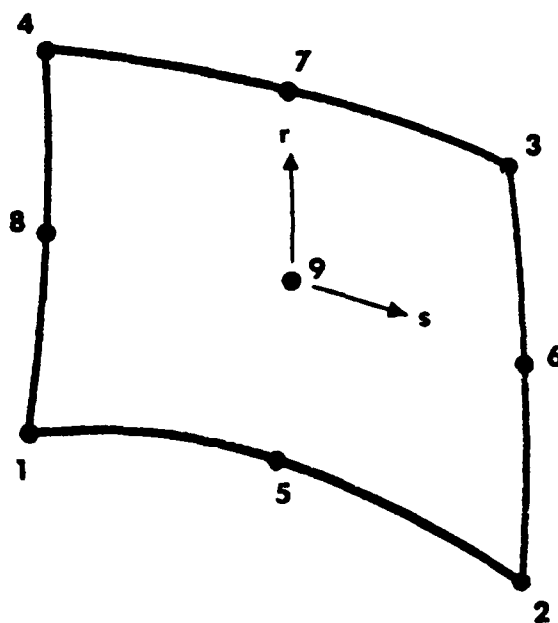


Figure 8.5.14 Nodal Connectivity for Variable-Node Plane Stress Element.

NOTES:

- (1) Repeat Card B-1 for each material property set to be defined. The n^{th} card entered in this section defines material property set n , for $n = 1, 2, \dots, \text{NMAT}$.
- (2) Mass densities are entered in a Force-Length-Time system of units consistent with those used elsewhere in the data. For example, in British units, mass density is entered in units of $\text{lbf-sec}^2/\text{in}^4$. The mass density of aluminum, for instance, would be entered as $\rho = (0.1 \text{ lb/in}^3)/(386.4 \text{ in/sec}^2) = 0.000259 \text{ lbf-sec}^2/\text{in}^4$.
- (3) If material nonlinearities are to be neglected, omit the yield stress as input. Default value set to 1.0×10^{12} .
- (4) The program attempts to follow the material stress strain curve as closely as possible, using a subincremental method of analyzing plastic flow. Each increment of time or load is divided into several "strain subincrements" at which material behavior is analyzed. $\text{DEMAX}(I)$ is the largest value of any incremental strain component which is permitted before stresses, strains, and the constitutive law are reevaluated. Default value set to 0.00020.
- (5) Applies only when $\text{IHARD}(I) = 3$ (combined hardening rule). Definition of γ is discussed in Chapter 2.
- (6) Isotropic hardening permits a uniform expansion of the yield locus in stress space; it predicts no Bauschinger effect, and is generally applicable in elastic-plastic problems involving nearly proportional systems of loading. Kinematic hardening allows the yield locus to translate in stress space, giving an "ideal" Bauschinger effect. The combined hardening rule, which permits both expansion and translation of the yield surface, is sometimes preferable for unloading and cyclic plasticity problems. Default hardening type is isotropic.
- (7) Uniaxial stress-strain data for a material are defined in Section 8.9, DATA CURVES. $\text{ISSC}(I)$ is the index of the particular data curve, describing the uniaxial stress-strain behavior of the material. Note that uniaxial material curves are piecewise linear functions, giving equivalent stress

equivalent plastic strain; that is, the required data in Section 8.9 defines

$$\sigma_{eq} \text{ vs. } (\epsilon - \sigma/E) \text{ for } \sigma_{eq} \geq \sigma_{yield}$$

- (8) Valid element numbers are 1, 2, ..., NELEM. Elements must be defined sequentially, but intermediate elements can be generated automatically (see Note 11, below). Card C-1 is repeated as needed to define all Type 9 elements in the model. Following the last element, a single blank card (setting IEL = 0) is entered to terminate input for Element Type 9.
- (9) The output code determines whether or not integration point stress output will be printed for element IEL. A blank field causes full printing for the element; an "N" in column 6 suppresses stress output.
- (10) Integration orders available for Element Type 9 and 1, 2, and 3 point Gaussian rules, corresponding to 1, 4, and 9 integration points per element, respectively. Locations of integration points for INT = 2 and 3 are listed in Tables 8.5.20 and 8.5.21, respectively. Default integration order is 3.
- (11) A nonzero value of KGEN on the second card of the pair causes elements between the last and current elements to be automatically generated. With the exception of node numbers, all elements generated are assigned the same data as the current element. Local node numbers for the previous element are incremented KGEN to generate each succeeding element. Node numbers for the current element (second card of the pair) need not be given. More than one element must be generated to use this feature. If element cards are omitted but KGEN = 0, a default value of 1 is used.
- (12) Local node numbers are defined as shown in Figure 8.5.14. Nodes 1-4 are required for all Type 9 elements, and each of nodes 5-9 is optional. The presence or absence of each node is automatically taken into account by the program.

TABLE 8.5.18
 INTEGRATION POINT LOCATIONS FOR VARIABLE-NODE
 PLANE STRESS ELEMENT WITH INT = 2

| Point | Nearest Node | r | s |
|-------|-----------------|-----|----|
| 1 | 1 | -h* | -h |
| 2 | 4 | -h | h |
| 3 | 2 | h | -h |
| 4 | 3 | h | h |

$$*h = 0.5773502691896$$

TABLE 8.5.19

INTEGRATION POINT LOCATIONS FOR VARIABLE-NODE
PLANE STRESS ELEMENT WITH INT = 3

| Point | r | s |
|-------|--------|------|
| 1 | $-h^*$ | $-h$ |
| 2 | $-h$ | 0 |
| 3 | $-h$ | h |
| 4 | 0 | $-h$ |
| 5 | 0 | 0 |
| 6 | 0 | h |
| 7 | h | $-h$ |
| 8 | h | 0 |
| 9 | h | h |

* $h = 0.7745966692415$

8.5.10 Data for Element Type 10

(Isoparametric Axisymmetric Element with 4-9 Nodes)

A. HEADER CARD, ELEMENT TYPE 10

| CARD | COL | DATA | DESCRIPTION | NOTES |
|------|-------|-------|---|-------|
| 1 | 1-5 | ITYPE | Element Type; Enter the Number "10" | - |
| | 6-10 | NMAT | Number of Material Property Sets (Maximum of 20) | - |
| | 11-15 | NELEM | Number of Elements of this Element Type | - |

- IMPORTANT:
- (1) Thermal Stress Analysis is not available with this element
 - (2) Axisymmetric models must be defined within the x-y plane; x corresponds to the radial coordinate.

B. MATERIAL PROPERTIES DATA, ELEMENT TYPE 10

(NMAT Cards are Required in this Section)

| CARD | COL | DATA | DESCRIPTION | NOTES |
|------|-------|----------|--|-------|
| 1 | 1-10 | EE(I) | Elastic Modulus | (1) |
| | 11-20 | PR(I) | Poisson's Ratio | - |
| | 21-30 | DNS(I) | Mass Density | (2) |
| | 31-40 | YLD(I) | Equivalent Stress at First Yield | (3) |
| | 41-50 | DEMAX(I) | Maximum Strain Subincrement | (4) |
| | 51-60 | GAMMA(I) | Ratio of Yield Surface Expansion to Translation, for Combined Strain Hardening Rule | (5) |
| | 61-65 | IHARD(I) | Strain Hardening Type Code =1: Isotropic Hardening =2: Kinematic Hardening =3: Combined Isotropic and Kinematic Hardening | |
| | 66-70 | ISSC(I) | Number of Data Curve Containing Uniaxial Stress-Strain Data for this Material | (7) |

C. ELEMENT DEFINITION DATA, ELEMENT TYPE 10

(A single blank card terminates input)

| CARD | COL | DATA | DESCRIPTION | NOTES |
|------|-------|------|---------------------------------------|-------|
| 1 | 1-5 | IEL | Element Number | (8) |
| | 6 | IOUT | Output Code (Blank or "N") | (9) |
| | 7-10 | IPR | Material Property Set | - |
| | 11-15 | INT | Order of Numerical Integration | (10) |
| | 16-20 | KGEN | Node Increment for Element Generation | (11) |
| | 21-25 | N(1) | Local Node Number 1 | (12) |
| | 26-30 | N(2) | Local Node Number 2 | |
| | 31-35 | N(3) | Local Node Number 3 | |
| | . | . | . | |
| | . | . | . | |
| | . | . | . | |
| | 61-65 | N(9) | Local Node Number 9 | |

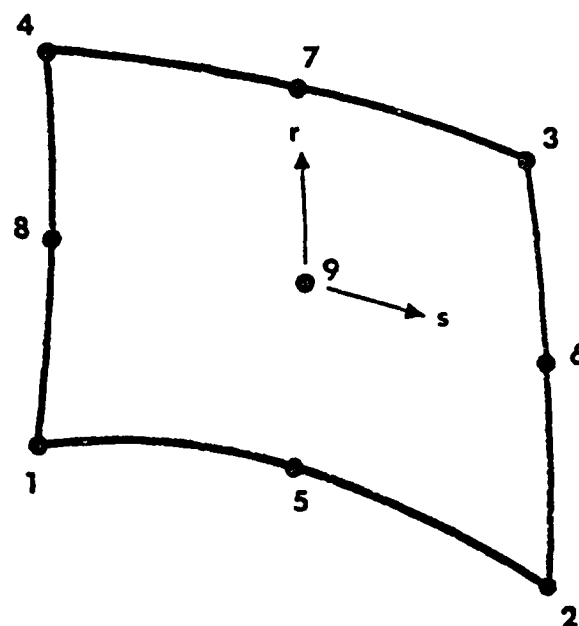


Figure 8.5.15. Nodal Connectivity for Variable-Node Axisymmetric Element.

NOTES:

- (1) Repeat Card B-1 for each material property set to be defined. The n^{th} card entered in this section defines material property set n , for $n = 1, 2, \dots, \text{NMAT}$.
- (2) Mass densities are entered in a Force-Length-Time system of units consistent with those used elsewhere in the data. For example, in British units, mass density is entered in units of $\text{lbf-sec}^2/\text{in}^4$. The mass density of aluminum, for instance, would be entered as $\rho = (0.1 \text{ lb/in}^3) / (386.4 \text{ in/sec}^2) = 0.000259 \text{ lbf-sec}^2/\text{in}^4$.
- (3) If material nonlinearities are to be neglected, omit the yield stress as input. Default value set to 1.0×10^{12} .
- (4) The program attempts to follow the material stress strain curve as closely as possible, using a subincremental method of analyzing plastic flow. Each increment of time or load is divided into several "strain subincrements" at which material behavior is analyzed. $\text{DEMAX}(I)$ is the largest value of any incremental strain component which is permitted before stresses, strains, and constitutive law are reevaluated. Default value set to 0.00020.
- (5) Applies only when $\text{IHARD}(I) = 3$ (combined hardening rule). Definition of γ is discussed in Chapter 2.
- (6) Isotropic hardening permits a uniform expansion of the yield locus in stress space; it predicts no Bauschinger effect, and is generally applicable in elastic-plastic problems involving nearly proportional systems of loading. Kinematic hardening allows the yield locus to translate in stress space, giving an "ideal" Bauschinger effect. The combined hardening rule, which permits both expansion and translation of the yield surface, is sometimes preferable for unloading and cyclic plasticity problems. Default hardening type is isotropic.
- (7) Uniaxial stress-strain data for a material are defined in Section 8.9, DATA CURVES. $\text{ISSC}(I)$ is the index of the particular data curve, describing the uniaxial stress-strain behavior of the current material. Note that uniaxial material curves are represented as piecewise linear functions, giving equivalent stress versus

equivalent plastic strain; that is, the required data in Section 8.9 defines

$$\sigma_{eq} \text{ vs. } (\epsilon - \sigma/E) \text{ for } \sigma_{eq} \geq \sigma_{yield}$$

- (8) Valid element numbers are 1, 2, ..., NELEM. Elements must be defined sequentially, but intermediate elements can be generated automatically (see Note 10, below). Card C-1 is repeated as needed to define all Type 9 elements in the model. Following the last element, a single blank card (setting IEL = 0) is entered to terminate input for Element Type 10.
- (9) The output code determines whether or not integration point stress output will be printed for element IEL. A blank field causes full printing for the element; an "N" in column 6 suppresses stress output.
- (10) Integration orders available for Element Type 9 are 1, 2, and 3 point Gaussian rules, corresponding to 1, 4, and 9 integration points per element, respectively. Locations of integration points for INT = 2 and 3 are listed in Tables 8.5.20 and 8.5.21, respectively. The default order is INT = 3.
- (11) A nonzero value of KGEN on the second card of the pair causes elements between the last and current elements to be automatically generated. With the exception of node numbers, all elements generated are assigned the same data as the current element. Local node numbers for the previous element are incremented KGEN to generate each succeeding element. Node numbers for the current element (second card of the pair) need not be given. More than one element must be generated to use this feature. If element cards are omitted but KGEN = 0, a default value of 1 is used.
- (12) Local node numbers are defined as shown in Figure 8.5.15. Nodes 1-4 are required for all Type 10 elements, and each of nodes 5-9 is optional. The presence or absence of each node is automatically taken into account by the program.

TABLE 8.5.20

INTEGRATION POINT LOCATIONS FOR VARIABLE-NODE
AXISYMMETRIC ELEMENT WITH INT = 2

| Point | Nearest Node | r | s |
|-------|-----------------|-----|----|
| 1 | 1 | -h* | -h |
| 2 | 4 | -h | h |
| 3 | 2 | h | -h |
| 4 | 3 | h | h |

$$*h = 0.5773502691896$$

TABLE 8.5.21

INTEGRATION POINT LOCATIONS FOR VARIABLE-NODE
AXISYMMETRIC ELEMENT WITH $INT = 3$

| Point | r | s |
|-------|--------|------|
| 1 | $-h^*$ | $-h$ |
| 2 | $-h$ | 0 |
| 3 | $-h$ | h |
| 4 | 0 | $-h$ |
| 5 | 0 | 0 |
| 6 | 0 | h |
| 7 | h | $-h$ |
| 8 | h | 0 |
| 9 | h | h |

* $h = 0.7745966692415$

8.5.11 Data for Element Type 11

(Three-Dimensional, Isoparametric Sixteen-Node Layered Shell)

A. HEADER CARD, ELEMENT TYPE 11

| CARD | COL | DATA | DESCRIPTION | NOTES |
|------|-------|-------|---|-------|
| 1 | 1-5 | ITYPE | Element Type; Enter the Number "11" | - |
| | 6-10 | NMAT | Number of Material Property Sets | - |
| | 11-15 | NELEM | Number of elements of this Element Type | - |
| | 16-20 | NLAM | Number of Laminate Cross-Section Definitions* | - |

B. MATERIAL PROPERTIES DATA, ELEMENT TYPE 11

- For each initially isotropic material, enter properties data from Section B-1, below (one card/material).
- For each elastic orthotropic material, enter properties data from Section B-2, below (two cards/material).
- NMAT material property sets should be defined in this data block.

*A laminate cross-section refers to a pattern of materials and their relative thickness which occur through the total thickness of a shell. Each unique combination must be defined as a separate "cross-section."

B-1. Isotropic Material Properties

| CARD | COL | DATA | DESCRIPTION | NOTES |
|------|-------|----------|-----------------------------------|-------|
| 1 | 1-10 | EE(I) | Elastic Modulus | (1) |
| | 11-20 | PR(I) | Poisson's Ratio | - |
| | 21-30 | DNS(I) | Mass Density | (2) |
| | 31-40 | ALPHA(I) | Coefficient of Thermal Expansion | (3) |
| | 41-50 | YLD(I) | Equivalent Stress at First Yield | (4) |
| | 51-60 | SLP(I) | Hardening Slope (Plastic Modulus) | (5) |

AD-A129 773

MAGNA (MATERIALLY AND GEOMETRICALLY NONLINEAR ANALYSIS)

6/8

PART I FINITE ELE. (U) DAYTON UNIV OH RESEARCH INST

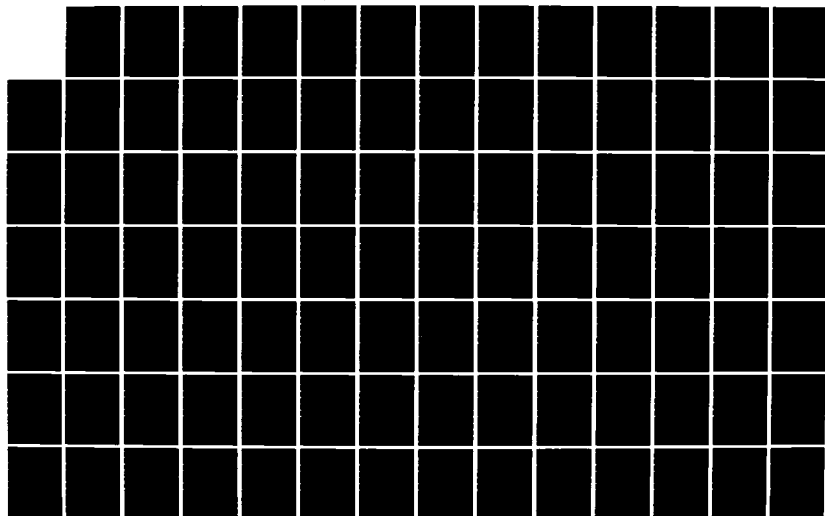
R A BROCKMAN DEC 82 UDR-TR-82-111 AFWAL-TR-82-3098-PT-1

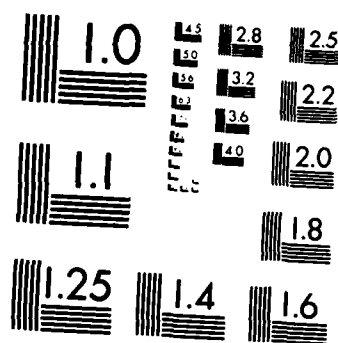
UNCLASSIFIED

F33615-80-C-3403

F/G 12/1

NL





MICROCOPY RESOLUTION TEST CHART
NATIONAL BUREAU OF STANDARDS-1963-A

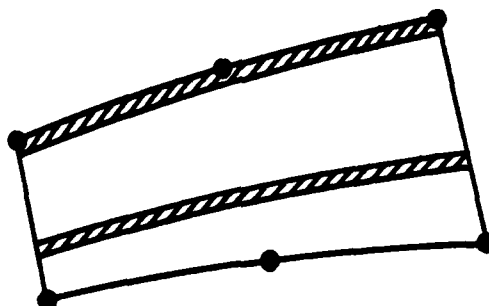
B-2. Orthotropic Material Properties

| CARD | COL | DATA | DESCRIPTION | NOTES |
|------|-------|-----------|---|-------|
| 1 | 1 | MTYPE | Literal "A" - Flag for Orthotropic Materials Data | - |
| | 2-10 | E1(I) | Elastic Modulus in Direction 1 | (6) |
| | 11-20 | E2(I) | Elastic Modulus in Direction 2 | - |
| | 21-30 | E3(I) | Elastic Modulus in Direction 3 | - |
| | 31-40 | G12(I) | Shear Modulus in Plane 1-2 | - |
| | 41-50 | G13(I) | Shear Modulus in Plane 1-3 | - |
| | 51-60 | G23(I) | Shear Modulus in Plane 2-3 | - |
| 2 | 1-10 | PR12(I) | Poisson's Ratio in Plane 1-2 | (7) |
| | 11-20 | PR13(I) | Poisson's Ratio in Plane 1-3 | - |
| | 21-30 | PR23(I) | Poisson's Ratio in Plane 2-3 | - |
| | 31-40 | DNS(I) | Mass Density | (2) |
| | 41-50 | ALPHA1(I) | Coefficient of Thermal Expansion in Direction 1 | (3) |
| | 51-60 | ALPHA2(I) | Coefficient of Thermal Expansion in Direction 2 | (3) |
| | 61-70 | ALPHA3(I) | Coefficient of Thermal Expansion in Direction 3 | (3) |

C. LAMINATE DEFINITION DATA, ELEMENT TYPE 11

- For each laminate cross-section definition, enter the data block below. NLAM laminate definitions should appear.
- At least one laminate definition is required in all problems.
- Card 1 below is repeated as necessary to define all NLAM cross-sections. For each laminate definition, Card 2 is repeated for each layer of the cross-section.

| CARD | COL | DATA | DESCRIPTION | NOTES |
|------|-------|-----------|--|-------|
| 1 | 1-5 | LAM | Laminate Definition Number | (8) |
| | 6-10 | NLAY(LAM) | Number of Layers (Min = 2, Max = 11) | (9) |
| 2 | 1-5 | LAYTYP | Layer Type =0: Variable Thickness =1: Constant Thickness | (10) |
| | 6-10 | MATL | Material Property Set for this Layer | - |
| | 11-20 | THICK | Layer Thickness (LAYTYP = 1) or Thickness Fraction (LAYTYP = 0) | (11) |
| | 21-30 | ANGLE | Orthotropic Material Axis Orientation for this Layer | (12) |



Variable-thickness (LAYTYP = 0)



Constant-thickness (LAYTYP = 1)

- Constant-thickness layers are of uniform thickness in the direction (approximately) normal to the layer
- Thicknesses of variable-thickness layers are distributed according to thickness fractions from the remaining thickness of an element
- All layers may have completely independent material properties and/or material axis orientations
- At least one layer must have variable thickness

Figure 8.5.16. Layer Type Definitions for Multilayered Shell Finite Element.

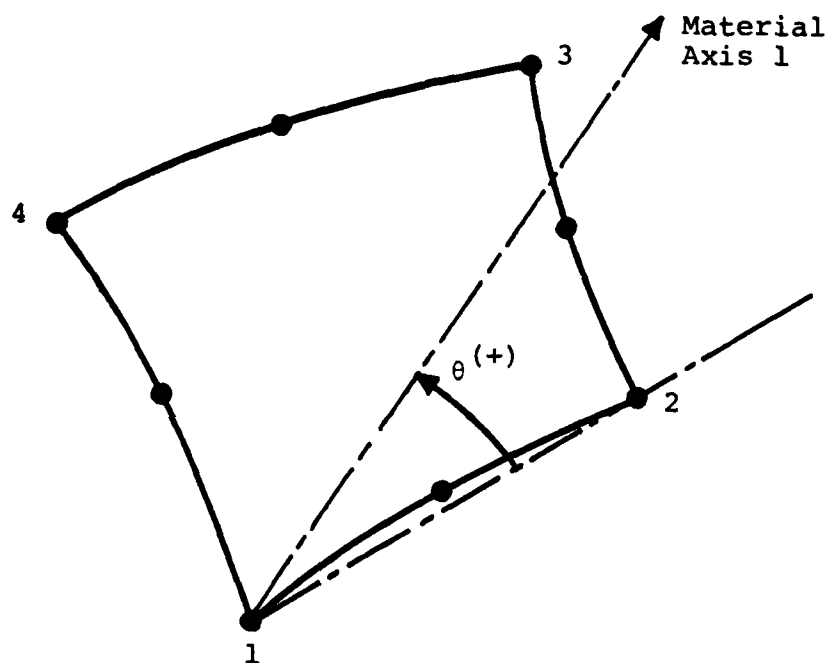


Figure 8.5.17. Definition of Orthotropic Material Axis Orientation for a Shell Layer.

D. ELEMENT DEFINITION DATA, ELEMENT TYPE 11

(A single blank card terminates input)

| CARD | COL | DATA | DESCRIPTION | NOTES |
|------|-------|---------|---------------------------------------|-------|
| 1 | 1-5 | IEL | Element Number | (13) |
| | 6 | IOUT | Output Code (Blank or "N") | (14) |
| | 7-10 | ILAM | Laminate Number for this Element | (15) |
| | 11-15 | INT | Order of Numerical Integration | (16) |
| | 16-20 | KGEN | Node Increment for Element Generation | (17) |
| | 21-25 | (Blank) | (Inactive Option) | - |
| | 26-30 | N(1) | Local Node Number 1 | (18) |
| | 31-35 | N(2) | Local Node Number 2 | - |
| | . | . | . | . |
| | . | . | . | . |
| | . | . | . | . |
| 2 | 75-80 | N(11) | Local Node Number 11 | - |
| | 1-5 | N(12) | Local Node Number 12 | - |
| | 6-10 | N(13) | Local Node Number 13 | - |
| | . | . | . | . |
| | . | . | . | . |
| | . | . | . | . |
| | 21-25 | N(16) | Local Node Number 16 | - |

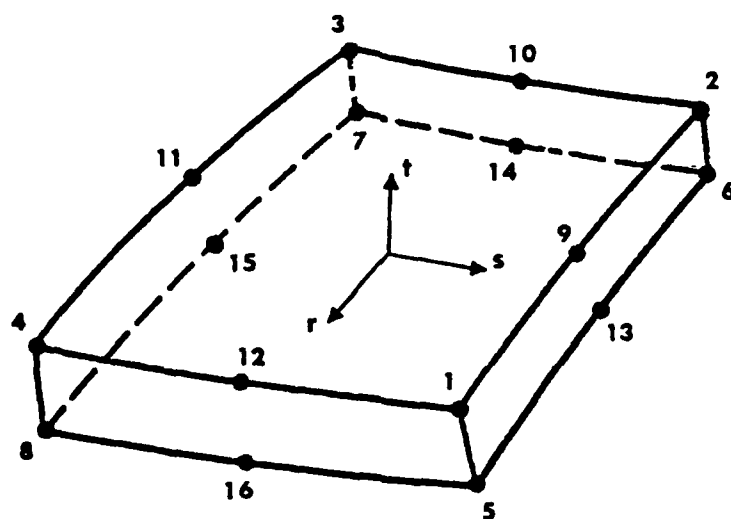


Figure 8.5.18. Nodal Connectivity for Sixteen-Node Layered Shell Element.

NOTES:

- (1) Repeat card set B-1 or B-2 for each material property set to be defined. The n^{th} card set entered in this section defines material property set n for $n = 1, 2, \dots, \text{NMAT}$.
- (2) Mass densities are entered in a Force-Length-Time system of units consistent with those used elsewhere in the data. For example, in British units, mass density is entered in units of $\text{lbf-sec}^2/\text{in}^4$. The mass density of aluminum, for instance, would be entered as $\rho = (0.1 \text{ lb/in}^3)/(386.4 \text{ in/sec}^2) = 0.000259 \text{ lbf-sec}^2/\text{in}^4$.
- (3) The coefficient of thermal expansion may be input but is not used. Thermal stress analysis is currently not available with Element Type 11.
- (4) Omit yield stress as input if material nonlinearities are to be neglected. Default value set to 1.0×10^{12} .
- (5) $\text{SLP}(I)$ represents the strain-hardening slope of the material in the plastic range, $d\sigma/d\varepsilon_p$. $\text{SLP}(I)$ may be determined from a bilinear representation of the material stress-strain curve (elastic modulus E , tangent modulus E_T) using the relation $\text{SLP}(I) = EE_T/(E - E_T)$. Isotropic strain hardening is assumed in all elastic-plastic materials with this element type.
- (6) Orthotropic material properties must be defined with respect to the principal directions of the material (e.g., parallel and perpendicular to the fiber directions, for a filamentary material). Elements in which the principal material directions are not aligned with the global coordinate axes are transformed to global coordinates using the laminate definition data of Section C.
- (7) The Poisson's ration $\text{PR}_{ij}(I)$ defines the lateral contraction in direction j due to a unit extension in direction i . Care should be taken to ensure that these values satisfy the symmetry conditions and other restrictions summarized in Chapter 2.

- (8) Each Type 11 element is defined by its nodal connections and by reference to one of the laminate definitions entered in this section. At least one laminate definition must appear in this input section.
- (9) "Layers" may refer to a true layered construction (multiple materials, or axis orientations), or may be defined to enhance resolution of yielded zones through the thickness of the shell. Each laminate must consist of at least two layers (they may be identical). Materials, thicknesses and material axes are entirely independent from layer to layer. Layers are numbered sequentially starting from the bottom layer (i.e., the layer nearest to the -t element surface).
- (10) LAYTYP = 1 specifies a layer whose thickness is constant over an entire element, even though the total element thickness may be variable. LAYTYP = 0 defines a layer whose thickness may vary quadratically over an element. These conventions are illustrated in Figure 8.5.16.
- (11) For LAYTYP = 1 (constant thickness layer), THICK defines the actual thickness for this layer. If LAYTYP = 0 (variable thickness) a "thickness fraction" is defined. The thickness of the layer at any point in an element is then
- $$t_{\text{layer}} = [t_{\text{total}} - \sum (\text{constant layer thicknesses})] \cdot \text{THICK}$$
- where t_{total} is computed from the node coordinates. The sum of all the thickness fraction values for LAYTYP = 0 layers is always scaled so that the sum of the thickness fractions is one.
- (12) The "3" direction of an orthotropic material is assumed to be in the shell thickness direction. The orientation of the orthotropic (1,2) axes is controlled by ANGLE, which is measured in degrees counter clockwise from a line connecting nodes 1 and 2 of an element (see Figure 8.5.17).
- (13) Valid element numbers are 1, 2, ..., NELEM. Elements must be defined sequentially, but intermediate elements can be generated automatically (see Note 17, below). Cards D-1 and D-2 are repeated as needed to define all Type 11 elements in the model. Following the last element, a single blank card (setting IEL = 0) is entered to terminate input for Element Type 11.

- (14) The output code determines whether or not integration point stress output will be printed for element IEL. A blank field causes full printing for the element; an "N" in column 6 suppresses stress output.
- (15) Each element must reference one of the laminate definitions entered in Section C. The top layer of the laminate is nearest the (+t) element surface (containing nodes 1 - 4).
- (16) Integration orders available for the element are 2 and 3 point Gaussian rules, corresponding to 4 and 9 integration points per element, respectively. Integration through the element thickness is always performed analytically. The default value of INT = 2 is suggested for general use. Locations of integration stations at the upper and lower surfaces of each layer are shown in Table 8.5.22.
- (17) A nonzero value of KGEN on the second card of a pair causes elements between the last and current elements to be generated automatically. With the exception of node numbers, all elements generated are assigned the same data as the current element. Local node numbers for the previous element are incremented by KGEN to generate each succeeding element. Node numbers for the current element need not be given. More than one element must be generated to use this feature. If element cards are omitted but KGEN = 0, a default value of 1 is used.
- (18) Local node numbering proceeds as shown in Figure 8.5.18.

TABLE 8.5.22

INTEGRATION POINT LOCATIONS FOR SIXTEEN-NODE
LAYERED SHELL ELEMENT

| Point | Nearest Nodes | r** | s** |
|-------|------------------|-----|-----|
| 1 | 1,5 | -h* | -h |
| 2 | 4,8 | -h | h |
| 3 | 2,6 | h | -h |
| 4 | 3,7 | h | h |

* $h = 0.5773502691896$

** A similar array of integration points is located
at the upper and lower surfaces of each layer.

8.5.12 Data for Element Type 12

(Three-Dimensional Isoparametric Curved Beam)

A. HEADER CARD, ELEMENT TYPE 12

| CARD | COL | DATA | DESCRIPTION | NOTES |
|------|-------|-------|---|-------|
| 1 | 1-5 | ITYPE | Element Type; Enter the Number "12" | - |
| | 6-10 | NMAT | Number of Material Property Sets (≤ 10) | - |
| | 11-15 | NELEM | Number of Elements of this Element Type | - |
| | 16-20 | NSEC | Number of Beam Section Properties (≤ 10) | - |

B. MATERIAL PROPERTIES DATA, ELEMENT TYPE 12

- For each material, enter properties data below (one card/material).
- NMAT material property sets should be defined in this data block.

| CARD | COL | DATA | DESCRIPTION | NOTES |
|------|-------|----------|----------------------------------|-------|
| 1 | 1-10 | E(I) | Elastic Modulus | - |
| | 11-20 | G(I) | Shear Modulus | (1) |
| | 21-30 | RHO(I) | Mass Density | (2) |
| | 31-40 | SY(I) | Yield Stress | (3) |
| | 41-50 | H(I) | Hardening Slope | (4) |
| | 51-60 | ALPHA(I) | Coefficient of Thermal Expansion | (5) |

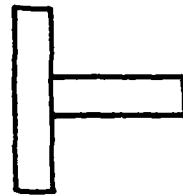
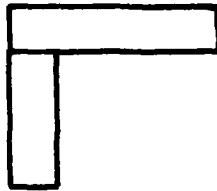
C. SECTION PROPERTIES DATA, ELEMENT TYPE 12

- For each beam section to be defined, enter geometric data below (2-5 cards/section).
- NSEC section properties should be defined in this data block.

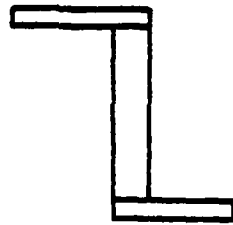
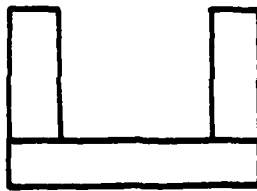
| CARD | COL | DATA | DESCRIPTION | NOTES |
|------|-------|------------|---|-------|
| 1 | 1-5 | ISEC | Section Property Number | (6) |
| | 6-10 | NSEG | Number of Segments in this Beam Cross-Section | (7) |
| | 11-20 | ZD(1) | Default local Z-Axis Orientation for this Cross-Section | (8) |
| | 21-30 | ZD(2) | | |
| | 31-40 | ZD(3) | | |
| 2 | 1-10 | YDIM(ISEG) | Segment Width | (9) |
| | 11-20 | ZDIM(ISEG) | Segment Depth | (9) |
| | 21-30 | YOFF(ISEG) | Segment Y-Offset | (10) |
| | 31-40 | ZOFF(ISEG) | Segment Z-Offset | (10) |



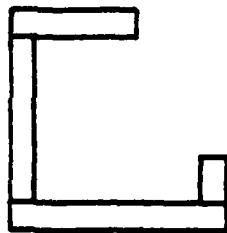
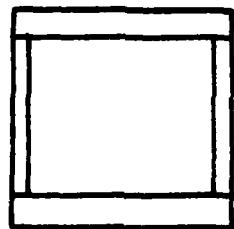
1 Segment



2 Segments



3 Segments



4 Segments

Figure 8.5.19. Some Typical Beam Sections Constructed from Rectangular Segments.

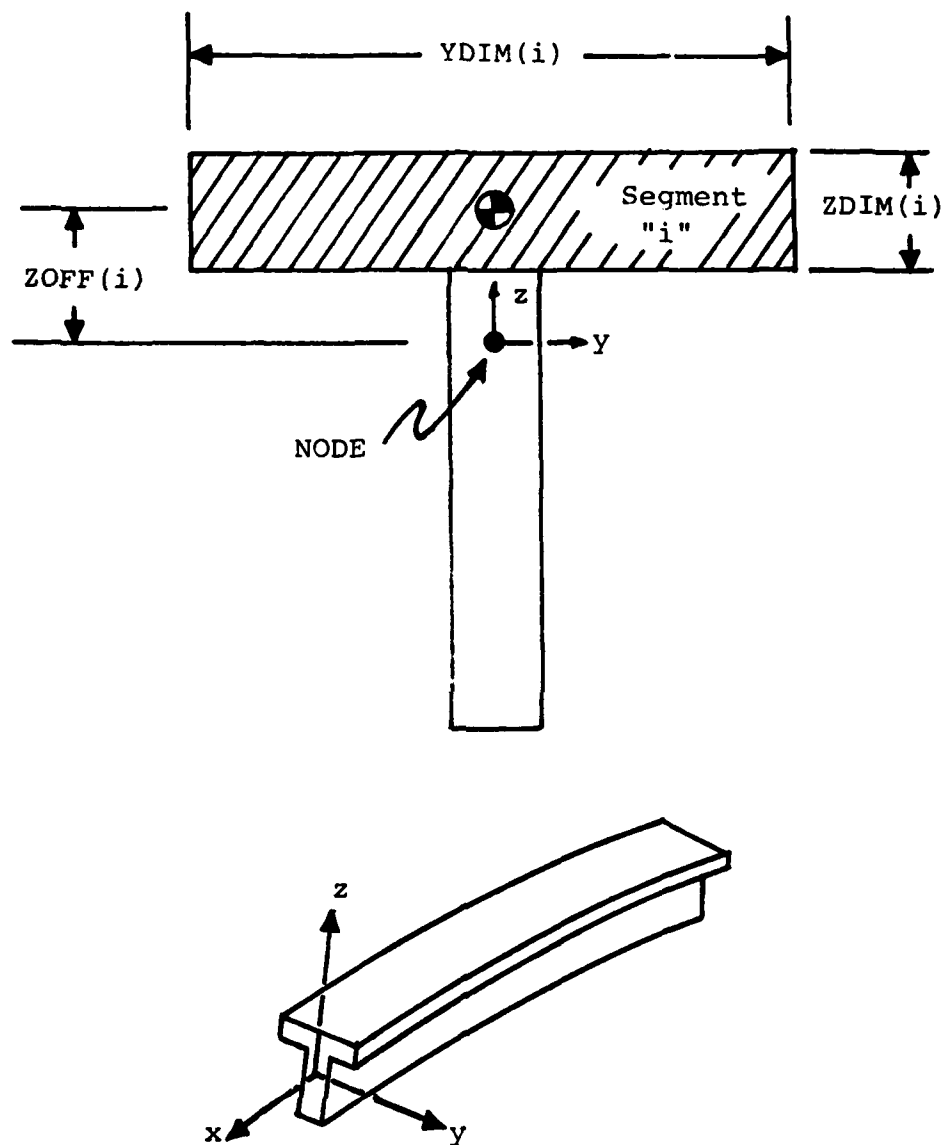
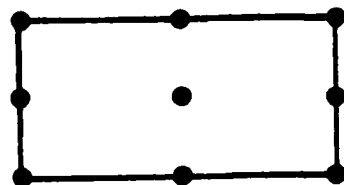
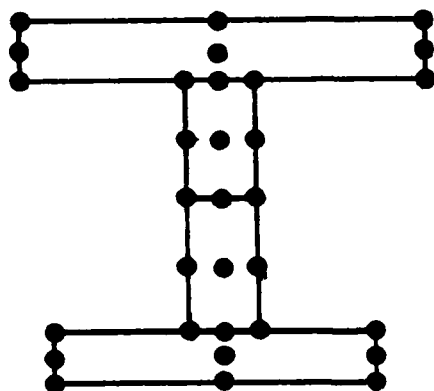


Figure 8.5.20. Beam Cross-Section Parameters.



1 Segment
9 Integration Points



4 Segments
36 Integration Points
(5 Overlap)

Figure 8.5.21. Cross-Sectional Integration Stations
in Curved Beam Element.

- Each of nodes "3" and "4" is optional
- Nodes "3" and "4" may be identical in curved elements

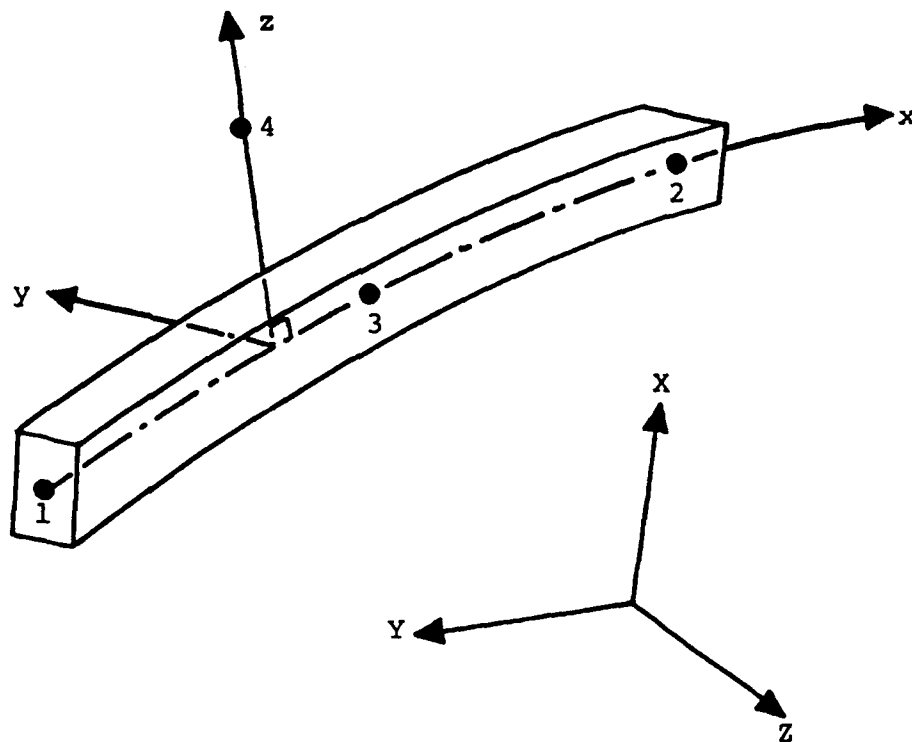
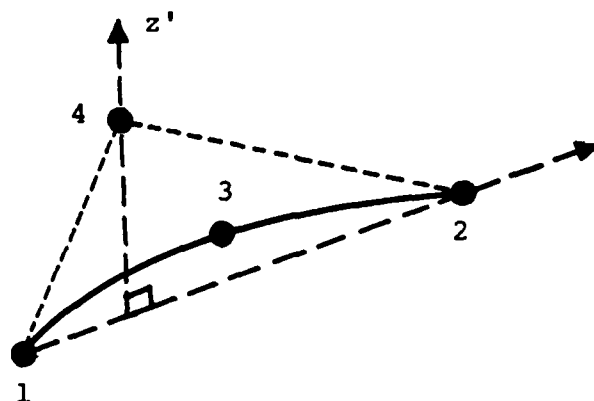


Figure 8.5.22. Connectivity and Local Axis Conventions for Beam Element.

D. ELEMENT DEFINITION DATA, ELEMENT TYPE 12

(A single blank card terminates input)

| CARD | COL | DATA | DESCRIPTION | NOTES |
|------|-------|------|---|-------|
| 1 | 1-5 | IEL | Element Number | (11) |
| | 6 | IOUT | Output Code (Blank or "N") | (12) |
| | 7-10 | MATL | Material Property Set Number | - |
| | 11-15 | ISEC | Section Property Number | (13) |
| | 16-20 | KGEN | Node Increment for Element Generation | (14) |
| | 21-25 | N(1) | Local Node Number 1 | (15) |
| | 26-30 | N(2) | Local Node Number 2 | - |
| | 31-35 | N(3) | Local Node Number 3 (Optional) | (16) |
| | 36-40 | N(4) | Auxiliary Node for Local Placement (Optional) | (17) |



RULES FOR LOCAL BEAM AXIS ORIENTATIONS

- Local X-axis is tangent to reference axis, proceeding from node 1 to node 2
- Local z'-axis is determined at any point on the reference axis by the following conventions:
 - (1) if node 4 is specified, z is oriented normal to the line connecting nodes 1 and 2, passing through node 4
 - (2) otherwise, the default z-axis orientation for the cross-section is used
 - (3) if neither of the above apply, the global Z axis is tried as the local z direction (followed by global X, then global Y).
- Local y is finally determined from $z' \otimes x$, and local z from $x \otimes y$

NOTES:

- (1) For beam elements, G may be specified independently of E , for the purpose of introducing shear correction factors, etc. Note that the value of G affects both the torsional behavior and the transverse shear deformation of the element.
- (2) Mass densities are specified per unit volume, in a Force-Length-Time system of units. For example, in British units, mass density is entered in $\text{lbf-sec}^2/\text{in}^4$.
- (3) Omit the yield stress as input if material nonlinearities are to be neglected. Default value set to 1.0×10^{12} .
- (4) $H(I)$ represents the strain-hardening slope of the material in the plastic range, $d\sigma/d\epsilon_p$. $H(I)$ may be determined from a bilinear representation of the material stress-strain curve (elastic modulus E , tangent modulus E_T) using the relation $H(I) = EE_T/(E - E_T)$. Isotropic strain hardening is assumed in all elastic-plastic materials with this element type.
- (5) The coefficient of thermal expansion may be input but is not used. Thermal stress analysis is currently not available with Element Type 12.
- (6) Section properties should be numbered from one through NSEC, and must be input in ascending order. Each Type 12 beam element is defined by its nodal connections, a material property reference, and reference to one of the section property definitions entered in this Section of input.
- (7) From one to four segments are permitted for each cross-section definition. Some typical cross-sections are shown in Figure 8.5.19.
- (8) All cross-section properties are defined in a local (y, z) coordinate system perpendicular to the beam axis. $ZD(1)$, $ZD(2)$, and $ZD(3)$ are components of a vector which defines the default local z -axis direction for elements in which the local directions are not specified elsewhere.

- (9) The size of each cross-section segment is defined by its width and depth in the local (y-z) system for an element. Each segment is rectangular, as shown in Figure 8.5.20. In nonlinear analysis, the segment definitions also determine the array of points used for stress storage and integration of beam internal forces (Figure 8.5.21.)
- (10) YOFF and ZOFF specify the distance of the centroid of a segment to the reference axis (through the nodes) of the beam. For a segment whose centroid coincides exactly with the nodes of the beam, YOFF and ZOFF are zero. Note that if NSEG > 1, YOFF or ZOFF will be nonzero for at least (NSEG - 1) segments.
- (11) Valid element numbers are 1, 2, ..., NELEM. Elements must be defined sequentially, but intermediate elements can be generated automatically (see Note 14, below). Card D-1 is repeated as needed to define all Type 12 elements in the model. Following the last element, a single blank card (setting IEL = 0) is entered to terminate input for Element Type 12.
- (12) The output code determines whether or not integration point stress output will be printed for element IEL. A blank field causes full printing for the element; on "N" in column 6 suppresses stress output.
- (13) Each element must reference one of the cross-section definitions entered in Section C. Note that offsets and local axis directions may be overridden by additional input on the element data cards.
- (14) A nonzero value of KGEN on the second card of a pair causes elements between the last and current elements to be generated automatically. With the exception of node numbers, all elements generated are assigned the same data as the current element. Local node numbers (if nonzero) for the previous element are incremented by KGEN to generate each succeeding element. Node numbers for the current element need not be given. More than one element must be generated to use this feature.
- (15) Local node numbering proceeds as shown in Figure 8.5.22.

- (16) The third local node (at mid-element) is optional and may be omitted. When node N(3) is not used, the element is straight and uses linear interpolation. When node N(3) is included, the element may be curved, and is based upon quadratic interpolation.
- (17) Node N(4) is an additional point used to determine the local axis directions of the beam element. The local (x,z) plane of the element is determined by nodes N(1), N(2), and N(4), as shown in Figure 8.5.20. and 8.5.22. In curved beam elements, node N(4) may be the same as node N(3); in this case, the local z-axis is located in the plane of the element, always perpendicular to the reference axis of the beam. If node N(4) is not specified, the default orientation of the cross-section is used, as input in Section C.

8.6 DATA FOR SURFACE CONTACT ANALYSIS

(Required for Nonlinear Analysis when IOPT(15)=1)

A. SIZING DATA

| CARD | COL | DATA | DESCRIPTION | NOTES |
|------|------|--------|--|-------|
| 1 | 1-5 | NSESET | Number of Surface Element Sets | (1) |
| | 6-10 | NSUREL | Total Number of Surface Elements to be Defined | - |

B. SURFACE ELEMENT SET LIMITS

- Repeat Card B-1 as required to define the last element in each surface element set (enter 16 values per line)

| CARD | COL | DATA | DESCRIPTION | NOTES |
|------|-------|-----------|------------------------|-------|
| 1 | 1-5 | IESET(1) | Last Element in Set 1 | (1) |
| | 6-10 | IESET(2) | Last Element in Set 2 | |
| | 11-15 | IESET(3) | Last Element in Set 3 | |
| | . | . | . | |
| | . | . | . | |
| | . | . | . | |
| | 76-80 | IESET(16) | Last Element in Set 16 | |

C. INTERACTION TABLE FOR SURFACE ELEMENT SETS

| CARD | COL | DATA | DESCRIPTION | NOTES |
|------|------|--------|---|-------|
| 1 | 1-5 | NENTRY | Number of Nonzero Entries in Interaction Table | (2) |
| 2 | 1-5 | ISLSET | Element Set for Slave Nodes | (3) |
| | 6-10 | IMSSET | Element Set for Master Surface Elements (>ISLSET) | (3) |

- Repeat Card C-2 as required to define all nonzero entries in the interaction table (i.e., NENTRY lines)

D. SURFACE ELEMENT DEFINITION DATA

| CARD | COL | DATA | DESCRIPTION | NOTES |
|------|-------|------|---------------------------------------|-------|
| 1 | 1-5 | IEL | Surface Element Number | (4) |
| | 6-10 | KGEN | Node Increment for Element Generation | (5) |
| | 11-15 | N(1) | Local Node Number 1 | (6) |
| | 16-20 | N(2) | Local Node Number 2 | |
| | 21-25 | N(3) | Local Node Number 3 | |
| | . | . | . | |
| | . | . | . | |
| | . | . | . | |
| | 51-55 | N(9) | Local Node Number 9 | |

- Repeat Card D-1 as required to define NSUREL Surface Elements.

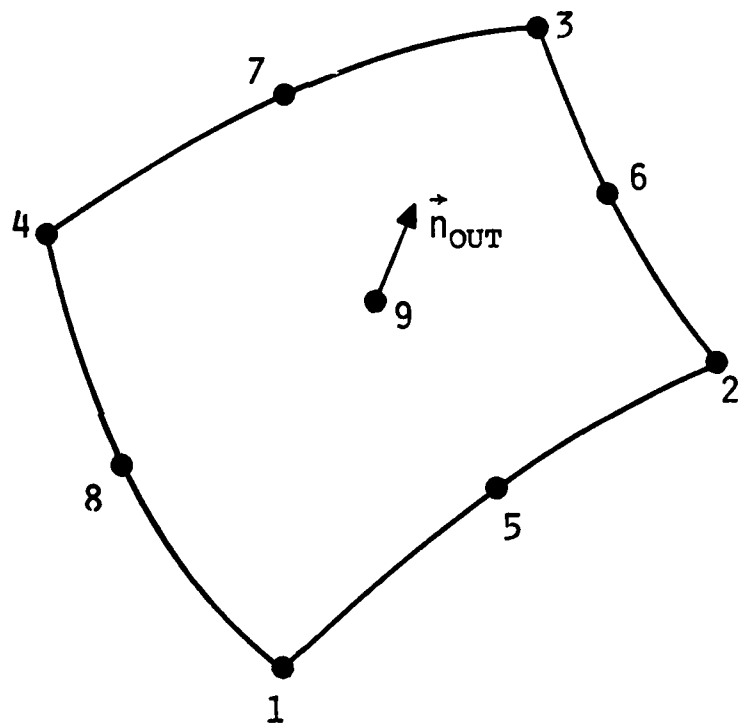


Figure 8.6.1. Connectivity for Variable-Node,
Three-Dimensional Contact Element

NOTES:

- (1) Surface Elements must be defined sequentially by sets; element sets are then used in Section C to define those combinations of elements which are to be examined for contact conditions. Elements 1, 2, ..., $IESET(1)$ belong to surface element set number 1, elements $IESET(1) + 1$ through $IESET(2)$ belong to Element Set 2, and so on. Thus, $IESET(I+1) > IESET(I)$ is always required, and $IESET(NSESET) = NSUREL$.
- (2) The interaction table defines combinations of surface element sets which are to be examined for possible contact. The maximum value of $NENTRY$ is $NSESET * (NSESET - 1) / 2$.
- (3) Each pair ($ISLSET, IMSSET$) defines a combination of surface element sets to be examined for possible contact at each step of the analysis. Each node of each element in set $ISLSET$ will be compared with every surface element in set $IMSSET$ to determine contact conditions. When contact is detected, constraints are applied to nodes in the slave node set to prevent motions which are not tangent to the surface element in $IMSSET$. Note that $ISLSET$ must always be less than $IMSSET$. Sets specified as slave node sets in one entry of the table may be assigned as master surface sets in subsequent entries, if required.
- (4) Card D-1 should be repeated as required to define all surface elements in the model. Elements need not be defined in sequential order; however, the highest-numbered element (element $NSUREL$) must be defined last. Input is finished when element $NSUREL$ has been defined.
- (5) A nonzero value of $KGEN$ on the second card of a pair causes intermediate elements to be generated by incrementing each nonzero node of the previous element by $KGEN$.
- (6) Local node point numbering for surface contact elements is shown in Figure 8.6.1. Nodes $N(1)$ through $N(4)$ are always required for each surface element. Each of the local nodes $N(5)$ through $N(9)$ are optional, and the absence or presence of each node is automatically taken into account in the program. Generally, the number of nodes used in a particular element will be the same as that on the corresponding surface of the structural finite element at the same location.

8.7 BOUNDARY CONDITIONS

(Required)

Boundary conditions can be supplied to the program in three ways*:

1. Constraint of a specified range of nodes (with specified increment) in selected nodal components. Used for homogeneous constraints (zero displacement) only.
2. Constraint of selected nodal components for a list of nodes. Used for homogeneous constraints only.
3. Linear, multivariable constraints between global displacement variables.

A. BOUNDARY CONDITION INPUT CONTROL DATA

| CARD | COL | DATA | DESCRIPTION | NOTES |
|------|-------|------|--|-------|
| 1 | 1-5 | NBC1 | Number of Type 1 Constraints | - |
| | 6-10 | NBC2 | Number of Type 2 Constraints | - |
| | 11-15 | - | (Blank) | - |
| | 16-20 | NLCC | Number of Linear Constraint Conditions | - |
| | 21-25 | MLCT | Maximum Number of Terms in a Single Linear Constraint Equation | - |

*Note that nonzero prescribed displacements may also be specified, as part of the nodal point force data in Section 8.10.

B. TYPE 1 CONSTRAINT DATA

(Range of nodes constrained in specified components)

- Omit this section if NBC1 = 0.

- Repeat cards 1 and 2 as required (NBC1 times).

| CARD | COL | DATA | DESCRIPTION | NOTES |
|------|-------|--------|------------------------------------|----------|
| 1 | 1-5 | N1 | Beginning Node Number | (1) |
| | 6-10 | N2 | Ending Node Number | - |
| | 11-15 | INCR | Node Number Increment | - |
| 2 | 1-5 | JD(1) | First Nodal Component Constrained | (1), (2) |
| | 6-10 | JD(2) | Second Nodal Component Constrained | - |
| | : | : | : | : |
| | : | : | : | : |
| | 46-50 | JD(10) | Tenth Nodal Component Constrained | - |

C. TYPE 2 CONSTRAINT DATA

(Specified Components Constrained at List of Nodes)

- Omit this Section if NBC2 = 0.

- Repeat cards 1 and 2 as required (NBC2 times).

| CARD | COL | DATA | DESCRIPTION | NOTES |
|------|-------|--------|------------------------------------|-------|
| 1 | 1-5 | JD(1) | First Nodal Component Constrained | (3) |
| | 6-10 | JD(2) | Second Nodal Component Constrained | - |
| | : | : | : | : |
| | : | : | : | : |
| | 46-50 | JD(10) | Tenth Nodal Component Constrained | - |
| 2 | 1-5 | ND(1) | First Node Constrained | (3) |
| | 6-10 | ND(2) | Second Node Constrained | - |
| | : | : | : | : |
| | : | : | : | : |
| | 46-50 | ND(10) | Tenth Node Constrained | - |

NOTES:

- (1) Nodes $N1$, $N1 + INCR$, $N1 + 2*INCR$, ..., $N2$ are constrained in nodal components $JD(1)$ through $JD(10)$. Note that the meaning of the nodal component numbers $JD(I)$ depends upon the solution variable set used (see Section 8.2, SOLUTION OPTIONS AND CONTROL PARAMETERS). For example, with $IOPT(1) = 1$, the Cartesian displacement components are $U = 1$, $V = 2$, $W = 3$. When $IOPT(1) = 2$, rotational freedoms are numbered $\theta_x = 4$, $\theta_y = 5$, $\theta_z = 6$.
- (2) IMPORTANT: When $IOPT(1) = 2$ (rotational degrees of freedom permitted), all rotations at nodes not connected to elements which use rotational degrees of freedom are automatically suppressed. For example, if both beam (Type 12) and solid (e.g., Type 8) elements are used in the model, rotational degrees of freedom will be activated only for nodes connected to the beam elements.
- (3) Each of the nodes $ND(1)$ are constrained in the specified components $JD(J)$; some of the $ND(I)$ and $JD(J)$ may be zero.

8.8 LINEAR CONSTRAINT DATA

(Optional for all analysis types)

Data entered in this section enforces linear constraint relationships between global degrees of freedom (e.g., to enforce skewed boundary conditions or rigid links within the model). The total number of constraints of this type, including both input and generated constraint equations, is defined in Section 8.7 (NLCC).

| CARD | COL | DATA | DESCRIPTION | NOTES |
|------|-------|--------|--|-------|
| 1 | 1-5 | NTERM | Number of Terms in the Current Constraint Equation | - |
| | 6-10 | NUMC | Number of Constraints to be Generated | (1) |
| | 11-15 | KGEN | Node Number Increment for Constraint Generation | (1) |
| 2 | 1-5 | NOD(1) | Node Number | (2) |
| | 6-10 | IC(1) | Direction | (2) |
| | 11-20 | XM(1) | Multiplier | (2) |
| | 21-25 | NOD(2) | Node Number | - |
| | 26-30 | IC(2) | Direction | |
| | 31-40 | XM(2) | Multiplier | |
| | . | . | . | |
| | . | . | . | |
| | . | . | . | |
| | 61-65 | NOD(4) | Node Number | |
| | 66-70 | IC(4) | Direction | |
| | 71-80 | XM(4) | Multiplier | |

- For each constraint, Card 2 is repeated as required to define all terms in the equation (four terms/card).
- Repeat Cards 1,2 until NLCC constraints have been defined.

NOTES:

- (1) The values NUMC and KGEN can be used to generate a series of linear constraints, when the number of terms, the nodal components, and multipliers are identical. NUMC constraints will be generated (including the one input), by incrementing each of the node numbers involved in the constraint by KGEN each time. IF NUMC = 0, only the input constraint is generated; if NUMC.GT.0 and KGEN = 0, KGEN is assigned a default value of one.
- (2) The node number NOD(I), and direction IC(I) = 1,2,3, and multiplier XM(I) define a single term of the linear constraint. The form of the constraint equation is then

$$\sum_{I=1}^{NTERM} XM(I) * U(I)$$

where U(I) is the global displacement degree of freedom defined at node NOD(I) in direction IC(I). Displacement degrees of freedom which appear in linear constraint equations must not be otherwise constrained.

8.9 DATA CURVES FOR NONLINEAR AND/OR DYNAMIC ANALYSIS

(Required for all nonlinear analyses and all transient dynamic analyses)

This section permits input of:

- Loading curves for nonlinear static analysis;
- Time-dependent loading functions for transient analysis;
- Time histories of prescribed nodal displacements;
- Uniaxial stress-strain data for elastic-plastic materials, in the form of equivalent stress versus plastic strain; and
- Temperature time-history data for thermal stress analysis.

Cards 2 through 7 below are repeated as required to define all data curves to be used in the analysis.

| CARD | COL | DATA | DESCRIPTION | NOTES |
|------|-------|-------|--|-------|
| 1 | 1-5 | NCURV | Number of Data Curves to be Defined | (1) |
| 2 | 1-5 | NC | Data Curve Identification Number | (2) |
| | 6-10 | NPT | Number of Point Pairs [X(I),Y(I)] Used to Define the Curve | (3) |
| | 11-80 | HED | Optional Alphanumeric Title | |
| 3 | 1-10 | X(1) | Abcissa for First Data Point | - |
| | 11-20 | Y(1) | Ordinate for First Data Point | - |
| | . | . | . | . |
| | . | . | . | . |
| | . | . | . | . |
| | 61-70 | X(4) | Abcissa for Fourth Data Point | - |
| 4-7 | 71-80 | Y(4) | Ordinate for Fourth Data Point | |
| | 1-80 | | Additional Pairs [X(I),Y(I)] as shown for Card 3 | (4) |

NOTES:

- (1) *Maximum number of data curves is fifty.*
- (2) *Data curves need not be numbered sequentially, but identification numbers must be between 1 and 50.*
- (3) *A maximum of twenty data points is permitted to define each curve.*
- (4) *Cards 4-7 are supplied only as needed to define all points on the curve. Unneeded cards should be omitted.*

8.10 EXTERNAL LOADS

(Required for all Static and Transient Dynamic Analyses)

External forces acting on the finite element model may be of two types:

- Concentrated forces (or imposed displacements) at nodal points, and
- Distributed volumetric or surface forces applied to selected elements.

These external forces are entered as data in Sections 8.10.1 (nodal loads), and 8.10.2 and 8.10.3 (distributed loads).

NOTE: Data must be entered in this Section for all static, harmonic, and transient dynamic analyses. The number of loading conditions (Section 8.10.1A) is always required in linear static analysis; if no nodal forces are to be prescribed in Section 8.10.1B or 8.10.1C, a single blank line should be entered to terminate nodal force input.

8.10.1 Concentrated Nodal Forces and Prescribed Displacements

- For all linear static and steady-state harmonic analyses, enter data from Section A and B below.
- For all nonlinear and/or transient dynamic analyses enter data from Section C below.

A. NUMBER OF LOADING CONDITIONS (LINEAR STATIC AND STEADY-STATE HARMONIC SOLUTIONS)

| CARD | COL | DATA | DESCRIPTION | NOTES |
|------|-----|------|------------------------------|-------|
| 1 | 1-5 | NLC | Number of Loading Conditions | (1) |

B. NODAL FORCES AND PRESCRIBED DISPLACEMENTS (LINEAR STATIC AND STEADY-STATE HARMONIC ANALYSIS)

- Repeat Card 1 as required to define all nodal loads and imposed displacements
- Input from this block is terminated with a single blank card. If no nodal forces are to be prescribed, enter a single blank card to terminate input.

| CARD | COL | DATA | DESCRIPTION | NOTES |
|------|-------|-------|---|-------|
| 1 | 1 | ITYPE | " " (Nodal Force) or "D" (Nodal Displacement) | (2) |
| | 2-5 | ICASE | Load Case Number (1-NLC) | - |
| | 6-10 | NØDE | Node Number at which Load is Applied (1=FX,2=FY,3=FZ,4=MX,5=MY,6=MZ) | - |
| | 11-15 | IDIR | Nodal Component Number | - |
| | 16-25 | P | Load or Displacement Magnitude | - |

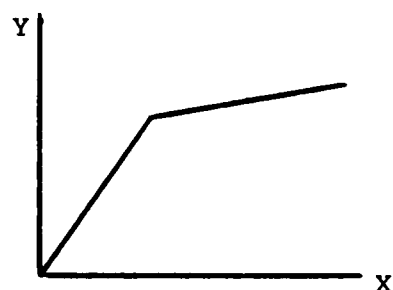
C. INCREMENTAL NODAL LOADS AND PRESCRIBED DISPLACEMENT DATA (NONLINEAR AND/OR TRANSIENT DYNAMIC ANALYSIS)

- Repeat Card 1 below as required
- Loads input is terminated with a single blank card. If no nodal forces are to be prescribed, enter a single blank card to terminate input.

| CARD | COL | DATA | DESCRIPTION | NOTES |
|------|-------|-------|---|-------|
| 1 | 1 | ITYPE | " " (Nodal Force) or "D" (Nodal Displacement) | (2) |
| | 2-5 | NODE | Node Point at which Load is Applied | - |
| | 6-10 | IC | Nodal Point Component in Direction of Load (1=FX,2=FY,3=FZ,4=MX,5=MY,6=MZ) | - |
| | 11-15 | NCURV | Identification Number of Data Curve Describing the Time Variation of the Load or Displacement | (3) |
| | 16-25 | SCALE | Scale Factor | (3) |

NOTES:

- (1) *The number of load cases is limited only by the available storage. In steady-state harmonic solutions, only one case is permitted (NLC = 1).*
- (2) *A blank field in column 1 (ITYPE) indicates that the input record describes an applied nodal force. For ITYPE = "D", the current input line defines a prescribed displacement at the node.*
- (3) *In nonlinear and transient dynamic analyses, all loads must be defined using DATA CURVE input (Section 8.9) to indicate dependence of the load upon time or load parameter. At each increment of the solution, data curve NCURV is interpolated at the current value of time to determine the total applied load at a particular node. Interpolated values are multiplied by SCALE and accumulated into the total loads vector. An example of the calculation of incremental loads data is shown in Figure 8.10.1. Prescribed displacements (ITYPE = "D") are interpolated and scaled in exactly the same way as nodal forces.*



DATA CURVE INPUT

$X(1)=0.$ $Y(1)=0.$
 $X(2)=2.$ $Y(2)=1000.$
 $X(3)=5.$ $Y(3)=1300.$

NODAL POINT LOADS INPUT

| <u>NODE</u> | <u>IC</u> | <u>SCALE</u> |
|-------------|-----------|--------------|
| 20 | 2 | 1.00 |
| 32 | 3 | 2.00 |
| 56 | 3 | 2.00 |

RESULTING NODAL FORCES VERSUS TIME

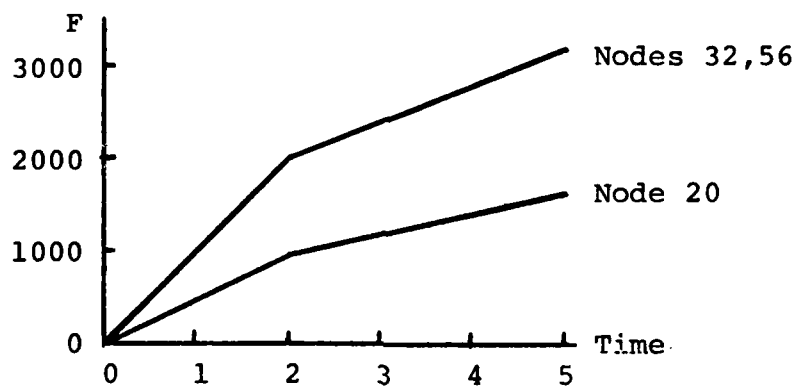


Figure 8.10.1. Example of Incremental Load Definition

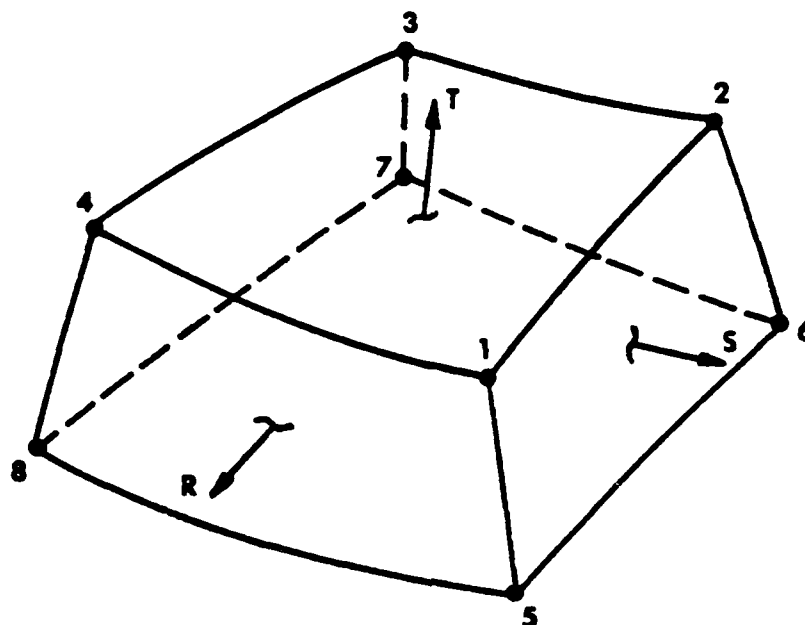
8.10.2 Distributed Element Forces

- Repeat Card 1 below as required to define all element surface pressures.
- Input in this block is terminated with a single blank card.

| CARD | COL | DATA | DESCRIPTION | NOTES |
|------|-------|--------|---|-------|
| 1 | 1-5 | IETYPE | Element Type Number | (1) |
| | 6-10 | IBEGIN | First Element to which Pressure is Applied | (2) |
| | 11-15 | IEND | Last Element to which Pressure is Applied (Default = IBEGIN) | (2) |
| | 16-20 | INCR | Element Number Increment (Default = 1) | (2) |
| | 21-25 | LTYPE | Loading Type and Direction Code | (3) |
| | 26-30 | ILIVE | Live Loads Flag =0: Dead Loading =1: Live Loading | (4) |
| | 31-35 | ICASE | Load Case Number (for Linear Static Analysis) or Data Curve Identification Number (Nonlinear and/or Dynamic Analysis) | (5) |
| | 36-45 | P | Load Magnitude (all loading types except centrifugal) | (6) |

TABLE 8.10.1
LOADING TYPE AND DIRECTION CODES (LTYPE)

| ELEMENT TYPE (I E T Y P E) | | | | | |
|----------------------------|----------------------|----------------------|--------------------------|----------------------|----------------------|
| LTYPE VALUE | 4 (TRUSS) | 3 or 9 (PLANAR) | 1, 2, 6, 7, 8 (SOLID) | 5 or 11 (SHELL) | 10 (AXISYM) |
| -1 | Body Force X | Body Force X | Body Force X | Body Force X | Body Force X |
| -2 | Body Force Y | Body Force Y | Body Force Y | Body Force Y | Body Force Y |
| -3 | Body Force Z | Body Force Z | Body Force Z | Body Force Z | N.A. |
| -4 | Centrifugal Force | Centrifugal Force | Centrifugal Force | Centrifugal Force | Centrifugal Force |
| 1 | N.A. | Line Load Edge 1 | Pressure Face 1 | Pressure Face 1 | Pressure Face 1 |
| 2 | N.A. | Line Load Edge 2 | Pressure Face 2 | Pressure Face 2 | Pressure Face 2 |
| 3 | N.A. | Line Load Edge 3 | Pressure Face 3 | Pressure Face 3 | Pressure Face 3 |
| 4 | N.A. | Line Load Edge 4 | Pressure Face 4 | Pressure Face 4 | Pressure Face 4 |
| 5 | N.A. | N.A. | Pressure Face 5 | Pressure Face 5 | N.A. |
| 6 | N.A. | N.A. | Pressure Face 6 | Pressure Face 6 | N.A. |



| SURFACE | LOCATION | CORNER NODES |
|---------|----------|---------------|
| 1 | $R = -1$ | 2 - 3 - 7 - 6 |
| 2 | $S = -1$ | 3 - 4 - 8 - 7 |
| 3 | $T = -1$ | 5 - 6 - 7 - 8 |
| 4 | $R = +1$ | 1 - 4 - 8 - 5 |
| 5 | $S = +1$ | 1 - 5 - 6 - 2 |
| 6 | $T = +1$ | 1 - 2 - 3 - 4 |

(ALL PRESSURES ARE POSITIVE OUTWARD)

Figure 8.10.2. Reference Surface Numbers for Pressure Loading on Three-Dimensional Solid and Shell Elements.

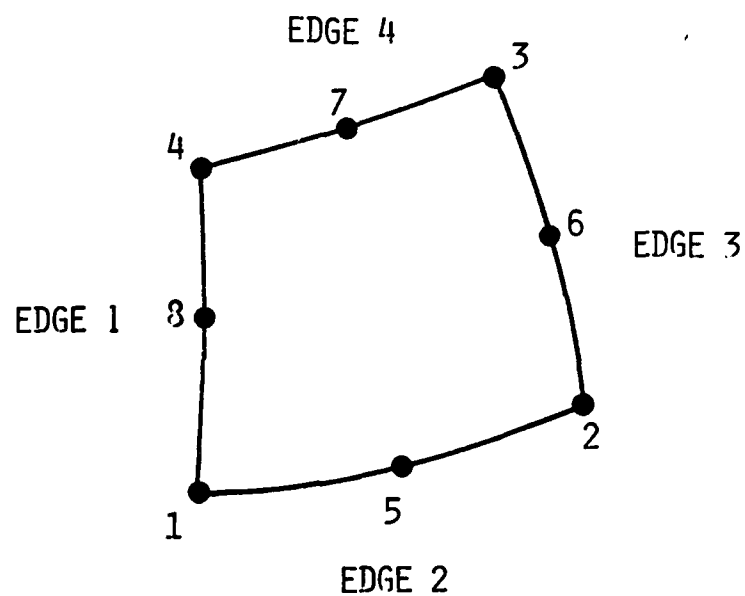


Figure 8.10.3 Edge Numbering for Two-Dimensional and Axisymmetric Distributed Loads.

NOTES:

- (1) The types of distributed loading which are valid for each element type are summarized in Table 8.10.1. Elements and element types may be listed in any order in this data block.
- (2) The specified loading is applied to elements IBEGIN, IBEGIN + INCR, ..., IEND. Element numbers on successive data cards need not be entered in any specific order, and element numbers may be repeated (e.g., when pressures act on more than one surface of an element).
- (3) Loading type and direction codes are summarized in Table 8.10.1. Surface and edge numbering for distributed loading are shown in Figures 8.10.2 and 8.10.3.
- (4) "Dead" loads (ILIVE = 0) are independent of the deformation of the element, and therefore are defined with reference to the undeformed element geometry. "Live" loads (ILIVE = 1) always act in the direction normal to the current element surface (as follower forces), and are defined as the force per unit deformed surface area, length or volume. Live loads are permitted only in nonlinear analysis (static or dynamic).
- (5) In linear static analysis, ICASE is interpreted as a loading condition number (the total number of load conditions, NLC, is defined in Section 8.10.1-A). For nonlinear or transient dynamic analysis types, ICASE is the number of the user-defined data curve which describes the time variation of this load. Data curves are defined in Section 8.9. In steady-state harmonic analysis, ICASE is not used.
- (6) Positive values of P define surface forces directed outward from the surface or edge in question. For linear static or harmonic analysis, P is simply the load magnitude; in nonlinear/dynamic solutions, the time-dependent function defined by data curve ICASE (see Note 5) is multiplied by P to obtain the loading value at any given time. This entry is ignored if LTYPE = -4 (centrifugal loading). If rotational body forces are to be generated, the axis of rotation and rotational speed must be defined in Section 8.10.3.

8.10.3 Centrifugal Loading Data

(Required for all analyses in which body forces due to rotation are included.)

| CARD | COL | DATA | DESCRIPTION | NOTES |
|------|-------|----------|--|-------|
| 1 | 1-10 | REFPT(1) | X-Coordinate of Reference Point on Axis of Rotation | (1) |
| | 11-20 | REFPT(2) | Y-Coordinate of Reference Point on Axis of Rotation | (1) |
| | 21-30 | REFPT(3) | Z-Coordinate of Reference Point on Axis of Rotation | (1) |
| | 31-40 | AXDIR(1) | X Component of Direction of Rotational Axis | (1) |
| | 41-50 | AXDIR(2) | Y Component of Direction of Rotational Axis | (1) |
| | 51-60 | AXDIR(3) | Z Component of Direction of Rotational Axis | (1) |
| | 61-70 | ØMEGA | Rotational Speed (or Scale Factor) | (2) |
| | 71-75 | ICURV | Data Curve Describing Time Variation of Rotational Speed | (2) |

NOTES:

- (1) The axis of rotation is defined by specifying the coordinates of an arbitrary point lying on the axis, and a vector describing the axis direction. REFPT(1)-(3) define the coordinates of the point, and AXDIR(1)-(3) the axis direction. The vector defined by AXDIR need not be normalized, but must have magnitude greater than zero. The rotational axis so defined will be used to generate centrifugal loading for all element loads having LTYPE = -4 in Section 8.10.2.
- (2) In linear static analysis, ØMEGA gives the rotational speed, while ICURV is unimportant. For nonlinear and/or dynamic analysis, ØMEGA is used as a scale factor; the function value interpolated from data curve ICURV at any time will be multiplied by ØMEGA to obtain the rotational velocity at that time. In both cases, the body force per unit volume is $\rho \omega^2 r$, where r is the perpendicular distance of a point from the axis of rotation. NOTE THAT ØMEGA MUST BE DEFINED WITH UNITS OF (RADIAN/UNIT TIME); e.g., a rotational speed of 100 cycles/sec would be specified by setting ØMEGA=200 π =628.31853.

8.11 HARMONIC FORCING FREQUENCIES

(Required *only* for steady-state harmonic solution)

- Repeat Card 1 as required (10 values/card) to define all forcing frequencies.
- NFREQ frequency values are required, as specified in Section 8.3.5.

| CARD | COL | DATA | DESCRIPTION | NOTES |
|------|-------|---------|-----------------------------|-------|
| 1 | 1-8 | FRQ(1) | Excitation Frequency No. 1 | (1) |
| | 9-16 | FRQ(2) | Excitation Frequency No. 2 | - |
| | . | . | . | - |
| | . | . | . | - |
| | . | . | . | - |
| | 73-80 | FRQ(10) | Excitation Frequency No. 10 | - |

NOTES:

- (1) The frequency values entered in this Section apply to all external forces given as data in Section 8.9. The form of the applied forces is $F = F_0 e^{i\omega t}$, where F_0 is defined by the nodal and element forces defined previously. Frequency values have units of cycles per unit time (cycles = radians/ 2π).

CHAPTER 9

USER SUBROUTINES

A number of user interfaces are provided in the MAGNA program for increased flexibility in modeling capabilities and data preparation. Most of these user interfaces are implemented in the form of user-supplied subroutines which permit the generation of data or user intervention at convenient points in the analysis. User-written subroutines are currently available for:

- generation of nodal coordinate data,
- transformations from user-defined coordinate systems,
- specifications of incremental nodal loads in nonlinear and/or dynamic analyses,
- definition of variable surface pressure loading,
- definition of initial velocity conditions in dynamic analysis,
- generation of nodal temperature distributions,
- specification of output parameters,
- definition of various nonlinear and anisotropic material models, and
- specification of damping properties for harmonic analysis.

A small COMMON area, labeled/USERC/, is also provided in the program for storing data which must be used repeatedly by user-written subroutines. An example of the use of this block for storing nodal degrees-of-freedom numbers appears in Section 9.3.

9.1 MESHG (GENERATE COORDINATES)

Coordinate data may optionally be generated or read in the user-supplied subroutine MESHG. This feature is useful in generating node point data for models with regular geometry, or in reading geometry data in non-standard card formats.

MESHG has the form:

```
SUBROUTINE MESHG (NØDES,NWØRK,MGEN,NTIN)

.
.
.

(code to read or generate coordinates)

.
.

RETURN

END
```

in which the formal parameters are:

NØDES = number of node points
NWØRK = (internal parameter)
MGEN = integer value input on CØØRDINATES card
NTIN = input file number

Whenever subroutine MESHG is supplied by the user, only the CØØRDINATES header card is read in the nodal point input section of the program. Additional input data required by the user-written routine MESHG can be inserted in the input stream in place of the usual nodal coordinate data. For example, nodal point coordinates prepared for other programs can be entered directly by supplying the proper READ directives in subroutine MESHG.

For each node whose coordinates are to be defined in MESHG, it is necessary to call the internal routine USRNOD, which places

the coordinate data in the proper storage area. Calls to USRNOD have the form

```
CALL USRNOD (NODE,X,Y,Z)
```

where

NODE = node point number, and

X,Y,Z = Cartesian coordinates.

Example 9.1-1

The simple MESHG routine shown below accepts as data a FORTRAN format specification, and then reads the coordinate data for each node in that format from the input data stream.

```
SUBROUTINE MESHG (NØDES,NWØRK,MGEN,NTIN)
  DIMENSION IFMT(20)
1  FORMAT (20A4)
  READ (NTIN,1) IFMT
  DØ 2 I = 1,NØDES
    READ (NTIN,IFMT) INØDE,X,Y,Z
    CALL USRNØD (INØDE,X,Y,Z)
2  CONTINUE
  RETURN
END
```

9.2 CTYPE (COORDINATE TRANSFORMATIONS)

User-defined coordinate systems can be defined in subroutine CTYPE to facilitate input data preparation. The form of this routine is as follows:

```
      SUBROUTINE CTYPE (ITYPE,X1,X2,X3)
      GØ TØ (1,2,3,4,5),ITYPE
1  CONTINUE
      .
      .
      .
      (coordinate system transformation, Type 1)
      .
      .
      .
      RETURN
2  CONTINUE
      .
      .
      .
      (coordinate system transformation, Type 2)
      .
      .
      .
      RETURN
      .
      .
      .
      (etc.)
      .
      .
      .
      END
```

Formal parameters are:

ITYPE = coordinate system type

X_i = on input, the i^{th} component in system ITYPE
on output, the i^{th} Cartesian component

The default version of CTYPE included in the program includes two default transformation types, (1) cylindrical, and (2) spherical, described in the table below.

| | | <u>Cylindrical</u> | <u>Spherical</u> |
|--------------|---|--------------------|---------------------------|
| ITYPE | = | 1 | 2 |
| Input X_i | = | R, θ, Z | R, ϕ, θ |
| Output X_i | = | X, Y, Z | X, Y, Z |
| X | = | $R \cos \theta$ | $R \sin \phi \cos \theta$ |
| Y | = | $R \sin \theta$ | $R \sin \phi \sin \theta$ |
| Z | = | Z | $R \cos \phi$ |

In the nodal coordinates input (Section 8.4), the value of ISYS (A,B,C,D,E or blank) determines which of the coordinate transformations in CTYPE is performed for a given node. If ISYS = blank, CTYPE is not called; when ISYS = A, CTYPE is called with ITYPE = 1; ISYS = B implies ITYPE = 2; etc.

9.3 ULØAD, USRLØD (INCREMENTAL LOADS)

In the incremental analysis of nonlinear and/or dynamic problems, it is often necessary to specify external loads whose magnitude or direction depends upon the deformed shape of a structure (or its rate of change). Typical examples include follower forces, structure-media interaction forces, and loading due to ballistic or soft-body impact on a structure. The user-written subroutine ULØAD (and, optionally, USRLØD) permits the introduction of any type of incremental loading into the analysis, including forces which may depend upon the current displacements or velocities.

The form of subroutine ULØAD is as follows:

```
SUBROUTINE ULØAD(P,WØRK,TIME,DT,
+             NTNØDV,NRDØF,NRCØDE,
+             NTDIS ,NRU  ,NRV  ,NIN,NØUT)
DIMENSION P(1),WØRK(1)
CØMMØN/MPART/N,IFILL(3),NWØRK
CØMMØN/DØF/NFVAR,NDPVPN,NDPN,MAXKØD
CØMMØN/VCARAY/LIST(20)
CØMMØN/CTRL/NØDES
.
.
.
(code to generate incremental loads)
.
.
.
RETURN
END
```

The form of subroutine USRLØD is arbitrary, since only ULØAD is called directly from MAGNA.

Formal parameters used in the subroutine to call ULØAD are defined as:

P = current vector of consistent nodal loads. The array dimension of P is N words, where N is in /MPART/. The array contains *total* force values to be applied in the next increment; values defined in ULØAD are to be added to the contents of P.

WORK = working vector available for use in ULØAD. The array dimension of WØRK is (NWORK-N), where N and NWØRK are contained in /MPART/. In most cases, the number of words in the array will be equal to the number of words of storage allocated in COMMON/BLANK/ (see Chapter 7), less the number of active degrees of freedom in the finite element model.

TIME = Current value of time, or load parameter.

DT = Time (or load parameter) increment.

NTNØDV = Device number of random-access file containing nodal degree-of-freedom tables.

NRDØF,NRCØDE = Random file record numbers at which nodal degree-of-freedom tables are stored.

NTDIS = Device number of random-access file containing current values of nodal displacements and velocities.

NRU = Record number for nodal displacements.

NRV = Record number for nodal velocities.

NIN = Input file number.

NØUT = Output file number.

Definitions of pertinent variables stored in labeled CØMMØN are:

1. CØMMØN /MPART/

N = number of active nodal degrees of freedom.

NWORK = number of words of array storage currently available in core. (NWØRK-N) gives the amount of array space available to the user in the vector WØRK.

2. `COMMON /DOF/`

NFVAR = number of field variables in the problem.
NDPVPN = number of nodal degrees of freedom (maximum)
per field variable.
NDPN = total number of degrees of freedom per node.
MAXKOD = parameter used in unpacking nodal degree of
freedom lists (see examples below).

3. `COMMON /VCARAY/`

LIST = integer array used to store degree-of-freedom
table for a particular node in unpacked form
(see example below).

4. `COMMON /CTRL/`

NODES = number of node points defined in the finite
element model.

The contents of the last three `COMMON` blocks will normally not be used in `ULOAD` unless the global degree of freedom number corresponding to a certain component of displacement at a node is unknown at the beginning of the analysis. If the degree of freedom of the model to which a user-defined load is to be applied is known (from a previous analysis, for example), the load may be applied directly, as shown in the following example.

Example 9.3-1

Consider a finite element model in which a follower force is to be directed at a particular nodal point (see Figure 9.3.1). The direction of the force is determined approximately by a vector from node A to node B. For simplicity, both nodes are assumed to remain on the X-Y plane at all times, so that the orientation of the force is a function of displacements U,V at both nodes.

Original coordinates of A and B are:

| Node | X ₀ | Y ₀ | Z ₀ |
|------|----------------|----------------|----------------|
| A | 10. | 1. | 0. |
| B | 10. | 0. | 0. |

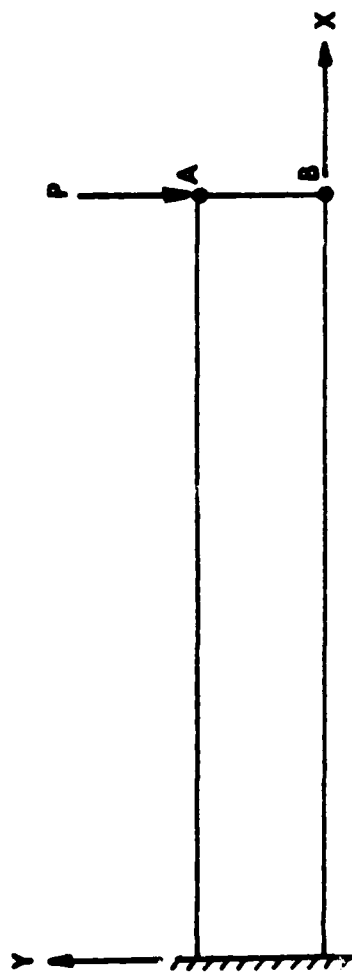


Figure 9.3.1 Finite Element Model for ULOAD Follower Force Example.

The relevant degrees of freedom, from a previous linear analysis, are known to be:

| <u>Node</u> | <u>Displacement</u> | <u>D.O.F. Number</u> |
|-------------|---------------------|----------------------|
| A | U_A | 20 |
| A | V_A | 21 |
| B | U_B | 31 |
| B | V_B | 32 |

The unit vector from A to B in the current position is, therefore, given by

$$n = \frac{(U_B - U_A) \hat{i} + (V_B - V_A - 1) \hat{j}}{\sqrt{(U_B - U_A)^2 + (V_B - V_A - 1)^2}} = n_x \hat{i} + n_y \hat{j},$$

and the components of force applied at node A will be

$$P_x = P n_x$$

$$P_y = P n_y$$

where P is the magnitude of the force. A version of ULØAD which demonstrates the retrieval of the current displacements and generates the current load is shown below.

```
SUBROUTINE ULØAD (P,WK,TIME,DT,NTNØDV,NRDØF,NRCØDE,NTDIS,
                  NRU,NRV,NIN,NØUT
```

```
  DIMENSION P(1),WK(1)
```

```
  COMMON /MPART/ N,IFILL(3),NWØRK
```

C

C

```
  EX. 9.3-1 : FØLLØWER FØRCE DIRECTED FRØM NØDE A TO B
```

C

C

```
  NØTE: ARRAY WK IS USED TØ STØRE CURRENT DISPLACEMENTS.
```

C

```
  DATA NUA,NVA,NUB,NVB/20,21,31,32/
```

```
  PTØTAL=100.0
```



```

C
C   CURRENT DISPLACEMENTS OBTAINED FROM RANDOM FILE
C   "NTDIS" AT RECORD "NRU".  NO. OF WORDS = "N".
C
C   CALL READMF (NTDIS,WK,N,NRU)
C
C   DISPLACEMENTS AT A,B,
C
C   UA = WK(NUA)
C   VA = WK(NVA)
C   UB = WK(NUB)
C   VB = WK(NVB)
C
C   UNIT VECTOR
C
C   XN = UB-UA
C   YN = VB-VA-1.0
C   C = SQRT(XN**2+ YN**2)
C   XN = XN/C
C   YN = YN/C
C
C   ADD LOADS TO VECTOR "P"
C
C   P(NUA) = P(NUA) + PTOTAL*XN
C   P(NVA) = P(NVA) + PTOTAL*YN
C
C   WRITE LOADS TO PRINTED OUTPUT FILE
C
C   WRITE (NOUT,100) TIME,P(NUA),P(NVA)
C   RETURN
100  FORMAT(/10X,26HLLOADS AT NODE A FOR TIME =,E15.8,
+       /10X,11HX-DIRECTION , E15.8,
+       /10X,11HY-DIRECTION , E15.8 )
C   END

```

In the example, current values of the nodal displacements are retrieved from record NRU of file NTDIS and stored in WK. In a dynamic problem, the corresponding velocities are stored at record NRV, so that velocity-dependent loadings could be specified as well. Note that the loads specified in ULØAD are current values of the *total* loads at the specified degrees of freedom; the *incremental* application of nodal loads is automatically accounted for elsewhere in the program.

In some cases, degree-of-freedom numbers for displacements at which incremental loads are to be generated are not known in advance and must be retrieved using data generated during the analysis. To accomplish this, the subroutine ULØAD is used to assign array storage for a second routine, USRLØD, so that workspace may be used for both real and integer variables. Example 9.3-2 illustrates this procedure.

Example 9.3-2

Figure 9.3.2 shows a structure supported by a series of discrete, nonlinear spring elements whose elastic response follows the load-deflection equation

$$F = k_0 w + k_1 w^3 ,$$

where w is the total extension. The nonlinear springs are applied at nodes 2,4,6,...,20 in the vertical (Z) direction; the corresponding nodal degree-of-freedom numbers are not known a priori. User subroutines ULØAD and USRLØD, listed below, are used to apply the proper forces at each node supported by a nonlinear spring.

```

SUBROUTINE ULØAD (P,WK,TIME,DT,NTNØDV,NRDØF,NRCØDE,NTDIS,
+
+               NRU,NRV,NIN,NØUT)
DIMENSION P(1),WK(1)
COMMON /MPART/N,IFILL(3),NWØRK
COMMON /CTRL /NØDES
C
C   EX. 9.3-2 : NØNLINEAR SPRING FØRCES

```

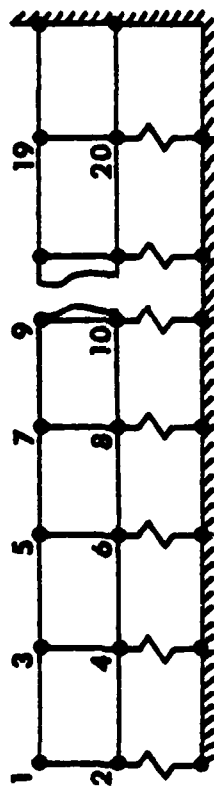


Figure 9.3.3.2 Beam Supported by Nonlinear Spring Elements.

```

C      ULØAD USED TØ SET UP ARRAYS FØR USRLØD
C
C      THREE ARRAYS (BESIDES P) ARE REQUIRED:
C
C      A. TWØ INTEGER ARRAYS, EACH OF LENGTH "NØDES" TØ
C          STØRE NØDAL D.Ø.F. TABLES
C
C      B. ØNE REAL ARRAY ØF LENGTH "N" FØR DISPLACEMENTS
C
C      N1 = START ØF ARRAY NDØF
C      N2 = START ØF ARRAY KØDE
C      N3 = START ØF ARRAY DISP
C      N4 = END ØF ARRAY DISP
C
      N1 = 1
      N2 = N1+NØDES
      N3 = N2+NØDES
      N4 = N3+N-1
      IF (N4.LE.(NWØRK-N)) GØ TØ 10
          NW = NWØRK-N
          WRITE (NØUT,100) N4,NW
100     FØRMAT (/10X,27HNØT ENØUGH STØRAGE IN ULØAD,
+          /10X,4HN4 =, I8,5X,4HNR =, I8)
      STOP
10     CALL USRLØD (P,WK(N1),WK(N2),WK(N3),TIME,DT,NTNØDV,
+          NRDØF,NRCØDE,NTDIS,NRU,NRV,NIN,NØUT)
      RETURN
      END
      SUBROUTINE USRLØD (P,NDØF,KØDE,DISP,TIME,DT,NTNØDV,
+          NRDØF,NRCØDE,NTDIS,NRU,NRV,NIN,NØUT)
      DIMENSION P(1),NDØF(1),KØDE(1),DISP(1)
      CØMMØN/MPART/N
      CØMMØN/DØF/NFVAR,NDPVPN,NDPN,MAXKØD
      CØMMØN/VCARAY/LIST(20)
      CØMMØN/CTRL/NØDES

```

```

C
C      EX. 9.3-2 : NONLINEAR SPRINGS
C
C      XK0=1000.0
C      XK1=124.5
C
C      WRITE(NOUT,10) TIME
10  FORMAT(/10X,32HNONLINEAR SPRING FORCES FOR TIME, E15.7,
          //10X,11HNODE FORCE,/1X)
C
C      READ CURRENT DISPLACEMENTS FROM RANDOM FILE "NTDIS"
C
C      CALL READMF (NTDIS,DISP,N,NRU)
C
C      READ NODAL DEGREES OF FREEDOM TABLES. THIS OPERATION IS
C      ALWAYS PERFORMED EXACTLY AS WRITTEN BELOW (2 STATEMENTS)
C
C      CALL READMF (NTNDV,NDOF,NODES,NRDOF)
C      CALL READMF (NTNDV,KODE,NODES,NRCODE)
C
C      COMPUTE SPRING FORCES AT EACH NODE
C
C      NN=3
C      DO 100 INOD=2,20,2
C
C      GET D.O.F. NUMBER FOR DISPLACEMENT COMPONENT "NN"
C      AT NODE "INOD". THIS OPERATION IS ALWAYS PERFORMED
C      EXACTLY AS WRITTEN BELOW (4 STATEMENTS). THE
C      DESIRED D.O.F. NUMBER IS DENOTED BY "IDOF" HERE.
C
C      NF=NDOF(INOD)
C      KD=KODE(INOD)
C      CALL UNPACK (NF,NDPN,MAXKOD,KD,LIST)
C      IDOF=LIST(NN)
C
C      GET DISPLACEMENT VALUE AND COMPUTE FORCE

```

C

```

W=DISP (IDØF)
FØRCE=XK0*W + XK1*(W**3)
P (IDØF)=P (IDØF)-FØRCE
WRITE (NØUT,50)INØD,FØRCE
50 FØRMAT (10X,I4,E12.5)
100 CØNTINUE
RETURN
END

```

The above example is intended to demonstrate the procedures involved in retrieving both the current solution parameters and the nodal degrees of freedom tables stored by the program. In practice, one would employ the more efficient procedure of determining the needed degree of freedom numbers only at the first increment, and storing the information for use in later computations. The labeled COMMON block /USERC/, whose length is unrestricted, can be utilized for this purpose (see Section 7.1.2). The form of subroutine ULØAD is as follows:

```

SUBRØUTINE ULØAD (P,WK,TIME,DT,NTNØDV,NRDØF,NRCØDE,
+
NTDIS,NRU,NRV,NIN,NØUT)
DIMENSION P(1),WK(1)
CØMMØN /USERC/ IDØF(10)
DATA KEY /0/
C
C DETERMINE IF FIRST INCREMENT
C
IF (KEY.NE.0) GØ TØ 10
KEY=1
C
C CALCULATIONS FOR FIRST INCREMENT
C
.
.
.

```

C
C INCREMENTAL LOADS CALCULATION
C

10 CONTINUE

·
·
·

RETURN

END

9.4 VINIT (INITIAL VELOCITY CONDITIONS)

The user subroutine VINIT is used to specify initial velocities at specified degrees of freedom in linear or nonlinear dynamic analyses. Degree of freedom numbers at which velocities are prescribed must be known explicitly. The subroutine has the form

```
SUBROUTINE VINIT (V,N)
DIMENSION V(N)
.
.
.
.
code to prescribe velocities
.
.
.
.
RETURN
END
```

in which the formal parameters are:

V = vector of velocity components at unconstrained degrees of freedom

N = total number of unconstrained degrees of freedom.

Subroutine VINIT is ignored in all static analyses, and in solutions which are being restarted from a previous checkpoint file. All initial velocities not specified in VINIT are automatically defined as zero.

Subroutine TEMGEN is a user-supplied routine which can be used to compute or define a reference temperature distribution throughout the finite element model. The resulting temperature values are interpreted as differences in temperature from the unstressed reference configuration. The temperature field can be made to vary proportionally with time by defining appropriate time functions (data curves), as described in Section 8.4 and 8.9.

DIMENSION X (4,NØDES)

```

      .
      .
      .
      .
      (code to generate temperature data)
      .
      .
      .
      .
RETURN
END

```

NODES = number of node points,
 X(1,I) = coordinate X at node I,
 X(2,I) = coordinate Y at node I,
 X(3,I) = coordinate Z at node I, and
 X(4,I) = temperature at node I.

9.5.1

Example 9.5-1

Consider a two-layer slab, in which Z is the thickness direction. The temperature field is

$$T(Z) = 200. + 65Z, \quad 0 \leq Z \leq 2,$$

$$T(Z) = 150. + 90Z, \quad 2 \leq Z \leq 6.$$

The corresponding temperature subroutine is shown below.

```
SUBROUTINE TEMGEN (NØDES,X)
DIMENSION X(4,NØDES)
DØ 1 I=1,NØDES
    Z=X(3,I)
    T=200.+65.*Z
    IF (Z.GT.2) T=150.+90.*Z
1  X(4,I)=T
    RETURN
END
```

9.6 UØUT (SPECIFY OUTPUT PARAMETERS)

The control of output to both the line printer and the postprocessor file (MPOST) is normally accomplished through the output frequency parameters entered in Section 8.2. In some situations, however, it may be desirable for MAGNA to produce output at irregular intervals during a nonlinear solution. Some typical instances are variable time step solutions, restart jobs, and problems in which the loading does not vary linearly with time. When circumstances dictate, the user-written subroutine UØUT may be used to request printer and/or postprocessor file output at arbitrary intervals in the analysis.

The general form of UØUT is as follows:

```
SUBROUTINE UØUT (ISTEP,TIME,IPRINT,IPØST)
.
.
.
(code to define output flags, IPRINT, IPOST)
.
.
.
RETURN
END
```

Formal parameters passed to UØUT are

ISTEP = current increment number
TIME = current time (or load parameter) value
IPRINT= line printer output flag
 (=1 for output; =0 for no output)
IPØST = postprocessor file output flag
 (=1 for output; =0 for no output)

On entry to the subroutine, IPRINT and IPØST contain default values assigned by the program. Both parameters may be redefined freely based upon the values of ISTEP and TIME. Note that under no circumstances should the parameters ISTEP and TIME be modified in UØUT.

Example 9.6-1

The sample version of UOUT shown below will request printed output at every other increment for times less than $t = 50.$, and at every fourth step thereafter. Output is written to the postprocessor file only after $t = 50.$, where every eighth increment is recorded.

```
      SUBROUTINE UOUT (ISTEP,TIME,IPRINT,IPOST)
      IF (TIME.GE.50.0) GO TO 10
C
C  TIME.LT.50 - PRINT EVERY OTHER STEP, NO MPOST OUTPUT
C
      IPOST = 0
      IPRINT = 0
      IF (MOD(ISTEP,2).EQ.0) IPRINT = 1
      RETURN
C
C  TIME.GT.50 - PRINT EVERY FOURTH STEP, AND
C  WRITE TO POST FILE EVERY EIGHTH STEP
C
10    IPOST = 0
      IPRINT = 0
      IF (MOD(ISTEP,8).EQ.0) IPOST = 1
      IF (MOD(ISTEP,4).EQ.0) IPRINT = 1
      RETURN
      END
```

9.7 NELASi (NONLINEAR ELASTIC MATERIAL LAW)

Four subroutines are available in MAGNA for the specification of nonlinear materials whose constitutive properties are not path-dependent (e.g., nonlinear elastic materials or elastic-plastic materials described by deformation theory).

They are:

NELAS1 - for one-dimensional elements (Type 4)

NELAS2 - for two-dimensional elements (Types 3 and 9)

NELAS3 - for three-dimensional elements (Types 1, 2, 6, 7 and 8)

NELASX - for axisymmetric elements (Type 10)

Each of the above user-written subroutines has the general form:

```
SUBROUTINE NELASi (IELTYP, IELNO, MATLNO, EPS, SIG, D)
  DIMENSION EPS(3), SIG(3), D(3,3)  [for NELAS2 only]
  DIMENSION EPS(6), SIG(6), D(6,6)  [for NELAS3 only]
  DIMENSION EPS(4), SIG(4), D(4,4)  [for NELASX only]
  .
  .
  .
  (code to define SIG and D)
  .
  .
  .
  RETURN
  END
```

in which the formal parameters are:

IELTYP = MAGNA element type

IELNO = element number

MATLNO = material property number

EPS = current Green's strain vector;

= ϵ (a scalar) for NELAS1

$= [\epsilon_x, \epsilon_y, \gamma_{xy}]$ for NELAS2
 $= [\epsilon_x, \epsilon_y, \epsilon_z, \gamma_{yz}, \gamma_{xz}, \gamma_{xy}]$ for NELAS3
 $= [\epsilon_x, \epsilon_y, \gamma_{xy}, \epsilon_z]$ for NELASX
 SIG = Piola-Kirchhoff stress vector, whose components correspond to those in EPS
 D = current tangent modulus matrix, such that $\Delta(\text{SIG}) = D \cdot \Delta(\text{EPS})$

The first four parameters (IELTYP, IELNO, MATLNO, EPS) are input to the routine and should not be modified. The total stresses in Lagrangian coordinates (SIG) and the instantaneous stress-strain coefficients (D) are to be computed by NELASi.

When these user subroutines are supplied, material properties should still be specified in the normal input data to ensure that the correct default values are set for certain internal material parameters. Material densities should be entered correctly, while the actual values specified for other properties are unimportant. When elastic-plastic materials are defined using the NELASi routines, it is recommended that no yield stress value be specified in the materials input data; this practice will prevent any attempt by the program to perform plasticity calculations prior to entering NELASi.

Example 9.7-1

The following example demonstrates the use of NELAS1 to define the stress-strain law for an elastic-plastic material, using the deformation theory of plasticity. The material has elastic modulus $E = 300,000$, yield stress $\sigma_y = 10,000$, and a plastic modulus $E_p = 27,000$.

```

SUBROUTINE NELAS1 (IELTYP, IELNO, MATLNO, EPS, SIG, D)
C
C   ELASTIC PROPERTIES
C
D = 300000.
SIG = D*EPS
IF (ABS(SIG).LE.10000.)RETURN

```

C
C ELASTIC-PLASTIC PROPERTIES (0.0333...=YIELD STRAIN)
D = 27000.
TEMP = EPS-0.333333333
IF (EPS.LT.0.0) TEMP=EPS+0.0333333333
SIG = 10000.
IF (EPS.LT.0.0) SIG=-SIG
SIG = SIG + D*TEMP
RETURN
END

9.8 USTØP (CONTROL POINT FOR JOB TERMINATION)

The lack of prior knowledge of structural response and the performance of a finite element program in computing it represents a potential source of difficulty in nonlinear analysis applications. In particular, the computing effort required for a given problem depends heavily upon the number of iteration cycles needed, the degree of material nonlinearity, and other factors which tend to be highly unpredictable. The user-written routine USTØP can be used to monitor the progress of a nonlinear solution, and optionally signal the termination of the job to avoid abnormal termination (due, for example, to CPU time limit errors).

USTØP is called once at the beginning of each complete increment of the solution. The general form of the subroutine is

```
SUBROUTINE USTØP (ISTEP,TIME,CPUTIM,ISTØP)
.
.
.
RETURN
END
```

in which the formal parameters are:

ISTEP - the pending solution increment number,

TIME - the time (or loading parameter) value corresponding to ISTEP,

CPUTIM - the current CPU time (in seconds) since the start of the job, and

ISTØP - a solution control flag (0 = continue, 1 = stop)

On entry to USTØP, all of the above parameters (including ISTØP) will be initialized. The value of ISTØP will be set to a value determined by the input solution parameters (number of time steps, etc.).

A common use of USTØP is to guard against abnormal termination due to time limit errors; in this case, the USTØP routine might be written as follows:

```
SUBROUTINE USTØP (ISTEP,TIME,CPUTIM,ISTØP)
  IF (CPUTIM.GE.1200)ISTØP=1
  RETURN
END
```

Note that the limiting value of CPUTIM should be determined so that sufficient time remains to perform another complete increment if ISTØP is not set to one.

Another approach might be to write USTØP such that the greatest possible number of solution increments are performed, without exceeding a certain CPU time limit. Subroutine USTØP is nearly the same in this case: the single statement ISTOP = 0, added as the first executable line, will force the solution to continue until the time limit is reached.

9.9 UPLASi (USER-DEFINED ELASTIC-PLASTIC MATERIAL LAW)

Three user-written subroutine interfaces exist in MAGNA for the definition of general incremental constitutive relations. These routines are:

UPLAS3 - for three-dimensional elements

UPLAS2 - for two-dimensional (plane stress) elements

UPLASX - for axisymmetric elements

The UPLASi routines may be used to implement material laws suitable for large or small deformations, including effects such as thermoplasticity, strain-rate sensitivity, or creep. Sufficient information is provided to the user subroutines to define constitutive equations expressed either in Lagrangian or Eulerian form, as appropriate.

The general form of subroutines UPLAS3, UPLAS2, and UPLASX is shown below.

```

SUBROUTINE UPLAS_ (NTYPE, IEL, INTPT, MATL, ISET,
+               TEMP, DTEMP, E, RHØ, TEC, G, XK,
+               RATIØ, DEMAX, S, DS, EPS, DEPS,
+               DG, DGINC, D, SEQ, EPQ, EP, ALPHA)
COMMON /DYNINT/ DUMMY(4), DT, TZERØ, TIME
DIMENSION E(m,m), TEC(n), S(m), DS(m), EPS(m), DEPS(m)
DIMENSION DG(3,k), DGINC(3,k), D(m,m), EP(m), ALPHA(m)

```

(user-written code)

```

RETURN
END

```

The parameters m,n,k are defined as follows:

```

UPLAS3 - m=6, n=6, k=3
UPLAS2 - m=3, n=1, k=2
UPLASX - m=4, n=1, k=2

```

Formal parameters for the subroutines UPLASi are defined below.

NTYPE = (input) element type code
 IELNØ = (input) element number
 INTPT = (input) integration point number for the element
 MATL = (input) material property number
 ISET = (output) flag for entry into UPLASi. On exit,
 ISET=0 indicates that no calculations were performed
 in the user-written routine; ISET=1 indicates that
 UPLASi has been used.
 TEMP = (input) current temperature increment during the
 current time or load step
 E = (input) elastic stress-strain matrix
 RHØ = (input) original material density
 TEC = (input) thermal expansion coefficient. In UPLAS3,
 TEC is a vector of length six, referred to global
 coordinate directions.
 G = (input) elastic shear modulus
 XK = (input/output) yield surface size, initialized to
 the input yield stress
 RATIØ = (input/output) ratio of yield surface expansion
 to translation, as input in materials data.
 DEMAX = (input/output) maximum strain subincrement size,
 as input in materials data
 S = (input/output) on entry, contains the stress at the
 beginning of the increment. On exit, must contain
 the stress at the end of the increment
 DS = (output) stress increment
 EPS = (input/output) on entry, contains the strains at
 the beginning of the increment. On exit, must
 contain the strain at the end of the increment
 DEPS = (input) increment of Green's strain for the
 current time or load step
 DG = (input) deformation gradient at the beginning of the
 increment
 DGINC = (input) incremental deformation gradient

D = (input/output) on entry, contains the stress-strain matrix at the end of the previous increment. On exit, must contain the stress-strain matrix at the end of the current increment.

SEQ = (input/output) effective stress, if applicable

EPQ = (input/output) effective plastic strain, if applicable

EP = (input/output) inelastic strain components (or other state variables as appropriate)

ALPHA = (input/output) additional space for storage of state variables at individual integration points.

Stress and strain components are stored in the following order:

UPLAS3 - σ_{xx} , σ_{yy} , σ_{zz} , σ_{yz} , σ_{xz} , σ_{xy}

UPLAS2 - σ_{xx} , σ_{yy} , σ_{xy}

UPLASX - σ_{xx} , σ_{yy} , σ_{xy} , σ_{zz}

This ordering must be maintained as well in the formulation of the stress-strain matrix D. The ordering convention for the total and incremental deformation gradients are

$$DG(I,J) = \frac{\partial x_I}{\partial X_J} = \delta_{IJ} + u_{I,J}$$

For the three-dimensional and axisymmetric elements, all coordinates and displacement values are referred to global directions; in the two-dimensional elements, a local system is used in which the z (or X_3) direction is normal to the element. For UPLASX (axisymmetric elements), the additional component $\partial x_3 / \partial X_3$ is stored in location DG(3,1).

The following operations are required within UPLASi:

- updating of the strains, $EPS(i)=EPS(i)+DEPS(I)$
- updating of the stresses, $S(I)=S(I)+DS(I)$
- setting ISET=1 is required whenever elastic-plastic computations are performed, to prevent conflicting calculations from being performed elsewhere in MAGNA.

If ISET=0 on exit from UPLASi, MAGNA will assume that no action has been taken by the user routine, and will perform stress and strain updating and elastic-plastic calculations as usual.

Several conventions should be noted for the proper operation of the UPLASi subroutines:

- strains supplied to the routine are "engineering" values, in which the shear strains are set to twice their tensorial (Green's strain) values;
- since the nonlinear formulation uses the total Lagrangian formulation, stresses output from UPLASi should be second Piola-Kirchhoff stresses, to ensure proper computation of the geometric stiffness;
- the modulus matrix D is necessary for correct computation of thermal "loads", and should always be computed in thermal problems;
- in nonlinear solutions using equilibrium iteration, UPLASi may be called several times per integration point. The initial values supplied to the routine are always those obtained from the last converged step, to avoid artificial "cycling" due to fluctuations in the estimated state of strain.

For the storage of state variables, several parameters are available whose values will be retained throughout the solution and which may be updated incrementally. In addition to the two vectors EP and ALPHA, which are specifically intended for the maintenance of state variables, the following parameters may be updated freely as needed: G, XK, RATIO, DEMAX, SEQ, and EPQ. Note that the values of SEQ and EP will appear in the integration point stress and strain output, since they normally contain the effective stress and the plastic strains, respectively.

9.10 UDAMP (STEADY-STATE DAMPING PROPERTIES)

The user-supplied subroutine UDAMP must be supplied in steady-state forced vibration analysis, to define elastic and damping properties of the materials to be analyzed. Optionally, this routine may be used to specify properties as functions of the excitation frequency (see Section 8.3.5).

The general form of the subroutine UDAMP is

```
SUBROUTINE UDAMP(IELTYP,MATL,FREQ,ETA,  
+               G,GO,IFDEP)
```

(user-written code)

```
RETURN
```

```
END
```

Formal parameters for subroutine UDAMP are as follows:

IELTYP = (input) element type code

MATL = (input) material property number

FREQ = (input) excitation frequency (cycles/time)

ETA = (output) material loss factor

G = (output) shear modulus at the current frequency

GO = (output) shear modulus for FREQ = 0

IFDEP = (input) flag for frequency dependent properties
(0 = no, 1 = yes)

For sinusoidal motions, the shear modulus of the material is assumed to be defined in the form $G^* = G(1 + \eta)$. G^* is complex-valued; the real part of G^* (that is, G) is the elastic property, while η defines the amount of intrinsic damping:

$$\eta = \frac{\text{energy dissipated per cycle}}{\text{energy stored per cycle}}$$

The values of G , G_0 , and η (G, GO, ETA) must be defined by the subroutine UDAMP. If the material properties are independent of

frequency (IFDEP = 0), then $G_0 = G$. When IFDEP = 1, both G and η (but not G_0) may be functions of the harmonic forcing frequency.

Since UDAMP is called for each element of the model, it is also possible to define properties which vary with temperature. To obtain the average element temperature, the additional declaration statement

COMMON/USERC/AVTEMP

can be included in the subroutine. On entry to UDAMP, the variable AVTEMP contains the average temperature for the current element.

9.11 UPRESS (VARIABLE SURFACE PRESSURES)

The user-supplied subroutine UPRESS is intended for the definition of distributed surface pressures which may vary as functions of both time and spatial position. Variable surface pressures may be defined for all three-dimensional solid and shell finite elements in MAGNA (Element Types 1, 2, 5, 6, 7, 8, and 11).

The general form of subroutine UPRESS is as follows:

```
SUBROUTINE UPRESS (ISTEP,TIME,X,Y,Z,ISURF,PRESS)
```

```
(user-written code to define PRESS)
```

```
RETURN
```

```
END
```

where the subroutine parameters are

ISTEP = current solution increment

TIME = current value of time or loading parameter

X,Y,Z = Cartesian coordinates of a point at which the pressure is to be specified

ISURF = surface number (1-6) on which the point lies

PRESS = output pressure value (positive outward)

Note that all elements for which UPRESS is to be used to define surface loading *must* be identified through the distributed loads input described in Section 8.10.2. The surface number (LTYPE) should be set to the appropriate value (1-6); note also that a data curve or load case number (ICASE) *must* be given as input.

In nonlinear analysis, the interpretation of the coordinates X,Y,Z which are passed to UPRESS depends upon the value of the live loads flag (ILIVE) on the pressure data card. If ILIVE = 0 (dead loading), the original coordinates of pressure sampling points are sent; when ILIVE = 1 (deformation-dependent loading), the X,Y,Z values are the updated coordinates for the current configuration.

The following simple example defines a hydrostatic pressure, with Z as the "depth" direction, which varies quadratically with time as

$$p(X,Y,Z,t) = (\gamma Z) \left(\frac{t}{2} + 2t^2 \right),$$

where $\gamma = 0.03613/\text{lb}/\text{in}^3$ (for water), and Z is in inches.

```
SUBROUTINE UPRESS (ISTEP,TIME,X,Y,Z,ISURF,PRESS)
DATA GAMMA/0.03613/
PRESS = GAMMA*Z*TIME*(0.5 + 2.0*TIME)
RETURN
END
```

9.12 UANIS2 - (Anisotropic Material Properties for 2-D Elements)

The user-written subroutine UANIS2 permits the definition of orthotropic, anisotropic, or other special material properties for two-dimensional finite elements (Element Types 3 and 9). UANIS2 is accessed by MAGNA during the input phase of an analysis, during which isotropic material properties defined as input data may be overridden selectively. Element stiffness formulation and stress recovery operations are fully consistent with the anisotropic properties specified in UANIS2.

The general form of subroutine UANIS2 is as follows:

```

      SUBROUTINE UANIS2 (IELTYP, MAXNOD, IELNUM, MATLNO, IGLOBL,
+                      XG      , YG      , ZG      , TRAN  , E      )
C
      DIMENSION XG(MAXNOD), YG(MAXNOD), ZG(MAXNOD)
      DIMENSION TRAN(3,3) , E(3,3)
C
      .
      .
      .
      (code to define anisotropic stress-strain coefficients, E)
      .
      .
C
      RETURN
      END
```

Formal parameters for subroutine UANIS2 are:

| | |
|--------|--|
| IELTYP | - MAGNA element type (3 or 9) |
| MAXNOD | - Maximum number of connected nodes (4 for Element Type 3, 9 for Element Type 9) |
| IELNUM | - Element sequence number (as defined in input) |
| MATLNO | - Material property number (as defined in input) |
| IGLOBL | - Flag for local (IGLOBL=1) or global (IGLOBL=2) coordinate system used for the current element. The global coordinate system (IGLOBL=2) is used only for Element Type 9, in elements which are oriented parallel to the global X-Y plane. The |

local coordinate system, used in all other cases, has x parallel to the direction from node 1 to node 2 of the element, and y perpendicular to the x direction in the plane of the element. All properties specified in UANIS2 must be referred to the coordinate system used for the element for correct results.

- XG,YG,ZG - Global coordinates X, Y, and Z, respectively, at each of the nodes connected to the current element. These values are provided for use in specifying anisotropic properties which may be dependent upon position or orientation.
- TRAN - Transformation matrix relating the local and global coordinates in the element. When IGLOBL=2, TRAN is an identity matrix; otherwise, TRAN is an orthogonal transformation matrix other than the identity. In either case, multiplication of the global coordinate values (X,Y,Z) by TRAN gives the local coordinate values (x,y,z) at the same point.
- E - Elastic stress-strain matrix, referred to the element coordinate system. The stresses are assumed to be ordered ($\sigma_x, \sigma_y, \sigma_{xy}$), and the strains ($\epsilon_x, \epsilon_y, \gamma_{xy}$), in which γ_{xy} is the engineering shear strain.

The following rules and conventions should be observed in using the user-written subroutine UANIS2:

- (1) Properties data for anisotropic elements should be defined in the normal MAGNA input, and overridden using UANIS2. A material number of "0" should NOT be input for such elements.

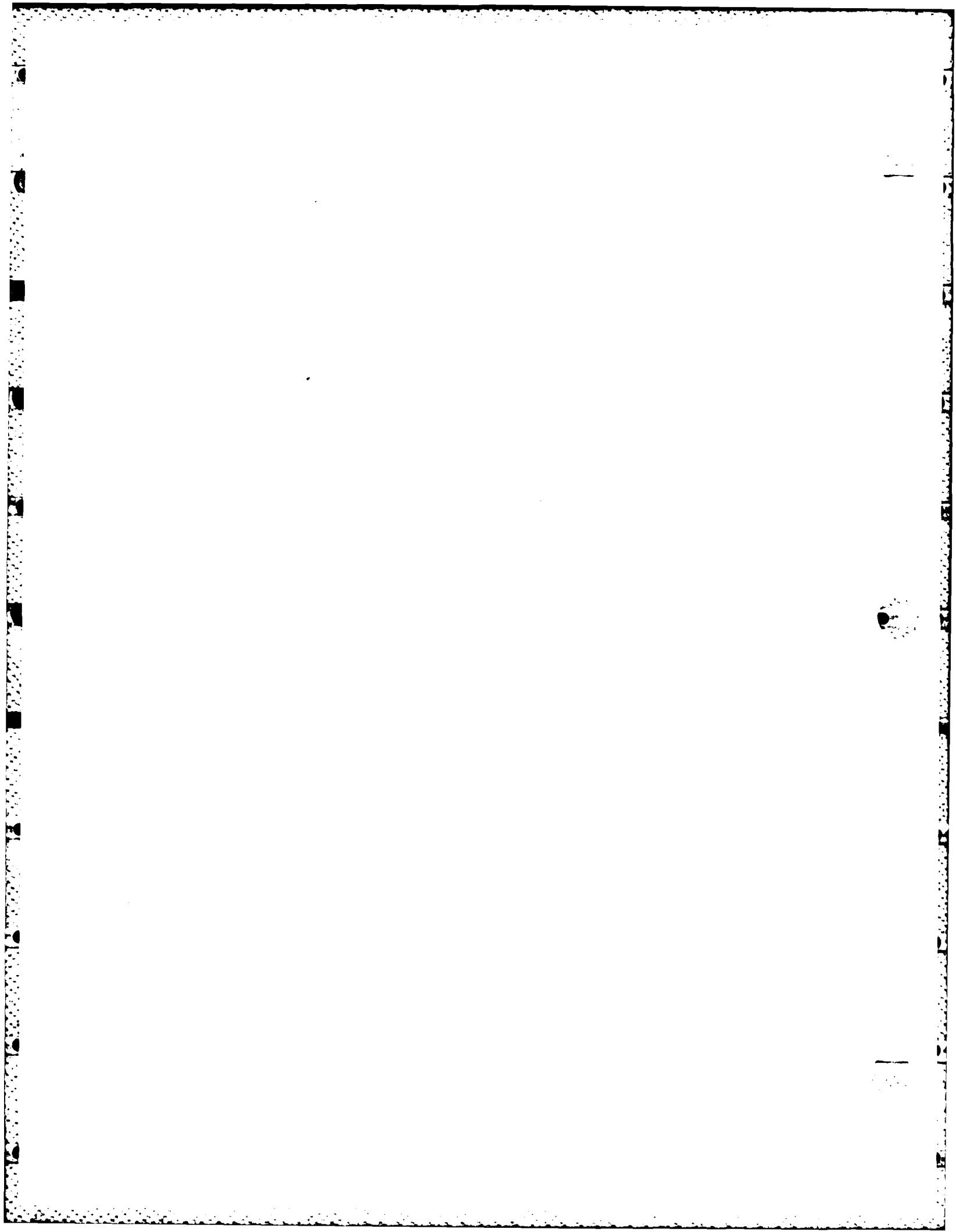
- (2) No subroutine parameters other than the stress-strain matrix "E" should be modified in UANIS2. Modification of other formal parameters could result in abnormal termination or incorrect results.
- (3) In nonlinear analysis, properties defined in UANIS2 are saved with the normal restart data; analysis restart runs can be made without supplying the subroutine if desired. Changes to subroutine UANIS2 made during analysis restarts will have no effect on the solution.
- (4) In transforming orthotropic properties from material to analysis coordinates, note that the strain values used in defining "E" must be engineering strains, for which the shear strain is twice the tensorial strain.

CHAPTER 10

PROGRAM OUTPUT

A general description of the MAGNA program printed output is given in this Chapter. Not all of the output referred to here will be obtained in a particular analysis, and in some instances, the output from linear and nonlinear solutions are necessarily different; where such differences occur, all possible forms of the printed information are discussed.

The first of the normal MAGNA outputs are the title page and the system notes page. These are self-explanatory and will not be discussed further here. Also, graphical output is obtained interactively (see Chapter 11) and is not part of the batch printer output.



10.1 STORAGE ALLOCATION MODULE (CDC MACHINE VERSION ONLY)

The MAGNA storage allocation utility module acts as a precompiler to the main finite element program, and is only activated when a STORAGE ALLOCATION card is supplied (Sections 7.1 and 7.2). Information printed by the storage allocation module includes

- (1) a summary of the program working storage, including actual, default and minimum values, and
- (2) an estimate of the total central memory requirements, in both decimal and octal values.

A sample of the storage module output is shown in Figure 10.1.1.

Output from the storage allocation utility can be used to verify that the STORAGE ALLOCATION card has been processed as expected, and that the central memory actually specified for the job is actually sufficient. Refer to the description of program working storage in Section 7.2 if difficulties are encountered in specifying the STORAGE ALLOCATION parameters.

Following the precompiler output, a FORTRAN compilation of the MAGNA main program appears. User-written subroutines are also compiled at this time and should be checked for coding errors.

18.08.31.

03/30/91

MAGNA / UPDGEN

WORKING ARRAY REDEFINITION

| LABELLED COMMON AREA | | LENGTH | DEFAULT | MINIMUM |
|----------------------|--------|---------|---------|---------|
| /BLANK/ | MAORC | - 32000 | 20000 | 12000 |
| /IDENT/ | MID | - 3400 | 2500 | 100 |
| /BLOX / | MNS | - 160 | 150 | 150 |
| /BLEQ / | MNS | - 160 | 150 | 150 |
| /INDXK/ | MINDXK | - 180 | 170 | 170 |

| | DECIMAL | OCTAL |
|----------------------------------|---------|--------|
| CENTRAL MEMORY (DEFAULT) . . . | 59004 | 165000 |
| ARRAY EXTENSIONS | 12930 | 031202 |
| CENTRAL MEMORY (ESTIMATED) . . . | 72834 | 216202 |

Figure 10.1.1.1 Output from Storage Allocation Module.

10.2 INPUT AND GENERATED DATA

The summary of model data, including both input and internally generated information, represents most of the MAGNA output generated prior to actually performing a solution. This output is intended to verify that the problem data has been read and interpreted correctly. Individual sections of this phase of the program output are described in the subsequent sections.

10.2.1 Input Data Listing (CDC and VAX Versions)

Immediately following the storage allocation module output and the user subroutine compilations (if any), a complete listing of the problem data is given, as it appears on the input file (TAPE5). The input listing should be inspected for keypunch errors, and checked with subsequent output to ensure that generated and/or defaulted data values have been assigned correctly.

10.2.2 Options and Solution Parameters

In this section of output, a label echo print of all initial data is printed, with default values inserted where appropriate. For nonlinear and natural frequency analyses, parameters governing the iterative solution are also printed at this time. If the job is to read or write restart files, a message is output verifying this fact and displaying the pertinent file labels and restart parameters. Runs in which the label or increment value on a previous restart tape has been incorrectly specified are terminated with an error message.

10.2.3 Nodal Coordinates

The nodal coordinate listing contains all input and generated values of the Cartesian coordinates x, y, z . Nodes for which no coordinate values have been assigned are flagged with a diagnostic message, and the value -9999.99999 is written for each coordinate. If thermal effects are to be included in

the solution, the temperature (as read or generated) at each node is also output, and the data curve number defining the temperature history is identified immediately following the coordinate listing.

10.2.4 Element Definition Data

Materials and element connectivity data are output, in order of element types, in this section of the MAGNA output. This portion of the printing should be examined to verify that:

- the element types have been specified in ascending order,
- the correct number of elements of each type have been read or generated,
- material numbers and integration orders are correct for all elements,
- all necessary moduli and densities (if required) have been specified,
- all elastic-plastic materials are assigned initially-isotropic properties, and
- stress-strain curve numbers have been properly assigned for all nonlinear materials.

The items listed above represent the most common errors made in this section of the data, and may generate errors which are otherwise difficult to trace. Orthotropic axis data can also be verified at this point, since the relative coordinates defining each local axis direction are printed explicitly.

Immediately following the regular element definition output, a summary of input parameters related to special surface contact elements is printed. This output consists of the number of surface elements and surface element sets, the element set limits, the active interaction table entries, and all input and generated contact element definitions. Particular care should be taken to verify that master/slave set entries in the interaction table are correctly defined, and that the orientation

of each contact element is such that the normal to the element is directed outward from the surface in question.

10.2.5 Boundary Conditions

Homogeneous nodal constraints are first written out exactly as input, with labeling to make possible errors more readily identifiable. A number of diagnostic messages may also appear, as described later in this chapter under Error and Warning Messages. Once all boundary conditions have been processed, a complete listing of unconstrained degrees of freedom for all nodes of the model is printed, as shown in the example below.

NODAL VARIABLE TABLES

| <u>Node</u> | <u>NFDF</u> | <u>Code</u> | <u>1</u> | <u>2</u> | <u>3</u> |
|-------------|-------------|-------------|----------|----------|----------|
| 1 | 1 | 3 | 1 | 2 | 0 |
| 2 | 3 | 3 | 3 | 4 | 0 |
| 3 | 5 | 4 | 0 | 0 | 5 |
| 4 | 6 | 7 | 6 | 7 | 8 |

At a particular node, NFDF specifies the number of the first nonzero (unconstrained) degree of freedom, CODE represents an internal variable used in packing the nodal equation tables, and the entries in columns 1, 2, 3 give the actual equation (degrees of freedom) number for the first, second and third variables at the node (in this case, the displacements u, v, w). This table can be used to check that all nodal constraints have been applied correctly, and if necessary to trace back subsequent errors in equation solving, etc., if an artificial instability exists in the model.

Linear (multipoint or tying) constraint data are the last items printed in the summary of boundary conditions for the model. The analyst should verify that the correct number of constraints appear if generation has been used, and that no previously constrained degrees of freedom appear in the specified constraints (a diagnostic is issued in this case).

10.2.6 Data Curves and Applied Loadings

The final portion of the input data summary lists the user-defined data curve input and applied nodal and element forces. This output is largely self-explanatory, and follows the input data sequence nearly line by line. Once these data have been output, input processing is complete and control is transferred to the appropriate solution branch in MAGNA. Note that output pertaining to matrix topology (Section 10.3) precedes this section of printing.

10.3 MATRIX TOPOLOGY AND PARTITIONING DATA

The matrix partitioning data printed immediately following the boundary conditions is one of the more important sections of output, since it gives a brief summary of the utilization of working storage within the program. Input/output times for large analyses can be drastically affected by the amount of array space, and the partitioning data output from MAGNA often can be used to determine the correct storage requirements for a given application.

The following parameters are always printed:

- Degrees of Freedom
- Number of Matrix Partitions
- Maximum Partition Size
- Work Area Available
- Work Area Used
- Maximum Half-Bandwidth
- Average Half-Bandwidth
- Apparent Population

The number of degrees of freedom is the final number of equations for the model; the length of /IDENT/ (see Chapter 7) must be at least as large as this value.

The next two items have to do with the splitting of system matrices into blocks (partitions) to perform a solution. The number of matrix partitions varies inversely with the working array space (/BLANK/ in Chapter 7) supplied to the program. A large number of partitions usually causes the CPU time for matrix assembly to increase dramatically, and leads to high I/O times during the assembly and solution steps. In nonlinear analyses, where these steps must be repeated many times, it is advisable to assign sufficient work space in /BLANK/ to keep the number of partitions relatively small (i.e., 25

or less). When the problem is large enough to force a larger number of partitions to be created, the length of /BLANK/ on the storage card should be specified as large as possible for the machine being used. The available work area and the array space actually used are printed as part of this summary; the program uses a special algorithm for each analysis type to make optimal use of the available working storage.

The final three items, bandwidths and population, are printed to provide a rough idea of the size of the system being solved. The maximum bandwidth is usually determined by linear constraints, which are the highest-numbered equations of the system; this value is relatively unimportant. Average bandwidth is a measure of how well the model has been numbered; very high values can force the creation of a large number of matrix partitions, which in extreme cases can affect the solution time dramatically. Finally, the apparent population is the number of entries in the system stiffness (or effective stiffness) matrix which are considered as nonzeros during the solution. The population is approximately given by the average half-bandwidth times the number of degrees of freedom.

If the optional matrix profile map has been selected (IOPT(7) = 1), this output is also given with the matrix partitioning data. The profile map indicates the pattern of nonzero terms in the system matrices, and provides an indication of the efficiency of storage utilization. An example is shown in Figure 10.3.1. The matrix map is always scaled to fit on two pages of printed output, so that each block of nonzero terms (indicated by "X" in the output) represents a submatrix whose size depends upon the total number of equations in the system. Diagonal submatrices are printed as "D" on the matrix profile map.

AD-A129 773

MAGNA (MATERIALLY AND GEOMETRICALLY NONLINEAR ANALYSIS) 7/8
PART I FINITE ELE. (U) DAYTON UNIV OH RESEARCH INST

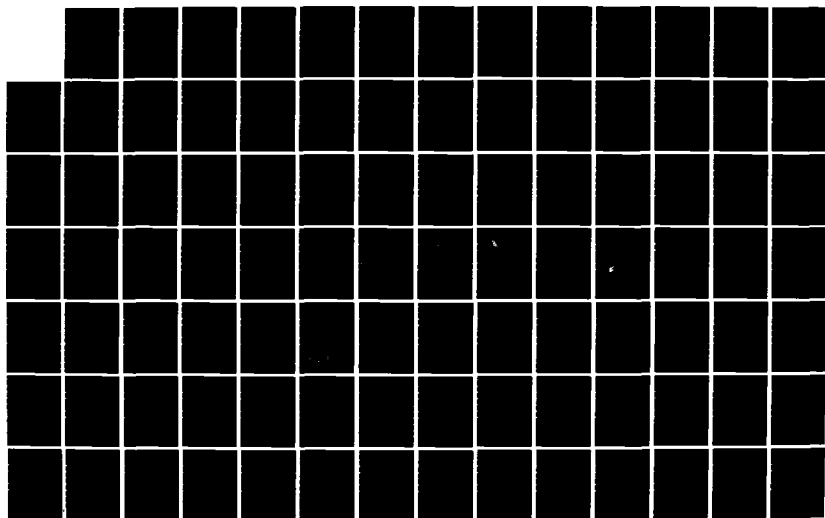
R A BROCKMAN DEC 82 UDR-TR-82-111 AFWAL-TR-82-3098-PT-1

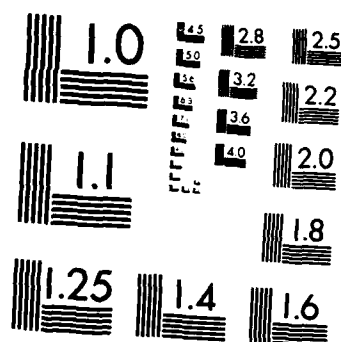
UNCLASSIFIED

F33615-80-C-3403

F/G 12/1

NL





MICROCOPY RESOLUTION TEST CHART
NATIONAL BUREAU OF STANDARDS-1963-A

100017 744104 10010 PLASTIC ANALYSIS, LINEAR STRAIN HARDENING
 100017 744104 10010 PLASTIC ANALYSIS, LINEAR STRAIN HARDENING
 100017 744104 10010 PLASTIC ANALYSIS, LINEAR STRAIN HARDENING

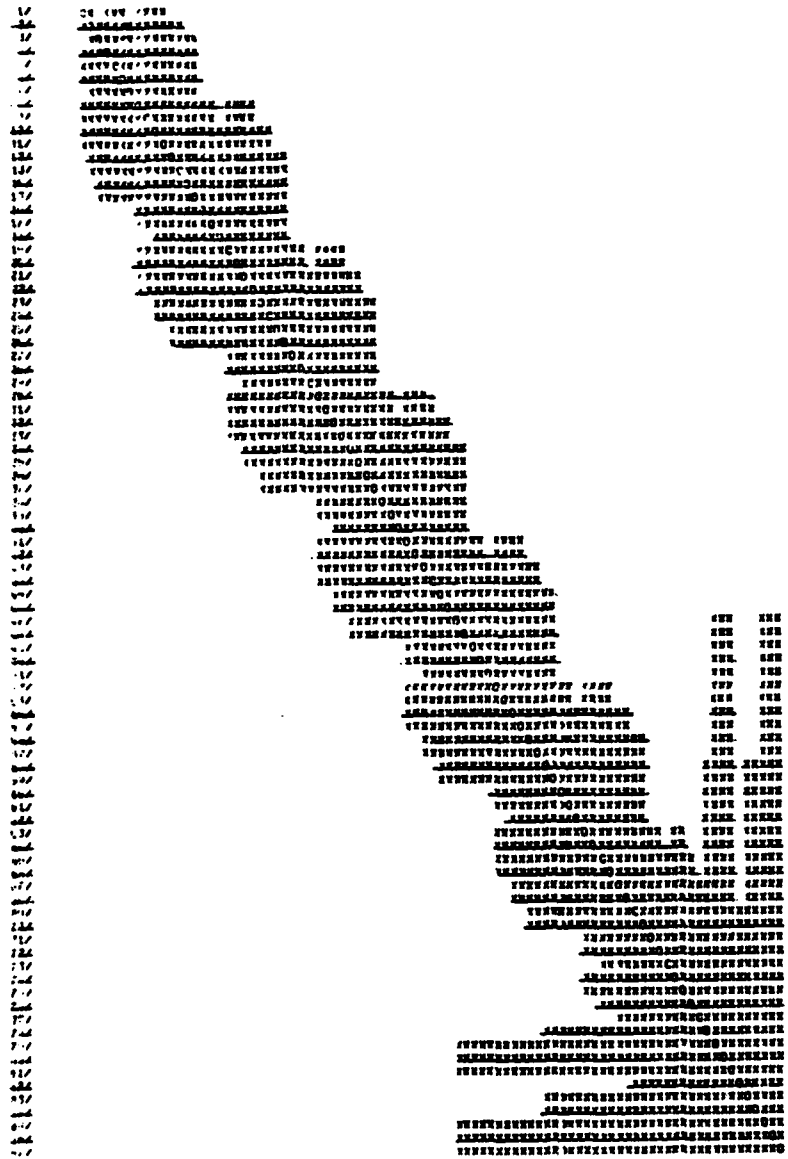


Figure 10.3.1 Matrix Profile Map Output.

10.4 ELEMENT GEOMETRIC PARAMETERS

In all linear analyses, and in nonlinear dynamic analysis, a summary of element geometry is output by MAGNA. This information is useful in isolating errors in coordinate and/or connectivity data which might not be obvious from geometry plots of the finite element mesh.

For all two- and three-dimensional elements, the following data are listed:

- element type and number,
- minimum, average and maximum Jacobian determinant values,
- element volume (area for 2-D elements), and
- element distortion ratio.

The Jacobian determinant values are characteristic of the mapping between physical and isoparametric coordinates, and should always be positive in elements of reasonable shape. Element areas or volumes are printed to permit identification of elements which are incorrectly defined or of unreasonable dimensions. Finally, unreasonably distorted elements can often be identified from the distortion ratio, defined as

$$8 (\min |J|) / \text{Vol.} \quad (3\text{-D Elements})$$

$$4 (\min |J|) / \text{Vol.} \quad (2\text{-D Elements})$$

in which $|J|$ is the Jacobian determinant. The distortion ratio is equal to one for elements which are parallelepipeds, and is less for more distorted elements. Elements having a distortion ratio less than about 0.25 are likely to result in local ill-conditioning and/or inaccuracy and may require redefinition as two or more elements.

10.5 ITERATIVE SOLUTION PARAMETERS

The progress of any nonlinear solution must be monitored continuously to ascertain the validity of the results and to detect convergence or divergence of successive approximations at a given loading or time value. During an iterative nonlinear solution, the MAGNA program uses two primary means of monitoring the progress of the iterations: residual (i.e., out-of-balance) forces and displacement corrections. Since both of these quantities are vectors for a multiple degree of freedom system, their "size" is measured using the Euclidean norm, denoted by $\| \underline{v} \| = \sqrt{\underline{v}^T \underline{v}}$. The force and displacement quantities monitored and printed during the solution are

$$FNORM = \| \underline{F}_{res} \| / \| \underline{F}_{ext} \|^2$$

and

$$DNORM = \| \Delta \underline{u}^{(i+1)} - \Delta \underline{u}^{(i)} \|^2$$

in which i denotes an iteration number during a given time or loading increment. Note that the quantity $FNORM$, being normalized with respect to the total external forces, is independent of the particular system of units being used, while $DNORM$ is measured in units of length. An exception occurs when the applied forces are zero, in which case the actual residual force norm is used for $FNORM$.

At each iteration cycle, the iteration number and current values of $FNORM$ and $DNORM$ are printed, along with appropriate diagnostic and/or informative messages. As the solution converges, both $FNORM$ and $DNORM$ will gradually decrease (in some cases following a few oscillations) until the force and displacement tolerances specified as iteration parameters (Section 8.3.1) are satisfied. In dynamic problems, and in those for which linear constraints have been specified, $FNORM$ will tend to converge to some constant value other than zero, due to inertial forces and to reactive forces which occur due to the presence of the constraints. For such analyses, residual force tolerances are applied to the *differences* in $FNORM$ between successive iterations.

It should be noted that one additional cycle of iteration is performed to complete the solution after convergence is achieved, so that the residual forces associated with the printed solution are often an order of magnitude or more smaller than the specified tolerance. Final residual forces and displacement corrections are displayed following the printed displacement and stress results for the increment, and labeled with NUMIT = 0.

Typical output for the iteration control variables appears as follows:

```

ITERATION CONTROL VARIABLES      INCREMENT = 4

NUMIT = 0      THE FOLLOWING ARE FINAL VALUES AT
                COMPLETION OF PREVIOUS INCREMENT
=====
NUMIT = 0      FNORM = .448E-09  DNORM = .553E-10
=====
NUMIT = 1      STIFFNESS TO BE REFORMED
                FNORM = .250+00  DNORM = .349E-01
                STIFFNESS TO BE REFORMED
NUMIT = 2      FNORM = .176E-03  DNORM = .348E-04
                STIFFNESS TO BE REFORMED
                NEXT ITERATION TO BE ACCEPTED

```

In the above example (taken from the analysis of Section 6.15), the values for NUMIT = 0 are final values for the third increment, and iterations for increment 4 begin at NUMIT = 1. The informative message "STIFFNESS TO BE REFORMED" appears at varying intervals in the solution, depending upon the type of iteration strategy requested. Convergence is indicated by the message "NEXT ITERATION TO BE ACCEPTED." Lack of convergence, which results in job termination, is signaled in this section of the output by one of the following diagnostics:

```

SOLUTION STOP - RESIDUAL FORCES INCREASING
SOLUTION STOP - DISPLACEMENT SOLUTION DIVERGING
SOLUTION STOP - NO CONVERGENCE IN MAXIT CYCLES

```

10.6 INCREMENTAL LOADS

At each increment of a nonlinear solution for which output is requested, the current external forces are printed immediately preceding the displacement solution. For concentrated nodal forces, which are obtained from the time function curves input in Section 8.9, the following information is printed:

NODE : node number at which force is applied,
COMPT : component (i.e., direction) of the force,
DOF : the global degree of freedom number, and
MAGNITUDE : value of total force.

Body forces, surface pressures and line loads are summarized element by element, in order of element type and number (this sorting is performed during the input stage). The following parameters are output for each distributed load:

- element type,
- element number,
- surface number, edge number, or body force direction,
- loading type ("LIVE" or "DEAD"),
- data curve number for this load,
- loaded volume, surface area, or edge length,
- loading magnitude.

For "live" loads, the distributed loading is applied per unit of deformed length, area, or volume; live pressures and line loads are assumed to act along the outward normal to the *deformed* surface or edge, and therefore may change direction during the course of the solution. "Dead" loading is always referred completely to the original geometry of an element.

10.7 DISPLACEMENT AND VELOCITY SOLUTIONS

Displacements are output by node and direction whenever printing is requested in a nonlinear or dynamic solution, for each loading condition in linear static analysis, and for each requested vibration mode in natural frequency problems. Velocities are also displayed in all dynamic analysis printouts. Output is given in the global Cartesian coordinate directions. When a nodal displacement (or velocity) is suppressed through boundary conditions, such constraint is indicated by an asterisk printed to the right of the corresponding displacement (velocity) value.

10.8 ELEMENT STRESSES AND STRAINS

In linear and nonlinear analysis, there are four categories of stress/strain output:

- One-Dimensional Elements,
- Two-Dimensional Elements,
- Three-Dimensional Elements, and
- Thin Plate and Shell Elements.

Within any of these categories, which are described separately in the following sections, the element stress output is virtually identical regardless of the element type. In all cases, the stress and strain quantities are those consistent with the Lagrangian formulation used throughout the program (see Section 2.1).

10.8.1 One-Dimensional Elements (Type 4)

The one-dimensional element, or truss, is an axial force element, and thus the state of stress is characterized by the stress parallel to the axis of the bar. Therefore, all stress and strain outputs are given in terms of a *local* coordinate directed from one end of the bar to the other.

In linear analysis, the output for each element consists of the following:

- element number,
- elastic modulus,
- element area,
- element length (undeformed),
- axial strain,
- axial stress, and
- total force (stress x area).

For each different material used, the most highly stressed element is also identified each time the stress output appears.

For nonlinear analysis, additional output is provided to describe possible material nonlinearities. Output parameters consist of:

- element number,
- element area,
- element length (undeformed),
- total axial strain,
- total plastic strain,
- axial stress,
- total force (stress x area),
- yield surface size, and
- yield surface translation.

The plastic strain as output by the program is defined as the residual strain which would exist if the element were unloaded perfectly elastically; that is,

$$\epsilon_p = \epsilon_{\text{total}} - \sigma/E$$

where E is the original elastic modulus. The yield surface size (i.e., the current "yield stress") and yield surface translation result from isotropic and kinematic strain-hardening effects, respectively.

10.8.2 Two-Dimensional and Axisymmetric Elements (Types 3, 9 and 10)

The two-dimensional elements in MAGNA are initially planar, although they may be arbitrarily oriented in space and may deform into a warped curvilinear shape. Due to the preferential orientation of the stress state, strain and stress output are normally given in a local system of coordinates parallel to the plane of the undeformed element. The reference coordinate directions are shown in Figure 10.8.1 for a typical element. The local x direction is determined from the first two corner nodes of the element; the local y axis lies in the plane defined

by nodes 1, 2 and 3 for the element, and is oriented perpendicular to local x. Since Element Type 9 is often used for true plane stress applications, output for Type 9 elements is given with respect to the *global* x,y coordinates, provided the element lies in a plane for which z is constant. When output is given in global directions, the axis type printed in the original element connectivity output is given as "GLO", rather than "LOC". For axisymmetric analysis (Element Type 10), stresses and strains are always output in the global system of coordinates.

All two-dimensional and axisymmetric elements in the program are numerically integrated, and, therefore, strain and stress outputs are given at the actual integration points of the element. The ordering of the integration points for 1, 2 and 3-point Gaussian quadrature rules is shown in Figure 10.8.2. Note that stress or strain results can be listed at the node points and/or plotted in contour or relief form over all or selected elements (see Chapter 11); this is usually the most useful and readily assimilated form of stress output. Having determined the most critical locations from stress or strain plots, the analyst can examine these portions of the model in greater detail using the printed output.

In linear analysis, the two-dimensional element output consists of:

- element and integration point numbers,
- strains ϵ_{xx} , ϵ_{yy} , γ_{xy} ,
- stresses σ_{xx} , σ_{yy} , σ_{xy} , and
- minimum and maximum principal stresses.

Circumferential (z-direction) strains and stresses will also be output for axisymmetric elements. The shear strain γ_{xy} is an "engineering shear strain" which is twice the tensorial value. The principal stress values are ordered algebraically (rather than by absolute value); that is,

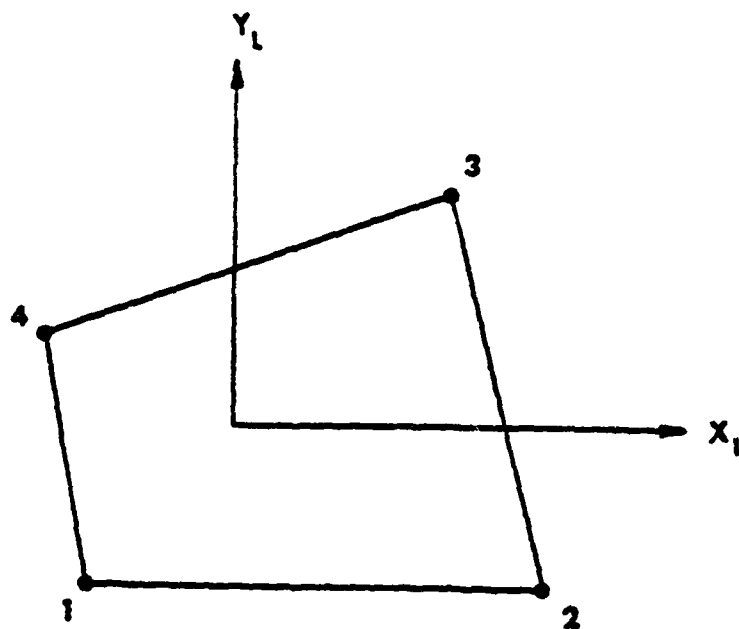


Figure 10.8.1 Local Coordinate Directions for Two-Dimensional Elements.

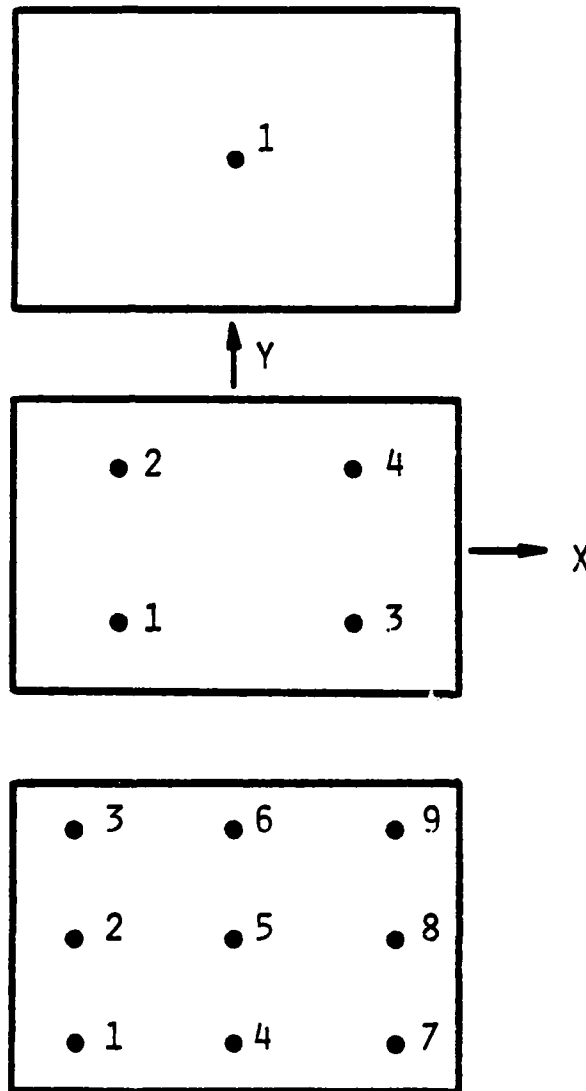


Figure 10.8.2 Integration Point Locations (INT=1,2,3) for Two-Dimensional Elements.

$$\sigma_{\max} = \frac{\sigma_{xx} + \sigma_{yy}}{2} + \sqrt{\left(\frac{\sigma_{xx} - \sigma_{yy}}{2}\right)^2 + \sigma_{xy}^2}$$

$$\sigma_{\min} = \frac{\sigma_{xx} + \sigma_{yy}}{2} - \sqrt{\left(\frac{\sigma_{xx} - \sigma_{yy}}{2}\right)^2 + \sigma_{xy}^2}$$

For each different material, the element having the largest von Mises effective stress is also identified and printed at the end of this segment of the output.

The element output for nonlinear problems is similar, but includes additional parameters which describe possible material nonlinearities. Besides the stress and strain quantities described above, the following data are printed at each integrating point:

- plastic strains $\epsilon_{xx}^P, \epsilon_{yy}^P, \gamma_{xy}^P$,
- yield function F ,
- relative error estimate f_R , and
- von Mises equivalent stress σ_{eq} .

The equivalent stress is given by

$$\sigma_{eq}^2 = (\sigma_1 - \sigma_2)^2 + \sigma_1 \sigma_2$$

in the plane stress case, where σ_1, σ_2 are the principal stresses at a point. The yield function F is

$$F = \sigma_{eq}^2 - k^2,$$

in which k represents the current yield surface diameter (i.e., the yield stress). Thus, the yield function is negative at a point if the material behaves elastically, and is equal to zero for plastic states. Due to numerical error accumulated during the solution, F will usually take on a small positive value for elastic-plastic points, rather than being exactly zero. Such truncation error is always expected to occur in plastic analysis, and the remaining output quantity, the relative error f_R , is

provided as a check that the amount of numerical error remains small. Define

$$f_R = F/k^2 ;$$

this quantity then describes the relative amount by which the computed stress state deviates from the yield surface. Note that, although a stress correction procedure is employed to adjust the computed stresses to lie on the yield surface, *the error f_R is evaluated before any stress corrections are applied.* Thus, the value of f_R is always larger than the final error associated with deviations from the current yield surface. Relative errors in the range of one or two tenths of a percent (.001 - .002) are normally acceptable, although the values are generally smaller in a well-behaved solution.

10.8.3 Three-Dimensional Elements (Types 1, 2, 6, 7 and 8)

The three-dimensional solid elements are arbitrarily shaped and oriented, and in general contain no preferential directions for strains or stresses. For this reason, the element output for all solid elements is referred to the global Cartesian system of coordinates.

As with the two-dimensional elements, all of the three-dimensional solids are isoparametric, numerically integrated elements. Printed output is given at the integration points, which are summarized for various orders of integration (1, 6, 8, 14 and 27 points) in Tables 10.8.1 through 10.8.5. For the 9-point integration available with Element Type 2, output is generated at the 2x2x2 Gauss points (Table 10.8.3). Averaged nodal stress/strain values and plotting on selected elements surfaces are also available with the graphics utility programs described in Chapter 11.

For linear analyses, three lines of printed output are produced per integration point. These consist of:

- Line 1 - element number
- integration point number
- strains ϵ_{xx} , ϵ_{yy} , ϵ_{zz} , γ_{yz} , γ_{xz} , γ_{xy}

TABLE 10.8.1

INTEGRATION POINT LOCATIONS FOR SOLID ELEMENTS
(1 Integration Point)

| Point | r | s | t |
|-------|---|---|---|
| 1 | 0 | 0 | 0 |

TABLE 10.8.2

INTEGRATION POINT LOCATIONS FOR SOLID ELEMENTS
(6 Integration Points)

| Point | r | s | t |
|-------|----|----|----|
| 1 | -1 | 0 | 0 |
| 2 | 0 | -1 | 0 |
| 3 | 0 | 0 | -1 |
| 4 | 1 | 0 | 0 |
| 5 | 0 | 1 | 0 |
| 6 | 0 | 0 | 1 |

TABLE 10.8.3

INTEGRATION POINT LOCATIONS FOR SOLID ELEMENTS
(8 Integration Points)

| Point | Nearest Node | r | s | t |
|-------|--------------|--------|------|------|
| 1 | 7 | $-h^*$ | $-h$ | $-h$ |
| 2 | 3 | $-h$ | $-h$ | h |
| 3 | 6 | $-h$ | h | $-h$ |
| 4 | 2 | $-h$ | h | h |
| 5 | 8 | h | $-h$ | $-h$ |
| 6 | 4 | h | $-h$ | h |
| 7 | 5 | h | h | $-h$ |
| 8 | 1 | h | h | h |

* $h = 0.5773502691896$

TABLE 10.8.4

INTEGRATION POINT LOCATIONS FOR SOLID ELEMENTS
(14 Integration Points)

| Point | r | s | t |
|-------|-------|----|----|
| 1 | *-a | 0 | 0 |
| 2 | a | 0 | 0 |
| 3 | 0 | -a | 0 |
| 4 | 0 | a | 0 |
| 5 | 0 | 0 | -a |
| 6 | 0 | 0 | a |
| 7 | ** -b | -b | -b |
| 8 | -b | b | -b |
| 9 | -b | -b | b |
| 10 | -b | b | b |
| 11 | b | -b | -b |
| 12 | b | b | -b |
| 13 | b | -b | b |
| 14 | b | b | b |

* a = 0.795822426

** b = 0.758786911

TABLE 10.8.5

INTEGRATION POINT LOCATIONS FOR SOLID ELEMENTS
(27 Integration Points)

| Point | Nearest Node | r | s | t |
|-------|--------------|-----|----|----|
| 1 | 7 | -h* | -h | -h |
| 2 | 19 | -h | -h | 0 |
| 3 | 3 | -h | -h | h |
| 4 | 14 | -h | 0 | -h |
| 5 | 24 | -h | 0 | 0 |
| 6 | 10 | -h | 0 | h |
| 7 | 6 | -h | h | -h |
| 8 | 18 | -h | h | 0 |
| 9 | 2 | -h | h | h |
| 10 | 15 | 0 | -h | -h |
| 11 | 25 | 0 | -h | 0 |
| 12 | 11 | 0 | -h | h |
| 13 | 26 | 0 | 0 | -h |
| 14 | 27 | 0 | 0 | 0 |
| 15 | 23 | 0 | 0 | h |
| 16 | 13 | 0 | h | -h |
| 17 | 22 | 0 | h | 0 |
| 18 | 9 | 0 | h | h |
| 19 | 8 | h | -h | -h |
| 20 | 20 | h | -h | 0 |
| 21 | 4 | h | -h | h |
| 22 | 16 | h | 0 | -h |
| 23 | 21 | h | 0 | 0 |
| 24 | 12 | h | 0 | h |
| 25 | 5 | h | h | -h |
| 26 | 17 | h | h | 0 |
| 27 | 1 | h | h | h |

* $h = 0.7745966692415$

Line 2 - stresses σ_{xx} , σ_{yy} , σ_{zz} , σ_{yz} , σ_{xz} , σ_{xy}

Line 3 - principal stresses σ_1 , σ_2 , σ_3

The shear strains γ_{ij} are "engineering" values which are twice the tensorial shear strains. In addition, the element having the highest von Mises effective stress for each material used is identified and printed. Note that, since yield stress values are not required as input in linear analyses, the effective stress can be computed correctly only for isotropic materials (for anisotropic material, the direction-dependent yield stress values usually appear in the definition of effective stress).

In nonlinear problems, four lines of output are provided per integration point:

Line 1 - total strains

Line 2 - plastic strains

Line 3 - total stresses

Line 4 - principal stresses.

Also, the yield function F , equivalent stress σ_{eq} , and estimated relative error f_R are output at each point; these quantities are defined and described in Section 10.8.2.

10.8.4 Thin Plate/Shell Elements (Type 5)

Output for the MAGNA thin shell element is presented in the local coordinates used for element stiffness formulation. These coordinate directions are determined in a similar manner to those used for the two-dimensional elements (Section 10.8.2), but are located in the element midsurface (Figure 10.8.3). Due to the simplicity of the element shape functions, the most accurate stress and strain values are those obtained at the element centroid; for this reason, all printed strain and stress values are evaluated at the center of the element for selected stations through the element thickness.

For linear problems, the output is labeled as follows:

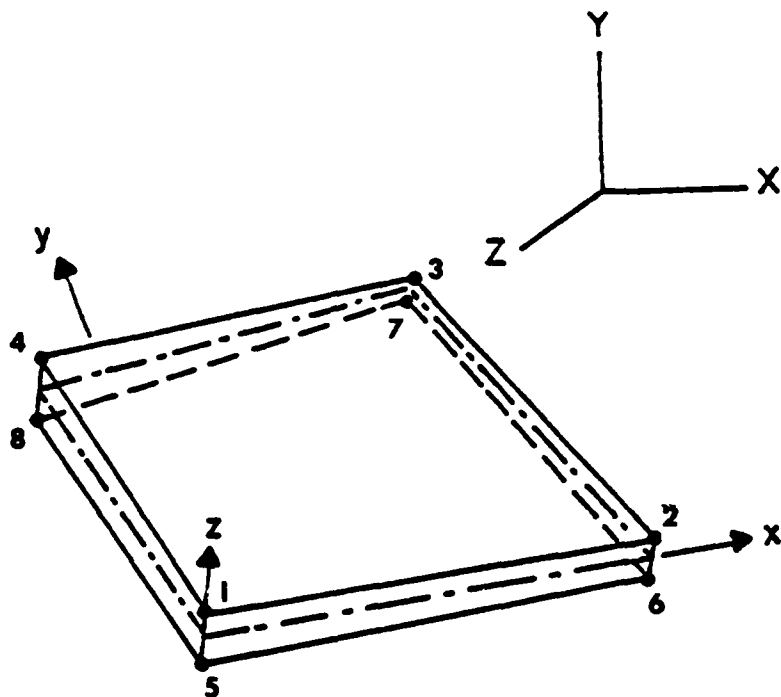


Figure 10.8.3 Local Coordinate Directions for Thin Shell Elements.

| <u>LABEL</u> | <u>QUANTITY</u> |
|--------------|--------------------------------------|
| EPS (U) | centroidal strains at upper surface |
| EPS (L) | centroidal strains at lower surface |
| UPPER | centroidal stresses at upper surface |
| MIDDLE | centroidal stresses at midsurface |
| LOWER | centroidal stresses at lower surface |

For each line of output, the xx, yy and xy components of strain or stress are given, along with maximum and minimum (principal) values. One set of the above output is printed for each shell element in the model.

In nonlinear analysis, two lines of output are produced at each sampling point through the element thickness, proceeding from the lower to the upper surface at the element centroid. These lines are labeled EPS(i) and SIG(i), where i denotes the number of the sampling point. In nonlinear elastic analyses, $1 \leq i \leq 3$, so that i = 1 denotes the lower face of element, i = 2 the midsurface, and i = 3 the upper surface. At each point, xx, yy, xy, maximum and minimum values of both strain and stress are given as output.

10.8.5 Layered Shell Elements (Type 11)

Strain and stress data for the layered shell is fully three dimensional, and are referred in the output to the global coordinate directions. All printed strains and stresses are listed by layers, with layer 1 being defined as the lower surface of the element ($t = -1$; see Figure 10.8.4).

In linear problems, strain and stress data is output for each layer at the corners of an element. Corners are labeled 1 through 4, corresponding to nodes 1-4 in Figure 10.8.4. Output lines for upper and lower surfaces of each layer are labeled "UP" and "LO", respectively. The output data consists of:

- element, corner, and layer numbers;
- strains $\epsilon_{xx}, \epsilon_{yy}, \epsilon_{zz}, \gamma_{yz}, \gamma_{xz}, \gamma_{xy}$;

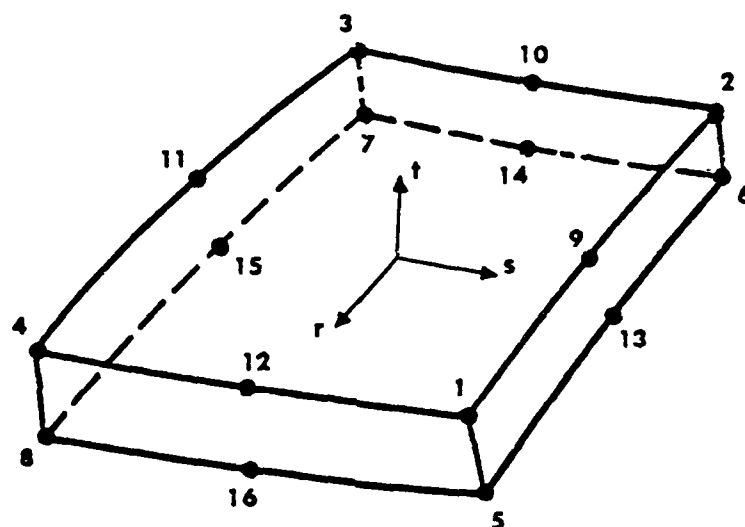


Figure 10.8.4. Node Numbers and Natural Coordinate Directions for Layered Shell Element.

- stresses σ_{xx} , σ_{yy} , σ_{zz} , σ_{yz} , σ_{xz} , σ_{xy} ;
- equivalent stresses σ_{eq} .

The shear strains γ_{ij} are engineering strains, which are twice the corresponding tensorial values.

Nonlinear strain and stress output for the layered shell element is similar to that for linear analysis; however, data are printed for integration points in each layer of an element. Within a particular layer and (upper or lower) surface, the integration points form a two-dimensional pattern (as in Figure 10.8.2). The precise locations of the integration points in terms of element natural coordinates are summarized in Table 10.8.6.

10.8.6 Beam Elements (Type 12)

The state of stress in the Type 12 curved beam element is characterized by a direct (axial and/or bending) stress, and two transverse shear stresses. Therefore, all element output is referred to the local coordinate system shown in Figure 10.8.5.

In linear problems, stresses are always distributed at most linearly over the beam cross-section and may be characterized exactly by stress resultants (forces and moments). The resultant quantities printed are:

- axial force (parallel to x);
- transverse shear forces in local y and z directions;
- twisting moment (moment about x); and
- bending moments about local y and z.

No strain data is printed for the beam element.

For nonlinear problems, the stresses may vary more than linearly over the cross-section, and shear stresses cannot be separated uniquely into contributions due to torsion and

- Each of nodes "3" and "4" is optional
- Nodes "3" and "4" may be identical in curved elements

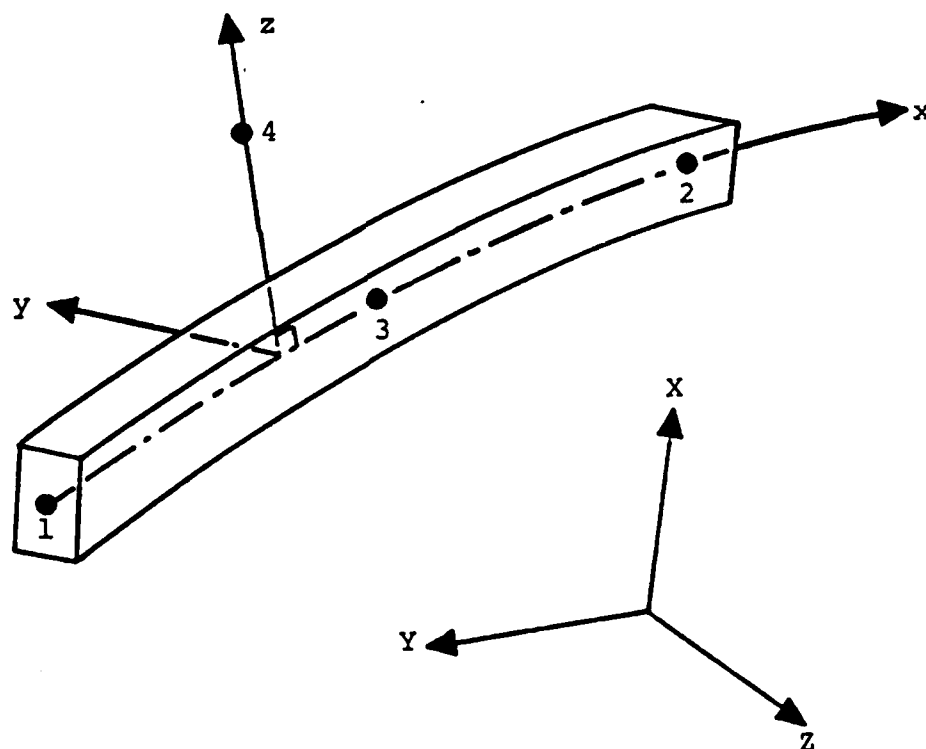


Figure 10.8.5. Local Coordinate Axes for Three-Dimensional, Curved Beam Element.

TABLE 10.8.6

INTEGRATION POINT LOCATIONS FOR SIXTEEN-NODE
LAYERED SHELL ELEMENT

| Point | Nearest Nodes | r** | s** |
|-------|------------------|-----|-----|
| 1 | 1,5 | -h* | -h |
| 2 | 4,8 | -h | h |
| 3 | 2,6 | h | -h |
| 4 | 3,7 | h | h |

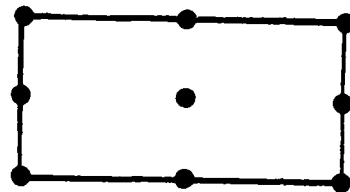
* $h = 0.5773502691896$

** A similar array of integration points is located
at the upper and lower surfaces of each layer.

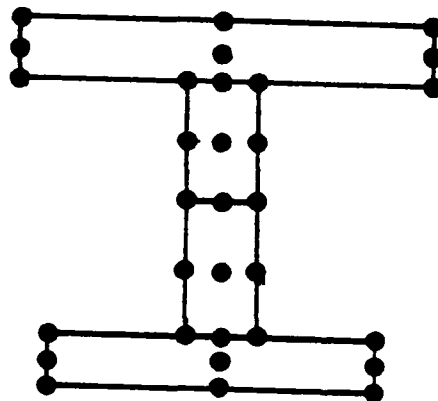
transverse shear strain. For this reason, local stresses are output in nonlinear analysis, rather than stress resultants. Within a cross-section, output for all integration points (identified by their local y,z coordinates) is printed, consisting of:

- element and integration point numbers;
- local coordinates of the integration point;
- stresses ϵ_{xx} , ϵ_{xy} , ϵ_{xz} ; and
- effective plastic strain ϵ_p .

A typical grid of integration points within the cross-section is shown in Figure 10.8.6. The number and location of these points depends upon the number of segments in the cross-section.



1 Segment
9 Integration Points



4 Segments
36 Integration Points
(5 Overlap)

Figure 10.8.6. Typical Integration Point Locations in Beam Element Cross-Section.

10.9 SOLUTION SUMMARY

At the end of every complete solution, a brief summary is displayed giving the total amounts of CPU time consumed in each stage of the analysis, as well as a summary of input/output resources used. This output is largely self-explanatory, and is used to determine the critical phases of the solution in terms of computing expense. An example of the solution time summary (in this case for a nonlinear static problem) is shown below.

SOLUTION TIME SUMMARY

| | |
|---|--------|
| INPUT AND TABLE SETUP | .406 |
| ELEMENT MATRICES, EQUILIBRIUM CORRECTION AND STRESS RECOVERY | 26.508 |
| MATRIX ASSEMBLIES | 1.601 |
| LOADS CALCULATIONS | .505 |
| EQUATION SOLUTIONS | 4.708 |
| DISPLACEMENT RECOVERY | 1.297 |
| TOTAL LOAD INCREMENTS | 9 |
| TOTAL ITERATION CYCLES | 23 |

SUMMARY OF SEQUENTIAL I/O OPERATIONS

| | |
|----------------------------------|--------|
| READ REQUESTS | 5601 |
| WRITE REQUESTS | 1953 |
| WORDS TRANSFERRED (INPUT) | 456357 |
| WORDS TRANSFERRED (OUTPUT) | 296469 |

For the VAX 11/780 version of MAGNA, any modification of the program storage or introduction of user-written subroutines requires that a new executable file be created. This revised executable file may be reused as required with the modified storage parameters and user routines intact. For this reason, a summary is also printed at the conclusion of the analysis run to record storage allocation parameters which are preset in the executable file used.

10.10 ERROR AND WARNING MESSAGES

The following is a summary of error and warning statements issued by the MAGNA program in addition to messages given by the operating system. These diagnostics fall in four general categories:

- (1) errors in model definition,
- (2) error conditions occurring during the actual solution,
- (3) errors due to exceedance of program capacity or invalid file operations, and
- (4) system-generated error messages.

The compilation of diagnostic messages below is divided into these four categories. Probable causes and corrective actions are listed whenever possible.

10.10.1 Model Definition Error Diagnostics

■ ERROR IN ELEMENT GEOMETRY TYPE = ... ELEMENT = ...

Error Type : Fatal

Meaning : Indicated element possesses a singular isoparametric mapping on the interior of the element, indicating an unreasonably distorted geometry.

Probable Cause : Error in connectivity for the element, or incorrect definition of coordinates of one or more nodes connected to the elements.

Corrective Action : Verify that the connectivity for the element is correct. If so, determine whether the coordinates of each node in the connectivity list have been correctly defined. If the connectivity and coordinates are correct, refine the model to give a less distorted shape for the element.

■ FOLLOWING ELEMENT IN ERROR (Shell Element Only)

Error Type : Nonfatal

Meaning : A thin shell element has been defined for which the isoparametric mapping is singular at one of the corners, indicating the possibility of unreasonable distortion.

Probable Cause : Error in connectivity or nodal coordinates for the element. In certain cases, this diagnostic may be issued when the element is correctly defined, for example, if two adjacent sides of the element are made coplanar.

Corrective Action : Check the element connectivity and the coordinates of each node connected to the element. If these are correct, refine the model to give a less distorted element shape.

■ WARNING - CONSTRAINED NODE IN ABOVE LIST IS UNDEFINED

Error Type : Nonfatal

Meaning : A boundary condition has been applied to a node whose number is greater than the number of nodes specified at the time of coordinate input. The constraint is processed but may cause an error.

Probable Cause : Incorrect definition of the number of nodes in the model, or keypunching or other error in the boundary condition input.

Corrective Action : Correct the constraint as required and rerun.

■ WARNING - SPECIFIED RANGE OF NODES NOT EVENLY DIVISIBLE BY INCREMENT

Error Type : Nonfatal

Meaning : A possible error has been detected in the generation of boundary conditions for a series of nodes.

Probable Cause : Error in starting or ending node numbers given for the constraint, or in the increment value.

Corrective Action : Check the list of nodal degrees of freedom in the output to verify that the correct nodes have been constrained. If extra nodes are constrained which were unintended, correct the input and rerun.

■ WARNING - UNDEFINED NODAL COMPONENT IN CONSTRAINT

Error Type : Nonfatal

Meaning : An undefined direction (component of displacement) has been referenced in a boundary condition. Although the undefined degree of freedom is simply ignored by the program, a constraint which was intended may not be applied if a keypunching error is involved.

Probable Cause : Usually due to keypunching error.

Corrective : Verify that all nodal degrees of
Action freedom to be constrained actually
have been suppressed, by checking
the final list of nodal degrees of
freedom. If this is not the case,
correct the error and rerun.

■ ERROR - SUPPRESSED DEGREE OF FREEDOM APPEARS IN
FOLLOWING CONSTRAINT

Error Type : Nonfatal

Meaning : An inactive displacement degree of
freedom is specified in a linear
constraint equation. The result may
not be intended. The superfluous
degree of freedom is ignored by the
program.

Probable : Incorrect specification either of the
Cause linear constraint or of the boundary
conditions at the node in question.

Corrective : Verify that both the linear constraint
Action and the boundary condition which
suppressed the degree of freedom are
correctly specified. If not, correct
and rerun.

■ LOAD INPUT ERROR, CODE =

Error Type : Nonfatal

Meaning : A nodal force has been incorrectly
specified, and will be ignored by the
program. Error codes are interpreted
as follows:

Code 1 : Undefined node

Code 10 : Undefined direction

Code 100 : Load applied to suppressed
degree of freedom

Code 1000 : Data curve number not
specified (nonlinear
analysis)

Code 10000 : Undefined loading condition
specified (linear analysis)

Error codes may be summed; for example,
CODE = 1010 indicates the occurrence
of two errors (code = 10 and code =
1000).

Probable : Error in loads input, boundary
Cause conditions, or specifications of the
number of loading conditions.

Corrective : Correct and rerun.
Action

■ ERROR - INDICATED ELEMENTS ARE UNDEFINED

Error Type : Nonfatal

Meaning : Pressure loads have been defined for
an element type which is not present
in the model. The specified pressures
are ignored.

Probable : Incorrect specification of element
Cause type in either element or distributed
loads data.

Corrective : Correct and rerun.
Action

■ ERROR - INVALID ELEMENT RANGE

Error Type : Nonfatal

Meaning : An element or series of elements
specified in pressure loads input
does not exist. The input line is
ignored.

Probable : Incorrect specification of element
Cause type, or starting/ending element
numbers.

Corrective : Correct and rerun.
Action

■ ERROR - INVALID SURFACE NUMBER

Error Type : Nonfatal

Meaning : Pressures have been specified on an
undefined element surface (≤ 0 , or > 6).
The input line is ignored.

Probable : Keypunching error or incorrect ordering
Cause of data.

Corrective : Correct and rerun.
Action

10.10.2 Solution Error Diagnostics

■ NONPOSITIVE PIVOT AT EQN VALUE =

Error Type : Nonfatal

Meaning : A non-positive diagonal element has been encountered during solution of the system equations, indicating that the stiffness (or effective stiffness) matrix is no longer positive definite.

Probable Cause : In linear analysis, this error generally indicates the presence of modeling errors not detected during input, or of possible ill-conditioning of the equations due to distorted elements, inadequate supports, or excessive use of reduced numerical integration. In nonlinear analysis, the presence of non-positive pivot values often signals the onset of either structural instability (due to passage through a limit point) or numerical instability (due to the rapid increase in plastic strains in a materially nonlinear analysis).

Corrective Action : For linear problems, check the model (e.g., by plotting) for unreasonable element distortion. If very large displacements are predicted, check for proper application of the boundary conditions or, when reduced integration is being used, increase the integration order in selected elements to stabilize the solution. In materially nonlinear problems, check for rapid increase of the plastic strains; if this is the case, specify a finer tolerance for iteration, decrease the step size, or both as required. If perfect plasticity has been assumed (no strain hardening), check to see if catastrophic collapse has occurred. When buckling is suspected (i.e., limit-point instability), the analysis can be rerun as a dynamic analysis with very large time steps, in which case inertial effects will stabilize the solution into the post-buckling range.

■ ZERO PIVOT AT EQN

Error Type : Fatal

Meaning : Same as above, except that a pivot value is exactly zero to machine precision.

Probable Cause : Usually due to insufficient boundary conditions, excessive use of reduced integration, or the occurrence of plastic collapse or limit-point instability.

Corrective Action : In linear problems, or in the first increment of nonlinear problems, insufficient supports are usually the problem. Check for the validity of the boundary conditions, or increase the order of numerical integration in strategically placed elements. In the later stages of a nonlinear analysis, collapse or instability is generally the source of trouble. These are corrected as outlined under the previous message.

■ BAD DIAGONAL I = D(I) =

Error Type : Fatal

Meaning : Eigenvalue solution has failed due to a zero or very small positive pivot value, indicating either a singularity or severe ill-conditioning in the model.

Probable Cause : Generally due to insufficient supports, excessive use of reduced integration, or highly distorted element shapes.

Corrective Action : Correct constraints, increase the order of element integration, or refine the model to eliminate unreasonable element geometry.

■ SOLUTION STOP - RESIDUAL FORCES INCREASING

■ SOLUTION STOP - DISPLACEMENT SOLUTION DIVERGING

■ SOLUTION STOP - NO CONVERGENCE IN MAXIT CYCLES

Error Type : Fatal

Meaning : The iterative solution for nonlinear equilibrium is nonconvergent or divergent at the current load level or time step. This lack of convergence is detected by large increases in out-of-balance forces, diverging estimates for the incremental displacements, or exceedance of a specified maximum number of cycles of iteration.

Probable : Usually due to the use of loading or time increments which are too large for the use of a simplified stiffness formulation (constant or averaged stiffness) in elements which are strongly nonlinear, or to an insufficient frequency of equilibrium iterations.

Corrective : Change the method of stiffness
Action formulation to full tangent stiffness in strongly nonlinear elements. Decrease the number of steps between stiffness recalculations and/or equilibrium iterations as required, or decrease the specified time or load increment value. Switching from modified Newton iterations to either full or combined Newton-Raphson iterations may also be helpful.

10.10.3 Central Memory and File Handling Errors

■ INSUFFICIENT LENGTH IN /..../

Error Type : Fatal

Meaning : One of the core-resident COMMON areas which determine the program capacity is not sufficient to process the problem.

Probable Cause : A large number of nodes, load cases, degrees of freedom or stiffness matrix partitions dictates the use of more array space.

Corrective Action : Modify the length of the indicated block of storage as indicated in Chapter 7.

■ WORK SPACE....INSUFFICIENT FOR MATRIX STORAGE

Error Type : Fatal

Meaning : The longest column of the stiffness (or effective stiffness) matrix is too long to be stored in high-speed memory.

Probable Cause : Insufficient array space, or poor node numbering of a large model.

Corrective Action : Renumber nodes if possible to reduce the local matrix bandwidth. Increase the length of COMMON/BLANK/ as indicated in Section 7.1.2.

■ INSUFFICIENT SPACE FOR ELEMENT FORCE DATA

■ INSUFFICIENT STORAGE FOR LOADS

Error Type : Fatal

Meaning : The program storage is insufficient for element or nodal force data.

Probable Cause : Large number of loading conditions in linear static analysis; very large number of surface pressure input lines.

Corrective Action : Reduce the number of load cases or pressure inputs (use generation features),

or increase the working storage in
COMMON/BLANK/ as outlined in
Chapter 7.

■ I/O ERROR UNIT =, SUBROUTINE =

Error Type : Fatal

Meaning : An irretrievable error has occurred
during transmission of data to or from
peripheral storage.

Probable Cause : In many instances, this type of error
occurs due to incorrect use of the
internal data generation features of
the program (e.g., causing too many
or too few elements to be generated,
etc.). If the input data has been
processed correctly, error is due to
an internal file-handling error.

Corrective Action : Verify that all input has been
specified and processed correctly.
If the problem persists, contact
installation analyst or the developer.

10.10.4 System Errors and Abnormal Termination

In some situations, modeling or data formatting
errors may not be trapped by the built-in data checks in MAGNA.
The usual result is an abnormal job termination due to one of
the three following types of run-time errors:

- (1) Arithmetic Overflow
- (2) Random Access File Errors
- (3) Sequential File Errors

Although the error messages generated by the system under these
conditions may vary widely, the error is usually recognizable:
for example, the arithmetic error will appear as a MODE error
on CDC or CRAY machines, divide check or overflow error on VAX,
etc. The sources of each of these types of problems under normal
conditions are summarized in the following paragraphs.

Arithmetic Errors. The most common sources of
arithmetic errors are:

1. Poisson's ratio declared as $\nu = 0.5$
2. Extensional modulus/moduli $E_i = 0.0$
3. A material property set is referenced, but not created
4. A nonlinear element has erroneous geometry.

Materials data should be checked to ensure that the Poisson's ratio is less than 0.5 for isotropic materials, that all moduli are positive, and that all materials used in element definitions have been defined previously. Errors in the materials data such as (1)-(3) will normally result in termination during the element input phase. The fourth type of arithmetic error generally results when a geometry error is not isolated by performing a preliminary *linear* analysis. This type of error typically occurs during the first cycle of element calculations; the preceding MAGNA output is the iteration information for INCREMENT=0 and NUMIT=0.

Random File Errors. The usual source of random file access errors is an erroneous reference to an undefined data curve. Care should be taken to verify that none of the following two conditions exist:

1. An elastic-plastic material is assigned a stress-strain curve number not defined in the data curves input.
2. A nodal or element load specification references an undefined data curve number.

Sequential File Errors. Sequential file errors (such as end-of-file condition or I/O list-exceeds-record-length) are sometimes caused by an incorrect use of element generation facilities, or by a failure to input element data in the proper sequence. The following conventions should be noted:

- the number of elements declared on the element type header(s) must match the number of elements defined;
- element types must be input in ascending order; and

- within element types, individual elements are numbered between 1 and the number of elements of a given type.

In most cases, a quick review of the element input echo will help to isolate the source of the problem.

10.11 STRAVG OUTPUT

STRAVG (Section 5.7) is a companion program to MAGNA which performs extrapolation of strain and stress values from integration points to the nodal points of the model, and finally generates continuous nodal strain and stress information. The nodal strain and stress data is useful for examining interior and/or surface stresses at easily identified points, for comparison with strain gauge data, and for the generation of contour and surface plots (Section 11.2). The data generated by STRAVG also permits the plotting of individual layer stresses in multilayered shell elements (Type 11).

The STRAVG utility is often executed as a part of the MAGNA analysis run, and its printed output is described in the following sections. Postprocessing files, which are also generated by STRAVG, are described separately in Section 5.7.

10.11.1 Model Parts Definitions

The first section of STRAVG output describes the definition of "parts" within the finite element model. A "part" is defined as any unique combination of element type and material number (or laminate number, for element Type 11). The definition of each part is summarized in a table such as the one shown below.

| Part No. | Elem. Type | Material No. |
|----------|------------|--------------|
| 1 | 7 | 1 |
| 2 | 7 | 2 |
| 3 | 8 | 1 |

A list of elements assigned to each model part is also output; within each part, elements are listed in sequential order (ascending element types and number) as defined in the original input data.

The significance of a model part as defined in STRAVG is that stress and strain values for adjacent elements are combined to generate nodal values *only* if the elements belong to the same part. Due to the differences in material properties

which exist between elements of different parts, discontinuities in strain and stress values will necessarily occur. By performing smoothing operations only within parts, such discontinuities are correctly accounted for in the data generated by STRAVG.

10.11.2 Nodal Strains and Stresses

The remaining output from STRAVG consists of nodal values for all components of strain and stress. These values are output for each increment, loading condition or mode shape written to the MPOST file by MAGNA (see Sections 5.7 and 8.2).

At each increment processed by STRAVG, nodal values are generated separately for each part, for all nodes connected to the part. The output is sorted by increments, then by parts, and finally by node number. For a particular part, only those node points connected to the part are printed; a node may appear more than once in the listing for each increment if it is connected to more than one part of the model. For each node, the printed output consists of the Green's strains (ϵ_{xx} , ϵ_{yy} , ϵ_{zz} , ϵ_{yz} , ϵ_{xz} , ϵ_{xy}) and Piola stresses (σ_{xx} , σ_{yy} , σ_{zz} , σ_{yz} , σ_{xz} , σ_{xy}).

10.11.3 Error Messages

Error messages are output from STRAVG in numeric form (e.g., "FATAL ERROR NUMBER 100"). The corresponding error descriptions are given in Table 10.11.1. The possible errors are of two types, file errors ("F" in the Table) and storage limit errors ("S" in the Table). File errors are typically encountered when the MPOST file generated in MAGNA is either nonexistent (not requested in the problem input) or incomplete (due to premature termination of MAGNA). Storage limit errors occur when the array areas in STRAVG are insufficient to process a problem. In the event a storage limit error occurs, a larger-capacity version of STRAVG should be requested from the installation analyst or the developer.

TABLE 10.11.1

STRAVG ERROR MESSAGES

| ERROR NO. | ROUTINE | DESCRIPTION | TYPE |
|-----------|---------|--|------|
| 50 | STRAVG | Storage exceeded (element data) | S |
| 60 | NCOUNT | Coordinate data not found | F |
| 70 | NCOUNT | Storage exceeded (nodal coordinate data) | S |
| 80 | WHINCR | Displacement data not found | F |
| 100 | GETMAT | Materials data not found | F |
| 102 | ELFILE | Element connectivity data not found | F |
| 105 | ELGEOM | Coordinate data missing or unusable | F |
| 108 | ELDISP | Nodal displacements not found | F |
| 109 | ELDISP | Displacement data missing or unusable | F |
| 200-204 | ELSUM | Element results data not found | F |
| 501 | DEFPRT | Storage exceeded (parts data) | S |

CHAPTER 11

PLOTTING UTILITIES

The MAGNA finite element program is supported by three types of plotting utilities:

- undeformed and deformed geometry plotting,
- contour and relief plotting of analysis results, and
- variable versus variable plotting.

On CDC computers, these graphics utilities are available with the Tektronix 4014 graphics terminal (or other PLOT-10¹ compatible hardware) and with the Hewlett-Packard 7221A four-color pen plotter. On the Hewlett-Packard plotter, transparencies for overhead projection can also be made directly. The Tektronix versions of the graphics utilities are also available on the Digital Equipment VAX 11/780.

Computer graphics utilities for use with MAGNA are divided into three physically distinct programs, GPLOT (geometry plotting), CPLOT (contour/relief plotting) and XYPLOT (variable versus variable plots), all of which can be accessed independently of MAGNA itself. Undeformed geometry plotting, which is done interactively, requires only the MAGNA data file, so that graphical verification of a finite element model can be obtained without submitting a large analysis run. Contour, relief, deformed geometry and x-y plots are produced interactively using the postprocessing files created by MAGNA (Section 5.7), so that decisions concerning which results are to be plotted may be made after the analysis is complete.

Commands, options and representative output from the graphics support programs are discussed in Section 11.1 through 11.3. Job control procedures necessary for accessing the programs are summarized in Section 11.4.

11.1 GPLOT - DEFORMED AND UNDEFORMED GEOMETRY PLOTTING

GPLOT is an interactive utility plotting program which accepts as input either a MAGNA data file (Chapter 8) or the MPOST postprocessor file (Section 5.7), for plotting undeformed and/or deformed geometry of a finite element model. A wide variety of options and features is available in GPLOT; these include

- orthogonal or perspective views,
- translations, rotations and/or reflections,
- labeling of nodes (all or selected surfaces) and elements,
- zooming, clipping and unscaling,
- exploded views, and
- plotting of selected elements by element type and number.

GPLOT is accessed using the command procedures described in Section 11.4. Prior to issuing the command to initiate execution, it is necessary only to attach the file to be plotted under the local (temporary) file name TAPE5. For the VAX 11/780 version of GPLOT, the file to be used for plotting is requested at the start of execution. GPLOT automatically retrieves all additional files which are required for execution, and returns them at the end of a session.

During execution, GPLOT is controlled by commands entered by the user which select options and define plotting parameters. Valid commands are summarized below. In each case, only the first four characters of the command need be entered. In alphabetical order, the commands recognized by GPLOT are:

- | | |
|-------------|--|
| <u>AXIS</u> | - select option to draw Cartesian axes |
| <u>CLIP</u> | - define "clip plane" position; used for situations in which eye position is inside the model. |
| <u>CUBE</u> | - define limits on points to be plotted, based on minimum and maximum values of X,Y,Z |

| | |
|-------------------|---|
| <u>DEFAULT</u> | - reset all parameters and options to their default values |
| <u>DEFORM</u> | - select geometry to be plotted: undeformed, deformed, or both |
| <u>DRAW</u> | - plot the model using current values of all parameters and options. |
| <u>ELEMENTS</u> | - specify plotting of selected elements only |
| <u>EYE</u> | - define viewing position in X,Y,Z coordinates |
| <u>HELP</u> | - display a list of valid commands |
| <u>LABEL</u> | - select labeling of nodes and/or elements |
| <u>NEW</u> | - initiate input of a different model (more than one model may be stored on a single data file) |
| <u>PROJECTION</u> | - select orthogonal or perspective view |
| <u>REFLECT</u> | - specify reflection of model with respect to a coordinate plane |
| <u>ROTATE</u> | - define rotations of model about coordinate axes |
| <u>SCALE</u> | - select scaling/unsaling of the plot |
| <u>SHRINK</u> | - select exploded view |
| <u>STOP</u> | - terminate execution |
| <u>SUMMARY</u> | - list of current values of all parameters and plot options |
| <u>TIME</u> | - display CPU time elapsed since sign-on |
| <u>TRANSLATE</u> | - define translations of the model along coordinate axes |
| <u>VERTICAL</u> | - select vertical axis direction |
| <u>ZOOM</u> | - define a portion of the model for "close-up" viewing using the cursor. |

In the command mode, a prompt symbol "*" is displayed whenever the program is ready to accept a new command. As commands are entered, additional input is requested as needed to define the

relevant parameters. Input requests are self-documenting and straightforward; one or two short sessions should be sufficient for the inexperienced user to become acclimated to the full range of capabilities of GPLOT. A sample terminal session using GPLOT is reproduced in Figure 11.1.1

COMMAND- ATTACH,P,PLOTPROC, ID=BRCKCHAM, MR=1.
AT CY= 900 SHAPTEL

COMMAND- ATTACH, TAPES, MAGNADATA, CY=1.

COMMAND- BEGIN, GPLOT, P.

BEGIN GPLOT - PRE/POST ANALYSIS GEOMETRY
PLOTTER FOR MAGNA PROGRAM.

ENTER THE CHARACTERS PER SECOND: 120
TERTRONIX OR HP PLOTTER(T.N): 1
TERTRONIX TERMINAL TYPES ---
0, 4800-1

1, 4810 / 4812 / 4813

2, 4814 / 4815

3, 4814 / 4815 (EM,GR,MOD.)

ENTER TERMINAL TYPE (0, 1, 2, 3).....: 3

MODEL INPUT FILE TYPES:

1 - INPUT DATA FILE

2 - POSTPROCESSOR (M-POST) FILE

ENTER FILE TYPE(1,2): 1

ENTER THE MODEL NUMBER

(= 1 IF ONLY ONE MODEL ON FILE): 1

COMMAND DESCRIPTION

AXES AXES DRAW AND LABEL
CLIP CLIP PLANE POSITION
CUBE SET MINIMA AND MAXIMA
DEFAULT SET DEFAULT VALUES
DEFORM DEFORMED MODEL REPRESENTATION
DRAW DRAW MODEL
ELEMENTS PLOTS ALL OR SELECTED ELEMENTS
EYE EYE POSITION
HELP LIST ALL COMMANDS
LABELS LABELS ELEMENTS AND/OR NODES
NEW NEW STRUCTURE
PROJECTION PROJECTION TYPE
REFLECT REFLECT A PLANE
ROTATE ROTATE MODEL ABOUT AXES
SCALE SCALE PLOT
SHRINK SHRINK ELEMENTS
STOP END PROGRAM
SUMMARY LIST ALL PARAMETER VALUES
TIME PRINT CPU TIME SINCE START OF SESSION
TRANSLATE TRANSLATE MODEL FROM ORIGIN
VERTICAL VERTICAL AXIS
ZOOM ZOOM ON THE MODEL
SITE SITE POSITION

*SUMM
LABEL AXES.....: NO
LABEL ELEMENTS.....: NO
LABEL NODES.....: NO
SCALE PLOT.....: YES
PLOT ALL ELEMENTS.....: YES
ZOOM OPTION.....: NO
AXIS VERTICAL.....: Z-AXIS
PLANE REFLECTED.....: NONE
PROJECTION TYPE.....: PERSPECTIVE
CLIP PLANE FACTOR.....: .8100
PLOT OPTION.....: UNDEFORMED
SHRINK FACTOR.....: 0.0000
EYE POSITION:
X-EYE= 100.0000
Y-EYE= 100.0000
Z-EYE= 100.0000
SITE POSITION:
XSITE= 0.0000
YSITE= 0.0000
ZSITE= 0.0000
ORIGIN TRANSLATION:
X= 0.0000
Y= 0.0000
Z= 0.0000
ROTATION:
X-ANGLE= 0.0000
Y-ANGLE= 0.0000
Z-ANGLE= 0.0000
CUBE MINIMA AND MAXIMA:
MINIMUM X 0.
MINIMUM Y 0.
MINIMUM Z 0.
STRUCTURE NUMBER.....: 1
UNDEFORMED MINIMA AND MAXIMA:
MINIMUM X 0.
MINIMUM Y 0.
MINIMUM Z 0.
*DRAW
MAXIMUM X 2.00000E+01
MAXIMUM Y 6.00000E-01
MAXIMUM Z 1.00000E+00
MAXIMUM X 2.00000E+01
MAXIMUM Y 6.00000E-01
MAXIMUM Z 1.00000E+00

Figure 11.1.1 Sample Terminal Session with GPLOT.

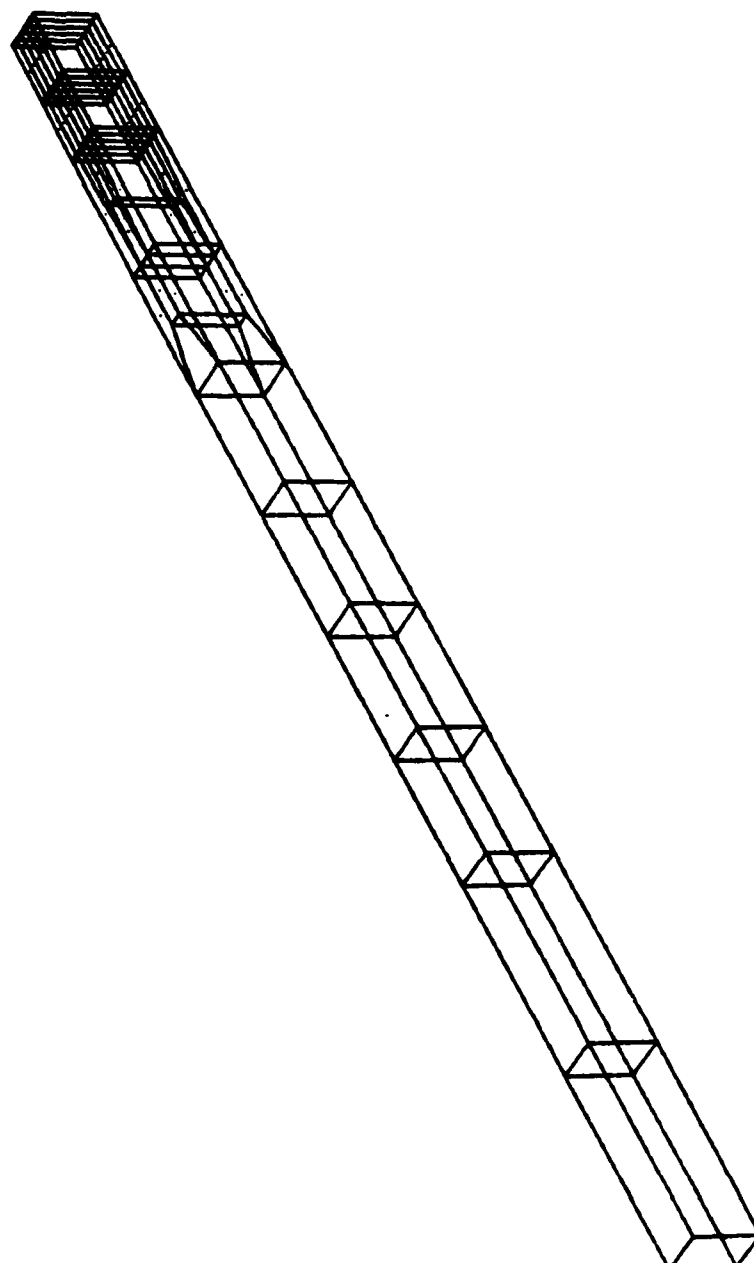


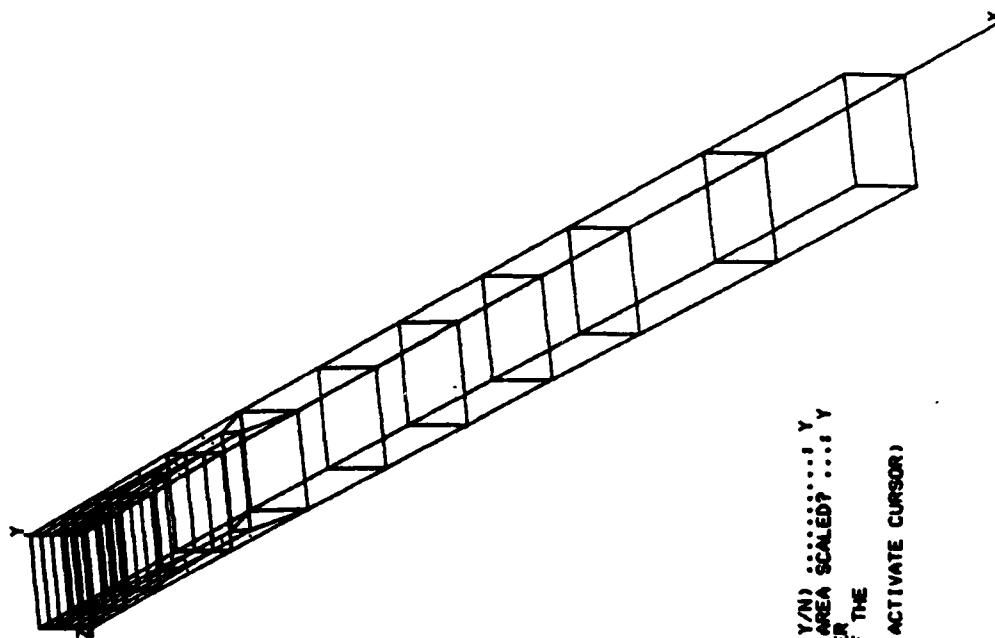
Figure 11.1.1.1 (continued)

```

*AXES      PLOT AND LABEL THE AXES?(Y,N) .....: Y
*EYE      ENTER THE EYE POSITION,
           XEYE, YEYE, ZEE .....: 100 40 20
*VERT     WHICH AXIS IS VERTICAL?
           ENTER 1 FOR X, 2 FOR Y, OR 3 FOR Z .....: 2
*PROJ     ENTER THE PROJECTION TYPE,
           PERSPECTIVE OR ORTHOGONAL(P,O) .....: P
*DRAW

```

Figure 11.1.1 (continued)



*ZOOM
 DO YOU WANT THE ZOOM OPTION(Y/N) : Y
 DO YOU WISH TO HAVE THE ZOOM AREA SCALED? Y
 DIGITIZE THE LOWER LEFT CORNER
 AND THE UPPER RIGHT CORNER OF THE
 ZOOM AREA
 (PRESS ANY KEY, THEN C/R, TO ACTIVATE CURSOR)

*DRAW

Figure 11.1.1 (continued)

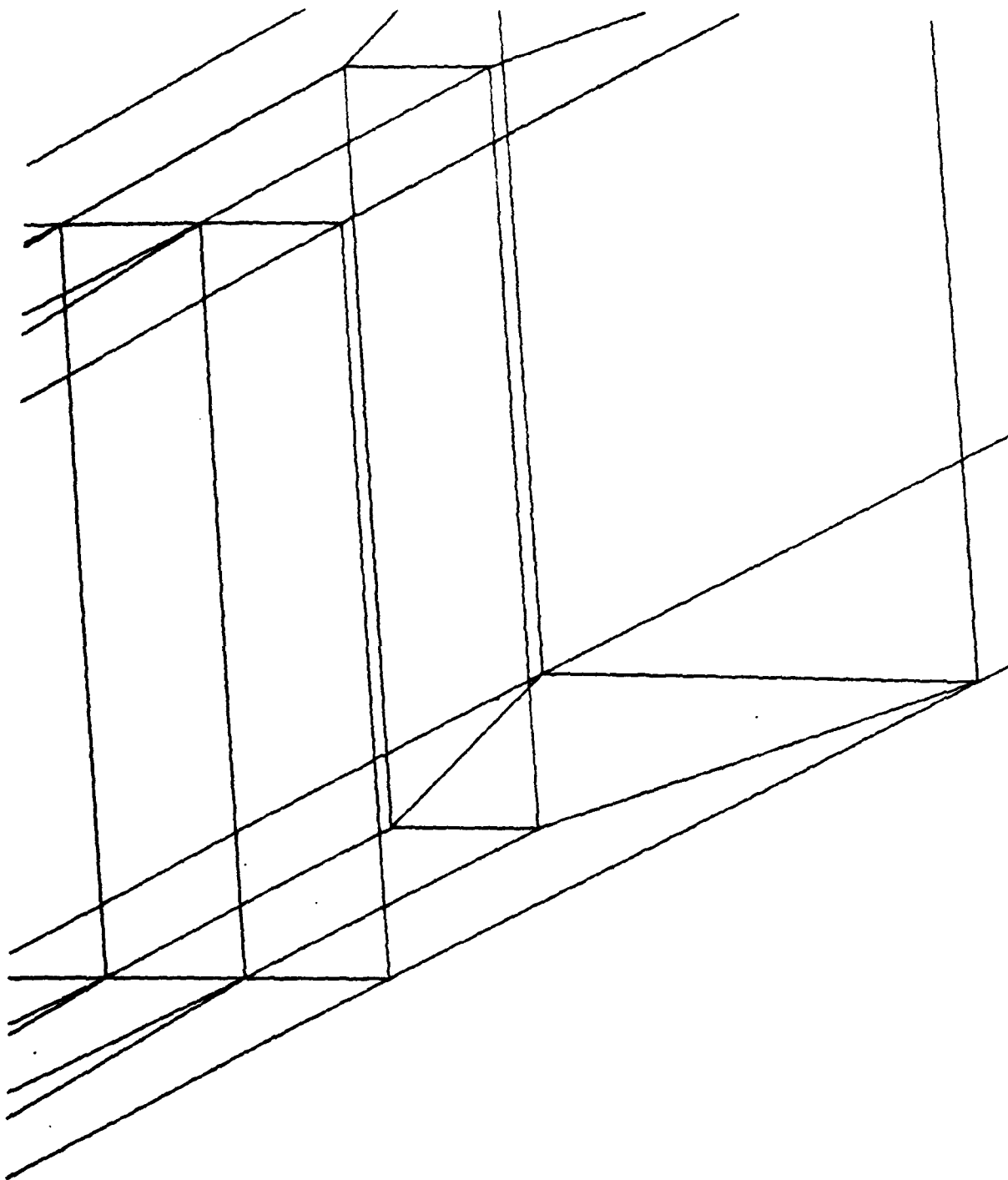


Figure 11.1.1.1 (continued)

```

*LABE
  LABEL THE ELEMENTS(Y,N) ..... N
  LABEL THE NODES(Y,N) ..... Y
  LABEL ALL THE SURFACES(Y,N) ..... Y
*DRAW

```

Figure 11.1.1 (continued)

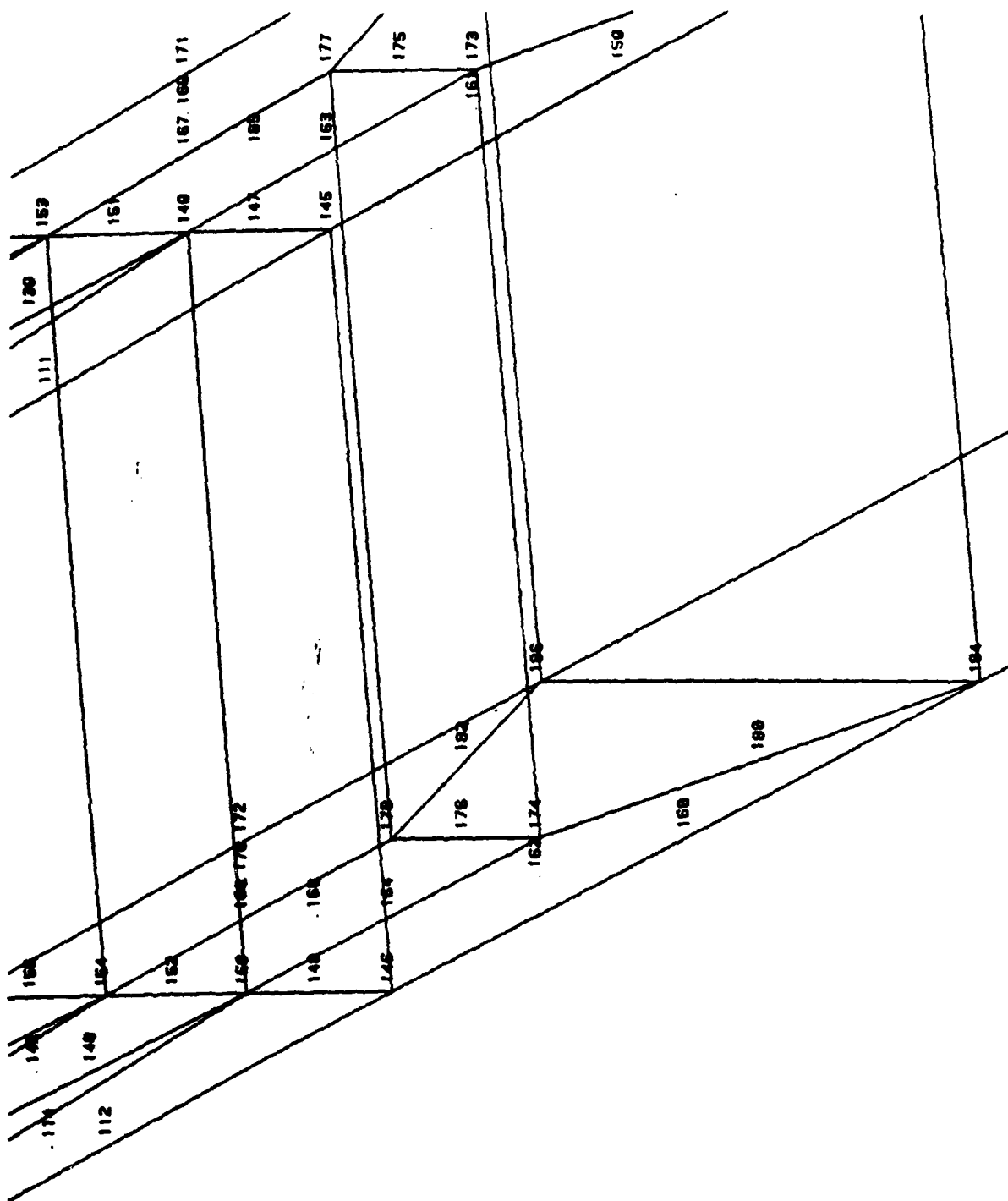


Figure 11.1.1 (continued)

11.1.1.11

*STOP

858788 MAXIMUM EXECUTION FL.
2.177 CP SECONDS EXECUTION TIME.

Figure 11.1.1 (continued)

11.2 CPLOT - CONTOUR AND RELIEF PLOTTING

CPLOT is an interactive graphics program designed for contour and relief plotting of analysis results (displacement, strain, stress) obtained using MAGNA. A contour plot displays lines on selected element surfaces along which the value of a particular function is constant; relief plots are obtained by projecting the values of a function above the plotting surface an amount proportional to their magnitude. CPLOT also permits superposition of both types of plots, or relief plotting of contour lines. Both types of plots may be superimposed on either the original geometry or the deformed geometry of a model. CPLOT accepts as input the APOST postprocessing file described in Section 5.7.

CPLOT is executed using the commands summarized in Section 11.4. Prior to entering the command to begin execution, it is necessary to attach the postprocessing file to be plotted under the local (temporary) file name TAPE99. On the VAX 11/780, the disk file name is requested by CPLOT following the start of execution. CPLOT automatically accesses all additional files which are required during execution, and returns them when the program is terminated.

As with GPLOT, the CPLOT program is controlled by alphanumeric commands, entered in response to the prompt symbol "?". Valid CPLOT commands are:

- ALEL - specify selected elements for plotting
- CLIP - specify CLIPping plane position (usually used for eye positions within the model)
- CONL - select labeling or no labeling of contour lines

- CORE - define Contour/Relief plot parameters; these include the type of plot, contour values, relief scale*, and number of relief lines per element
- CUBE - define minimum and maximum x,y,z coordinates to be plotted
- DEFO - select geometry (undeformed, deformed) to be plotted and scale displacements. Contour and relief plots may be drawn on either the undeformed or deformed geometry
- ENTE - specify plotting of ENTire Element (for 3-D element types), rather than plotting surfaces only
- EXIT - terminate execution
- EXPL - select EXPLoded view
- EYEP - specify viewing (EYE) Position
- HELP - display list of valid commands and options
- LABE - select option to plot title block, outline the finished plot, and print contour label values
- LAXS - specify plotting of Cartesian axes
- LELE - select element numbering options
- MOVI - force plotting limits to be fixed at the values entered in CUBE for a series of plots; normally used for setting up a series of frames for animation or for overlaid transparencies
- NEWD - used to set up a NEW Data set (from the same model) for plotting (displacements, stress or strain component).
- NINC - select a New INCrement to be plotted
- NODE - select option for NODE point numbering
- PLOT - PLOT the model using current values of all parameters and options

*The "relief scale" is the number of units of length to be assigned to the largest function value to be plotted. This scale controls the height of the relief plot above the plotting surface.

- PROJ - select PROJection type (orthogonal or perspective)
- REFL - specify REFlection of plot about a coordinate plane
- RESE - RESEt all parameters and options to default values
- SITE - define physical coordinate values to be located at the center of the finished plot; normally used to recenter a plotting region "clipped off" using the CUBE command
- STEP - modify STEP size used in following contour lines through an element; normally used to increase resolution on contour lines which are poorly represented with the default step size
- SUBT - enter a one-line SUBtitle on a labeled plot
- SUMM - print a SUMMary of current parameter values and options
- SURF - select the SURFace of solid elements on which contouring or relief plotting is to be done. Surfaces (numbered in the same manner as for element pressure loads) are specified by element type. SURF is also used to select a specific layer for plotting, with layered shell elements (Type 11).
- TIME - print CPU TIME elapsed since sign-on.
- VERT - specify VERTical axis direction
- ZOOM - input plotting limits via the cursor to obtain close-up views, or to turn this option off after use

At the start of execution, the RESE and NEWD commands are automatically executed to establish the default parameter values and to ready the first data set for plotting.

In addition to the usual contour/relief plots of displacement, strain or stress in the model, it is interesting to note that CPLOT can be used to obtain useful representations of deformed structural geometry. For instance, by setting contour values which are out-of-range, and selecting the deformed option, one can produce deformed geometry plots of selected surfaces of the model. Another example is the use of relief

plots on the deformed geometry, with the relief scale set to zero (function values not projected above the surface); by specifying a relatively large number of lines per element (5-8 or more), deformed plots are obtained which can be made to produce a "shaded" effect which emphasizes the patterns of deformation to a greater extent than the usual deformed geometry plot.

As with GPLOT, the CPLOT program can be utilized by even inexperienced users with a minimum of orientation, since the commands are largely self-explanatory; the interactive mode of operation of the program permits the repetition of selected plots with various options, parameter values and viewing positions to obtain the best form of presentation of results. A short sample terminal session with CPLOT is reproduced in Figure 11.2.1.

```

COMMAND- ATTACH P, PLOTPROC, ID=BROCKMAN, NR=1.
AT CY= 000 SH-APPL
COMMAND- ATTACH TAPE0, MAGNAPOST, ID=BROCKMAN
AT CY= 001 SH-APPL
COMMAND- BEGIN, CPlot2, P.

```

```

*****
BEGIN CPlot (CONTOUR / RELIEF PLOTTING)
*****
ENTER CHARACTERS PER SECOND-----128

```

```

TEKTRONIX TERMINAL TYPES ---
0. 4000-1
1. 4010 / 4012 / 4013
2. 4014 / 4015 / 4052
3. 4014 / 4015 (ENH.BR.MOD.)
4. 4114

```

```

ENTER TERMINAL TYPE (0.1.2.3.4): 4

```

```

ENTER COMMANDS

```

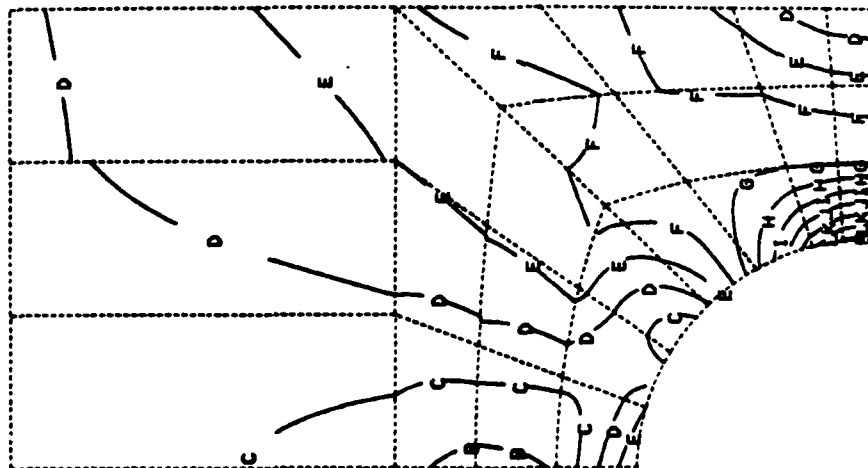
```

PVERT WHICH AXIS VERTICAL(1=X,2=Y,3=Z) .....: 2
TEYE
KEYE 100.0000TEYE 100.0000ZEYE 100.0000
CHANGE THESE VALUES? (Y,N).....: Y
ENTER THE EYE POSITION
KEYE,TEYE,ZEYE .....: 0 0 10000
771TL
OUTLINE AND LABEL THE PLOT? (Y,N).....: Y
TCORE
OPTION 1: CONTOUR ONLY
OPTION 2: RELIEF ONLY
OPTION 3: BOTH
ENTER THE PLOT OPTION (1,2,3).....: 1
MINIMUM VALUE ---1 3.3600E-01 MAXIMUM VALUE---1 6.260000E+00
ENTER THE CONTOUR VALUES (MIN, MAX, INCR).....: 0 6.5 .5
LABEL CONTOUR? (Y,N).....: Y
ENTER CONTOUR LABEL DISTANCE (-1. -1.) 0. CENTER...: 0
DO YOU WANT TO SEE THE CURRENT LABEL VALUES?N
ENTER THE RELIEF (AND/OR)CONTOUR SCALE.....: 0
TORAM

```

Figure 11.2.1 Sample Terminal Session with CPlot.

PERFORATED TENSION STRIP, PLASTIC ANALYSIS, LINEAR STRAIN HARDENING
 MAX. LOAD = YIELD STRESS X MINIMUM SECTION WIDTH UNITS KGF/MM/SEC
 8-NODE PLANE STRESS ELEMENTS (TYPE 8) 3X3 INTEGRATION



CONTOUR PLOT OF
 MODEL STRESSES

COMPONENT = SEQ

MAXIMUM = 8.500E+00
 MINIMUM = 0.
 INTERVAL = 5.000E-01
 CORE SCALE = 0.
 PERSPECTIVE VIEW

EYE POSITION

XEYE = 0.
 YEYE = 0.
 ZEYE = 1.000E+04

INCREMENT = 1
 TIME = 1.250E-01

PLOT OPTION = UNDEFORMED

UNIVERSITY OF DAYTON
 RESEARCH INSTITUTE

03/03/93

CONTOUR LABEL VALUES

A = 0.
 B = 5.000E-01
 C = 1.000E+00
 D = 1.500E+00
 E = 2.000E+00
 F = 2.500E+00
 G = 3.000E+00
 H = 3.500E+00
 I = 4.000E+00
 J = 4.500E+00
 K = 5.000E+00
 L = 5.500E+00
 M = 6.000E+00
 N = 6.500E+00



Figure 11.2.1 (continued)

11.3 XYPLOT - VARIABLE VERSUS VARIABLE PLOTTING

XYPLOT is an interactive graphics program which can be used to construct two-dimensional plots of one (or more) dependent variables versus a single independent quantity. Most of the plot specification parameters are under user control, including:

- physical dimensions of the plot,
- number and values of axis tic marks,
- output formats for axis label values,
- axis and plot titles, and
- line and symbol types.

The program is particularly useful on the Hewlett-Packard 7221A and similar plotters, since each part of the plot can be drawn before proceeding to the next. XYPLOT accepts input data either from a specially prepared plot file or directly from the terminal, and, therefore, can be used for producing plots of data from any source.

When x-y plots of MAGNA results are required, two utility programs, WRTFIL and WTFILA, may be used to extract analysis data from the MPOST and APOST files respectively. WRTFIL, which accesses the MPOST file, can retrieve displacement data or average element stresses versus time, and is most useful for plotting displacement histories at selected nodes of a model. WTFILA extracts results from the APOST postprocessor file for selected node points. Using WTFILA, plot files can be generated for any combination(s) of the following data:

- increment number
- time value
- displacement components (u,v,w)
- absolute displacement magnitude
- strain components (E_{xx} , E_{yy} , ..., E_{xy})

- unit extensions (U_x, U_y, U_z)
- stress components ($\sigma_{xx}, \sigma_{yy}, \dots, \sigma_{xy}$)
- von Mises effective stress

Other variable-versus-variable plots can be produced using XYPLOT directly, with input provided at the keyboard or on free-formatted input files. Manually-prepared file input to XYPLOT follows the simple format described in Table 11.3.1. For specialized applications, it is also useful to write a short program to extract the needed data from a MAGNA postprocessor file (see Section 5.7), and write it to an XYPLOT input file.

Sample plots produced using XYPLOT are reproduced in Figures 11.3.1 through 11.3.3.

TABLE 11.3.1
XYPLOT FILE INPUT SEQUENCE

| Data Item | Description |
|--|--------------------------------------|
| N | Number of plots |
| n_1 | Number of data points for plot no. 1 |
| x_1, y_1 x_2, y_2 \vdots x_{n_1}, y_{n_1} | Data for plot no. 1 |
| n_2 | Number of data points for plot no. 2 |
| x_1, y_1 x_2, y_2 \vdots x_{n_2}, y_{n_2} | Data for plot no. 2 |
| \vdots | \vdots |
| n_N | Number of data points for plot no. N |
| x_1, y_1 x_2, y_2 \vdots x_{n_N}, y_{n_N} | Data for plot no. N |

File Type : Sequential, Formatted
 Formats : Data in free format; data items
 separated by commas or blanks

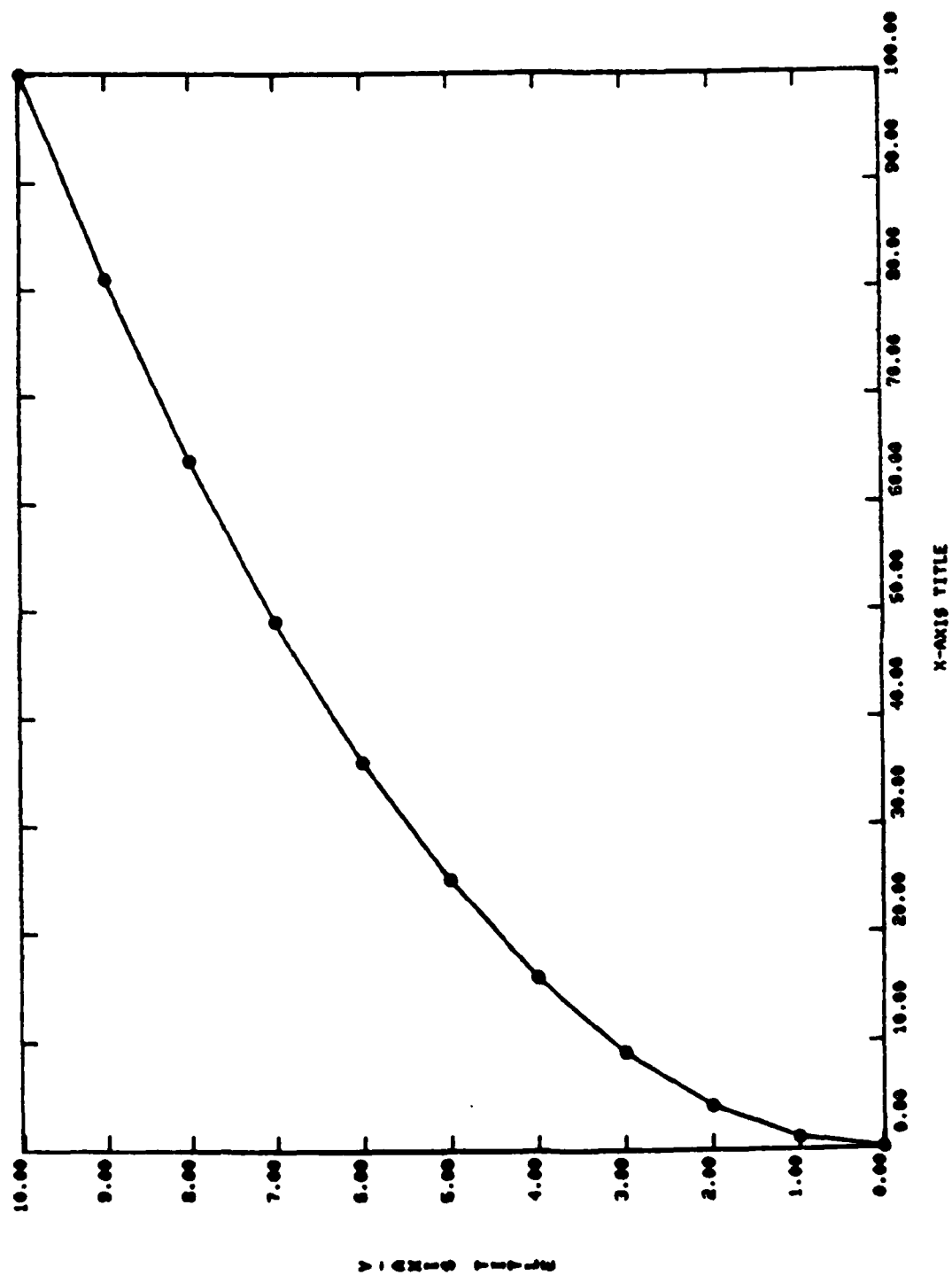


Figure 11.3.1 X-Y Plot (Sample No. 1).

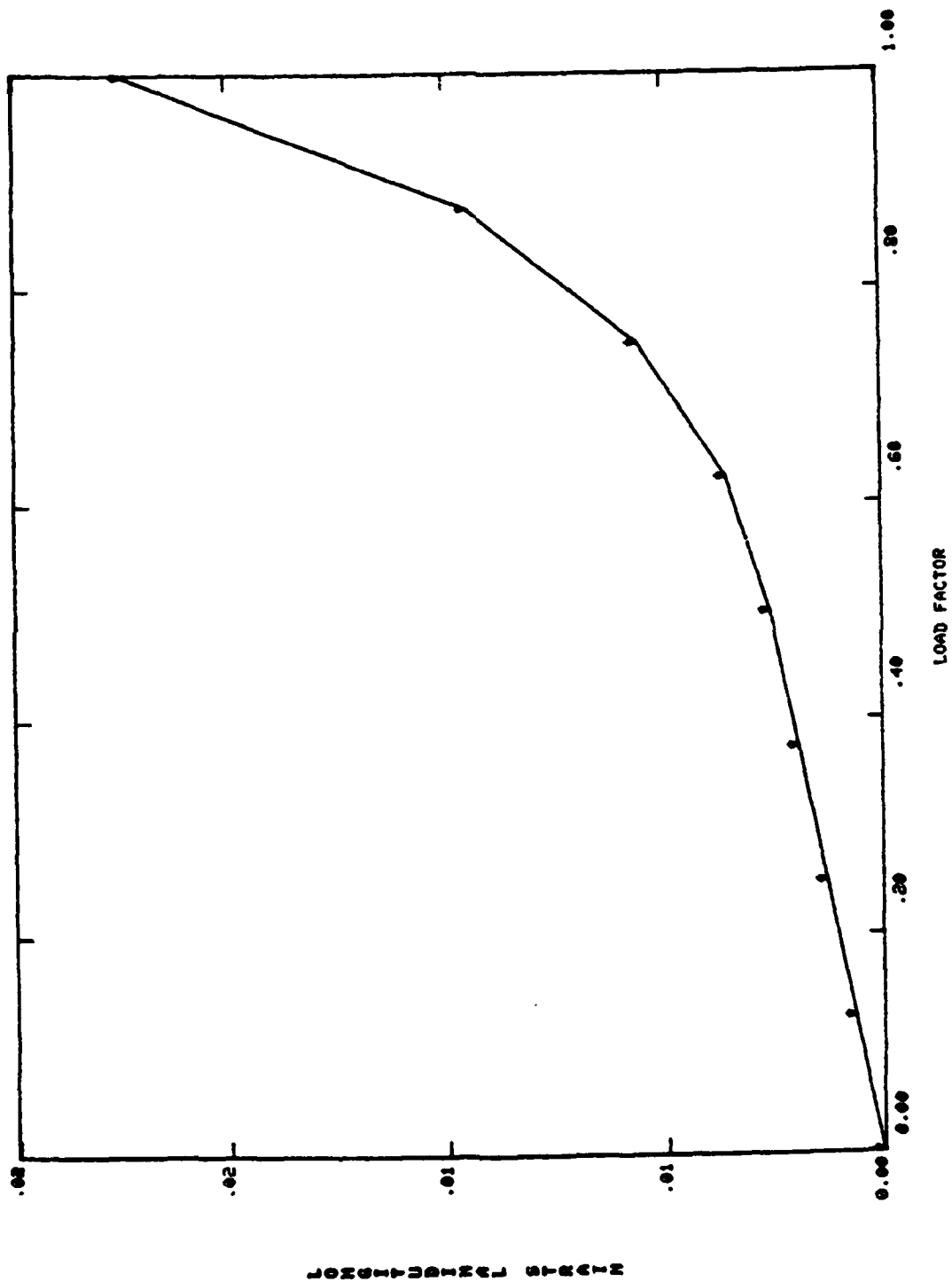


Figure 11.3.2 X-Y Plot (Sample No. 2).

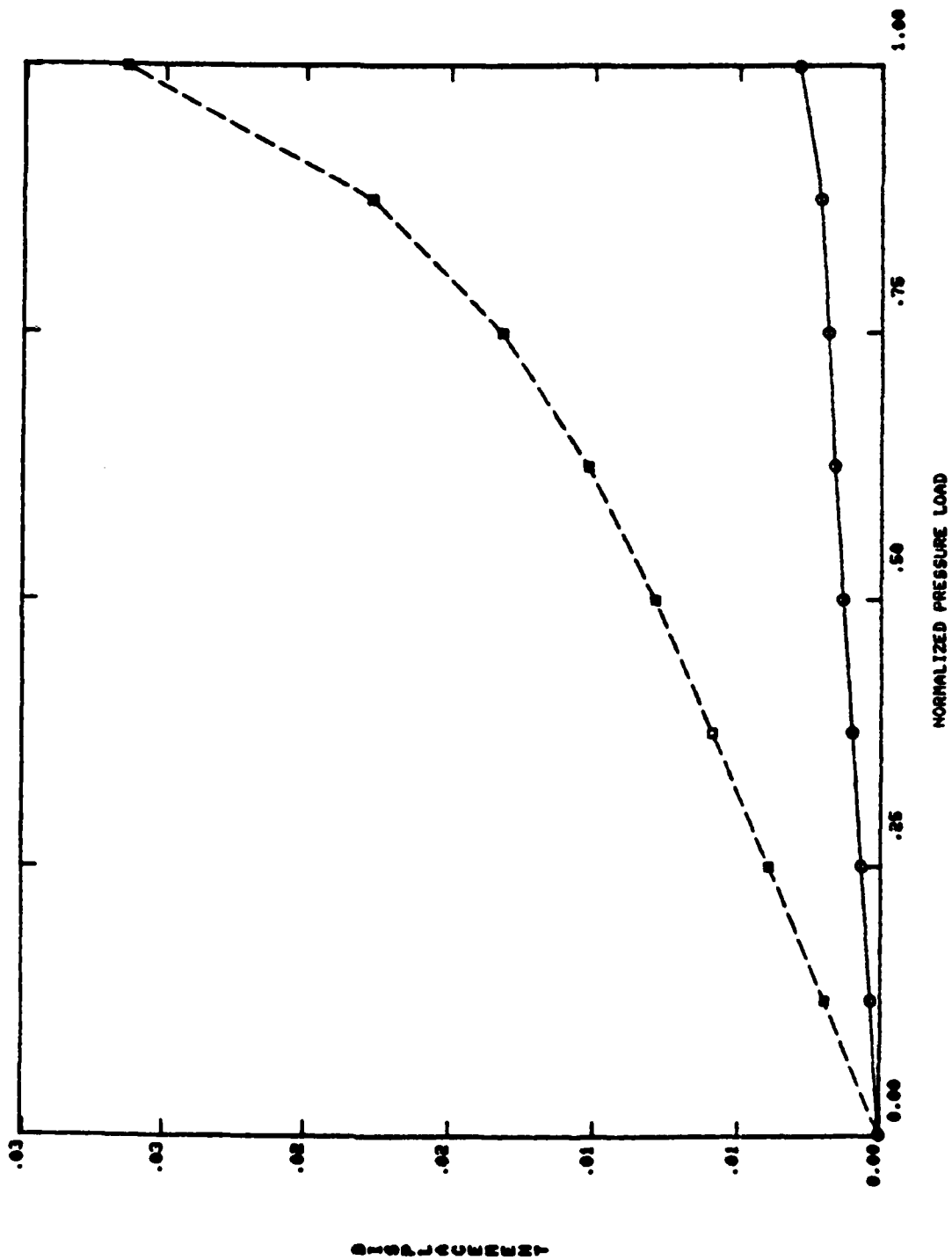


Figure 11.3.3 X-Y Plot (Sample No. 3).

11.4 PROCEDURES FOR ACCESSING GPLOT, CPLOT AND XYPLOT

Each of the plotting utility programs described in this Chapter is executed through a separate (control language) procedure. These procedures automatically access the required program and library files, and return them upon completion of the run.

On the VAX-11/780, the plotting programs can be accessed by simply entering

```
RUN[MAGNA.RAB]GPLOT
```

or

```
RUN[MAGNA.RAB]CPLOT
```

The names of files containing data to be plotted will be requested by GPLOT and CPLOT after the RUN command is issued. In the case of XYPLOT, the WRTFIL (or WTFILA) utility can be used to read an MPOST (or APOST) postprocessor file, and extract displacement, strain, stress or other data for XYPLOT. The required commands are

```
RUN[MAGNA.RAB]WRTFIL (or WTFILA)
```

```
·  
·  
·
```

```
RUN[MAGNA.RAB]XYPLOT
```

WRTFIL and WTFILA generate a (formatted) disk file XYSCRØ.DAT, which is properly formatted for XYPLOT. Alternatively, XYPLOT may be used alone to plot from an existing XYSCRØ.DAT datafile, or from keyboard data input. Run-time procedures for all of the plotting programs may be accessed on CDC computers, by attaching a single file:

```
ATTACH,P,PLOTPROC,ID=BROCKMAN,MR=1.
```

The actual filename required (PLOTPROC,ID=BROCKMAN is used above) may be installation dependent.

Prior to the execution of GPLOT, a MAGNA input file or MPOST postprocessor file must be attached under the local

(temporary) file name TAPE5. If the data to be plotted resides on an input file and a user-written mesh generation program is being used, this routine should also be attached, as file MESHG. To initiate execution, then, the following sequence of commands is typical:

```
ATTACH,TAPE5,MYDATAFILE.  
ATTACH,MESHG,MYGENERATOR. (optional)  
ATTACH,P,PLOTPROC,ID=BROCKMAN,MR=1.  
BEGIN,GPLOT,P.
```

For plotting on Tektronix 4010 series graphics terminals, the above sequence can be followed exactly. On Hewlett-Packard equipment, the BEGIN command must be modified slightly:

```
BEGIN,GPLOT,P,HP.
```

CPlot, the contour/relief plotter, accepts as input only the MAGNA APOST postprocessor file. Prior to execution, the postprocessing file must be attached under the local file name TAPE99. The command sequence necessary to begin execution is of the form

```
ATTACH,TAPE99,APOSTFILE.  
ATTACH,P,PLOTPROC,ID=BROCKMAN,MR=1.  
BEGIN,CPlot,P.  
(or BEGIN,CPlot,P,HP.)
```

For variable-versus-variable plots on the CDC computer, the XYPlot program is executed by entering

```
BEGIN,XYPlot,P.
```

or

```
BEGIN,XYPlot,P,HP.
```

If a plotting file has been prepared prior to the execution of XYPlot, this file should be attached as local file XYSCRØ prior to entering the BEGIN command. If results are to be extracted from an MPOST postprocessor file directly (using WRTFIL), the appropriate commands are

```
ATTACH,TAPE99,MPOST  
ATTACH,P,PLOTPROC,ID=BROCKMAN,MR=1.  
BEGIN,WRTFIL,P.)  
(or BEGIN,WRTFIL,P,HP.)
```

The procedure WRTFIL automatically transfers control to XYPLOT for plotting once the data has been selected from the postprocessor file. To extract results from the APOST file using WTFILA, and then perform x-y plotting, the required sequence of commands is

```
ATTACH,APOST
ATTACH,P,PLOTPROC,ID=BROCKMAN,MR=1.
BEGIN,WTFILA,P.
.
.
.
BEGIN,XYPLOT,P.
(or BEGIN,XYPLOT,P,HP.)
```


CHAPTER 12

GUIDELINES FOR EFFECTIVE MODELING

The conduct of a practical nonlinear analysis requires a considerable amount of judgment and insight on the part of the analyst. Many decisions must be made concerning the modeling detail to be used, the options to be exercised, and the general strategy upon which the solution is to be based. While a great deal of experience is necessary in making optimum use of any nonlinear solution program, several general observations can readily be made concerning good modeling practices and the effective choice of solution options and procedures. In the remainder of this chapter, some general guidelines which have proved to lead to effective modeling with MAGNA are outlined. While some of these suggestions are particular to the solution methods employed in MAGNA, the majority can be understood to represent good modeling practice in a more general sense.

12.1 ANALYSIS OPTIONS

In many instances, the scope of an analytical study or some prior knowledge of the structural response will be sufficient to dictate the analysis option to be used and will give the needed information concerning time or load incrementation. Unfortunately, such cases are exceptional, and in the general case it is frequently necessary to study a problem in depth using several different analysis options.

The use of linear analysis to gain insight to the requirements for nonlinear analysis, and the performance of static analysis as a precursor to extended-time dynamic solutions, cannot be overemphasized. When relatively little is known about the nonlinear dynamic response of a structure, for example, the following progression of analyses may be in order:

- (a) linear static solution, to determine the order of magnitude of the response and to discern the possible importance of material nonlinearity,
- (b) nonlinear static analysis, to assess the influence of large displacement effects upon load path redistribution and to estimate the degree of "stiffening" or "softening" under the loads of interest,
- (c) natural frequency solution, for use in estimating time step values for dynamic solution, and finally,
- (d) nonlinear dynamic analysis, to actually solve the problem of interest.

Obviously, not all of these steps are necessary in every application. However, the information obtained from a less complex form of analysis than that for which final results are sought can often prevent a great deal of difficulty by revealing unexpected characteristics of the structural response. In some situations, a preliminary linear analysis may reveal that a nonlinear analysis is in fact not even necessary.

In some applications, the choice of analysis option may not be obvious even though the expected response is reasonably well-defined. An important example of this is in static postbuckling analysis. Though the loading is slowly applied, the most expedient means of extending a solution into the postbuckling range with MAGNA is to exercise the nonlinear *dynamic* option, using very large time increments. For postbuckling response (which is frequently characterized by a loss of positive definiteness of the tangent stiffness) the dynamic analysis uses inertial effects to stabilize the numerical solution, while the use of large time steps minimizes the effect of inertia upon the values of the computed displacements. Thus, a nonlinear static analysis can be used to isolate the critical load, and a restarted dynamic analysis performed to follow the response into the postbuckled region.

12.2 NODE POINT AND ELEMENT NUMBERING

One of the simplest ways of improving the efficiency of a linear or nonlinear analysis is through effective numbering of the finite element model. The solution of equations in MAGNA is performed using a profile storage scheme (also called variable bandwidth, skyline or active column storage), in which the system of equations

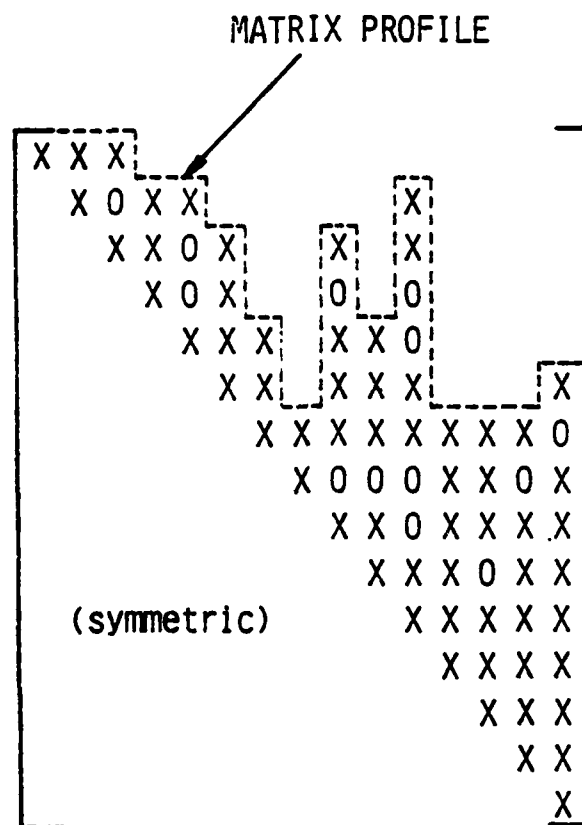
$$\underline{\underline{K}}\underline{\underline{X}} = \underline{\underline{F}} \quad (12.1)$$

is factored in the form

$$\underline{\underline{L}}\underline{\underline{D}}\underline{\underline{L}}^T \underline{\underline{X}} = \underline{\underline{F}} \quad (12.2)$$

as described in Chapter 4. The upper triangular portion of $\underline{\underline{K}}$ is stored as shown in Figure 12.2.1. In any column of $\underline{\underline{K}}$, only those entries below the first nonzero element of the column are stored and manipulated during the solution. The envelope of nonzero entries in $\underline{\underline{K}}$ (called the skyline or profile of $\underline{\underline{K}}$) is small in a well-numbered model, thus minimizing the number of operations performed during the solution.

To assess the effectiveness of a numbering scheme, one could imagine the model as having one degree of freedom per node, and note that nonzero entries in the matrix occur wherever two different nodes are connected within a single finite element. An example of a truss-like structure is shown in Figure 12.2.2, with two different node numbering schemes. For the case in which node 1 is connected to all of the higher-numbered nodes, a full matrix results, and numbering in this fashion should obviously be avoided. In general, effective node numbering involves minimizing the number of connections from low-numbered nodes to higher-numbered nodes. Since numbering of the elements does not affect the matrix profile, any convenient scheme for numbering the elements may be adopted without affecting the efficiency of the solution.



X = NONZERO ENTRY
 0 = ZERO ENTRY
 = ZERO ENTRY

Figure 12.2.1 Variable Bandwidth Matrix Storage.

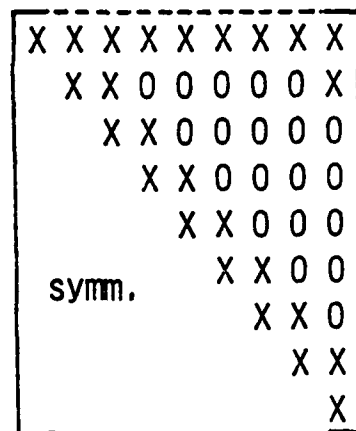
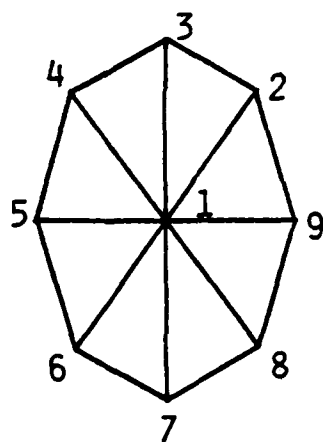
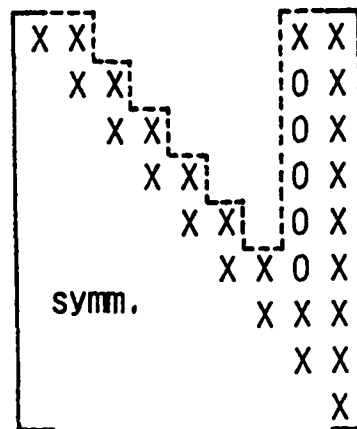
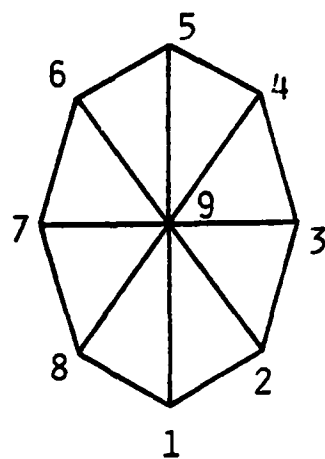


Figure 12.2.2 Effect of Node Point Numbering on Matrix Profile.

In models having a fairly regular pattern of nodes (e.g., rectangular solids, aircraft wings, etc.), the usual rules which should be observed for bandwidth minimization (i.e., "number the shortest directions first") will generally result in an adequate numbering for the profile solution. For more general models, numbering will typically begin in one corner of the mesh and proceed across the grid along directions having a relatively small number of nodes. Due to the method of storage used in MAGNA, local increases in bandwidth are not of particular concern. Therefore, if convenience in generating a series of nodes results in a somewhat wider bandwidth at a few nodes of the model, solution efficiency is minimally affected.

12.3 SELECTION OF ELEMENT TYPES AND OPTIONS

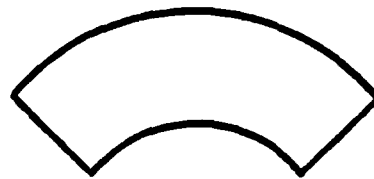
Computational efficiency is of primary concern in most practical nonlinear analyses, since the cost of analysis invariably influences modeling detail (and, therefore, accuracy). A wide variety of element types, integration rules and element formulations are provided in MAGNA for three-dimensional analysis, and effective use of these options can result in considerable savings in computer resources.

In one- and two-dimensional problems, and in thin plate or shell analysis, the choice of an element type is relatively straightforward. For three-dimensional or thick shell problems, however, MAGNA offers a wide variety of element options, and the proper choice of element configuration, integration order and stiffness formulation is important in terms of analysis accuracy and efficiency. Although the engineering judgment of the analyst must ultimately prevail in the selection of element types and options for specific applications, some suggestions for choosing the appropriate element form in a few general problem classes are offered in the following paragraphs.

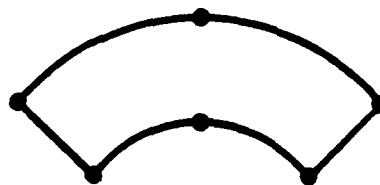
Fully three-dimensional continua, such as valve bodies, pistons, foundations or slabs, generally require elements with a similar node pattern in each direction. Examples are the eight, twenty and twenty-seven node brick elements (Types 2, 6 and 1, respectively). Element types 1 and 7 are often useful in transitioning between these different types of elements. It should be observed that the eight-node solid element (Type 2) is incapable of representing complex states of stress unless a very fine mesh is used; the higher-order (quadratic) solids are nearly always superior for general use. For most analyses of solid continua, reduced numerical integration is not necessary and in fact may reduce the accuracy of materially nonlinear solutions. When Gaussian integration is used, the $2 \times 2 \times 2$ rule is suggested for eight-node elements and a $3 \times 3 \times 3$ rule is generally appropriate for the quadratic solids. The

non-Gaussian integration rules available with all solid elements in MAGNA (6-point and 9-point rules for Element Type 2, and 14-point rule for all others) are highly recommended; these integration formulas give good accuracy and reliability at a substantially lower cost than the Gaussian quadrature formulas.

Thick shells are one of the most common classes of engineering structures. Components of this type include pressure vessels, turbine blades, aircraft transparencies, arch dams and floor and bridge slabs. Such structures may certainly be analyzed using the 20 or 27-node elements; however, some simplification is often possible since the state of strain across the thickness of the shell is adequately described by simple *linear* shape functions. Element Type 8, which uses quadratic shape functions over the element surfaces and linearly varying displacements through the thickness, is most often appropriate in this case. Either a $2 \times 2 \times 2$ integration (the most commonly used) or the 14-point quadrature rule can be used effectively with the sixteen node element (Type 8). If a different nodal pattern is desired, one of the variable-node elements (Types 1 and 7) can be used to construct an appropriate element. One example is the eighteen ($3 \times 3 \times 2$) node Lagrangian thick shell element, which is a subcase of Element Type 1. Since the response of moderately thick shells generally involves a certain amount of bending, the use of Element Type 2 (8-node brick) is not recommended, since bending deformation cannot occur in these linear-displacement elements without introducing significant transverse shear strains (Figure 12.3.1). When Type 2 elements are used for such an application, selective (9-point) integration should be used. Regardless of the element configuration used, care should be taken to construct elements with "reasonable" length-to-thickness ratios. A conservative guideline is to use elements whose maximum length-to-thickness ratio is 100:1 or less, to avoid numerical ill-conditioning which might result from extreme element thinness.



ELEMENT IN PURE BENDING



QUADRATIC ELEMENT APPROXIMATION



LINEAR ELEMENT APPROXIMATION

Figure 12.3.1 Approximation of Bending Deformation Using Eight-Node Solid Elements.

In plate and shell analysis, two element types (5 and 11) are available in MAGNA. The eight-node (Type 5) shell element provides good results for shells with small to moderate initial curvature, but may be poorly-behaved in coarse meshes when inplane deformations are important. In particular, the inplane bending (cross-bending) response of Element Type 5 is relatively poor; the higher-order Type 11 shell is preferred when inplane bending is important.

The sixteen-node shell (Type 11) represents both inplane and bending deformations with high accuracy, when the stiffnesses of the shell layers are similar in magnitude. Application of the Type 11 shell to layered constructions with widely dissimilar layer properties (such as thick sandwich panels, or the plastic-interlayer construction typical of aircraft transparencies) should be approached with extreme caution. Since displacements vary only linearly through the element thickness, stiff layers tend to dominate the transverse shear behavior, and bending rigidity may be overestimated; the extent to which this effect is manifested in the behavior of a model depends strongly upon the wall construction and upon the types of boundary conditions. In such pathological cases, the specification of orthotropic material properties in the stronger layers to eliminate excessive transverse shear stiffness is sometimes a useful device.

Finally, a note regarding reduced numerical integration is appropriate, since this device is often used to improve the bending flexibility of thick or moderately thin shell models composed of three-dimensional solid elements. The use of inexact integration produces an "artificial" element flexibility which compensates for the overestimate of element rigidity typical of displacement finite elements. Inexactly integrated quadratic elements (e.g., 20-node brick with 2x2x2 quadrature) produce good results and in fact are much less expensive than exactly integrated elements, but the existence of *zero-energy deformation modes, or mechanisms*, which could lead to meaningless results is possible. *The use of a preliminary natural frequency analysis to verify that no such mechanisms exist is strongly encouraged in all applications involving reduced integration.*

12.4 USE OF EQUILIBRIUM ITERATION

The choice of an equilibrium iteration option determines the manner in which the nonlinear finite element system is solved by MAGNA. In some types of problems, the use of iteration is unnecessary, while in other cases a solution cannot be obtained without it. The remainder of this section is intended to classify some of these problem types and to suggest appropriate iteration strategies wherever possible.

The equilibrium iteration methods available in MAGNA are based upon full and modified Newton-Raphson techniques, and a combination of these. Figure 12.4.1 shows the processes of full and modified Newton iteration for a single degree-of-freedom system, where iteration is performed at a constant value of the applied loading. For the system shown, the tangent stiffness simply corresponds to the instantaneous slope of the load-deflection path. In (full) Newton-Raphson iteration, the slope (stiffness) is adjusted at each iteration cycle, so that convergence occurs rapidly. Modified Newton iterations are always based upon the stiffness computed at the beginning of the step, and for this reason are sometimes called "constant stiffness" iterations. For systems having many degrees of freedom, updating of the stiffness matrix at each iteration requires a considerable amount of additional computation in return for the fast rate of convergence. It should also be observed that the domain of convergence is also improved with full Newton iteration; that is, an initial estimate of the solution which is relatively poor is often sufficient when full Newton iterations are used, while modified Newton iteration may diverge from the correct result. A third iteration strategy, combined Newton-Raphson iteration, is also available in the program. The combined iteration method is designed to retain the best features of the full and modified iterations (Figure 12.4.2).

In general, the modified Newton-Raphson iteration is effective only in mildly nonlinear problems, or when rather

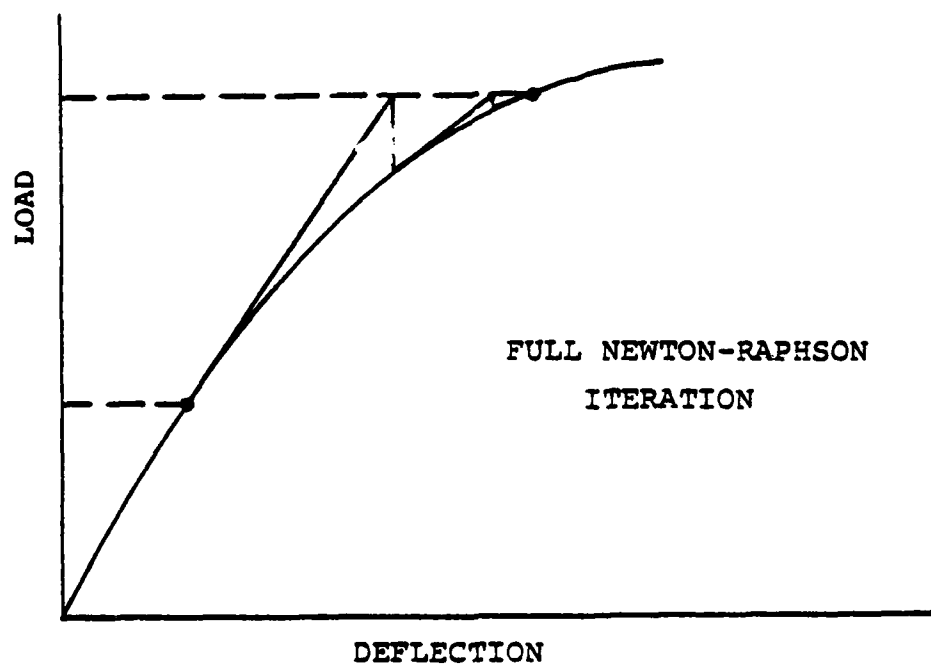
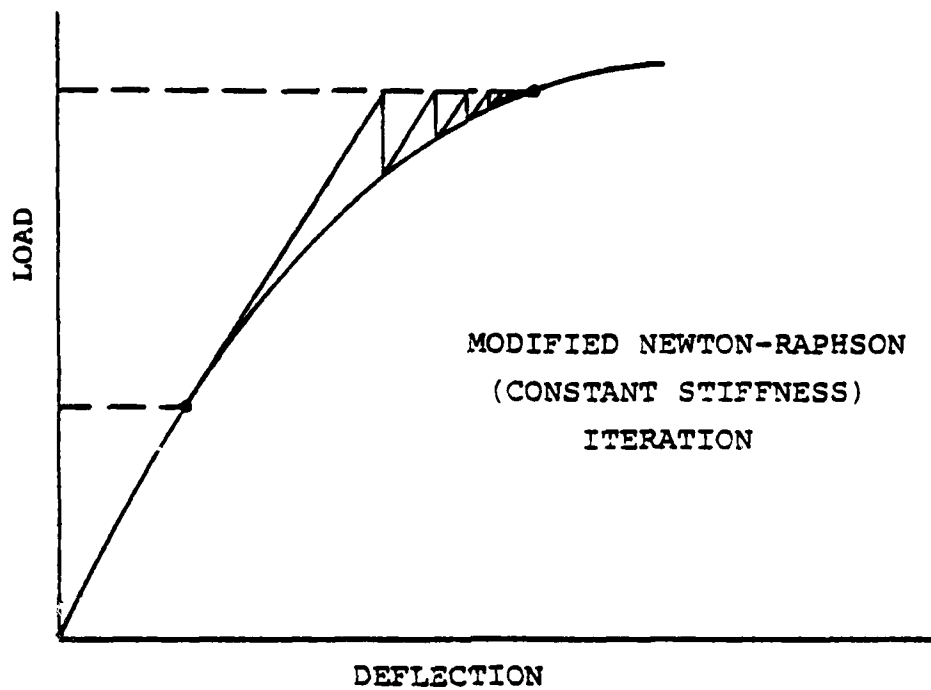


Figure 12.4.1 Newton-Raphson and Modified Newton Iteration Schemes.

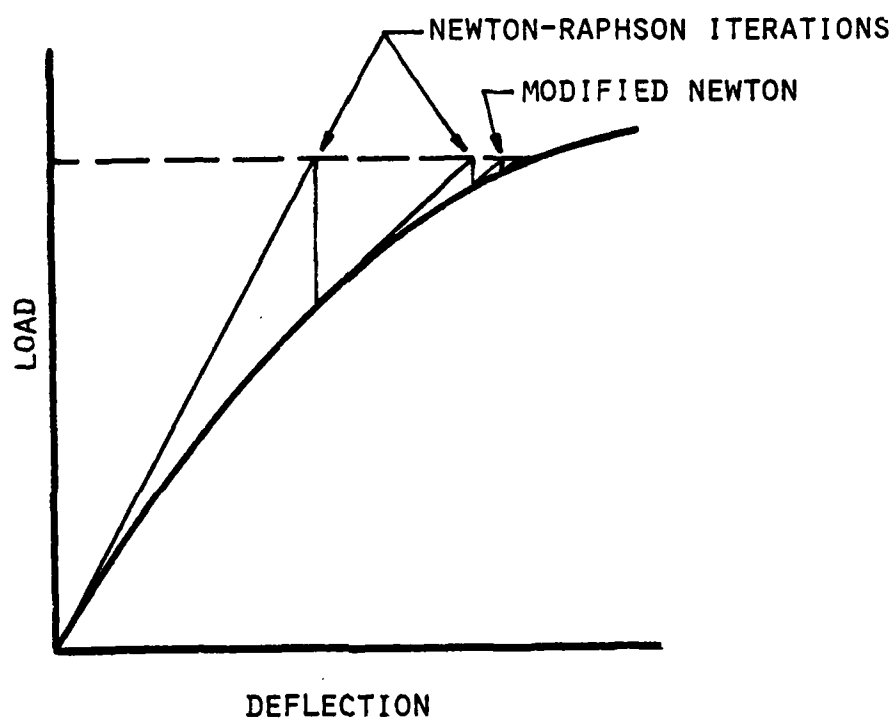


Figure 12.4.2 Combined Iteration Technique.

small increments of loading are used. For most applications, the combined Newton iteration strategy is the most cost-effective means of solution, provided moderately sized increments of time or loading are chosen. A full Newton-Raphson method is superior for highly geometrically nonlinear problems (particularly when large rotations are involved), and for analyses using very large increment sizes. Thus, if a solution for the entire history of loading is required, a natural approach is to employ moderate loading increments in conjunction with the modified Newton solution. A problem involving primarily geometric nonlinearities and for which only a final solution is required would be better solved in relatively large increments using full Newton-Raphson iteration. Dynamic analyses, in which time increment sizes are generally limited by accuracy considerations, are most appropriately solved with combined iteration in almost every instance.

In materially nonlinear analysis, due to the path dependence of the problem, care must be exercised in the iterative solution to ensure that the increment size is not excessive even though convergence appears satisfactory. The incremental solution is incapable of detecting any changes in relative magnitude among the incremental components of strain. That is, the individual strain components are constrained to behave proportionally within any single increment, and the solution increment must be made small enough that this constraint is acceptable, whether or not equilibrium iterations are used. Plastic analyses involving unloading also require special consideration, due to the dependence of the tangent stiffness upon the location and magnitude of the external forces. When unloading (or any abrupt change in loading history) occurs, it is advisable that the increment during which this event takes place be made rather small to avoid possible divergence of the solution. The effect of using large load increments in segments of the solution during which highly nonproportional loading is present is illustrated in Figure 12.4.3.

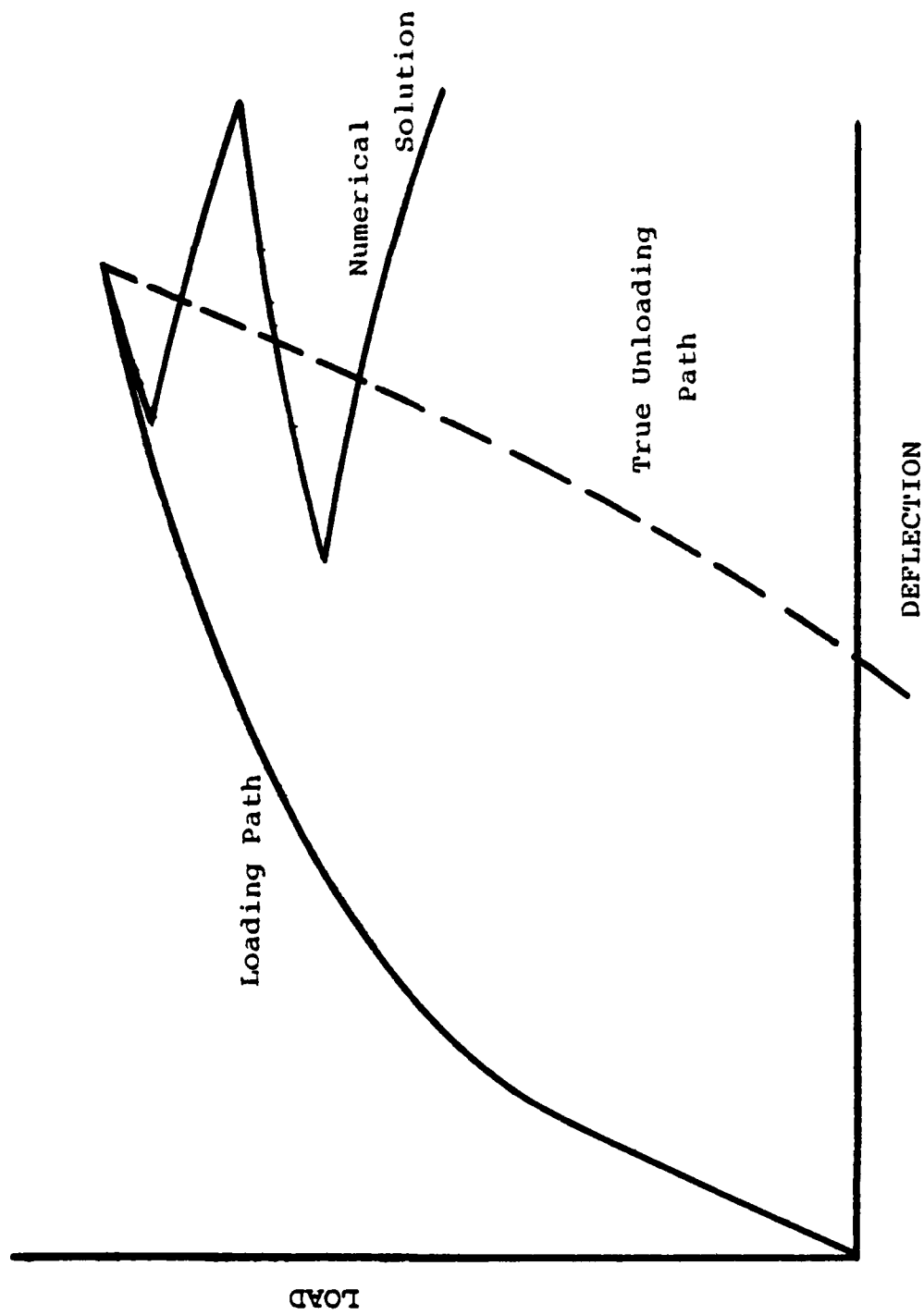


Figure 12.4.3 Effect of Large Loading Step upon Nonlinear Solution during Load Reversal.

For geometrically nonlinear analyses in which large incremental rotations are involved, the use of equilibrium iteration at frequent intervals in the solution is particularly important. Due to the total Lagrangian formulation used in MAGNA, finite incremental rotations tend to introduce artificial stresses which, when uncorrected, produce an artificial geometric stiffness and lead to the "ratcheting" behavior pictured in Figure 12.4.4. The most effective means of avoiding such inaccuracies in large rotation problems is the full Newton-Raphson procedure. In addition, MAGNA includes a "large rotation iteration" option which is designed to systematically eliminate the detrimental effects of artificial geometric stiffening during equilibrium iteration; this scheme is user-selectable, by setting the iteration parameter LRGROT (see Section 8.3) to a nonzero value. When The LRGROT option is invoked, geometric stiffnesses are suppressed in the tangent modulus calculation for three-dimensional elements, until a converged state of equilibrium is obtained.

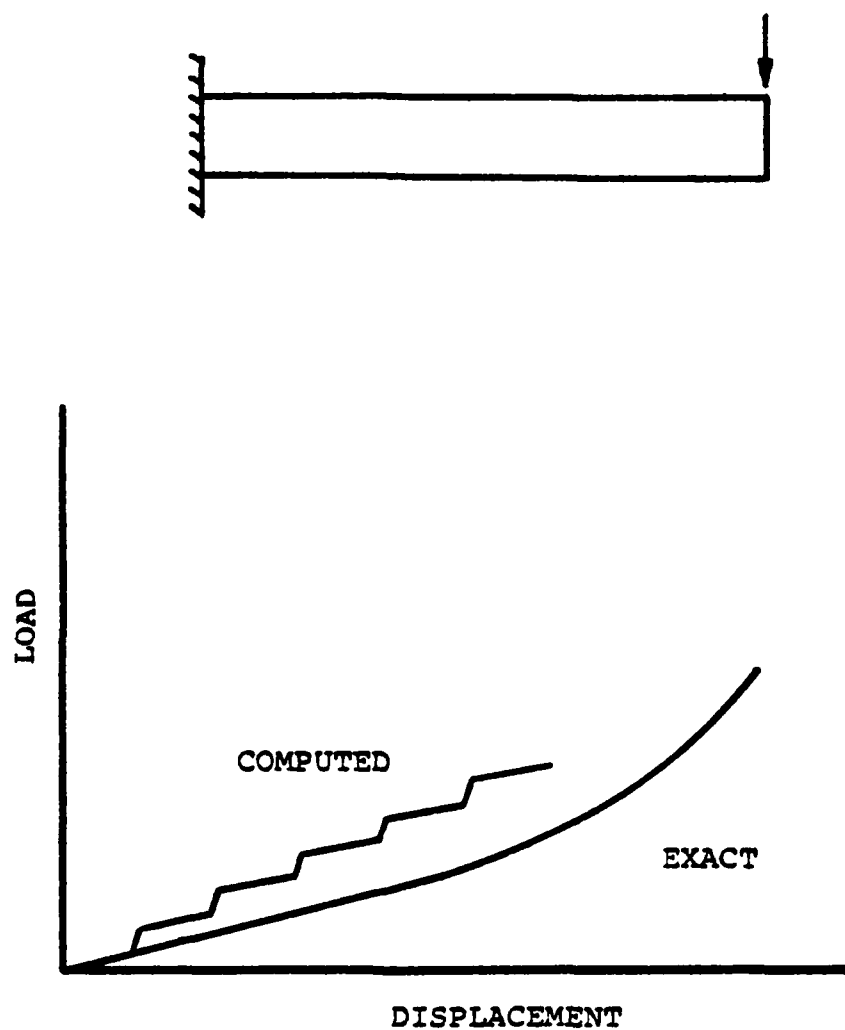


Figure 12.4.4 Ratcheting Effect (due to Large Rotations)
in Solution without Equilibrium Iterations.

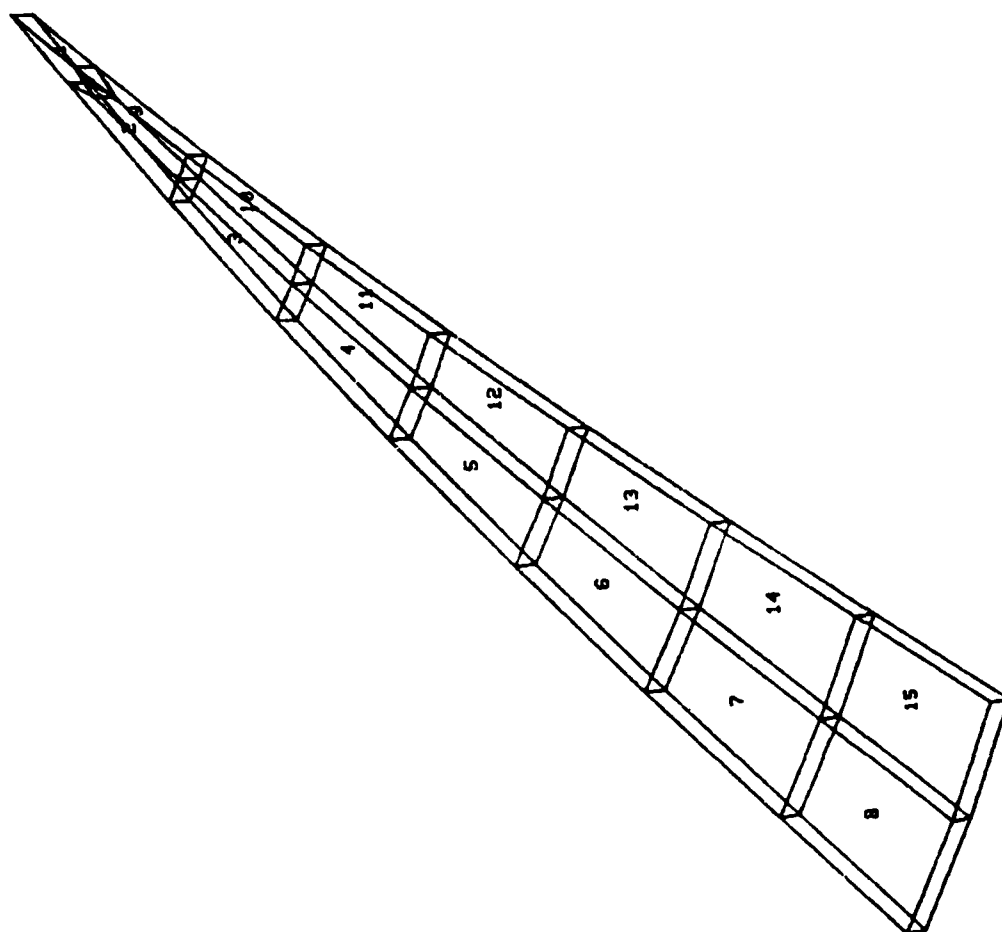
APPENDIX

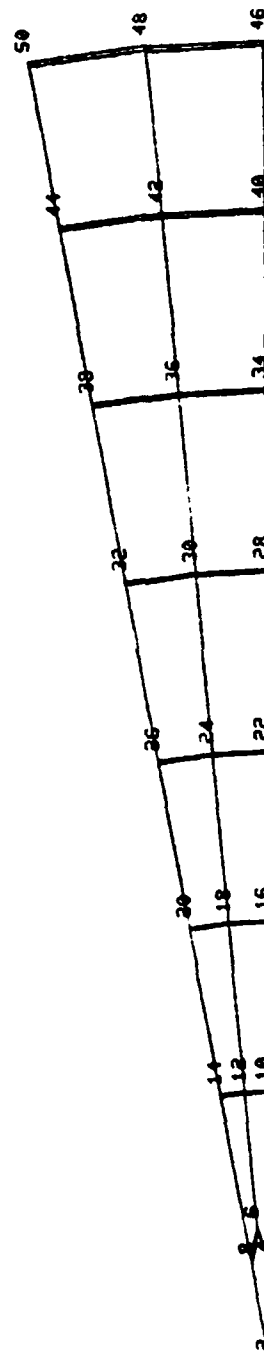
Several input data decks are listed in this Appendix to clarify the actual form of the problem data expected by MAGNA. In each case, pertinent data concerning the type of analysis and features used are given, along with geometry plots of the undeformed finite element model.

Input Deck Example #1

Shallow Spherical Cap Under Apex Load (Section 6.2)

Type of Analysis Nonlinear Static
Number of Increments 50
Equilibrium Iteration None
Coordinate Data Spherical Coordinates
Element Type 5 (15 Elements)
Linear Constraints 14 (2 Terms Each)
Data Curves 1 (Applied Loading)
External Forces Nodal Loads





NONLINEAR STATIC ANALYSIS
 SPHERICAL CAP R=4.76, T=0.01576 10-DEGREE SECTOR
 15 SHELL ELEMENTS (TYPE 5) MAX. LOAD=100.

1 1 1 2 0 1

30 1

0. 0.

COORDINATES 50

| | | | |
|-----|---------|------|-----|
| 18 | 4.75212 | 0. | 0. |
| 28 | 4.76789 | 0. | 0. |
| 38 | 4.75212 | 0.8 | 0. |
| 48 | 4.76789 | 0.8 | 0. |
| 58 | 4.75212 | 1.09 | 5. |
| 68 | 4.76789 | 1.09 | 5. |
| 78 | 4.75212 | 0.8 | 10. |
| 88 | 4.76789 | 0.8 | 10. |
| 98 | 4.75212 | 2.2 | 0. |
| 108 | 4.76789 | 2.2 | 0. |
| 118 | 4.75212 | 2.2 | 5. |
| 128 | 4.76789 | 2.2 | 5. |
| 138 | 4.75212 | 2.2 | 10. |
| 148 | 4.76789 | 2.2 | 10. |
| 158 | 4.75212 | 3.6 | 0. |
| 168 | 4.76789 | 3.6 | 0. |
| 178 | 4.75212 | 3.6 | 5. |
| 188 | 4.76789 | 3.6 | 5. |
| 198 | 4.75212 | 3.6 | 10. |
| 208 | 4.76789 | 3.6 | 10. |

| | | | |
|-----|---------|------|-----|
| 218 | 4.75212 | 5. | 0. |
| 228 | 4.76788 | 5. | 0. |
| 238 | 4.75212 | 5. | 5. |
| 248 | 4.76788 | 5. | 5. |
| 258 | 4.75212 | 5. | 10. |
| 268 | 4.76788 | 5. | 10. |
| 278 | 4.75212 | 6.5 | 0. |
| 288 | 4.76788 | 6.5 | 0. |
| 298 | 4.75212 | 6.5 | 5. |
| 308 | 4.76788 | 6.5 | 5. |
| 318 | 4.75212 | 6.5 | 10. |
| 328 | 4.76788 | 6.5 | 10. |
| 338 | 4.75212 | 8. | 0. |
| 348 | 4.76788 | 8. | 0. |
| 358 | 4.75212 | 8. | 5. |
| 368 | 4.76788 | 8. | 5. |
| 378 | 4.75212 | 8. | 10. |
| 388 | 4.76788 | 8. | 10. |
| 398 | 4.75212 | 9.5 | 0. |
| 408 | 4.76788 | 9.5 | 0. |
| 418 | 4.75212 | 9.5 | 5. |
| 428 | 4.76788 | 9.5 | 5. |
| 438 | 4.75212 | 9.5 | 10. |
| 448 | 4.76788 | 9.5 | 10. |
| 458 | 4.75212 | 10.9 | 0. |
| 468 | 4.76788 | 10.9 | 0. |
| 478 | 4.75212 | 10.9 | 5. |
| 488 | 4.76788 | 10.9 | 5. |
| 498 | 4.75212 | 10.9 | 10. |
| 508 | 4.76788 | 10.9 | 10. |

| | | | | | | | | | | | | | | | | | | | |
|----|---|----|---|---|---|---|---|---|---|---|---|---|---|---|---|---|---|---|---|
| 5 | 1 | 15 | | | | | | | | | | | | | | | | | |
| 1 | 1 | 1 | 1 | 1 | 1 | 1 | 1 | 1 | 1 | 1 | 1 | 1 | 1 | 1 | 1 | 1 | 1 | 1 | 1 |
| 2 | 1 | 1 | 1 | 1 | 1 | 1 | 1 | 1 | 1 | 1 | 1 | 1 | 1 | 1 | 1 | 1 | 1 | 1 | 1 |
| 3 | 1 | 1 | 1 | 1 | 1 | 1 | 1 | 1 | 1 | 1 | 1 | 1 | 1 | 1 | 1 | 1 | 1 | 1 | 1 |
| 4 | 1 | 1 | 1 | 1 | 1 | 1 | 1 | 1 | 1 | 1 | 1 | 1 | 1 | 1 | 1 | 1 | 1 | 1 | 1 |
| 5 | 1 | 1 | 1 | 1 | 1 | 1 | 1 | 1 | 1 | 1 | 1 | 1 | 1 | 1 | 1 | 1 | 1 | 1 | 1 |
| 6 | 1 | 1 | 1 | 1 | 1 | 1 | 1 | 1 | 1 | 1 | 1 | 1 | 1 | 1 | 1 | 1 | 1 | 1 | 1 |
| 7 | 1 | 1 | 1 | 1 | 1 | 1 | 1 | 1 | 1 | 1 | 1 | 1 | 1 | 1 | 1 | 1 | 1 | 1 | 1 |
| 8 | 1 | 1 | 1 | 1 | 1 | 1 | 1 | 1 | 1 | 1 | 1 | 1 | 1 | 1 | 1 | 1 | 1 | 1 | 1 |
| 9 | 1 | 1 | 1 | 1 | 1 | 1 | 1 | 1 | 1 | 1 | 1 | 1 | 1 | 1 | 1 | 1 | 1 | 1 | 1 |
| 10 | 1 | 1 | 1 | 1 | 1 | 1 | 1 | 1 | 1 | 1 | 1 | 1 | 1 | 1 | 1 | 1 | 1 | 1 | 1 |
| 11 | 1 | 1 | 1 | 1 | 1 | 1 | 1 | 1 | 1 | 1 | 1 | 1 | 1 | 1 | 1 | 1 | 1 | 1 | 1 |
| 12 | 1 | 1 | 1 | 1 | 1 | 1 | 1 | 1 | 1 | 1 | 1 | 1 | 1 | 1 | 1 | 1 | 1 | 1 | 1 |
| 13 | 1 | 1 | 1 | 1 | 1 | 1 | 1 | 1 | 1 | 1 | 1 | 1 | 1 | 1 | 1 | 1 | 1 | 1 | 1 |
| 14 | 1 | 1 | 1 | 1 | 1 | 1 | 1 | 1 | 1 | 1 | 1 | 1 | 1 | 1 | 1 | 1 | 1 | 1 | 1 |
| 15 | 1 | 1 | 1 | 1 | 1 | 1 | 1 | 1 | 1 | 1 | 1 | 1 | 1 | 1 | 1 | 1 | 1 | 1 | 1 |

| | | | | |
|----|------------|----|------------|---|
| 4 | 0 | 0 | 14 | 2 |
| 1 | 2 | 1 | | |
| 1 | 2 | | | |
| 3 | 39 | 6 | | |
| 2 | | | | |
| 4 | 40 | 6 | | |
| 2 | | | | |
| 45 | 50 | 1 | | |
| 1 | 2 | 3 | | |
| 2 | | | | |
| 7 | 1-17364818 | 7 | 2.98480776 | |
| 2 | | | | |
| 8 | 1-17364818 | 8 | 2.98480776 | |
| 2 | | | | |
| 13 | 1-17364818 | 13 | 2.98480776 | |
| 2 | | | | |
| 14 | 1-17364818 | 14 | 2.98480776 | |
| 2 | | | | |
| 19 | 1-17364818 | 19 | 2.98480776 | |
| 2 | | | | |
| 20 | 1-17364818 | 20 | 2.98480776 | |

AD-A129 773

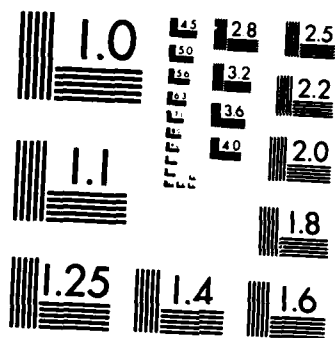
MAGNA (MATERIALLY AND GEOMETRICALLY NONLINEAR ANALYSIS)
PART I FINITE ELE. (U) DAYTON UNIV OH RESEARCH INST
R A BROCKMAN DEC 82 UDR-TR-82-111 AFWL-TR-82-3098-PT-1
F33615-80-C-3403 F/G 12/1

8/8

UNCLASSIFIED

NL





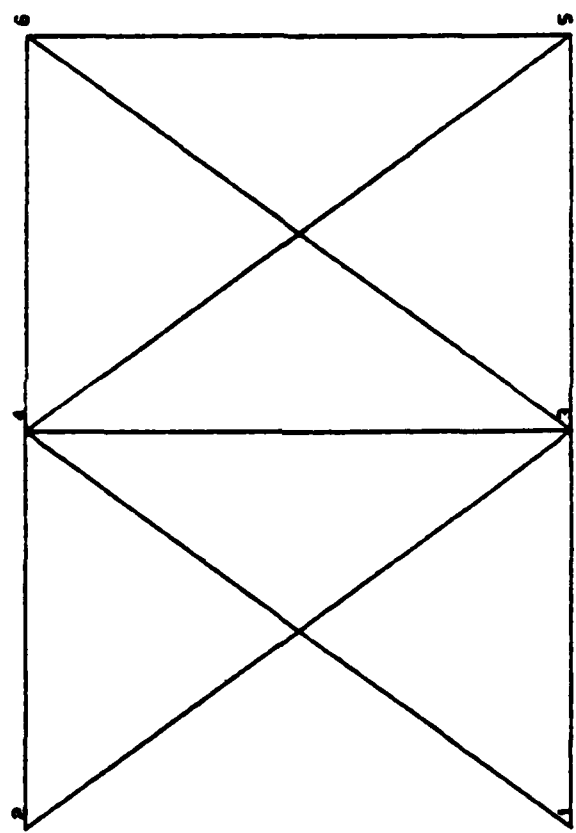
MICROCOPY RESOLUTION TEST CHART
NATIONAL BUREAU OF STANDARDS-1963-A

[illegible]

Input Deck Example #2

Elastic-Plastic Two-Bay Truss (Section 6.7)

Type of Analysis Nonlinear Static
Number of Increments 25
Equilibrium Iteration None
Coordinate Data Cartesian Coordinates
Element Type 4 (10 Elements)
Data Curves 2 (Stress-Plastic Strain
and Applied Loading)
External Forces Nodal Loads



| | | | | | | | |
|----|----|---|---|---|----|---|---|
| 1 | 1 | 1 | 2 | 2 | 0 | 1 | 1 |
| 25 | 1 | | | | | | |
| | 1. | | | | 0. | | |

A.11

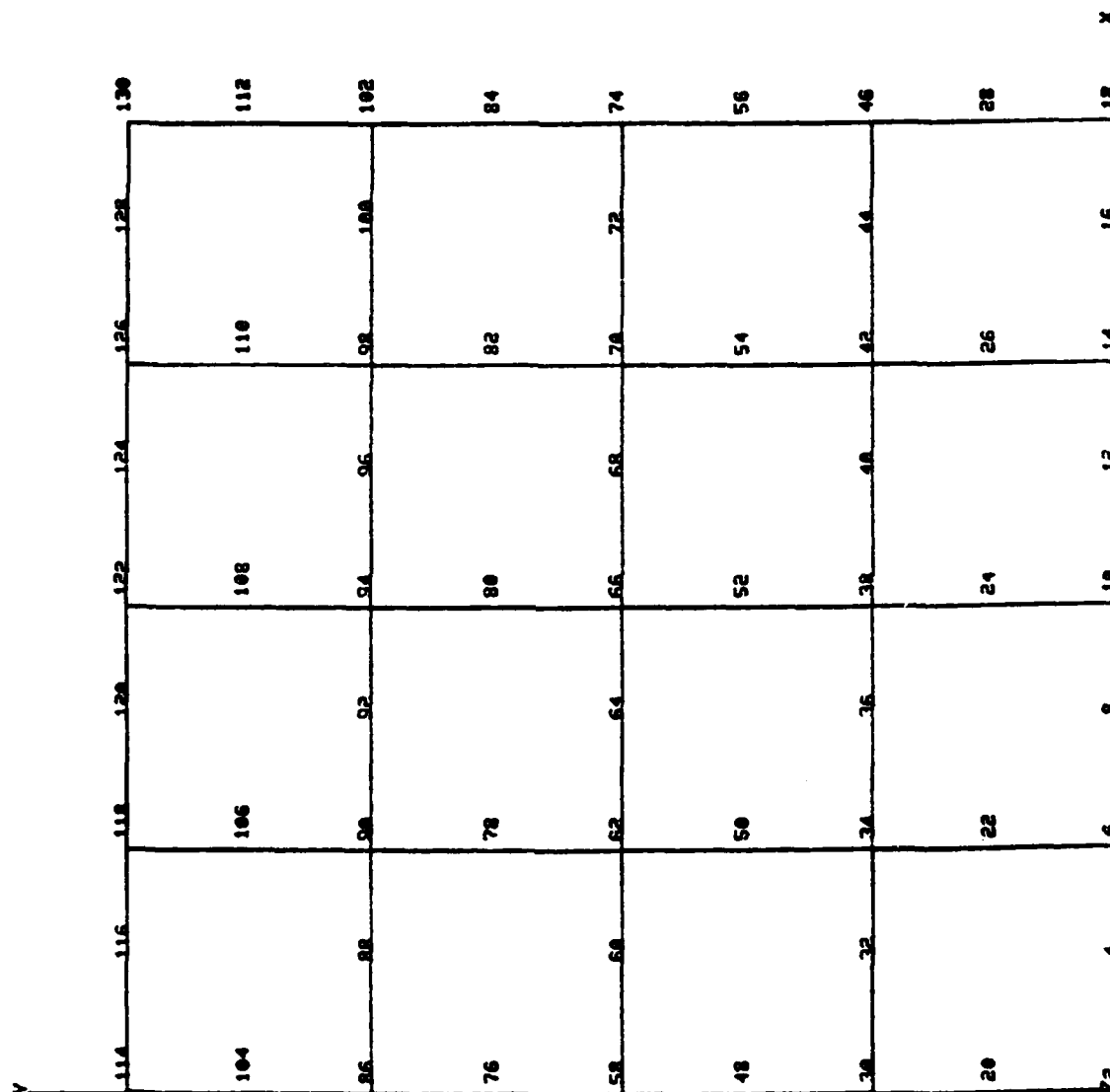
| | 2 | 1 | 2 | 1 | 2 | 3 | 3 | 2 | 1 | 10 | EPS=(S/E)*(1+(3/7))*(S/40520)**6) | | | | | | |
|--|---|---|---|---|---|---|---|---|---|--------|-----------------------------------|--------|--------|--------|-------|--------|-------|
| | | | | | | | | | | 0. | 2500. | .00021 | 3000. | .00062 | 3500. | .00111 | 3800. |
| | | | | | | | | | | .00174 | 40520. | .00362 | 4500. | .00568 | 4800. | .00756 | 5000. |
| | | | | | | | | | | .04747 | 6500. | .20306 | 8000. | | | | |
| | | | | | | | | | | 2 | LOADING | | | | | | |
| | | | | | | | | | | 0. | 0. | 25. | 10000. | | | | |
| | | | | | | | | | | 5 | 2 | 2 | -1.0 | | | | |

Input Deck Example #3

Postbuckling of a Simply-Supported Plate (Section 6.14)

Type of Analysis Nonlinear Dynamic
Number of Increments 20
Equilibrium Iteration Combined Newton-Raphson
Coordinate Data Cartesian Coordinates
Element Type 8 (16 Elements)
Data Curves 2 (Applied Loading)
External Forces Nodal Loads and Surface
Pressures

| | | | |
|----|----|----|----|
| 16 | 15 | 14 | 13 |
| 12 | 11 | 10 | 9 |
| 8 | 7 | 6 | 5 |
| 4 | 3 | 2 | 1 |



SIMPLY SUPPORTED SQUARE PLATE, COMPRESSION BUCKLING, DOUBLE SYMM.
 (16) 16-NODE ELEMENTS (TYPE 8) REDUCED INTEGRATION
 CLASSICAL SOLN. $4X=11.3$ LB/IN (226 P.S.I.) FOR CRITICAL LOAD

1 2 1 2 1 1 0 0 1
 20 1
 1000. 0

3 1 10 0.10 0.000050

COORDINATES 139

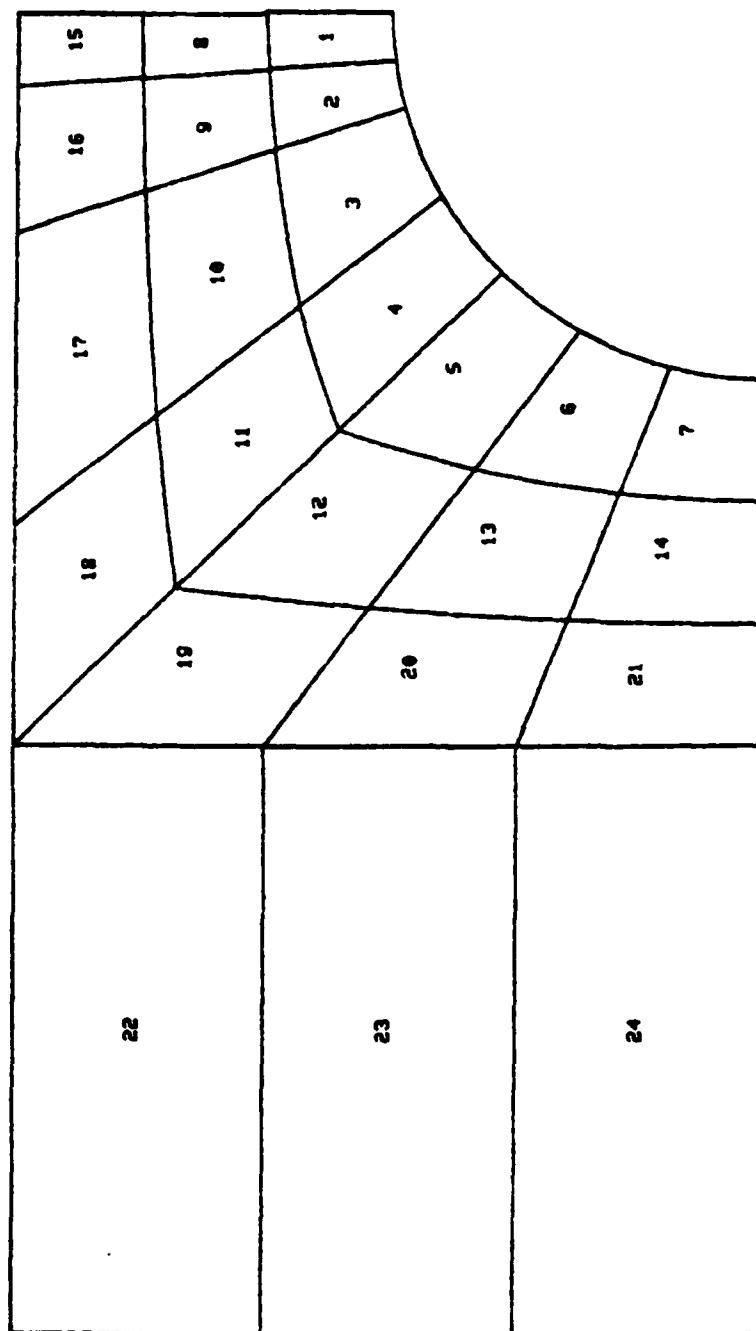
| | | | | |
|----|---|-----|------|-----|
| 17 | 2 | 10. | | |
| 18 | 2 | 10. | | .05 |
| 19 | | | 1.25 | .05 |
| 27 | 2 | 10. | 1.25 | |
| 20 | | | 1.25 | .05 |
| 28 | 2 | 10. | 1.25 | .05 |
| 29 | | | 2.5 | |
| 45 | 2 | 10. | 2.5 | .05 |
| 30 | | | 2.5 | .05 |
| 46 | 2 | 10. | 2.5 | |
| 47 | | | 3.75 | |
| 55 | 2 | 10. | 3.75 | |
| 48 | | | 3.75 | .05 |
| 56 | 2 | 10. | 3.75 | .05 |
| 57 | | | 5. | |
| 73 | 2 | 10. | 5. | |
| 58 | | | 5. | .05 |
| 74 | 2 | 10. | 5. | .05 |
| 75 | | | 6.25 | |
| 83 | 2 | 10. | 6.25 | |

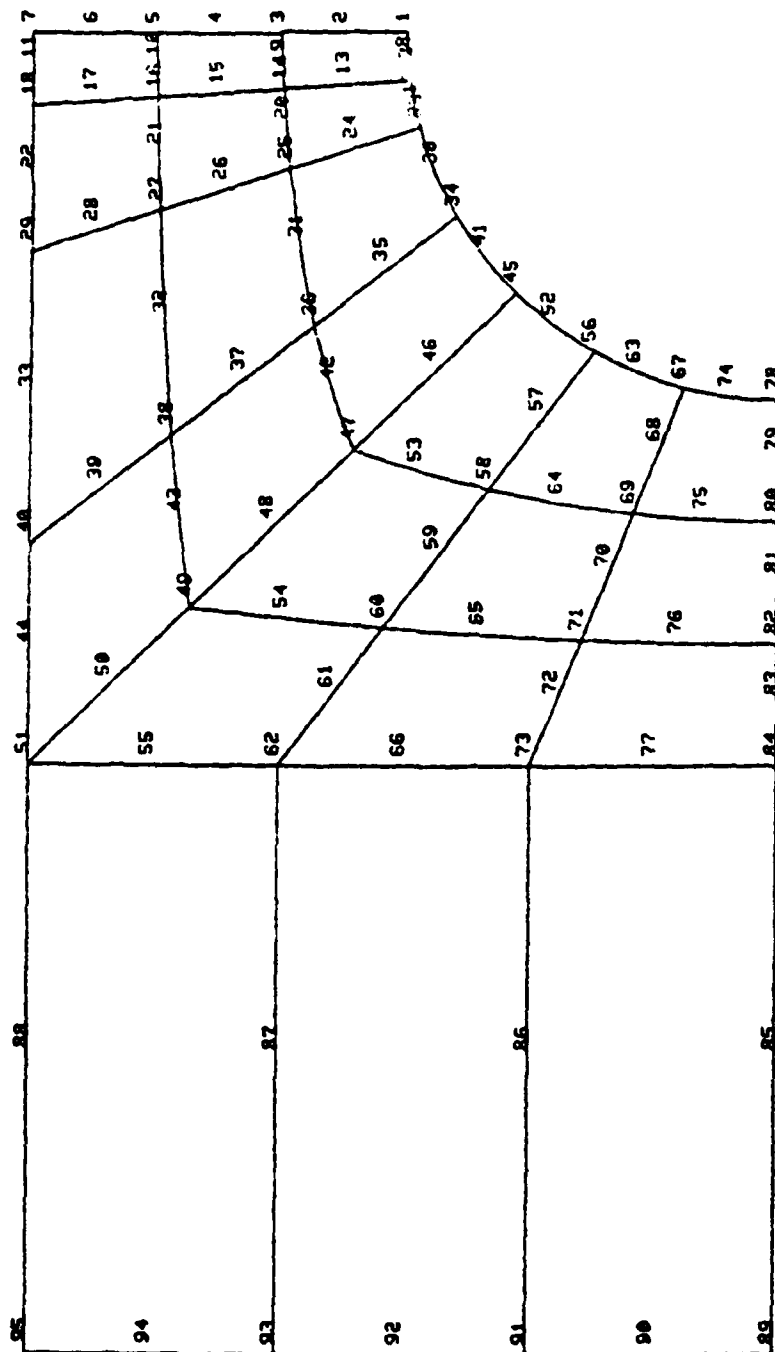
| | | | |
|-----|-----|--|--------------------------------------|
| 8 | | | |
| 1 | 18 | 1 | |
| 2 | | | |
| 1 | 113 | 28 | |
| 1 | | | |
| 2 | 114 | 28 | |
| 1 | | | |
| 19 | 103 | 28 | |
| 1 | | | |
| 20 | 104 | 28 | |
| 1 | | | |
| 113 | 130 | 1 | |
| 3 | | | |
| 17 | 129 | 28 | |
| 3 | | | |
| 27 | 111 | 28 | |
| 3 | | | |
| 2 | | | |
| 1 | 2 | PRESSURE P = 210 + T/100 (10 PSI STEP) | |
| | 0. | 210. | 20000. |
| | | | 410. |
| 2 | 2 | TRIGGER? LOAD = CONSTANT 0.01 | |
| | 0. | 0.01 | 20000. |
| | | | 0.01 |
| 1 | 3 | -1. | CENT. LOAD TO TRIGGER TRANSV. DISPL. |
| | | 2 | |
| 8 | 13 | 16 | 1 1 0 1 -1. |

Input Deck Example #4

Elastic-Plastic Analysis of a Perforated Strip (Section 6.15)

Type of Analysis Nonlinear Static
Number of Increments 2
Equilibrium Iteration Combined Newton-Raphson
Coordinate Data Cartesian/Cylindrical
Element Type 9 (24 Elements)
Data Curves 2 (Stress-Strain and Applied
Loading)
External Forces Nodal Loads





PERFORATED TENSION STRIP, PLASTIC ANALYSIS, LINEAR STRAIN HARDENING
 MAX. LOAD = YIELD STRESS X MINIMUM SECTION WIDTH UNITS KGF/MM/SEC
 8-NODE PLANE-STRESS-ELEMENTS (TYPE 9) 3X3 INTEGRATION

1 1 2 2 0 1 1 0 0 0 1

2

0.

0.

3 1 20 0.1 1.E-20

COORDINATES

95

1A

5.

7

10.

8A

5.

11

10.

12A

5.

18

10.

19A

5.

22

10.

23A

5.

29

10.

30A

5.

33

10.

34A

5.

40

10.

41A

5.

44

10.

45A

5.

51

10.

52A

5.

55

1

8.333333

10.

| | | |
|-----|------------|------|
| 56A | 5. | 60. |
| 62 | 1 6.666667 | 10. |
| 63A | 5. | 67.5 |
| 66 | 1 5. | 10. |
| 67A | 5. | 75. |
| 73 | 1 3.333333 | 10. |
| 74A | 5. | 82.5 |
| 77 | 1 1.666667 | 10. |
| 78A | 5. | 90. |
| 84 | 1 0. | 10. |
| 85 | 0. | 14. |
| 88 | 1 10. | 14. |
| 89 | 0. | 18. |
| 95 | 1 10. | 18. |

| | | | | | | | | | |
|-------|---|----|-----|----|------|-------|----|----|----|
| 9 | 1 | 24 | 0.2 | 0. | 24.3 | .0002 | 0. | 1 | 2 |
| 7000. | 1 | 3 | 1 | 3 | 14 | 12 | 2 | 9 | 13 |
| 1 | 1 | 3 | 11 | 3 | 5 | 16 | 4 | 10 | 15 |
| 7 | 1 | 3 | 11 | 3 | 5 | 16 | 4 | 10 | 15 |
| 8 | 1 | 3 | 11 | 3 | 5 | 16 | 4 | 10 | 15 |
| 14 | 1 | 3 | 11 | 3 | 5 | 16 | 4 | 10 | 15 |
| 15 | 1 | 3 | 11 | 3 | 5 | 16 | 4 | 10 | 15 |
| 21 | 1 | 3 | 11 | 3 | 5 | 16 | 4 | 10 | 15 |
| 22 | 1 | 3 | 11 | 3 | 5 | 16 | 4 | 10 | 15 |
| 23 | 1 | 3 | 11 | 3 | 5 | 16 | 4 | 10 | 15 |
| 24 | 1 | 3 | 11 | 3 | 5 | 16 | 4 | 10 | 15 |

REFERENCES

SECTION 2.1:

1. S. Yaghmai, "Incremental Analysis of Large Deformations in Mechanics of Solids, with Application to Axisymmetric Shells of Revolution," Ph.D. Dissertation, Dept. of Civil Engineering, University of California, Berkeley, 1969.
2. D. P. Mondkar and G. H. Powell, "Finite Element Analysis of Nonlinear Static and Dynamic Response," Int. J. Num. Meth. Engng., Vol. 11, pp. 499-520, 1977.
3. L. E. Malvern, Introduction to the Mechanics of a Continuous Medium, Prentice-Hall, 1969.
4. J. T. Oden, Finite Elements of Nonlinear Continua, McGraw-Hill, 1972.
5. C. Truesdell and W. Noll, "The Nonlinear Field Theories of Mechanics, in Encyclopedia of Physics, Vol. 3, Springer-Verlag, New York, 1965.
6. P. Sharifi and D. N. Yates, "Nonlinear Thermo-Elastic-Plastic and Creep Analysis by the Finite Element Method," AIAA J., Vol. 12, No. 9, 1975.

SECTION 2.2:

1. G. Strang and G. J. Fix, An Analysis of the Finite Element Method, Prentice-Hall, 1973.

SECTION 2.3:

1. L. E. Malvern, Introduction to the Mechanics of a Continuous Medium, Prentice-Hall, 1969.
2. C. T. Wang, Applied Elasticity, McGraw-Hill, 1953.
3. S. W. Key, J. H. Biffle, and R. D. Krieg, "A Study of the Computational and Theoretical Differences of Two Finite Strain Elastic-Plastic Constitutive Models," in Formulations and Computational Algorithms in Finite Element Analysis, Bathe, Oden and Wunderlich, editors, MIT Press, 1977.

4. B. Hunsaker, W. E. Haisler, and J. A. Stricklin, "On the Use of Two Hardening Rules of Plasticity in Incremental and Pseudo-Force Analysis," in Constitutive Equations in Viscoplasticity: Computational and Engineering Aspects, AMD Volume 20, ASME Publications, New York, 1976.
5. A. Mendelson, Plasticity: Theory and Applications, Macmillan, New York, 1968.
6. Y. Yamada, T. Kawai, N. Yoshimura, and T. Sakurai, "Analysis of the Elastic-Plastic Problems by the Matrix Displacement Method," Proceedings of Structural Mechanics, AFFDL-TR-68-150, Wright-Patterson Air Force Base, Ohio, 1969.
7. H. Ziegler, "A Modification of Prager's Workhardening Rule," Zeitschrift fuer Angewandte Mathematik und Physik, Vol. 9a, pp 260-276, Sept. 1958.
8. W. Prager, "The Theory of Plasticity: A Survey of Recent Achievements," Proceedings of the Institution of Mechanical Engineers, Vol. 169, No. 21, pp 41-57, 1955.
9. M. Tanaka, "Large-Deflection Analysis of Elastic-Plastic Circular Plates with Combined Isotropic and Kinematic Hardenings," Ingenieur-Archiv, Vol. 41, pp 342-356, 1972.
10. D. Bushnell, "A Subincremental Strategy for Solving Problems Involving Large Deflections, Plasticity and Creep," in Constitutive Equations in Viscoplasticity: Computational and Engineering Aspects, AMD Volume 20, ASME Publications, New York, 1976.
11. R. M. Jones, Mechanics of Composite Materials, Scripta Book Company, Washington, D.C. 1975.

SECTION 3.3

1. B. M. Irons, "Quadrature Rules for Brick Based Finite Elements," in International Journal for Numerical Methods in Engineering, Vol. 3, No. 2, pp. 293-294.

SECTION 3.4:

1. R. A. Brockman, "A Penalty Function Approach for the Nonlinear Finite Element Analysis of Thin Shells," Ph.D. Dissertation, University of Dayton, Dayton, Ohio, July 1979.

SECTION 4.2:

1. N. Newmark, "A Method of Computation for Structural Dynamics," Proceedings of the A.S.C.E., Journal of the Engineering Mechanics Division, Vol. 85, pp 67-94, 1959.
2. K. J. Bathe and E. L. Wilson, Numerical Methods in Finite Element Analysis, Prentice-Hall, Englewood Cliffs, N. J., 1975.

SECTION 4.3:

1. R. L. Fox, Optimization Methods in Engineering Design, Addison-Wesley, 1971.

SECTION 4.5:

1. A. Jennings, "A Direct Iteration Method of Obtaining the Latent Roots and Vectors of a Symmetric Matrix," Proc. Cambridge Phil. Soc., Vol. 63, pp 755-765, 1967.
2. H. Rutishauser, "Computational Aspects of F. L. Bauer's Simultaneous Iteration Method," Num. Math., Vol. 13, pp 4-13, 1969.
3. R. B. Coor and A. Jennings, "A Simultaneous Iteration Algorithm for Symmetric Eigenvalue Problems," Int. J. Num. Meth. Engng., Vol. 10, pp. 647-663, 1976.

SECTION 6.1:

1. R. Winter and H. S. Levine, "Experiments on Large Plastic Deformations of Circular Plates with Work Hardening," Grumman Research Dept. Report RE-502, Grumman Aerospace Corp., July 1975.
2. B. Hunsaker, W. E., Haisler, and J. A. Stricklin, "On the Use of Two Hardening Rules of Plasticity in Incremental and Pseudo-Force Analysis," in Constitutive Equations in Viscoplasticity: Computational and Engineering Aspects, AMD Vol. 20, ASME Publications, New York, 1976.

SECTION 6.2:

1. O. C. Zienkiewicz and G. C. Nayak, "A General Approach to Problems of Plasticity and Large Deformation Using Isoparametric Elements," Proceedings of the Third Conference on Matrix Methods in Structural Mechanics, AFFDL-TR-71-160, Wright-Patterson Air Force Base, Ohio, pp 881-928, 1973.
2. Anon., MARC-CDC User Information Manual, Publication No. 17311700, Revision H, Vol. III, Control Data Corp., Minneapolis, Minn., October 1974.
3. D. P. Mondkar and G. H. Powell, "Finite Element Analysis of Nonlinear Static and Dynamic Response," Int. J. Num. Meth. Engng., Vol. 11, pp 499-520, 1977.
4. K. J. Bathe, H. Ozdemir, and E. L. Wilson, "Static and Dynamic Geometric and Material Nonlinear Analysis," Report No. UC-SESM-74-4, University of California, Berkeley, 1974.

SECTION 6.4:

1. J. S. Humphreys, "On Dynamic Snap Buckling of Shallow Arches," AIAA Journal, Vol. 4, pp 878-886, 1966.
2. K. J. Bathe, H. Ozdemir, and E. L. Wilson, "Static and Dynamic Geometric and Material Nonlinear Analysis," Report No. UC-SESM-74-4, University of California, Berkeley, 1974.

SECTION 6.5:

1. R. M. Watt, "AFFDL F-16 Canopy Bird Impact Test (Final Checked Data)," Data Package, Project V415-18A, Volume I, Von Karman Gas Dynamics Facility, Arnold Engineering Development Center, Arnold Air Force Station, Tennessee, June 1977.

SECTION 6.6:

1. S. P. Timoshenko and J. N. Goodier, Theory of Elasticity, McGraw-Hill, 1970.

SECTION 6.7:

1. D. P. Mondkar and G. H. Powell, "Static and Dynamic Analysis of Nonlinear Structures," Report No. EERC-75-10, University of California, Berkeley, 1975.
2. J. E. Goldberg and R. M. Richard, "Analysis of Nonlinear Structures," Proceedings A.S.C.E., Journal of the Structural Division, Vol. 89, pp 333-351, 1963.
3. A. K. Noor, "Nonlinear Analysis of Space Trusses," Proceedings A.S.C.E., Journal of the Structural Division, Vol. 100, pp 533-546, 1974.

SECTION 6.8:

1. J. N. Dickson, "Analysis of Bonded Joints in Laminated Composite Materials with Linear Stress-Strain Behavior," Report No. ER 10854, Lockheed Georgia Co., November 1970.
2. J. N. Dickson and T. M. Hsu, "Computer Programs for the Analysis of Bonded Joints," Report No. ER 10856, Lockheed Georgia Co., April 1971.
3. M. Goland and E. Reissner, "The Stresses in Cemented Joints," Transactions of the A.S.M.E., Journal of Applied Mechanics, Vol. 11, No. 1, pp 17-26, March 1974.

SECTION 6.9:

1. G. R. Monforton, "Discrete Element, Finite Displacement Analysis of Anisotropic Sandwich Shells,: Report No. 39, Division of Solid Mechanics, Structures and Mechanics and Design, Case Western Reserve University, 1970.
2. H. P. Kan and J. C. Huang, "Large Deflections of Rectangular Sandwich Plates," AIAA Journal, Vol. 5, pp 1706-1708, 1967.

SECTION 6.10:

1. E. Deutsch, "Das Knicken von Bogenträgern bei Unsymmetrischer Belastung," Der Bauingenieur, Vol. 21, pp 353-360, 1940.
2. D. A. DaDeppo and R. Schmidt, "Instability of Clamped-Hinged Circular Arches Subjected to a Point Load," Transactions of the A.S.M.E., Journal of Applied Mechanics, Vol. 42, pp 894-896, 1975.

SECTION 6.11:

1. S. Timoshenko and S. Woinowsky-Krieger, Theory of Plates and Shells, Second Edition, McGraw-Hill, New York, 1959.

SECTION 6.12:

1. N. J. Hoff, "Bending and Buckling of Rectangular Sandwich Plates, NACA-TN-225, 1950.
2. F. J. Plantema, Sandwich Construction, Wiley, New York, 1966.
3. R. A. Brockman, "Stability of Flat, Simply-Supported Rectangular Sandwich Panels Subjected to Combined Inplane Loadings," AFFDL-TR-76-14, Vol. I, Wright-Patterson Air Force Base, Ohio, 1976.
4. K. H. Boller, "Buckling Loads of Flat Sandwich Panels in Compression: The Buckling of Flat Sandwich Panels with Edges Simply Supported," Report No. 1525-A, Forest Products Laboratory, Madison, Wisconsin, 1947.

5. G. R. Monforton, "Discrete Element, Finite Displacement Analysis of Anisotropic Sandwich Shells," Report No. 39, Division of Solid Mechanics, Structures and Mechanical Design, Case Western Reserve University, 1970.

SECTION 6.13:

1. A. Pica, R. D. Wood, and E. Hinton, "Finite Element Analysis of Geometrically Nonlinear Plate Behavior using a Mindlin Formulation, J. Computers and Structures, Vol. 11, pp. 203-216, 1980.

SECTION 6.14:

1. S. P. Timoshenko and J. M. Gere, Theory of Elastic Stability, McGraw-Hill, 1961.

SECTION 6.15:

1. K. J. Bathe, H. Ozdemir and E. L. Wilson, "Static and Dynamic Geometric and Material Nonlinear Analysis," Report No. UCSESM-74-4, University of California, Berkeley, 1974.
2. P. S. Theocaris, and E. Marketos, "Elastic-Plastic Analysis of Perforated Thin Strips of a Strain-Hardening Material," J. Mechanics and Physics of Solids, Vol. 12, pp. 377-390, 1964.

SECTION 6.16:

1. R. M. Jones, Mechanics of Composite Materials, Scripta Book Co., 1975.

SECTION 6.17:

1. V. B. Venkayya and J. P. Eimermacher, "Recessed Head Fastener Strength Evaluation Program," Technical Memorandum FBR-77-43, Wright-Patterson Air Force Base, Ohio, 1977.
2. E. Bannik, G. Bowman and F. Sandow, "Fastener Recess Evaluation," Wright-Patterson Air Force Base, Ohio, October, 1977.

SECTION 6.18:

1. ———, "The NASTRAN User's Manual," Report No. N78-29506, National Aeronautics and Space Administration, Washington, D.C., July 1976.
2. ———, "ANSYS User's Manual," Swanson Analysis Systems, Inc., July, 1979.
3. NISA (Numerically Integrated Elements for System Analysis), Engineering Mechanics Research Corp., Troy, Michigan.

SECTION 6.20:

1. D. P. Mondkar and G. H. Powell, "Finite Element Analysis of Nonlinear Static and Dynamic Response," Int. J. Num. Meth. Engng., Vol. 11, pp. 499-520, 1977.
2. G. Weeks, "Temporal Operators for Nonlinear Structural Dynamics Problems," J. Eng. Mech. Div., ASCE, Vol. 98, pp. 1087-1104, 1972.

SECTION 11.0:

1. ———, "PLOT-10 Terminal Control System User's Manual," Document No. 062-1474-00, Tektronix, Beaverton, Oregon, 1974.

END

FILMED

8-83

DTIC